Acoustics and Aerodynamic Sound

Music, calm speech, whispering leaves fluttering in a breeze are pleasant and desirable sounds. Noise, howling gales, explosions and screeching traffic are less so. A quantitative understanding of the sources of all such sounds can be obtained by careful analysis of the mechanical equations of motion. This is provided by *Acoustics and Aerodynamic Sound*, which serves as a short, one-semester introduction to acoustics and aerodynamic sound at the advanced undergraduate and graduate levels.

Sound is treated as a branch of fluid mechanics, which is possible because students embarking on an advanced course in acoustics will be familiar with this topic. It is also desirable because an ability to relate acoustic events to hydrodynamic phenomena provides insight into acoustic principles, in particular into the role of vorticity in the mechanics of sound production by vibrating bodies and in the scattering and diffraction of sound.

MICHAEL HOWE has more than 30 years of experience in research on fluid mechanics, acoustics, random vibration, and structural mechanics. He is the author of more than 200 refereed journal articles on these and related subjects. His books include *Acoustics of Fluid-Structure Interactions*; *The Theory of Vortex Sound*; *Hydrodynamics and Sound*; and *Mathematical Methods for Mechanical Sciences.*

His expertise in acoustics has been recognised by the American Society of Mechanical Engineers, which awarded him the Per Bruel Gold Medal (2000); the American Institute of Aeronautics and Astronautics, which awarded him the Aero-Acoustics Medal (2001); and the Institute of Acoustics, which awarded him the Rayleigh Medal (2007).

Downloaded from https://www.cambridge.org/core. Charité Universitätsmedizin Berlin, on 20 Dec 2021 at 10:08:46, subject to the Cambridge Core terms of use, available at https://www.cambridge.org/core/terms. https://doi.org/10.1017/CBO9781107360273

Downloaded from https://www.cambridge.org/core. Charité Universitätsmedizin Berlin, on 20 Dec 2021 at 10:08:46, subject to the Cambridge Core terms of use, available at https://www.cambridge.org/core/terms. https://doi.org/10.1017/CBO9781107360273

Acoustics and Aerodynamic Sound

MICHAEL HOWE
Boston University

CAMBRIDGE
UNIVERSITY PRESS

Downloaded from https://www.cambridge.org/core. Charité Universitätsmedizin Berlin, on 20 Dec 2021 at 10:08:46, subject to the Cambridge Core terms of use, available at https://www.cambridge.org/core/terms. https://doi.org/10.1017/CBO9781107360273

CAMBRIDGE
UNIVERSITY PRESS

32 Avenue of the Americas, New York, NY 10013-2473, USA

Cambridge University Press is part of the University of Cambridge.

It furthers the University's mission by disseminating knowledge in the pursuit of education, learning and research at the highest international levels of excellence.

www.cambridge.org
Information on this title: www.cambridge.org/9781107044401

© Michael Howe 2015

This publication is in copyright. Subject to statutory exception and to the provisions of relevant collective licensing agreements, no reproduction of any part may take place without the written permission of Cambridge University Press.

First published 2015

Printed in the United States of America

A catalog record for this publication is available from the British Library.

Library of Congress Cataloging in Publication Data
Howe, Michael (Acoustical engineer)
Acoustics and aerodynamic sound / Michael Howe, Boston University.
pages cm
Includes bibliographical references and index.
ISBN 978-1-107-04440-1 (hardback)
1. Acoustical engineering. I. Title.
TA365.H695 2014
620.2–dc23 2014024212

ISBN 978-1-107-04440-1

Cambridge University Press has no responsibility for the persistence or accuracy of URLs for external or third-party Internet Web sites referred to in this publication and does not guarantee that any content on such Web sites is, or will remain, accurate or appropriate.

Downloaded from https://www.cambridge.org/core. Charité Universitätsmedizin Berlin, on 20 Dec 2021 at 10:08:46, subject to the Cambridge Core terms of use, available at https://www.cambridge.org/core/terms. https://doi.org/10.1017/CBO9781107360273

In memoriam Dorothy Howe

1921–2014

Downloaded from https://www.cambridge.org/core. Charité Universitätsmedizin Berlin, on 20 Dec 2021 at 10:08:47, subject to the Cambridge Core terms of use, available at https://www.cambridge.org/core/terms. https://doi.org/10.1017/CBO9781107360273

Downloaded from https://www.cambridge.org/core. Charité Universitätsmedizin Berlin, on 20 Dec 2021 at 10:08:47, subject to the Cambridge Core terms of use, available at https://www.cambridge.org/core/terms. https://doi.org/10.1017/CBO9781107360273

Contents

Preface *page* xiii

1 Introduction 1
1.1 Sources of sound 1
1.2 Equations of motion of a fluid 2
1.2.1 The material derivative 2
1.2.2 Equation of continuity 2
1.2.3 Momentum equation 3
1.2.4 Energy equation 3
1.2.5 Equation of state 4
1.2.6 Crocco's equation 5
1.3 Sound waves in an ideal fluid 6
1.3.1 The wave equation for an ideal fluid 7
1.3.2 Speed of sound 9
1.3.3 Plane waves 9
1.4 Low-frequency pulsations of a sphere 13
1.4.1 Acoustic compactness 13
1.4.2 Radiation from an acoustically compact pulsating sphere 14
1.5 The point source 16
1.5.1 Sound produced by a point source 16
1.5.2 Singular behaviour at $\mathbf{x} = 0$ 17
1.5.3 Impulsive point source 18
1.6 Free space Green's function 19
1.6.1 The retarded potential 19
1.6.2 Green's function in one or two space dimensions: Method of descent 20

Downloaded from https://www.cambridge.org/core. Charité Universitätsmedizin Berlin, on 20 Dec 2021 at 10:08:46, subject to the Cambridge Core terms of use, available at https://www.cambridge.org/core/terms. https://doi.org/10.1017/CBO9781107360273

1.7 Initial value problem for the wave equation 21
1.7.1 Sound radiated from a spherical region of initial high pressure 24
1.8 Monopoles, dipoles and quadrupoles 25
1.8.1 The monopole 25
1.8.2 Dipole sources and dipole distributions 27
1.8.3 Quadrupoles 28
1.8.4 Solution of the general linear acoustic equation 29
1.8.5 Vibrating sphere 30
1.9 Acoustic energy equation 32
1.9.1 Calculation of the energy flux 33
1.9.2 Power radiated by a vibrating sphere 34
1.9.3 Energy radiated during the sudden release of high-pressure air 35
1.10 Calculation of the acoustic far field 37
1.10.1 Dipole source distributions 38
1.10.2 Quadrupole source distributions 39
1.10.3 Example 40
1.10.4 Multipole expansion of the field of a compact source 41
1.10.5 Transition to the far field 41
Problems 1 42

2 More on Green's Function 47
2.1 Kirchhoff's formula 47
2.1.1 Volume and surface integral transformations 48
2.1.2 First derivation of Kirchhoff's formula 49
2.1.3 Sound generation by a compact vibrating body 51
2.1.4 Generalised Kirchhoff formula 52
2.1.5 Example: Green's function for a plane boundary 54
2.1.6 Kirchhoff's formula for the velocity potential 55
2.1.7 Determinancy of the sound 55
2.2 Advanced potentials 56
2.2.1 Kirchhoff's formula 57
2.3 The time-harmonic wave equation 58
2.3.1 Time-harmonic Green's function 59
2.3.2 Dipole and quadrupole sources 60
2.3.3 Kirchhoff's formula in the frequency domain 60
2.4 The reciprocal theorem 61
2.5 The compact Green's function 63

Downloaded from https://www.cambridge.org/core. Charité Universitätsmedizin Berlin, on 20 Dec 2021 at 10:08:46, subject to the Cambridge Core terms of use, available at https://www.cambridge.org/core/terms. https://doi.org/10.1017/CBO9781107360273

2.5.1 Time-harmonic compact Green's function 63
2.6 The sphere and cylindrical bodies 67
2.6.1 Compact Green's function for a sphere 67
2.6.2 Cylindrical bodies: The circular cylinder 70
2.6.3 The rigid strip 72
2.7 Symmetric compact Green's function 74
2.8 Radiation and scattering by a compact body 77
2.8.1 Low-frequency radiation 77
2.8.2 Low-frequency sound produced by an arbitrary vibrating body 79
2.8.3 Rayleigh scattering: Scattering of sound by a compact body 81
2.9 Compact Green's function reference 84
2.9.1 Special cases 84
2.9.1a Wall with compact surface irregularity 84
2.9.1b Half-plane: $x_1 < 0,\ x_2 = 0, -\infty < x_3 < \infty$ 85
2.9.1c Half-plane with two-dimensional sources 87
2.9.1d Infinite duct 87
2.9.1e Open end of a duct 88
2.9.1f Circular disc 90
2.9.1g Circular aperture 90
2.9.2 Compact Green's function in two dimensions 91
2.A Appendix: Ideal incompressible flow in two dimensions 93
2.A.1 The complex potential 93
2.A.2 Conformal transformation 96
2.A.3 Equation of motion of a vortex 97
2.A.4 Numerical integration of the vortex path equation 100
Problems 2 100

3 Piston and Diffraction Problems 104
3.1 Radiation from a baffled piston 104
3.1.1 Time-harmonic oscillations 106
3.1.2 Pressure on the axis of symmetry 108
3.1.3 The Fresnel zone 110
3.1.4 Reaction force on the piston 113
3.1.5 Example (Rayleigh 1945) 115
3.2 Diffraction 115
3.2.1 Circular aperture in a plane, rigid screen 118
3.2.2 Babinet's principle 119
3.2.3 Example: Diffraction by a circular disc 120

Downloaded from https://www.cambridge.org/core. Charité Universitätsmedizin Berlin, on 20 Dec 2021 at 10:08:46, subject to the Cambridge Core terms of use, available at https://www.cambridge.org/core/terms. https://doi.org/10.1017/CBO9781107360273

3.2.4 Diffraction by a straight edge 121
3.3 Diffraction by a compact aperture 124
3.3.1 Conductivity of the aperture 125
3.3.2 Conductivity of a circular aperture 126
3.3.3 Transmission of sound through an aperture 127
3.3.4 Compact Green's function for an aperture 129
3.3.5 The bias flow screen 131
3.3.6 The complex conductivity 135
3.3.7 Dissipation by vorticity production 138
Problems 3 140

4 Aerodynamic Sound 143
4.1 Lighthill's acoustic analogy 143
4.2 The v^8-law 146
4.3 Curle's theory 150
4.3.1 Curle's equation 150
4.3.2 Sound produced by turbulence near a compact rigid body 152
4.3.3 The Ffowcs Williams–Hawkings equation (1969) 153
4.3.4 Influence of surface vibration 154
4.4 Vorticity 155
4.4.1 Kinetic energy of incompressible flow 155
4.4.2 Vortex lines and angular velocity 157
4.4.3 The vorticity equation 158
4.4.4 The Biot–Savart formula 160
4.5 Vorticity as a source of sound 162
4.6 The vortex sound equation 164
4.6.1 Reformulation of Lighthill's equation 165
4.6.2 Vortex sound at low Mach numbers 166
4.6.3 Sound generation by a spinning vortex pair (Powell 1963) 167
4.6.4 Example: Method of stationary phase 169
4.7 Vortex-surface interaction noise 170
4.7.1 Example: Sound produced by vortex motion near a half-plane (Crighton 1972) 173
4.8 Radiation from an acoustically compact body 176
4.8.1 Radiation in two dimensions 178
4.9 Influence of vortex shedding 179
4.9.1 Blade-vortex interaction noise in two dimensions 181

Downloaded from https://www.cambridge.org/core. Charité Universitätsmedizin Berlin, on 20 Dec 2021 at 10:08:46, subject to the Cambridge Core terms of use, available at https://www.cambridge.org/core/terms. https://doi.org/10.1017/CBO9781107360273

4.9.2 Comparison with airfoil-gust interaction theory: Kutta condition 184
4.10 Linear theory of vortex-airfoil interaction noise 186
4.10.1 Blade-vortex interactions in three dimensions 188
4.A Appendix: Surface force in incompressible flow 192
4.A.1 Surface force expressed in terms of vorticity 192
4.A.2 Solid body in translational motion 193
4.A.3 Surface force in irrotational flow with sources 194
Problems 4 195

5 Aperture and Duct Problems 205
5.1 Rayleigh's approximation for the conductivity 205
5.1.1 Circular aperture in a thin screen (Rayleigh 1870) 205
5.1.2 Annular aperture 209
5.1.3 Minimum of a ratio of quadratic functions 211
5.2 Impulsive motion of an incompressible fluid 212
5.2.1 Remarks on Kelvin's theorem (1879) 213
5.3 Duct problems 214
5.3.1 Circular aperture in a duct (Fock 1941) 214
5.3.2 Rayleigh's method applied to Fock's problem 216
5.3.3 Example: Sound transmission through a baffle-plate aperture 218
5.3.4 Duct with an annular aperture 220
5.3.5 Example: Analytical approximations for the annular aperture 222
5.4 The end correction 223
5.4.1 Cylindrical duct with a small axisymmetric opening 225
5.4.2 End correction for a flanged duct (Rayleigh 1870) 228
5.5 Duct of variable diameter 230
5.6 Effect of mean flow 232
5.6.1 The Cummings–Fant equation 232
5.6.2 Linearisation of the dissipation integral 234
5.6.3 Time-harmonic sound 235
5.6.4 Absorption at an annular aperture 235
5.7 Sound produced by a synthetic jet 237
5.7.1 Representation of the monopole sound 238
5.7.2 Green's function and the calculation of p_s and p_ω 239
5.7.3 Cummings–Fant equation 241
5.7.4 Time-harmonic piston motion 242
Problems 5 245

Downloaded from https://www.cambridge.org/core. Charité Universitätsmedizin Berlin, on 20 Dec 2021 at 10:08:46, subject to the Cambridge Core terms of use, available at https://www.cambridge.org/core/terms. https://doi.org/10.1017/CBO9781107360273

6 Solutions of Starred Problems 250
6.1 Problems 1 250
6.2 Problems 2 255
6.3 Problems 3 264
6.4 Problems 4 268
6.5 Problems 5 281

Bibliography 287
Index 291

Downloaded from https://www.cambridge.org/core. Charité Universitätsmedizin Berlin, on 20 Dec 2021 at 10:08:46, subject to the Cambridge Core terms of use, available at https://www.cambridge.org/core/terms. https://doi.org/10.1017/CBO9781107360273

Preface

An introductory account is given of the theory of the production and propagation of sound and its interactions with solid structures. It is intended for a one-semester course on acoustics at the advanced undergraduate or graduate level, and is therefore shorter than most of the standard texts – many important applications are omitted, such as speech and musical acoustics, ultrasonic imaging, and thermoacoustics. Sound is treated as a branch of fluid mechanics, which is possible because most students embarking on an advanced course are likely to have some familiarity with fluid mechanics or be sufficiently mature to assimilate the review material provided in the text. It is also desirable because an ability to relate acoustic events to hydrodynamic phenomena provides valuable insight into acoustic principles, in particular into the role of 'vorticity' in the mechanics of sound production by vibrating bodies and in the scattering and diffraction of sound. Any homogeneous fluid that has kinetic energy independent of moving boundaries must possess vorticity, a quantity that propagates by convection and molecular diffusion, and that therefore undergoes relatively little displacement during a typical acoustic cycle; the existence of vorticity signifies the presence of possible sources of sound, and its production occurs when sound is dissipated.

Chapter 1 forms a stand-alone introduction to theoretical acoustics, and is suitable together with material from §§2.1, 2.3, 2.4, 3.1, 3.2, 4.1–4.3, for a 'short course' on acoustics and aerodynamic sound. A general discussion of the Kirchhoff integral representation and generalisations is given in Chapter 2, with particular emphasis on sound sources of various types near an acoustically 'compact' body or section of a larger solid boundary, including the influence of surface vibration and scattering. Chapter 3 deals with the sound radiated by a baffled piston, Kirchhoff diffraction theory, and interactions of sound with apertures and perforated screens. Lighthill's theory of aerodynamic sound and its extensions to sound production by 'vortex-surface interactions'

Downloaded from https://www.cambridge.org/core. Charité Universitätsmedizin Berlin, on 20 Dec 2021 at 10:08:47, subject to the Cambridge Core terms of use, available at https://www.cambridge.org/core/terms. https://doi.org/10.1017/CBO9781107360273.001

are presented in Chapter 4. Methods for treating the interaction of sound with small apertures, constrictions and duct open ends are discussed in Chapter 5, including nonlinear jetting and absorption by vorticity production – inspired by Rayleigh's application of Kelvin's general 'minimum energy' principle to impulsively started fluid motion. Sections numbered with an asterisk may be omitted on a first reading.

No discussion is given of experiments required to validate the theory, nor is there any account of applications to practical noise control problems. The latter are very well treated in several standard engineering handbooks. Similarly, little or no attention is given to specialities such as ray theory and the geometrical theory of diffraction, nonlinear effects of propagation, or the influence on propagation and sound generation of high-speed flows and combusting flows. Electrical analogies involving 'lumped parameter' models also are avoided. Nevertheless, the book provides a self-consistent treatment of the more familiar processes of propagation, scattering, diffraction and production of sound.

The reader is assumed to possess a working knowledge of vector calculus including Cartesian tensor notation, and of rudimentary generalised functions ('delta' function, etc.). A good appreciation of the subject requires the student to work through the problems at the end of each chapter, which should be within the capabilities of most students working alone. Some of the problems are perhaps better treated as short end-of-term projects. Solutions of 'starred' problems are outlined in Chapter 6.

Michael Howe

Downloaded from https://www.cambridge.org/core. Charité Universitätsmedizin Berlin, on 20 Dec 2021 at 10:08:47, subject to the Cambridge Core terms of use, available at https://www.cambridge.org/core/terms. https://doi.org/10.1017/CBO9781107360273.001

1
Introduction

1.1 Sources of sound

Music, calm speech, whispering leaves fluttering in a breeze are pleasant and desirable sounds. Noise, howling gales, explosions and screeching traffic are less so. A quantitative understanding of the *sources* of all such sounds can be obtained by careful analysis of the mechanical equations of motion. Most sources are very complex, frequently involving ill-defined turbulent and perhaps combusting flows and their interactions with vibrating structures, and the energy released as sound tends to be a tiny fraction of that of the structural and hydrodynamic motions. Our analysis must correctly and reliably account for this general *inefficiency* of sound generation, because small errors in source modelling can lead to very large errors in acoustic prediction.

In this book we shall consider only the simplest case in which the fluid can be regarded as continuous and locally homogeneous at all levels of subdivision. The motion of the fluid will be defined when the velocity and the thermodynamic state are specified for each of the *fluid particles* of which it may be supposed to consist. The distinctive fluid property possessed by both liquids and gases is that these fluid particles can move freely relative to one another under the influence of applied forces or other externally imposed changes at the boundaries of the fluid. Five scalar partial differential equations are required to determine these motions. They are statements of conservation of mass, momentum and energy, and they are to be solved subject to appropriate *boundary* and *initial* conditions. These equations will be used to formulate and analyse a wide range of problems; our main task will be to simplify these problems to obtain a thorough understanding of source mechanisms together with a quantitative description of the subsequent propagation of the sound including, possibly, its reflection, scattering and diffraction at solid boundaries.

A general introduction to acoustics is presented in this chapter; it forms the basis for the treatment of the fluid-structure interaction problems examined

Downloaded from https://www.cambridge.org/core. Charité Universitätsmedizin Berlin, on 20 Dec 2021 at 10:08:47, subject to the Cambridge Core terms of use, available at https://www.cambridge.org/core/terms. https://doi.org/10.1017/CBO9781107360273.002

in the rest of the book. The classical acoustic wave equation is derived from the general equations of motion. Particular solutions, methods of solution and applications are then discussed, principally for situations in which acoustic sources radiate into an unbounded fluid.

1.2 Equations of motion of a fluid

The state of a fluid at time t and position $\mathbf{x} = (x_1, x_2, x_3)$ is defined when the velocity $\mathbf{v}$ and any two thermodynamic variables are specified. These quantities are governed by equations describing conservation of mass, momentum and energy, supplemented by a thermodynamic equation of state.

1.2.1 The material derivative

Let v_i denote the component of fluid velocity $\mathbf{v}$ in the x_i direction, and consider the rate at which any function $F(\mathbf{x}, t)$ varies *following the motion* of a fluid particle (a material point moving with the fluid). Let the particle be at $\mathbf{x}$ at time t, and at $\mathbf{x} + \delta\mathbf{x}$ a short time later at time $t + \delta t$, where $\delta\mathbf{x} = \mathbf{v}(\mathbf{x}, t)\delta t + \cdots$. At the new position of the fluid particle

$$F(\mathbf{x} + \delta\mathbf{x}, t + \delta t) = F(\mathbf{x}, t) + v_j \delta t \frac{\partial F}{\partial x_j}(\mathbf{x}, t) + \delta t \frac{\partial F}{\partial t}(\mathbf{x}, t) + \cdots,$$

where the repeated suffix j implies summation over $j = 1, 2, 3$. The limiting value of $(F(\mathbf{x} + \delta\mathbf{x}, t + \delta t) - F(\mathbf{x}, t))/\delta t$ as $\delta t \to 0$ defines the material (or 'Lagrangian') derivative DF/Dt of F:

$$\frac{DF}{Dt} = \frac{\partial F}{\partial t} + v_j \frac{\partial F}{\partial x_j} \equiv \frac{\partial F}{\partial t} + \mathbf{v} \cdot \nabla F. \tag{1.2.1}$$

DF/Dt measures the time rate of change of F as seen by an observer moving with the fluid particle that occupies position $\mathbf{x}$ at time t.

1.2.2 Equation of continuity

A fluid particle of volume V and mass density ρ has a total mass of $\rho V \equiv (\rho V)(\mathbf{x}, t)$, where $\mathbf{x}$ denotes the position of the centroid of V at time t (Figure 1.2.1). Conservation of mass requires that $D(\rho V)/Dt = 0$, that is, that

$$\frac{1}{\rho}\frac{D\rho}{Dt} + \frac{1}{V}\frac{DV}{Dt} = 0. \tag{1.2.2}$$

Now $\frac{1}{V}\frac{DV}{Dt} = \frac{1}{V}\oint_S \mathbf{v} \cdot d\mathbf{S}$, where the integration is over the closed material surface S forming the boundary of V, on which the vector surface element $d\mathbf{S}$ is directed *out* of V. It is the fractional rate of increase of the volume of the

Downloaded from https://www.cambridge.org/core. Charité Universitätsmedizin Berlin, on 20 Dec 2021 at 10:08:47, subject to the Cambridge Core terms of use, available at https://www.cambridge.org/core/terms. https://doi.org/10.1017/CBO9781107360273.002

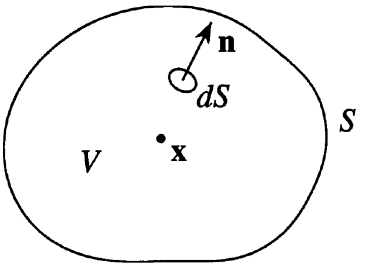

Figure 1.2.1

fluid particle, and becomes equal to $\operatorname{div}\mathbf{v}$ as $V \to 0$. In this limit (1.2.2) can therefore be cast in any of the following equivalent forms of the *equation of continuity*

$$\left.\begin{aligned} \tfrac{1}{\rho}\tfrac{D\rho}{Dt} + \operatorname{div}\mathbf{v} &= 0, \\ \tfrac{\partial\rho}{\partial t} + \operatorname{div}(\rho\mathbf{v}) &= 0, \\ \tfrac{\partial\rho}{\partial t} + \tfrac{\partial}{\partial x_j}(\rho v_j) &= 0. \end{aligned}\right\} \tag{1.2.3}$$

1.2.3 Momentum equation

The momentum equation is derived in a similar manner by consideration of the rate of change of momentum $D(\rho V\mathbf{v})/Dt \equiv (\rho V)D\mathbf{v}/Dt$ of a fluid particle subject to pressure p and **viscous** forces acting on the surface S of V, and body forces $\mathbf{F}$ per unit volume within V. It is sufficient for our purposes to quote the form of the resulting *Navier–Stokes equation*

$$\rho\frac{D\mathbf{v}}{Dt} = -\nabla p - \eta\operatorname{curl}\boldsymbol{\omega} + \left(\eta' + \frac{4}{3}\eta\right)\nabla\operatorname{div}\mathbf{v} + \mathbf{F}, \tag{1.2.4}$$

where $\boldsymbol{\omega} = \operatorname{curl}\mathbf{v}$ is the **vorticity**, and η and η' are respectively the **shear** and **bulk** coefficients of viscosity, which generally vary with pressure, temperature and position in the fluid. Viscous forces are important predominantly close to solid boundaries, where the frictional drag is governed by the shear viscosity η. It is then a good approximation to adopt the *Stokesian* model in which the contribution of the bulk viscosity is ignored.

Values of ρ, η and $\nu = \eta/\rho$ (the 'kinematic' viscosity) for air and water at 10°C and one atmosphere pressure are given in Table 1.2.1.

1.2.4 Energy equation

Consideration of the transfer of heat by molecular diffusion across the moving material boundary S of the fluid particle of Figure 1.2.1, and of the generation

Downloaded from https://www.cambridge.org/core. Charité Universitätsmedizin Berlin, on 20 Dec 2021 at 10:08:47, subject to the Cambridge Core terms of use, available at https://www.cambridge.org/core/terms. https://doi.org/10.1017/CBO9781107360273.002

Table 1.2.1

	ρ kg/m^3	η kg/ms	ν m^2/s
Air	1.23	$1.764\ 10^{-5}$	$1.433\ 10^{-5}$
Water	1000	$1.284\ 10^{-3}$	$1.284\ 10^{-6}$

of heat by frictional dissipation within its interior volume V leads to the energy equation

$$\rho T \frac{Ds}{Dt} = 2\eta \left(e_{ij} - \frac{1}{3} e_{kk} \delta_{ij} \right)^2 + \eta' e_{kk}^2 + \operatorname{div}\left(\kappa \nabla T \right), \tag{1.2.5}$$

where $\rho T\, Ds/Dt$ is the time rate of change following a fluid particle of the heat gained per unit volume. T, s are respectively the absolute temperature and specific entropy (i.e. entropy per unit mass), κ is the thermal conductivity of the fluid, and

$$e_{ij} = \frac{1}{2} \left(\frac{\partial v_i}{\partial x_j} + \frac{\partial v_j}{\partial x_i} \right) \tag{1.2.6}$$

is the rate of strain tensor, which accounts for changes in shape of the fluid particle. Because $e_{kk} \equiv \operatorname{div} \mathbf{v}$, the term involving the bulk coefficient of viscosity η' in (1.2.5) determines the dissipative production of heat during compressions and rarefactions of the fluid.

To understand the significance of the rate of strain tensor, observe that the velocity $\mathbf{v}'$ relative to the centroid of the moving fluid particle at vector distance $\mathbf{x}'$ from its centroid, is given to first order by

$$\begin{aligned} v_i' = x_j' \frac{\partial v_i}{\partial x_j} \;&\equiv\; x_j' \frac{1}{2} \left(\frac{\partial v_i}{\partial x_j} + \frac{\partial v_j}{\partial x_i} \right) + x_j' \frac{1}{2} \left(\frac{\partial v_i}{\partial x_j} - \frac{\partial v_j}{\partial x_i} \right) \\ &= \frac{1}{2} \frac{\partial}{\partial x_i'} \left(e_{jk} x_j' x_k' \right) + \frac{1}{2} \left(\boldsymbol{\omega} \wedge \mathbf{x}' \right)_i \end{aligned} \tag{1.2.7}$$

where e_{ij} and the vorticity $\boldsymbol{\omega}$ are evaluated at the centroid. The term in $\boldsymbol{\omega}$ therefore represents relative *rigid body rotation* of the particle about the centroid, at angular velocity $\frac{1}{2}\boldsymbol{\omega}$, with no change of shape. The gradient term, however, represents an *irrotational* distortion of V, and is responsible for frictional forces and the conversion of mechanical energy into heat.

1.2.5 Equation of state

In the presence of velocity and pressure gradients a fluid cannot be in strict thermodynamic equilibrium, so that thermodynamic variables require special

Downloaded from https://www.cambridge.org/core. Charité Universitätsmedizin Berlin, on 20 Dec 2021 at 10:08:47, subject to the Cambridge Core terms of use, available at https://www.cambridge.org/core/terms. https://doi.org/10.1017/CBO9781107360273.002

interpretation. The density ρ and the total internal energy e per unit mass can be defined in the usual way for a very small fluid particle without the need for thermodynamic equilibrium, such that ρ and ρe are the mass and internal energy per unit volume. The pressure and all other thermodynamic quantities are then defined by means of the same functions of ρ and e that would be used for a system in thermal equilibrium, and the relations between the thermodynamic variables are then the same as for a fluid in local thermodynamic equilibrium, defined by equations of the form

$$p = p(\rho, s), \quad p = p(\rho, T), \quad s = s(\rho, T), \quad \text{etc.} \tag{1.2.8}$$

The equations of state (1.2.8) permit any thermodynamic variable to be expressed in terms of any two variables, such as the density and temperature, although in applications it may be more convenient to use other such equations. There is no dissipation when sound propagates in an *ideal fluid*: $Ds/Dt = 0$ and it is usual to assume *homentropic* motion $s = s_o$ = constant. This permits the fluid motion to be determined from the equations of continuity and momentum and the equation of state $p = p(\rho, s_o)$, the energy equation being ignored. In more general situations it is necessary to retain the energy equation to account for coupling between macroscopic motions and the internal energy of the fluid.

Note, however, that the *thermodynamic pressure* $p = p(\rho, e)$ defined in this way is generally no longer the sole source of *normal stress* on any surface drawn in the fluid. This is the case in a fluid of non-zero bulk viscosity ($\eta' \neq 0$), whose molecules possess rotational (or other internal) degrees of freedom whose relaxation time required for the re-establishment of thermal equilibrium after, say, a compression, is large relative to the equilibration time of the translational degrees of freedom. When compressed (during an interval in which $\operatorname{div} \mathbf{v} < 0$) the temperature must rise, but the corresponding increase in the rotational energy lags slightly behind that of the molecular translational energy responsible for normal stress; the thermodynamic pressure p accordingly is smaller than the true normal stress (which equals $p - \eta' \operatorname{div} \mathbf{v}$). For most acoustic problems such discrepancies are sufficiently small to be neglected in a first approximation and will not be considered further.

1.2.6 Crocco's equation

The momentum equation (1.2.4) can be recast by introducing the specific enthalpy $w = e + p/\rho$ of the fluid, in terms of which the first law of thermodynamics supplies the relation

Downloaded from https://www.cambridge.org/core. Charité Universitätsmedizin Berlin, on 20 Dec 2021 at 10:08:47, subject to the Cambridge Core terms of use, available at https://www.cambridge.org/core/terms. https://doi.org/10.1017/CBO9781107360273.002

$$dw = \frac{dp}{\rho} + T\,ds. \tag{1.2.9}$$

The vector identity $(\mathbf{v}\cdot\nabla)\mathbf{v} = \boldsymbol{\omega}\wedge\mathbf{v} + \nabla\left(\frac{1}{2}v^2\right)$ and (1.2.9) permit the momentum equation to be put in **Crocco's** form

$$\frac{\partial\mathbf{v}}{\partial t} + \nabla B = -\boldsymbol{\omega}\wedge\mathbf{v} + T\nabla s - \nu\,\mathrm{curl}\,\boldsymbol{\omega} + \left(\nu' + \tfrac{4}{3}\nu\right)\nabla\,\mathrm{div}\,\mathbf{v} + \frac{\mathbf{F}}{\rho}, \tag{1.2.10}$$

where $\nu' = \eta'/\rho$ and

$$B = w + \tfrac{1}{2}v^2 \tag{1.2.11}$$

is the **total enthalpy**. In a **perfect gas** $w = c_pT = \gamma p/(\gamma-1)\rho$, where c_p is the specific heat at constant pressure and $\gamma = c_p/c_v$, c_v being the specific heat at constant volume.

Crocco's equation finds application in the acoustics of turbulent, heat conducting flows.

1.3 Sound waves in an ideal fluid

The intensity of an acoustic pressure p in air (relative to the mean atmospheric pressure p_o) is usually measured in decibels by the quantity

$$20\times\log_{10}\left(\frac{|p|}{p_{ref}}\right),$$

where the reference pressure $p_{ref} = 2\times10^{-5}$ Pa. Thus, $p = p_o \equiv 1$ atmosphere ($= 10^5$ Pa) is equivalent to 194 dB. A very loud sound $\sim$ 120 dB corresponds to

$$\frac{p}{p_o} \approx \frac{2\times10^{-5}}{10^5}\times10^{\left(\frac{120}{20}\right)} = 2\times10^{-4} \ll 1.$$

Similarly, for a 'deafening' sound of 160 dB, $p/p_o \sim 0.02$. This corresponds to a pressure of about 0.3 lbs/in^2, and is loud enough for 'nonlinear effects' to begin to be important.

The passage of a sound wave in the form of a pressure fluctuation is accompanied by a back-and-forth motion of the fluid in the direction of propagation at the *acoustic particle velocity* v, say. It will be seen (§1.3.3) that

$$\text{acoustic particle velocity} \approx \frac{\text{acoustic pressure}}{\rho_o \times \text{speed of sound}},$$

where ρ_o is the mean air density. The 'speed of sound' in air is about 340 m/sec. Thus, $v \sim 5$ cm/sec at 120 dB; at 160 dB $v \sim 5$ m/sec.

Downloaded from https://www.cambridge.org/core. Charité Universitätsmedizin Berlin, on 20 Dec 2021 at 10:08:47, subject to the Cambridge Core terms of use, available at https://www.cambridge.org/core/terms. https://doi.org/10.1017/CBO9781107360273.002

1.3.1 The wave equation for an ideal fluid

In most applications the acoustic pressure is very small relative to p_o, and sound propagation is studied by linearising the equations of motion. We consider first the simplest case of sound propagation in an *ideal fluid* – that is, a homogeneous, inviscid, non–heat-conducting fluid of mean pressure p_o and density ρ_o, which is at rest in the absence of the sound. The energy equation (1.2.5) implies that $Ds/Dt = 0$ so that sound propagation is homentropic (*adiabatic*) with $s = s_o \equiv s(p_o, \rho_o) =$ constant throughout fluid. The implication is that, in an ideal fluid there is negligible dissipation of the organised mechanical energy of the sound by heat and momentum transfer by molecular diffusion between neighbouring fluid particles.

The departures of the pressure and density from their undisturbed values are denoted by p', ρ' where $p'/p_o \ll 1$, $\rho'/\rho_o \ll 1$. The linearised form of the momentum equation (1.2.4) for an ideal fluid ($\eta = \eta' = 0$) then becomes

$$\rho_o \frac{\partial \mathbf{v}}{\partial t} + \nabla p' = \mathbf{F}. \tag{1.3.1}$$

Before linearising the continuity equation (1.2.3) it is useful to make an artificial generalisation by inserting a **volume source** distribution $q(\mathbf{x}, t)$ on the right-hand side:

$$\frac{1}{\rho}\frac{D\rho}{Dt} + \operatorname{div} \mathbf{v} = q; \tag{1.3.2}$$

q is the rate of increase of fluid volume per unit volume of the fluid, and might represent, for example, the effect of volume pulsations of a small body in the fluid (§1.4). The linearised equation is then

$$\frac{1}{\rho_o}\frac{\partial \rho'}{\partial t} + \operatorname{div} \mathbf{v} = q. \tag{1.3.3}$$

Eliminate $\mathbf{v}$ between (1.3.1) and (1.3.3):

$$\frac{\partial^2 \rho'}{\partial t^2} - \nabla^2 p' = \rho_o \frac{\partial q}{\partial t} - \operatorname{div} \mathbf{F}. \tag{1.3.4}$$

An equation determining the pressure p' alone in terms of q and $\mathbf{F}$ is obtained by invoking the homentropic approximation $p = p(\rho, s_o)$, where $p_o = p(\rho_o, s_o)$ in the undisturbed state. Therefore

$$p_o + p' = p(\rho_o + \rho', s_o) \approx p(\rho_o, s_o) + \rho' \frac{\partial p}{\partial \rho}(\rho, s_o), \tag{1.3.5}$$

Downloaded from https://www.cambridge.org/core. Charité Universitätsmedizin Berlin, on 20 Dec 2021 at 10:08:47, subject to the Cambridge Core terms of use, available at https://www.cambridge.org/core/terms. https://doi.org/10.1017/CBO9781107360273.002

where the derivative is evaluated at the undisturbed value ρ_o of the density. It has the dimensions of (velocity)^2 and its square root defines the *speed of sound*

$$c_o = \sqrt{\left(\frac{\partial p}{\partial \rho}\right)_s}, \tag{1.3.6}$$

where differentiation is performed at $s = s_o$, and evaluated at $\rho = \rho_o$. In air $c_o \approx 340$ m/s; in water $c_o \approx 1500$ m/s.

From (1.3.5): $\rho' = p'/c_o^2$, and substitution for ρ' in (1.3.4) yields the inhomogeneous wave equation

$$\left(\frac{1}{c_o^2}\frac{\partial^2}{\partial t^2} - \nabla^2\right) p = \rho_o \frac{\partial q}{\partial t} - \operatorname{div} \mathbf{F}, \tag{1.3.7}$$

where the prime $'$ on the acoustic pressure has been discarded. This equation governs the production of sound waves by the volume source q and the force $\mathbf{F}$. When these terms are absent the equation describes sound propagation from sources on the boundaries of the fluid, such as the vibrating cone of a loudspeaker.

The volume source q and (with the exception of gravity) the body force $\mathbf{F}$ would never appear in a complete description of sound generation in a real fluid. They are introduced only when we *think* we understand how to 'model' mathematically the real sources of sound in terms of idealised volume sources and forces. But this can be dangerous and misleading – small errors in specifying the sources often result in very large errors in the predicted sound, because only a tiny fraction of the available energy of a vibrating fluid or structure actually radiates away as sound.

When $\mathbf{F} = \mathbf{0}$ equation (1.3.1) implies the existence of a velocity potential φ such that $\mathbf{v} = \nabla\varphi$, in terms of which the perturbation pressure is given by

$$p = -\rho_o \frac{\partial \varphi}{\partial t}. \tag{1.3.8}$$

It follows from this and (1.3.7) (with $\mathbf{F} = \mathbf{0}$) that the velocity potential is the solution of

$$\left(\frac{1}{c_o^2}\frac{\partial^2}{\partial t^2} - \nabla^2\right) \varphi = -q(\mathbf{x}, t), \tag{1.3.9}$$

where causality has been invoked to discard any time-independent constants of integration in passing from (1.3.7) to (1.3.9). Equation (1.3.9) is the wave equation of classical acoustics.

In the 'propagation zone,' where the source terms $q = 0$, $\mathbf{F} = \mathbf{0}$, the velocity $\mathbf{v}$ and the perturbations in p, ρ (and in other thermodynamic quantities such as the temperature T, internal energy e and enthalpy w, but *not* the specific entropy

Downloaded from https://www.cambridge.org/core. Charité Universitätsmedizin Berlin, on 20 Dec 2021 at 10:08:47, subject to the Cambridge Core terms of use, available at https://www.cambridge.org/core/terms. https://doi.org/10.1017/CBO9781107360273.002

Table 1.3.1 *Speed of sound and acoustic wavelength*

	c_o				λ at 1 kHz	
	m/s	f/s	km/h	mph	metres	feet
Air	340	1100	1225	750	0.3	1
Water	1500	5000	5400	3400	1.5	5

s, which remains constant and equal to s_o) propagate as sound governed by the homogeneous form of (1.3.9). The velocity fluctuation **v** produced by the passage of the wave is the **acoustic particle velocity**.

1.3.2 Speed of sound

In a perfect gas $p = \rho \mathrm{R} T$ and $s = c_v \ln(p/\rho^\gamma)$, where $\mathrm{R} = c_p - c_v$ is the gas constant, and in the linearised approximation

$$c_o = \sqrt{\gamma p_o/\rho_o} = \sqrt{\gamma \mathrm{R} T_o}. \tag{1.3.10}$$

The wavelength λ of sound of frequency f Hz is the distance travelled by the sound in one period $1/f$, that is, $\lambda = c_o/f$. Typical approximate speeds of sound in air and in water, and the corresponding acoustic wavelength at $f = 1$ kHz are given in Table 1.3.1.

1.3.3 Plane waves

A plane acoustic wave propagating in the x direction satisfies

$$\left(\frac{1}{c_o^2}\frac{\partial^2}{\partial t^2} - \frac{\partial^2}{\partial x^2}\right)\varphi = 0, \tag{1.3.11}$$

which has the general solution (D'Alembert 1747)

$$\varphi = \Phi\left(t - \frac{x}{c_o}\right) + \Psi\left(t + \frac{x}{c_o}\right), \tag{1.3.12}$$

where Φ, Ψ are arbitrary functions that respectively represent waves travelling at speed c_o without change of form in the positive and negative x directions. The acoustic particle velocity $\mathbf{v} = \nabla\varphi$ is parallel to the propagation direction (the waves are 'longitudinal').

The solutions (1.3.12) and the linearised (source-free) equations of motion can be used to show that fluctuations in v, p, ρ', T' and w' in a plane wave propagating parallel to the x-axis in a perfect gas are related by

Downloaded from https://www.cambridge.org/core. Charité Universitätsmedizin Berlin, on 20 Dec 2021 at 10:08:47, subject to the Cambridge Core terms of use, available at https://www.cambridge.org/core/terms. https://doi.org/10.1017/CBO9781107360273.002

$$v = \pm\frac{p}{\rho_o c_o}, \quad \rho' = \frac{p}{c_o^2}, \quad T' = \frac{p}{\rho_o c_p}, \quad w' = \frac{p}{\rho_o}, \tag{1.3.13}$$

where v is measured in the positive x direction and the $\pm$ sign is taken according as the wave propagates in the positive or negative x direction.

Example 1 Waves in a uniform tube generated by an oscillating piston The end $x = 0$ of an infinitely long, uniform tube is closed by a smoothly sliding piston executing small amplitude normal oscillations at velocity $u_o(t)$ (Figure 1.3.1a). If x increases along the tube, linear acoustic theory and the requirement that sound waves must propagate to $x = +\infty$, away from the piston, imply that $p = p(t - x/c_o)$. At $x = 0$ the velocities of the fluid and piston are the same, so that

$$u_o(t) \equiv \frac{p(t)}{\rho_o c_o}, \qquad \therefore \quad p = \rho_o c_o u_o(t - x/c_o) \text{ for } x > 0.$$

In practice a solution of this kind, where energy is confined by the tube to propagate in waves of constant cross-section, becomes progressively invalid as x increases, because of the accumulation of small effects of flow nonlinearity. Nonlinear analysis reveals that at a point in the wave where the particle velocity is v the wave actually propagates at speed $c_o + v$, so that wave elements where v is large and positive produce 'wave steepening,' resulting ultimately in the formation of 'shock waves.' This type of behaviour is important, for example, for waves generated in a long railway tunnel by the piston effect of an entering high-speed train.

Example 2 Reflection at a closed end (Figure 1.3.1b) Let the plane wave $p = p_I(t - x/c_o)$ approach from $x < 0$ the closed, rigid end at $x = 0$ of a uniform, semi-infinite tube. The reflected pressure $p_R(t + x/c_o)$ is determined by the condition that the (normal) fluid velocity must vanish at $x = 0$. Therefore, $p_I(t)/\rho_o c_o - p_R(t)/\rho_o c_o = 0$, and the overall pressure within the tube is given by

$$p = p_I(t - x/c_o) + p_I(t + x/c_o), \quad x < 0.$$

Reflection at the rigid end causes 'pressure doubling at the wall,' where $p = 2p_I(t)$.

Example 3 Reflection at an open end (Figure 1.3.1c) When the wavelength of the sound is large compared to the radius R of an open ended circular cylindrical tube, the first approximation to the condition satisfied by the acoustic pressure at the open end ($x = 0$) is that the overall pressure

Downloaded from https://www.cambridge.org/core. Charité Universitätsmedizin Berlin, on 20 Dec 2021 at 10:08:47, subject to the Cambridge Core terms of use, available at https://www.cambridge.org/core/terms. https://doi.org/10.1017/CBO9781107360273.002

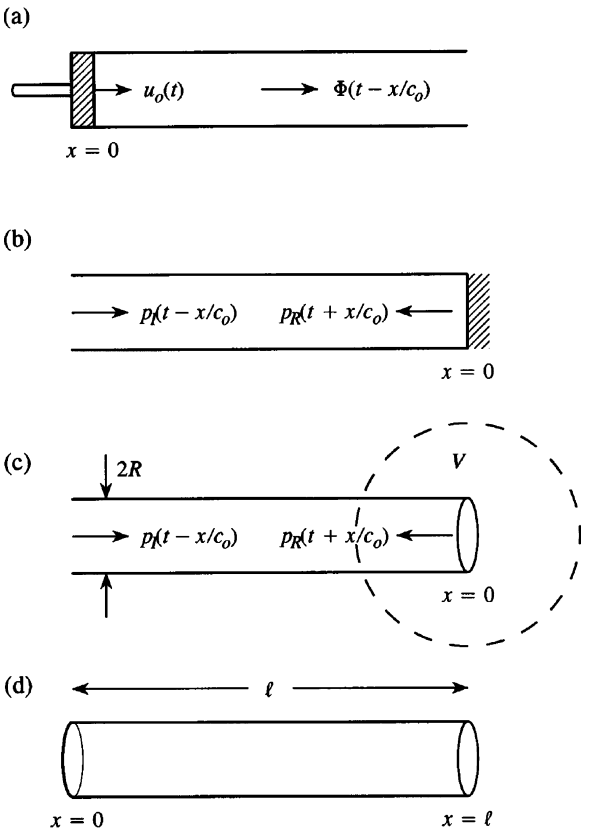

Figure 1.3.1

$p = 0$. Indeed, because of the free expansion of the fluid outside the tube, the pressure outside may be assumed to vanish compared to the incident pressure $p_I(t - x/c_o) \sim p_I(t)$. Then, integration of the linearised momentum equation over the fluid contained in a spherical region V of radius R_s, where $R \ll R_s \ll \lambda =$ the acoustic wavelength, reveals that

$$\pi R^2 p \approx \frac{\partial}{\partial t} \int_V \rho_o v_1 \, d^3\mathbf{x} \sim \frac{f V p_I(t)}{c_o},$$

where $v_1 \sim O(p_I(t)/\rho_o c_o)$ is the particle velocity parallel to the tube, p is the net pressure within the tube close to the open end, and f is the frequency of the sound.

Downloaded from https://www.cambridge.org/core. Charité Universitätsmedizin Berlin, on 20 Dec 2021 at 10:08:47, subject to the Cambridge Core terms of use, available at https://www.cambridge.org/core/terms. https://doi.org/10.1017/CBO9781107360273.002

Therefore, near the open end

$$p \sim \frac{fV}{\pi R^2 c_o} p_I(t) \sim \frac{R_s^3}{R^2 \lambda} p_I(t) \ll p_I(t) \quad \text{as} \quad \lambda = \frac{c_o}{f} \to \infty.$$

Thus, relative to the incident pressure, the pressure at the open end when $\lambda \gg R$ may be assumed to vanish. The pressure wave reflected back into the tube at the end is therefore approximately $-p_I(t + x/c_o)$,

$$p \approx p_I(t - x/c_o) - p_I(t + x/c_o), \quad x < 0,$$

and the acoustic particle velocity in the mouth of the tube $\approx 2p_I(t)/\rho_o c_o$, twice that attributable to the incident wave alone.

Example 4 Low frequency resonant oscillations in a pipe with open ends (Figure 1.3.1d) A pressure wave of complex amplitude $p_\pm$ and radian frequency ω propagating in the $\pm x$ direction has the representation $p = p_\pm \mathrm{e}^{-i\omega(t \mp x/c_o)}$, where the real part is to be taken. Therefore, the combination

$$p = p_+ \mathrm{e}^{-i\omega(t - x/c_o)} + p_- \mathrm{e}^{-i\omega(t + x/c_o)}$$

will vanish at the open end $x = 0$ provided $p_- = -p_+$. The pressure also vanishes at $x = \ell$ when the frequency satisfies

$$\mathrm{e}^{i\omega\ell/c_o} - \mathrm{e}^{-i\omega\ell/c_o} = 0, \quad \text{i.e.} \quad \sin(k_o \ell) = 0$$

where $k_o = \omega/c_o$ is called the **acoustic wavenumber**. This equation accordingly determines the 'resonance frequencies' of an open-ended tube of length ℓ in the low frequency approximation in which the pressure is assumed to vanish at the ends, *viz.*

$$f = \frac{\omega}{2\pi} \approx \frac{n\, c_o}{2\ell}, \quad n = 1,\ 2,\ 3,\ \ldots\ .$$

Thus, the minimum resonance frequency of a pipe of length $\ell = 1$ m is about 170 Hz ($c_o \sim 340$ m/s in air). The wavelength of this sound is $c_o/f \equiv 2\pi/k_o = 2\ell = 2$ m does not depend on the speed of sound.

The simple, one-dimensional theory neglects energy losses from the ends of the tube by radiation into the ambient atmosphere, and neglects also viscous and thermal losses in 'acoustic boundary layers' at the walls of the tube. These cause the wave amplitude to decay after several wave periods, so that resonant oscillations within the tube actually persist only for a finite time after the source of excitation is removed.

Downloaded from https://www.cambridge.org/core. Charité Universitätsmedizin Berlin, on 20 Dec 2021 at 10:08:47, subject to the Cambridge Core terms of use, available at https://www.cambridge.org/core/terms. https://doi.org/10.1017/CBO9781107360273.002

1.4 Low-frequency pulsations of a sphere

1.4.1 Acoustic compactness

Small amplitude motion in an ideal fluid produced by radial pulsations of a spherical body of mean radius a with the centre at the origin is *irrotational* (i.e. $\mathbf{v} = \nabla\varphi$, see Figure 1.4.1) and satisfies the homogeneous equation

$$\frac{1}{c_o^2}\frac{\partial^2\varphi}{\partial t^2} - \nabla^2\varphi = 0, \quad r = |\mathbf{x}| > a. \tag{1.4.1}$$

Let the oscillations occur at frequency ω (proportional to $e^{-i\omega t}$, for example) so that the characteristic wavelength of the sound generated by the motion is $\lambda = 2\pi/k_o$, where $k_o = \omega/c_o$ is the acoustic wavenumber. The sphere is said to be **acoustically compact** if the frequency is small enough that $k_o a \ll 1$, which means that the radius a is a small fraction of λ. More generally, a body is acoustically compact when its characteristic dimension is small compared to the wavelengths of the sound waves it is producing or with which it interacts.

When $a \ll \lambda$ the fluid motion close to the sphere changes significantly over distances $\sim O(a)$. In this region the two terms on the left of (1.4.1) are respectively of orders $k_o^2\varphi$ and φ/a^2 (because $\partial/\partial t \sim \omega$) where $(k_o a)^2 \ll 1$. The unsteady motion in the immediate neighbourhood of the sphere is therefore governed by the **Laplace** equation obtained by discarding the first term on the left of (1.4.1):

$$\nabla^2\varphi = 0, \quad r \sim a. \tag{1.4.2}$$

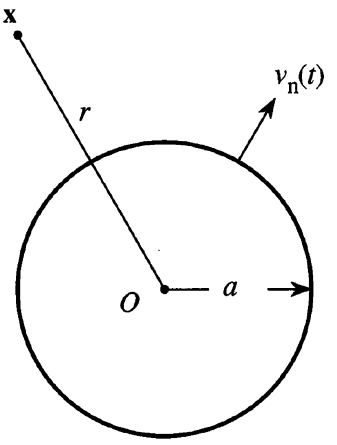

Figure 1.4.1

Downloaded from https://www.cambridge.org/core. Charité Universitätsmedizin Berlin, on 20 Dec 2021 at 10:08:47, subject to the Cambridge Core terms of use, available at https://www.cambridge.org/core/terms. https://doi.org/10.1017/CBO9781107360273.002

This is just the continuity equation $\operatorname{div} \mathbf{v} = 0$ for *incompressible flow*. The corresponding pressure and density perturbations δp and $\delta\rho$ satisfy

$$\delta\rho \approx \frac{\delta p}{c_o^2}.$$

In incompressible, irrotational flow pressure changes are produced by the action of external forces (at boundaries, etc.), but the density must remain fixed. Thus, the formal limit of incompressible motion corresponds to setting $c_o = \infty$.

1.4.2 Radiation from an acoustically compact pulsating sphere

Let the normal velocity on the mean position $r = a$ of the surface of the sphere be $v_n(t)$. We have to solve equation (1.4.1) subject to the (linearised) boundary condition

$$\frac{\partial\varphi}{\partial r} = v_n(t) \quad \text{on} \quad r = a, \quad \text{where} \quad r = |\mathbf{x}|.$$

The solution must be spherically symmetric, so that we may put

$$\nabla^2\varphi \equiv \frac{1}{r^2}\frac{\partial}{\partial r}\left(r^2\frac{\partial}{\partial r}\right)\varphi \equiv \frac{1}{r}\frac{\partial^2}{\partial r^2}(r\varphi)\,.$$

Equation (1.4.1) can therefore be reduced to the *one-dimensional* wave equation for $r\varphi$

$$\frac{1}{c_o^2}\frac{\partial^2}{\partial t^2}(r\varphi) - \frac{\partial^2}{\partial r^2}(r\varphi) = 0, \quad r > a. \tag{1.4.3}$$

The general solution $r\varphi = \Phi(t - r/c_o) + \Psi(t + r/c_o)$, for arbitrary functions Φ and Ψ, yields

$$\varphi = \frac{\Phi\left(t - \frac{r}{c_o}\right)}{r} + \frac{\Psi\left(t + \frac{r}{c_o}\right)}{r}, \quad r > a. \tag{1.4.4}$$

The terms on the right represent respectively spherically symmetric disturbances propagating in the directions of increasing and decreasing values of r at the speed of sound c_o. Causality requires the incoming wave to be omitted, that is, that $\Psi \equiv 0$, because $\Psi(t + r/c_o)/r$ necessarily represents sound arriving from $r = \infty$, which is impossible for pulsations that started at some finite time in the past or in the absence of a distant spherical reflecting surface. This statement of the causality principle is equivalent to imposing a *radiation condition* that sound waves must propagate *away* from their source.

Downloaded from https://www.cambridge.org/core. Charité Universitätsmedizin Berlin, on 20 Dec 2021 at 10:08:47, subject to the Cambridge Core terms of use, available at https://www.cambridge.org/core/terms. https://doi.org/10.1017/CBO9781107360273.002

The outgoing wave function Φ is determined from the condition $\partial\varphi/\partial r = v_n(t)$ at $r = a$, which gives

$$v_n(t) = \frac{\partial}{\partial r}\left(\frac{\Phi\left(t - \frac{r}{c_o}\right)}{r}\right)_{r=a} = -\frac{1}{a^2}\Phi\left(t - \frac{a}{c_o}\right) - \frac{1}{ac_o}\frac{\partial\Phi}{\partial t}\left(t - \frac{a}{c_o}\right). \tag{1.4.5}$$

The two terms on the right are, respectively, the hydrodynamic and acoustic components of $\partial\varphi/\partial r$, the latter vanishing in the incompressible limit $c_o \to \infty$. For a compact sphere a typical component of $\Phi(t) \propto \mathrm{e}^{-i\omega t}$ of radian frequency ω satisfies $k_o a \ll 1$, in which case

$$\mathrm{e}^{-i\omega(t-a/c_o)} \simeq \mathrm{e}^{-i\omega t} \quad \text{and} \quad \frac{a}{c_o}\frac{\partial}{\partial t} \sim k_o a \ll 1.$$

Therefore, the time delay a/c_o on the right of (1.4.5) can be neglected and the time-derivative term discarded, giving $\Phi(t) \simeq -a^2 v_n(t)$, and

$$\varphi \simeq -\frac{a^2 v_n(t - r/c_o)}{r}, \quad r > a.$$

It is more convenient to express this in terms of the volume flux $Q(t) = 4\pi a^2 v_n(t)$ (also called the 'volume velocity'), which is the rate of volume outflow from the sphere:

$$\varphi \simeq -\frac{Q(t - r/c_o)}{4\pi r}, \quad r > a. \tag{1.4.6}$$

The corresponding acoustic pressure fluctuations are

$$p = -\rho_o\frac{\partial\varphi}{\partial t} = \frac{\rho_o}{4\pi r}\frac{\partial Q}{\partial t}\left(t - \tfrac{r}{c_o}\right).$$

The pressure and potential both decay like $1/r$ with distance from the sphere, which is typical of all sound waves spreading in unbounded three-dimensional space. The pressure at time t observed at a distant point r depends on the value of the volume velocity Q at the earlier time $t - r/c_o$, where $r/c_o \sim (r - a)/c_o$ is the time of travel of sound from the sphere; $t - r/c_o$ is called the **retarded time**. The pressure is non-zero only if the volume velocity varies with time, whereas the potential φ continues to represent a steady (and *incompressible*) outflow of fluid when $Q =$ constant. In the incompressible limit ($c_o \to \infty$) the pressure

$$p = \frac{\rho_o}{4\pi r}\frac{\partial Q(t)}{\partial t}$$

still decays like $1/r$, but exhibits the unphysical characteristic of changing instantaneously everywhere when $\partial Q/\partial t$ changes its value.

Downloaded from https://www.cambridge.org/core. Charité Universitätsmedizin Berlin, on 20 Dec 2021 at 10:08:47, subject to the Cambridge Core terms of use, available at https://www.cambridge.org/core/terms. https://doi.org/10.1017/CBO9781107360273.002

The outgoing wave solution (1.4.6) is typical of all compact, pulsating bodies; the far field sound can always be expressed in that form in terms of the corresponding volume velocity $Q(t)$ of the body.

1.5 The point source

1.5.1 Sound produced by a point source

The sound generated by a *volume* point source of strength $Q(t)$ at the origin is the solution of equation (1.3.9) when $q(\mathbf{x}, t) = Q(t)\delta(\mathbf{x})$:

$$\left(\frac{1}{c_o^2}\frac{\partial^2}{\partial t^2} - \nabla^2\right)\varphi = -Q(t)\delta(\mathbf{x}), \quad \text{where } \delta(\mathbf{x}) = \delta(x_1)\delta(x_2)\delta(x_3). \quad (1.5.1)$$

The source strength q is the 'rate of production of fluid volume' per unit volume, so that the net volumetric outflow from the source is

$$\int_{-\infty}^{\infty} q(\mathbf{x}, t)\, d^3\mathbf{x} = \int_{-\infty}^{\infty} Q(t)\delta(\mathbf{x})\, d^3\mathbf{x} = Q(t).$$

The causal solution must be spherically symmetric of the outgoing form

$$\varphi = \frac{\Phi\,(t - r/c_o)}{r}, \quad r = |\mathbf{x}| > 0, \quad (1.5.2)$$

for a suitable wave function Φ, which can be determined by extension of the argument leading to Laplace's equation (1.4.2). The source occupies an infinitesimal region of space and is therefore compact for any component of $Q(t) \propto \mathrm{e}^{-i\omega t}$ of finite frequency, which produces sound of wavelength $\lambda = 2\pi/k_o > 0$. Therefore, as $r \to 0$ the potential $\varphi \approx \Phi(t)/r$ satisfies the incompressible limit of equation (1.5.1)

$$\nabla^2\varphi = Q(t)\delta(\mathbf{x}).$$

$\Phi(t)$ is found by integrating both sides of this equation over the interior of a sphere of infinitesimal radius $r = R$, using the divergence theorem on the left: $\int_{r<R} \nabla^2\varphi d^3\mathbf{x} = \oint_S \nabla\varphi \cdot d\mathbf{S}$, where S is the surface of the sphere. Then

$$\oint_S \nabla\varphi \cdot d\mathbf{S} \equiv \left(\frac{-\Phi(t)}{R^2}\right) \times (4\pi R^2) = Q(t)$$

$$\therefore \quad \Phi(t) = -\frac{Q(t)}{4\pi}. \quad (1.5.3)$$

Hence, the solution of equation (1.5.1) becomes

$$\varphi = -\frac{Q\,(t - r/c_o)}{4\pi r}. \quad (1.5.4)$$

Downloaded from https://www.cambridge.org/core. Charité Universitätsmedizin Berlin, on 20 Dec 2021 at 10:08:47, subject to the Cambridge Core terms of use, available at https://www.cambridge.org/core/terms. https://doi.org/10.1017/CBO9781107360273.002

This agrees with the potential (1.4.6) of sound produced by a pulsating, compact sphere of the same volume velocity, and indicates that the effect of such a sphere at large distances $r \gg a$ can be modelled by replacing the sphere by a point source of the same strength $Q(t)$ = rate of change of the volume of the sphere. This conclusion is valid for any compact pulsating body, not just a sphere.

1.5.2 Singular behaviour at* $\mathbf{x} = 0$

The argument leading to formula (1.5.3) for the wave function $\Phi(t)$ implicitly requires that $k_o R \ll 1$ ($k_o = \omega/c_o$) for all of the different frequency components of $Q(t)$. But the frequency decomposition of an impulsive source, for which $\partial Q/\partial t \to \infty$, usually involves frequencies ω of all orders, for some of which $k_o R \to \infty$ for any $R \neq 0$. To avoid this contradiction the general outgoing solution (1.5.2) must be extended down to the source at $r = 0$, where it is undefined, by writing

$$\varphi = \frac{\Phi\left(t - \frac{r}{c_o}\right)}{r} = \lim_{\epsilon \to 0} \frac{\Phi\left(t - \frac{r}{c_o}\right)}{(r^2 + \epsilon^2)^{\frac{1}{2}}}, \quad r \geq 0. \tag{1.5.5}$$

Let us substitute this into the left-hand side of equation (1.5.1) and examine what happens as $\epsilon \to 0$.

By direct calculation we find

$$\nabla^2 \varphi = \frac{1}{r}\frac{\partial^2}{\partial r^2}(r\varphi) = -\frac{3\epsilon^2 \Phi(t - r/c_o)}{(r^2+\epsilon^2)^{\frac{5}{2}}} - \frac{2\epsilon^2 \Phi'(t - r/c_o)}{c_o r (r^2+\epsilon^2)^{\frac{3}{2}}} + \frac{\Phi''(t - r/c_o)}{c_o^2 (r^2+\epsilon^2)^{\frac{1}{2}}}$$

$$\frac{1}{c_o^2}\frac{\partial^2 \varphi}{\partial t^2} = \frac{\Phi''(t - r/c_o)}{c_o^2 (r^2+\epsilon^2)^{\frac{1}{2}}}$$

$$\therefore \quad \frac{1}{c_o^2}\frac{\partial^2 \varphi}{\partial t^2} - \nabla^2 \varphi = \frac{3\epsilon^2 \Phi(t - r/c_o)}{(r^2+\epsilon^2)^{\frac{5}{2}}} + \frac{2\epsilon^2 \Phi'(t - r/c_o)}{c_o r (r^2+\epsilon^2)^{\frac{3}{2}}}, \tag{1.5.6}$$

where the primes denote differentiation with respect to the argument of Φ. Both terms on the right of (1.5.6) vanish as $\epsilon \to 0$ when $r > 0$, but they are undefined as $\epsilon \to 0$ when $r = 0$. They must therefore be interpreted as generalised functions (Lighthill 1958).

First, for any smoothly varying 'test' function $f(\mathbf{x})$ and any volume V enclosing the origin, as $\epsilon \to 0$

$$\int_V \frac{3\epsilon^2 f(\mathbf{x}) d^3\mathbf{x}}{(r^2+\epsilon^2)^{\frac{5}{2}}} \to f(\mathbf{0}) \int_{-\infty}^{\infty} \frac{3\epsilon^2 d^3\mathbf{x}}{(r^2+\epsilon^2)^{\frac{5}{2}}} = f(\mathbf{0}) \int_0^{\infty} \frac{12\pi\epsilon^2 r^2 dr}{(r^2+\epsilon^2)^{\frac{5}{2}}} = 4\pi f(\mathbf{0}),$$

Downloaded from https://www.cambridge.org/core. Charité Universitätsmedizin Berlin, on 20 Dec 2021 at 10:08:47, subject to the Cambridge Core terms of use, available at https://www.cambridge.org/core/terms. https://doi.org/10.1017/CBO9781107360273.002

where the value of the last integral is independent of ϵ. This is the defining property of $4\pi\delta(\mathbf{x})$, where $\delta(\mathbf{x})$ is the three-dimensional δ-function. Similarly, as $\epsilon \to 0$,

$$\int_V \frac{2\epsilon^2 f(\mathbf{x}) d^3\mathbf{x}}{r(r^2+\epsilon^2)^{\frac{3}{2}}} \to f(\mathbf{0}) \int_{-\infty}^{\infty} \frac{2\epsilon^2 d^3\mathbf{x}}{r(r^2+\epsilon^2)^{\frac{3}{2}}} = f(\mathbf{0}) \int_0^{\infty} \frac{8\pi\epsilon^2 r dr}{(r^2+\epsilon^2)^{\frac{3}{2}}}$$
$$= 8\pi\epsilon f(\mathbf{0}) \to 0.$$

The limiting value of the right-hand side of (1.5.6) as $\epsilon \to 0$ is therefore $4\pi\Phi(t)\delta(\mathbf{x})$, which coincides with the source term in equation (1.5.1) provided $\Phi(t) = -Q(t)/4\pi$. This confirms the general validity of the heuristic argument of §1.5.1, and reveals that the correct interpretation of the solution

$$\varphi = -\frac{Q(t - r/c_o)}{4\pi r}$$

of Equation (1.5.1) is

$$\varphi = -\lim_{\epsilon\to 0} \frac{Q(t - r/c_o)}{4\pi(r^2+\epsilon^2)^{\frac{1}{2}}}, \quad r \geq 0,$$

and that

$$\nabla^2\left(\frac{-1}{4\pi r}\right) = \lim_{\epsilon\to 0} \nabla^2\left(\frac{-1}{4\pi(r^2+\epsilon^2)^{\frac{1}{2}}}\right) = \lim_{\epsilon\to 0} \frac{3\epsilon^2}{4\pi(r^2+\epsilon^2)^{\frac{5}{2}}} = \delta(\mathbf{x}). \tag{1.5.7}$$

1.5.3 Impulsive point source

For the 'impulsive' point source $q = \delta(\mathbf{x})\delta(t)$ equation (1.3.9) becomes

$$\left(\frac{1}{c_o^2}\frac{\partial^2}{\partial t^2} - \nabla^2\right)\varphi = -\delta(\mathbf{x})\delta(t). \tag{1.5.8}$$

The source vanishes except during an infinitesimal instant at $t = 0$. The *causal* solution (with outgoing wave behaviour) is spherically symmetric and non-zero only for $t > 0$. It is found by setting $Q(t) = \delta(t)$ in the solution (1.5.4) of Equation (1.5.1):

$$\varphi(\mathbf{x}, t) = -\frac{1}{4\pi r}\delta\left(t - \frac{r}{c_o}\right) \equiv -\frac{1}{4\pi|\mathbf{x}|}\delta\left(t - \frac{|\mathbf{x}|}{c_o}\right). \tag{1.5.9}$$

The sound wave consists of a singular spherical pulse that is non-zero only on the surface of the sphere $r = c_o t > 0$ expanding at the speed of sound; it vanishes *everywhere* for $t < 0$.

Downloaded from https://www.cambridge.org/core. Charité Universitätsmedizin Berlin, on 20 Dec 2021 at 10:08:47, subject to the Cambridge Core terms of use, available at https://www.cambridge.org/core/terms. https://doi.org/10.1017/CBO9781107360273.002

1.6 Free space Green's function

The free space Green's function $G(\mathbf{x}, \mathbf{y}, t, \tau)$ is the *causal* solution of the wave equation generated by the impulsive point source $\delta(\mathbf{x}-\mathbf{y})\delta(t-\tau)$, located at the point $\mathbf{x}=\mathbf{y}$ at time $t=\tau$. The usual convention in acoustics, however, is to reverse the sign of the source (by putting $q(\mathbf{x}, t) = -\delta(\mathbf{x}-\mathbf{y})\delta(t-\tau)$). The formula for G is then obtained from the solution (1.5.9) for a source at $\mathbf{x}=\mathbf{0}$ at $t=0$ simply by reversing the sign and replacing $\mathbf{x}$ by $\mathbf{x}-\mathbf{y}$ and t by $t-\tau$. In other words, if

$$\left(\frac{1}{c_o^2}\frac{\partial^2}{\partial t^2} - \nabla^2\right) G = \delta(\mathbf{x}-\mathbf{y})\delta(t-\tau), \quad \text{where } G = 0 \quad \text{for } t < \tau, \tag{1.6.1}$$

then

$$G(\mathbf{x}, \mathbf{y}, t, \tau) = \frac{1}{4\pi|\mathbf{x}-\mathbf{y}|}\delta\left(t-\tau-\frac{|\mathbf{x}-\mathbf{y}|}{c_o}\right). \tag{1.6.2}$$

This represents an impulsive, spherically symmetric wave expanding from the source at $\mathbf{y}$ at the speed of sound. The wave amplitude decreases inversely with distance $|\mathbf{x}-\mathbf{y}|$ from the source point $\mathbf{y}$.

1.6.1 The retarded potential

Green's function is the fundamental building block for solutions of the inhomogeneous wave Equation (1.3.7) of linear acoustics in an unbounded medium. Let us write this equation in the form

$$\left(\frac{1}{c_o^2}\frac{\partial^2}{\partial t^2} - \nabla^2\right) p = \mathcal{F}(\mathbf{x}, t), \tag{1.6.3}$$

where the generalised source $\mathcal{F}(\mathbf{x}, t)$ is assumed to be generating waves that propagate away from the source region, in accordance with the radiation condition.

This source distribution can be regarded as a distribution of impulsive point sources of the type on the right of Equation (1.6.1), because

$$\mathcal{F}(\mathbf{x}, t) = \iint_{-\infty}^{\infty} \mathcal{F}(\mathbf{y}, \tau)\delta(\mathbf{x}-\mathbf{y})\delta(t-\tau)d^3\mathbf{y}d\tau.$$

The outgoing wave solution for each constituent source of strength

$$\mathcal{F}(\mathbf{y}, \tau)\delta(\mathbf{x}-\mathbf{y})\delta(t-\tau)d^3\mathbf{y}d\tau \text{ is } \mathcal{F}(\mathbf{y}, \tau)G(\mathbf{x}, \mathbf{y}, t, \tau)d^3\mathbf{y}d\tau,$$

Downloaded from https://www.cambridge.org/core. Charité Universitätsmedizin Berlin, on 20 Dec 2021 at 10:08:47, subject to the Cambridge Core terms of use, available at https://www.cambridge.org/core/terms. https://doi.org/10.1017/CBO9781107360273.002

so that by adding these individual contributions we obtain

$$p(\mathbf{x},t) = \iint_{-\infty}^{\infty} \mathcal{F}(\mathbf{y},\tau) G(\mathbf{x},\mathbf{y},t,\tau)\, d^3\mathbf{y}\, d\tau \tag{1.6.4}$$

$$= \frac{1}{4\pi} \iint_{-\infty}^{\infty} \frac{\mathcal{F}(\mathbf{y},\tau)}{|\mathbf{x}-\mathbf{y}|} \delta\left(t - \tau - \frac{|\mathbf{x}-\mathbf{y}|}{c_o}\right) d^3\mathbf{y}\, d\tau \tag{1.6.5}$$

$$\text{i.e. } p(\mathbf{x},t) = \frac{1}{4\pi} \int_{-\infty}^{\infty} \frac{\mathcal{F}\left(\mathbf{y}, t - \frac{|\mathbf{x}-\mathbf{y}|}{c_o}\right)}{|\mathbf{x}-\mathbf{y}|} d^3\mathbf{y}. \tag{1.6.6}$$

The integral formula (1.6.6) is called a **retarded potential**; it represents the pressure at position $\mathbf{x}$ and time t as a linear superposition of contributions from sources at positions $\mathbf{y}$ that radiated at the earlier times $t - |\mathbf{x}-\mathbf{y}|/c_o$, $|\mathbf{x}-\mathbf{y}|/c_o$ being the time of travel of sound waves from $\mathbf{y}$ to $\mathbf{x}$.

1.6.2 Green's function in one or two space dimensions: Method of descent*

The Green's function for *plane* waves that propagate in one dimension (in a uniform duct, for example) say parallel to the x_1-axis, is the causal solution $G(x_1, y_1, t, \tau)$ of

$$\left(\frac{1}{c_o^2}\frac{\partial^2}{\partial t^2} - \frac{\partial^2}{\partial x_1^2}\right) G = \delta(x_1 - y_1)\delta(t-\tau), \quad \text{where } G = 0 \text{ for } t < \tau. \tag{1.6.7}$$

This equation can be obtained formally by integrating the corresponding three-dimensional equation (1.6.1) over the plane of uniformity $-\infty < x_2,\ x_3 < \infty$. This is Hadamard's (1952) *method of descent* to a lower space dimension. Using the formula (1.6.2) for G in three dimensions, we find that (1.6.7) is satisfied by

$$G(x_1, y_1, t, \tau) = \iint_{-\infty}^{\infty} \frac{1}{4\pi|\mathbf{x}-\mathbf{y}|} \delta\left(t - \tau - \frac{|\mathbf{x}-\mathbf{y}|}{c_o}\right) dy_2 dy_3$$

$$= \int_0^{\infty} \delta\left(t - \tau - \frac{\sqrt{|x_1 - y_1|^2 + \mu^2}}{c_o}\right) \frac{\mu\, d\mu}{2\sqrt{|x_1 - y_1|^2 + \mu^2}}$$

$$= \frac{c_o}{2} \mathrm{H}\left(t - \tau - \frac{|x_1 - y_1|}{c_o}\right), \tag{1.6.8}$$

where $\mathrm{H}(x)$ is the Heaviside unit step function ($= 1, 0$ according as $x \gtrless 0$).

In two dimensions, sound waves propagate 'cylindrically' as functions of (x_1, x_2) and t, and Green's function can be found by descent, by integrating the three-dimensional formula over $-\infty < x_3 < \infty$ to obtain the solution

Downloaded from https://www.cambridge.org/core. Charité Universitätsmedizin Berlin, on 20 Dec 2021 at 10:08:47, subject to the Cambridge Core terms of use, available at https://www.cambridge.org/core/terms. https://doi.org/10.1017/CBO9781107360273.002

$$G(\mathbf{x}, \mathbf{y}, t, \tau) = \frac{\mathrm{H}(t - \tau - |\mathbf{x} - \mathbf{y}|/c_o)}{2\pi\sqrt{(t-\tau)^2 - |\mathbf{x}-\mathbf{y}|^2/c_o^2}}, \quad \mathbf{x} = (x_1, x_2),\ \mathbf{y} = (y_1, y_2), \tag{1.6.9}$$

of

$$\left(\frac{1}{c_o^2}\frac{\partial^2}{\partial t^2} - \nabla^2\right) G = \delta(x_1 - y_1)\delta(x_2 - y_2)\delta(t - \tau), \quad G = 0 \text{ for } t < \tau. \tag{1.6.10}$$

In three dimensions G consists of a spherically spreading singular pulse that vanishes everywhere except at the wavefront. The corresponding one-dimensional Green's function is finite and consists of two simple discontinuities propagating in both directions from the source at the speed of sound, to the rear of which the amplitude is constant and equal to $c_o/2$. The behaviour of G in two dimensions exhibits certain intermediate characteristics: the wavefront consists of a circular cylindrical singular pulse radiating outwards from the source at the speed of sound, but followed by a slowly decaying tail extending back to the source point where its amplitude decreases like $1/(t-\tau)$. From the viewpoint of an observer in three dimensions, the two-dimensional source $\delta(x_1 - y_1)\delta(x_2 - y_2)\delta(t - \tau)$ is equivalent to a uniform, infinitely long 'line' source (parallel to the x_3 axis). The tail can be attributed to the arrival of sound from distant points on this line source, which persists for all time after the passage of the wave front, which can be regarded as produced by components of the line source in the immediate neighbourhood of its intersection with the x_1x_2 plane.

1.7* Initial value problem for the wave equation

Our first application of the retarded potential integral is to the solution of 'Cauchy's problem,' in which it is required to calculate the sound at times $t > 0$ in terms of the state of the acoustic medium at $t = 0$. This includes, for example, the problem of the sound produced by the sudden rupture of a closed material envelope containing air at high pressure (a 'bursting' balloon). Alternatively, the state of a system of sound waves generated by sources in the distant past might be specified at $t = 0$ and it is desired to determine their subsequent propagation.

The nature of the required initial data can be deduced directly from the homogeneous form (where $\mathcal{F} \equiv 0$) of the wave equation (1.6.3), whose solution is required for $t > 0$. To do this the equation is multiplied by the Heaviside function $\mathrm{H}(t)$, making use of the identity

$$\mathrm{H}(t)\frac{\partial^2 p}{\partial t^2} = \frac{\partial^2}{\partial t^2}\Big(p\mathrm{H}(t)\Big) - \frac{\partial}{\partial t}\Big(\delta(t)p\Big) - \delta(t)\frac{\partial p}{\partial t}.$$

Downloaded from https://www.cambridge.org/core. Charité Universitätsmedizin Berlin, on 20 Dec 2021 at 10:08:47, subject to the Cambridge Core terms of use, available at https://www.cambridge.org/core/terms. https://doi.org/10.1017/CBO9781107360273.002

Then Equation (1.6.3), with $\mathcal{F}(\mathbf{x}, t) \equiv 0$, becomes

$$\left(\frac{1}{c_o^2}\frac{\partial^2}{\partial t^2} - \nabla^2\right)(p\mathrm{H}) = \frac{1}{c_o^2}\frac{\partial}{\partial t}\Big(\delta(t)\,p\Big) + \frac{1}{c_o^2}\delta(t)\frac{\partial p}{\partial t}. \tag{1.7.1}$$

This equation is formally valid for all time $-\infty < t < \infty$, with $p\mathrm{H}(t) \equiv 0$ for $t < 0$. The outgoing wave solution calculated using the retarded potential (1.6.6) determines $p(\mathbf{x}, t)\mathrm{H}(t) \equiv p(\mathbf{x}, t)$ for $t > 0$ in terms of the initial pressure and velocity distributions:

$$p = f(\mathbf{x}), \quad \frac{\partial p}{\partial t} \equiv -\rho_o c_o^2 \mathrm{div}\,\mathbf{v} = g(\mathbf{x}) \quad \text{at } t = 0, \tag{1.7.2}$$

where $f(\mathbf{x})$, $g(\mathbf{x})$ represent the prescribed initial values ($\partial p/\partial t = -\rho_o c_o^2 \mathrm{div}\,\mathbf{v}$ is the linearised continuity equation).

To evaluate the retarded potential integral for $t > 0$ we start from (1.6.5):

$$p(\mathbf{x}, t) = \frac{1}{4\pi c_o^2}\iint\left(\frac{\partial}{\partial \tau}\Big(f(\mathbf{y})\delta(\tau)\Big) + g(\mathbf{y})\delta(\tau)\right) \times \delta\left(t - \tau - \frac{|\mathbf{x}-\mathbf{y}|}{c_o}\right)\frac{d^3\mathbf{y}\,d\tau}{|\mathbf{x}-\mathbf{y}|}. \tag{1.7.3}$$

Introduce polar coordinates ($r = |\mathbf{x} - \mathbf{y}|, \theta, \phi$), with origin at the observer position $\mathbf{x}$, so that $\mathrm{d}^3\mathbf{y} = r^2 dr\, d\sigma$, where $d\sigma = \sin\theta\, d\theta d\phi$ is the solid angle element. Then the integral involving $f(\mathbf{y})$ becomes

$$\begin{aligned}
&\frac{1}{4\pi c_o^2}\iint\frac{\partial}{\partial\tau}\Big(f(r,\sigma)\delta(\tau)\Big)\delta\left(t-\tau-\frac{r}{c_o}\right)r\,dr\,d\sigma\,d\tau \\
&= \frac{1}{4\pi c_o^2}\frac{\partial}{\partial t}\int f(r,\sigma)\,\delta\left(t-\frac{r}{c_o}\right)r\,dr\,d\sigma \\
&= \frac{\partial}{\partial t}\oint t f(c_o t, \sigma)\,\frac{d\sigma}{4\pi} \\
&= \frac{\partial}{\partial t}\Big(t\,\bar{f}(c_o t)\Big),
\end{aligned}$$

where

$$\bar{f}(c_o t) = \oint f(c_o t, \sigma)\,\frac{d\sigma}{4\pi}$$

is the mean value of $f(\mathbf{y}) \equiv f(r, \sigma)$ on the surface of a sphere of radius $r = c_o t$ centred on the observer position $\mathbf{x}$ (P in Figure 1.7.1).

Combining this with a similar calculation for the term in $g(\mathbf{y})$, leads to Poisson's (1819) solution

$$p(\mathbf{x}, t) = \frac{\partial}{\partial t}\Big(t\,\bar{f}(c_o t)\Big) + t\,\bar{g}(c_o t). \tag{1.7.4}$$

Downloaded from https://www.cambridge.org/core. Charité Universitätsmedizin Berlin, on 20 Dec 2021 at 10:08:47, subject to the Cambridge Core terms of use, available at https://www.cambridge.org/core/terms. https://doi.org/10.1017/CBO9781107360273.002

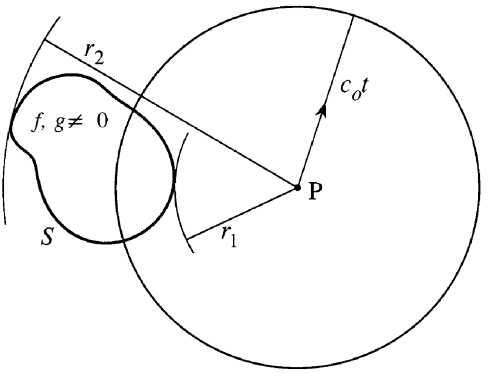

Figure 1.7.1

If the initial values $f(\mathbf{x})$, $g(\mathbf{x})$ of the pressure and its time derivative are non-zero only within a finite region bounded by a closed surface S (Figure 1.7.1), the mean values on the right of (1.7.4) vanish except when the expanding spherical surface $r = c_o t$ cuts across S. The pressure perturbation at P *outside* S is therefore non-zero only for $r_1 < c_o t < r_2$, where r_1, r_2 are the respective radii of the smallest and largest spheres centred on P that just touch S. The acoustic pressure radiating from S is therefore non-zero only within a shell-like region of space; at time t the outer surface of this shell is the *envelope* of the family of spheres of radius $c_o t$ whose centres lie on S. Equation (1.7.4) also gives the solution for an observer *within* S. For sufficiently small time the 'inner' envelope of the expanding family of spheres forms a wavefront collapsing into the interior of S – this eventually crosses itself, emerges from the 'other side' of S and expands to form the inner boundary of the radiating shell.

Note that the right-hand side of (1.7.1) can be cast in the form of the general source $\rho_o \partial q/\partial t - \operatorname{div} \mathbf{F}$ of the linear acoustic equation (1.3.7), where $q(\mathbf{x}, t)$, $\mathbf{F}(\mathbf{x}, t)$ are the *impulsive* volume source and body force distributions

$$q(\mathbf{x}, t) = \frac{1}{\rho_o c_o^2}\, p(\mathbf{x}, 0)\delta(t), \quad \mathbf{F}(\mathbf{x}, t) = \rho_o \mathbf{v}(\mathbf{x}, 0)\delta(t), \tag{1.7.5}$$

and where the formula for $\mathbf{F}$ is obtained from the linearised continuity equation

$$\frac{1}{c_o^2}\frac{\partial p}{\partial t} + \operatorname{div}(\rho_o \mathbf{v}) = 0.$$

Also, when the initial disturbance is non-zero only within a finite region bounded by the surface S the linearised momentum Equation (1.3.1) implies

Downloaded from https://www.cambridge.org/core. Charité Universitätsmedizin Berlin, on 20 Dec 2021 at 10:08:47, subject to the Cambridge Core terms of use, available at https://www.cambridge.org/core/terms. https://doi.org/10.1017/CBO9781107360273.002

that, at any point $\mathbf{x}$ *outside* S, $\nabla \int_0^\infty p(\mathbf{x}, t)dt = -\rho_o[\mathbf{v}(\mathbf{x}, t)]_{t=0}^\infty \equiv 0$, because $\mathbf{v} = 0$ before and after the passage of the sound wave. Therefore

$$\int_0^\infty p(\mathbf{x}, t)dt \equiv \int_{r_1/c_o}^{r_2/c_o} p(\mathbf{x}, t)dt = 0 \quad \text{for all } \mathbf{x}, \tag{1.7.6}$$

because the integrand vanishes (like $1/|\mathbf{x}|$) at infinitely large distances from S. Thus, the acoustic pressure variation at $\mathbf{x}$ during the time interval $r_1/c_o < t < r_2/c_o$ occupied by the wave must always involve equal and opposite net compressions and rarefactions. This conclusion is true for waves propagating in three and two dimensions, but not for one-dimensional propagation. It is illustrated by the example in §1.7.1.

1.7.1 Sound radiated from a spherical region of initial high pressure

Let the initial uniform high pressure $f(\mathbf{x}) = p_0 > 0$ be confined to stationary fluid in the interior of a sphere S of radius a, so that $g(\mathbf{x}) = 0$. Evidently, for the exterior point P in Figure 1.7.2 at distance r from the centre O of the sphere, $r_1 = r - a$, $r_2 = r + a$, and the pressure at P is non-zero only for $r - a < c_o t < r + a$. During this time

$$\bar{f}(c_o t) = \frac{\bar{\sigma}\, p_0}{4\pi},$$

where $\bar{\sigma} = \int_0^{2\pi} d\phi \int_0^{\Theta(t)} \sin\theta\, d\theta = 2\pi\{1 - \cos\Theta(t)\}$ is the solid angle subtended at P by the spherical cap AB formed by the intersection of S and the sphere of radius $c_o t$ centred on P. Hence, using the cosine formula ($a^2 = r^2 + c_o^2 t^2 - 2rc_o t\cos\Theta$) for the triangle OAP, we find

$$\bar{f}(c_o t) = \frac{p_0}{4rc_o t}\Big(a^2 - (c_o t - r)^2\Big)\Big(\mathrm{H}(c_o t - r + a) - \mathrm{H}(c_o t - r - a)\Big),$$

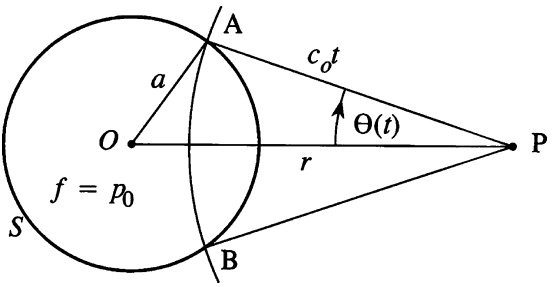

Figure 1.7.2

Downloaded from https://www.cambridge.org/core. Charité Universitätsmedizin Berlin, on 20 Dec 2021 at 10:08:47, subject to the Cambridge Core terms of use, available at https://www.cambridge.org/core/terms. https://doi.org/10.1017/CBO9781107360273.002

and therefore

$$p(r,t) = \frac{\partial}{\partial t}\Big(t\,\bar{f}(c_o t)\Big)$$
$$= -\frac{p_0}{2r}(c_o t - r)\Big(\mathrm{H}(c_o t - r + a) - \mathrm{H}(c_o t - r - a)\Big),\ r > a, \quad (1.7.7)$$

which represents an outgoing spherical wave confined to the shell $c_o t - a < r < c_o t + a$ that decreases in amplitude like $1/r$.

A similar calculation performed when P lies *within* the initial high pressure region ($r < a$) gives

$$p(r,t) = p_0\left(1 - \frac{(c_o t + r)}{2r}\mathrm{H}(c_o t + r - a) + \frac{(c_o t - r)}{2r}\mathrm{H}(c_o t - r - a)\right), \quad r < a. \quad (1.7.8)$$

The pressure at r inside S remains equal to p_0 until the arrival of the *rarefaction wave* (the second term in the large brackets) at time $t = (a - r)/c_o$, which is subsequently 'reflected' from the centre $r = 0$ as a compression wave, after the passage of which the pressure is reduced to zero.

The sequence of events is illustrated in Figure 1.7.3, where the non-dimensional pressure p/p_0 is plotted against r/a for a set of increasing values of $c_o t/a$. The perturbation pressure is initially uniform within S at $c_o t/a = 0$ and vanishes elsewhere. Compression and rarefaction waves radiate respectively into the exterior and interior of S as $c_o t/a$ increases towards 1 . When $c_o t/a \sim 1$ the negative rarefaction peak becomes very large, and ultimately $p/p_0 \to -\delta(c_o t/a - 1)$ at $r = 0$. Long before this happens in a real fluid, however, the large rarefaction is suppressed by nonlinear actions that increase the propagation speed of the higher pressure sections of the inward propagating wave, thereby inhibiting the formation of a deep negative pressure. After reflection at $r = 0$ when $c_o t/a = 1$ the whole disturbance becomes an outgoing 'N-wave' occupying a shell of thickness $2a$; the compression wavefront is at $r = c_o t + a$ and there is a pressure null within the shell at $r = c_o t$. Spherical spreading causes the wave amplitude to decrease like $1/r$. It also follows from (1.7.7) and (1.7.8) that $\int_0^\infty p(r,t)dt = 0$, even though the initial pressure distribution $p_0 > 0$ within $r < a$.

1.8 Monopoles, dipoles and quadrupoles

1.8.1 The monopole

A *volume* point source $Q(t)\delta(\mathbf{x})$ of the type considered in §1.5.1 as a model for a pulsating sphere is also called a point *monopole*. It generates the outgoing wave solution

Downloaded from https://www.cambridge.org/core. Charité Universitätsmedizin Berlin, on 20 Dec 2021 at 10:08:47, subject to the Cambridge Core terms of use, available at https://www.cambridge.org/core/terms. https://doi.org/10.1017/CBO9781107360273.002

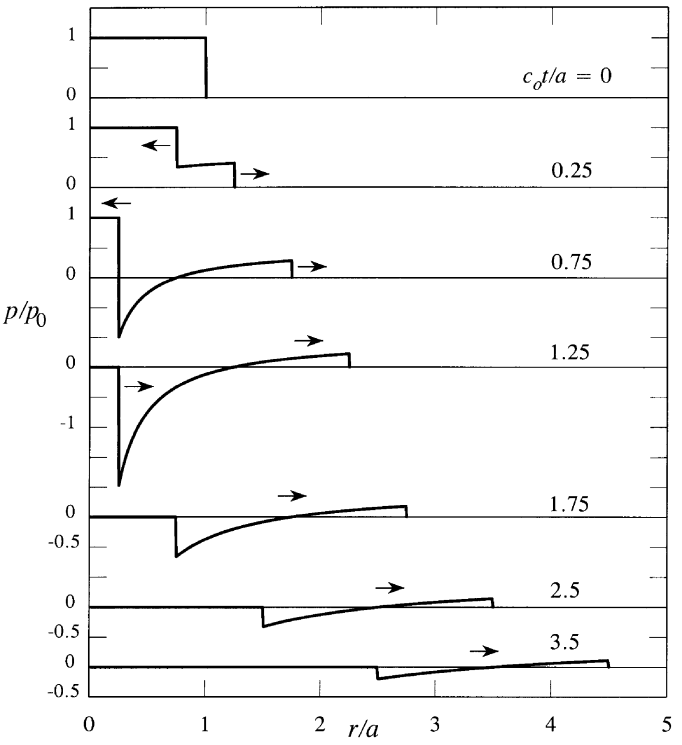

Figure 1.7.3

$$\varphi(\mathbf{x}, t) = \frac{-Q\left(t - \frac{|\mathbf{x}|}{c_o}\right)}{4\pi |\mathbf{x}|}$$

of Equation (1.5.1). This formula also follows directly from the retarded potential solution (1.6.6) of Equation (1.6.3) for the acoustic pressure, by replacing p by φ in (1.6.6) and setting $\mathcal{F}(\mathbf{y}, \tau) = -Q(\tau)\delta(\mathbf{y})$. When expressed in terms of the acoustic pressure $(-\rho_o \partial\varphi/\partial t)$ we have

$$p(\mathbf{x}, t) = \frac{\rho_o}{4\pi |\mathbf{x}|} \frac{\partial Q}{\partial t}\left(t - \frac{|\mathbf{x}|}{c_o}\right). \tag{1.8.1}$$

The potential generated by a *distributed* monopole source $q(\mathbf{x}, t)$ satisfies

$$\left(\frac{1}{c_o^2}\frac{\partial^2}{\partial t^2} - \nabla^2\right)\varphi = -q(\mathbf{x}, t),$$

Downloaded from https://www.cambridge.org/core. Charité Universitätsmedizin Berlin, on 20 Dec 2021 at 10:08:47, subject to the Cambridge Core terms of use, available at https://www.cambridge.org/core/terms. https://doi.org/10.1017/CBO9781107360273.002

which is a special case of the general equation (1.6.3), with solution

$$\varphi(\mathbf{x},t) = -\frac{1}{4\pi}\int_{-\infty}^{\infty}\frac{q\left(\mathbf{y},t-\frac{|\mathbf{x}-\mathbf{y}|}{c_o}\right)}{|\mathbf{x}-\mathbf{y}|}d^3\mathbf{y}. \tag{1.8.2}$$

It is usually only meaningful to speak of $q(\mathbf{x},t)$ as a monopole source distribution if it is acoustically compact and when the net volume outflow $\int_{-\infty}^{\infty} q(\mathbf{x},t)\,d^3\mathbf{x} \neq 0$, for example, when the outflow is caused by combustion. The distribution will otherwise turn out to be equivalent to a collection of less acoustically efficient, higher-order 'multipoles' (see §1.10.4), that is, of dipoles, quadrupoles, and so on, to be discussed next.

1.8.2 Dipole sources and dipole distributions

Let $\mathbf{f} = \mathbf{f}(t)$ be a time-dependent vector, then a 'source' on the right of the acoustic pressure Equation (1.6.3) of the type

$$\mathcal{F}(\mathbf{x},t) = \operatorname{div}\Big(\mathbf{f}(t)\delta(\mathbf{x})\Big) \equiv \frac{\partial}{\partial x_j}\Big(f_j(t)\delta(\mathbf{x})\Big) \tag{1.8.3}$$

is called a *point dipole* (at the origin). The repeated subscript j implies a summation over $j = 1,\ 2,\ 3$. Equation (1.3.7) shows that it is equivalent to a singular force density $\mathbf{F}(\mathbf{x},t) = -\mathbf{f}(t)\delta(\mathbf{x})$ per unit volume applied to the fluid at the origin.

The sound produced by the dipole can be calculated from (1.6.6), but it is easier to use (1.6.5):

$$p(\mathbf{x},t) = \frac{1}{4\pi}\iint_{-\infty}^{\infty}\frac{\partial}{\partial y_j}\Big(f_j(\tau)\delta(\mathbf{y})\Big)\frac{\delta\left(t-\tau-\frac{|\mathbf{x}-\mathbf{y}|}{c_o}\right)}{|\mathbf{x}-\mathbf{y}|}d^3\mathbf{y}d\tau.$$

Integrate by parts with respect to each y_j (recalling that $\delta(\mathbf{y}) = 0$ at $y_j = \pm\infty$), and note that

$$\frac{\partial}{\partial y_j}\frac{\delta\left(t-\tau-\frac{|\mathbf{x}-\mathbf{y}|}{c_o}\right)}{|\mathbf{x}-\mathbf{y}|} = -\frac{\partial}{\partial x_j}\frac{\delta\left(t-\tau-\frac{|\mathbf{x}-\mathbf{y}|}{c_o}\right)}{|\mathbf{x}-\mathbf{y}|}.$$

Then

$$p(\mathbf{x},t) = \frac{1}{4\pi}\iint_{-\infty}^{\infty} f_j(\tau)\delta(\mathbf{y})\frac{\partial}{\partial x_j}\left(\frac{\delta\left(t-\tau-\frac{|\mathbf{x}-\mathbf{y}|}{c_o}\right)}{|\mathbf{x}-\mathbf{y}|}\right)d^3\mathbf{y}d\tau$$

$$= \frac{1}{4\pi}\frac{\partial}{\partial x_j}\iint_{-\infty}^{\infty} f_j(\tau)\delta(\mathbf{y})\left(\frac{\delta\left(t-\tau-\frac{|\mathbf{x}-\mathbf{y}|}{c_o}\right)}{|\mathbf{x}-\mathbf{y}|}\right)d^3\mathbf{y}d\tau$$

Downloaded from https://www.cambridge.org/core. Charité Universitätsmedizin Berlin, on 20 Dec 2021 at 10:08:47, subject to the Cambridge Core terms of use, available at https://www.cambridge.org/core/terms. https://doi.org/10.1017/CBO9781107360273.002

i.e.

$$p(\mathbf{x},t)=\frac{\partial}{\partial x_j}\left(\frac{f_j\left(t-\frac{|\mathbf{x}|}{c_o}\right)}{4\pi|\mathbf{x}|}\right). \tag{1.8.4}$$

The same procedure shows that for a *distributed* dipole $\mathcal{F}(\mathbf{x},t)=\operatorname{div}\mathbf{f}(\mathbf{x},t)$ on the right of Equation (1.6.3), the acoustic pressure is

$$p(\mathbf{x},t)=\frac{1}{4\pi}\frac{\partial}{\partial x_j}\int_{-\infty}^{\infty}\frac{f_j\left(\mathbf{y},t-\frac{|\mathbf{x}-\mathbf{y}|}{c_o}\right)}{|\mathbf{x}-\mathbf{y}|}d^3\mathbf{y}. \tag{1.8.5}$$

A point dipole at the origin orientated in the direction of a unit vector $\mathbf{n}$ is equivalent to two point monopoles of equal but opposite strengths placed a short distance apart (much smaller than the acoustic wavelength) on opposite sides of the origin on a line through the origin parallel to $\mathbf{n}$. For example, if $\mathbf{n}$ is parallel to the x_1 axis and the sources are distance ϵ apart (Figure 1.8.1a), the two monopoles would be

$$\begin{aligned}Q(t)\left\{\delta\left(x_1-\tfrac{\epsilon}{2}\right)-\delta\left(x_1+\tfrac{\epsilon}{2}\right)\right\}\delta(x_2)\delta(x_3)&\approx-\epsilon\,Q(t)\delta'(x_1)\delta(x_2)\delta(x_3)\\&\equiv-\frac{\partial}{\partial x_1}\Big(\epsilon\,Q(t)\delta(\mathbf{x})\Big).\end{aligned}$$

This is a fluid *volume* dipole. The relation $p=-\rho_o\partial\varphi/\partial t$ implies that the equivalent dipole source in the pressure Equation (1.3.7) or (1.6.3) is

$$\mathcal{F}\;\equiv\;-\operatorname{div}\mathbf{F}=-\,\rho_o\frac{\partial}{\partial x_1}\left(\epsilon\frac{\partial Q}{\partial t}(t)\delta(\mathbf{x})\right).$$

1.8.3 Quadrupoles

A source distribution involving two space derivatives is locally equivalent to a combination of four monopoles whose net volume source strength is zero, and is called a quadrupole. A general quadrupole has the form

$$\mathcal{F}(\mathbf{x},t)=\frac{\partial^2 T_{ij}}{\partial x_i\partial x_j}(\mathbf{x},t) \tag{1.8.6}$$

in Equation (1.6.3). The argument above leading to expression (1.8.5) can be applied twice to show that the corresponding acoustic pressure is

$$p(\mathbf{x},t)=\frac{1}{4\pi}\frac{\partial^2}{\partial x_i\partial x_j}\int_{-\infty}^{\infty}\frac{T_{ij}(\mathbf{y},t-|\mathbf{x}-\mathbf{y}|/c_o)}{|\mathbf{x}-\mathbf{y}|}\,d^3\mathbf{y}. \tag{1.8.7}$$

A point quadrupole is equivalent to a quartet of point monopoles of zero net strength, as exemplified in Figure 1.8.1b. When $\epsilon\ll\lambda$ (the acoustic wavelength) the combination reduces to

Downloaded from https://www.cambridge.org/core. Charité Universitätsmedizin Berlin, on 20 Dec 2021 at 10:08:47, subject to the Cambridge Core terms of use, available at https://www.cambridge.org/core/terms. https://doi.org/10.1017/CBO9781107360273.002

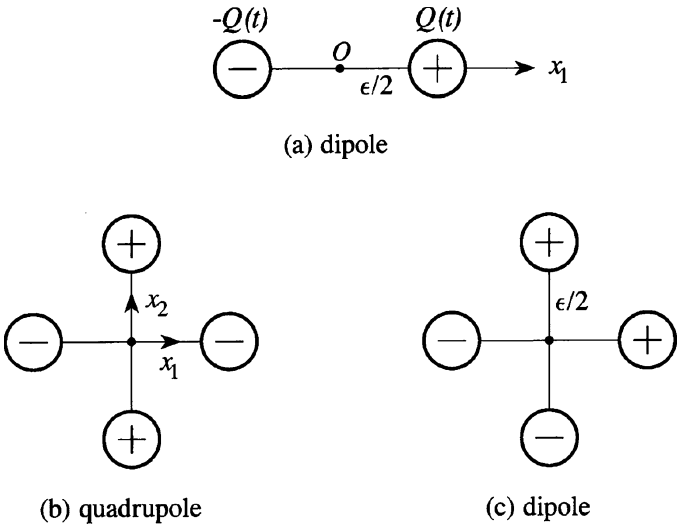

Figure 1.8.1

$$\left(-\frac{\partial^2}{\partial x_1^2}+\frac{\partial^2}{\partial x_2^2}\right)\frac{\epsilon^2 Q(t)\delta(\mathbf{x})}{4}.$$

However, not all compact arrangements of four sources of zero net strength are quadrupoles; that shown in Figure 1.8.1c is equivalent to the dipole

$$-\left(\frac{\partial}{\partial x_1}+\frac{\partial}{\partial x_2}\right)\epsilon Q(t)\delta(\mathbf{x}).$$

1.8.4 Solution of the general linear acoustic equation

The sources on the right of the general linear acoustic Equation (1.3.7)

$$\left(\frac{1}{c_o^2}\frac{\partial^2}{\partial t^2}-\nabla^2\right)p=\rho_o\frac{\partial q}{\partial t}-\operatorname{div}\mathbf{F}$$

are respectively of monopole and dipole type. The solution with outgoing wave behaviour is therefore

$$p(\mathbf{x},t)=\frac{\rho_o}{4\pi}\frac{\partial}{\partial t}\int_{-\infty}^{\infty}\frac{q(\mathbf{y},t-|\mathbf{x}-\mathbf{y}|/c_o)}{|\mathbf{x}-\mathbf{y}|}\,d^3\mathbf{y}$$
$$-\frac{1}{4\pi}\frac{\partial}{\partial x_j}\int_{-\infty}^{\infty}\frac{F_j(\mathbf{y},t-|\mathbf{x}-\mathbf{y}|/c_o)}{|\mathbf{x}-\mathbf{y}|}\,d^3\mathbf{y}. \qquad (1.8.8)$$

Downloaded from https://www.cambridge.org/core. Charité Universitätsmedizin Berlin, on 20 Dec 2021 at 10:08:47, subject to the Cambridge Core terms of use, available at https://www.cambridge.org/core/terms. https://doi.org/10.1017/CBO9781107360273.002

1.8.5 Vibrating sphere

Let a rigid sphere of radius a execute small amplitude oscillations at speed $U(t)$ in the x_1 direction (Figure 1.8.2a) at sufficiently low frequencies that it may be assumed to be acoustically compact. Take the coordinate origin at the mean position of the centre. The sphere 'pushes' fluid away from its advancing front hemisphere, and the retreating rear hemisphere draws in fluid from its wake. The sphere therefore resembles a dipole source, and it is shown in §2.8.1 that the motion induced in an ideal fluid is equivalent to that produced by a point volume dipole of strength $2\pi a^3 U(t)$ at the position of its centre directed along the x_1-axis. The velocity potential is the solution of

$$\left(\frac{1}{c_o^2}\frac{\partial^2}{\partial t^2} - \nabla^2\right)\varphi = \frac{\partial}{\partial x_1}\left(2\pi a^3 U(t)\delta(\mathbf{x})\right). \tag{1.8.9}$$

By analogy with (1.8.3) and (1.8.4), we have

$$\varphi(\mathbf{x}, t) = \frac{\partial}{\partial x_1}\left(\frac{2\pi a^3 U\left(t - \frac{|\mathbf{x}|}{c_o}\right)}{4\pi|\mathbf{x}|}\right). \tag{1.8.10}$$

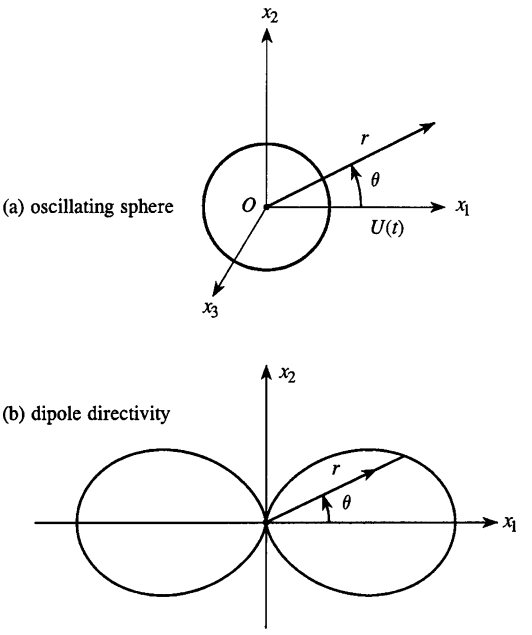

Figure 1.8.2

Downloaded from https://www.cambridge.org/core. Charité Universitätsmedizin Berlin, on 20 Dec 2021 at 10:08:47, subject to the Cambridge Core terms of use, available at https://www.cambridge.org/core/terms. https://doi.org/10.1017/CBO9781107360273.002

Now

$$\frac{\partial}{\partial x_j}|\mathbf{x}| = \frac{x_j}{|\mathbf{x}|}. \tag{1.8.11}$$

Applying this formula for $j = 1$, we find (putting $r = |\mathbf{x}|$ and $x_1 = r\cos\theta$)

$$\varphi = \underbrace{-\frac{a^3\cos\theta}{2r^2}U\left(t - \frac{r}{c_o}\right)}_{\textbf{near field}} \underbrace{-\frac{a^3\cos\theta}{2c_o r}\frac{\partial U}{\partial t}\left(t - \frac{r}{c_o}\right)}_{\textbf{far field}} \tag{1.8.12}$$

The 'near field' term is dominant at sufficiently small distances r that

$$\frac{1}{r} \gg \frac{1}{c_o}\frac{1}{U}\frac{\partial U}{\partial t} \sim \frac{f}{c_o}$$

where f is the characteristic frequency of the oscillations of the sphere. But sound of frequency f travels a distance

$$c_o/f = \lambda \equiv \text{ one acoustic wavelength}$$

in one period of oscillation $1/f$. Hence, the near field term is dominant when

$$r \ll \lambda.$$

The motion becomes incompressible when $c_o \to \infty$. In this limit the solution reduces entirely to the near field term, which is also called the *hydrodynamic* near field; it decreases in amplitude like $1/r^2$ as $r \to \infty$.

The 'far field' is the 'acoustic' region that exists only when the fluid is compressible. It consists of propagating sound waves, carrying energy away from the sphere, and takes over from the near field when $r \gg \lambda$. There is an intermediate zone where $r \sim \lambda$ in which the solution is in a state of transition from the near to the far field. This accords with the assumption that the sphere is *compact* and can be replaced by the point dipole: the motion close to the sphere is essentially the same as if the fluid is incompressible, that is, the diameter of the sphere is much smaller than the acoustic wavelength ($a \ll \lambda$).

The *intensity* of the sound generated by the sphere in the far field is proportional to φ^2:

$$\varphi^2 \sim \frac{a^6}{4c_o^2 r^2}\left(\frac{\partial U}{\partial t}\right)^2_{t-\frac{r}{c_o}} \cos^2\theta, \quad r \to \infty.$$

The dependence on θ determines the *directivity* of the sound. For the dipole it has the 'figure of eight' pattern illustrated in Figure 1.8.2b, with peaks in directions parallel to the dipole axis ($\theta = 0,\ \pi$); there are radiation 'nulls' at $\theta = \frac{\pi}{2}$ (the curve should be imagined to be rotated about the x_1 axis).

Downloaded from https://www.cambridge.org/core. Charité Universitätsmedizin Berlin, on 20 Dec 2021 at 10:08:47, subject to the Cambridge Core terms of use, available at https://www.cambridge.org/core/terms. https://doi.org/10.1017/CBO9781107360273.002

1.9 Acoustic energy equation

The acoustic energy equation in a *stationary* ideal fluid is obtained by taking the scalar product of the velocity $\mathbf{v}$ and linearised momentum equation (1.3.1). The result is written

$$\frac{\partial}{\partial t}\left(\frac{1}{2}\rho_o v^2\right) + \operatorname{div}\Big(p\,\mathbf{v}\Big) - p\operatorname{div}\mathbf{v} = \mathbf{v}\cdot\mathbf{F}.$$

The term $p\operatorname{div}\mathbf{v}$ on the left is rendered in a more useful form by substitution for $\operatorname{div}\mathbf{v}$ from the linearised equation of continuity (1.3.3)

$$\operatorname{div}\mathbf{v} = q - \frac{1}{\rho_o}\frac{\partial\rho}{\partial t} = q - \frac{1}{\rho_o c_o^2}\frac{\partial p}{\partial t}.$$

The required energy equation is then obtained in the form

$$\frac{\partial\mathcal{E}}{\partial t} + \operatorname{div}\Big(p\,\mathbf{v}\Big) = pq + \mathbf{v}\cdot\mathbf{F}, \tag{1.9.1}$$

where

$$\mathcal{E} = \frac{1}{2}\rho_o v^2 + \frac{1}{2}\frac{p^2}{\rho_o c_o^2} \tag{1.9.2}$$

is the acoustic energy density, the terms on the right being respectively the kinetic energy and the compressional potential energy per unit volume. The divergence in Equation (1.9.1) is the acoustic power radiated out of unit volume of fluid, and the sources on the right are energy production rates of the volume sources $q(\mathbf{x},t)$ and force distribution $\mathbf{F}(\mathbf{x},t)$. The energy balance is perhaps more clearly exhibited by integration of the energy equation over the fluid region within a large and fixed closed surface S (Figure 1.9.1) that contains all of the acoustic sources. Application of the divergence theorem yields

$$\frac{\partial}{\partial t}\int\mathcal{E}\,d^3\mathbf{x} + \oint_S p\mathbf{v}\cdot d\mathbf{S} = \int (pq + \mathbf{v}\cdot\mathbf{F})\,d^3\mathbf{x}, \tag{1.9.3}$$

which equates the sum of the rate of accumulation of energy within S and the energy flux out through S to the rate of working of the acoustic sources.

In these formulae the perturbation quantities p and $\mathbf{v}$ must be calculated from the *linearised* acoustic equations. In particular, it is clear from the derivation of (1.9.1) that the pressure p in the compressional potential energy $p^2/2\rho_o c_o^2$ and in the energy flux vector $p\mathbf{v}$ is the linear excess of the total pressure over the mean background pressure – possible contributions to these quantities from the mean pressure must be specifically excluded. Thus, if V is the volume occupied by unit mass of the fluid, then $\rho V = 1$, and the compressional energy *per unit mass* is to be calculated from the formula $-\int_{V_o}^{V} p'\,dV$, where $V_o = 1/\rho_o$ is the volume occupied by unit mass in the absence of the sound, and p' is the perturbation pressure produced by the volumetric change $V - V_o$.

Downloaded from https://www.cambridge.org/core. Charité Universitätsmedizin Berlin, on 20 Dec 2021 at 10:08:47, subject to the Cambridge Core terms of use, available at https://www.cambridge.org/core/terms. https://doi.org/10.1017/CBO9781107360273.002

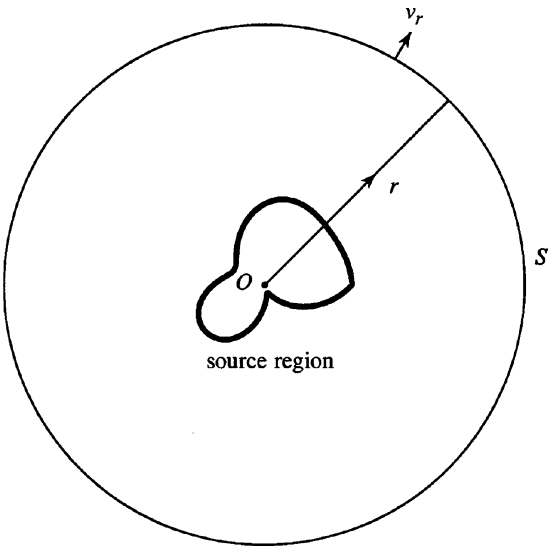

Figure 1.9.1

Then the acoustic compressional energy per unit volume is (using the linearised adiabatic formula $dp' = c_o^2 d\rho$)

$$-\rho_o \int_{V_o}^{V} p'\, dV = -\rho_o \int_{\rho_o}^{\rho} p'\, d\left(\frac{1}{\rho}\right) = \frac{1}{\rho_o c_o^2} \int_0^p p'\, dp' = \frac{1}{2}\frac{p^2}{\rho_o c_o^2}.$$

1.9.1 Calculation of the energy flux

At large distances r from a source region we generally have

$$p(\mathbf{x}, t) \sim \frac{\rho_o \Phi\left(\theta, \phi, t - \frac{r}{c_o}\right)}{r}, \quad r \to \infty, \tag{1.9.4}$$

where the function Φ depends on the nature of the source distribution, and θ and ϕ are polar angles determining the directivity of the sound. From the radial component of the linearised momentum equation

$$\begin{aligned}\frac{\partial v_r}{\partial t} &= -\frac{1}{\rho_o}\frac{\partial p}{\partial r} \\ &\equiv \frac{1}{r^2}\Phi\left(\theta, \phi, t - \frac{r}{c_o}\right) + \frac{1}{c_o r}\frac{\partial \Phi}{\partial t}\left(\theta, \phi, t - \frac{r}{c_o}\right).\end{aligned} \tag{1.9.5}$$

The first term in the second line can be neglected when $r \to \infty$, and therefore

$$v_r \sim \frac{1}{c_o r}\Phi\left(\theta, \phi, t - \frac{r}{c_o}\right) \equiv \frac{p}{\rho_o c_o}. \tag{1.9.6}$$

Downloaded from https://www.cambridge.org/core. Charité Universitätsmedizin Berlin, on 20 Dec 2021 at 10:08:47, subject to the Cambridge Core terms of use, available at https://www.cambridge.org/core/terms. https://doi.org/10.1017/CBO9781107360273.002

By considering the θ and ϕ components of the momentum equation we can show that the corresponding velocity components v_θ, v_ϕ, say, decrease faster than $1/r$ as $r \to \infty$. We therefore conclude from this and (1.9.6) that the 'acoustic particle velocity' is normal to the acoustic wavefronts (the spherical surfaces $r = c_o t$). In other words: the far field sound consists of 'longitudinal waves' in which the fluid particles oscillate backwards and forwards along the local direction of propagation of the sound.

The **acoustic power** Π radiated by the source distribution is given by the surface integral of equation (1.9.3), which we can take in the form

$$\Pi = \oint_S p v_r \, dS = \oint_S \frac{p^2}{\rho_o c_o} \, dS, \tag{1.9.7}$$

where the surface of integration S is that of a large sphere of radius r centred on the source region. Because the surface area $= 4\pi r^2$ we only need to know the pressure and velocity correct to order $1/r$ on S in order to evaluate the integral. Smaller contributions (such as that determined by the first term in the second line of (1.9.5)) decrease too fast as r increases to supply a finite contribution to the integral as $r \to \infty$.

In acoustic problems we are therefore usually satisfied if we can calculate the pressure and velocity in the acoustic far field correct to order $1/r$; this will always permit the evaluation of the radiated sound power. The formula $v_r = p/\rho_o c_o$ is applicable at large distances from the sources, where the wavefronts can be regarded as *locally plane*, but it is true identically for plane sound waves. In the latter case, and for spherical waves on the surface of the large sphere of Figure 1.9.1, the quantity

$$I = p v_r = \frac{p^2}{\rho_o c_o} \tag{1.9.8}$$

is called the **acoustic intensity**. It is the rate of transmission of acoustic energy per unit area of wavefront. For a plane wave $\mathcal{E} = p^2/\rho_o c_o^2$, so that $I = c_o \mathcal{E}$, that is, the plane wave energy flux is equal to the energy density multiplied by the speed of sound.

1.9.2 Power radiated by a vibrating sphere

Put $U(t) = U_o \cos(\omega t)$ in formula (1.8.12) for the velocity potential φ produced by an acoustically compact sphere vibrating in the x_1 direction at speed $U(t)$. In the far field

$$p = -\rho_o \frac{\partial \varphi}{\partial t} \sim -\frac{\rho_o a^3 \omega^2 U_o \cos\theta}{2 c_o r} \cos\left\{\omega\left(t - \tfrac{r}{c_o}\right)\right\}$$

Downloaded from https://www.cambridge.org/core. Charité Universitätsmedizin Berlin, on 20 Dec 2021 at 10:08:47, subject to the Cambridge Core terms of use, available at https://www.cambridge.org/core/terms. https://doi.org/10.1017/CBO9781107360273.002

$$\therefore\ \Pi = \oint_S \frac{p^2\,dS}{\rho_o c_o} = \frac{\rho_o a^6 \omega^4 U_o^2}{4c_o^3}\cos^2\left\{\omega\left(t-\tfrac{r}{c_o}\right)\right\}\int_0^{2\pi} d\phi \int_0^{\pi}\cos^2\theta\sin\theta\,d\theta$$

$$= \frac{\pi}{3}(k_o a)^3 a^3 \omega \rho_o U_o^2 \cos^2\left\{\omega\left(t-\tfrac{r}{c_o}\right)\right\},$$

$$\text{i.e.}\quad \langle\Pi\rangle = \frac{\pi}{6}(k_o a)^3 a^3 \omega \rho_o U_o^2 = \frac{(k_o a)^3}{4}\,\omega\left(\tfrac{1}{2}m_o U_o^2\right),\quad m_o = \frac{4\pi a^3 \rho_o}{3},$$

where the angle brackets denote a time average and m_o is the mass of fluid displaced by the sphere. The term $\omega\left(\frac{1}{2}m_o U_o^2\right)$ is a measure of the rate of change of the *hydrodynamic* energy (the local fluctuating power) of the gross fluid motion adjacent to the vibrating sphere. Because the sphere is acoustically compact (i.e. $k_o a \ll 1$), only a tiny fraction of this power actually radiates as sound, determined by the value of the efficiency factor $(k_o a)^3$.

1.9.3 Energy radiated during the sudden release of high-pressure air

The initial value problem of §1.7.1 involves the production of sound by the sudden release of high pressure air from a spherical region with surface S : $|\mathbf{x}| = a$. The initial pressure excess within S is p_o, and the corresponding potential energy is therefore

$$\int_{|\mathbf{x}|<a} \frac{p_o^2}{2\rho_o c_o^2}\,d^3\mathbf{x} = \frac{4\pi a^3}{3}\frac{p_o^2}{2\rho_o c_o^2}, \tag{1.9.9}$$

which must be radiated in the sound field.

Let us verify the consistency of this assertion with the energy Equation (1.9.3). All of the wave energy will radiate through a distant closed surface S_∞, and integration of (1.9.3) over all times implies that

$$\int_{-\infty}^{\infty}\oint_{S_\infty} p\mathbf{v}\cdot d\mathbf{S}\,dt = \int_{-\infty}^{\infty}\int_{|\mathbf{x}|<a}(pq+\mathbf{v}\cdot\mathbf{F})\,d^3\mathbf{x}\,dt. \tag{1.9.10}$$

Outside the source region the pressure is given by Equation (1.7.7), and the power radiated through S_∞ is therefore

$$\Pi = \oint_{S_\infty}\frac{p^2}{\rho_o c_o}\,dS$$

$$= 4\pi r^2\left(\frac{p_o^2}{4r^2\rho_o c_o}(c_o t - r)^2\right)\Big(\mathrm{H}(c_o t - r + a) - \mathrm{H}(c_o t - r - a)\Big).$$

Downloaded from https://www.cambridge.org/core. Charité Universitätsmedizin Berlin, on 20 Dec 2021 at 10:08:47, subject to the Cambridge Core terms of use, available at https://www.cambridge.org/core/terms. https://doi.org/10.1017/CBO9781107360273.002

Thus, the total radiated acoustic energy E determined by the left-hand side of (1.9.10) is

$$E = \frac{\pi p_0^2}{\rho_o c_o} \int_{(r-a)/c_o}^{(r+a)/c_o} (c_o t - r)^2 \, dt = \frac{2\pi a^3}{3} \frac{p_0^2}{\rho_o c_o^2},$$

in agreement with Equation (1.9.9).

Similarly, from Equations (1.7.5) we have $\mathbf{F} = 0$ and

$$q = \frac{p_0}{\rho_o c_o^2} \delta(t) \mathrm{H}(a - r).$$

When this is multiplied by the interior time-dependent acoustic pressure (1.7.8), it follows from (1.9.10) that E is also given by $E = \int_{-\infty}^{\infty} \int_{|\mathbf{x}|<a} pq \, d^3\mathbf{x} \, dt$. To evaluate the integral recall that the radiated pressure is the causal solution of Equation (1.7.1), and what is actually calculated is *not* p but $p\mathrm{H}(t)$. Thus,

$$\begin{aligned} E &= \frac{p_0^2}{\rho_o c_o^2} \int_{-\infty}^{\infty} \int_{|\mathbf{x}|<a} \mathrm{H}(t)\, \delta(t) \left(1 - \frac{(c_o t + r)}{2r} \mathrm{H}(c_o t + r - a) \right. \\ &\qquad \left. + \frac{(c_o t - r)}{2r} \mathrm{H}(c_o t - r - a) \right) d^3\mathbf{x} \, dt \\ &\equiv \frac{p_0^2}{\rho_o c_o^2} \int_{-\infty}^{\infty} \int_{|\mathbf{x}|<a} \mathrm{H}(t)\, \delta(t) d^3\mathbf{x} \, dt = \frac{4\pi a^3}{3} \frac{p_0^2}{\rho_o c_o^2} \int_{-\infty}^{\infty} \mathrm{H}(t)\, \delta(t) \, dt \\ &= \frac{4\pi a^3}{3} \frac{p_0^2}{\rho_o c_o^2} \left[\tfrac{1}{2} \mathrm{H}^2(t) \right]_{-\infty}^{\infty} = \frac{2\pi a^3}{3} \frac{p_0^2}{\rho_o c_o^2}, \end{aligned}$$

which also agrees with (1.9.9).

The integration with respect to time has made use of the result $d\mathrm{H}(t)/dt = \delta(t)$. Readers uncomfortable with this formal step should observe that the solution of the initial value problem (1.7.1) can be carried through with negligible change of details, by replacing $\mathrm{H}(t)$ and $\delta(t)$ by their corresponding 'small-ϵ' approximations

$$\mathrm{H}_\epsilon(t) = \frac{1}{2} + \frac{1}{\pi} \tan^{-1}\left(\frac{t}{\epsilon}\right), \quad \delta_\epsilon(t) = \frac{\epsilon}{\pi(\epsilon^2 + t^2)}, \quad \epsilon > 0,$$

in which case $\int_{-\infty}^{\infty} \mathrm{H}_\epsilon(t)\, \delta_\epsilon(t) \, dt = [\tfrac{1}{2} \mathrm{H}_\epsilon^2(t)]_{-\infty}^{\infty} = \tfrac{1}{2}$.

Downloaded from https://www.cambridge.org/core. Charité Universitätsmedizin Berlin, on 20 Dec 2021 at 10:08:47, subject to the Cambridge Core terms of use, available at https://www.cambridge.org/core/terms. https://doi.org/10.1017/CBO9781107360273.002

1.10 Calculation of the acoustic far field

We now discuss the approximations necessary to evaluate the sound in the far field from the retarded potential representation:

$$p(\mathbf{x}, t) = \frac{1}{4\pi} \int_{-\infty}^{\infty} \frac{\mathcal{F}\left(\mathbf{y}, t - \frac{|\mathbf{x}-\mathbf{y}|}{c_o}\right)}{|\mathbf{x}-\mathbf{y}|} d^3\mathbf{y}. \tag{1.10.1}$$

Assume that $\mathcal{F}(\mathbf{x}, t) \neq 0$ only within a finite source region (Figure 1.10.1), and take the coordinate origin O within the region.

When $|\mathbf{x}| \to \infty$ and $\mathbf{y}$ lies within the source region (so that $|\mathbf{x}| \gg |\mathbf{y}|$)

$$\begin{aligned} |\mathbf{x}-\mathbf{y}| &\equiv \left\{ \left(|\mathbf{x}| - \frac{\mathbf{x}\cdot\mathbf{y}}{|\mathbf{x}|} \right)^2 + \frac{|\mathbf{x}\wedge\mathbf{y}|^2}{|\mathbf{x}|^2} \right\}^{\frac{1}{2}} \\ &= \left(|\mathbf{x}| - \frac{\mathbf{x}\cdot\mathbf{y}}{|\mathbf{x}|} \right) \left\{ 1 + \frac{|\mathbf{x}\wedge\mathbf{y}|^2/|\mathbf{x}|^2}{(|\mathbf{x}| - \mathbf{x}\cdot\mathbf{y}/|\mathbf{x}|)^2} \right\}^{\frac{1}{2}} \\ &\approx |\mathbf{x}| - \frac{\mathbf{x}\cdot\mathbf{y}}{|\mathbf{x}|} + \frac{|\mathbf{x}\wedge\mathbf{y}|^2}{2|\mathbf{x}|^3} + \cdots \end{aligned} \tag{1.10.2}$$

$$\text{i.e., } |\mathbf{x}-\mathbf{y}| \approx |\mathbf{x}| - \frac{\mathbf{x}\cdot\mathbf{y}}{|\mathbf{x}|} \quad \text{when} \quad \frac{|\mathbf{y}|}{|\mathbf{x}|} \ll 1. \tag{1.10.3}$$

$$\text{Similarly,} \quad \frac{1}{|\mathbf{x}-\mathbf{y}|} \approx \frac{1}{\left(|\mathbf{x}| - \frac{\mathbf{x}\cdot\mathbf{y}}{|\mathbf{x}|}\right)} = \frac{1}{|\mathbf{x}|}\left(1 + \frac{\mathbf{x}\cdot\mathbf{y}}{|\mathbf{x}|^2} + \cdots\right)$$

$$\therefore \quad \frac{1}{|\mathbf{x}-\mathbf{y}|} \approx \frac{1}{|\mathbf{x}|} + \frac{\mathbf{x}\cdot\mathbf{y}}{|\mathbf{x}|^3} \quad \text{when} \quad \frac{|\mathbf{y}|}{|\mathbf{x}|} \ll 1. \tag{1.10.4}$$

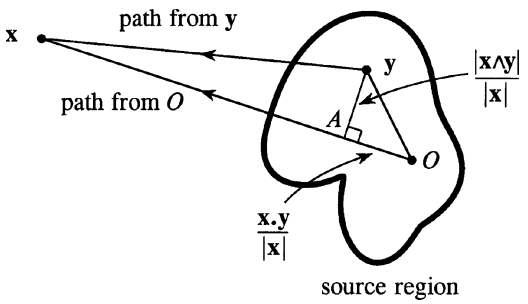

Figure 1.10.1

Downloaded from https://www.cambridge.org/core. Charité Universitätsmedizin Berlin, on 20 Dec 2021 at 10:08:47, subject to the Cambridge Core terms of use, available at https://www.cambridge.org/core/terms. https://doi.org/10.1017/CBO9781107360273.002

The approximation (1.10.4) shows that, in order to obtain the far field approximation of the solution (1.10.1) that behaves like $1/r = 1/|\mathbf{x}|$ as $|\mathbf{x}| \to \infty$, it is sufficient to replace $|\mathbf{x} - \mathbf{y}|$ in the denominator of the integrand by $|\mathbf{x}|$. However, in the argument of the source strength $\mathcal{F}$ it is important to retain possible *phase differences* between the sound waves generated by components of the source distribution at different locations $\mathbf{y}$; we therefore replace $|\mathbf{x} - \mathbf{y}|$ in the retarded time by the right-hand side of (1.10.3). Hence,

$$p(\mathbf{x}, t) \approx \frac{1}{4\pi |\mathbf{x}|} \int_{-\infty}^{\infty} \mathcal{F}\left(\mathbf{y}, t - \frac{|\mathbf{x}|}{c_o} + \frac{\mathbf{x} \cdot \mathbf{y}}{c_o |\mathbf{x}|}\right) d^3\mathbf{y}, \quad |\mathbf{x}| \to \infty. \tag{1.10.5}$$

This is called the *Fraunhofer approximation*.

The source region may extend over many characteristic acoustic wavelengths of the sound. By retaining the contribution $\mathbf{x} \cdot \mathbf{y}/c_o|\mathbf{x}|$ to the retarded time we ensure that any *interference* between waves generated at different positions within the source region is correctly described by the far field approximation. In Figure 1.10.1 the acoustic travel time $|\mathbf{x} - \mathbf{y}|/c_o$ from a source point $\mathbf{y}$ to the far field point $\mathbf{x}$ is equal to that from the point labelled A to $\mathbf{x}$ when $|\mathbf{x}| \to \infty$. Indeed, the travel time over OA is $\mathbf{x} \cdot \mathbf{y}/c_o|\mathbf{x}|$, and $|\mathbf{x}|/c_o - \mathbf{x} \cdot \mathbf{y}/c_o|\mathbf{x}|$ equals $|\mathbf{x} - \mathbf{y}|/c_o$ with an error of order $|\mathbf{x} \wedge \mathbf{y}|^2/2c_o|\mathbf{x}|^3 \to 0$ when $|\mathbf{x}| \to \infty$.

1.10.1 Dipole source distributions

By applying the far field formula (1.10.5) to a dipole source $\mathcal{F}(\mathbf{x}, t) = \operatorname{div} \mathbf{f}(\mathbf{x}, t)$ we obtain (from (1.8.5))

$$p(\mathbf{x}, t) \approx \frac{1}{4\pi} \frac{\partial}{\partial x_j} \left[\frac{1}{|\mathbf{x}|} \int_{-\infty}^{\infty} f_j \left(\mathbf{y}, t - \frac{|\mathbf{x}|}{c_o} + \frac{\mathbf{x} \cdot \mathbf{y}}{c_o |\mathbf{x}|}\right) d^3\mathbf{y} \right]$$

$$\approx \frac{1}{4\pi |\mathbf{x}|} \frac{\partial}{\partial x_j} \int_{-\infty}^{\infty} f_j \left(\mathbf{y}, t - \frac{|\mathbf{x}|}{c_o} + \frac{\mathbf{x} \cdot \mathbf{y}}{c_o |\mathbf{x}|}\right) d^3\mathbf{y}, \quad |\mathbf{x}| \to \infty, \tag{1.10.6}$$

because the differential operator $\partial/\partial x_j$ need not be applied to $1/|\mathbf{x}|$ as this would give a contribution decreasing like $1/r^2$ at large distances from the dipole.

However, it is useful to make a further transformation that replaces $\partial/\partial x_j$ by the *time derivative* $\partial/\partial t$, which is usually more easily estimated in applications. To do this we observe that

Downloaded from https://www.cambridge.org/core. Charité Universitätsmedizin Berlin, on 20 Dec 2021 at 10:08:47, subject to the Cambridge Core terms of use, available at https://www.cambridge.org/core/terms. https://doi.org/10.1017/CBO9781107360273.002

$$\begin{aligned}\frac{\partial f_j}{\partial x_j}\left(\mathbf{y}, t-\frac{|\mathbf{x}|}{c_o}+\frac{\mathbf{x}\cdot\mathbf{y}}{c_o|\mathbf{x}|}\right) &= \frac{\partial f_j}{\partial t}\left(\mathbf{y}, t-\frac{|\mathbf{x}|}{c_o}+\frac{\mathbf{x}\cdot\mathbf{y}}{c_o|\mathbf{x}|}\right)\\ &\quad\times\frac{\partial}{\partial x_j}\left(t-\frac{|\mathbf{x}|}{c_o}+\frac{\mathbf{x}\cdot\mathbf{y}}{c_o|\mathbf{x}|}\right)\\ &= \frac{\partial f_j}{\partial t}\left(\mathbf{y}, t-\frac{|\mathbf{x}|}{c_o}+\frac{\mathbf{x}\cdot\mathbf{y}}{c_o|\mathbf{x}|}\right)\\ &\quad\times\left(-\frac{x_j}{c_o|\mathbf{x}|}+\frac{y_j}{c_o|\mathbf{x}|}-\frac{(\mathbf{x}\cdot\mathbf{y})x_j}{c_o|\mathbf{x}|^3}\right)\\ &\approx -\frac{x_j}{c_o|\mathbf{x}|}\frac{\partial f_j}{\partial t}\left(\mathbf{y}, t-\frac{|\mathbf{x}|}{c_o}+\frac{\mathbf{x}\cdot\mathbf{y}}{c_o|\mathbf{x}|}\right) \text{ as } |\mathbf{x}|\to\infty.\end{aligned}$$

Hence, the far field of a distribution of dipoles $\mathcal{F}(\mathbf{x}, t) = \operatorname{div}\mathbf{f}(\mathbf{x}, t)$ is given by

$$p(\mathbf{x}, t) = \frac{-x_j}{4\pi c_o|\mathbf{x}|^2}\frac{\partial}{\partial t}\int_{-\infty}^{\infty} f_j\left(\mathbf{y}, t-\frac{|\mathbf{x}|}{c_o}+\frac{\mathbf{x}\cdot\mathbf{y}}{c_o|\mathbf{x}|}\right)d^3\mathbf{y}. \tag{1.10.7}$$

Note that

$$\frac{x_j}{|\mathbf{x}|^2} = \frac{x_j}{|\mathbf{x}|}\frac{1}{|\mathbf{x}|},$$

where $x_j/|\mathbf{x}|$ is the jth component of the *unit vector* $\mathbf{x}/|\mathbf{x}|$. Thus, the additional factor of $x_j/|\mathbf{x}|$ in (1.10.7) does not change the rate of decay of the sound with distance from the source (which is still like $1/r$) but it does affect the *directivity*.

A comparison of (1.10.6) and (1.10.7) leads to the following rule for interchanging space and time derivatives *in the acoustic far field*

$$\frac{\partial}{\partial x_j} \longleftrightarrow -\frac{1}{c_o}\frac{x_j}{|\mathbf{x}|}\frac{\partial}{\partial t}. \tag{1.10.8}$$

1.10.2 Quadrupole source distributions

For the quadrupole (1.8.6)

$$\mathcal{F}(\mathbf{x}, t) = \frac{\partial^2 T_{ij}}{\partial x_i \partial x_j}(\mathbf{x}, t)$$

and

$$p(\mathbf{x}, t) = \frac{1}{4\pi}\frac{\partial^2}{\partial x_i \partial x_j}\int_{-\infty}^{\infty}\frac{T_{ij}(\mathbf{y}, t-|\mathbf{x}-\mathbf{y}|/c_o)}{|\mathbf{x}-\mathbf{y}|}\,d^3\mathbf{y}.$$

By applying (1.10.5) and the rule (1.10.8), we find that the acoustic far field is given by

Downloaded from https://www.cambridge.org/core. Charité Universitätsmedizin Berlin, on 20 Dec 2021 at 10:08:47, subject to the Cambridge Core terms of use, available at https://www.cambridge.org/core/terms. https://doi.org/10.1017/CBO9781107360273.002

$$p(\mathbf{x},t) \approx \frac{x_i x_j}{4\pi c_o^2 |\mathbf{x}|^3} \frac{\partial^2}{\partial t^2} \int_{-\infty}^{\infty} T_{ij}\left(\mathbf{y}, t - \frac{|\mathbf{x}|}{c_o} + \frac{\mathbf{x}\cdot\mathbf{y}}{c_o|\mathbf{x}|}\right) d^3\mathbf{y}, \quad |\mathbf{x}| \to \infty. \tag{1.10.9}$$

1.10.3 Example

For the (1,2) *point* quadrupole

$$\mathcal{F}(\mathbf{x},t) = \frac{\partial^2}{\partial x_1 \partial x_2}\left(T(t)\delta(\mathbf{x})\right)$$

equation (1.10.9) shows that in the acoustic far field

$$p(\mathbf{x},t) \approx \frac{x_1 x_2}{4\pi c_o^2 |\mathbf{x}|^3} \frac{\partial^2 T}{\partial t^2}\left(t - \frac{|\mathbf{x}|}{c_o}\right), \quad |\mathbf{x}| \to \infty.$$

If we use spherical polar coordinates, such that

$$x_1 = r\cos\theta, \; x_2 = r\sin\theta\cos\phi, \; x_3 = r\sin\theta\sin\phi,$$

we can write the pressure in the form

$$p(\mathbf{x},t) \approx \frac{\sin 2\theta \cos\phi}{8\pi c_o^2 |\mathbf{x}|} \frac{\partial^2 T}{\partial t^2}\left(t - \frac{|\mathbf{x}|}{c_o}\right), \quad |\mathbf{x}| \to \infty.$$

The directivity of the sound ($\propto p^2$) is therefore represented by $\sin^2 2\theta \cos^2\phi$. Its shape is plotted in Figure 1.10.2 for radiation in the x_1x_2-plane ($\phi = 0, \; \pi$). The four-lobe 'clover leaf' pattern is characteristic of a quadrupole T_{ij} for which $i \neq j$.

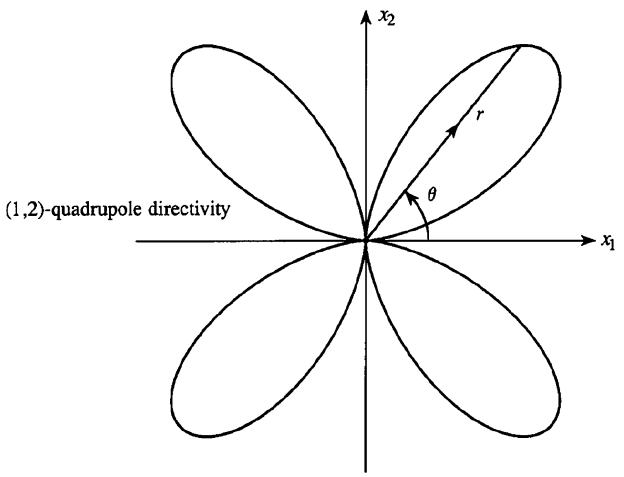

Figure 1.10.2

Downloaded from https://www.cambridge.org/core. Charité Universitätsmedizin Berlin, on 20 Dec 2021 at 10:08:47, subject to the Cambridge Core terms of use, available at https://www.cambridge.org/core/terms. https://doi.org/10.1017/CBO9781107360273.002

1.10.4 Multipole expansion of the field of a compact source

Phase variations $\mathbf{x}\cdot\mathbf{y}/c_o|\mathbf{x}|$ of sound arriving from different parts of a generalised source $\mathcal{F}(\mathbf{x},t)$ are small if the source region is acoustically compact. Therefore, the far field approximation ($|\mathbf{x}|\to\infty$) (1.10.5) reduces to that of a point monopole at the origin:

$$\begin{aligned} p(\mathbf{x},t) &\approx \frac{1}{4\pi|\mathbf{x}|}\int_{-\infty}^{\infty}\mathcal{F}\left(\mathbf{y},t-\frac{|\mathbf{x}|}{c_o}+\frac{\mathbf{x}.\mathbf{y}}{c_o|\mathbf{x}|}\right)\,d^3\mathbf{y} \\ &\approx \frac{1}{4\pi|\mathbf{x}|}\int_{-\infty}^{\infty}\mathcal{F}\left(\mathbf{y},t-\frac{|\mathbf{x}|}{c_o}\right)\,d^3\mathbf{y}. \end{aligned}$$

This gives the principal component of the radiating sound unless it should happen that the overall source strength is null, that is, unless $\int_{-\infty}^{\infty}\mathcal{F}(\mathbf{y},t)\;d^3\mathbf{y}=0$. The amplitude of sound waves in the far field is then crucially dependent on the existence of small phase mismatches between the contributions from different parts of the source region, and must be determined by expanding the Fraunhofer approximation in powers of $\mathbf{x}\cdot\mathbf{y}/c_o|\mathbf{x}|$. The result is formally equivalent to representing the sound as the superposition of the fields of a series of point sources at the origin of increasing multipole order,

$$\begin{aligned} p(\mathbf{x},t)\approx{}& \frac{1}{4\pi|\mathbf{x}|}\int_{-\infty}^{\infty}\mathcal{F}\left(\mathbf{y},t-\frac{|\mathbf{x}|}{c_o}\right)\,d^3\mathbf{y} \\ &+\frac{x_i}{4\pi c_o|\mathbf{x}|^2}\frac{\partial}{\partial t}\int_{-\infty}^{\infty}y_i\mathcal{F}\left(\mathbf{y},t-\frac{|\mathbf{x}|}{c_o}\right)\,d^3\mathbf{y} \\ &+\frac{x_ix_j}{8\pi c_o^2|\mathbf{x}|^3}\frac{\partial^2}{\partial t^2}\int_{-\infty}^{\infty}y_iy_j\mathcal{F}\left(\mathbf{y},t-\frac{|\mathbf{x}|}{c_o}\right)\,d^3\mathbf{y}+\cdots \\ ={}&\text{monopole}+\text{dipole}+\text{quadrupole}+\cdots \end{aligned} \tag{1.10.10}$$

Each term in this 'multipole expansion' is nominally of order $\omega\ell/c_o=k_o\ell\ll1$ relative to its predecessor, where $\omega\sim\partial/\partial t$ is the characteristic source frequency and $\ell\sim$ the diameter of the source region. The expansion is therefore halted at the first non-zero term (see Problem 1.16 at the end of this chapter).

1.10.5 Transition to the far field

The Fraunhofer approximation (1.10.5) for the acoustic far field requires that $|\mathbf{x}|$ be sufficiently large that the term $|\mathbf{x}\wedge\mathbf{y}|^2/2|\mathbf{x}|^3$ on the right of (1.10.2) can be ignored in approximating the retarded time. This may not be valid even when

Downloaded from https://www.cambridge.org/core. Charité Universitätsmedizin Berlin, on 20 Dec 2021 at 10:08:47, subject to the Cambridge Core terms of use, available at https://www.cambridge.org/core/terms. https://doi.org/10.1017/CBO9781107360273.002

$|\mathbf{x}| \gg |\mathbf{y}|$ for applications involving very high frequency source distributions, when it may be necessary to replace (1.10.5) by the *Fresnel* formula

$$p(\mathbf{x},t) \approx \frac{1}{4\pi|\mathbf{x}|}\int_{-\infty}^{\infty} \mathcal{F}\left(\mathbf{y}, t - \frac{|\mathbf{x}|}{c_o} + \frac{\mathbf{x}\cdot\mathbf{y}}{c_o|\mathbf{x}|} - \frac{|\mathbf{x}\wedge\mathbf{y}|^2}{2c_o|\mathbf{x}|^3}\right) d^3\mathbf{y}. \quad (1.10.11)$$

Ultimately as $|\mathbf{x}| \to \infty$ the Fraunhofer approximation must become applicable, when waves arriving from the source have parallel wavefronts propagating in the direction $\mathbf{x}/|\mathbf{x}|$.

The retarded time correction can be important at high frequencies within a region at intermediate but large distances $|\mathbf{x}|$ from the source where the pressure is governed by interference between spherical waves with nonparallel wavefronts arriving from different parts of the source. This is the *Fresnel zone* – the region where wavefront curvature is important. For a source of diameter $\sim \ell$ and characteristic radian frequency ω it is determined by the condition that $\omega|\mathbf{x}\wedge\mathbf{y}|^2/2c_o|\mathbf{x}|^3$ is not small, where

$$|\mathbf{x}| < R_o \sim \frac{\pi\ell^2}{\lambda}, \quad \lambda = \frac{2\pi}{k_o}, \quad (1.10.12)$$

that is, where $\ell/\lambda > |\mathbf{x}|/\ell \gg 1$. The distance $|\mathbf{x}| = R_o \sim \pi\ell^2/\lambda$ from the source region may therefore be interpreted as marking the beginning of the (Fraunhofer) far field.

Problems 1

1.1.* Derive the relations (1.3.13) for plane sound waves.

1.2. Calculate the low frequency resonances for one-dimensional sound waves in a tube of length ℓ (Figure 1.3.1d) when the tube is (i) closed at $x = 0$ and open at $x = \ell$, (ii) closed at both ends.

1.3.* Use the trial solution $\varphi = \Phi(t - |x|/c_o)$ to solve the problem

$$\left(\frac{1}{c_o^2}\frac{\partial^2}{\partial t^2} - \frac{\partial^2}{\partial x^2}\right)\varphi = \delta(x)\delta(t), \quad -\infty < x < \infty,$$

where $\varphi = 0$ for $t < 0$.

1.4. When the body force $\mathbf{F} = \rho\mathbf{g}$ in Equation (1.3.1), where $\mathbf{g}$ is the acceleration due to gravity, show that in the adiabatic approximation the linearised acoustic wave equation becomes

$$\frac{1}{\rho_o c_o^2}\frac{\partial^2 p'}{\partial t^2} - \frac{\partial}{\partial x_j}\left(\frac{1}{\rho_o}\frac{\partial p'}{\partial x_j}\right) = \frac{\partial q}{\partial t} - \operatorname{div}\left(\frac{p'\mathbf{g}}{\rho_o c_o^2}\right),$$

Downloaded from https://www.cambridge.org/core. Charité Universitätsmedizin Berlin, on 20 Dec 2021 at 10:08:47, subject to the Cambridge Core terms of use, available at https://www.cambridge.org/core/terms. https://doi.org/10.1017/CBO9781107360273.002

where $p' = p - p_o$, and the mean pressure, density, and sound speed $p_o,\ \rho_o,\ c_o$ vary with depth in the atmosphere. Deduce that the gravitational term on the right-hand side can be neglected provided $\omega \gg g/c_o$, where ω is a typical acoustic frequency.

1.5.* Consider the initial value problem (1.7.1), (1.7.2) in which the pressure $p = p_0 =$ constant and $\partial p/\partial t = 0$ at time $t = 0$ in $0 < x_1 < h$. Show that Poisson's solution (1.7.4) predicts plane wave propagation parallel to the x_1 direction, and that the pressure wave radiating through a typical exterior point P distance r_1 from the source region has amplitude $\frac{1}{2}p_0$, arrives at time $t = r_1/c_o$ and occupies a plane 'shell' of thickness h.

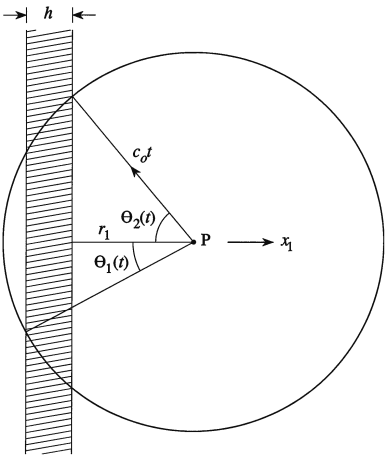

1.6. The initial value problem for one-dimensional propagation of sound parallel to the x axis in unbounded fluid is governed by

$$\left(\frac{1}{c_o^2}\frac{\partial^2}{\partial t^2} - \frac{\partial^2}{\partial x^2}\right)(p\mathrm{H}) = \frac{1}{c_o^2}\frac{\partial}{\partial t}\Big(\delta(t)f(x)\Big) + \frac{1}{c_o^2}\delta(t)g(x), \quad -\infty < x < \infty,$$

where $\mathrm{H} \equiv \mathrm{H}(t)$ is the Heaviside step function and $f(x),\ g(x)$ are the respective values of p and $\partial p/\partial t$ at $t = 0$. Use Green's function (1.6.8) to derive D'Alembert's solution

Downloaded from https://www.cambridge.org/core. Charité Universitätsmedizin Berlin, on 20 Dec 2021 at 10:08:47, subject to the Cambridge Core terms of use, available at https://www.cambridge.org/core/terms. https://doi.org/10.1017/CBO9781107360273.002

$$p(x,t) = \frac{1}{2}\Big(f(x-c_o t)+f(x-c_o t)\Big) + \frac{1}{2c_o}\int_{x-c_o t}^{x+c_o t} g(y)\,dy, \quad t>0.$$

1.7. At time $t = 0$ a plane acoustic wave $p = P(x - c_o t)$ propagating in unbounded fluid satisfies $p = P(x)$, $\partial p/\partial t = -c_o P'(x)$ (the prime denoting differentiation with respect to the argument). Verify that Poisson's solution (1.7.4) predicts that $p = P(x - c_o t)$ when $t > 0$.

1.8.* A plane sound wave $p = p_I \cos\{\omega(t - x_1/c_o)\}$ is incident from $x_1 = -\infty$ on the open end $x_1 = 0$ of a uniform, semi-infinite duct of radius R, as in Figure 1.3.1c. Show that when $k_o R \ll 1$ ($k_o = \omega/c_o$) the volume velocity at the open end is $Q(t) = (2\pi R^2 p_I/\rho_o c_o)\cos(\omega t)$, and that the acoustic pressure in free space at distance $r \gg R$ from the open end is given by

$$p = -\frac{k_o R^2 p_I}{2r}\sin\left[\omega\left(t-\frac{r}{c_o}\right)\right], \quad r\to\infty.$$

Deduce that a fraction $(k_o R)^2$ of the incident wave energy is radiated into free space.

1.9. A plane wave $p = p_I e^{-i\omega(t-x/c_o)}$ propagates from $x = -\infty$ in an infinitely long tube of uniform cross-section A containing a thin piston of the same cross-section at $x = 0$ of mass m, which is free to move in the tube without friction. Show that the plane waves reflected and transmitted by the piston have the respective amplitudes

$$\frac{p_I}{\left(1+\frac{4\rho_o^2 A^2}{k_o^2 m^2}\right)^{\frac{1}{2}}} \quad \text{and} \quad \frac{p_I}{\left(1+\frac{k_o^2 m^2}{4\rho_o^2 A^2}\right)^{\frac{1}{2}}}, \quad k_o = \frac{\omega}{c_o}.$$

1.10. Show that the kinetic and potential energy densities for a plane wave $p = p(t - x/c_o)$ are equal.

1.11. Verify that the sum of the kinetic and potential energies is constant for plane waves in a uniform tube closed at both ends.

1.12.* A sphere of mean radius a pulsates at frequency ω with *small* amplitude, uniform radial velocity $ue^{-i\omega t}$ (u = constant). Show that in an ideal compressible fluid the velocity potential at distance r from the centre of the sphere is

$$\varphi = \frac{-Q_o\, e^{-i\omega\{t-(r-a)/c_o\}}}{4\pi r(1-ik_o a)},$$

where $k_o = \omega/c_o$ and $Q_o = 4\pi a^2 u$.

Write down the compact limit of this formula and the *inhomogeneous* wave equation of which it is the solution.

Downloaded from https://www.cambridge.org/core. Charité Universitätsmedizin Berlin, on 20 Dec 2021 at 10:08:47, subject to the Cambridge Core terms of use, available at https://www.cambridge.org/core/terms. https://doi.org/10.1017/CBO9781107360273.002

1.13. Show that the resonant frequencies ω of time-harmonic radial acoustic waves in the region between two rigid concentric spheres of radii a and b are the solutions of the equation

$$(k_o^2 ab + 1)\sin\{k_o(b-a)\} - k_o(b-a)\cos\{k_o(b-a)\} = 0, \quad k_o = \frac{\omega}{c_o}.$$

1.14.* The velocity potential of sound produced in an ideal compressible fluid when a sphere of mean radius a pulsates with *small* amplitude radial velocity $u\cos(\omega t)$ (u = constant) is given at distance r from its centre by (Question 1.12)

$$\varphi = \mathrm{Re}\left\{\frac{-a^2 u\, \mathrm{e}^{-i\omega\{t-(r-a)/c_o\}}}{r(1-ik_o a)}\right\}, \quad k_o = \frac{\omega}{c_o}.$$

Show that the mean acoustic power radiated by the sphere is

$$\Pi_a = \left(\frac{(k_o a)^2}{1+(k_o a)^2}\right) 4\pi a^2 c_o \tfrac{1}{2}\rho_o u^2 \,.$$

Deduce the compact ($k_o a \ll 1$) and non-compact ($k_o a \gg 1$) limits of this formula.

1.15. A rigid sphere of radius a vibrates at frequency ω with *small* amplitude velocity $U_o \mathrm{e}^{-i\omega t}$ (U_o = constant) in the x_1 direction. Use the trial solution

$$\varphi = A\,\frac{\partial}{\partial x_1}\left(\frac{\mathrm{e}^{-i\omega(t-|\mathbf{x}|/c_o)}}{|\mathbf{x}|}\right)$$

to show that in an ideal compressible fluid the velocity potential at $\mathbf{x}$ is

$$\varphi = \frac{a^3 U_o}{\{1+(1-ik_o a)^2\}}\,\frac{\partial}{\partial x_1}\left(\frac{\mathrm{e}^{-i\omega\{t-(|\mathbf{x}|-a)/c_o\}}}{|\mathbf{x}|}\right),$$

where the coordinate origin is at the undisturbed position of the centre of the sphere.

1.16.* Consider the outgoing wave solution of

$$\left(\frac{1}{c_o^2}\frac{\partial^2}{\partial t^2} - \nabla^2\right)\varphi = \frac{\mathrm{sgn}(x)\mathrm{H}(a-|\mathbf{x}|)U(t)}{a}, \quad a > 0,$$

where $U(t)$ is known as a function of time. If the source region $|\mathbf{x}| < a$ is acoustically compact, show that

$$\varphi(\mathbf{x},t) \simeq \frac{a^3\cos\theta}{8c_o|\mathbf{x}|}\frac{\partial U}{\partial t}\left(t-\frac{|\mathbf{x}|}{c_o}\right), \quad |\mathbf{x}| \to \infty,$$

where $\cos\theta = x/|\mathbf{x}|$.

Downloaded from https://www.cambridge.org/core. Charité Universitätsmedizin Berlin, on 20 Dec 2021 at 10:08:47, subject to the Cambridge Core terms of use, available at https://www.cambridge.org/core/terms. https://doi.org/10.1017/CBO9781107360273.002

1.17.* A *volume* point source of strength $q_o(t)$ translates at *constant, subsonic* velocity $\mathbf{U}$. The velocity potential $\varphi(\mathbf{x}, t)$ of the radiated sound is the outgoing solution of

$$\left(\frac{1}{c_o^2}\frac{\partial^2}{\partial t^2} - \nabla^2\right)\varphi = -q_o(t)\delta(\mathbf{x} - \mathbf{U}t).$$

Show that

$$\varphi(\mathbf{x}, t) = \frac{-q_o(t - R/c_o)}{4\pi R(1 - M\cos\Theta)}, \quad M = \frac{U}{c_o},$$

where R is the distance of the reception point $\mathbf{x}$ from the source position *at the time of emission* of the sound received at $\mathbf{x}$ at time t, and Θ is the angle between $\mathbf{U}$ and the direction of propagation of this sound.

Downloaded from https://www.cambridge.org/core. Charité Universitätsmedizin Berlin, on 20 Dec 2021 at 10:08:47, subject to the Cambridge Core terms of use, available at https://www.cambridge.org/core/terms. https://doi.org/10.1017/CBO9781107360273.002

2

More on Green's Function

2.1 Kirchhoff's formula

The retarded potential integral (1.6.6)

$$p(\mathbf{x}, t) = \frac{1}{4\pi} \int_{-\infty}^{\infty} \frac{\mathcal{F}\left(\mathbf{y}, t - \frac{|\mathbf{x}-\mathbf{y}|}{c_o}\right)}{|\mathbf{x} - \mathbf{y}|} d^3\mathbf{y}$$

represents the causal solution of the general linear acoustic equation

$$\left(\frac{1}{c_o^2}\frac{\partial^2}{\partial t^2} - \nabla^2\right) p = \rho_o \frac{\partial q}{\partial t} - \operatorname{div} \mathbf{F} \tag{2.1.1}$$

in an unbounded fluid. The solution is actually valid in a bounded region for all times before the first arrival of sound waves at the physical boundary. At later times, the boundary will be subject unsteady pressures, so that each of its surface elements exerts a force on the fluid, and might therefore be expected to behave as an additional acoustic *dipole source*. Similarly, the normal component of the acoustic particle velocity of sound waves arriving at the boundary will be opposed by an effective surface velocity dependent in magnitude and phase on the mechanical properties of the boundary – as a result, each surface element will also behave as an acoustic *monopole*. It appears, therefore, that the solution of the acoustic equation in fluid with boundary S can be obtained by augmenting the retarded potential solution in the absence of boundaries by contributions from continuous distributions of monopole and dipole sources on S.

This is the essence of Kirchhoff's (1882) formula for sound generation in a bounded medium. We shall give two derivations. The first (§2.1.2) is an extension of the intuitive method of Chapter 1, where Green's function (1.6.2) is interpreted as the sound produced by an impulsive point source at position $\mathbf{y}$ at time τ. In the second approach (§2.2), Green's function is regarded as an

Downloaded from https://www.cambridge.org/core. Charité Universitätsmedizin Berlin, on 20 Dec 2021 at 10:08:47, subject to the Cambridge Core terms of use, available at https://www.cambridge.org/core/terms. https://doi.org/10.1017/CBO9781107360273.003

advanced potential propagating in space and time as a function of $(\mathbf{y}, \tau)$, so that the spherical wave (1.6.2) ultimately converges on the observation point $(\mathbf{x}, t)$ as τ increases to t and vanishes thereafter.

2.1.1 Volume and surface integral transformations

We establish first a transformation formula between surface and volume integrals that simplifies the discussion of surface source distributions.

Let V denote the fluid region outside a closed control surface S (Figure 2.1.1) defined by the equation

$$f(\mathbf{x}) = 0, \quad \text{where} \begin{cases} f(\mathbf{x}) > 0 & \text{for } \mathbf{x} \text{ in } V, \\ f(\mathbf{x}) < 0 & \text{for } \mathbf{x} \text{ inside } S, \end{cases}$$

so that the Heaviside step function $\mathrm{H}(f) = 1$ for $\mathbf{x}$ in V, and 0 for $\mathbf{x}$ inside S. Then, for an arbitrary function $\Phi(\mathbf{x})$ defined in V and on S,

$$\int_{-\infty}^{\infty} \Phi(\mathbf{x}) \nabla \mathrm{H} d^3\mathbf{x} = \oint_S \Phi(\mathbf{x})\, \mathbf{n} dS \equiv \oint_S \Phi(\mathbf{x})\, d\mathbf{S} \tag{2.1.2}$$

where $\mathrm{H} = \mathrm{H}(f)$ and $\mathbf{n}$ is the unit normal on S directed into V.

The equality (2.1.2) is obtained by noting that $\nabla \mathrm{H}(f) \equiv \delta(f)\, \nabla f$ is non-zero only on S, on which $\mathbf{n} = \nabla f / |\nabla f|$ is the outward unit normal. The volume integral is therefore confined to the region between the inner and outer faces of a shell of infinitesimal thickness (between the broken line surfaces in

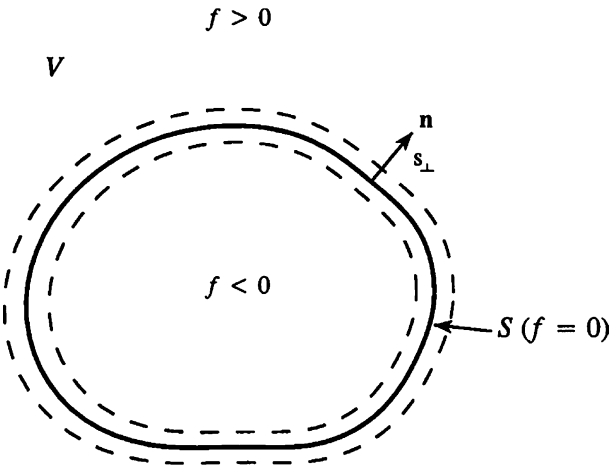

Figure 2.1.1

Downloaded from https://www.cambridge.org/core. Charité Universitätsmedizin Berlin, on 20 Dec 2021 at 10:08:47, subject to the Cambridge Core terms of use, available at https://www.cambridge.org/core/terms. https://doi.org/10.1017/CBO9781107360273.003

Figure 2.1.1) that just encloses S, and within which the volume element can be written $d^3\mathbf{x} = ds_\perp dS$, where $s_\perp = 0$ on S and $s_\perp$ is measured parallel to $\mathbf{n}$. Because $f = 0$ on S, we have $f(s_\perp) \approx s_\perp f'(0)$ for small values of $s_\perp$, so that

$$\delta(f) = \delta\Big(s_\perp f'(0)\Big) = \frac{\delta(s_\perp)}{|f'(0)|} \equiv \frac{\delta(s_\perp)}{|\nabla f|}$$

and therefore

$$\int_{-\infty}^{\infty} \Phi(\mathbf{x}) \nabla \mathrm{H} d^3\mathbf{x} \equiv \int_{-\infty}^{\infty} \Phi(\mathbf{x}) \nabla f \delta(f) d^3\mathbf{x} = \int_{-\infty}^{\infty} \Phi(\mathbf{x}) \frac{\nabla f}{|\nabla f|} \delta(s_\perp) ds_\perp dS$$
$$= \oint_S \Phi(\mathbf{x})\, \mathbf{n} dS.$$

2.1.2 *First derivation of Kirchhoff's formula*

Kirchhoff's formula is a representation of the solution of equation (2.1.1) when the acoustic medium is confined by a set of boundaries or control surfaces. Consider the case of a single, *fixed* closed surface S defined by an equation $f(\mathbf{x}) = 0$, such that $f(\mathbf{x}) > 0$ in the fluid region V outside S that extends to infinity (Figure 2.1.2). S may be assumed to enclose a physical boundary (a 'solid body' with boundary S) or may merely constitute a control surface used to isolate a fixed region of space containing both solid bodies and fluid or just fluid (perhaps a fluid region undergoing, say, a chemical reaction within which linear acoustic theory is not applicable).

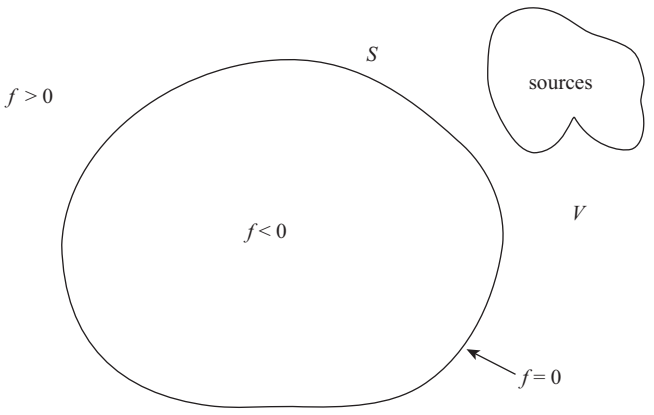

Figure 2.1.2

Downloaded from https://www.cambridge.org/core. Charité Universitätsmedizin Berlin, on 20 Dec 2021 at 10:08:47, subject to the Cambridge Core terms of use, available at https://www.cambridge.org/core/terms. https://doi.org/10.1017/CBO9781107360273.003

Multiply the linear acoustic equation (2.1.1) by $\mathrm{H} \equiv \mathrm{H}(f)$ and form the inhomogeneous equation for the new variable $\mathrm{H}p$ by use of the identities

$$\mathrm{H}\nabla^2 p \equiv \nabla^2(\mathrm{H}p) - \nabla \cdot (p\nabla \mathrm{H}) - \nabla \mathrm{H} \cdot \nabla p,$$

$$\mathrm{H}\frac{\partial^2 p}{\partial t^2} \equiv \frac{\partial^2(\mathrm{H}p)}{\partial t^2},$$

$$\mathrm{H}\left(\rho_o \frac{\partial q}{\partial t} - \operatorname{div} \mathbf{F}\right) \equiv \rho_o \frac{\partial(\mathrm{H}q)}{\partial t} - \operatorname{div}(\mathrm{H}\mathbf{F}) + \nabla \mathrm{H} \cdot \mathbf{F}.$$

Then

$$\begin{aligned}\left(\frac{1}{c_o^2}\frac{\partial^2}{\partial t^2} - \nabla^2\right)(\mathrm{H}p) &= \rho_o \frac{\partial(\mathrm{H}q)}{\partial t} - \operatorname{div}(\mathrm{H}\mathbf{F}) \\ &\quad + \nabla \mathrm{H} \cdot (-\nabla p + \mathbf{F}) - \operatorname{div}(p\nabla \mathrm{H}) \\ &= \rho_o \frac{\partial(\mathrm{H}q)}{\partial t} - \operatorname{div}(\mathrm{H}\mathbf{F}) \\ &\quad + \nabla \mathrm{H} \cdot \rho_o \frac{\partial \mathbf{v}}{\partial t} - \operatorname{div}(p\nabla \mathrm{H}) \qquad (2.1.3)\end{aligned}$$

where the linearised momentum equation $\rho_o \partial \mathbf{v}/\partial t = -\nabla p + \mathbf{F}$ has been used in passing from the first to the second equality. The first two terms on the right-hand side are the usual monopole and dipole sources distributed within the fluid but restricted to the region outside S where $\mathrm{H}(f) = 1$. The third and last source terms, however, are confined to the surface S at which $\nabla \mathrm{H} \neq 0$, and are respectively equivalent to *monopole* and *dipole* sources distributed on S. Equation (2.1.3) is formally valid *everywhere*, including the region within S where $\mathrm{H}(f) = 0$, and determines $\mathrm{H}p$ in terms of the surface sources and the prescribed volume sources and force distribution in V.

Kirchhoff's formula is the causal solution of (2.1.3) valid throughout all space and can be written down by analogy with the solution (1.8.8) in the absence of boundaries:

$$\begin{aligned}(\mathrm{H}p)(\mathbf{x}, t) &= \frac{\rho_o}{4\pi}\frac{\partial}{\partial t}\oint_S \frac{v_n(\mathbf{y}, t - |\mathbf{x}-\mathbf{y}|/c_o)}{|\mathbf{x}-\mathbf{y}|}\, dS(\mathbf{y}) \\ &\quad - \frac{1}{4\pi}\frac{\partial}{\partial x_j}\oint_S \frac{p(\mathbf{y}, t - |\mathbf{x}-\mathbf{y}|/c_o)}{|\mathbf{x}-\mathbf{y}|} n_j\, dS(\mathbf{y}) \\ &\quad + \frac{\rho_o}{4\pi}\frac{\partial}{\partial t}\int_V \frac{q(\mathbf{y}, t - |\mathbf{x}-\mathbf{y}|/c_o)}{|\mathbf{x}-\mathbf{y}|}\, d^3\mathbf{y} \\ &\quad - \frac{1}{4\pi}\frac{\partial}{\partial x_j}\int_V \frac{F_j(\mathbf{y}, t - |\mathbf{x}-\mathbf{y}|/c_o)}{|\mathbf{x}-\mathbf{y}|}\, d^3\mathbf{y}, \qquad (2.1.4)\end{aligned}$$

Downloaded from https://www.cambridge.org/core. Charité Universitätsmedizin Berlin, on 20 Dec 2021 at 10:08:47, subject to the Cambridge Core terms of use, available at https://www.cambridge.org/core/terms. https://doi.org/10.1017/CBO9781107360273.003

where v_n is the normal component of velocity on S directed into V, and the integral transformation formula (2.1.2) has been used to obtain the surface integrals.

The solution is valid throughout the whole of space, including that contained within S where $\mathrm{H}p \equiv 0$. In other words, the combined values of the retarded source integrals on the right hand side must vanish when $\mathbf{x}$ is inside S. This implies that the surface values of the pressure and the normal velocity v_n cannot be independent, and cannot therefore be prescribed arbitrarily in any particular application.

2.1.3 Sound generation by a compact vibrating body

A rigid body with closed surface S and volume Δ executes small amplitude translational oscillations at velocity $\mathbf{U}(t)$ at sufficiently low frequency that the body is acoustically compact (Figure 2.1.3). The radiated sound is given by Kirchhoff's formula (2.1.4) with $q = 0,\ \mathbf{F} = 0$.

Because the vibrating body exerts an unsteady force on the fluid it might be expected that the radiation will be of dipole order, as for the vibrating sphere discussed in §1.8.5.

Take the coordinate origin within the body. In the acoustic far field $|\mathbf{x}-\mathbf{y}|$ can then be replaced by $|\mathbf{x}|$ in the denominators of the integrands, and the operator $\partial/\partial x_j \to -(x_j/c_o|\mathbf{x}|)\,\partial/\partial t$ for the surface pressure integral. As $|\mathbf{x}| \to \infty$,

$$p(\mathbf{x},t) \approx \frac{\rho_o}{4\pi|\mathbf{x}|}\frac{\partial}{\partial t}\oint_S v_n\left(\mathbf{y}, t - \frac{|\mathbf{x}|}{c_o} + \frac{\mathbf{x}\cdot\mathbf{y}}{c_o|\mathbf{x}|}\right) dS + \frac{x_j}{4\pi c_o|\mathbf{x}|^2}\frac{\partial}{\partial t}\oint_S p\left(\mathbf{y}, t - \frac{|\mathbf{x}|}{c_o} + \frac{\mathbf{x}\cdot\mathbf{y}}{c_o|\mathbf{x}|}\right) n_j\, dS.$$

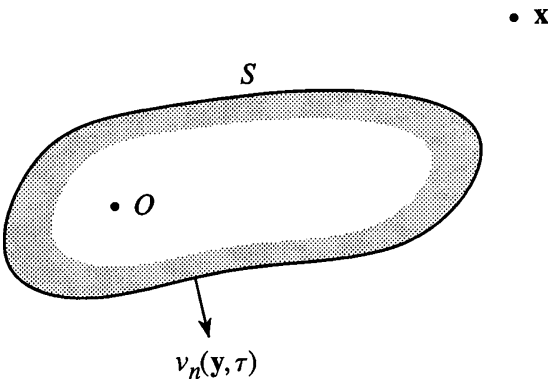

Figure 2.1.3

Downloaded from https://www.cambridge.org/core. Charité Universitätsmedizin Berlin, on 20 Dec 2021 at 10:08:47, subject to the Cambridge Core terms of use, available at https://www.cambridge.org/core/terms. https://doi.org/10.1017/CBO9781107360273.003

Put $v_n = U_j n_j$ and consider the two-term multipole expansion (§1.10.4)

$$\frac{\rho_o}{4\pi|\mathbf{x}|}\frac{\partial}{\partial t}\oint_S v_n\left(\mathbf{y}, t-\frac{|\mathbf{x}|}{c_o}+\frac{\mathbf{x}\cdot\mathbf{y}}{c_o|\mathbf{x}|}\right)dS$$
$$\approx \frac{\rho_o}{4\pi|\mathbf{x}|}\oint_S \frac{\partial U_j}{\partial t}\left(t-\frac{|\mathbf{x}|}{c_o}\right)n_j dS + \frac{\rho_o x_i}{4\pi c_o|\mathbf{x}|^2}\oint_S \frac{\partial^2 U_j}{\partial t^2}\left(t-\frac{|\mathbf{x}|}{c_o}\right)y_i n_j dS$$
$$= 0 + \frac{\rho_o x_i}{4\pi c_o|\mathbf{x}|^2}\frac{\partial^2 U_j}{\partial t^2}\left(t-\frac{|\mathbf{x}|}{c_o}\right)\oint_S y_i n_j dS = \frac{\Delta\rho_o x_j}{4\pi c_o|\mathbf{x}|^2}\frac{\partial^2 U_j}{\partial t^2}\left(t-\frac{|\mathbf{x}|}{c_o}\right).$$

The monopole vanishes because the body is incompressible; the final integral has been evaluated by the divergence theorem, which transforms it into an integral over the volume Δ of the body:

$$\oint_S y_i n_j dS = \int_\Delta \frac{\partial y_i}{\partial y_j} d^3\mathbf{y} = \Delta\delta_{ij}.$$

The expansion in powers of $(\mathbf{x}\cdot\mathbf{y}/c_o|\mathbf{x}|)\partial/\partial t$ is equivalent to expanding in powers of a small compactness parameter $k_o\ell$ ($\equiv \omega\ell/c_o$), where ω is a typical frequency of oscillation and ℓ is the characteristic diameter of the body, and this approximation determines the contribution from the surface velocity correct to *dipole* order. The surface pressure integral already represents a dipole, so that it is sufficient to neglect the variations $\mathbf{x}\cdot\mathbf{y}/c_o|\mathbf{x}|$ on S of the retarded time. Hence we can write:

$$p(\mathbf{x},t) \approx \frac{x_j}{4\pi c_o|\mathbf{x}|^2}\left[m_o\frac{d^2U_j}{dt^2}+\frac{dF_j}{dt}\right], \quad |\mathbf{x}|\to\infty, \tag{2.1.5}$$

where the square brackets [ ] denote evaluation at the retarded time $t-|\mathbf{x}|/c_o$, $m_o = \rho_o\Delta$ is the fluid mass displaced by the body, and $F_j(t) = \oint_S p(\mathbf{y},t)n_j\,dS$ is the unsteady force *exerted on the fluid* by the body. The radiation (2.1.5) is equivalent to that generated by a point dipole $-\operatorname{div}(\mathbf{f}\delta(\mathbf{x}))$, where $\mathbf{f} = m_o d\mathbf{U}/dt + \mathbf{F}$ is the force required to produce the same fluid motion when the material of the body is replaced by the displaced mass m_o.

2.1.4 Generalised Kirchhoff formula

Kirchhoff's formula is derived using the free space Green's function (1.6.2). But equation (2.1.3) can also be solved in terms of any Green's function $G(\mathbf{x},\mathbf{y},t-\tau)$ that satisfies equation (1.6.1) in the region V outside S provided it exhibits outgoing wave behaviour. This is useful when S coincides with a solid boundary on which the properties of G can be prescribed.

Introduce an additional control surface S_+ on which $f(\mathbf{x}) = 0$, such that $f(\mathbf{x}) \gtrless 0$ according as $\mathbf{x}$ lies outside or within S_+. The body with surface

Downloaded from https://www.cambridge.org/core. Charité Universitätsmedizin Berlin, on 20 Dec 2021 at 10:08:47, subject to the Cambridge Core terms of use, available at https://www.cambridge.org/core/terms. https://doi.org/10.1017/CBO9781107360273.003

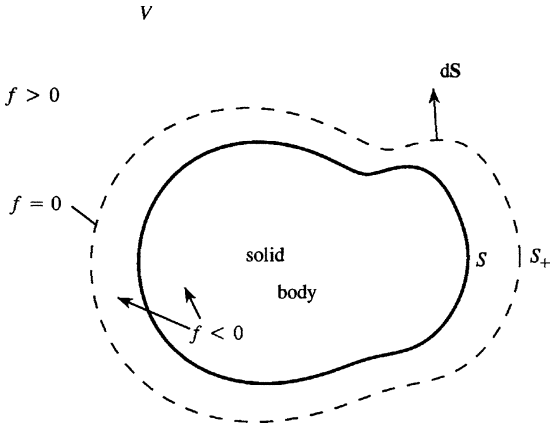

Figure 2.1.4

S is assumed to be enclosed within S_+, and S_+ is subsequently allowed to shrink down to coincide with S (Figure 2.1.4). Then, in the fluid (region V outside S)

$$(\mathrm{H}p)(\mathbf{x},t) = \iint G(\mathbf{x},\mathbf{y},t-\tau)\left(\rho_o \frac{\partial(\mathrm{H}q)}{\partial\tau} - \operatorname{div}(\mathrm{H}\mathbf{F}) + \nabla\mathrm{H}\cdot\rho_o\frac{\partial\mathbf{v}}{\partial\tau} - \operatorname{div}(p\nabla\mathrm{H})\right)(\mathbf{y},\tau)\,d^3\mathbf{y}d\tau,$$

where the integrations are over V and all retarded times τ. This formally determines $\mathrm{H}p$ in the whole of V, including the region between S and S_+ where $\mathrm{H}p \equiv 0$; but except in the case where G is the free space Green's function (1.6.2), the integral for $\mathrm{H}p$ does not vanish within S (see §2.2.1). The integral is simplified in the usual way by application of the divergence theorem, observing that $\partial G/\partial\tau = -\partial G/\partial t$ and that there are no contributions from integrations over S where all source terms are null. Thus, when $S_+ \to S$ we find for $\mathbf{x}$ in V

$$p(\mathbf{x},t) = \iint_V \left(\frac{\partial G}{\partial t}\rho_o q + \frac{\partial G}{\partial \mathbf{y}}\cdot\mathbf{F}\right) d^3\mathbf{y}d\tau + \iint_S \left(\frac{\partial G}{\partial t}\rho_o v_n + \frac{\partial G}{\partial y_n}p\right) dS(\mathbf{y})d\tau. \tag{2.1.6}$$

where $G = G(\mathbf{x},\mathbf{y},t-\tau)$, and q, $\mathbf{F}$, v_n and p are expressed as functions of $(\mathbf{y},\tau)$. The first integral is the contribution from volume sources and forces within the fluid; the surface integral gives similarly the contribution from the

Downloaded from https://www.cambridge.org/core. Charité Universitätsmedizin Berlin, on 20 Dec 2021 at 10:08:47, subject to the Cambridge Core terms of use, available at https://www.cambridge.org/core/terms. https://doi.org/10.1017/CBO9781107360273.003

surface volume sources of strength v_n per unit area and the normal surface forces of strength p per unit area.

In applications the value on S of $G(\mathbf{x}, \mathbf{y}, t-\tau)$ or $\partial G(\mathbf{x}, \mathbf{y}, t-\tau)/\partial y_n$ or a linear combination of these quantities is chosen to simplify the surface integral terms, as illustrated by the following case of a plane boundary.

2.1.5 Example: Green's function for a plane boundary

Let the fluid occupy the semi-infinite region $x_2 > 0$ bounded by a plane surface S: $x_2 = 0$ (Figure 2.1.5). For a **hard wall** we choose G to satisfy $\partial G/\partial x_n \equiv \partial G/\partial x_2 = 0$ on $x_2 = 0$. This is done by the 'method of images', by augmenting the free space Green's function by the field of an image source $\delta(\mathbf{x}-\bar{\mathbf{y}})\delta(t-\tau)$ located 'within the wall' at $\bar{\mathbf{y}} = (y_1, -y_2, y_3)$. Then

$$G(\mathbf{x}, \mathbf{y}, t-\tau) = \frac{1}{4\pi|\mathbf{x}-\mathbf{y}|}\delta\left(t-\tau-\frac{|\mathbf{x}-\mathbf{y}|}{c_o}\right) + \frac{1}{4\pi|\mathbf{x}-\bar{\mathbf{y}}|}\delta\left(t-\tau-\frac{|\mathbf{x}-\bar{\mathbf{y}}|}{c_o}\right). \tag{2.1.7}$$

This satisfies $\partial G/\partial x_2 = 0$ on $x_2 = 0$; it also satisfies $\partial G/\partial y_2 = 0$ for $y_2 = 0$ because the formula is unchanged when $\mathbf{x}$ and $\mathbf{y}$ are interchanged.

When $x_2 = 0$ coincides with a plane, **pressure release** surface on which it is convenient to take $G(\mathbf{x}, \mathbf{y}, t-\tau) = 0$ for either $\mathbf{x}$ or $\mathbf{y}$ on S, we place an equal but *opposite* image source at $\bar{\mathbf{y}}$, giving

$$G(\mathbf{x}, \mathbf{y}, t-\tau) = \frac{1}{4\pi|\mathbf{x}-\mathbf{y}|}\delta\left(t-\tau-\frac{|\mathbf{x}-\mathbf{y}|}{c_o}\right) - \frac{1}{4\pi|\mathbf{x}-\bar{\mathbf{y}}|}\delta\left(t-\tau-\frac{|\mathbf{x}-\bar{\mathbf{y}}|}{c_o}\right). \tag{2.1.8}$$

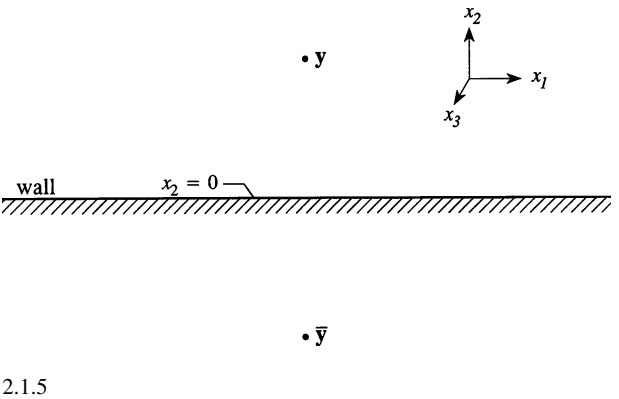

Figure 2.1.5

Downloaded from https://www.cambridge.org/core. Charité Universitätsmedizin Berlin, on 20 Dec 2021 at 10:08:47, subject to the Cambridge Core terms of use, available at https://www.cambridge.org/core/terms. https://doi.org/10.1017/CBO9781107360273.003

This can be used in problems involving sound propagation in water adjacent to a free plane surface (an interface with air, for example).

2.1.6 Kirchhoff's formula for the velocity potential

Kirchhoff's formula (2.1.6) for the acoustic pressure is easily modified in an obvious manner to obtain the corresponding representation for the velocity potential φ, which is governed by

$$\left(\frac{1}{c_o^2}\frac{\partial^2}{\partial t^2} - \nabla^2\right)\varphi = -q(\mathbf{x}, t). \tag{2.1.9}$$

We now have

$$\left(\frac{1}{c_o^2}\frac{\partial^2}{\partial t^2} - \nabla^2\right)(\mathrm{H}\varphi) = -\mathrm{H}q(\mathbf{x}, t) - \nabla\mathrm{H}\cdot\nabla\varphi - \mathrm{div}\,(\varphi\nabla\mathrm{H}),$$

and for points $\mathbf{x}$ within the fluid we find

$$\varphi(\mathbf{x}, t) \;=\; -\iint_V Gq\, d^3\mathbf{y}d\tau \;-\; \iint_S \left(G\frac{\partial\varphi}{\partial y_n} - \frac{\partial G}{\partial y_n}\varphi\right) dS(\mathbf{y})d\tau, \tag{2.1.10}$$

where $G = G(\mathbf{x}, \mathbf{y}, t-\tau)$ and q, $\partial\varphi/\partial y_n \equiv v_n$ and φ are expressed as functions of $(\mathbf{y}, \tau)$.

2.1.7* Determinancy of the sound

Kirchhoff's formula determines the acoustic field in terms of the prescribed sources and the values of v_n and the pressure p (or velocity potential φ) on S. The surface data are redundant, however, because a knowledge of p (or φ) alone or of v_n alone on S is actually sufficient to completely determine the sound.

Let us illustrate this for equation (2.1.9). Suppose that $\Phi = \varphi_1 - \varphi_2$, where φ_1, φ_2 are two possible solutions with outgoing wave behaviour satisfying identical conditions on S. Then $\Phi(\mathbf{x}, t)$ satisfies the homogeneous form of (2.1.9), $(\partial^2/c_o^2\partial t^2 - \nabla^2)\Phi = 0$, with total acoustic energy

$$W = \frac{\rho_o}{2}\int_V \left\{\frac{1}{c_o^2}\left(\frac{\partial\Phi}{\partial t}\right)^2 + (\nabla\Phi)^2\right\} d^3\mathbf{x}, \tag{2.1.11}$$

where V is the fluid region outside S bounded by a large surface Σ enclosing all sources and sufficiently distant that no sound has arrived at time t. It follows that

Downloaded from https://www.cambridge.org/core. Charité Universitätsmedizin Berlin, on 20 Dec 2021 at 10:08:47, subject to the Cambridge Core terms of use, available at https://www.cambridge.org/core/terms. https://doi.org/10.1017/CBO9781107360273.003

$$\frac{dW}{dt} = \rho_o \int_V \left\{ \frac{1}{c_o^2} \frac{\partial \Phi}{\partial t} \frac{\partial^2 \Phi}{\partial t^2} + \nabla \Phi \cdot \nabla \left(\frac{\partial \Phi}{\partial t} \right) \right\} d^3\mathbf{x}$$

$$= \rho_o \int_V \left\{ \frac{\partial \Phi}{\partial t} \left(\frac{1}{c_o^2} \frac{\partial^2 \Phi}{\partial t^2} - \nabla^2 \Phi \right) + \nabla \cdot \left(\frac{\partial \Phi}{\partial t} \nabla \Phi \right) \right\} d^3\mathbf{x}$$

$$= -\rho_o \oint_S \frac{\partial \Phi}{\partial t} \frac{\partial \Phi}{\partial x_n} dS,$$

where the divergence theorem is applied on the last line to obtain the surface integral over S – there being no contribution from Σ on which $\Phi(\mathbf{x}, t) \equiv 0$.

If the sources responsible for the sound vanish for $t \leq t_o$, then $W(t_o) = 0$ and, when Φ is replaced by $\varphi_1 - \varphi_2$,

$$W(t) = -\rho_o \int_{t_o}^{t} dt \oint_S \left(\frac{\partial \varphi_1}{\partial t} - \frac{\partial \varphi_2}{\partial t} \right) \left(\frac{\partial \varphi_1}{\partial x_n} - \frac{\partial \varphi_2}{\partial x_n} \right) dS.$$

This implies that $W(t) \equiv 0$ whenever either the value of φ alone or of $v_n = \partial\varphi/\partial x_n$ alone is specified on S, because the corresponding condition is satisfied separately by φ_1 and φ_2. Therefore, Φ must be constant in V because the integrand of (2.1.11) is non-negative, i.e. $\varphi_1 = \varphi_2 +$ constant, where the constant vanishes because $\varphi_1 = \varphi_2 = 0$ on Σ.

This establishes the uniqueness of the outgoing wave solution, and also that the specification of either φ or $\partial\varphi/\partial x_n$ on S is sufficient to determine that solution. Kirchhoff's formula (2.1.10) is therefore strictly an alternative, *integral equation* transformation of the partial differential equation (2.1.9). When, for example, the normal velocity is known on S, Kirchhoff's formula determines the velocity potential within the fluid only when φ is also known on S, but φ cannot be prescribed arbitrarily on S. The difficulty is avoided if Green's function G in (2.1.10) is required to satisfy $\partial G/\partial y_n = 0$ on S.

2.2* Advanced potentials

Green's function

$$G(\mathbf{x}, \mathbf{y}, t - \tau) = \frac{1}{4\pi |\mathbf{x} - \mathbf{y}|} \delta \left(t - \tau - \frac{|\mathbf{x} - \mathbf{y}|}{c_o} \right), \qquad (2.2.1)$$

has been interpreted as the outgoing wave solution of the inhomogeneous wave equation (1.6.1) produced by an impulsive point source located at $\mathbf{y}$ at time τ. However, it is clear that $G(\mathbf{x}, \mathbf{y}, t - \tau)$ also satisfies the 'adjoint' wave problem

$$\left(\frac{1}{c_o^2} \frac{\partial^2}{\partial \tau^2} - \frac{\partial^2}{\partial y_j^2} \right) G = \delta(\mathbf{y} - \mathbf{x}) \delta(\tau - t), \quad G = 0 \text{ for } \tau > t, \qquad (2.2.2)$$

Downloaded from https://www.cambridge.org/core. Charité Universitätsmedizin Berlin, on 20 Dec 2021 at 10:08:47, subject to the Cambridge Core terms of use, available at https://www.cambridge.org/core/terms. https://doi.org/10.1017/CBO9781107360273.003

in which propagation occurs as a function of $\mathbf{y}$ and τ and the source-like singularity on the right hand side is at a fixed location $\mathbf{x}$ at time t. In this case, however, the spherical wave (2.2.1) sweeps through the whole of space as τ increases from $-\infty$ before ultimately *converging* on, and disappearing at the source point $\mathbf{x}$ at $\tau = t$. The retarded potential integral solution (1.6.5) then represents the pressure field at $(\mathbf{x}, t)$ in terms of the values of the source function $\mathcal{F}(\mathbf{y}, \tau)$ encountered by the collapsing spherical wave at the retarded times $t - |\mathbf{x} - \mathbf{y}|/c_o$ during its convergence to $\mathbf{x}$.

This interpretation of Green's function as an 'advanced potential' solution of the wave equation forms the basis of the following, more traditional derivation of Kirchhoff's formula.

2.2.1 Kirchhoff's formula

It is required to determine the solution of the general linear wave equation (2.1.1) at a given point $\mathbf{x}$ at time t in infinite space bounded internally by one or more fixed and closed surfaces S, typified by Figure 2.1.2. We use $(\mathbf{y}, \tau)$ to denote an arbitrary space-time point in the medium, in terms of which equation (2.1.1) becomes

$$\left(\frac{1}{c_o^2}\frac{\partial^2}{\partial\tau^2} - \frac{\partial^2}{\partial y_j^2}\right) p = \rho_o \frac{\partial q}{\partial \tau} - \frac{\partial F_j}{\partial y_j}, \tag{2.2.3}$$

where the suffix notation is used to emphasise implied dependence on the independent variables $(\mathbf{y}, \tau)$.

Let Green's function $G(\mathbf{x}, \mathbf{y}, t - \tau)$ be an advanced potential solution of equation (2.2.2). This might be the usual free space Green's function with 'incoming' wave behaviour, but it may also be modified to satisfy suitable conditions on S. Multiply equation (2.2.3) by $G(\mathbf{x}, \mathbf{y}, t - \tau)$; subtract the result from the product of $p(\mathbf{y}, \tau)$ and equation (2.2.2). After simplification we find

$$\frac{1}{c_o^2}\frac{\partial}{\partial\tau}\left(p\frac{\partial G}{\partial\tau} - G\frac{\partial p}{\partial\tau}\right) + \frac{\partial}{\partial y_j}\left(G\frac{\partial p}{\partial y_j} - p\frac{\partial G}{\partial y_j}\right) + \rho_o\frac{\partial q}{\partial\tau}G - \frac{\partial F_j}{\partial y_j}G$$
$$= p(\mathbf{y}, \tau)\,\delta(\mathbf{y} - \mathbf{x})\delta(\tau - t) \tag{2.2.4}$$

This equation is now integrated over $-\infty < \tau < \infty$ and over the whole of the spatial region V bounded by S and a distant closed control surface Σ containing all of the sources. For the first term on the left,

$$\int_{-\infty}^{\infty}\frac{\partial}{\partial\tau}\left(p\frac{\partial G}{\partial\tau} - G\frac{\partial p}{\partial\tau}\right)d\tau = \left[p\frac{\partial G}{\partial\tau} - G\frac{\partial p}{\partial\tau}\right]_{-\infty}^{\infty} \equiv 0,$$

Downloaded from https://www.cambridge.org/core. Charité Universitätsmedizin Berlin, on 20 Dec 2021 at 10:08:47, subject to the Cambridge Core terms of use, available at https://www.cambridge.org/core/terms. https://doi.org/10.1017/CBO9781107360273.003

because G, $\partial G/\partial\tau$ both vanish at $\tau = \infty$ and $p(\mathbf{y},\tau)$, $\partial p(\mathbf{y},\tau)/\partial\tau$ must vanish at $\tau = -\infty$ if the action of the acoustic sources begins at some finite time in the past.

Next, using the divergence theorem

$$\int_V \left(\frac{\partial}{\partial y_j}\left(G\frac{\partial p}{\partial y_j} - p\frac{\partial G}{\partial y_j}\right) - \frac{\partial F_j}{\partial y_j}G\right) d^3\mathbf{y}$$
$$= \oint_S \left(-G\left(\frac{\partial p}{\partial y_n} - F_n\right) + p\frac{\partial G}{\partial y_n}\right) dS(\mathbf{y}) + \int_V F_j\frac{\partial G}{\partial y_j} d^3\mathbf{y},$$

where the surface integral is over S with y_n measured in the normal direction from S into the fluid. There can be no contribution from Σ, because $p(\mathbf{y},\tau)$ and $\mathbf{F}$ may be assumed to vanish when Σ is infinitely distant, before the arrival of the sound, and therefore on any surface Σ that encloses S and all of the sources. Finally, the momentum equation can be used to replace $\partial p/\partial y_n - F_n$ by $-\rho_o \partial v_n/\partial\tau$.

Hence, when $\mathbf{x}$ lies in the fluid region V (and because $\partial G/\partial\tau = -\partial G/\partial t$) the integrated form of (2.2.4) becomes

$$p(\mathbf{x},t) = \iint_V \left(\frac{\partial G}{\partial t}\rho_o q + \frac{\partial G}{\partial \mathbf{y}}\cdot\mathbf{F}\right) d^3\mathbf{y}d\tau$$
$$+ \iint_S \left(\frac{\partial G}{\partial t}\rho_o v_n + \frac{\partial G}{\partial y_n}p\right) dS(\mathbf{y})d\tau, \qquad (2.2.5)$$

which is the generalised Kirchhoff formula (2.1.6). The terms on the right-hand side sum to zero when $\mathbf{x}$ lies within S provided G is the free space Green's function (2.2.1), when the δ-function singularity on the right of (2.2.2) is outside the region of integration V. But for a Green's function that satisfies a non–free field boundary condition on S, the δ-function in (2.2.2) is replaced by at least one new singularity as a function of $\mathbf{y}$ in V as $\mathbf{x}$ moves out of V, which leads generally to the prediction of a non-zero value for the right-hand side of (2.2.5) when $\mathbf{x}$ lies within S (see, for example, the plane boundary Green's functions (2.1.7), (2.1.8)).

2.3 The time-harmonic wave equation

A function $f(t)$ and its *Fourier transform* $\hat{f}(\omega)$ are related by

$$\hat{f}(\omega) = \frac{1}{2\pi}\int_{-\infty}^{\infty} f(t)\mathrm{e}^{i\omega t}dt, \quad f(t) = \int_{-\infty}^{\infty}\hat{f}(\omega)\mathrm{e}^{-i\omega t}d\omega. \qquad (2.3.1)$$

Let $\hat{\varphi} = \hat{\varphi}(\mathbf{x},\omega)$ and $\hat{q} = \hat{q}(\mathbf{x},\omega)$ be the respective Fourier transforms of the velocity potential and volume source in equation (2.1.9). By taking the Fourier

Downloaded from https://www.cambridge.org/core. Charité Universitätsmedizin Berlin, on 20 Dec 2021 at 10:08:47, subject to the Cambridge Core terms of use, available at https://www.cambridge.org/core/terms. https://doi.org/10.1017/CBO9781107360273.003

transform of (2.1.9), noting that $\partial^2\varphi/\partial t^2 = \int_{-\infty}^{\infty} -\omega^2\hat{\varphi}(\mathbf{x},\omega)\mathrm{e}^{-i\omega t}d\omega$, we are led to study the time-harmonic wave equations

$$(\nabla^2 + k_o^2)\hat{\varphi} = 0, \quad (\nabla^2 + k_o^2)\hat{\varphi} = \hat{q}(\mathbf{x},\omega), \quad k_o = \frac{\omega}{c_o}. \tag{2.3.2}$$

They are known respectively as the Helmholtz equation and the *inhomogeneous* Helmholtz equation.

2.3.1 Time-harmonic Green's function

Green's function $\hat{G}(\mathbf{x},\mathbf{y},\omega)$ for the Helmholtz equation is the particular solution for $\hat{q} = \delta(\mathbf{x}-\mathbf{y})$, i.e.

$$(\nabla^2 + k_o^2)\hat{G} = \delta(\mathbf{x}-\mathbf{y}). \tag{2.3.3}$$

If we take the Fourier transform of the corresponding equation

$$\left(\frac{1}{c_o^2}\frac{\partial^2}{\partial t^2} - \nabla^2\right) G = \delta(\mathbf{x}-\mathbf{y})\delta(t-\tau)$$

for the *time domain* Green's function $G(\mathbf{x},\mathbf{y},t-\tau)$, we find

$$(\nabla^2 + k_o^2)\left\{\int_{-\infty}^{\infty} G(\mathbf{x},\mathbf{y},t-\tau)\,\mathrm{e}^{i\omega t}\,dt\right\} = -\,\mathrm{e}^{i\omega\tau}\,\delta(\mathbf{x}-\mathbf{y}),$$

and, therefore, that $\hat{G}(\mathbf{x},\mathbf{y},\omega)$ and $G(\mathbf{x},\mathbf{y},t-\tau)$ satisfy the reciprocal relations

$$\hat{G}(\mathbf{x},\mathbf{y},\omega) = -\int_{-\infty}^{\infty} G(\mathbf{x},\mathbf{y},t-\tau)\mathrm{e}^{i\omega(t-\tau)}\,dt, \tag{2.3.4}$$

$$G(\mathbf{x},\mathbf{y},t-\tau) = -\frac{1}{2\pi}\int_{-\infty}^{\infty} \hat{G}(\mathbf{x},\mathbf{y},\omega)\mathrm{e}^{-i\omega(t-\tau)}\,d\omega. \tag{2.3.5}$$

The *free space* (time-harmonic) Green's function $\hat{G}(\mathbf{x},\mathbf{y},\omega)$, with outgoing wave behaviour, is obtained by substituting the corresponding free space time-domain Green's function (§1.6)

$$G(\mathbf{x},\mathbf{y},t-\tau) = \frac{1}{4\pi|\mathbf{x}-\mathbf{y}|}\delta\left(t-\tau-\frac{|\mathbf{x}-\mathbf{y}|}{c_o}\right)$$

into the integrand of (2.3.4), which yields

$$\hat{G}(\mathbf{x},\mathbf{y},\omega) = \frac{-\mathrm{e}^{ik_o|\mathbf{x}-\mathbf{y}|}}{4\pi|\mathbf{x}-\mathbf{y}|}. \tag{2.3.6}$$

Downloaded from https://www.cambridge.org/core. Charité Universitätsmedizin Berlin, on 20 Dec 2021 at 10:08:47, subject to the Cambridge Core terms of use, available at https://www.cambridge.org/core/terms. https://doi.org/10.1017/CBO9781107360273.003

The solution $\hat{\varphi}(\mathbf{x}, \omega)$ of the second of equations (2.3.2) in an unbounded medium is therefore

$$\hat{\varphi}(\mathbf{x}, \omega) = \int_{-\infty}^{\infty} \hat{G}(\mathbf{x}, \mathbf{y}, \omega)\hat{q}(\mathbf{y}, \omega)d^3\mathbf{y} \equiv \frac{-1}{4\pi}\int_{-\infty}^{\infty} \frac{\hat{q}(\mathbf{y}, \omega)\mathrm{e}^{ik_o|\mathbf{x}-\mathbf{y}|}}{|\mathbf{x}-\mathbf{y}|}d^3\mathbf{y}. \tag{2.3.7}$$

2.3.2 Dipole and quadrupole sources

The method of integration by parts described in §1.8 can be used to show that the corresponding solutions for the dipole and quadrupole sources

$$\hat{q}(\mathbf{x}, \omega) = \frac{\partial f_j}{\partial x_j}(\mathbf{x}, \omega) \quad \text{and} \quad \hat{q}(\mathbf{x}, \omega) = \frac{\partial^2 T_{ij}}{\partial x_i \partial x_j}(\mathbf{x}, \omega) \tag{2.3.8}$$

are, respectively,

$$\hat{\varphi}(\mathbf{x}, \omega) = \frac{-1}{4\pi}\frac{\partial}{\partial x_j}\int_{-\infty}^{\infty} \frac{f_j(\mathbf{y}, \omega)\mathrm{e}^{ik_o|\mathbf{x}-\mathbf{y}|}}{|\mathbf{x}-\mathbf{y}|}d^3\mathbf{y}, \tag{2.3.9}$$

and

$$\hat{\varphi}(\mathbf{x}, \omega) = \frac{-1}{4\pi}\frac{\partial^2}{\partial x_i \partial x_j}\int_{-\infty}^{\infty} \frac{T_{ij}(\mathbf{y}, \omega)\mathrm{e}^{ik_o|\mathbf{x}-\mathbf{y}|}}{|\mathbf{x}-\mathbf{y}|}d^3\mathbf{y}. \tag{2.3.10}$$

Example For a point dipole at the origin orientated in the x_1-direction

$$\hat{q}(\mathbf{x}, \omega) = \frac{\partial}{\partial x_1}\Big(f_1\delta(\mathbf{x})\Big),$$

$$\therefore \quad \hat{\varphi}(\mathbf{x}, \omega) = \frac{-1}{4\pi}\frac{\partial}{\partial x_1}\int_{-\infty}^{\infty} \frac{f_1\delta(\mathbf{y})\mathrm{e}^{ik_o|\mathbf{x}-\mathbf{y}|}}{|\mathbf{x}-\mathbf{y}|}d^3\mathbf{y} \approx \frac{-ik_o x_1 f_1 \mathrm{e}^{ik_o|\mathbf{x}|}}{4\pi|\mathbf{x}|^2}, \ |\mathbf{x}| \to \infty. \tag{2.3.11}$$

2.3.3 Kirchhoff's formula in the frequency domain

Take the Fourier transform of the equations in §2.1.6 to express the inhomogeneous Helmholtz equation (the second of equations (2.3.2)) in the form

$$(\nabla^2 + k_o^2)(\mathrm{H}\hat{\varphi}) = \mathrm{H}\hat{q} + \nabla\mathrm{H}\cdot\nabla\hat{\varphi} + \mathrm{div}\,(\hat{\varphi}\nabla\mathrm{H}),$$

together with the corresponding integral solution

$$\hat{\varphi}(\mathbf{x}, \omega) = \int_V \hat{G}\hat{q}\, d^3\mathbf{y} + \oint_S \left(\hat{G}\frac{\partial\hat{\varphi}}{\partial y_n} - \frac{\partial\hat{G}}{\partial y_n}\hat{\varphi}\right) dS(\mathbf{y}). \tag{2.3.12}$$

Downloaded from https://www.cambridge.org/core. Charité Universitätsmedizin Berlin, on 20 Dec 2021 at 10:08:47, subject to the Cambridge Core terms of use, available at https://www.cambridge.org/core/terms. https://doi.org/10.1017/CBO9781107360273.003

2.4 The reciprocal theorem

Point source solutions of the Helmholtz equation satisfy a *reciprocal theorem*, which is a special case of a very general theorem of mechanics first used with great effect in acoustics by Lord Rayleigh (1945).

Consider the two acoustic problems illustrated in Figure 2.4.1, in which sound of frequency ω is generated by two equal unit point sources at $\mathbf{x} = \mathbf{y}$ and $\mathbf{x} = \mathbf{y}'$ in the presence of a solid body S. Let the respective velocity potentials generated by these sources be $\hat{G}(\mathbf{x}, \mathbf{y}, \omega)$ and $\hat{G}(\mathbf{x}, \mathbf{y}', \omega)$, where

$$\left(\nabla^2 + k_o^2\right)\hat{G}(\mathbf{x}, \mathbf{y}, \omega) = \delta(\mathbf{x} - \mathbf{y}), \tag{2.4.1}$$

$$\left(\nabla^2 + k_o^2\right)\hat{G}(\mathbf{x}, \mathbf{y}', \omega) = \delta(\mathbf{x} - \mathbf{y}'). \tag{2.4.2}$$

Assume also that $\hat{G}(\mathbf{x}, \mathbf{y}, \omega)$ and $\hat{G}(\mathbf{x}, \mathbf{y}', \omega)$ satisfy the following general linear conditions on S

$$\frac{\partial \hat{G}}{\partial x_n}(\mathbf{x}, \mathbf{y}, \omega) = \frac{\hat{G}(\mathbf{x}, \mathbf{y}, \omega)}{\mathcal{Z}(\mathbf{x}, \omega)}, \quad \frac{\partial \hat{G}}{\partial x_n}(\mathbf{x}, \mathbf{y}', \omega) = \frac{\hat{G}(\mathbf{x}, \mathbf{y}', \omega)}{\mathcal{Z}(\mathbf{x}, \omega)}, \quad \text{for } \mathbf{x} \text{ on } S, \tag{2.4.3}$$

where x_n is measured in the normal direction from S *into the fluid* and $\mathcal{Z} \equiv \mathcal{Z}(\mathbf{x}, \omega)$ is the surface 'impedance'. For a *rigid* surface $\mathcal{Z} = \infty$.

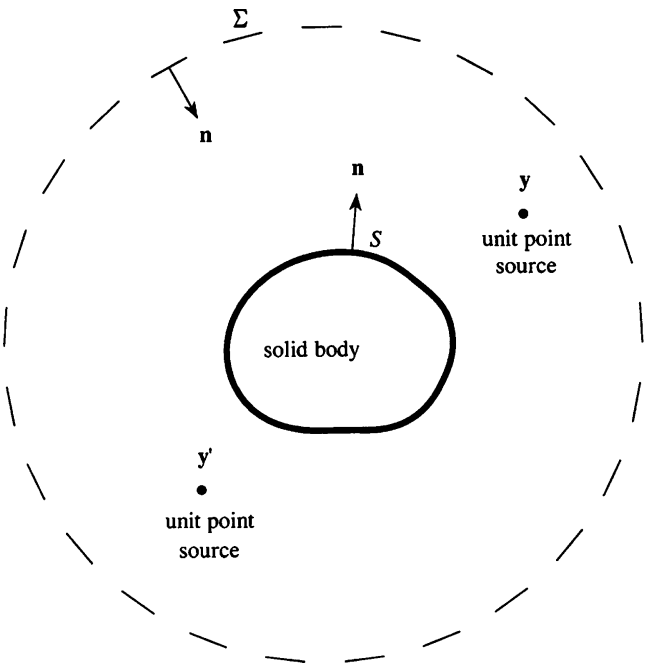

Figure 2.4.1

Downloaded from https://www.cambridge.org/core. Charité Universitätsmedizin Berlin, on 20 Dec 2021 at 10:08:47, subject to the Cambridge Core terms of use, available at https://www.cambridge.org/core/terms. https://doi.org/10.1017/CBO9781107360273.003

In the acoustic far field, at large distances from S, both solutions must exhibit the characteristics of outgoing sound waves, such that (with implied time dependence $\mathrm{e}^{-i\omega t}$)

$$\hat{G}(\mathbf{x},\mathbf{y},\omega) \sim \frac{f(\theta,\phi)\mathrm{e}^{ik_o r}}{r}, \quad \hat{G}(\mathbf{x},\mathbf{y}',\omega) \sim \frac{f'(\theta,\phi)\mathrm{e}^{ik_o r}}{r}, \quad r \equiv |\mathbf{x}| \to \infty, \tag{2.4.4}$$

where the coordinate origin is taken in the neighbourhood of S. The angular dependencies of the far field radiations are determined by the factors $f(\theta,\phi)$, $f'(\theta,\phi)$, that depend on the polar angles θ, ϕ defining the orientation of the far field point $\mathbf{x}$ and on the details of the interaction with S of the volume flow from each source.

The **reciprocal theorem** states that

$$\hat{G}(\mathbf{y},\mathbf{y}',\omega) = \hat{G}(\mathbf{y}',\mathbf{y},\omega), \tag{2.4.5}$$

that the potential at $\mathbf{y}$ produced by a point source at $\mathbf{y}'$ is the same as the potential at $\mathbf{y}'$ produced by an equal point source at $\mathbf{y}$.

Proof This uses the method of §2.2.1. Multiply equation (2.4.1) by $\hat{G}(\mathbf{x},\mathbf{y}',\omega)$ and equation (2.4.2) by $\hat{G}(\mathbf{x},\mathbf{y},\omega)$, subtract the resulting equations and integrate over the volume bounded by the surface S and by a large surface Σ in the acoustic far field. The identity

$$\begin{aligned}\hat{G}(\mathbf{x},\mathbf{y}',\omega)\nabla^2\hat{G}(\mathbf{x},\mathbf{y},\omega) - \hat{G}(\mathbf{x},\mathbf{y},\omega)\nabla^2\hat{G}(\mathbf{x},\mathbf{y}',\omega)\\ = \ \mathrm{div}\left(\hat{G}(\mathbf{x},\mathbf{y}',\omega)\nabla\hat{G}(\mathbf{x},\mathbf{y},\omega) - \hat{G}(\mathbf{x},\mathbf{y},\omega)\nabla\hat{G}(\mathbf{x},\mathbf{y}',\omega)\right)\end{aligned}$$

and the divergence theorem permit the volume integral of the term obtained from the left hand sides of (2.4.1) and (2.4.2) to be expressed as surface integrals over S and Σ, whereas the integrals involving the δ-functions can be evaluated explicitly. Hence,

$$\begin{aligned}\oint_{S+\Sigma}\left(\hat{G}(\mathbf{x},\mathbf{y},\omega)\frac{\partial\hat{G}}{\partial x_n}(\mathbf{x},\mathbf{y}',\omega) - \hat{G}(\mathbf{x},\mathbf{y}',\omega)\frac{\partial\hat{G}}{\partial x_n}(\mathbf{x},\mathbf{y},\omega)\right)dS\\ = \hat{G}(\mathbf{y},\mathbf{y}',\omega) - \hat{G}(\mathbf{y}',\mathbf{y},\omega).\end{aligned}$$

The surface integral over S vanishes because of the impedance conditions (2.4.3). The surface integral over Σ vanishes because of conditions (2.4.4) and because $\partial\theta/\partial x_n$ and $\partial\phi/\partial x_n$ are each of order $1/r$ as $r \to \infty$, and therefore

$$\begin{aligned}\frac{\partial\hat{G}}{\partial x_n}(\mathbf{x},\mathbf{y},\omega) &\sim f(\theta,\phi)\frac{ik_o\mathrm{e}^{ik_o r}}{r}\frac{\partial r}{\partial x_n},\\ \frac{\partial\hat{G}}{\partial x_n}(\mathbf{x},\mathbf{y}',\omega) &\sim f'(\theta,\phi)\frac{ik_o\mathrm{e}^{ik_o r}}{r}\frac{\partial r}{\partial x_n}, \quad \text{as } r \to \infty.\end{aligned}$$

This proves the theorem.

Downloaded from https://www.cambridge.org/core. Charité Universitätsmedizin Berlin, on 20 Dec 2021 at 10:08:47, subject to the Cambridge Core terms of use, available at https://www.cambridge.org/core/terms. https://doi.org/10.1017/CBO9781107360273.003

The result is usually expressed by the simple reciprocal property

$$\hat{G}(\mathbf{x}, \mathbf{y}, \omega) = \hat{G}(\mathbf{y}, \mathbf{x}, \omega). \tag{2.4.6}$$

2.5 The compact Green's function

The surface integrals in the generalised Kirchhoff formula (2.1.6) are absent when the surface S is rigid (so that $v_n = 0$) and when $\partial G/\partial y_n = 0$ on S. The solution of the sound generation problem can then be expressed in the elementary form

$$p(\mathbf{x}, t) = \int_{-\infty}^{\infty} \int_V \mathcal{F}(\mathbf{y}, \tau) G(\mathbf{x}, \mathbf{y}, t - \tau) d^3\mathbf{y} d\tau$$

without the need to consider explicit contributions from surface sources on S.

The main difficulty in using this formula is the calculation of a Green's function satisfying $\partial G/\partial y_n = 0$ for $\mathbf{y}$ on S, which, by reciprocity, implies also that $\partial G/\partial x_n = 0$ for $\mathbf{x}$ on S. Although it is always possible in principle, exact analytical representations are known only for solid bodies of very simple shapes (such as spheres, circular cylinders and half-planes). However, a relatively simple and general approximation for the modified Green's function is easily obtained for applications in which the typical wavelength of the sound produced by the sources $\mathcal{F}(\mathbf{x}, t)$ is *large compared to one or more principal dimensions* of the solid body S. This is called the *compact Green's function*. We have already seen that the influence of a solid body on the production of sound by neighbouring sources is equivalent to an additional distribution of monopole and dipole sources on S. For a rigid body, the compact Green's function determines a first approximation for these monopole and dipole distributions, and obviates the need to evaluate surface integrals.

2.5.1 Time-harmonic compact Green's function

For a typical frequency ω of the sound, the wavelength $\lambda \sim 2\pi/k_o$ is large compared to a characteristic dimension ℓ of the solid body provided $k_o\ell \ll 1$. To exploit this condition we consider first the compact approximation for the time-harmonic Green's function for the problem of Figure 2.5.1. We have to solve

$$\left(\nabla^2 + k_o^2\right)\hat{G}(\mathbf{x}, \mathbf{y}, \omega) = \delta(\mathbf{x} - \mathbf{y}), \quad \frac{\partial \hat{G}}{\partial x_n} = 0 \text{ on } S, \tag{2.5.1}$$

when the rigid body S is acoustically compact. The time-dependent Green's function $G(\mathbf{x}, \mathbf{y}, t - \tau)$ is obtained in terms of $\hat{G}(\mathbf{x}, \mathbf{y}, \omega)$ by formal application of equation (2.3.5).

Downloaded from https://www.cambridge.org/core. Charité Universitätsmedizin Berlin, on 20 Dec 2021 at 10:08:47, subject to the Cambridge Core terms of use, available at https://www.cambridge.org/core/terms. https://doi.org/10.1017/CBO9781107360273.003

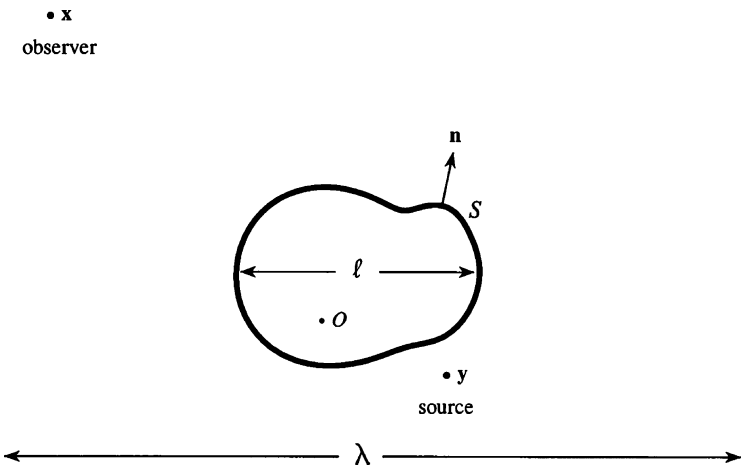

Figure 2.5.1

The objective in applications is usually the calculation of the sound radiated to large distances in terms of sources very close to the body. Let ℓ denote the characteristic diameter of the body, and take the coordinate origin at O within S. The source point $\mathbf{y}$ is assumed to be close to S (so that $|\mathbf{y}| \sim \ell$) and the observer at $\mathbf{x}$ is in the acoustic far field. The compactness condition therefore implies that

$$k_o \ell \ll 1 \quad \text{and} \quad k_o |\mathbf{y}| \ll 1.$$

In these circumstances, because $\hat{G}(\mathbf{y}, \mathbf{x}, \omega) = \hat{G}(\mathbf{x}, \mathbf{y}, \omega)$, the compact approximation for $\hat{G}(\mathbf{x}, \mathbf{y}, \omega)$ can be found very easily from the solution of the *reciprocal* problem:

$$\left(\frac{\partial^2}{\partial y_1^2} + \frac{\partial^2}{\partial y_2^2} + \frac{\partial^2}{\partial y_3^2} + k_o^2 \right) \hat{G}(\mathbf{x}, \mathbf{y}, \omega) = \delta(\mathbf{y} - \mathbf{x}), \tag{2.5.2}$$

where $\partial \hat{G} / \partial y_n = 0$ on S, and the δ-function singularity is at the fixed far field point $\mathbf{x}$. The solution is required only for $\mathbf{y}$ in the neighbourhood of S.

Put

$$\begin{aligned} \hat{G}(\mathbf{x}, \mathbf{y}, \omega) &= \hat{G}_o(\mathbf{x}, \mathbf{y}, \omega) + \hat{G}'(\mathbf{x}, \mathbf{y}, \omega) \\ &\equiv \frac{-\mathrm{e}^{ik_o|\mathbf{x}-\mathbf{y}|}}{4\pi |\mathbf{x} - \mathbf{y}|} + \hat{G}'(\mathbf{x}, \mathbf{y}, \omega) \end{aligned}$$

where $\hat{G}_o(\mathbf{x}, \mathbf{y}, \omega)$ denotes the spherical wave solution (2.3.6) when the presence of the solid is ignored. Then $\hat{G}'(\mathbf{x}, \mathbf{y}, \omega)$ is the velocity potential of the motion produced when this wave impinges on S.

Downloaded from https://www.cambridge.org/core. Charité Universitätsmedizin Berlin, on 20 Dec 2021 at 10:08:47, subject to the Cambridge Core terms of use, available at https://www.cambridge.org/core/terms. https://doi.org/10.1017/CBO9781107360273.003

When $|\mathbf{x}| \to \infty$, the approximations

$$|\mathbf{x}-\mathbf{y}| \approx |\mathbf{x}| - \frac{\mathbf{x}\cdot\mathbf{y}}{|\mathbf{x}|} \equiv |\mathbf{x}| - \frac{x_j y_j}{|\mathbf{x}|}, \quad \text{and} \quad \frac{1}{|\mathbf{x}-\mathbf{y}|} \approx \frac{1}{|\mathbf{x}|} + \frac{\mathbf{x}\cdot\mathbf{y}}{|\mathbf{x}|^3} \approx \frac{1}{|\mathbf{x}|}$$

and the condition $k_o y_j \sim k_o \ell \ll 1$ imply that

$$\hat{G}_o(\mathbf{x},\mathbf{y},\omega) \equiv \frac{-\mathrm{e}^{ik_o|\mathbf{x}-\mathbf{y}|}}{4\pi|\mathbf{x}-\mathbf{y}|} \approx \frac{-\mathrm{e}^{ik_o|\mathbf{x}|}}{4\pi|\mathbf{x}|} \times \mathrm{e}^{-\frac{ik_o x_j y_j}{|\mathbf{x}|}}$$

$$\approx \frac{-\mathrm{e}^{ik_o|\mathbf{x}|}}{4\pi|\mathbf{x}|}\left(1 - \frac{ik_o x_j y_j}{|\mathbf{x}|} + O(k_o\ell)^2\right) \tag{2.5.3}$$

The linear dependence on y_j in the second line of this formula represents the first approximation (of order $k_o\ell$) in a power series expansion of rapidly decreasing terms that describes the variation of $\hat{G}_o(\mathbf{x},\mathbf{y},\omega)$ close to the body. Thus, regarded as a function of $\mathbf{y}$,

$$\hat{G}_o(\mathbf{x},\mathbf{y},\omega) = \frac{-\mathrm{e}^{ik_o|\mathbf{x}|}}{4\pi|\mathbf{x}|} + \frac{\mathrm{e}^{ik_o|\mathbf{x}|}}{4\pi|\mathbf{x}|}\frac{ik_o x_j y_j}{|\mathbf{x}|} + \cdots$$
$$\equiv \text{constant} + U_j y_j + \cdots, \tag{2.5.4}$$
$$\text{where} \quad U_j = \frac{\mathrm{e}^{ik_o|\mathbf{x}|}}{4\pi|\mathbf{x}|}\frac{ik_o x_j}{|\mathbf{x}|},$$

can be regarded as the velocity potential of a *uniform flow* at velocity U_j impinging on the solid.

At distances $|\mathbf{y}| \gg \ell$ from S the distortion of this flow produced by the body must be small. Let it be represented by the velocity potential

$$\hat{G}'(\mathbf{x},\mathbf{y},\omega) = -U_j\varphi_j^*(\mathbf{y}) + O(k_o\ell)^2, \quad \text{where} \quad \varphi_j^*(\mathbf{y}) \to 0 \text{ when } |\mathbf{y}| \gg \ell.$$

The function φ_j^* has the dimensions of length and $\varphi_j^* \sim O(\ell)$ near S (Batchelor 1967). Therefore

$$\hat{G}(\mathbf{x},\mathbf{y},\omega) = \hat{G}_o(\mathbf{x},\mathbf{y},\omega) + \hat{G}'(\mathbf{x},\mathbf{y},\omega) = \frac{-\mathrm{e}^{ik_o|\mathbf{x}|}}{4\pi|\mathbf{x}|} + U_j\Big(y_j - \varphi_j^*(\mathbf{y})\Big) + \cdots, \tag{2.5.5}$$

where the terms shown explicitly represent a potential flow past the rigid surface S.

Near S equation (2.5.2) is satisfied separately by $\hat{G}_o(\mathbf{x},\mathbf{y},\omega)$ and $\hat{G}'(\mathbf{x},\mathbf{y},\omega)$ with the right hand side replaced by zero (because $\mathbf{x}$ is in the far field). Hence

$$U_j\nabla^2\varphi_j^*(\mathbf{y}) + O(k_o\ell)^2 = 0.$$

But $U_j\varphi_j^*(\mathbf{y}) = O(k_o\ell)$, and therefore, *correct to the neglect of small terms of order* $O(k_o\ell)^2$,

Downloaded from https://www.cambridge.org/core. Charité Universitätsmedizin Berlin, on 20 Dec 2021 at 10:08:47, subject to the Cambridge Core terms of use, available at https://www.cambridge.org/core/terms. https://doi.org/10.1017/CBO9781107360273.003

$$\nabla^2\varphi_j^*(\mathbf{y}) = 0, \quad \text{and therefore} \quad \nabla^2\Big(y_j - \varphi_j^*(\mathbf{y})\Big) = 0,$$

where the rigid surface condition requires

$$\frac{\partial}{\partial y_n}\Big(y_j - \varphi_j^*(\mathbf{y})\Big) = 0 \text{ on } S. \tag{2.5.6}$$

In summary: when $\mathbf{x}$ is in the acoustic far field and $\mathbf{y}$ is close to the body

$$\hat{G}(\mathbf{x},\mathbf{y},\omega) = \frac{-\mathrm{e}^{ik_o|\mathbf{x}|}}{4\pi|\mathbf{x}|}\left(1 - \frac{ik_o x_i}{|\mathbf{x}|}\Big(y_i - \varphi_i^*(\mathbf{y})\Big) + \ O(k_o\ell)^2\right), \quad \mathbf{y} \sim \mathrm{O}(\ell),\ |\mathbf{x}| \to \infty. \tag{2.5.7}$$

The first term in the large brackets is the contribution from the spherical wave $\hat{G}_o(\mathbf{x},\mathbf{y},\omega)$ evaluated at $\mathbf{y} = \mathbf{0}$. The next term is $\mathrm{O}(k_o\ell)$ and includes a component $-ik_o x_j y_j/|\mathbf{x}|$ from $\hat{G}_o(\mathbf{x},\mathbf{y},\omega)$ plus a correction $-ik_o x_j\varphi_j^*(\mathbf{y})/|\mathbf{x}|$ produced by S.

The vector field

$$\mathbf{Y}(\mathbf{y}) \equiv \mathbf{y} - \boldsymbol{\varphi}^*(\mathbf{y}) \tag{2.5.8}$$

is called the **Kirchhoff vector** for the rigid body S; the jth component

$$Y_j(\mathbf{y}) \equiv y_j - \varphi_j^*(\mathbf{y})$$

satisfies Laplace's equation $\nabla^2 Y_j = 0$ with $\partial Y_j/\partial y_n = 0$ on S, and can be interpreted as the velocity potential of incompressible flow past S that has unit speed in the j-direction at large distances from S. The function $\varphi_j^*(\mathbf{y})$ decays with distance from S, and satisfies

$$\frac{\partial\varphi_j^*}{\partial y_n}(\mathbf{y}) = n_j \ \text{ on } S, \tag{2.5.9}$$

because $\partial y_j/\partial y_n \equiv n_i\partial y_j/\partial y_i = n_i\delta_{ij} = n_j$. Hence $\varphi_j^*(\mathbf{y})$ is the instantaneous velocity potential of the motion that would be produced by translational motion of S as a *rigid body* at unit speed in the j-direction.

Definition

$$\hat{G}(\mathbf{x},\mathbf{y},\omega) = \frac{-\mathrm{e}^{ik_o|\mathbf{x}|}}{4\pi|\mathbf{x}|}\left(1 - \frac{ik_o x_j}{|\mathbf{x}|}\Big(y_j - \varphi_j^*(\mathbf{y})\Big)\right), \quad \mathbf{y} \sim \mathrm{O}(\ell),\ |\mathbf{x}| \to \infty, \tag{2.5.10}$$

is called the (time-harmonic) compact Green's function for source points $\mathbf{y}$ near the body and observer positions $\mathbf{x}$ in the acoustic far field.

In §2.7, we shall introduce a very much more elegant representation of the compact Green's function that greatly expands its utility.

Downloaded from https://www.cambridge.org/core. Charité Universitätsmedizin Berlin, on 20 Dec 2021 at 10:08:47, subject to the Cambridge Core terms of use, available at https://www.cambridge.org/core/terms. https://doi.org/10.1017/CBO9781107360273.003

2.6 The sphere and cylindrical bodies

2.6.1 Compact Green's function for a sphere

Let the sphere have radius a and take the coordinate origin O at its centre (Figure 2.6.1). The jth component of the Kirchhoff vector $Y_j(\mathbf{y}) = y_j - \varphi_j^*(\mathbf{y})$ is the velocity potential of incompressible flow past the sphere having unit speed in the j-direction at large distances from the sphere.

When $j = 1$ the flow is symmetric about the y_1-axis. Take spherical polar coordinates (r, ϑ, ϕ) with ϑ measured from the positive y_1-axis. Then $y_1 = r\cos\vartheta$, and condition (2.5.9) becomes

$$\frac{\partial \varphi_1^*}{\partial r} = \cos\vartheta \quad \text{at} \quad r = a. \tag{2.6.1}$$

The axisymmetric Laplace equation

$$\left(\frac{1}{r^2}\frac{\partial}{\partial r}\left(r^2\frac{\partial}{\partial r}\right) + \frac{1}{r^2\sin\vartheta}\frac{\partial}{\partial\vartheta}\left(\sin\vartheta\frac{\partial}{\partial\vartheta}\right)\right)\varphi_1^* = 0,$$

is satisfied by the trial solution $\varphi_1^* = \Psi(r)\cos\vartheta$ provided

$$r^2\frac{d^2\Psi}{dr^2} + 2r\frac{d\Psi}{dr} - 2\Psi = 0.$$

The solutions of this equation are proportional to r^n where n is a root of the quadratic equation

$$n^2 + n - 2 = 0, \quad \text{i.e. } n = -2,\ 1,$$

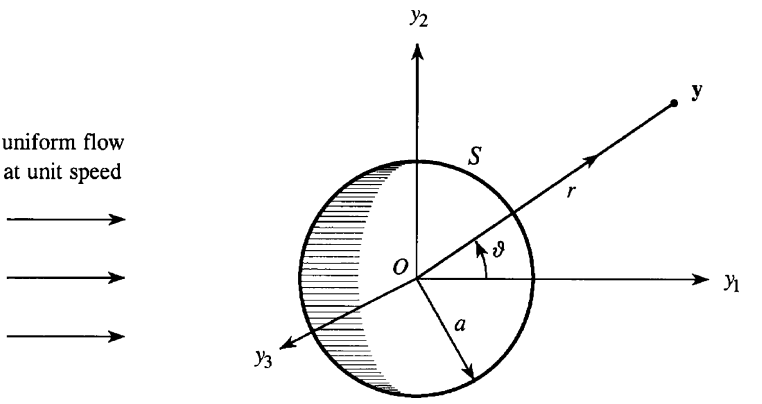

Figure 2.6.1

Downloaded from https://www.cambridge.org/core. Charité Universitätsmedizin Berlin, on 20 Dec 2021 at 10:08:47, subject to the Cambridge Core terms of use, available at https://www.cambridge.org/core/terms. https://doi.org/10.1017/CBO9781107360273.003

so that

$$Y_1 \equiv y_1 - \varphi_1^* = r\cos\vartheta - \left(Ar + \frac{B}{r^2}\right)\cos\vartheta, \quad \text{where } A \text{ and } B \text{ are constants.}$$

The condition that $\varphi_1^* \to 0$ as $r \to \infty$ implies that $A = 0$, and condition (2.6.1) supplies $B = -a^3/2$. Therefore,

$$Y_1 = r\cos\vartheta + \frac{a^3}{2r^2}\cos\vartheta \equiv y_1\left(1 + \frac{a^3}{2r^3}\right).$$

Because of the symmetry of the sphere it is also clear that

$$Y_2 = y_2\left(1 + \frac{a^3}{2r^3}\right), \quad Y_3 = y_3\left(1 + \frac{a^3}{2r^3}\right), \quad r = |\mathbf{y}|.$$

Thus, the compact Green's function (2.5.10) for the sphere is

$$\hat{G}(\mathbf{x}, \mathbf{y}, \omega) = \frac{-\mathrm{e}^{ik_o|\mathbf{x}|}}{4\pi|\mathbf{x}|}\left\{1 - \frac{ik_o x_j y_j}{|\mathbf{x}|}\left(1 + \frac{a^3}{2|\mathbf{y}|^3}\right)\right\}, \quad \mathbf{y} \sim \mathrm{O}(a), \ |\mathbf{x}| \to \infty. \tag{2.6.2}$$

This represents the far field acoustic potential produced by a point source at $\mathbf{y}$ close to the sphere. Because $k_o|\mathbf{y}|$ is small the second term in the brace brackets is always *small* compared to 1. This appears to suggest that, after all, the sphere has a relatively small influence on the production of sound! This is certainly true for monopole sources, but most sources of interest in applications are dipoles or quadrupoles, and in these circumstances we shall see that it is the small, second term that determines the leading order contribution to the far field sound.

Example 1 Determine the far field sound generated by a dipole source close to a stationary, rigid sphere of radius $a \ll \lambda =$ acoustic wavelength. With the origin at the centre of the sphere, we consider the outgoing wave solution of

$$\left(\nabla^2 + k_o^2\right)\hat{\varphi} = f_1\frac{\partial}{\partial x_1}\{\delta(x_1 - L)\delta(x_2)\delta(x_3)\}, \quad \text{where } \frac{\partial\hat{\varphi}}{\partial x_n} = 0 \text{ on } |\mathbf{x}| = a.$$

The dipole is orientated in the x_1-direction (Figure 2.6.2) and lies on the x_1-axis at $(L, 0, 0)$. The solution is given by (2.3.12) with $\partial\hat{\varphi}/\partial y_n = 0$, $\partial\hat{G}/\partial y_n = 0$ on the sphere:

$$\hat{\varphi}(\mathbf{x}, \omega) = \int f_1\frac{\partial}{\partial y_1}\{\delta(y_1 - L)\delta(y_2)\delta(y_3)\}\,\hat{G}(\mathbf{x}, \mathbf{y}, \omega)d^3\mathbf{y},$$

where the integration is over the fluid. The source term is zero everywhere except at $(L, 0, 0)$. To evaluate the integral we write

Downloaded from https://www.cambridge.org/core. Charité Universitätsmedizin Berlin, on 20 Dec 2021 at 10:08:47, subject to the Cambridge Core terms of use, available at https://www.cambridge.org/core/terms. https://doi.org/10.1017/CBO9781107360273.003

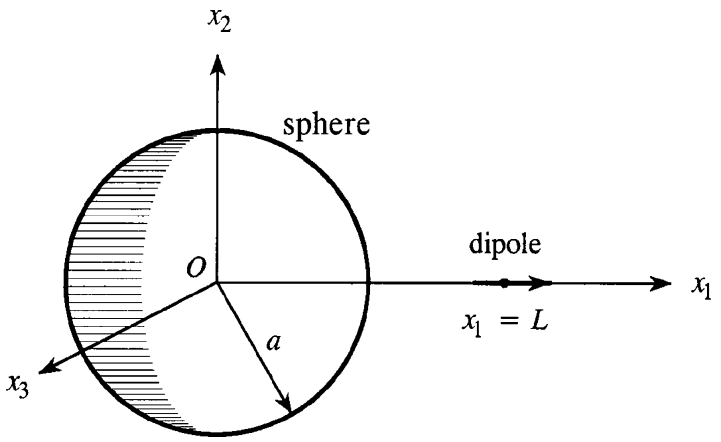

Figure 2.6.2

$$\hat{\varphi}(\mathbf{x},\omega) = f_1 \int \frac{\partial}{\partial y_1}\left\{\hat{G}(\mathbf{x},\mathbf{y},\omega)\delta(y_1 - L)\delta(y_2)\delta(y_3)\right\} d^3\mathbf{y}$$
$$- f_1 \int \delta(y_1 - L)\delta(y_2)\delta(y_3)\frac{\partial \hat{G}}{\partial y_1}(\mathbf{x},\mathbf{y},\omega) d^3\mathbf{y}.$$

The first integral is zero because $\delta(y_1 - L) = 0$ on the boundaries of the region of integration,

$$\therefore \quad \hat{\varphi}(\mathbf{x},\omega) = -f_1 \left(\frac{\partial \hat{G}}{\partial y_1}(\mathbf{x},\mathbf{y},\omega)\right)_{\mathbf{y}=(L,0,0)}. \tag{2.6.3}$$

Thus far the calculation is exact. To determine the solution in the far field given that the sphere is acoustically compact we use the compact approximation (2.6.2) for $\hat{G}(\mathbf{x},\mathbf{y},\omega)$. We see immediately that the differentiation with respect to y_1 will be applied only to the 'small' second term in the brace brackets of (2.6.2), giving

$$\hat{\varphi}(\mathbf{x},\omega) = \frac{-ik_o f_1 x_j e^{ik_o|\mathbf{x}|}}{4\pi|\mathbf{x}|^2}\left\{\frac{\partial}{\partial y_1}\left[y_j\left(1 + \frac{a^3}{2|\mathbf{y}|^3}\right)\right]\right\}_{\mathbf{y}=(L,0,0)}$$

$$= \frac{-ik_o f_1 x_1 e^{ik_o|\mathbf{x}|}}{4\pi|\mathbf{x}|^2}\left(1 - \frac{a^3}{L^3}\right)$$

$$= \frac{-ik_o f_1 \cos\theta e^{ik_o|\mathbf{x}|}}{4\pi|\mathbf{x}|}\left(1 - \frac{a^3}{L^3}\right), \quad |\mathbf{x}| \to \infty, \quad k_o a \ll 1,$$

Downloaded from https://www.cambridge.org/core. Charité Universitätsmedizin Berlin, on 20 Dec 2021 at 10:08:47, subject to the Cambridge Core terms of use, available at https://www.cambridge.org/core/terms. https://doi.org/10.1017/CBO9781107360273.003

where θ is the angle between the x_1-axis and the $\mathbf{x}$ direction (so that $x_1 = |\mathbf{x}| \cos\theta$).

By setting $a = 0$ in this formula we recover the far field (2.3.11) of a dipole source in the absence of the sphere. The presence of the sphere accordingly *reduces* the amplitude of the sound relative to that produced by a free field dipole. The amplitude is zero when $L \to a$. In this limit the surface of the sphere is effectively plane in the vicinity of the dipole and an equal and opposite 'image dipole' is formed in the sphere. The net radiation is therefore equivalent to that produced by a *quadrupole source*, and to calculate the sound in this case it would be necessary to use a more accurate approximation to $\hat{G}(\mathbf{x}, \mathbf{y}, \omega)$. This conclusion applies only to dipoles orientated *radially* with respect to the sphere (see Question 2.1 of **Problems 2**), but it is true for *any* compact rigid surface when a dipole orientated in the direction of the local surface normal approaches the surface.

2.6.2 Cylindrical bodies: The circular cylinder

The expansion procedure of §2.5 for the compact body of Figure 2.5.1 can be extended to a cylindrical body of *compact cross-section*. Figure 2.6.3 illustrates the case of an infinite circular cylinder of radius a whose axis lies along the y_3-axis, and whose diameter $2a \sim \ell$ is acoustically compact. The source point $\mathbf{y}$ is adjacent to the cylinder and for the moment (see §2.7) is assumed to be

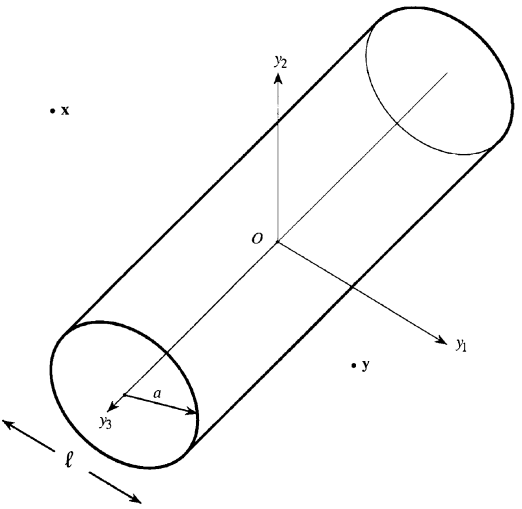

Figure 2.6.3

Downloaded from https://www.cambridge.org/core. Charité Universitätsmedizin Berlin, on 20 Dec 2021 at 10:08:47, subject to the Cambridge Core terms of use, available at https://www.cambridge.org/core/terms. https://doi.org/10.1017/CBO9781107360273.003

within an axial distance $|y_3| \ll \lambda$ from the coordinate origin O. In this region the expansion (2.5.7) remains valid with $\varphi_3^*(\mathbf{y}) \equiv 0$, because the impinging flow described by the velocity potential (2.5.4) for $j = 3$ is unaffected by the cylinder.

Hence, we can take

$$\hat{G}(\mathbf{x}, \mathbf{y}, \omega) = \frac{-e^{ik_o|\mathbf{x}|}}{4\pi|\mathbf{x}|}\left(1 - \frac{ik_o x_j Y_j}{|\mathbf{x}|}\right), \quad \mathbf{y} \sim O(\ell), \ |\mathbf{x}| \to \infty, \tag{2.6.4}$$

where the Kirchhoff vector $\mathbf{Y}$ has the components

$$Y_1 = y_1 - \varphi_1^*(\mathbf{y}), \quad Y_2 = y_2 - \varphi_2^*(\mathbf{y}), \quad Y_3 = y_3. \tag{2.6.5}$$

The potentials $\varphi_j^*(\mathbf{y})$ $(j = 1, 2)$ for a circular cylinder of radius a can be found by the method of §2.6.1. For $j = 1$ the flow is symmetric about the y_1-axis and is independent of the spanwise coordinate y_3 (Figure 2.6.4). Using polar coordinates $(y_1, y_2) = r(\cos\vartheta, \sin\vartheta)$, the condition (2.5.9) becomes $\partial\varphi_1^*/\partial r = \cos\vartheta$ for $r = a$, which suggests the trial solution $\varphi_1^* = \Psi(r)\cos\vartheta$ of the polar form of Laplace's equation

$$\left(\frac{1}{r}\frac{\partial}{\partial r}\left(r\frac{\partial}{\partial r}\right) + \frac{1}{r^2}\frac{\partial^2}{\partial\vartheta^2}\right)\varphi_1^* = 0.$$

Proceeding as in §2.6.1 for the sphere, we find $\Psi = -a^2/r$ and

$$\varphi_1^* = -\frac{a^2\cos\vartheta}{r} = -\frac{a^2 y_1}{r^2},$$

and similarly $\varphi_2^* = -a^2 y_2/r^2$.

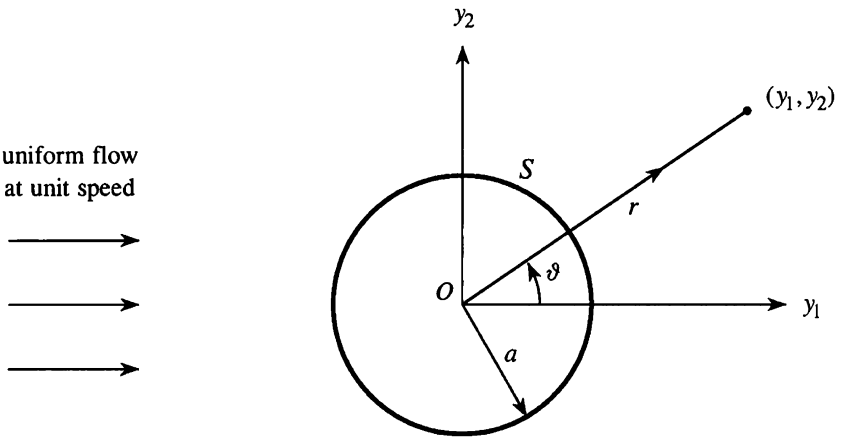

Figure 2.6.4

Downloaded from https://www.cambridge.org/core. Charité Universitätsmedizin Berlin, on 20 Dec 2021 at 10:08:47, subject to the Cambridge Core terms of use, available at https://www.cambridge.org/core/terms. https://doi.org/10.1017/CBO9781107360273.003

The compact Green's function for the circular cylinder is therefore

$$\hat{G}(\mathbf{x}, \mathbf{y}, \omega) = \frac{-\mathrm{e}^{ik_o|\mathbf{x}|}}{4\pi|\mathbf{x}|}\left(1 - \frac{ik_o x_j Y_j}{|\mathbf{x}|}\right), \quad \mathbf{y} \sim \mathrm{O}(\ell), \ |\mathbf{x}| \to \infty, \tag{2.6.6}$$

where

$$Y_j = y_j\left(1 + \frac{a^2}{y_1^2 + y_2^2}\right), \quad j = 1, 2; \quad Y_3 = y_3. \tag{2.6.7}$$

2.6.3 The rigid strip

The rigid strip of 'chord' $2a$ and infinite span provides a simple model of a sharp-edged airfoil. In Figure 2.6.5 the airfoil occupies $-a < y_1 < a$, $y_2 = 0$, $-\infty < y_3 < \infty$. The airfoil has no influence on uniform ideal flow in the y_1-direction, nor on one in the y_3-direction, so that $\varphi_1^*(\mathbf{y}) \equiv 0$ and $\varphi_3^*(\mathbf{y}) \equiv 0$.

The potential $\varphi_2^*(\mathbf{y}) \equiv \varphi_2^*(y_1, y_2)$ can be determined by the method of conformal transformation (see Appendix 2.A). If $z = y_1 + iy_2$, the upper and lower surfaces of the strip occupied by the airfoil in the z-plane are mapped onto the circular cylinder $|\zeta| = a$ in the ζ-plane by the transformation

$$\zeta = z + \sqrt{z^2 - a^2}.$$

Because $\zeta \sim 2z$ as $|z| \to \infty$ a uniform flow at unit speed in the y_2-direction in the z-plane at large distances from the airfoil corresponds to a uniform flow

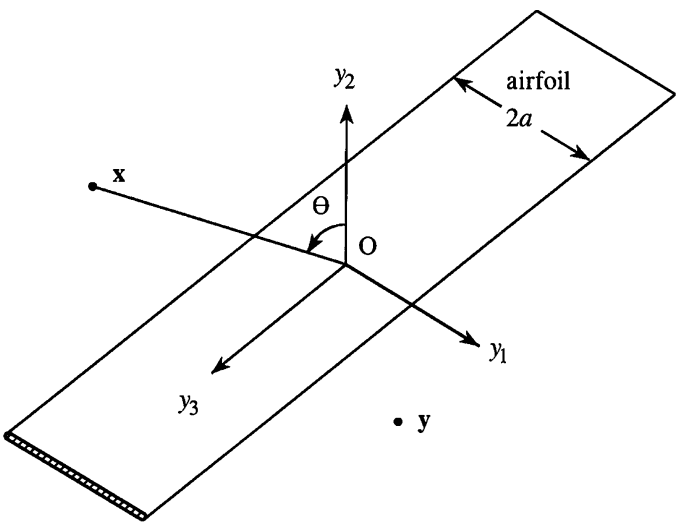

Figure 2.6.5

Downloaded from https://www.cambridge.org/core. Charité Universitätsmedizin Berlin, on 20 Dec 2021 at 10:08:47, subject to the Cambridge Core terms of use, available at https://www.cambridge.org/core/terms. https://doi.org/10.1017/CBO9781107360273.003

at speed $\frac{1}{2}$ in the direction of the imaginary ζ-axis at large distances from the cylinder. From Example 3 of §2.A (with $U = \frac{1}{2}$) the potential $Y_2 = y_2 - \varphi_2^*(y_1, y_2) = \operatorname{Re} w(z)$, where w is the complex potential

$$w(z) = -\frac{i}{2}\left(\zeta - \frac{a^2}{\zeta}\right) = -\frac{i}{2}\left(z + \sqrt{z^2 - a^2} - \frac{a^2}{z + \sqrt{z^2 - a^2}}\right)$$
$$= -i\sqrt{z^2 - a^2}.$$

Thus, the compact Green's function for a strip, with source near the origin, is

$$\hat{G}(\mathbf{x}, \mathbf{y}, \omega) = \frac{-e^{ik_o|\mathbf{x}|}}{4\pi|\mathbf{x}|}\left(1 - \frac{ik_o x_j Y_j}{|\mathbf{x}|}\right), \quad \mathbf{y} \sim O(a), \ |\mathbf{x}| \to \infty, \tag{2.6.8}$$

where

$$Y_1 = y_1, \quad Y_2 = \operatorname{Re}\left(-i\sqrt{z^2 - a^2}\right), \quad Y_3 = y_3, \quad z = y_1 + iy_2. \tag{2.6.9}$$

The streamlines of flow past the strip defined by the velocity potential $Y_2(\mathbf{y})$ crowd together and change very rapidly near the sharp edges (Figure 2.6.6). This is an indication that a dipole or quadrupole source (or any higher order multipole) near an edge can be an important source of sound, because ∇Y_2 becomes very large at the edge.

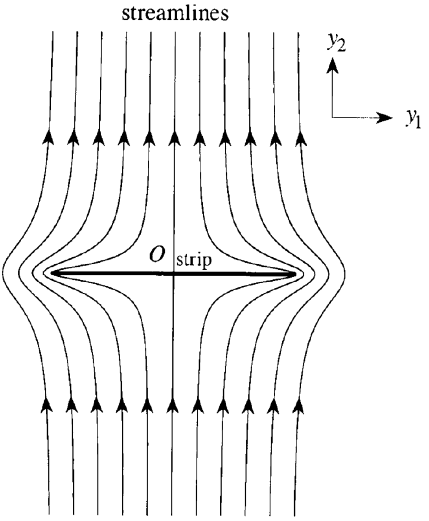

Figure 2.6.6

Downloaded from https://www.cambridge.org/core. Charité Universitätsmedizin Berlin, on 20 Dec 2021 at 10:08:47, subject to the Cambridge Core terms of use, available at https://www.cambridge.org/core/terms. https://doi.org/10.1017/CBO9781107360273.003

Example 2 Calculate the far field velocity potential when

$$\left(\nabla^2 + k_o^2\right)\hat{\varphi} = f_2 \frac{\partial}{\partial x_2}\left[\delta(x_1 - L)\delta(x_2)\delta(x_3)\right], \quad L > a, \quad k_o L \ll 1,$$

$$\text{where} \quad \frac{\partial \varphi}{\partial x_2} = 0 \ \text{ on the airfoil } \ -a < x_1 < a, \ x_2 = 0, \ -\infty < x_3 < \infty.$$

The dipole source is orientated in the x_2-direction and is positioned just to the right of the edge at $y_1 = a$ in Figure 2.6.5. The solution is given by the following form of equation (2.6.3)

$$\hat{\varphi}(\mathbf{x}, \omega) = -f_2 \left(\frac{\partial \hat{G}}{\partial y_2}(\mathbf{x}, \mathbf{y}, \omega)\right)_{\mathbf{y}=(L,0,0)} \approx -\frac{i f_2 k_o x_2 \mathrm{e}^{ik_o|\mathbf{x}|}}{4\pi |\mathbf{x}|^2}\left(\frac{\partial Y_2}{\partial y_2}\right)_{\mathbf{y}=(L,0,0)}$$

where, from (2.6.9),

$$\begin{aligned}\frac{\partial Y_2}{\partial y_2} &= \mathrm{Re}\left(-i\frac{\partial}{\partial y_2}\sqrt{z^2 - a^2}\right), \quad z = y_1 + iy_2 \\ &= \mathrm{Re}\left(\frac{z}{\sqrt{z^2 - a^2}}\right),\end{aligned}$$

$$\begin{aligned}\therefore \quad \hat{\varphi}(\mathbf{x}, \omega) &\approx -\frac{i f_2 k_o x_2 \mathrm{e}^{ik_o|\mathbf{x}|}}{4\pi |\mathbf{x}|^2}\frac{L}{\sqrt{L^2 - a^2}} \\ &= -\frac{i f_2 k_o L \cos\Theta \mathrm{e}^{ik_o|\mathbf{x}|}}{4\pi |\mathbf{x}|\sqrt{L^2 - a^2}}, \quad |\mathbf{x}| \to \infty,\end{aligned}$$

where $\Theta = \cos^{-1}(x_2/|\mathbf{x}|)$ is the angle between the normal to the strip and the radiation direction $(\mathbf{x}/|\mathbf{x}|)$ indicated in Figure 2.6.5.

The amplitude of the sound is increased by a factor $L/\sqrt{L^2 - a^2}$ relative to that produced by the same dipole in free space, and is unbounded as $L \to a$, when the dipole approaches the edge.

2.7 Symmetric compact Green's function

The definition (2.5.10) of the compact Green's function can be recast to exhibit the reciprocal nature of the source and observer positions $\mathbf{y}$ and $\mathbf{x}$. To do this we first observe that, for a body of characteristic diameter ℓ, when $\mathbf{y} \sim O(\ell)$,

$$Y_j(\mathbf{y}) = y_j - \varphi_j^*(\mathbf{y}) \sim O(\ell),$$

and therefore that $k_o Y_j \ll 1$. Hence

$$\hat{G}(\mathbf{x}, \mathbf{y}, \omega) \approx \frac{-\mathrm{e}^{ik_o|\mathbf{x}|}}{4\pi |\mathbf{x}|}\left(1 - \frac{ik_o x_j Y_j}{|\mathbf{x}|}\right) \equiv \frac{-\mathrm{e}^{ik_o|\mathbf{x}|}}{4\pi |\mathbf{x}|}\left(1 - \frac{ik_o \mathbf{x}\cdot\mathbf{Y}}{|\mathbf{x}|}\right)$$

Downloaded from https://www.cambridge.org/core. Charité Universitätsmedizin Berlin, on 20 Dec 2021 at 10:08:47, subject to the Cambridge Core terms of use, available at https://www.cambridge.org/core/terms. https://doi.org/10.1017/CBO9781107360273.003

$$\approx \frac{-1}{4\pi|\mathbf{x}|} e^{ik_o|\mathbf{x}| - \frac{ik_o \mathbf{x}\cdot\mathbf{Y}}{|\mathbf{x}|}},$$

$$\approx \frac{-e^{ik_o|\mathbf{x}-\mathbf{Y}|}}{4\pi|\mathbf{x}|}, \quad \mathbf{Y} \sim O(\ell), \quad |\mathbf{x}| \to \infty, \tag{2.7.1}$$

where on the last line we have used the usual far field approximation (1.10.3)

$$|\mathbf{x} - \mathbf{Y}| \approx |\mathbf{x}| - \frac{\mathbf{x}\cdot\mathbf{Y}}{|\mathbf{x}|}, \quad |\mathbf{x}| \to \infty.$$

Now let $\mathbf{X}(\mathbf{x})$ denote the Kirchhoff vector for the body expressed in terms of $\mathbf{x}$, i.e.

$$X_j(\mathbf{x}) = x_j - \varphi_j^*(\mathbf{x}). \tag{2.7.2}$$

Then, because $\varphi_j^*(\mathbf{x}) \to 0$ as $|\mathbf{x}| \to \infty$, we also have $|\mathbf{X}| \sim |\mathbf{x}|$ as $|\mathbf{x}| \to \infty$, and therefore from (1.10.3) and (1.10.4)

$$\left.\begin{array}{rcl} |\mathbf{X}-\mathbf{Y}| & \approx & |\mathbf{x}| - \frac{\mathbf{x}\cdot\mathbf{Y}}{|\mathbf{x}|} \\ \frac{1}{|\mathbf{X}-\mathbf{Y}|} & \approx & \frac{1}{|\mathbf{x}|} + \frac{\mathbf{x}\cdot\mathbf{Y}}{|\mathbf{x}|^3} \approx \frac{1}{|\mathbf{x}|} \end{array}\right\} \quad \text{when } |\mathbf{x}| \to \infty. \tag{2.7.3}$$

Thus, to the same approximation, (2.7.1) can be written

$$\hat{G}(\mathbf{x}, \mathbf{y}, \omega) \approx \frac{-e^{ik_o|\mathbf{X}-\mathbf{Y}|}}{4\pi|\mathbf{X}-\mathbf{Y}|}, \quad \mathbf{Y} \sim O(\ell), \quad |\mathbf{x}| \to \infty.$$

This result is the basis of our revised definition of the

Time-harmonic compact Green's function

$$\hat{G}(\mathbf{x}, \mathbf{y}, \omega) = \frac{-e^{ik_o|\mathbf{X}-\mathbf{Y}|}}{4\pi|\mathbf{X}-\mathbf{Y}|}, \tag{2.7.4}$$

where $\mathbf{X} = \mathbf{x} - \boldsymbol{\varphi}^*(\mathbf{x})$, $\mathbf{Y} = \mathbf{y} - \boldsymbol{\varphi}^*(\mathbf{y})$ are the Kirchhoff vectors for the body expressed respectively in terms of $\mathbf{x}$ and $\mathbf{y}$. The components X_j and Y_j are the velocity potential of incompressible flow past the body having unit speed in the j-direction at large distances from the body; φ_j^* is the velocity potential of the incompressible flow that would be produced by rigid body motion of S at unit speed in the j-direction.

Our generalised definition clearly satisfies the reciprocal theorem. Also, because of the symmetrical way in which $\mathbf{x}$ and $\mathbf{y}$ enter this formula we

Downloaded from https://www.cambridge.org/core. Charité Universitätsmedizin Berlin, on 20 Dec 2021 at 10:08:47, subject to the Cambridge Core terms of use, available at https://www.cambridge.org/core/terms. https://doi.org/10.1017/CBO9781107360273.003

may now remove any restriction on the position of the coordinate origin. The approximation is valid for arbitrary source and observer locations provided that *at least one of them* lies in the far field of the body. When *both* $\mathbf{x}$ and $\mathbf{y}$ are in the far field (so that $\mathbf{X} \sim \mathbf{x}$ and $\mathbf{Y} \sim \mathbf{y}$) predictions made with the compact Green's function will be the same as when the body is *absent*. This is because, for distant sources the amplitude of the sound scattered by a compact rigid object is $\mathrm{O}((k_o\ell)^2)$ smaller than the incident sound, that is, it is of *quadrupole* intensity (§2.8.3). When $\mathbf{x}$ is close to the body the source must be in the far field; $\hat{G}(\mathbf{x}, \mathbf{y}, \omega)$ then determines the modification by the body of low frequency sound received by an observer near the body.

The definition (2.7.4) is easily recalled because it is an obvious generalisation of the free space Green's function (2.3.6). In applications, it is necessary to remember also that it is valid only for determining the leading order approximation to the surface monopole and dipole sources induced on the body by neighbouring sources in the fluid. In practice, this means that when used in calculations $\hat{G}(\mathbf{x}, \mathbf{y}, \omega)$ will normally be expanded to **first order only** in the Kirchhoff source vector $\mathbf{Y}(\mathbf{y})$.

We can go further and use the formula (2.3.5) relating Green's functions for the wave equation and the Helmholtz equation to derive the compact approximation for the wave equation Green's function:

$$\begin{aligned} G(\mathbf{x}, \mathbf{y}, t-\tau) &= -\frac{1}{2\pi}\int_{-\infty}^{\infty} \hat{G}(\mathbf{x}, \mathbf{y}, \omega)\mathrm{e}^{-i\omega(t-\tau)}d\omega \\ &\approx \frac{1}{8\pi^2|\mathbf{X}-\mathbf{Y}|}\int_{-\infty}^{\infty} \mathrm{e}^{-i\omega\left(t-\tau-\frac{|\mathbf{X}-\mathbf{Y}|}{c_o}\right)}d\omega \\ &= \frac{1}{4\pi|\mathbf{X}-\mathbf{Y}|}\delta\left(t-\tau-\frac{|\mathbf{X}-\mathbf{Y}|}{c_o}\right). \end{aligned}$$

This remarkable result is formally identical with the classical free space Green's function (1.6.2) with $\mathbf{X}$, $\mathbf{Y}$ substituted for $\mathbf{x}$, $\mathbf{y}$. However, its use is subject to the same restrictions as (2.7.4), and it will be valid only when applied to time-dependent source terms producing sound whose wavelength is large compared to the characteristic body dimension ℓ. With this understanding we can define the

Compact Green's function for the wave equation

$$G(\mathbf{x}, \mathbf{y}, t-\tau) = \frac{1}{4\pi|\mathbf{X}-\mathbf{Y}|}\delta\left(t-\tau-\frac{|\mathbf{X}-\mathbf{Y}|}{c_o}\right), \tag{2.7.5}$$

where $\mathbf{X} = \mathbf{x} - \boldsymbol{\varphi}^*(\mathbf{x})$, $\mathbf{Y} = \mathbf{y} - \boldsymbol{\varphi}^*(\mathbf{y})$ are Kirchhoff vectors for the body. The components X_j and Y_j are the velocity potential of incompressible flow past the body having unit speed in the j-direction at large distances from the body;

Downloaded from https://www.cambridge.org/core. Charité Universitätsmedizin Berlin, on 20 Dec 2021 at 10:08:47, subject to the Cambridge Core terms of use, available at https://www.cambridge.org/core/terms. https://doi.org/10.1017/CBO9781107360273.003

φ_j^* is the velocity potential of the incompressible flow that would be produced by rigid body motion of S at unit speed in the j-direction.

2.8 Radiation and scattering by a compact body

2.8.1 Low-frequency radiation

Consider again the sound produced by a vibrating compact body discussed in §2.1.3, where the acoustic far field pressure (2.1.5) involves the unsteady force $F_i(t)$ exerted on the fluid by the body, but with no explicit representation for $\mathbf{F}$. The compact Green's function (2.7.5) for the wave equation will now be used to give a complete theory of the low frequency sound produced by a vibrating body. The maximum frequency of the vibrations must be small enough to ensure that the body (or its cross-section, in the case of vibrating a cylinder) is acoustically compact.

Let the surface S (Figure 2.8.1) vibrate with normal velocity $\partial\varphi/\partial x_n = v_n(\mathbf{x}, t)$. In the absence of sources and body forces and when G is chosen such that $\partial G/\partial y_n = 0$ on S, the generalised Kirchhoff formula (2.1.10) for the velocity potential supplies:

$$\varphi(\mathbf{x}, t) = -\iint_S G(\mathbf{x}, \mathbf{y}, t-\tau) v_n(\mathbf{y}, \tau)\, dS(\mathbf{y}) d\tau.$$

At low frequencies the first approximation to the far field sound is obtained by replacing $G(\mathbf{x}, \mathbf{y}, t-\tau)$ by its compact approximation (2.7.5). The details are given here; they illustrate the general procedure that should be adopted when using the compact Green's function (in particular, the technique of expanding to first order in $\mathbf{Y}$):

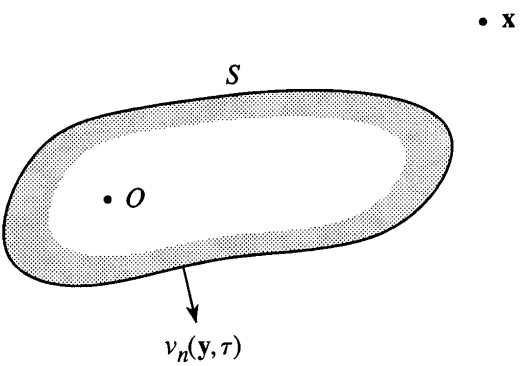

Figure 2.8.1

Downloaded from https://www.cambridge.org/core. Charité Universitätsmedizin Berlin, on 20 Dec 2021 at 10:08:47, subject to the Cambridge Core terms of use, available at https://www.cambridge.org/core/terms. https://doi.org/10.1017/CBO9781107360273.003

$$\begin{aligned}\varphi(\mathbf{x},t) &\approx -\int_{-\infty}^{\infty}\oint_S \frac{v_n(\mathbf{y},\tau)}{4\pi|\mathbf{X}-\mathbf{Y}|}\delta\left(t-\tau-\frac{|\mathbf{X}-\mathbf{Y}|}{c_o}\right)dS(\mathbf{y})d\tau,\\ &= -\frac{1}{4\pi|\mathbf{x}|}\int_{-\infty}^{\infty}\oint_S v_n(\mathbf{y},\tau)\delta\left(t-\tau-\frac{|\mathbf{x}|}{c_o}+\frac{\mathbf{x}\cdot\mathbf{Y}}{c_o|\mathbf{x}|}\right)dS(\mathbf{y})d\tau\\ &\qquad \left(\mathbf{X}\sim\mathbf{x}\text{ as }|\mathbf{x}|\to\infty\right)\\ &\approx -\frac{1}{4\pi|\mathbf{x}|}\int_{-\infty}^{\infty}\oint_S v_n(\mathbf{y},\tau)\\ &\qquad\times\left\{\delta\left(t-\tau-\frac{|\mathbf{x}|}{c_o}\right)+\delta'\left(t-\tau-\frac{|\mathbf{x}|}{c_o}\right)\frac{x_jY_j}{c_o|\mathbf{x}|}\right\}dS(\mathbf{y})d\tau,\end{aligned}$$

where the prime denotes differentiation with respect to time. Performing the integration with respect to τ:

$$\begin{aligned}\varphi(\mathbf{x},t) \approx &-\frac{1}{4\pi|\mathbf{x}|}\oint_S v_n\left(\mathbf{y},t-\frac{|\mathbf{x}|}{c_o}\right)dS(\mathbf{y})\\ &-\frac{x_j}{4\pi c_o|\mathbf{x}|^2}\frac{\partial}{\partial t}\oint_S v_n\left(\mathbf{y},t-\frac{|\mathbf{x}|}{c_o}\right)Y_j(\mathbf{y})dS(\mathbf{y}).\end{aligned}$$

The first integral is a *monopole* sound wave that is non-zero only if the volume enclosed by S is *pulsating*. It is then the most important component of the far field – the second integral is smaller by a factor $\sim O(\omega\ell/c_o) \ll 1$ (because $\partial/\partial t \sim \omega$ and $Y_j \sim \ell$).

The monopole term vanishes for a *rigid body* executing small amplitude translational oscillations at velocity $\mathbf{U}(t)$, say. Then

$$v_n(\mathbf{y},\tau) = \mathbf{n}(\mathbf{y})\cdot\mathbf{U}(\tau) = n_i(\mathbf{y})U_i(\tau),$$

where $\mathbf{n}(\mathbf{y})$ is the surface normal directed into the fluid. Making the substitution $Y_j = y_j - \varphi_j^*(\mathbf{y})$ in the second integral we obtain an acoustic field of *dipole* type, given by

$$\varphi(\mathbf{x},t) \approx -\frac{x_j}{4\pi c_o|\mathbf{x}|^2}\frac{\partial U_i}{\partial t}\left(t-\frac{|\mathbf{x}|}{c_o}\right)\oint_S n_i(\mathbf{y})Y_j(\mathbf{y})dS(\mathbf{y}) \tag{2.8.1}$$

$$= -\frac{x_j}{4\pi c_o|\mathbf{x}|^2}\frac{\partial U_i}{\partial t}\left(t-\frac{|\mathbf{x}|}{c_o}\right)\oint_S [n_iy_j - n_i\varphi_j^*]\,dS,\ |\mathbf{x}|\to\infty. \tag{2.8.2}$$

Example The vibrating sphere Consider a rigid sphere of radius a centred at the origin and oscillating in the x_1-direction at velocity $U(t)$ (Figure 2.8.2). Then $\mathbf{U} = (U,0,0)$, and it is only necessary to take $i = 1$ in (2.8.1) or (2.8.2).

Downloaded from https://www.cambridge.org/core. Charité Universitätsmedizin Berlin, on 20 Dec 2021 at 10:08:47, subject to the Cambridge Core terms of use, available at https://www.cambridge.org/core/terms. https://doi.org/10.1017/CBO9781107360273.003

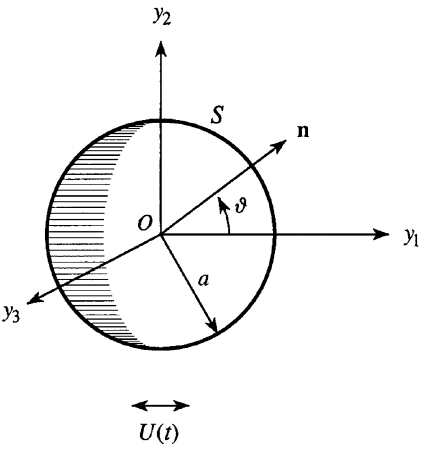

Figure 2.8.2

Using spherical polar coordinates (r, ϑ, ϕ) with $\mathbf{y} = r(\cos\vartheta, \sin\vartheta\cos\phi, \sin\vartheta\sin\phi)$, we have

$$\left.\begin{aligned} \mathbf{Y} &\equiv \mathbf{y}\left(1+\frac{a^3}{2|\mathbf{y}|^3}\right) = \frac{3a}{2}(\cos\vartheta, \sin\vartheta\cos\phi, \sin\vartheta\sin\phi) \\ n_1 &= \cos\vartheta \end{aligned}\right\} \text{ on the sphere}$$

Hence

$$\begin{aligned} \oint_S n_1 Y_j dS &= \frac{3a^3}{2}\oint_S (\cos\vartheta, \sin\vartheta\cos\phi, \sin\vartheta\sin\phi)\cos\vartheta\sin\vartheta d\vartheta d\phi \\ &= \begin{cases} 2\pi a^3, & j=1, \\ 0, & j=2,\ 3, \end{cases} \end{aligned}$$

and (2.8.1) therefore becomes

$$\varphi(\mathbf{x}, t) \approx -\frac{a^3\cos\theta}{2c_o|\mathbf{x}|}\frac{\partial U}{\partial t}(t-|\mathbf{x}|/c_o), \quad |\mathbf{x}|\to\infty, \quad \text{and} \quad \frac{x_1}{|\mathbf{x}|} = \cos\theta. \quad (2.8.3)$$

This agrees with the far field result obtained in §1.8.5, and confirms the model used there in which the vibrating sphere was replaced by a point dipole of strength $2\pi a^3 U(t)$ at its centre.

2.8.2 Low-frequency sound produced by an arbitrary vibrating body

The radiation from a vibrating compact rigid body can be expressed more generally in terms of the *added mass tensor* M_{ij} (Batchelor 1967), defined by the surface integral

Downloaded from https://www.cambridge.org/core. Charité Universitätsmedizin Berlin, on 20 Dec 2021 at 10:08:47, subject to the Cambridge Core terms of use, available at https://www.cambridge.org/core/terms. https://doi.org/10.1017/CBO9781107360273.003

$$M_{ij} = -\rho_o \oint_S n_i \varphi_j^* dS.$$

Condition (2.5.9), that $\partial\varphi_i^*/\partial y_n = n_i$ on S, implies that $M_{ij} = M_{ji}$, because

$$M_{ij} = -\rho_o \oint_S n_i \varphi_j^* dS = -\rho_o \oint_S \frac{\partial \varphi_i^*}{\partial y_n} \varphi_j^* dS \equiv -\rho_o \oint_S \varphi_i^* \frac{\partial \varphi_j^*}{\partial y_n} dS = M_{ji}. \tag{2.8.4}$$

The final integral is deduced from the second by reference to Figure 2.4.1, recalling that $\nabla^2\varphi_j^* = \nabla^2\varphi_i^* = 0$, and applying the divergence theorem as follows:

$$\oint_{S+\Sigma} \left(\frac{\partial \varphi_i^*}{\partial y_n} \varphi_j^* - \varphi_i^* \frac{\partial \varphi_j^*}{\partial y_n} \right) dS = \int_{\text{fluid}} \left(\varphi_i^* \nabla^2 \varphi_j^* - \varphi_j^* \nabla^2 \varphi_i^* \right) d^3\mathbf{y} \equiv 0.$$

The integration over Σ vanishes as the surface recedes to infinity because (Batchelor 1967)

$$\varphi_{i,j}^*(\mathbf{y}) \sim O\left(\frac{1}{|\mathbf{y}|^2}\right) \quad \text{as} \quad |\mathbf{y}| \to \infty.$$

When the body moves in an ideal, *incompressible* fluid in the absence of vorticity ($\boldsymbol{\omega} = \operatorname{curl} \mathbf{v}$), the force F_i it exerts on the fluid in the i-direction can be calculated in terms of the velocity potential φ from the formula $F_i = -\rho_o \frac{d}{dt} \oint_S \varphi\, n_i\, dS$ (§4.A.3 with $q = 0$). For an isolated body, φ_j^* is the velocity potential produced by motion of the body at unit speed in the j direction. Therefore, for translational motion at velocity U_j we can put $\varphi = U_j \varphi_j^*$, so that

$$F_i(t) = -\rho_o \frac{d}{dt} \oint_S U_j \varphi_j^* n_i\, dS \;\equiv\; -\rho_o \frac{dU_j}{dt} \oint_S \varphi_j^* n_i\, dS \;=\; M_{ij} \frac{dU_j}{dt}, \tag{2.8.5}$$

because φ_j^* does not depend on time on the non-rotating surface S of the body. For a body of mass m, this means that when an external force $\mathcal{F}_i$ acts through its centre of mass, the equation of motion of the body can be written

$$\left(m\delta_{ij} + M_{ij}\right) \frac{dU_j}{dt} = \mathcal{F}_i.$$

The added mass tensor determines the effective mass of fluid that accompanies the body in its accelerated motion. The inertia of this fluid and that of the body must be overcome by the force $\boldsymbol{\mathcal{F}}$ when the body accelerates. In general, however, a *couple* must also be applied to the translating body to counter a rotational torque also exerted on the body by the fluid.

Let us now apply these concepts to determine from (2.8.2) the sound pressure produced by a rigid compact body executing small amplitude translational

Downloaded from https://www.cambridge.org/core. Charité Universitätsmedizin Berlin, on 20 Dec 2021 at 10:08:47, subject to the Cambridge Core terms of use, available at https://www.cambridge.org/core/terms. https://doi.org/10.1017/CBO9781107360273.003

oscillations at velocity $\mathbf{U}(t)$. The acoustic pressure is given in the far field by $p = -\rho_o \partial\varphi/\partial t$ (§1.3), and therefore

$$p(\mathbf{x},t) = \frac{x_j}{4\pi c_o |\mathbf{x}|^2} \frac{\partial^2 U_i}{\partial t^2}\left(t - \frac{|\mathbf{x}|}{c_o}\right) \times \left\{\rho_o \oint_S n_i y_j dS - \rho_o \oint_S n_i \varphi_j^* dS\right\}, \quad |\mathbf{x}| \to \infty. \tag{2.8.6}$$

The first integral is evaluated by the divergence theorem (as in §2.1.3): $\rho_o \oint_S n_i y_j dS = \rho_o \Delta \delta_{ij} \equiv m_o \delta_{ij}$, where m_o is the mass of fluid displaced by the body. The second integral is the added mass tensor M_{ij}.

Thus, the acoustic pressure can be expressed in either of the forms

$$\begin{aligned} p(\mathbf{x},t) &\approx \frac{x_i}{4\pi c_o |\mathbf{x}|^2}\left(m_o \delta_{ij} + M_{ij}\right)\frac{\partial^2 U_j}{\partial t^2}\left(t - \frac{|\mathbf{x}|}{c_o}\right) \\ &= \frac{x_i}{4\pi c_o |\mathbf{x}|^2}\left(m_o \frac{\partial^2 U_i}{\partial t^2} + \frac{\partial F_i}{\partial t}\right)\left(t - \frac{|\mathbf{x}|}{c_o}\right), \quad |\mathbf{x}| \to \infty, \end{aligned} \tag{2.8.7}$$

where the second line follows from (2.8.5), F_i being the force exerted by the body on the fluid in the i-direction.

For a sphere of radius a oscillating at speed $U(t)$ in the x_1-direction

$$m_o = \frac{4}{3}\pi a^3 \rho_o \quad \text{and} \quad M_{ij} = \frac{1}{2} m_o \delta_{ij}$$

$$\therefore \quad p(\mathbf{x},t) \approx \frac{x_i}{4\pi c_o |\mathbf{x}|^2}\left(m_o \delta_{ij} + \frac{1}{2} m_o \delta_{ij}\right)\frac{\partial^2 U_j}{\partial t^2}\left(t - \frac{|\mathbf{x}|}{c_o}\right), \quad |\mathbf{x}| \to \infty.$$

$$= \frac{\rho_o a^3 \cos\theta}{2 c_o |\mathbf{x}|}\frac{\partial^2 U}{\partial t^2}\left(t - \frac{|\mathbf{x}|}{c_o}\right),$$

which is equivalent to (2.8.3).

2.8.3 *Rayleigh scattering: Scattering of sound by a compact body*

The scattered radiation produced when long wavelength sound impinges on a fixed, rigid body is equivalent in the far field to that generated by a combination of monopole and dipole sources. Let the incident wave be propagating in the x_1-direction and be given by

$$p = p_{\mathrm{I}}(t - x_1/c_o),$$

and let $p_{\mathrm{s}}(\mathbf{x},t)$ denote the scattered pressure. Then p_{s} satisfies the homogeneous wave equation

$$\left(\frac{1}{c_o^2}\frac{\partial^2}{\partial t^2} - \nabla^2\right) p_{\mathrm{s}} = 0,$$

Downloaded from https://www.cambridge.org/core. Charité Universitätsmedizin Berlin, on 20 Dec 2021 at 10:08:47, subject to the Cambridge Core terms of use, available at https://www.cambridge.org/core/terms. https://doi.org/10.1017/CBO9781107360273.003

and the acoustic particle velocity $\mathbf{v}_s$ of the scattered sound is given by $\rho_o \partial \mathbf{v}_s/\partial t = -\nabla p_s$.

The scattered pressure at large distances from the body is given by the generalised Kirchhoff formula (2.1.6) and the compact Green's function in the form

$$p_s(\mathbf{x}, t) \approx \rho_o \frac{\partial}{\partial t} \oint\!\!\!\!\!\!\int_S G(\mathbf{x}, \mathbf{y}, t-\tau) v_{sn}(\mathbf{y}, \tau)\, dS(\mathbf{y}) d\tau,$$

where v_{sn} is the component of $\mathbf{v}_s$ on the surface S of the body in the direction of the outward normal.

Now

$$v_{sn} + v_{In} = 0 \quad \text{on } S$$

where $\mathbf{v}_I = (v_I, 0, 0)$ is the incident wave particle velocity, and $v_I = p_I/\rho_o c_o$. Take the coordinate origin at O within S and expand the compact Green's function to dipole order, to find

$$\begin{aligned} p_s(\mathbf{x}, t) \approx & -\frac{\rho_o}{4\pi |\mathbf{x}|} \frac{\partial}{\partial t} \oint_S v_{In}([t] - y_1/c_o)\, dS(\mathbf{y}) \\ & - \frac{\rho_o x_j}{4\pi c_o |\mathbf{x}|^2} \frac{\partial^2}{\partial t^2} \oint_S Y_j(\mathbf{y}) v_{In}([t] - y_1/c_o)\, dS(\mathbf{y}), \quad |\mathbf{x}| \to \infty, \end{aligned} \tag{2.8.8}$$

where $[t] = t - |\mathbf{x}|/c_o$.

The continuity equation $\operatorname{div} \mathbf{v}_I = (-1/\rho_o c_o^2)\partial p_I/\partial t$ satisfied by the incident wave implies that

$$\begin{aligned} \oint_S v_{In}([t] - y_1/c_o)\, dS(\mathbf{y}) &= -\int_\Delta \frac{1}{\rho_o c_o^2} \frac{\partial p_I}{\partial t}([t] - y_1/c_o)\, d^3\mathbf{y} \\ &\approx -\frac{m_o}{\rho_o^2 c_o^2} \frac{\partial p_I}{\partial t}([t]), \end{aligned}$$

where the volume integration is over the compact interior of S (of volume Δ) across which variations of the retarded time are neglected, and $m_o = \rho_o \Delta$ is the mass of fluid displaced by the body.

Similarly, setting $v_{In} = (p_I/\rho_o c_o) n_1$ in the second integral of (2.8.8), we find

$$\oint_S Y_j(\mathbf{y}) v_{In}([t] - y_1/c_o)\, dS(\mathbf{y}) = \frac{1}{\rho_o c_o} \oint_S Y_j(\mathbf{y}) n_1(\mathbf{y}) p_1([t] - y_1/c_o)\, dS(\mathbf{y}).$$

When retarded time variations in this integral are neglected the resulting approximations for the two integrals in (2.8.8) are both second order in the

Downloaded from https://www.cambridge.org/core. Charité Universitätsmedizin Berlin, on 20 Dec 2021 at 10:08:47, subject to the Cambridge Core terms of use, available at https://www.cambridge.org/core/terms. https://doi.org/10.1017/CBO9781107360273.003

'compactness parameter' $\omega\ell/c_o \ll 1$, where ℓ is the effective diameter of the body and ω is a typical frequency.

$$\therefore \quad \oint_S Y_j(\mathbf{y}) v_{In}([t] - y_1/c_o)\, dS(\mathbf{y}) \approx \frac{p_I([t])}{\rho_o^2 c_o} \left(m_o \delta_{1j} + M_{1j}\right).$$

Hence (2.8.8) becomes

$$p_s \approx \frac{1}{4\pi\rho_o c_o^2 |\mathbf{x}|} \left\{ m_o - \left(m_o \cos\theta + \frac{x_j M_{1j}}{|\mathbf{x}|} \right) \right\} \left[\frac{\partial^2 p_I}{\partial t^2} \right], \quad |\mathbf{x}| \to \infty, \tag{2.8.9}$$

where $\cos\theta = x_1/|\mathbf{x}|$, the square brackets denote evaluation at the retarded time $t - |\mathbf{x}|/c_o$, and the two terms in the curly brackets represent respectively radiation of monopole and dipole type. But, both of these components are of the same nominal *quadrupole* magnitude $\sim O(k_o^2 \ell^2) \ll 1$ relative to the incident wave, where $k_o = \omega/c_o$.

In the particular case of the **sphere** of Figure 2.8.3, we have $M_{ij} = \frac{1}{2} m_o \delta_{ij}$, and therefore

$$p_s \approx \frac{m_o}{4\pi\rho_o c_o^2 |\mathbf{x}|} \left(1 - \tfrac{3}{2}\cos\theta\right) \left[\frac{\partial^2 p_I}{\partial t^2} \right], \quad |\mathbf{x}| \to \infty.$$

The directivity factor $\left(1 - \frac{3}{2}\cos\theta\right)^2$ is plotted in Figure 2.8.4.

The scattered acoustic power increases as $(k_o\ell)^4$, i.e. as the fourth power of the frequency. This prompted Rayleigh (1873) to attribute the formation of *harmonic echoes* to scattering by an assemblage of compact bodies: 'When a composite note, such as that proceeding from the human throat, impinges on the obstacle, its components are diverted in very different proportions. A group of small obstacles will return the first harmonic, or octave, sixteen times more powerfully than the fundamental. After this, it is not hard to understand how a wood, which may be considered to be made up of a great number of obstacles,

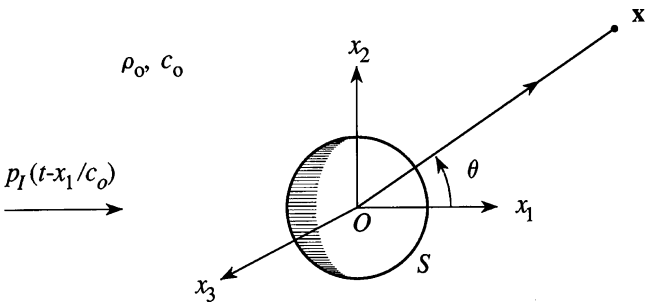

Figure 2.8.3

Downloaded from https://www.cambridge.org/core. Charité Universitätsmedizin Berlin, on 20 Dec 2021 at 10:08:47, subject to the Cambridge Core terms of use, available at https://www.cambridge.org/core/terms. https://doi.org/10.1017/CBO9781107360273.003

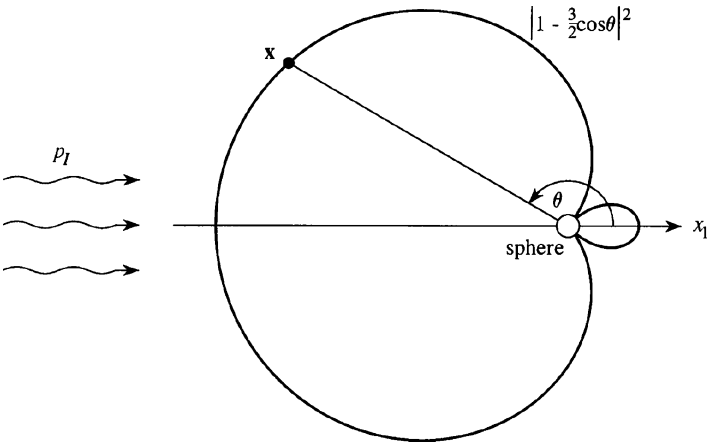

Figure 2.8.4

many of which in two or three of their dimensions, are small in comparison with the wavelength, returns a sound which appears to be raised an octave.' Similarly, for sound incident on a nominally plane wall 'covered with small projections, there would be a diffused echo, due to the projections in which the higher elements preponderated, and an ordinary echo, obeying the law of reflection, in which the lower elements would preponderate.'

2.9 Compact Green's function reference

General form: *Compact bodies and cylindrical bodies of compact cross-section*

$$G(\mathbf{x},\mathbf{y},t-\tau)=\frac{1}{4\pi|\mathbf{X}-\mathbf{Y}|}\delta\left(t-\tau-\frac{|\mathbf{X}-\mathbf{Y}|}{c_o}\right) \tag{2.9.1}$$

$$\left.\begin{aligned}\mathbf{X}&=\mathbf{x}-\boldsymbol{\varphi}^*(\mathbf{x})\\ \mathbf{Y}&=\mathbf{y}-\boldsymbol{\varphi}^*(\mathbf{y})\end{aligned}\right\}\text{ Kirchhoff vectors for the body.}$$

$X_3 = x_3,\ Y_3 = y_3$, for a cylindrical body of *compact cross-section* parallel to the x_3 direction.

2.9.1 Special cases

2.9.1a Wall with compact surface irregularity Let the wall coincide with $x_2 = 0$ with fluid in $x_2 > 0$ (Figure 2.9.1):

$$G(\mathbf{x},\mathbf{y},t-\tau)=\frac{1}{4\pi|\mathbf{X}-\mathbf{Y}|}\delta\left(t-\tau-\frac{|\mathbf{X}-\mathbf{Y}|}{c_o}\right)+\frac{1}{4\pi|\bar{\mathbf{X}}-\mathbf{Y}|}\delta\left(t-\tau-\frac{|\bar{\mathbf{X}}-\mathbf{Y}|}{c_o}\right), \tag{2.9.2}$$

Downloaded from https://www.cambridge.org/core. Charité Universitätsmedizin Berlin, on 20 Dec 2021 at 10:08:47, subject to the Cambridge Core terms of use, available at https://www.cambridge.org/core/terms. https://doi.org/10.1017/CBO9781107360273.003

Table 2.9.1 *Canonical examples*

body	X_1	X_2	X_3
sphere of radius a centre at origin	$x_1\left(1+\frac{a^3}{2\lvert\mathbf{x}\rvert^3}\right)$	$x_2\left(1+\frac{a^3}{2\lvert\mathbf{x}\rvert^3}\right)$	$x_3\left(1+\frac{a^3}{2\lvert\mathbf{x}\rvert^3}\right)$
circular cylinder of radius a coaxial with the x_3-axis	$x_1\left(1+\frac{a^2}{x_1^2+x_2^2}\right)$	$x_2\left(1+\frac{a^2}{x_1^2+x_2^2}\right)$	x_3
strip airfoil $-a<x_1<a,\ x_2=0,$ $-\infty<x_3<\infty$	x_1	$\mathrm{Re}(-i\sqrt{z^2-a^2})$ $z=x_1+ix_2$	x_3

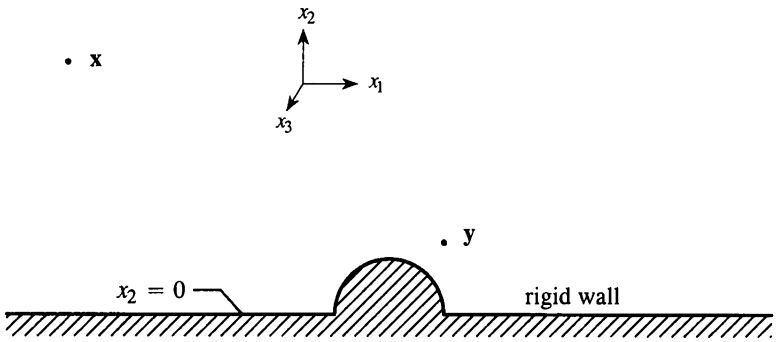

Figure 2.9.1

where

$$\left.\begin{aligned} Y_1 &= y_1-\varphi_1^*(\mathbf{y}), \quad Y_2=y_2, \quad Y_3=y_3-\varphi_3^*(\mathbf{y}) \\ X_1 &= x_1-\varphi_1^*(\mathbf{x}), \quad X_2=x_2, \quad X_3=x_3-\varphi_3^*(\mathbf{x}) \end{aligned}\right\} \tag{2.9.3}$$

and $\bar{\mathbf{X}}=(X_1,-X_2,X_3)$. $X_1(\mathbf{x})$, $X_3(\mathbf{x})$ are the velocity potentials of flows parallel to the wall past the surface irregularity having unit speeds respectively in the x_1 and x_3 directions as $|\mathbf{x}|\to\infty$.

$Y_3=y_3$, $X_3=x_3$ for a two-dimensional irregularity uniform in the x_3-direction.

2.9.1b Half-plane: $x_1<0$, $x_2=0$, $-\infty<x_3<\infty$. The compact Green's function is defined for a source at $\mathbf{y}$ *whose distance from the edge* is small compared to the acoustic wavelength. Use the cylindrical polar coordinates $\mathbf{x}=(r\cos\theta, r\sin\theta, x_3)$, $\mathbf{y}=(r_o\cos\theta_o, r_o\sin\theta_o, y_3)$, and let $\mathbf{i}_3$ be a unit vector in the x_3-direction (parallel to the edge, Figure 2.9.2).

Downloaded from https://www.cambridge.org/core. Charité Universitätsmedizin Berlin, on 20 Dec 2021 at 10:08:47, subject to the Cambridge Core terms of use, available at https://www.cambridge.org/core/terms. https://doi.org/10.1017/CBO9781107360273.003

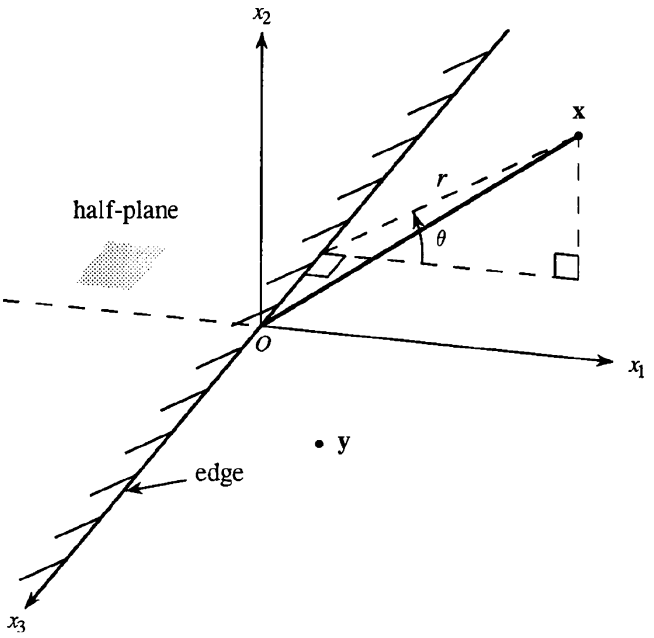

Figure 2.9.2

Then

$$\hat{G}(\mathbf{x}, \mathbf{y}, \omega) = \hat{G}_0(\mathbf{x}, \omega) + \hat{G}_1(\mathbf{x}, \mathbf{y}, \omega) + \ldots, \tag{2.9.4}$$

where, for $|\mathbf{x} - y_3\mathbf{i}_3| \to \infty$ and $k_o\sqrt{y_1^2 + y_2^2} \ll 1$,

$$\begin{aligned}\hat{G}_0(\mathbf{x}, \mathbf{y}, \omega) &= \frac{-1}{4\pi|\mathbf{x} - y_3\mathbf{i}_3|}\mathrm{e}^{ik_o|\mathbf{x}-y_3\mathbf{i}_3|},\\ \hat{G}_1(\mathbf{x}, \mathbf{y}, \omega) &= \frac{-1}{\pi\sqrt{2\pi i}}\frac{\sqrt{k_o}\varphi^*(\mathbf{x})\varphi^*(\mathbf{y})}{|\mathbf{x} - y_3\mathbf{i}_3|^{3/2}}\mathrm{e}^{ik_o|\mathbf{x}-y_3\mathbf{i}_3|},\end{aligned} \tag{2.9.5}$$

and

$$\varphi^*(\mathbf{x}) = \sqrt{r}\sin(\theta/2), \quad \varphi^*(\mathbf{y}) = \sqrt{r_o}\sin(\theta_o/2). \tag{2.9.6}$$

$\varphi^*(\mathbf{x})$ is a velocity potential of incompressible flow around the edge of the half-plane in the anticlockwise sense (with parabolic streamlines, cf. Figure 4.7.3), expressed in terms of polar coordinates $(x_1, x_2) = r(\cos\theta, \sin\theta)$ (and similarly for $\varphi^*(\mathbf{y})$).

The component $\hat{G}_0$ of $\hat{G}$ represents the radiation from a point source at $\mathbf{y}$ when scattering is neglected; $\hat{G}_1$ is the first correction due to presence of the half-plane, and

Downloaded from https://www.cambridge.org/core. Charité Universitätsmedizin Berlin, on 20 Dec 2021 at 10:08:47, subject to the Cambridge Core terms of use, available at https://www.cambridge.org/core/terms. https://doi.org/10.1017/CBO9781107360273.003

$$G_1(\mathbf{x},\mathbf{y},t-\tau)$$
$$= -\frac{1}{2\pi}\int_{-\infty}^{\infty}\hat{G}_1(\mathbf{x},\mathbf{y},\omega)\mathrm{e}^{-i\omega(t-\tau)}d\omega$$
$$= \frac{1}{\pi^2\sqrt{2c_o}}\frac{\varphi^*(\mathbf{x})\varphi^*(\mathbf{y})}{|\mathbf{x}-y_3\mathbf{i}_3|^{3/2}}\frac{\partial}{\partial t}\left(\frac{\mathrm{H}(t-\tau-|\mathbf{x}-y_3\mathbf{i}_3|/c_o)}{\sqrt{t-\tau-|\mathbf{x}-y_3\mathbf{i}_3|/c_o}}\right). \quad (2.9.7)$$

2.9.1c Half-plane with two-dimensional sources This is for the *two-dimensional* problem of Figure 2.9.2, where source conditions are uniform in the x_3-direction, and

$$\left(\frac{1}{c_o^2}\frac{\partial^2}{\partial t^2}-\nabla^2\right)G=\delta(x_1-y_1)\delta(x_2-y_2)\delta(t-\tau),\ \ G=0\text{ for }t<\tau. \quad (2.9.8)$$

When the 'line' source at $\mathbf{y}=(y_1,y_2)$ is close to the edge of the half-plane in Figure 2.9.2 the corresponding compact Green's function is obtained by the method of descent (§1.6.2), by integration of (2.9.5) over $-\infty<y_3<\infty$, using the *method of stationary phase* for $k_o\sqrt{x_1^2+x_2^2}\to\infty$ (see §4.6.4), and then using formula (2.3.5) to calculate $G(\mathbf{x},\mathbf{y},t-\tau)\approx G_0(\mathbf{x},t-\tau)+G_1(\mathbf{x},\mathbf{y},t-\tau)+\cdots$. The first term in the expansion that involves $\mathbf{y}$ is

$$G_1(\mathbf{x},\mathbf{y},t-\tau)\approx\frac{\varphi^*(\mathbf{x})\varphi^*(\mathbf{y})}{\pi|\mathbf{x}|}\delta(t-\tau-|\mathbf{x}|/c_o),\ \ |\mathbf{x}|\to\infty, \quad (2.9.9)$$

where $\mathbf{x}=(x_1,x_2)$, $\mathbf{y}=(y_1,y_2)$ and φ^* is defined as in (2.9.6).

2.9.1d Infinite duct Only plane waves can propagate in a cylindrical duct of cross-sectional area A when the characteristic wavelength of sound is large compared with the diameter $\sim\sqrt{A}$, even if the source region is highly three-dimensional. The corresponding compact Green's function satisfies the one dimensional wave equation when the cross-sectional area is *uniform*. Taking the x_1-direction along the axis of the duct (Figure 2.9.3a), we have

$$G(\mathbf{x},\mathbf{y},t-\tau)=\frac{c_o}{2A}\mathrm{H}\left(t-\tau-\frac{|x_1-y_1|}{c_o}\right),\quad |\mathbf{x}-\mathbf{y}|\gg\sqrt{A}. \quad (2.9.10)$$

For a uniform duct with an acoustically compact section of variable cross-section (e.g., the 'neck' of Figure 2.9.3b), the compact Green's function is

$$G(\mathbf{x},\mathbf{y},t-\tau)=\frac{c_o}{2A}\mathrm{H}\left(t-\tau-\frac{|X_1-Y_1|}{c_o}\right),\quad |\mathbf{x}-\mathbf{y}|\gg\sqrt{A}, \quad (2.9.11)$$

where $X_1(\mathbf{x})$ and $Y_1(\mathbf{y})$ denote the velocity potential of incompressible flow along the duct having unit speed at large distances from the neck.

Downloaded from https://www.cambridge.org/core. Charité Universitätsmedizin Berlin, on 20 Dec 2021 at 10:08:47, subject to the Cambridge Core terms of use, available at https://www.cambridge.org/core/terms. https://doi.org/10.1017/CBO9781107360273.003

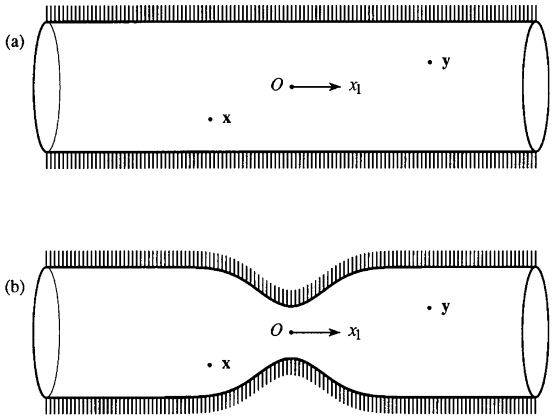

Figure 2.9.3

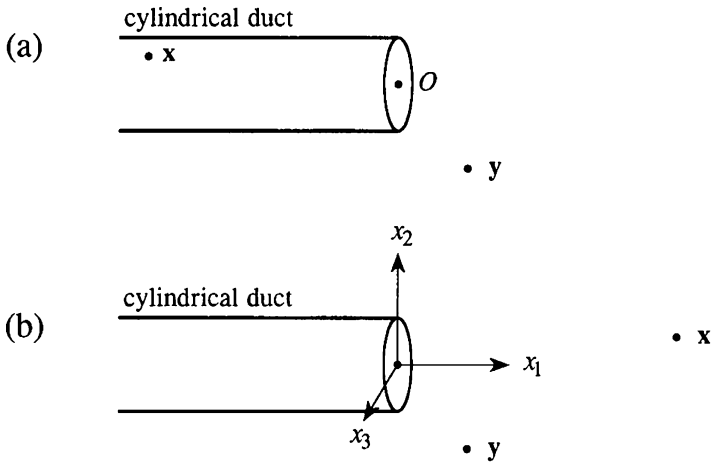

Figure 2.9.4

2.9.1e Open end of a duct The geometry is illustrated in Figure 2.9.4a. Within the duct, several diameters from the entrance, the cross-sectional area is uniform and equal to A. The entrance geometry can be arbitrary, not necessarily that of the uniform cylinder shown in the figure. Take the coordinate origin in the entrance plane of the duct, with the negative x_1-axis lying along the axis of the duct. Then, there are two cases:

(i) Propagation into the duct: Figure 2.9.4a

The source at **y** is near the duct entrance and an observer at **x** is within the duct (or *vice versa*), when the characteristic acoustic wavelength is large compared to the duct diameter

Downloaded from https://www.cambridge.org/core. Charité Universitätsmedizin Berlin, on 20 Dec 2021 at 10:08:47, subject to the Cambridge Core terms of use, available at https://www.cambridge.org/core/terms. https://doi.org/10.1017/CBO9781107360273.003

$$G(\mathbf{x},\mathbf{y},t-\tau)\approx\frac{c_o}{2A}\left\{\mathrm{H}\left[t-\tau-\frac{|\varphi^*(\mathbf{x})-\varphi^*(\mathbf{y})|}{c_o}\right]-\mathrm{H}\left[t-\tau+\frac{\varphi^*(\mathbf{x})+\varphi^*(\mathbf{y})}{c_o}\right]\right\},\quad(2.9.12)$$

where the velocity potential $\varphi^*(\mathbf{x})$ describes incompressible flow from the duct, and satisfies

$$\left.\begin{array}{ll}\varphi^*(\mathbf{x}) & \approx x_1-\ell_E \quad \text{when } |x_1|\gg\sqrt{A} \text{ within the duct,}\\ & \approx -A/4\pi|\mathbf{x}| \text{ when } |\mathbf{x}|\gg\sqrt{A} \text{ outside the duct,}\end{array}\right\}\quad(2.9.13)$$

in which ℓ_E is the 'end correction' of the duct ($\approx 0.61R$ for an unflanged circular cylinder of radius $R=\sqrt{A/\pi}$, see §5.4.1).

(ii) Propagation out of the duct: Figure 2.9.4b

When either the source or observer is located at a large distance from the duct entrance in *free space*

$$G(\mathbf{x},\mathbf{y},t-\tau)=\frac{1}{4\pi|\mathbf{X}-\mathbf{Y}|}\delta\left(t-\tau-\frac{(|\mathbf{X}(\mathbf{x})-\mathbf{Y}(\mathbf{y})|-[\varphi^*(\mathbf{x})+\varphi^*(\mathbf{y})])}{c_o}\right),\quad(2.9.14)$$

where φ^* is defined as in (2.9.13), and $\mathbf{X}(\mathbf{x})$, $\mathbf{Y}(\mathbf{y})$ denote the Kirchhoff vector whose i-component is the velocity potential of flow past the stationary surface formed by the duct entrance; they have unit speed in the i-direction at large distances from the entrance outside the duct and are exponentially small within the duct.

For a uniform, thin-walled cylindrical duct

$$\mathbf{X}(\mathbf{x})\equiv\Big(x_1-\varphi^*(\mathbf{x}),X_2(\mathbf{x}),X_3(\mathbf{x})\Big),\quad \mathbf{Y}(\mathbf{y})\equiv\Big(y_1-\varphi^*(\mathbf{y}),Y_2(\mathbf{y}),Y_3(\mathbf{y})\Big).$$

When $y_1\to-\infty$ within the duct,

$$G(\mathbf{x},\mathbf{y},t-\tau)=\frac{1}{4\pi|\mathbf{x}|}\delta\Big(t-\tau-(|\mathbf{x}|-y_1)/c_o\Big),\quad |\mathbf{x}|\to\infty.\quad(2.9.15)$$

Formulae for $\varphi^*(\mathbf{x})$

For a thin-walled circular cylinder of radius R

$$\frac{\partial\varphi^*}{\partial x_1}(\mathbf{x})=\frac{1}{2}-\frac{1}{2\pi}\int_0^\infty \mathrm{I}_0\left(\frac{\lambda\varpi}{R}\right)\left(\frac{2\mathrm{K}_1(\lambda)}{\mathrm{I}_1(\lambda)}\right)^{\frac{1}{2}}\sin\left\{\lambda\left(\frac{x_1}{R}+\mathcal{Z}(\lambda)\right)\right\}d\lambda,$$

$$\mathcal{Z}(\lambda)=\frac{1}{\pi}\int_0^\infty \ln\left(\frac{\mathrm{K}_1(\mu)\mathrm{I}_1(\mu)}{\mathrm{K}_1(\lambda)\mathrm{I}_1(\lambda)}\right)\frac{d\mu}{\mu^2-\lambda^2},$$

Downloaded from https://www.cambridge.org/core. Charité Universitätsmedizin Berlin, on 20 Dec 2021 at 10:08:47, subject to the Cambridge Core terms of use, available at https://www.cambridge.org/core/terms. https://doi.org/10.1017/CBO9781107360273.003

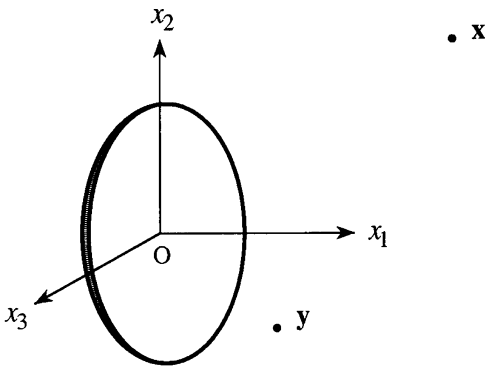

Figure 2.9.5

where the origin is at the centre of the duct exit, $\varpi = \sqrt{x_2^2 + x_3^2} < R$, and $\mathrm{I}_0,\ \mathrm{I}_1,\ \mathrm{K}_1$ are modified Bessel functions.

2.9.1f Circular disc: thin, rigid, of radius a with centre at the origin and orientated normal to the x_1-axis (Figure 2.9.5).

$$\left.\begin{aligned} &Y_1 = y_1 + \tfrac{2a\,\mathrm{sgn}(y_1)}{\pi}\int_0^\infty \left(\tfrac{\sin(\xi a)}{\xi a} - \cos(\xi a)\right)\tfrac{\mathrm{e}^{-\xi|y_1|}\mathrm{J}_0(\xi\varpi)d\xi}{\xi},\quad \varpi = \sqrt{y_2^2 + y_3^2},\\ &Y_2 = y_2,\quad Y_3 = y_3. \end{aligned}\right\} \tag{2.9.16}$$

In particular, just to the left and right of the plane of symmetry

$$Y_1 \equiv -\varphi_1^* = \pm\frac{2}{\pi}\mathrm{H}(a-\varpi)\sqrt{a^2-\varpi^2},\ \ y_1 = \pm 0.$$

2.9.1g Circular aperture of radius a, centre at the origin in a thin rigid, plane wall $x_1 = 0$ (Figure 2.9.6; see also §3.3.4). The source at $\mathbf{y}$ is close to the aperture on *either side* of the wall; $\mathbf{x}$ is in the far field on the side $x_1 > 0$.

$$G(\mathbf{x},\mathbf{y},t-\tau) = \frac{1}{2\pi|\mathbf{x}|}\left(1 + \frac{\varphi^*(\mathbf{y})}{\ell}\right)\delta\left(t - \tau - \frac{|\mathbf{x}|}{c_o}\right) \tag{2.9.17}$$

$$\varphi^*(\mathbf{y}) = -\frac{a\,\mathrm{sgn}(y_1)}{2}\int_0^\infty \frac{\sin(\xi a)}{\xi}\mathrm{e}^{-\xi|y_1|}\mathrm{J}_0(\xi\varpi)d\xi - \ell\mathrm{H}(-y_1)$$

where $\varpi = \sqrt{y_2^2 + y_3^2}$, and

$$\varphi^*(\mathbf{y}) \to \begin{cases} -\frac{A}{2\pi|\mathbf{y}|}, & y_1 \to +\infty \\ \frac{A}{2\pi|\mathbf{y}|} - \ell, & y_1 \to -\infty, \end{cases},\quad A = \pi a^2,\ \ell = \frac{\pi a}{2}.$$

Downloaded from https://www.cambridge.org/core. Charité Universitätsmedizin Berlin, on 20 Dec 2021 at 10:08:47, subject to the Cambridge Core terms of use, available at https://www.cambridge.org/core/terms. https://doi.org/10.1017/CBO9781107360273.003

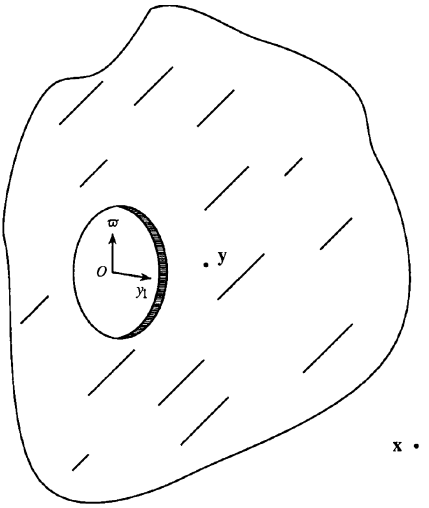

Figure 2.9.6

The function $\varphi^*(\mathbf{y})$ is the velocity potential of ideal, incompressible flow through the aperture (from $y_1 < 0$ to $y_1 > 0$) with unit mean speed in the plane of the aperture and net flux $\int_{y_1=+0} \frac{\partial \varphi^*}{\partial y_1}\, dS = A$.

2.9.2 Compact Green's function in two dimensions

For two-dimensional cylindrical boundary geometry with generators parallel to the x_3 axis

$$G(\mathbf{x}, \mathbf{y}, t-\tau) = \frac{1}{4\pi |\mathbf{X}-\mathbf{Y}|}\delta\left(t - \tau - \frac{|\mathbf{X}-\mathbf{Y}|}{c_o}\right),$$
$$X_{1,2} = x_{1,2} - \varphi^*_{1,2}(\mathbf{x}), \quad Y_{1,2} = y_{1,2} - \varphi^*_{1,2}(\mathbf{y}),$$
$$X_3 = x_3, \quad Y_3 = y_3.$$

When the source distribution does not depend on x_3 the corresponding *two-dimensional* compact Green's function G_2 can be derived by the method of descent (§1.6.2), by integration over $-\infty < x_3 < \infty$.

Set $\xi = x_3 - y_3$, $\bar{\mathbf{x}} = (x_1, x_2)$ and let $|\bar{\mathbf{x}}| = (x_1^2 + x_2^2)^{\frac{1}{2}} \to \infty$. Take the origin of coordinates within the cylindrical body, then

Downloaded from https://www.cambridge.org/core. Charité Universitätsmedizin Berlin, on 20 Dec 2021 at 10:08:47, subject to the Cambridge Core terms of use, available at https://www.cambridge.org/core/terms. https://doi.org/10.1017/CBO9781107360273.003

$$G_2 \approx \frac{1}{4\pi}\int_{-\infty}^{\infty}\delta\left(t-\tau-\frac{\sqrt{|\bar{\mathbf{x}}|^2+\xi^2}}{c_o}+\frac{\bar{\mathbf{x}}\cdot\mathbf{Y}}{c_o\sqrt{|\bar{\mathbf{x}}|^2+\xi^2}}\right) \times \frac{d\xi}{\sqrt{|\bar{\mathbf{x}}|^2+\xi^2}} \quad \text{as } |\bar{\mathbf{x}}|\to\infty,$$

where $\bar{\mathbf{x}}\cdot\mathbf{Y} = x_1Y_1 + x_2Y_2$ is independent of ξ. Expand the δ-function to first order in $\mathbf{Y}$:

$$G_2 \approx \frac{1}{4\pi}\int_{-\infty}^{\infty}\delta\left(t-\tau-\frac{\sqrt{|\bar{\mathbf{x}}|^2+\xi^2}}{c_o}\right)\frac{d\xi}{\sqrt{|\bar{\mathbf{x}}|^2+\xi^2}} + \frac{\bar{\mathbf{x}}\cdot\mathbf{Y}}{4\pi c_o}\int_{-\infty}^{\infty}\delta'\left(t-\tau-\frac{\sqrt{|\bar{\mathbf{x}}|^2+\xi^2}}{c_o}\right)\frac{d\xi}{(|\bar{\mathbf{x}}|^2+\xi^2)}$$

$$= \frac{\mathrm{H}(t-\tau-|\bar{\mathbf{x}}|/c_o)}{2\pi\sqrt{(t-\tau)^2-|\bar{\mathbf{x}}|^2/c_o^2}} + \frac{\bar{\mathbf{x}}\cdot\mathbf{Y}}{2\pi c_o}\frac{\partial}{\partial t}\int_0^{\infty}\delta\left(t-\tau-\frac{\sqrt{|\bar{\mathbf{x}}|^2+\xi^2}}{c_o}\right)\frac{d\xi}{(|\bar{\mathbf{x}}|^2+\xi^2)}.$$

For the second integral

$$\int_0^{\infty}\delta\left(t-\tau-\frac{\sqrt{|\bar{\mathbf{x}}|^2+\xi^2}}{c_o}\right)\frac{d\xi}{(|\bar{\mathbf{x}}|^2+\xi^2)} = \left\{\frac{\mathrm{H}(t-\tau-|\bar{\mathbf{x}}|/c_o)}{(|\bar{\mathbf{x}}|^2+\xi^2)\left|\frac{\partial}{\partial\xi}\frac{\sqrt{|\bar{\mathbf{x}}|^2+\xi^2}}{c_o}\right|}\right\}_{\xi=\sqrt{c_o^2(t-\tau)^2-|\bar{\mathbf{x}}|^2}} = \frac{\mathrm{H}(t-\tau-|\bar{\mathbf{x}}|/c_o)}{(t-\tau)\sqrt{c_o^2(t-\tau)^2-|\bar{\mathbf{x}}|^2}}.$$

Hence

$$G_2(\bar{\mathbf{x}},\bar{\mathbf{y}},t-\tau) = \frac{\mathrm{H}(t-\tau-|\bar{\mathbf{x}}|/c_o)}{2\pi\sqrt{(t-\tau)^2-|\bar{\mathbf{x}}|^2/c_o^2}} + \frac{\bar{\mathbf{x}}\cdot\mathbf{Y}}{2\pi c_o}\frac{\partial}{\partial t}\left(\frac{\mathrm{H}(t-\tau-|\bar{\mathbf{x}}|/c_o)}{(t-\tau)\sqrt{c_o^2(t-\tau)^2-|\bar{\mathbf{x}}|^2}}\right) \quad (2.9.18)$$

G_2 has an infinite peak at the wavefront where $t-\tau-|\bar{\mathbf{x}}|/c_o = 0$ followed by a slowly decaying 'tail'. At any point $\bar{\mathbf{x}}$ in the far field the first sound arrives from the nearest point on the line source of (1.6.10), after propagating along a ray perpendicular to the source over a distance equal to $|\bar{\mathbf{x}}|$, and therefore after a time delay $|\bar{\mathbf{x}}|/c_o$; but the observer at $\bar{\mathbf{x}}$ receives sound continuously after the

Downloaded from https://www.cambridge.org/core. Charité Universitätsmedizin Berlin, on 20 Dec 2021 at 10:08:47, subject to the Cambridge Core terms of use, available at https://www.cambridge.org/core/terms. https://doi.org/10.1017/CBO9781107360273.003

passage of this wavefront, generated at more distant sections of the infinitely long line source; the wavefront arrives at time $\tau + |\bar{\mathbf{x}}|/c_o$, and at a later time t sound is received from those source points whose distance from $\bar{\mathbf{x}}$ is equal to $c_o(t-\tau)$.

The far field representation (2.9.18) can be approximated further by expanding about the wavefront (where $t - \tau = |\bar{\mathbf{x}}|/c_o$) which contains most of the acoustic energy. Just to the rear of the wavefront

$$(t-\tau)\sqrt{c_o^2(t-\tau)^2 - |\bar{\mathbf{x}}|^2} \equiv (t-\tau)\sqrt{c_o(t-\tau)+|\bar{\mathbf{x}}|}\sqrt{c_o(t-\tau)-|\bar{\mathbf{x}}|}$$
$$\approx \frac{|\bar{\mathbf{x}}|}{c_o}\sqrt{2|\bar{\mathbf{x}}|}\sqrt{c_o(t-\tau)-|\bar{\mathbf{x}}|}, \quad \text{for} \quad t-\tau \sim \frac{|\bar{\mathbf{x}}|}{c_o}.$$

Therefore, the 'dipole' component of the two-dimensional compact Green's function (2.9.18) becomes

$$G_2(\bar{\mathbf{x}}, \bar{\mathbf{y}}, t-\tau) \approx \frac{\bar{\mathbf{x}}\cdot\mathbf{Y}}{2\pi\sqrt{2c_o}|\bar{\mathbf{x}}|^{\frac{3}{2}}}\frac{\partial}{\partial t}\left\{\frac{\mathrm{H}(t-\tau-|\bar{\mathbf{x}}|/c_o)}{\sqrt{t-\tau-|\bar{\mathbf{x}}|/c_o}}\right\}, \quad |\bar{\mathbf{x}}| \to \infty. \tag{2.9.19}$$

For a cylindrical irregularity on a flat wall $x_2 = 0$ (Figure 2.9.1), the dipole component of the two-dimensional compact Green's function is

$$G_2(\bar{\mathbf{x}}, \bar{\mathbf{y}}, t-\tau) \approx \frac{x_1 Y_1}{\pi\sqrt{2c_o}|\bar{\mathbf{x}}|^{\frac{3}{2}}}\frac{\partial}{\partial t}\left\{\frac{\mathrm{H}(t-\tau-|\bar{\mathbf{x}}|/c_o)}{\sqrt{t-\tau-|\bar{\mathbf{x}}|/c_o}}\right\}, \quad |\bar{\mathbf{x}}| \to \infty, \tag{2.9.20}$$

where $Y_1 \equiv Y_1(y_1, y_2)$ is the velocity potential of incompressible flow past the cylinder in a direction parallel to the wall (with unit speed at large distances). The dipole is parallel to the wall and perpendicular to the cylinder axis, and the effect of the wall is to generate an equal 'image' dipole that just *doubles* the magnitude of the sound relative to the corresponding dipole (2.9.19) in the absence of the wall.

2.A Appendix: Ideal incompressible flow in two dimensions

2.A.1 The complex potential

Let $w(z) = \varphi(x, y) + i\psi(x, y)$ $(z = x + iy)$ be *regular* (analytic) in a region $\mathcal{D}$ of the complex z-plane. The real and imaginary parts $\varphi(x, y)$ and $\psi(x, y)$ satisfy Laplace's equation: $(\partial^2/\partial x^2 + \partial^2/\partial y^2)(\varphi, \psi) = 0$ in $\mathcal{D}$.

A function $f(z)$ regular in $\mathcal{D}$ defines a (conformal) transformation $\zeta = f(z)$ of $\mathcal{D}$ into a region $\mathcal{D}'$ in the plane of $\zeta = \xi + i\eta$, the boundary of $\mathcal{D}$ mapping onto the boundary of $\mathcal{D}'$. If $\mathcal{W}(\zeta)$ is regular in $\mathcal{D}'$ with real and imaginary parts $\Phi(\xi, \eta)$, $\Psi(\xi, \eta)$, then $(\partial^2/\partial\xi^2 + \partial^2/\partial\eta^2)(\Phi, \Psi) = 0$ in $\mathcal{D}'$ and the transformation $\zeta = f(z)$ defines a corresponding function $w(z) \equiv \varphi(x, y) +$

Downloaded from https://www.cambridge.org/core. Charité Universitätsmedizin Berlin, on 20 Dec 2021 at 10:08:47, subject to the Cambridge Core terms of use, available at https://www.cambridge.org/core/terms. https://doi.org/10.1017/CBO9781107360273.003

$i\psi(x, y) = \mathcal{W}(f(z)) \equiv \Phi(\xi(x, y), \eta(x, y)) + i\Psi(\xi(x, y), \eta(x, y))$ which is regular in $\mathcal{D}$. That is: the solutions Φ and Ψ of Laplace's equation in $\mathcal{D}'$ are also solutions of Laplace's equation in $\mathcal{D}$.

Irrotational motion of an ideal, incompressible fluid in planes parallel to the xy-plane can be represented by a *complex potential* $w(z) = \varphi(x, y) + i\psi(x, y)$, in terms of which the velocity $\mathbf{v} = \nabla\varphi = (\partial\varphi/\partial x, \partial\varphi/\partial y)$. ψ is called the *stream function*, and the family of curves $\psi(x, y) =$ constant define the instantaneous system of streamlines of the flow. The real and imaginary parts $\varphi(x, y)$, $\psi(x, y)$ satisfy Laplace's equation and the Cauchy–Riemann equations:

$$\frac{\partial\varphi}{\partial x} = \frac{\partial\psi}{\partial y}, \quad \frac{\partial\varphi}{\partial y} = -\frac{\partial\psi}{\partial x},$$

so that $\nabla\varphi \cdot \nabla\psi = 0$, that is, the streamlines intersect the 'equipotentials' $\varphi =$ constant at right angles. If $\mathbf{v} = (u, v)$, these equations imply that the *complex velocity*

$$w'(z) = \frac{\partial\varphi}{\partial x} - i\frac{\partial\varphi}{\partial y} \equiv u - iv.$$

Example 1 $w = Uz$, $U =$ real constant, defines uniform flow at speed U along streamlines parallel to the x-direction: $\varphi = Ux, \quad \psi = Uy$.

Example 2

$$w = U\left(z + \frac{a^2}{z}\right), \quad U = \text{ real constant}, \quad |z| > a > 0,$$

represents steady flow past a rigid cylinder of radius a with centre at the origin (Figure 2.A.1; cf. §2.6.2). At large distances $w \to Uz$, where the motion becomes uniform at speed U parallel to the x-axis. In terms of the polar form $z = re^{i\theta}$, the velocity potential $\varphi = \text{Re}\, w(z)$ is

$$\varphi = U\cos\theta\left(r + \frac{a^2}{r}\right).$$

Example 3

$$w = -iU\left(z - \frac{a^2}{z}\right),$$

$$U = \text{real constant}, \quad |z| > a > 0, \quad \left(\varphi = U\sin\theta\left(r + \frac{a^2}{r}\right)\right),$$

describes potential flow in the y-direction past a rigid cylinder of radius a with centre at the origin.

Downloaded from https://www.cambridge.org/core. Charité Universitätsmedizin Berlin, on 20 Dec 2021 at 10:08:47, subject to the Cambridge Core terms of use, available at https://www.cambridge.org/core/terms. https://doi.org/10.1017/CBO9781107360273.003

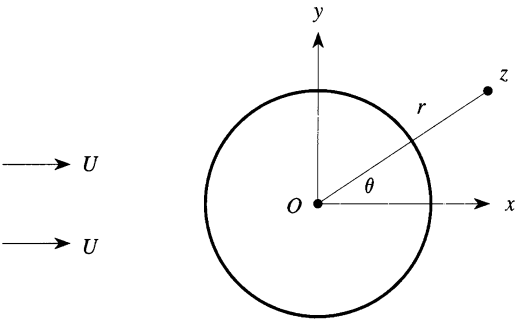

Figure 2.A.1

Example 4

$$w = -\frac{i\Gamma}{2\pi}\ln z, \quad \left(\varphi = \frac{\Gamma\theta}{2\pi},\ \psi = -\frac{\Gamma}{2\pi}\ln r,\ \ z = re^{i\theta}\right),$$

is regular except at $z = 0$, and describes the irrotational flow outside a *line vortex* of strength Γ concentrated at $z = 0$. The streamlines are circles centred at $z = 0$, and the flow speed is $\partial\varphi/r\partial\theta = \Gamma/2\pi r$ in the anticlockwise direction (for $\Gamma > 0$). The circulation $\int_C \mathbf{v}\cdot d\mathbf{x} = \Gamma$, where C is any contour encircling the vortex once, and the contour is traversed in the *positive* direction (with the *interior on the left*). When the vortex is at $z_0 = x_0 + iy_0$

$$w = -\frac{i\Gamma}{2\pi}\ln(z - z_0).$$

Example 5

$$w = -\frac{i\Gamma}{2\pi}\ln(z - z_0) + \frac{i\Gamma}{2\pi}\ln(z - z_0^*),$$

represents the flow produced by two line vortices of circulations $\pm\Gamma$ respectively at $z_0 = x_0 + iy_0,\ z_0^* = x_0 - iy_0$ (Figure 2.A.2). The stream function $\psi = \mathrm{Im}\, w = 0$ on the x-axis, which is therefore a streamline of the flow, on which $\partial\varphi/\partial y = 0$. In the region $y > 0$ the potential describes the flow produced by a vortex of strength Γ at z_0 *adjacent to a rigid wall* at $y = 0$ (which is accounted for by an equal and opposite 'image' vortex). Each vortex translates parallel to the wall at speed $u = \Gamma/4\pi y_o$ determined by the velocity potential of its image. The mean value of the local rotational flow produced by the 'self-potential' of each vortex (Example 4) vanishes on the vortex axis, and cannot therefore cause it to translate.

Downloaded from https://www.cambridge.org/core. Charité Universitätsmedizin Berlin, on 20 Dec 2021 at 10:08:47, subject to the Cambridge Core terms of use, available at https://www.cambridge.org/core/terms. https://doi.org/10.1017/CBO9781107360273.003

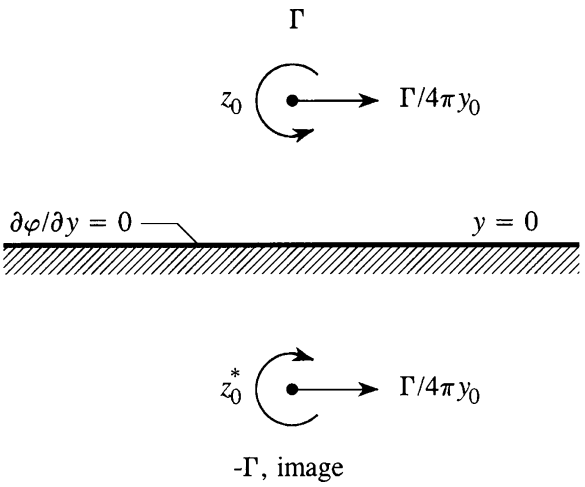

Figure 2.A.2

2.A.2 Conformal transformation

Let the flow past a system of rigid boundaries in the z-plane be represented by means of a conformal transformation $\zeta = f(z)$ by an equivalent flow in the ζ-plane. Point source and vortex singularities of the flow are *preserved* under the transformation. If, for example, $\zeta = \zeta_0$ is the image of a vortex of strength Γ at $z = z_0$, the complex potential in the neighbourhood of ζ_0 (where $\zeta - \zeta_0 \approx f'(z_0)(z - z_0)$) is determined by

$$\begin{aligned} \mathcal{W}(\zeta) \;=\; w(z) &= \frac{-i\Gamma}{2\pi} \ln(z - z_0) + \text{terms finite at } z_0 \\ &= \frac{-i\Gamma}{2\pi} \ln\left(\frac{\zeta - \zeta_0}{f'(z_0)}\right) + \text{terms finite at } \zeta_0 \\ &= \frac{-i\Gamma}{2\pi} \ln(\zeta - \zeta_0) + \text{terms finite at } \zeta_0. \end{aligned}$$

The vortex in the z-plane therefore maps into an equal vortex at the image point in the ζ-plane.

Example 6 The transformation $\zeta = i\sqrt{z}$ maps the z-plane cut along the negative real axis (so that $-\pi < \arg z < \pi$) onto the upper half-plane of $\zeta = \xi + i\eta$ (as in Figure 2.A.3). The complex potential of flow in the positive ξ-direction parallel to the boundary $\eta = 0$ in the ζ-plane corresponds to flow around the edge of the semi-infinite plane $x < 0$, $y = 0$, in the clockwise sense, and has the general representation $\mathcal{W} = \alpha\zeta$, where the constant $\alpha > 0$.

Downloaded from https://www.cambridge.org/core. Charité Universitätsmedizin Berlin, on 20 Dec 2021 at 10:08:47, subject to the Cambridge Core terms of use, available at https://www.cambridge.org/core/terms. https://doi.org/10.1017/CBO9781107360273.003

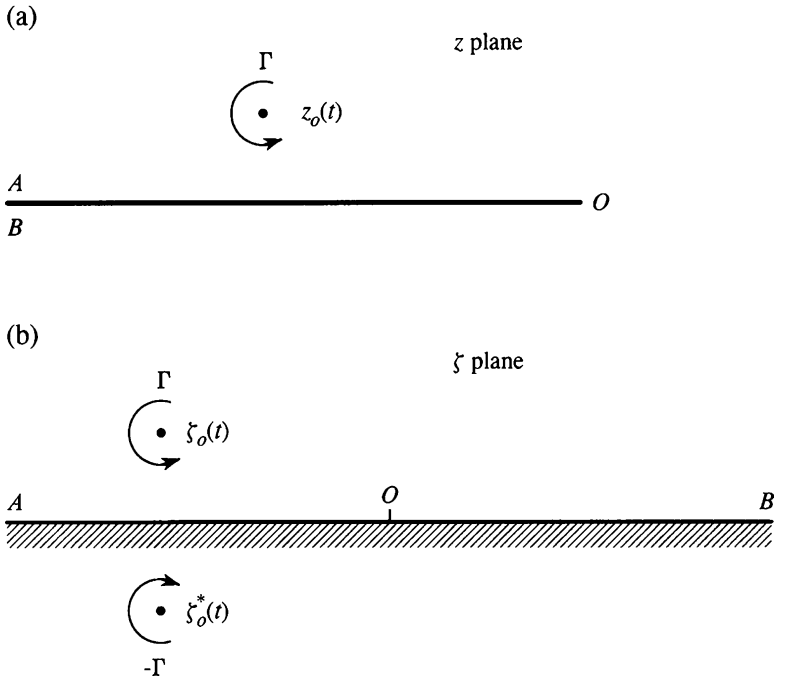

Figure 2.A.3

In the z-plane

$$w = i\alpha\sqrt{z} \equiv -\alpha\sqrt{r}\sin\left(\frac{\theta}{2}\right) + i\alpha\sqrt{r}\cos\left(\frac{\theta}{2}\right), \quad -\pi < \theta < \pi,$$

where $z = re^{i\theta}$. The streamlines are the parabolas $\sqrt{r}\cos\left(\frac{\theta}{2}\right) = \text{constant}$ (see Figure 4.7.3).

2.A.3 Equation of motion of a vortex

A line vortex is convected at the local velocity at its axis (§4.4). For a vortex of strength Γ at $z = z_o(t)$ in the z plane, the velocity is infinite as the core is approached because of the singular velocity induced by its 'self-potential' $-(i\Gamma/2\pi)\ln(z - z_o)$. But the rotational flow around the core cannot induce motion of the core, and this potential must be removed from the complex potential $w(z)$ of the entire flow before calculating the convection velocity of the vortex.

In applications the complex potential $w(z)$ usually occurs in the form

$$w(z) = -\frac{i\Gamma}{2\pi}\ln\Big(\zeta(z) - \zeta(z_o)\Big) + F(z) \qquad (2.A.1)$$

Downloaded from https://www.cambridge.org/core. Charité Universitätsmedizin Berlin, on 20 Dec 2021 at 10:08:47, subject to the Cambridge Core terms of use, available at https://www.cambridge.org/core/terms. https://doi.org/10.1017/CBO9781107360273.003

where $\zeta(z)$, $F(z)$ are regular functions of z in the neighbourhood of the vortex at $z = z_o$. In particular, when $|z - z_o|$ is small

$$\zeta(z) = \zeta(z_o) + (z - z_o)\zeta'(z_o) + \frac{(z - z_o)^2}{2}\zeta''(z_o) + \cdots$$

where the primes denote differentiation with respect to z. Thus, subtracting the self-potential from $w(z)$ we find, near the vortex,

$$\begin{aligned} W(z) &= w(z) + \frac{i\Gamma}{2\pi}\ln(z - z_o) \\ &= -\frac{i\Gamma}{2\pi}\ln\Big(\zeta(z) - \zeta(z_o)\Big) + \frac{i\Gamma}{2\pi}\ln(z - z_o) + F(z) \\ &\approx -\frac{i\Gamma}{2\pi}\ln\left[\zeta'(z_o) + \frac{1}{2}\zeta''(z_o)(z - z_o)\right] + F(z). \end{aligned} \tag{2.A.2}$$

The complex velocity of the vortex is $W'(z_o) \equiv \{W'(z)\}_{z=z_o}$, that is, setting $z_o = x_o + iy_o$,

$$\frac{dz_o^*}{dt} \equiv \frac{dx_o}{dt} - i\frac{dy_o}{dt} = W'(z_o).$$

Using (2.A.2), this becomes

$$\frac{dx_o}{dt} - i\frac{dy_o}{dt} = -\frac{i\Gamma\zeta''(z_o)}{4\pi\zeta'(z_o)} + F'(z_o). \tag{2.A.3}$$

The real and imaginary parts of this equation supply two nonlinear first order ordinary differential equations for the position $(x_o(t), y_o(t))$ of the vortex at time t.

Example 7 Motion of a line vortex of strength $\Gamma > 0$ adjacent to a rigid half-plane lying along the negative real axis ($x < 0$, $y = 0$; Figure 2.A.3a).

The transformation

$$\zeta = i\sqrt{z}, \quad z = x_1 + ix_2, \quad -\pi < \arg z < \pi, \tag{2.A.4}$$

maps the fluid region $-\pi < \arg z < \pi$ into the upper half $\mathrm{Im}\,\zeta > 0$ of the ζ-plane (Figure 2.A.3b). Let the vortex at $z_o(t)$ map into a vortex at $\zeta = \zeta_o(t)$. The velocity potential $w(\zeta)$ of the motion in the ζ-plane is found by introducing an image vortex of strength $-\Gamma$ at $\zeta = \zeta_o^*(t)$ (as in Example 5), in which case

$$w = \frac{-i\Gamma}{2\pi}\ln(\zeta - \zeta_o) + \frac{i\Gamma}{2\pi}\ln(\zeta - \zeta_o^*).$$

Downloaded from https://www.cambridge.org/core. Charité Universitätsmedizin Berlin, on 20 Dec 2021 at 10:08:47, subject to the Cambridge Core terms of use, available at https://www.cambridge.org/core/terms. https://doi.org/10.1017/CBO9781107360273.003

In the z-plane this becomes

$$w(z) = -\frac{i\Gamma}{2\pi}\ln\Big(\zeta(z) - \zeta(z_o)\Big) + \frac{i\Gamma}{2\pi}\ln\Big(\zeta(z) - \zeta^*(z_o)\Big),$$

which is of the form (2.A.1). Hence, the equation of motion (2.A.3) becomes

$$\frac{dx_o}{dt} - i\frac{dy_o}{dt} = \frac{i\Gamma}{8\pi z_o} + \frac{i\Gamma}{4\pi\sqrt{z_o}[\sqrt{z_o} + (\sqrt{z_o})^*]}.$$

Put $z_o = re^{i\theta}$, then the real and imaginary parts of the equation are

$$\frac{dx_o}{dt} \equiv \cos\theta\frac{dr}{dt} - r\sin\theta\frac{d\theta}{dt} = \frac{\Gamma}{8\pi r}\left(\sin\theta + \tan\frac{\theta}{2}\right),$$

$$\frac{dy_o}{dt} \equiv \sin\theta\frac{dr}{dt} + r\cos\theta\frac{d\theta}{dt} = -\frac{\Gamma}{8\pi r}(\cos\theta + 1).$$

Therefore

$$\frac{dr}{dt} = -\frac{\Gamma}{8\pi r}\tan\frac{\theta}{2}, \quad \frac{d\theta}{dt} = -\frac{\Gamma}{4\pi r^2} \tag{2.A.5}$$

$$\text{i.e.} \qquad r\frac{d\theta}{dr} = 2\cot\frac{1}{2}\theta$$

$$\therefore \quad r = \ell\sec\frac{1}{2}\theta, \quad \ell = \text{constant}. \tag{2.A.6}$$

This is the polar equation of the trajectory plotted in Figure 4.7.2 (Chapter 4). The constant length ℓ is equal to the distance of closest approach of the vortex to the edge of the half-plane, which occurs at $\theta = 0$. Substituting for r in the second of equations (2.A.5), we find

$$\sec^2\left(\frac{1}{2}\theta\right)\frac{d\theta}{dt} = -\frac{\Gamma}{4\pi\ell^2}, \qquad \therefore \quad \theta = 2\tan^{-1}\left(-\frac{\Gamma t}{8\pi\ell^2}\right),$$

where time is measured from the instant at which $\theta = 0$. The dependence of r on t is now obtained by substituting into (2.A.6).

Collecting together these results, we have:

$$r = \ell\sqrt{1 + \left(\frac{Ut}{\ell}\right)^2}, \quad \theta = 2\tan^{-1}\left(-\frac{Ut}{\ell}\right);$$

$$\frac{x_o}{\ell} = \frac{1 - (Ut/\ell)^2}{\sqrt{1 + (Ut/\ell)^2}}, \quad \frac{y_o}{\ell} = \frac{-2Ut/\ell}{\sqrt{1 + (Ut/\ell)^2}}, \quad \text{where } U = \frac{\Gamma}{8\pi\ell}. \tag{2.A.7}$$

Downloaded from https://www.cambridge.org/core. Charité Universitätsmedizin Berlin, on 20 Dec 2021 at 10:08:47, subject to the Cambridge Core terms of use, available at https://www.cambridge.org/core/terms. https://doi.org/10.1017/CBO9781107360273.003

Thus, (for $\Gamma > 0$) the vortex starts above the half-plane at $t = -\infty$ at $x_o = -\infty$, $y_o = 2\ell$ and translates towards the edge, initially at speed U parallel to the plane. It crosses the x-axis at $t = 0$ at $x_o = \ell$, and proceeds along a symmetrical path below the half-plane (see Figure 4.7.2).

2.A.4 Numerical integration of the vortex path equation

It is usually necessary to integrate equation (2.A.3) numerically. The time and space variables should first be non-dimensionalised with respect to convenient time and length scales defined by the problem. The integration is started from a prescribed point on the trajectory through which the vortex is required to pass.

Consider integration by means of a fourth-order *Runge–Kutta* procedure. Write the equation of motion (2.A.3) in the form

$$\frac{dz_o}{dt} = f^*(z_o), \quad \text{where} \quad f(z_o) = -\frac{i\Gamma\zeta''(z_o)}{4\pi\zeta'(z_o)} + F'(z_o),$$

and let h be a suitably small integration time step (which need not be constant). Assume that at time t_n the vortex is at $z_o(t_n) = z_o^n$. To determine the complex position z_o^{n+1} at time $t_{n+1} = t_n + h$ we evaluate

$$k_1 = hf^*(z_o^n), \quad k_2 = hf^*\left(z_o^n + \frac{1}{2}k_1\right),$$

$$k_3 = hf^*\left(z_o^n + \frac{1}{2}k_2\right), \quad k_4 = hf^*\left(z_o^n + k_3\right),$$

and then find

$$z_o^{n+1} = z_o^n + \frac{1}{6}\left(k_1 + 2k_2 + 2k_3 + k_4\right).$$

Problems 2

2.1. Use the compact Green's function to solve

$$\left(\nabla^2 + k_o^2\right)\hat{\varphi} = f_2\frac{\partial}{\partial x_2}\left[\delta(x_1 - L)\delta(x_2)\delta(x_3)\right],$$

$$\text{where} \quad \frac{\partial\varphi}{\partial x_n} = 0 \text{ on } |\mathbf{x}| = a,$$

for the sound radiated by an azimuthally orientated dipole adjacent to a compact, rigid sphere.

2.2. Use the compact Green's function to solve

$$\left(\nabla^2 + k_o^2\right)\hat{\varphi} = f_1\frac{\partial}{\partial x_1}\left[\delta(x_1 - L)\delta(x_2)\delta(x_3)\right],$$

$$\text{where} \quad \frac{\partial\varphi}{\partial x_n} = 0 \text{ on } (x_1^2 + y_2^2)^{\frac{1}{2}} = a,$$

Downloaded from https://www.cambridge.org/core. Charité Universitätsmedizin Berlin, on 20 Dec 2021 at 10:08:47, subject to the Cambridge Core terms of use, available at https://www.cambridge.org/core/terms. https://doi.org/10.1017/CBO9781107360273.003

for the sound radiated by a radially orientated dipole adjacent to a rigid circular cylinder of compact cross-section.

2.3. Repeat Question 2.2 for the dipoles

$$f_2 \frac{\partial}{\partial x_2}\left[\delta(x_1 - L)\delta(x_2)\delta(x_3)\right], \quad f_3 \frac{\partial}{\partial x_3}\left[\delta(x_1 - L)\delta(x_2)\delta(x_3)\right].$$

2.4.* The constant strength dipole

$$q(\mathbf{x}, t) = f_2 \frac{\partial}{\partial x_2}\left(\delta(x_1 - Ut)\delta(x_2 - h)\delta(x_3)\right), \quad f_2 = \text{constant}$$

translates at *constant* velocity U past a fixed rigid cylinder of radius $a < h$ whose axis coincides with the x_3-axis. Show that when $M = U/c_o \ll 1$, the far field acoustic potential determined by equation (2.1.9) is given by

$$\varphi \approx \frac{f_2 M a^2}{2\pi|\mathbf{x}|(h^2 + U^2[t]^2)^3} \times \left\{\frac{x_1 h}{|\mathbf{x}|}(3U^2[t]^2 - h^2) + \frac{x_2 U[t]}{|\mathbf{x}|}(3h^2 - U^2[t]^2)\right\},$$

where $[t] = t - \dfrac{|\mathbf{x}|}{c_o}$.

2.5.* The volume source

$$q(\mathbf{x}, t) = q_o \delta(x_1 - Ut)\delta(x_2 - h)\delta(x_3), \quad q_o = \text{constant}$$

translates at *constant* velocity U past a fixed rigid sphere of radius $a < h$ whose centre is at the origin. Determine from equation (2.1.9) the far field acoustic perturbation of the velocity potential produced by the sphere given that $M = U/c_o \ll 1$.

2.6.* The point source $q(\mathbf{x}, t) = q_o \delta(x_1 - Ut)\delta(x_2)\delta(x_3)$, ($q_o$ = constant) convects along the axis of symmetry of the necked duct shown in Figure 2.9.3b at constant, low Mach number speed U. If the cross-sectional area of the duct is denoted by $S(x_1)$, where $S(x_1) \to A$, $x_1 \to \pm\infty$, use the approximations

$$X_1 = A\int_0^{x_1} \frac{d\xi}{S(\xi)}, \quad Y_1 = A\int_0^{y_1} \frac{d\xi}{S(\xi)},$$

to calculate the acoustic pressure radiated from the neck during the passage of the source.

2.7. In incompressible flow the velocity potential generated by a distribution of sources $q(\mathbf{x}, t)$ near a rigid body is determined by the solution of

$$\nabla^2 \varphi = q(\mathbf{x}, t).$$

Downloaded from https://www.cambridge.org/core. Charité Universitätsmedizin Berlin, on 20 Dec 2021 at 10:08:47, subject to the Cambridge Core terms of use, available at https://www.cambridge.org/core/terms. https://doi.org/10.1017/CBO9781107360273.003

Show that the monopole and dipole components of the solution at large distances from the body in an unbounded fluid (in the *hydrodynamic* far field) can be calculated using the following incompressible limit of the compact Green's function

$$G(\mathbf{x}, \mathbf{y}, t-\tau) = \frac{-\delta(t-\tau)}{4\pi|\mathbf{X}-\mathbf{Y}|}.$$

2.8. A rigid body translates without rotation in the j-direction at velocity $U_j(t)$ in an ideal, incompressible fluid at rest at infinity . Show that the velocity potential is

$$\Phi = U_j \varphi_j^*.$$

In a fixed reference frame the pressure can be calculated from Bernoulli's equation:

$$\frac{\partial \Phi}{\partial t} + \frac{p}{\rho_o} + \frac{1}{2}(\nabla\Phi)^2 = 0.$$

Use these results to prove formula (2.8.5) for the force exerted on the fluid by the body.

2.9.* A compact rigid disc of radius a executes small amplitude vibrations at velocity $U(t)$ normal to itself. In the undisturbed state it lies in the plane $x_1 = 0$ with its centre at the origin. If $\varphi_1^*(\mathbf{x}) = \mp(2/\pi)\sqrt{a^2 - x_2^2 - x_3^2}$ on the faces $x_1 = \pm 0$, $\sqrt{x_2^2 + x_3^2} < a$ of the disc, show that the acoustic pressure generated by the motion is given by

$$p(\mathbf{x}, t) \approx \frac{2\rho_o a^3 \cos\theta}{3\pi c_o |\mathbf{x}|} \frac{\partial^2 U}{\partial t^2}(t - |\mathbf{x}|/c_o), \quad |\mathbf{x}| \to \infty, \quad \cos\theta = \frac{x_1}{|\mathbf{x}|}.$$

2.10. Show that the acoustic pressure p_s scattered when a sound wave $p_I(\mathbf{x}, t)$ is incident on a compact, stationary rigid body of volume Δ is determined at large distances by the outgoing solution of

$$\left(\frac{1}{c_o^2}\frac{\partial^2}{\partial t^2} - \nabla^2\right) p_s = \rho_o \frac{\partial}{\partial t}\big(q\delta(\mathbf{x})\big) - \operatorname{div}\big(\mathbf{f}\delta(\mathbf{x})\big),$$

$$q = \frac{\Delta}{\rho_o c_o^2}\frac{\partial p_I}{\partial t}; \quad \mathrm{f}_i = (m_o\delta_{ij} + M_{ij})\frac{1}{\rho_o}\frac{\partial p_I}{\partial x_j},$$

where the coordinate origin is within the body and m_o is the mass of fluid displaced by the body. The monopole strength q is equal and opposite to the volume flux into a surface that just encloses the body produced by the incident sound alone; $\mathbf{f}$ is the net force exerted on the fluid by the body.

Downloaded from https://www.cambridge.org/core. Charité Universitätsmedizin Berlin, on 20 Dec 2021 at 10:08:47, subject to the Cambridge Core terms of use, available at https://www.cambridge.org/core/terms. https://doi.org/10.1017/CBO9781107360273.003

2.11.* Let the sphere in the Rayleigh scattering problem of Figure 2.8.3 have mass m and be free to execute small amplitude translational motions parallel to the x_1 axis under the influence of the incident wave. Show that the scattered pressure is then given by

$$p_s \approx \frac{m_o}{4\pi\rho_o c_o^2|\mathbf{x}|}\left(1-\frac{3(m-m_o)}{(2m+m_o)}\cos\theta\right)\left[\frac{\partial^2 p_{\mathrm{I}}}{\partial t^2}\right], \quad |\mathbf{x}|\to\infty,$$

where the square brackets denote evaluation at the retarded time.

2.12.* Calculate the trajectories of a vortex pair consisting of two parallel line vortices of strengths $\pm\Gamma$ moving under their mutual induction towards a rigid plane parallel to the line of centres of the vortices.

2.13.* Show that the transformation $\zeta = \sqrt{z^2/a^2+1},\ a>0$ maps the upper z-plane cut by a thin rigid barrier along the imaginary axis between $z=0$ and $z=ia$ onto the upper ζ-plane. Hence deduce that a line vortex Γ at $z=z_o(t)$ traverses a path determined by the equation

$$\frac{dz_o^*}{dt} = -\frac{i\Gamma}{4\pi}\left\{\frac{a^2}{z_o(z_o^2+a^2)} - \frac{2z_o}{z_o^2+a^2-|z_o^2+a^2|}\right\},$$

provided the fluid is at rest at infinity.

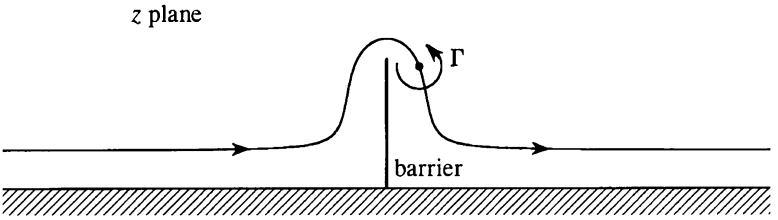

Downloaded from https://www.cambridge.org/core. Charité Universitätsmedizin Berlin, on 20 Dec 2021 at 10:08:47, subject to the Cambridge Core terms of use, available at https://www.cambridge.org/core/terms. https://doi.org/10.1017/CBO9781107360273.003

3

Piston and Diffraction Problems

3.1 Radiation from a baffled piston

A compact vibrating body radiates sound of dipole strength (§2.1.3). Thus the acoustic pressure produced by a small disc of radius a vibrating back and forth at normal velocity $U(t)$ (Figure 3.1.1; see Question 2.9, **Problems 2**) is given by

$$p(\mathbf{x}, t) \approx \frac{2\rho_o a^3 \cos\theta}{3\pi c_o r} \frac{\partial^2 U}{\partial t^2}(t - r/c_o), \quad r \equiv |\mathbf{x}| \to \infty, \quad \cos\theta = \frac{x_1}{|\mathbf{x}|}.$$

This is smaller by a factor of order $k_o a = \omega a/c_o$ ($\ll 1$) than the monopole radiation from a small sphere of the same radius pulsating at normal velocity U and frequency $\omega \sim \partial/\partial t$. The sound produced by the disc is attributable to equal and opposite monopoles on its front and back faces – one forces fluid out of the way of the advancing disc and the other draws in an equal flux of fluid in its wake. Their acoustic pressures almost cancel in the far field, but there is a residual dipole pressure dependent on the small difference in the effective travel times of sound from the front and back faces.

The compact disc is a good model for studying sound production by a loudspeaker cone. In an open environment it is a very poor radiator compared, for example, to the monopole sound of a spherical speaker. Cancellation between the front and back monopoles is usually prevented by placing the cone in an opening (with sealed edges) in the side of a box-like enclosure, so that only the front of the cone can radiate. The same increase in radiation efficiency is achieved when the disc is placed within a circular aperture of slightly larger radius cut into a large, plane 'baffle', much larger than the characteristic wavelength of the sound, so that the disc vibrates without friction and leakage at its edge. Such a disc is called a 'baffled piston'.

Let the exposed piston face S_p, say, and the baffle occupy the plane $x_1 = 0$ in the undisturbed state (Figure 3.1.2). This plane will be identified with the surface S of the generalised Kirchhoff formula (2.1.6), with $q = 0$, $\mathbf{F} = 0$. The

Downloaded from https://www.cambridge.org/core. Charité Universitätsmedizin Berlin, on 20 Dec 2021 at 10:08:47, subject to the Cambridge Core terms of use, available at https://www.cambridge.org/core/terms. https://doi.org/10.1017/CBO9781107360273.004

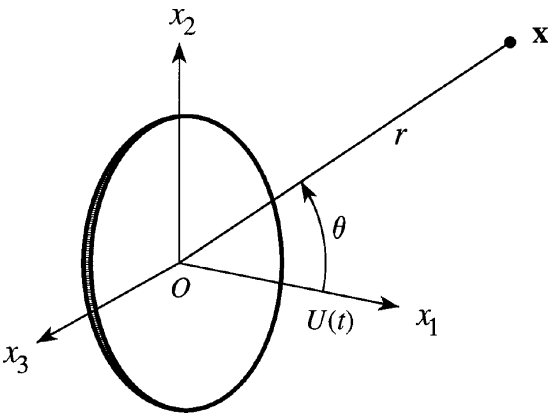

Figure 3.1.1

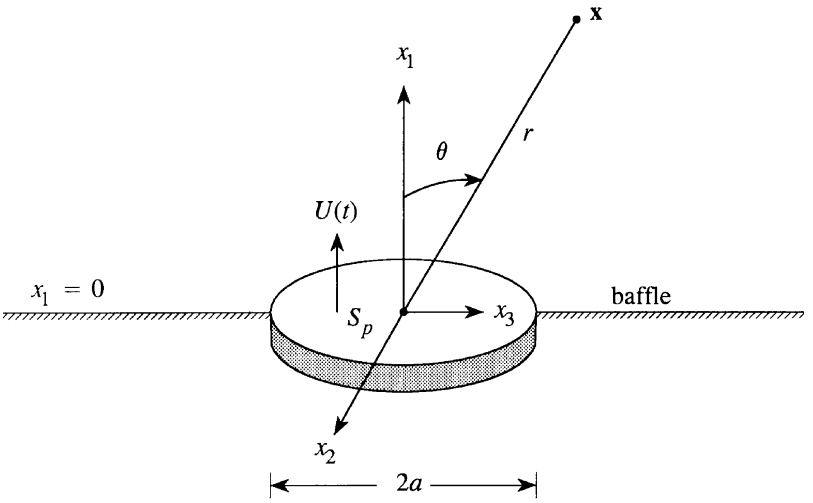

Figure 3.1.2

normal velocity $v_n(\mathbf{x}, t)$ vanishes on S except on S_p, where it is assumed that $v_n(\mathbf{x}, t) = U(t)$. The unknown surface pressure on S is eliminated by taking G to be the rigid wall Green's function (2.1.7), in the form

$$G(\mathbf{x}, \mathbf{y}, t-\tau) = \frac{1}{4\pi|\mathbf{x}-\mathbf{y}|}\delta\left(t-\tau-\frac{|\mathbf{x}-\mathbf{y}|}{c_o}\right) + \frac{1}{4\pi|\bar{\mathbf{x}}-\mathbf{y}|}\delta\left(t-\tau-\frac{|\bar{\mathbf{x}}-\mathbf{y}|}{c_o}\right), \tag{3.1.1}$$

where $\bar{\mathbf{x}} = (-x_1, x_2, x_3)$ and $\partial G/\partial y_1 = 0$ on $y_1 = 0$.

Downloaded from https://www.cambridge.org/core. Charité Universitätsmedizin Berlin, on 20 Dec 2021 at 10:08:47, subject to the Cambridge Core terms of use, available at https://www.cambridge.org/core/terms. https://doi.org/10.1017/CBO9781107360273.004

The pressure in $x_1 > 0$ is then given by *Rayleigh's integral*

$$p(\mathbf{x}, t) = \rho_o \frac{\partial}{\partial t} \oint_{y_1=0} G(\mathbf{x}, \mathbf{y}, t-\tau) v_n(\mathbf{y}, \tau)\, dy_2 dy_3 d\tau$$

$$= \frac{\rho_o}{2\pi} \frac{\partial}{\partial t} \oint_{S_p} U\left(t - \frac{|\mathbf{x}-\mathbf{y}|}{c_o}\right) \frac{dy_2 dy_3}{|\mathbf{x}-\mathbf{y}|}, \tag{3.1.2}$$

where S_p is the region $y_2^2 + y_3^2 < a^2,\ y_1 = 0$ for a piston of radius a.

3.1.1 Time-harmonic oscillations

In the far field (3.1.2) becomes (§1.10)

$$p(\mathbf{x}, t) \approx \frac{\rho_o}{2\pi |\mathbf{x}|} \frac{\partial}{\partial t} \oint_{S_p} U\left(t - \frac{|\mathbf{x}|}{c_o} + \frac{\mathbf{x}\cdot\mathbf{y}}{c_o|\mathbf{x}|}\right) dy_2 dy_3, \quad |\mathbf{x}| \to \infty.$$

Retarded time variations $\mathbf{x}\cdot\mathbf{y}/c_o|\mathbf{x}|$ can be neglected on S_p when the piston is compact. The pressure is then given by the monopole formula

$$p(\mathbf{x}, t) \approx \frac{\rho_o}{2\pi |\mathbf{x}|} \frac{\partial Q}{\partial t}\left(t - \frac{|\mathbf{x}|}{c_o}\right), \quad |\mathbf{x}| \to \infty, \tag{3.1.3}$$

where $Q(t) = \pi a^2 U(t)$ is the volume source strength of the piston. The pressure has *twice* the amplitude of a source of equal strength radiating into free space (cf. (1.8.1)), and the power radiated by the piston is four times that from a free field source into the half-space $x_1 > 0$.

The omni-directional behaviour is absent at higher frequencies, when phase variations across the face of the piston cannot be ignored. If we set $U(t) = \int_{-\infty}^{\infty} \hat{U}(\omega) e^{-i\omega t} d\omega$ and consider the acoustic pressure $\hat{p}(\mathbf{x}, \omega) e^{-i\omega t}$ for each frequency ω, equation (3.1.2) becomes

$$\hat{p}(\mathbf{x}, \omega) = \frac{-i\omega\rho_o \hat{U}}{2\pi} \oint_{S_p} e^{ik_o|\mathbf{x}-\mathbf{y}|} \frac{dy_2 dy_3}{|\mathbf{x}-\mathbf{y}|} \quad (k_o = \omega/c_o)$$

$$\approx \frac{-i\omega\rho_o \hat{U} e^{ik_o|\mathbf{x}|}}{2\pi|\mathbf{x}|} \oint_{S_p} e^{-ik_o \mathbf{x}\cdot\mathbf{y}/|\mathbf{x}|}\, dy_2 dy_3 \ \ (|\mathbf{x}| \to \infty)$$

$$= \frac{-i\omega\rho_o \hat{U} e^{ik_o|\mathbf{x}|}}{2\pi|\mathbf{x}|} \int_0^a d\varpi \int_0^{2\pi} \varpi\, e^{-ik_o \varpi \sin\theta \cos\phi} d\phi\,, \tag{3.1.4}$$

where θ defines the direction to the observer at $\mathbf{x}$ in the far field (Figure 3.1.2), $\varpi = (y_2^2 + y_3^2)^{\frac{1}{2}}$, and ϕ is the angle between the vectors $(0, y_2, y_3),\ (0, x_2, x_3)$

Downloaded from https://www.cambridge.org/core. Charité Universitätsmedizin Berlin, on 20 Dec 2021 at 10:08:47, subject to the Cambridge Core terms of use, available at https://www.cambridge.org/core/terms. https://doi.org/10.1017/CBO9781107360273.004

in the plane of the baffle. The double integral is evaluated as follows (Abramowitz & Stegun 1970):

$$\int_0^{2\pi} \mathrm{e}^{-ik_o\varpi \sin\theta\cos\phi}\,d\phi = 2\int_0^{\pi} \cos(k_o\varpi \sin\theta\cos\phi)\,d\phi$$
$$= 2\pi \mathrm{J}_0(k_o\varpi \sin\theta)$$

$$2\pi\int_0^a \varpi \mathrm{J}_0(k_o\varpi \sin\theta)\,d\varpi = \frac{2\pi}{(k_o\sin\theta)^2}\int_0^{k_o a\sin\theta} \xi \mathrm{J}_0(\xi)\,d\xi$$
$$= \pi a^2 \frac{2\mathrm{J}_1(k_o a\sin\theta)}{k_o a\sin\theta},$$

where J_0, J_1 are Bessel functions, and the formula $\int z\mathrm{J}_0(z)\,dz = z\mathrm{J}_1(z)$ has been used. Hence

$$\hat{p}(\mathbf{x},\omega) \approx -\frac{i\omega\rho_o\hat{Q}}{2\pi|\mathbf{x}|}\left(\frac{2\mathrm{J}_1(k_o a\sin\theta)}{k_o a\sin\theta}\right)\mathrm{e}^{ik_o|\mathbf{x}|}, \quad |\mathbf{x}|\to\infty, \tag{3.1.5}$$

where $\hat{Q}(\omega) = \pi a^2\hat{U}(\omega)$ is the Fourier transform of the piston source strength. In the compact limit $\mathrm{J}_1(k_o a\sin\theta) \sim \frac{1}{2}k_o a\sin\theta$, and (3.1.5) reduces to the Fourier transform of the compact approximation (3.1.3): $\hat{p}_o(\mathbf{x},\omega) = -(i\omega\rho_o\hat{Q}/2\pi|\mathbf{x}|)\mathrm{e}^{ik_o|\mathbf{x}|}$, say, so that

$$\frac{\hat{p}(\mathbf{x},\omega)}{\hat{p}_o(\mathbf{x},\omega)} \approx \frac{2\mathrm{J}_1(k_o a\sin\theta)}{k_o a\sin\theta}. \tag{3.1.6}$$

This compares the acoustic pressure at frequency ω and direction θ to the monopole pressure produced by a point-sized piston of the same strength. The pressure radiated in the normal direction is always equal to the compact limit, because $2\mathrm{J}_1(k_o a\sin\theta)/k_o a\sin\theta \to 1$ as $\theta\to 0$. The result can also be expressed as a ratio of the acoustic intensities (1.9.8) $I(\theta) = |\hat{p}(\mathbf{x},\omega)|^2/\rho_o c_o$ and $I_o = |\hat{p}_o(\mathbf{x},\omega)|^2/\rho_o c_o$, namely,

$$\frac{I(\theta)}{I_o} = \left(\frac{2\mathrm{J}_1(k_o a\sin\theta)}{k_o a\sin\theta}\right)^2. \tag{3.1.7}$$

$10\times\log_{10}(I(\theta)/I_o)$ dB is plotted in Figure 3.1.3 for several values of $k_o a = 2\pi a/\lambda$ = piston circumference/acoustic wavelength. The piston behaves as a monopole for $2\pi a < \lambda$, but the wave pattern becomes directive when the circumference exceeds about three wavelengths, and when $2\pi a/\lambda > 3.83$ (the first positive zero of $\mathrm{J}_1(z)$) radiation 'lobes' develop separated by nulls in the directivity. Most of the energy radiates in the main lobe, for $\sin\theta < 3.83/k_o a = 0.61\lambda/a$. The lobe maxima decrease with angular distance from the principal lobe at $\theta = 0$ and their number increases with $k_o a$. This is typical of the directivity patterns of a single cone loud-speaker.

Downloaded from https://www.cambridge.org/core. Charité Universitätsmedizin Berlin, on 20 Dec 2021 at 10:08:47, subject to the Cambridge Core terms of use, available at https://www.cambridge.org/core/terms. https://doi.org/10.1017/CBO9781107360273.004

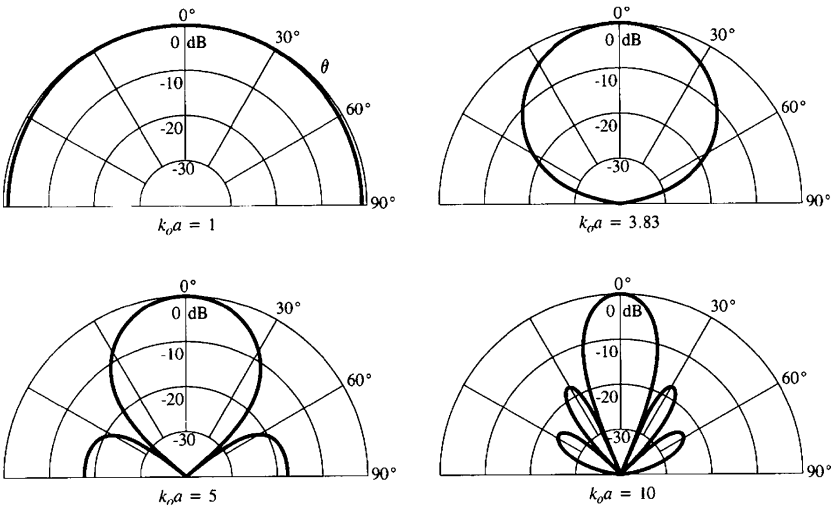

Figure 3.1.3

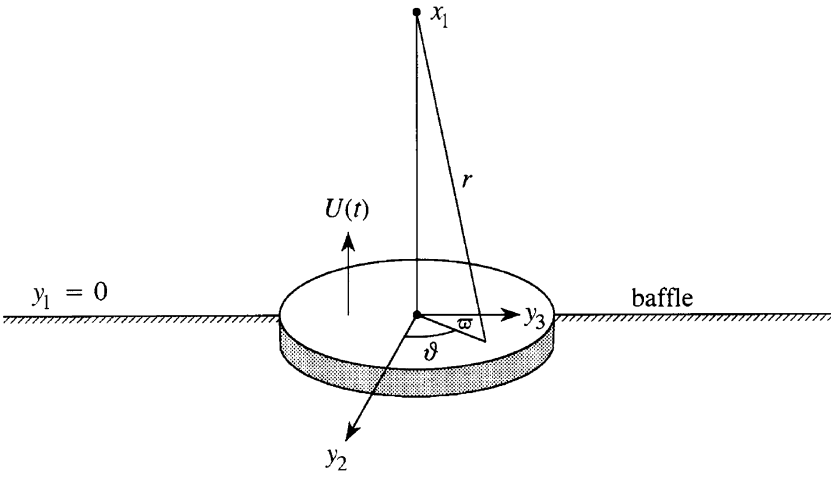

Figure 3.1.4

3.1.2 Pressure on the axis of symmetry

Rayleigh's integral (3.1.2) can be evaluated explicitly for points $\mathbf{x} = (x_1, 0, 0)$ on the axis of symmetry of the piston (Figure 3.1.4). Introduce polar coordinates $y_2 = \varpi \cos\vartheta$, $y_3 = \varpi \sin\vartheta$, $dy_2 dy_3 = \varpi d\varpi d\vartheta$, $(0 < \vartheta < 2\pi,\ 0 < \varpi < a)$. The relation $r^2 \equiv |\mathbf{x} - \mathbf{y}|^2 = x_1^2 + \varpi^2$ implies that $\varpi d\varpi = rdr$, where $x_1 < r < (x_1^2 + a^2)^{\frac{1}{2}}$, and (3.1.2) therefore yields the exact formula

Downloaded from https://www.cambridge.org/core. Charité Universitätsmedizin Berlin, on 20 Dec 2021 at 10:08:47, subject to the Cambridge Core terms of use, available at https://www.cambridge.org/core/terms. https://doi.org/10.1017/CBO9781107360273.004

$$p(\mathbf{x},t)=\frac{\rho_o}{2\pi}\frac{\partial}{\partial t}\oint_{S_p} U\left(t-\frac{r}{c_o}\right)drd\vartheta=-\rho_o c_o\int_{x_1}^{\sqrt{x_1^2+a^2}}\frac{\partial U}{\partial r}\left(t-\frac{r}{c_o}\right)dr$$

$$=\rho_o c_o\,U\left(t-\frac{x_1}{c_o}\right)-\rho_o c_o\,U\left(t-\frac{(x_1^2+a^2)^{\frac{1}{2}}}{c_o}\right). \tag{3.1.8}$$

The first term on the right is like a plane wave generated by a piston in a uniform duct (§1.3.3, Example 1). The second represents an axisymmetric disturbance propagating from the circular edge of the piston. The pressure ultimately decreases like $1/x_1$, and the transition to the far field occurs when x_1 is large enough that

$$U\left(t-\frac{(x_1^2+a^2)^{\frac{1}{2}}}{c_o}\right)\approx U\left(t-\frac{x_1}{c_o}-\frac{a^2}{2c_o x_1}\right)$$

$$\approx U\left(t-\frac{x_1}{c_o}\right)-\frac{a^2}{2c_o x_1}\frac{\partial U}{\partial t}\left(t-\frac{x_1}{c_o}\right).$$

The approximation (3.1.3), which is valid on the axis of symmetry, is recovered when this is substituted into (3.1.8).

The far field emerges when $x_1\gg a$ and also at sufficiently large distances $x_1>k_o a^2/2$ that depend on the frequency $\omega\sim(1/U)\partial U/\partial t$. $R_o\equiv k_o a^2/2=\pi a^2/\lambda$ can be regarded as the distance beyond which the Fraunhofer approximation becomes applicable (§1.10.5). At shorter distances (within the 'Fresnel zone') large fluctuations of pressure can occur by interference between the two waves of (3.1.8). Thus, for time-harmonic piston velocity $\hat{U}(\omega)\mathrm{e}^{-i\omega t}$ (3.1.8) becomes

$$\hat{p}(\mathbf{x},\omega)=\rho_o c_o\hat{U}\left(\mathrm{e}^{ik_o x_1}-\mathrm{e}^{ik_o(x_1^2+a^2)^{\frac{1}{2}}}\right)$$

$$=-2i\rho_o c_o\hat{U}\mathrm{e}^{ik_o\{x_1+(x_1^2+a^2)^{\frac{1}{2}}\}/2}\sin\left(\frac{k_o}{2}\left((x_1^2+a^2)^{\frac{1}{2}}-x_1\right)\right) \tag{3.1.9}$$

$$\approx-2i\rho_o c_o\hat{U}\mathrm{e}^{ik_o x_1}\sin\left(\frac{R_o}{2x_1}\right),\quad\text{for } x_1\gg a.$$

Destructive interference between the plane wave $\rho_o c_o\hat{U}\mathrm{e}^{ik_o x_1}$ and the axisymmetric edge wave occurs where the argument of the sine in (3.1.9) is a multiple of π, at

$$\frac{x_1}{R_o}=\frac{(a/\lambda)^2-n^2}{2n\pi(a/\lambda)^2}\left(\sim\frac{1}{2n\pi}\ \text{ for } x_1\gg a\right),\quad\text{where } 1\le n\le\left[a/\lambda\right],$$

where $[x]$ denotes the greatest integer not greater than x, the case $n=1$ being farthest from the piston. Similarly, wave reinforcement where

Downloaded from https://www.cambridge.org/core. Charité Universitätsmedizin Berlin, on 20 Dec 2021 at 10:08:47, subject to the Cambridge Core terms of use, available at https://www.cambridge.org/core/terms. https://doi.org/10.1017/CBO9781107360273.004

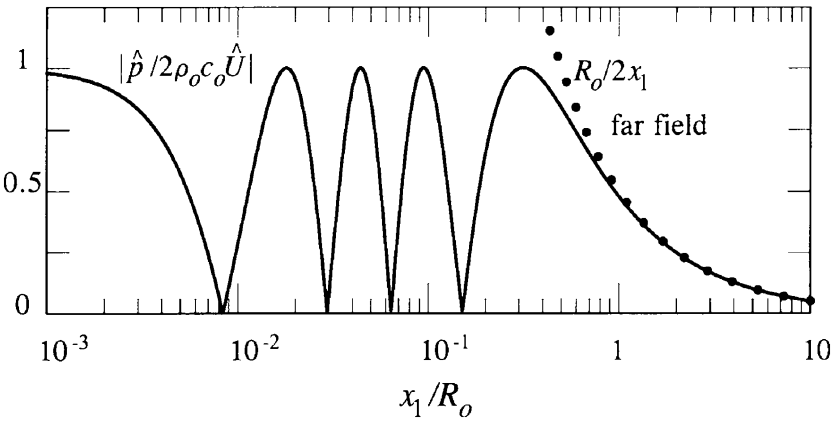

Figure 3.1.5

$|\hat{p}(\mathbf{x},\omega)/2\rho_o c_o \hat{U}| = 1$ is found at values of x_1 where the argument of the sine is an odd multiple of $\pi/2$:

$$\frac{x_1}{R_o} = \frac{(a/\lambda)^2 - (n-\frac{1}{2})^2}{2(n-\frac{1}{2})\pi(a/\lambda)^2} \left(\sim \frac{1}{(2n-1)\pi} \quad \text{for } x_1 \gg a \right),$$

$$\text{where } 1 \le n \le \left[\tfrac{1}{2} + \tfrac{a}{\lambda} \right].$$

The last peak ($n = 1$) at $x_1 \sim 0.3R_o$ marks the onset of the far field – at larger distances the propagation path difference between the edge and plane waves ($= (x_1^2 + a^2)^{\frac{1}{2}} - x_1 \sim a^2/2x_1$) becomes progressively smaller and their residual difference governs the decay in the far field. This is clear from Figure 3.1.5, where $|\hat{p}(\mathbf{x},\omega)/2\rho_o c_o \hat{U}|$ is plotted against x_1/R_o for $k_o a/2\pi = 4.5$ ($R_o \sim 14a$), so that there are 4 pressure nulls along the axis of symmetry within the Fresnel zone. Also plotted is the far field limit $|\hat{p}(\mathbf{x},\omega)/2\rho_o c_o \hat{U}| \approx R_o/2x_1$. The transition to the far field is complete at $x_1 \approx R_o$.

3.1.3 The Fresnel zone*

The large pressure fluctuations on the piston axis when $k_o a \gg 1$ occur because waves from the edge of the circular piston arrive *in phase* at a given point on the axis, reinforcing to produce a pressure amplitude of the same magnitude as the plane wave $\rho_o c_o\, U(t - x_1/c_o)$. This reinforcement is weaker at off-axis points, and at very high frequencies destructive interference can reduce the edge wave contribution so that within the Fresnel zone $x_1 \ll R_o$ the pressure is dominated by the plane wave at off-axis points within the circular cylindrical beam formed by the projection of the piston cross-section $x_1 > 0$, $(x_2^2 + x_3^2)^{\frac{1}{2}} < a$. The pressure outside the 'beam' decays very rapidly with radial distance $(x_2^2 + x_3^2)^{\frac{1}{2}}$.

Downloaded from https://www.cambridge.org/core. Charité Universitätsmedizin Berlin, on 20 Dec 2021 at 10:08:47, subject to the Cambridge Core terms of use, available at https://www.cambridge.org/core/terms. https://doi.org/10.1017/CBO9781107360273.004

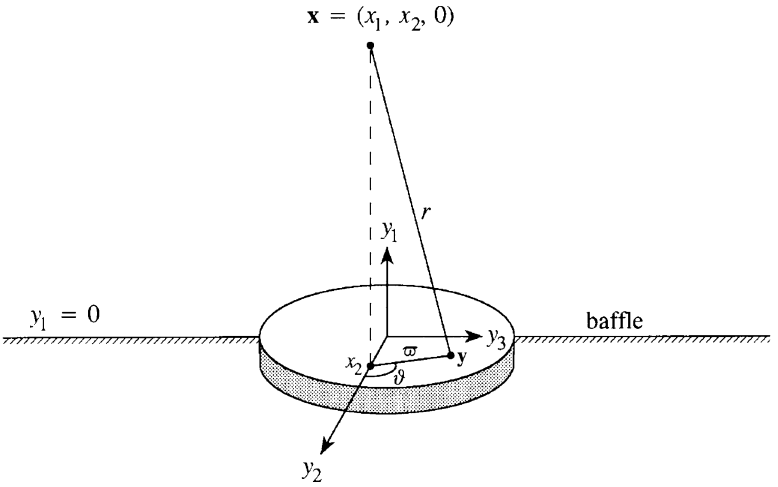

Figure 3.1.6

Let us consider the pressure at a typical point $\mathbf{x} = (x_1, x_2, 0)$, where $0 < x_2 < a$ within the main beam of the Fresnel zone (Figure 3.1.6). Starting from equation (3.1.2), introduce polar coordinates (ϖ, ϑ) on the face of the piston with the origin shifted to $\mathbf{y} = (0, x_2, 0)$ (the normal projection of $\mathbf{x}$ onto the piston) such that $dy_2 dy_3 = \varpi d\varpi d\vartheta$, $(0 < \vartheta < 2\pi,\ 0 < \varpi < \varpi_{\max}(\vartheta))$, where $\varpi_{\max}(\vartheta)$ is the distance along the ϑ direction from the new origin to the edge of the piston. Put $r = |\mathbf{x} - \mathbf{y}| = (x_1^2 + \varpi^2)^{\frac{1}{2}}$, $\varpi d\varpi = rdr$ where $x_1 < r < r_{\max}(\vartheta) = (x_1^2 + \varpi_{\max}^2(\vartheta))^{\frac{1}{2}}$. Then

$$
\begin{aligned}
p(\mathbf{x}, t) &= \frac{\rho_o}{2\pi} \frac{\partial}{\partial t} \oint_{S_p} U\left(t - \frac{r}{c_o}\right) dr d\vartheta \\
&= -\frac{\rho_o c_o}{2\pi} \int_0^{2\pi} d\vartheta \int_{x_1}^{r_{\max}(\vartheta)} \frac{\partial U}{\partial r}\left(t - \frac{r}{c_o}\right) dr \\
&= \rho_o c_o\, U\left(t - \frac{x_1}{c_o}\right) - \frac{\rho_o c_o}{2\pi} \int_0^{2\pi} U\left(t - \frac{r_{\max}(\vartheta)}{c_o}\right) d\vartheta.
\end{aligned}
$$

For time-harmonic piston velocity $\hat{U}(\omega)\mathrm{e}^{-i\omega t}$ this becomes

$$
\frac{\hat{p}(\mathbf{x}, \omega)}{\rho_o c_o \hat{U}} = \mathrm{e}^{ik_o x_1} - \frac{1}{2\pi} \int_0^{2\pi} \mathrm{e}^{ik_o r_{\max}(\vartheta)}\, d\vartheta, \tag{3.1.10}
$$

where inspection of Figure 3.1.6 and the cosine formula $a^2 = x_2^2 + \varpi_{\max}^2 + 2x_2 \varpi_{\max} \cos\vartheta$ yield

Downloaded from https://www.cambridge.org/core. Charité Universitätsmedizin Berlin, on 20 Dec 2021 at 10:08:47, subject to the Cambridge Core terms of use, available at https://www.cambridge.org/core/terms. https://doi.org/10.1017/CBO9781107360273.004

$$r_{\max} = \left(x_1^2 + a^2 + x_2 \left(x_2 \cos 2\vartheta - 2\cos\vartheta \sqrt{a^2 - x_2^2 \sin^2\vartheta} \right) \right)^{\frac{1}{2}}.$$

Let $0 < x_2/a < 1$. In the region $a \ll x_1 \ll R_o \equiv k_o a^2/2$ of the Fresnel zone $r_{\max}$ can be approximated by

$$r_{\max} \approx (x_1^2 + a^2)^{\frac{1}{2}} + \frac{x_2}{2(x_1^2 + a^2)^{\frac{1}{2}}} \left(x_2 \cos 2\vartheta - 2\cos\vartheta \sqrt{a^2 - x_2^2 \sin^2\vartheta} \right),$$

correct to relative order $\sim a^2/x_1^2$. Then (3.1.10) becomes

$$\frac{\hat{p}(\mathbf{x}, \omega)}{\rho_o c_o \hat{U}} = \mathrm{e}^{ik_o x_1} - \mathrm{e}^{ik_o (x_1^2 + a^2)^{\frac{1}{2}}} \frac{1}{\pi} \int_0^\pi \mathrm{e}^{ik_o a^2 \Theta / 2(x_1^2 + a^2)^{\frac{1}{2}}} \, d\vartheta, \qquad (3.1.11)$$

where

$$\Theta = \mu \left(\mu \cos 2\vartheta - 2\cos\vartheta \sqrt{1 - \mu^2 \sin^2\vartheta} \right), \quad 0 < \mu = x_2/a < 1.$$

In the Fresnel zone $k_o a^2/2(x_1^2 + a^2)^{\frac{1}{2}} \approx R_o/x_1 \gg 1$, and the integrand $\sim \mathrm{e}^{i(R_o/x_1)\Theta}$ oscillates rapidly as ϑ increases from 0 to π; successive intervals of integration therefore interfere destructively and give cancelling contributions except in the vicinity of $\vartheta = 0,\ \pi$ at which $\partial\Theta/\partial\vartheta = 0$, and where Θ varies slowly. The integral can then be approximated by the *method of stationary phase*, by expansion of the integrand about these points. Omitting the details of the calculation (see §4.6.4), we find

$$\frac{\hat{p}(\mathbf{x}, \omega)}{\rho_o c_o \hat{U}} \approx \mathrm{e}^{ik_o x_1} - \frac{1}{2} \left(\frac{(x_1^2 + a^2)^{\frac{1}{2}}}{\pi R_o} \frac{a}{x_2} \right)^{\frac{1}{2}} \times \left\{ \frac{a}{a - x_2} \mathrm{e}^{i(k_o |\mathbf{x}|_{\min} + \frac{\pi}{4})} + \frac{a}{a + x_2} \mathrm{e}^{i(k_o |\mathbf{x}|_{\max} - \frac{\pi}{4})} \right\}, \qquad (3.1.12)$$

where $|\mathbf{x}|_{\min,\max} = (x_1^2 + (a \mp x_2)^2)^{\frac{1}{2}}$ are the respective distances of $\mathbf{x}$ from the stationary points $\vartheta = 0,\ \pi$ on the edge of the piston. In other words, the edge generated part of the sound is received at $\mathbf{x}$ from the vicinities of farthest and nearest points on the edge, where the rate at which $r_{\max}$ changes with position on the circumference is stationary ($\partial r_{\max}/\partial\vartheta = 0$).

This formula shows that the edge wave contribution is small within the Fresnel zone where $x_1/R_o \ll x_2/a$. It extends to all off-axis points the conclusion that the influence of the edge generated wave is much reduced within the main beam of the Fresnel zone when R_o/x_1 is sufficiently large. However, the approximation (3.1.12) fails near the axis of symmetry $x_2 = 0$, for the obvious reason that edge waves arriving on the piston axis from the circumference

Downloaded from https://www.cambridge.org/core. Charité Universitätsmedizin Berlin, on 20 Dec 2021 at 10:08:47, subject to the Cambridge Core terms of use, available at https://www.cambridge.org/core/terms. https://doi.org/10.1017/CBO9781107360273.004

of the piston reinforce rather than interfere. When $\frac{x_1}{R_o}\frac{a}{x_2} \ll 1$, but $\frac{x_2}{a} \to 0$ equation (3.1.12) becomes

$$\hat{p}(\mathbf{x},\omega) = \rho_o c_o \hat{U} \left\{ \mathrm{e}^{ik_o x_1} - \mathrm{e}^{ik_o (x_1^2+a^2)^{\frac{1}{2}}} \left(\frac{(x_1^2+a^2)^{\frac{1}{2}}}{\pi R_o} \frac{a}{x_2} \right)^{\frac{1}{2}} \right.$$
$$\left. \times \cos\left(\frac{2R_o}{(x_1^2+a^2)^{\frac{1}{2}}} \frac{x_2}{a} - \frac{\pi}{4} \right) \right\}. \qquad (3.1.13)$$

Now $\Theta \approx -2\mu\cos\vartheta$ when $\mu = x_2/a$ is small, and when this approximation is made in (3.1.11) we find

$$\hat{p}(\mathbf{x},\omega) = \rho_o c_o \hat{U} \left\{ \mathrm{e}^{ik_o x_1} - \mathrm{e}^{ik_o (x_1^2+a^2)^{\frac{1}{2}}} \mathrm{J}_0 \left(\frac{2R_o}{(x_1^2+a^2)^{1/2}} \frac{x_2}{a} \right) \right\}.$$

This coincides with the on-axis formula (3.1.9) when $x_2 = 0$, because $\mathrm{J}_0(0) = 1$, and provides the correct 'inner' limit of (3.1.13), to which it reduces when $\frac{x_1}{R_o}\frac{a}{x_2} \ll 1$.

Formula (3.1.12) fails when $x_2 \to a$, when $\mathbf{x}$ lies on the edge of the Fresnel zone beam, in which case a more careful analysis is required. At very high frequencies the region $x_2 > a$ is outside the main acoustic beam when $k_o a \to \infty$. According to edge diffraction theory, the transition across the edge of the beam into the acoustic 'shadow' in $x_2 > a$ occurs over a distance $\sim a\sqrt{x_1/R_o}$ (cf. §3.2.4).

3.1.4 Reaction force on the piston

The reaction of the air in front of the piston produces an opposing force $F_p = \oint_{S_p} p\, dS(\mathbf{x})$ (in the negative x_1 direction in Figure 3.1.6) given for time-harmonic motion (using (3.1.4)) by

$$F_p = \frac{-i\omega\rho_o \hat{U}}{2\pi} \oint_{S_p} \oint_{S_p} \frac{\mathrm{e}^{ik_o|\mathbf{x}-\mathbf{y}|}}{|\mathbf{x}-\mathbf{y}|}\, dS(\mathbf{y})\, dS(\mathbf{x}),$$

the integrations being over the surface of the piston. Now, because of the symmetry of the integrand

$$\oint_{S_p} \oint_{S_p} \Big(\cdot \Big)\, dS(\mathbf{y})\, dS(\mathbf{x})$$
$$= \oint_{|\mathbf{x}|<a} dS(\mathbf{x}) \oint_{|\mathbf{y}|<|\mathbf{x}|} \Big(\cdot \Big)\, dS(\mathbf{y}) + \oint_{|\mathbf{x}|<a} dS(\mathbf{x}) \oint_{|\mathbf{y}|>|\mathbf{x}|} \Big(\cdot \Big)\, dS(\mathbf{y})$$
$$= 2 \oint_{|\mathbf{x}|<a} dS(\mathbf{x}) \oint_{|\mathbf{y}|<|\mathbf{x}|} \Big(\cdot \Big)\, dS(\mathbf{y}). \qquad (3.1.14)$$

Downloaded from https://www.cambridge.org/core. Charité Universitätsmedizin Berlin, on 20 Dec 2021 at 10:08:47, subject to the Cambridge Core terms of use, available at https://www.cambridge.org/core/terms. https://doi.org/10.1017/CBO9781107360273.004

Let $r = |\mathbf{x} - \mathbf{y}|$ and introduce polar coordinates (r, θ) for the $\mathbf{y}$ integration with pole at $\mathbf{x}$, then

$$\oint_{|\mathbf{y}|<|\mathbf{x}|} \Big(\cdot\Big)\, dS(\mathbf{y}) = \int_{-\frac{\pi}{2}}^{\frac{\pi}{2}} d\theta \int_0^{2|\mathbf{x}|\cos\theta} \mathrm{e}^{ik_o r}\, dr$$
$$= \frac{i\pi}{k_o}\Big(1 - \mathrm{J}_0(2k_o|\mathbf{x}|) - i\mathbf{H}_0(2k_o|\mathbf{x}|)\Big)$$

where $\mathbf{H}_0(x) = \frac{2}{\pi}\int_0^{\frac{\pi}{2}} \sin(x\cos\theta)\, d\theta$ is the Struve function of order 0 (Abramowitz & Stegun 1970),

$$\therefore \quad F_p = \rho_o c_o \hat{U}\, 2\pi \int_0^a \Big(1 - \mathrm{J}_0(2k_o\varpi) - i\mathbf{H}_0(2k_o\varpi)\Big)\varpi\, d\varpi$$

$$= \rho_o c_o \hat{U}\pi a^2 \left(1 - \frac{\mathrm{J}_1(2k_o a)}{k_o a} - i\,\frac{\mathbf{H}_1(2k_o a)}{k_o a}\right) \tag{3.1.15}$$

where $\mathrm{J}_1(x)$, $\mathbf{H}_1(x)$ $\Big(= \frac{2x}{\pi}\int_0^{\frac{\pi}{2}} \sin(x\cos\theta)\sin^2\theta\, d\theta\Big)$ are Bessel and Struve functions of order 1.

The real and imaginary parts of $F_p/\rho_o c_o \hat{U}\,\pi a^2$ are plotted in Figure 3.1.7. The limiting values at high and low values of $k_o a$ are

$$F_p \approx \rho_o c_o \hat{U}\pi a^2 \begin{cases} 1 - 2i/\pi k_o a, & k_o a \gg 1 \\ (k_o a)^2/2 - 8ik_o a/3\pi, & k_o a \ll 1 \end{cases} \tag{3.1.16}$$

At very high frequencies ($k_o a \to \infty$) the piston generates locally plane, parallel waves just in front of its surface, with acoustic particle velocity $\hat{U}$ and pressure $\hat{p} = \rho_o c_o \hat{U}$, so that $F_p = \rho_o c_o \hat{U}\pi a^2$ (cf. §1.3.3, Example 1).

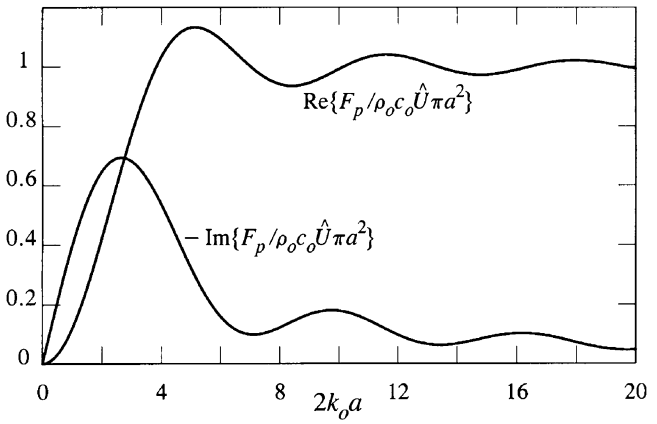

Figure 3.1.7

Downloaded from https://www.cambridge.org/core. Charité Universitätsmedizin Berlin, on 20 Dec 2021 at 10:08:47, subject to the Cambridge Core terms of use, available at https://www.cambridge.org/core/terms. https://doi.org/10.1017/CBO9781107360273.004

3.1.5 Example (Rayleigh 1945)

Let the piston have mass M and let its motion be restrained by a linear restoring force such that the natural frequency of vibration is Ω in the absence of fluid loading. When acted upon by a force $F\mathrm{e}^{-i\omega t}$ (in the $+x_1$ direction) the equation of motion will be

$$\left(M + \frac{\rho_o \pi a}{k_o^2}\mathbf{H}_1(2k_o a)\right)\frac{d^2\xi}{dt^2} + \rho_o c_o \pi a^2 \left(1 - \frac{\mathrm{J}_1(2k_o a)}{k_o a}\right)\frac{d\xi}{dt} + M\Omega^2\xi = F\mathrm{e}^{-i\omega t},$$

where ξ is the displacement of the piston in the x_1 direction. In the compact limit $k_o a \ll 1$,

$$\mathbf{H}_1(2k_o a) \sim \frac{8(k_o a)^2}{3\pi}, \quad \mathrm{J}_1(2k_o a) \sim k_o a - \frac{(k_o a)^3}{2},$$

and the equation of motion becomes

$$(M + M_a)\frac{d^2\xi}{dt^2} + \frac{\rho_o c_o \pi a^2 (k_o a)^2}{2}\frac{d\xi}{dt} + M\Omega^2\xi = F\mathrm{e}^{-i\omega t}. \qquad (3.1.17)$$

where $M_a = \frac{8\rho_o a^3}{3}$ is the added mass of the piston. The term in $d\xi/dt$ represents damping due to radiation losses.

3.2 Diffraction

Sound waves in free space at large distances from sources propagate locally along straight lines or 'rays' at right angles to the wavefronts. Deviations from rectilinear propagation can occur by refraction in regions of non-uniform temperature, where the speed of sound is variable, or by reflection from a surface or from a boundary across which the mean temperature and density change. A departure from rectilinear propagation not attributable to such effects is usually called diffraction, and typically involves interaction with one or more edges of a large surface, such as the edge of a screen, or a sharp-edged aperture in a screen. At high frequencies diffraction produces acoustic 'shadows', the boundaries of which are diffuse rather than geometrically sharp, and across which the acoustic amplitude is oscillatory because of interference between wavelets diffracted from different elements of the incident wavefront not blocked by the diffracting surface. At lower frequencies at which the wavelength is larger than the diffracting body the sound is usually said to be 'scattered' – in Rayleigh scattering (§2.8.3), for example, only a small fraction of the incident wave energy is diffracted out of the main line of propagation of the incident sound.

The typical diffraction problem is illustrated in Figure 3.2.1. A source of sound Q is separated from an observer P by a hard screen S_s with a small

Downloaded from https://www.cambridge.org/core. Charité Universitätsmedizin Berlin, on 20 Dec 2021 at 10:08:47, subject to the Cambridge Core terms of use, available at https://www.cambridge.org/core/terms. https://doi.org/10.1017/CBO9781107360273.004

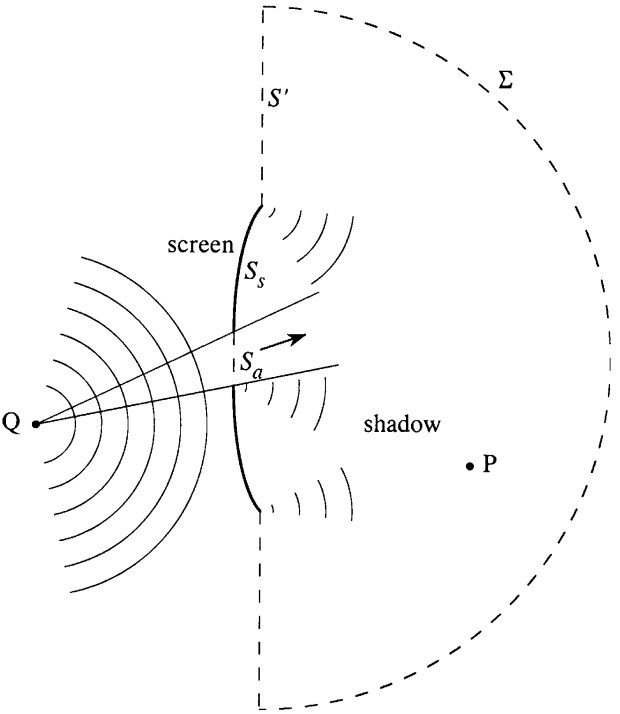

Figure 3.2.1

aperture. Sound reaches P via the aperture and possibly also by diffraction around the edges of the screen. The acoustic wavelength is assumed to be much smaller than the screen, the aperture, and the source and observer distances from the screen, so that straight line propagation of wavefronts along 'rays' from Q would imply that no sound is received at P unless P and Q are in 'line of sight' through the aperture. Problems of this kind are too difficult to solve in full generality, and are usually treated by *Kirchhoff's diffraction theory*. This is an approximation derived from Kirchhoff's formula (§2.1) that formalises *Huygens' principle* that the future development of a wavefront can be found by assuming that each point on the front emits a spherical wave, and that the position of the new front at a later time is determined by the envelope of these waves. The theory is approximate because boundary conditions are imposed on the screen S_s, on its artificial extension S', and within the plane of the aperture S_a, that are only approximately correct.

Let S be the closed surface enclosing P consisting of the aperture plane S_a, the side of the screen S_s facing P, a convenient lateral extension S' that meets at infinity a control surface Σ that completes the closure of S. Kirchhoff's formula

Downloaded from https://www.cambridge.org/core. Charité Universitätsmedizin Berlin, on 20 Dec 2021 at 10:08:47, subject to the Cambridge Core terms of use, available at https://www.cambridge.org/core/terms. https://doi.org/10.1017/CBO9781107360273.004

(2.1.6) with $q = 0$, $\mathbf{F} = 0$ gives the pressure at P in terms of conditions on S in the form

$$p(\mathbf{x}, t) = \iint\!\!\!\!\!\!\bigcirc_S \left(\frac{\partial G}{\partial t}(\mathbf{x}, \mathbf{y}, t - \tau)\rho_o v_n(\mathbf{y}, \tau) + \frac{\partial G}{\partial y_n}(\mathbf{x}, \mathbf{y}, t - \tau) p(\mathbf{y}, \tau) \right) dS(\mathbf{y}) d\tau, \tag{3.2.1}$$

where G is an appropriate Green's function. This formula can be used to calculate the pressure anywhere within S provided the boundary values v_n and p are known.

In Kirchhoff's original theory G is the free space Green's function (1.6.2) and v_n and p are assumed to vanish on S_s, because it is in the acoustic 'shadow' of the source Q. On S_a (the aperture) and S', v_n and p are assumed to take the values they would have in the absence of the screen. The section Σ is sufficiently distant that no sound arrives there in a finite time (in the case of time-harmonic waves the contribution from Σ vanishes because of the radiation condition, as in the proof of the reciprocal theorem in §2.4). These approximations are reasonable and at very high frequencies predictions agree well with experiment, because the wavelength is a very small fraction of the aperture radius and errors in the assumed boundary values produced by the presence of the screen are confined to neighbourhoods of the edge a few wavelengths wide, and make only a small contribution to the Kirchhoff integral.

However, the boundary conditions imposed on S_s, S_a and S' are mutually inconsistent because it can be shown, that if p and v_n both vanish over any section of S (for all times) the pressure p must vanish everywhere within S. This indicates that a solution derived from the assumed boundary values is unlikely to reproduce those boundary values. The inconsistency can be removed for a hard screen (on which $v_n \equiv 0$) by choosing Green's function to have vanishing normal derivative on S. Equation (3.2.1) then reduces to

$$p(\mathbf{x}, t) = \rho_o \frac{\partial}{\partial t} \iint\!\!\!\!\!\!\bigcirc_{S_a + S'} G(\mathbf{x}, \mathbf{y}, t - \tau) v_n(\mathbf{y}, \tau)\, dS(\mathbf{y}) d\tau, \tag{3.2.2}$$

which is an explicit statement of *Huygens' principle* – the sound incident on the aperture (S_a or S') propagates beyond the aperture as if every element $dS(\mathbf{y})$ emits a spherical wave whose initial amplitude and phase are those of the incident wave. Because of this remaining approximation, in which v_n is replaced by its value for the incident wave, the assumed boundary conditions are strictly incorrect (near edges), so that although predictions are applicable at larges distances from the screen and aperture, they remain unreliable within a few wavelengths of S_a and S', where the theory correctly reproduces the prescribed normal velocity v_n, but not the surface pressure.

Downloaded from https://www.cambridge.org/core. Charité Universitätsmedizin Berlin, on 20 Dec 2021 at 10:08:47, subject to the Cambridge Core terms of use, available at https://www.cambridge.org/core/terms. https://doi.org/10.1017/CBO9781107360273.004

3.2.1 Circular aperture in a plane, rigid screen

Diffraction problems of this kind are important in specialised laboratory applications involving, for example, high frequency acoustic imaging. Let the screen coincide with the plane $x_1 = 0$ with an aperture of radius a with centre at the origin (Figure 3.2.2). Consider the simplest case of a plane sound wave of pressure $p = p_I(t - x_1/c_o)$ at normal incidence on the screen from $x_1 < 0$. Kirchhoff's integral formula (3.2.1) is reduced to the form (3.2.2) involving integration over the aperture alone by use of the rigid wall Green's function (2.1.7)

$$G(\mathbf{x}, \mathbf{y}, t-\tau) = \frac{1}{4\pi|\mathbf{x}-\mathbf{y}|}\delta\left(t-\tau-\frac{|\mathbf{x}-\mathbf{y}|}{c_o}\right) + \frac{1}{4\pi|\bar{\mathbf{x}}-\mathbf{y}|}\delta\left(t-\tau-\frac{|\bar{\mathbf{x}}-\mathbf{y}|}{c_o}\right), \tag{3.2.3}$$

where $\bar{\mathbf{x}} = (-x_1, x_2, x_3)$ and $\partial G/\partial y_1 = 0$ on $y_1 = 0$. The diffracted pressure at the point P at $\mathbf{x}$ to the right of the screen ($x_1 > 0$) is then given by

$$p(\mathbf{x}, t) = \frac{\rho_o}{2\pi}\frac{\partial}{\partial t}\int_{y_1=0} \frac{v_n(\mathbf{y}, t-|\mathbf{x}-\mathbf{y}|/c_o)}{|\mathbf{x}-\mathbf{y}|}\, dS(\mathbf{y}).$$

In the absence of the screen $v_n = p_I(t)/\rho_o c_o$, and Kirchhoff's approximation yields

$$p(\mathbf{x}, t) = \frac{1}{2\pi c_o}\frac{\partial}{\partial t}\int_{S_a} \frac{p_I(t-|\mathbf{x}-\mathbf{y}|/c_o)}{|\mathbf{x}-\mathbf{y}|}\, dy_2 dy_3. \tag{3.2.4}$$

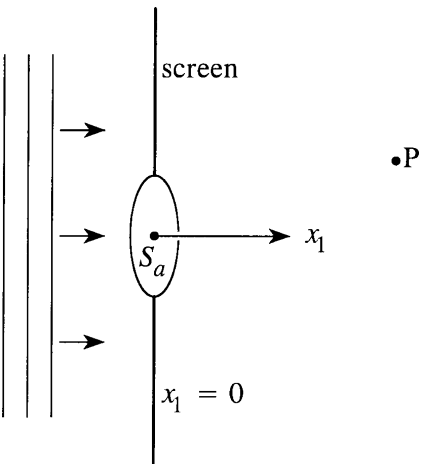

Figure 3.2.2

Downloaded from https://www.cambridge.org/core. Charité Universitätsmedizin Berlin, on 20 Dec 2021 at 10:08:47, subject to the Cambridge Core terms of use, available at https://www.cambridge.org/core/terms. https://doi.org/10.1017/CBO9781107360273.004

This is identical in form with equation (3.1.2) for the sound produced by a piston of normal velocity $U(t) = p_I(t)/\rho_o c_o$. The characteristics of the sound transmitted through the aperture can therefore be deduced from the discussion of the circular piston in §3.1. There are certain important differences, however. First, equation (3.1.2) provides the *exact* linear theory solution for the piston, whereas the diffraction solution is applicable only at *high frequencies* $k_o a \gg 1$. Second, the diffracted solution is valid only in the Fresnel and Fraunhofer far fields where $k_o x_1 \gg 1$, and not near the boundaries. For example, the method leading to equation (3.1.8) implies that the transmitted pressure on the axis of the aperture is given by

$$p(\mathbf{x}, t) = p_I\left(t - \frac{x_1}{c_o}\right) - p_I\left(t - \frac{(x_1^2 + a^2)^{\frac{1}{2}}}{c_o}\right), \quad x_1 > 0, \tag{3.2.5}$$

where the incident wave $p_I(t - x_1/c_o)$ is supplemented by a diffracted wave from the edge of the aperture. This formula gives the erroneous prediction $p = p_I(t) - p_I(t - a/c_o)$ at the boundary point $x_1 = 0$, at the centre of the aperture, although the normal velocity $v_1 = p_I(t)/\rho_o c_o$ is correctly predicted. This is on the boundary S where we expect the solution to fail because of the imposition of the Kirchhoff boundary conditions.

3.2.2 Babinet's principle

Two diffraction problems 1 and 2 are *complementary* if aperture 1 and screen 2 are congruent and *vice versa*. Thus, the complement of the problem of Figure 3.2.1 is obtained by replacing the broken line 'open' sections S_a and S' of S by screen, and the screen section S_s by aperture.

Let $p_o(\mathbf{x}, t)$ denote the pressure at P in the absence of all screens, and let $p_1(\mathbf{x}, t)$, $p_2(\mathbf{x}, t)$ be the respective corresponding pressures for problems 1 and 2. Then Babinet's principle asserts, that within the approximation of Kirchhoff diffraction theory

$$p_o(\mathbf{x}, t) = p_1(\mathbf{x}, t) + p_2(\mathbf{x}, t).$$

This is proved by adding the corresponding representations (3.2.2) of $p_1(\mathbf{x}, t)$, $p_2(\mathbf{x}, t)$ in terms of the *same* Green's function $G(\mathbf{x}, \mathbf{y}, t - \tau)$ and the boundary values of v_n determined by the incident wave, consistently with the Kirchhoff approximation. The result is the *exact* representation at P of the incident wave, uninfluenced by diffraction, in terms of the incident velocity on a fluid control surface that coincides with S.

Downloaded from https://www.cambridge.org/core. Charité Universitätsmedizin Berlin, on 20 Dec 2021 at 10:08:47, subject to the Cambridge Core terms of use, available at https://www.cambridge.org/core/terms. https://doi.org/10.1017/CBO9781107360273.004

3.2.3 Example: Diffraction by a circular disc

Let the disc have radius a with centre at $\mathbf{x} = 0$ orientated with its normal in the x_1 direction (Figure 3.2.3). A high frequency plane wave $p = p_I(t - x_1/c_o)$ is incident from $x_1 < 0$.

(i) Diffracted field behind the disc

The pressure in $x_1 > 0$ is given by equation (3.2.4) with the integration over the infinite aperture $(y_2^2 + y_3^2)^{\frac{1}{2}} > a$. The influence of the disc must be negligible when $x_1 \gg a$ outside the Fresnel zone, as the 'shadow' of the disc becomes diffuse and ultimately disappears, and the pressure everywhere differs negligibly from that of the incident wave. Of interest is the behaviour on the axis of the disc, where coherent contributions from waves diffracted at the edge of the disc reinforce. Setting $r = |\mathbf{x} - \mathbf{y}|$ for $\mathbf{x}$ on the axis of symmetry, we find

$$p(\mathbf{x}, t) = -\int_{(x_1^2+a^2)^{\frac{1}{2}}}^{\infty} \frac{\partial p_I}{\partial r}(t - r/c_o)\, dr = p_I\left(t - \frac{(x_1^2+a^2)^{\frac{1}{2}}}{c_o}\right),$$

there being no contribution from $p_I(t - r/c_o)$, $r \to \infty$ in the 'infinite past' before the arrival of the incident wave. This formula could have been written down from Babinet's principle using formula (3.2.5). According to §3.1 interference reduces the influence of the edge diffracted waves at off-axis points within the Fresnel zone. At very high frequencies, this would imply that the Fresnel zone of the disc is silent except very close to the axis where

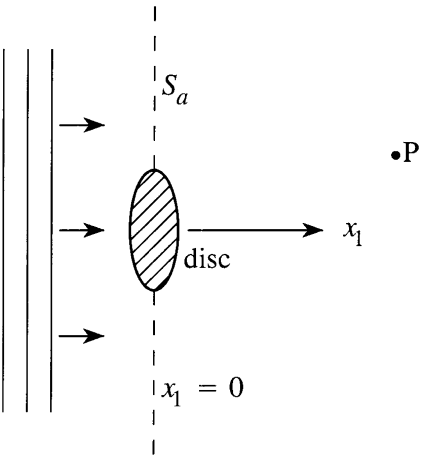

Figure 3.2.3

Downloaded from https://www.cambridge.org/core. Charité Universitätsmedizin Berlin, on 20 Dec 2021 at 10:08:47, subject to the Cambridge Core terms of use, available at https://www.cambridge.org/core/terms. https://doi.org/10.1017/CBO9781107360273.004

the pressure is the same as in the incident wave. A similar result is obtained on the axis of symmetry of any axisymmetric body, such as a sphere. It was first predicted by Poisson, and subsequently observed as a 'bright spot' in an experiment performed by Arago and Fresnel on the diffraction of light by a disc.

(ii) Diffracted field in front of the disc

The diffracted pressure $p'(\mathbf{x}, t)$ in $x_1 < 0$ is given by

$$p'(\mathbf{x}, t) = \frac{\rho_o}{2\pi} \frac{\partial}{\partial t} \int_{y_1=-0} \frac{v_n'(\mathbf{y}, t - |\mathbf{x} - \mathbf{y}|/c_o)}{|\mathbf{x} - \mathbf{y}|} \, dS(\mathbf{y}),$$

where the integration is over the left-hand side $y_1 = -0$ of the open aperture S_a and the disc in Figure 3.2.3, facing the incident wave. The normal velocity v_n' is equal and opposite to the acoustic particle velocity $p_I(t)/\rho_o c_o$ of the incident wave on the rigid surface ($x_1 = -0$) of the disc, but vanishes on S_a, through which the incident wave passes unimpeded.

The overall pressure for $x_1 < 0$ is therefore given by

$$p(\mathbf{x}, t) = p_I(t - x_1/c_o) + \frac{1}{2\pi c_o} \frac{\partial}{\partial t} \int_{(y_2^2+y_3^2)^{\frac{1}{2}}<a} \frac{p_I(t - |\mathbf{x} - \mathbf{y}|/c_o)}{|\mathbf{x} - \mathbf{y}|} \, dS(\mathbf{y}).$$

The 'back-diffracted' pressure has all the characteristics of the diffracted radiation of a piston or aperture of normal velocity $p_I(t)/\rho_o c_o$. In the Fraunhofer far field (as $x_1 \to -\infty$) the radiation from the disc has the directional characteristics of the piston shown in Figure 3.1.3 for different frequencies of the incident wave. Similarly, on the axis of the disc the integral is easily evaluated in the usual way to give

$$p(\mathbf{x}, t) = p_I\left(t - \tfrac{x_1}{c_o}\right) + p_I\left(t + \tfrac{x_1}{c_o}\right) - p_I\left(t - \tfrac{(x_1^2+a^2)^{\frac{1}{2}}}{c_o}\right), \quad x_1 < 0.$$

3.2.4 Diffraction by a straight edge*

The canonical problem of the diffraction of sound by the straight edge of a semi-infinite screen (Figure 3.2.4) is amenable to exact analytical treatment. It is known, however, that predictions for this problem based on Kirchhoff's approximation agree well with the exact theory except at positions well within the shadow zone, behind the screen.

Let the screen coincide with the half-plane $x_2 = 0$, $x_1 < 0$ and consider the simplest case of a plane wave $\hat{p} = \hat{p}_I e^{ik_o x_2}$ with implied time dependence $e^{-i\omega t}$, incident normally from $x_2 < 0$. Using the hard wall Green's function,

Downloaded from https://www.cambridge.org/core. Charité Universitätsmedizin Berlin, on 20 Dec 2021 at 10:08:47, subject to the Cambridge Core terms of use, available at https://www.cambridge.org/core/terms. https://doi.org/10.1017/CBO9781107360273.004

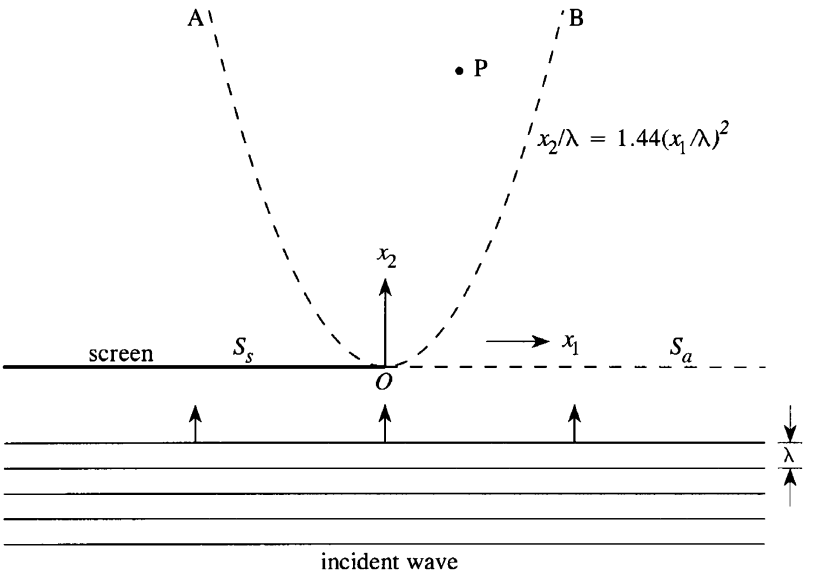

Figure 3.2.4

the pressure at P in $x_2 > 0$ is given according to Kirchhoff's theory by the following form of (3.2.4)

$$\hat{p}(\mathbf{x}, \omega) = \frac{-ik_o\hat{p}_I}{2\pi}\int_{-\infty}^{\infty} dy_3 \int_0^{\infty} \frac{e^{ik_o\{x_2^2+(y_1-x_1)^2+(y_3-x_3)^2\}^{\frac{1}{2}}}\, dy_1}{\{x_2^2+(y_1-x_1)^2+(y_3-x_3)^2\}^{\frac{1}{2}}},$$

in which we have used the relation $\hat{v}_n = \hat{p}_I/\rho_o c_o$.

When $k_o x_2 \gg 1$ and $x_1 > 0$ the main contribution to the integral is from the neighbourhood of the stationary point $(y_1, y_3) = (x_1, x_3)$ of the exponent. When $x_1 < 0$ the y_1 integral is dominated by the contribution from the vicinity of the edge $y_1 = 0$. In either case, the integral can be approximated by

$$\hat{p}(\mathbf{x}, \omega) = \frac{-ik_o\hat{p}_I e^{ik_o x_2}}{2\pi x_2}\int_{-\infty}^{\infty} dy_3 \int_0^{\infty} e^{i(k_o/2x_2)\{(y_1-x_1)^2+(y_3-x_3)^2\}}\, dy_1, \qquad k_o x_2 \gg 1,$$

This can be expressed in terms of the complex Fresnel integral (Abramowitz & Stegun 1970)

Downloaded from https://www.cambridge.org/core. Charité Universitätsmedizin Berlin, on 20 Dec 2021 at 10:08:47, subject to the Cambridge Core terms of use, available at https://www.cambridge.org/core/terms. https://doi.org/10.1017/CBO9781107360273.004

$$F(z) = \int_0^z \mathrm{e}^{\frac{i\pi}{2}\xi^2}\, d\xi, \tag{3.2.6}$$

which satisfies $F(-z) = -F(z)$, $F(+\infty) = \mathrm{e}^{\frac{i\pi}{4}}/\sqrt{2}$. By putting $u = (y_1 - x_1)\sqrt{k_o/\pi x_2}$, $v = (y_3 - x_3)\sqrt{k_o/\pi x_2}$ we find

$$\hat{p}(\mathbf{x}, \omega) \approx \frac{-i\,\hat{p}_I \mathrm{e}^{ik_o x_2}}{2} \int_{-\infty}^{\infty} \mathrm{e}^{\frac{i\pi}{2}v^2} dv \int_{-x_1\sqrt{\frac{k_o}{\pi x_2}}}^{\infty} \mathrm{e}^{\frac{i\pi}{2}u^2} du$$

$$= \frac{\hat{p}_I \mathrm{e}^{ik_o x_2}}{2} \left[1 + 2^{\frac{1}{2}} \mathrm{e}^{-\frac{i\pi}{4}} F\left(x_1 \sqrt{\frac{k_o}{\pi x_2}} \right) \right]. \tag{3.2.7}$$

$F(z)$ is conveniently calculated by use of the formulae (Abramowitz & Stegun 1970)

$$F(z) = \frac{\mathrm{e}^{\frac{i\pi}{4}}}{2^{\frac{1}{2}}} - \Big(g(z) + i f(z) \Big) \mathrm{e}^{\frac{i\pi}{2}z^2},$$

where $f(0) = g(0) = \dfrac{1}{2}$ and $f(z) \sim \dfrac{1}{\pi z}$, $g(z) \sim \dfrac{1}{(\pi z)^3}$, $z \to +\infty$.

Interpolation between these limiting values for f and g can be made using the rational approximations

$$\left.\begin{aligned} f(z) &\simeq \frac{1 + 0.926z}{2 + 1.792z + 3.104z^2} \\ g(z) &\simeq \frac{1}{2 + 4.142z + 3.492z^2 + 6.67z^3} \end{aligned}\right\} z > 0. \tag{3.2.8}$$

Thus, when $x_1\sqrt{k_o/\pi x_2}$ becomes large and positive

$$\hat{p}(\mathbf{x}, \omega) \sim \hat{p}_I \mathrm{e}^{ik_o x_2} - \frac{\hat{p}_I}{x_1} \left(\frac{x_2}{2\pi k_o} \right)^{\frac{1}{2}} \mathrm{e}^{i\{k_o(x_1^2 + x_2^2)^{\frac{1}{2}} + \frac{\pi}{4}\}}, \quad x_1 > 0.$$

In the 'shadow zone' $x_1 < 0$ when $|x_1|\sqrt{k_o/\pi x_2} \gg 1$,

$$\hat{p}(\mathbf{x}, \omega) \sim -\frac{\hat{p}_I}{x_1} \left(\frac{x_2}{2\pi k_o} \right)^{\frac{1}{2}} \mathrm{e}^{i\{k_o(x_1^2 + x_2^2)^{\frac{1}{2}} + \frac{\pi}{4}\}}, \quad x_1 < 0.$$

These approximations cease to be applicable in the transition region across the geometrical shadow boundary $x_1 = 0$, where the approximations (3.2.8) can be used to calculate $\hat{p}(\mathbf{x}, \omega)$. The result of this calculation is shown in Figure 3.2.5, in which $20 \times \log_{10}(|\hat{p}/\hat{p}_I|)$ (dB) is plotted against $x_1(2/\lambda x_2)^{\frac{1}{2}} \equiv x_1(k_o/\pi x_2)^{\frac{1}{2}}$. On the geometrical boundary $x_1 = 0$, $|\hat{p}/\hat{p}_I| = \frac{1}{2}$ and the sound level is reduced by just over 6 dB. The pressure fluctuates as the boundary is

Downloaded from https://www.cambridge.org/core. Charité Universitätsmedizin Berlin, on 20 Dec 2021 at 10:08:47, subject to the Cambridge Core terms of use, available at https://www.cambridge.org/core/terms. https://doi.org/10.1017/CBO9781107360273.004

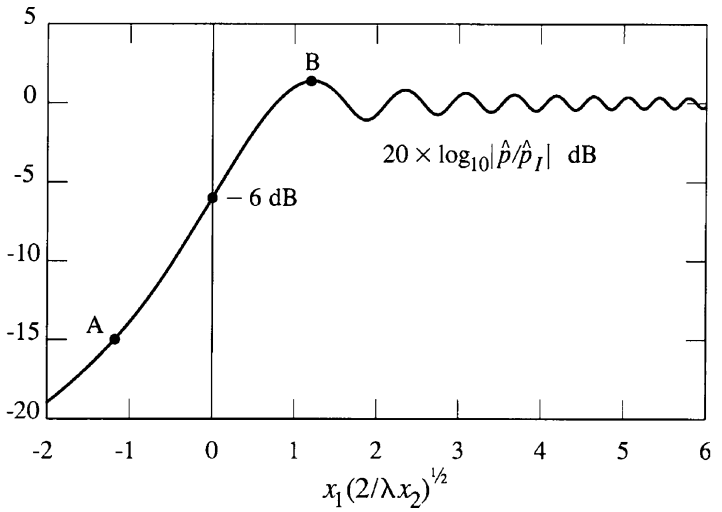

Figure 3.2.5

approached from $x_1 > 0$ and attains a maximum of about 1.37 dB (the point labelled B in the figure) at $x_1(2/\lambda x_2)^{\frac{1}{2}} \approx 1.2$. The pressure level is reduced by 15 dB within the shadow at $x_1(2/\lambda x_2)^{\frac{1}{2}} \approx -1.18$, at the point labelled A. The broken line curve in Figure 3.2.4 is the parabola

$$\frac{x_2}{\lambda} = \frac{2}{(1.18)^2}\left(\frac{x_1}{\lambda}\right)^2 \quad \left(\simeq 1.44\left(\frac{x_1}{\lambda}\right)^2\right).$$

The left-hand leg OA corresponds to the -15 dB level within the shadow zone; the leg OB gives the approximate position of the 1.37 dB pressure peak.

Comparison of the Kirchhoff approximation with the exact solution of the diffraction problem (Noble 1958) reveals that (3.2.7) underestimates the amplitude of the diffracted waves, but that the error is less than 10% for propagation directions within about $\pm 25°$ from the geometrical shadow boundary $x_1 = 0$, and vanishes for $x_1 = 0$.

3.3 Diffraction by a compact aperture

The diffracted pressure produced by a sound wave incident on a compact aperture in a thin screen is the monopole

$$p(\mathbf{x}, t) \approx \frac{\rho_o}{2\pi|\mathbf{x}|}\frac{\partial Q}{\partial t}\left(t - \frac{|\mathbf{x}|}{c_o}\right), \quad |\mathbf{x}| \to \infty, \tag{3.3.1}$$

where $Q(t)$ is the volume velocity through the aperture *towards* the observer at the far field point $\mathbf{x}$, the coordinate origin being taken at the centroid of the aperture. When the flow within the aperture can be regarded as ideal and

Downloaded from https://www.cambridge.org/core. Charité Universitätsmedizin Berlin, on 20 Dec 2021 at 10:08:47, subject to the Cambridge Core terms of use, available at https://www.cambridge.org/core/terms. https://doi.org/10.1017/CBO9781107360273.004

irrotational Q can be calculated in terms of the incident acoustic pressure and the aperture *conductivity*.

3.3.1 Conductivity of the aperture

Consider ideal flow through the aperture produced by local acoustic pressures $p_{\pm}(t)$ on the 'left' and 'right' of the screen (Figure 3.3.1). These pressures may be regarded as uniform in the regions labelled A and B that are far from the aperture but well within an acoustic wavelength of the aperture, and the motion close to and within the aperture can be taken as incompressible with velocity potential $\varphi(\mathbf{x}, t)$. Let the aperture have cross-sectional area A and let the mean velocity at this cross-section be $U(t)$, so that the volume velocity $Q = AU$. Then, for the *incompressible* motion we can put

$$\varphi(\mathbf{x}, t) = \alpha(t) + U(t)\varphi^*(\mathbf{x}), \tag{3.3.2}$$

where the time-dependent function $\alpha(t)$ will be determined by the pressures $p_{\pm}(t)$. The function φ^* depends only on the aperture geometry; it represents the velocity potential of flow through the aperture from left to right having unit mean speed in the mid-plane of the aperture. By the addition of a suitable constant it may be assumed to satisfy

$$\varphi^*(\mathbf{x}) \to \begin{cases} -\frac{A}{2\pi|\mathbf{x}|}, & x_1 \to +\infty \\ \frac{A}{2\pi|\mathbf{x}|} - \ell, & x_1 \to -\infty, \end{cases} \tag{3.3.3}$$

where the coordinate origin is taken at O within the aperture.

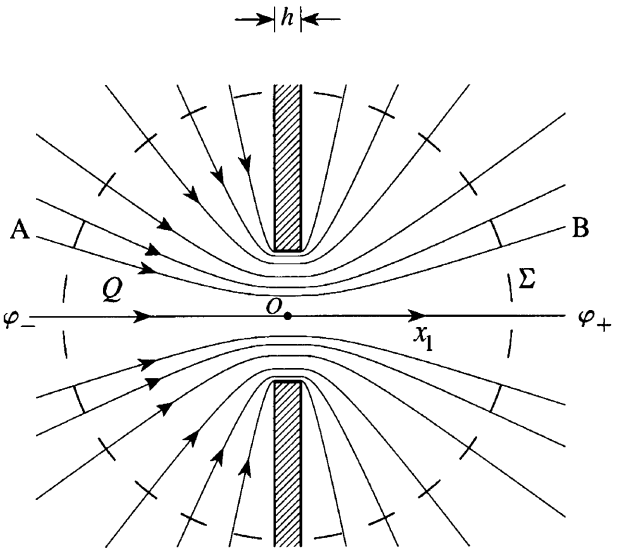

Figure 3.3.1

Downloaded from https://www.cambridge.org/core. Charité Universitätsmedizin Berlin, on 20 Dec 2021 at 10:08:47, subject to the Cambridge Core terms of use, available at https://www.cambridge.org/core/terms. https://doi.org/10.1017/CBO9781107360273.004

The constant ℓ is a characteristic length dependent on the aperture shape and thickness of the screen. To understand its significance, observe from (3.3.2), (3.3.3) that the limiting values $\varphi_\pm(t)$ of φ respectively as $x_1 \to \pm\infty$ satisfy

$$\varphi_+ - \varphi_- = \ell U. \tag{3.3.4}$$

By expressing this result in terms of the corresponding pressures $p_\pm = -\rho_o \partial\varphi_\pm/\partial t$, and the volume velocity $Q = AU$ we find

$$\rho_o \ell \frac{dQ}{dt} = A\Big(p_-(t) - p_+(t)\Big). \tag{3.3.5}$$

Hence, ℓ is the *effective length of the slug of fluid of mass $\rho_o \ell A$ involved in the unsteady motion through the aperture* produced by the sound.

Equation (3.3.4) can also be written in the form of *Ohm's law*

$$\varphi_+ - \varphi_- = Q\frac{\ell}{A} = \frac{Q}{K_o} \tag{3.3.6}$$

which determines the current Q of an electrical element in terms of the potential difference $\varphi_+ - \varphi_-$ and the 'resistance' ℓ/A, or in terms of $\varphi_+ - \varphi_-$ and the 'conductivity' $K_o \equiv A/\ell$.

The kinetic energy of the flow through the aperture is $T = \frac{1}{2}\rho_o \int_V (\nabla\varphi)^2 d^3\mathbf{x}$, where V is the fluid contained within the spherical control surface Σ in Figure 3.3.1. Thus, using the divergence theorem and recalling that $\nabla^2\varphi = 0$,

$$\begin{aligned} T &= \tfrac{1}{2}\rho_o \int_V \Big(\operatorname{div}(\varphi\,\nabla\varphi) - \varphi\,\nabla^2\varphi\Big)\, d^3\mathbf{x} \\ &= \tfrac{1}{2}\rho_o \oint_\Sigma \varphi\,\nabla\varphi \cdot d\mathbf{S} \equiv \tfrac{1}{2}\rho_o(\varphi_+ - \varphi_-)Q, \end{aligned}$$

where $d\mathbf{S}$ is the surface element on Σ directed away from the aperture. Hence, from (3.3.6), the kinetic energy of the aperture motion can be written

$$T = \frac{\rho_o Q^2}{2K_o}. \tag{3.3.7}$$

This result is often used in the numerical determination of K_o from the principle, that when the volume velocity Q is prescribed the kinetic energy of motion through the aperture is a *minimum* when the flow is irrotational (Chapter 5).

3.3.2 Conductivity of a circular aperture

For a circular aperture of radius a in a thin screen of negligible thickness (§2.9.1g)

$$\varphi^*(\mathbf{x}) = -\operatorname{sgn}(x_1)\,\frac{a}{2}\int_0^\infty \frac{\sin(\xi a)}{\xi} e^{-\xi|x_1|} J_0(\xi\varpi)\, d\xi - \mathrm{H}(-x_1)\ell,$$

$$\varpi = (x_2^2 + x_3^2)^{\frac{1}{2}}.$$

Downloaded from https://www.cambridge.org/core. Charité Universitätsmedizin Berlin, on 20 Dec 2021 at 10:08:47, subject to the Cambridge Core terms of use, available at https://www.cambridge.org/core/terms. https://doi.org/10.1017/CBO9781107360273.004

By symmetry φ^* is constant within the plane of the aperture, and continuity of φ^* at $x_1 = 0,\ \varpi < a$ implies that

$$\ell = a\int_0^\infty \frac{\sin(\xi a)}{\xi} \mathrm{J}_0(\xi\varpi)\, d\xi = \frac{\pi a}{2}, \quad \therefore \quad K_o = \frac{\pi a^2}{\ell} = 2a. \tag{3.3.8}$$

When the screen has finite thickness h the increase in φ^* in passing from the negative ($x_1 = -h/2$) to the positive end ($x_1 = +h/2$) of the aperture $\simeq h$, because φ^* represents a flow *at unit speed* within the aperture of cross-section A. To a good approximation (when $h > a$) it can be assumed that the contribution to the slug length ℓ from each end of the aperture is the same as the length $8a/3\pi$ determining the added mass of a circular, baffled piston (§3.1.5; see also §5.4.2). Hence

$$\ell \simeq h + \frac{16a}{3\pi}, \quad \therefore \quad K_o = \frac{A}{\ell} \simeq \frac{\pi a^2}{h + \frac{16a}{3\pi}}.$$

This approximation implies that $K_o \simeq 1.85a$ when $h = 0$, instead of its exact, thin screen value $K_o = 2a$.

3.3.3 Transmission of sound through an aperture

Let the aperture and screen thickness be compact, and consider a plane wave $p = p_I(t - x_1/c_o)$ incident on the screen at $x_1 = 0$ from $x_1 < 0$ (Figure 3.3.2). In the absence of the aperture there is a reflected wave $p_R = p_I(t + x_1/c_o)$, and no waves in $x_1 > 0$. The volume velocity $Q(t)$ through the aperture produces a spherical wave (3.3.1) in $x_1 > 0$; there is also a spherical wave of opposite sign radiated back into $x_1 < 0$. Q is determined in terms of p_I by equation (3.3.5) (with $p_- = p_I(t) + p_R(t),\ p_+ = 0$):

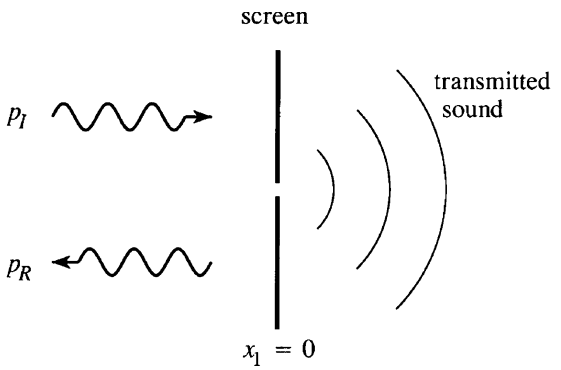

Figure 3.3.2

Downloaded from https://www.cambridge.org/core. Charité Universitätsmedizin Berlin, on 20 Dec 2021 at 10:08:47, subject to the Cambridge Core terms of use, available at https://www.cambridge.org/core/terms. https://doi.org/10.1017/CBO9781107360273.004

$$\rho_o \ell \frac{dQ}{dt} = A\Big(p_I(t) + p_R(t)\Big) = 2Ap_I(t), \quad \therefore \quad \rho_o \frac{dQ}{dt} = 2K_o p_I(t). \tag{3.3.9}$$

The spherical wave transmitted through the aperture is therefore given by

$$p(\mathbf{x}, t) \approx \frac{K_o\, p_I\left(t - \frac{|\mathbf{x}|}{c_o}\right)}{\pi |\mathbf{x}|}, \quad |\mathbf{x}| \gg a, \quad x_1 > 0. \tag{3.3.10}$$

The interaction of the incident wave p_I with the aperture leads to a transfer of a small quantity of incident wave energy to the energy radiated as spherical waves on both sides of the screen. This is investigated by using the near field *uniform* and *compressive* components of the spherical waves to correct the aperture flux equation (3.3.5). Thus in $x_1 > 0$ near the aperture equation (3.3.10) implies that

$$p(\mathbf{x}, t) \sim \frac{K_o p_I(t)}{\pi |\mathbf{x}|} - \frac{K_o}{\pi c_o} \frac{\partial p_I}{\partial t}(t),$$

so that the corrected value of p_+ is

$$p_+ = -\frac{K_o}{\pi c_o} \frac{dp_I(t)}{dt} = -\frac{\rho_o}{2\pi c_o} \frac{d^2 Q(t)}{dt^2}$$

Similarly, the spherical wave radiating into $x_1 < 0$ is given by (3.3.10) with the sign reversed, so that $p_- = 2p_I + (\rho_o/2\pi c_o) d^2Q(t)/dt^2$. Hence, (3.3.5) becomes

$$\rho_o \ell \frac{dQ}{dt} = 2Ap_I(t) + \frac{\rho_o A}{\pi c_o} \frac{d^2 Q}{dt^2}.$$

This is transformed into an energy equation by multiplication by Q/A, and recalling that $\ell K_o = A$:

$$\frac{d}{dt}\left(\frac{\rho_o Q^2}{2K_o}\right) = 2p_I Q - \frac{\rho_o}{\pi c_o}\left(\frac{dQ}{dt}\right)^2 + \frac{\rho_o}{\pi c_o} \frac{d}{dt}\left(Q \frac{dQ}{dt}\right). \tag{3.3.11}$$

The left hand side is the time rate of change of the kinetic energy within and near the aperture. It follows also that

$$2\langle p_I(t) Q(t) \rangle = \left\langle \frac{\rho_o}{\pi c_o} \left(\frac{dQ(t)}{dt}\right)^2 \right\rangle, \tag{3.3.12}$$

where the angle brackets $\langle\ \rangle$ denote a time average. The left-hand side is the rate of working of the incident and reflected waves (p_I, p_R) at the aperture. The right-hand side is the mean power radiated by the spherical waves $= \oint_S \langle p^2/\rho_o c_o \rangle dS$ calculated using (3.3.1), where S is the surface of a large sphere centred on the aperture.

Downloaded from https://www.cambridge.org/core. Charité Universitätsmedizin Berlin, on 20 Dec 2021 at 10:08:47, subject to the Cambridge Core terms of use, available at https://www.cambridge.org/core/terms. https://doi.org/10.1017/CBO9781107360273.004

3.3.4* Compact Green's function for an aperture

The compact Green's function is required in order to investigate real fluid effects during diffraction at an aperture. It is given in §2.9.1g for a circular aperture in a thin screen, and its derivation is now outlined as a simple generalisation of the method of §2.5, avoiding the frequency domain and working directly with advanced potentials.

Consider an observer at $\mathbf{x}$ in the far field in the region V_+ ($x_1 > 0$) of Figure 3.3.3. When the aperture is absent $G = G_o$, where

$$G_o = \frac{1}{4\pi|\mathbf{x}-\mathbf{y}|}\delta\left(t-\tau-\frac{|\mathbf{x}-\mathbf{y}|}{c_o}\right) + \frac{1}{4\pi|\bar{\mathbf{x}}-\mathbf{y}|}\delta\left(t-\tau-\frac{|\bar{\mathbf{x}}-\mathbf{y}|}{c_o}\right), \quad \bar{\mathbf{x}} = (-x_1, x_2, x_3).$$

Let the acoustically compact, spherical control surface S (with interior V_o) be centred on the aperture and be large compared to the aperture diameter – so that $|\mathbf{y}| \ll |\mathbf{x}|$ and $k_o|\mathbf{y}| \ll 1$ when $\mathbf{y}$ lies in V_o, where $k_o = \omega/c_o \sim (1/c_o)\partial/\partial\tau$ and ω is a characteristic source frequency. Then, for $\mathbf{y}$ in V_+ near S

$$G \simeq G_o(\mathbf{x}, \mathbf{y}, t-\tau) + \frac{1}{2\pi|\mathbf{y}|}\Phi\left(\tau+\frac{|\mathbf{y}|}{c_o}\right)$$
$$\simeq \frac{1}{2\pi|\mathbf{x}|}\delta\left(t-\tau-\frac{|\mathbf{x}|}{c_o}\right) + \frac{\Phi(\tau)}{2\pi|\mathbf{y}|}, \tag{3.3.13}$$

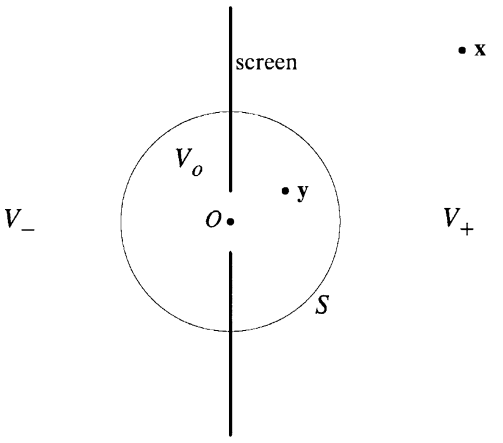

Figure 3.3.3

Downloaded from https://www.cambridge.org/core. Charité Universitätsmedizin Berlin, on 20 Dec 2021 at 10:08:47, subject to the Cambridge Core terms of use, available at https://www.cambridge.org/core/terms. https://doi.org/10.1017/CBO9781107360273.004

where $\Phi(\tau+|\mathbf{y}|/c_o)/2\pi|\mathbf{y}|$ is an advanced potential converging on the aperture and associated with motion through the aperture, and the second line is the first term in the expansion of this potential in powers of $k_o|\mathbf{y}| \ll 1$.

Similarly, in the region V_- on the left-hand side of the screen, close to S

$$G = \frac{1}{2\pi|\mathbf{y}|}\Psi\left(\tau + \frac{|\mathbf{y}|}{c_o}\right) \simeq \frac{\Psi(\tau)}{2\pi|\mathbf{y}|}. \tag{3.3.14}$$

Within and near the aperture, in region V_o, we can put

$$G \simeq \alpha(\tau) + \beta(\tau)\varphi^*(\mathbf{y}), \tag{3.3.15}$$

for suitably defined functions $\alpha(\tau)$, $\beta(\tau)$, where $\varphi^*(\mathbf{y})$ is defined in §3.3.2 as in (2.9.17).

The 'inner' approximation (3.3.15) must match the corresponding near field approximations (3.3.13), (3.3.14) across S. The matching conditions are obtained using the limiting behaviours of $\varphi^*(\mathbf{y})$ given in (3.3.3), leading to the equations

$$\begin{aligned}
\alpha(\tau) &= \frac{1}{2\pi|\mathbf{x}|}\delta\left(t-\tau-\frac{|\mathbf{x}|}{c_o}\right),\\
A\beta(\tau) + \Phi(\tau) &= 0,\\
\ell\beta(\tau) - \alpha(\tau) &= 0,\\
A\beta(\tau) - \Psi(\tau) &= 0.
\end{aligned}$$

Thus, $\beta(\tau) = \alpha(\tau)/\ell$, and substituting for $\alpha(\tau)$, $\beta(\tau)$ in (3.3.15) yields the compact approximation

$$G(\mathbf{x},\mathbf{y},t-\tau) = \frac{1}{2\pi|\mathbf{x}|}\left(1+\frac{\varphi^*(\mathbf{y})}{\ell}\right)\delta\left(t-\tau-\frac{|\mathbf{x}|}{c_o}\right) \tag{3.3.16}$$

for sources within and near the aperture. This represents a spherical, monopole wave generated by the source at $\mathbf{y}$ and by the volume flux through the aperture induced by the source.

Note also that, because $K_o = A/\ell$,

$$\Phi(\tau) = -\Psi(\tau) \simeq \frac{-K_o}{2\pi|\mathbf{x}|}\delta\left(t-\tau-\frac{|\mathbf{x}|}{c_o}\right).$$

This implies that for source points $\mathbf{y}$ in V_- on the left of the screen,

Downloaded from https://www.cambridge.org/core. Charité Universitätsmedizin Berlin, on 20 Dec 2021 at 10:08:47, subject to the Cambridge Core terms of use, available at https://www.cambridge.org/core/terms. https://doi.org/10.1017/CBO9781107360273.004

$$G(\mathbf{x}, \mathbf{y}, t-\tau) = \frac{K_o}{(2\pi|\mathbf{y}|)(2\pi|\mathbf{x}|)}\,\delta\left(t-\tau-\frac{|\mathbf{y}|}{c_o}-\frac{|\mathbf{x}|}{c_o}\right).$$

Therefore, the acoustic pressure at $\mathbf{x}$ ($x_1 > 0$) produced by a point source of strength $Q_I(t)$ at $\mathbf{y}$ on the left of the screen is given by

$$p(\mathbf{x}, t) \simeq \frac{K_o}{\pi|\mathbf{x}|}\,\frac{\rho_o}{4\pi|\mathbf{y}|}\,\frac{\partial Q_I}{\partial t}\left(t-\frac{|\mathbf{y}|}{c_o}-\frac{|\mathbf{x}|}{c_o}\right),$$

which is an obvious generalisation of formula (3.3.10) when the incident plane wave $p_I(t)$ at the aperture is replaced by the incident spherical wave

$$\frac{\rho_o}{4\pi|\mathbf{y}|}\,\frac{\partial Q_I}{\partial t}\left(t-\frac{|\mathbf{y}|}{c_o}\right).$$

3.3.5 The bias flow screen*

A steady mean pressure differential maintained across a screen with a small aperture produces a nominally steady *bias flow*. When the motion is at high Reynolds number, it is uninfluenced by viscosity except near the aperture edge, where the flow separates to form a jet. Vorticity generated at the edge by incident sound is swept away in the jet, and damping occurs by the transfer of acoustic energy to the kinetic energy of the jet. A bias flow screen with multiple apertures can therefore be used to enhance the attenuation of sound by vorticity production (§3.3.7).

Suppose that $x_1 < 0$ is the high pressure side of the screen and consider again the problem of a plane sound wave at normal incidence from $x_1 < 0$. An approximate representation of the influence of the jet for a circular aperture is obtained using the model of Figure 3.3.4. The jet is treated as smooth irrotational flow bounded by an axisymmetric shear layer idealised as a vortex sheet S_J (a 'free streamline'; Batchelor 1967). The jet rapidly contracts in cross-section to a uniform cylindrical form a short distance downstream of the aperture with cross-sectional area σA, where σ is the *contraction ratio* and $A = \pi a^2$ is the aperture area. If P_o denotes the mean pressure drop across the screen, the asymptotic jet speed in this downstream section is $U_\sigma = \sqrt{2P_o/\rho_o}$. This is also the mean tangential component of velocity at all points along the jet adjacent to the vortex sheet and just within the jet, where the mean pressure is uniform and constant.

The acoustic pressure wave generated at the aperture has two components $p(\mathbf{x}, t) = p_A(\mathbf{x}, t) + p_\sigma(\mathbf{x}, t)$, corresponding respectively to the diffracted pressure (3.3.10) produced in the absence of the jet, and that generated by the

Downloaded from https://www.cambridge.org/core. Charité Universitätsmedizin Berlin, on 20 Dec 2021 at 10:08:47, subject to the Cambridge Core terms of use, available at https://www.cambridge.org/core/terms. https://doi.org/10.1017/CBO9781107360273.004

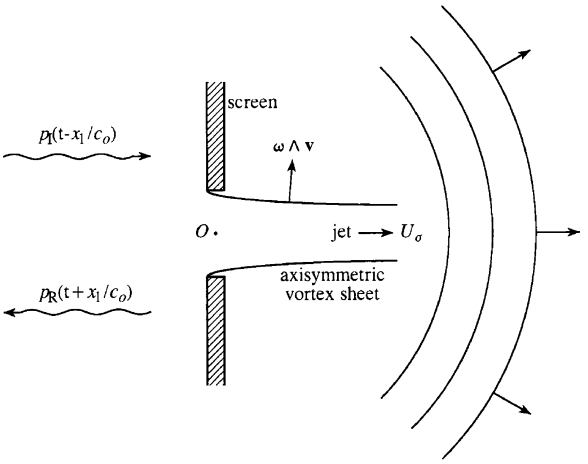

Figure 3.3.4

interaction of the volume flux Q with the jet. The latter is calculated using the vortex sound formula (4.7.4). Hence, to the right of the screen in $x_1 > 0$,

$$\left.\begin{aligned} p_A(\mathbf{x},t) &\approx \tfrac{K_o}{\pi|\mathbf{x}|}\, p_I\left(t-\tfrac{|\mathbf{x}|}{c_o}\right), \\ p_\sigma(\mathbf{x},t) &\approx -\rho_o \int_V (\boldsymbol{\omega}\wedge\mathbf{v})(\mathbf{y},\tau)\cdot \tfrac{\partial G}{\partial \mathbf{y}}(\mathbf{x},\mathbf{y},t-\tau)d^3\mathbf{y}d\tau \end{aligned}\right\} |\mathbf{x}|\to\infty, \tag{3.3.17}$$

where G is the aperture compact Green's function and $\boldsymbol{\omega} = \operatorname{curl}\mathbf{v}$ is the jet vorticity. The integration is over all regions where $\boldsymbol{\omega} \neq 0$.

The main contribution to the integral in (3.3.17) is from the neighbourhood of the aperture where $\nabla\varphi^*(\mathbf{y})$ (in the Green's function (3.3.16)) is significantly different from zero. In this region the vorticity will be approximated by

$$\boldsymbol{\omega}(\mathbf{x},t) = \{U_\sigma + u_\sigma(t)\}\delta(s_\perp)\mathbf{i}_\phi(\mathbf{x}),$$

where $u_\sigma(t)$ is the perturbation jet velocity just inside the vortex sheet produced by the incident sound, $s_\perp$ is distance measured in the direction of the *outward* normal from the vortex sheet, and $\mathbf{i}_\phi$ is a unit vector tangential to a circular vortex line orientated in the *clockwise* direction when looking along the jet from the aperture (Figure 3.3.5). The vorticity is convected at the mean of the velocities on the two sides of the vortex sheet, that is, at $\mathbf{v} = \frac{1}{2}\{U_\sigma + u_\sigma(t)\}\mathbf{t}$ where $\mathbf{t} = \mathbf{t}(\mathbf{x})$ is the unit tangential vector shown in the figure. The perturbation value of the vortex source is therefore

Downloaded from https://www.cambridge.org/core. Charité Universitätsmedizin Berlin, on 20 Dec 2021 at 10:08:47, subject to the Cambridge Core terms of use, available at https://www.cambridge.org/core/terms. https://doi.org/10.1017/CBO9781107360273.004

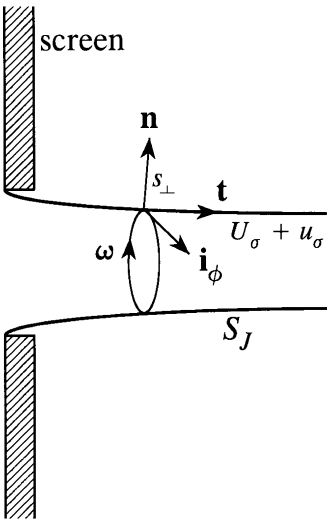

Figure 3.3.5

$$\boldsymbol{\omega} \wedge \mathbf{v} = \tfrac{1}{2}\Big((U_\sigma + u_\sigma(t))^2 - U_\sigma^2\Big)\delta(s_\perp)\mathbf{i}_\phi \wedge \mathbf{t} \approx U_\sigma u_\sigma(t)\delta(s_\perp)\mathbf{n}, \quad (3.3.18)$$

where $\mathbf{n} = \mathbf{i}_\phi \wedge \mathbf{t}$ is the outward unit normal on the jet boundary.

This is a quasi-static approximation, according to which modulation of the jet by the incident sound occurs sufficiently slowly that the jet may be assumed to pass through a continuous sequence of nominally steady states with slowly varying asymptotic jet speed $U_\sigma + u_\sigma(t)$. In particular, the variation of u_σ with distance from the aperture is neglected, implying that the 'wavelength' $\sim 2\pi U_\sigma/\omega$ (at frequency ω) of the vorticity variations along the jet is large compared to the aperture radius, that is, it is formally a low *Strouhal* number approximation: $\omega\ell/U_\sigma \ll 1$. When the result (3.3.18) and the compact Green's function (3.3.16) are substituted into the second of (3.3.17) we find

$$p_\sigma(\mathbf{x}, t) \approx -\frac{\rho_o U_\sigma}{2\pi\ell|\mathbf{x}|}\, u_\sigma\left(t - \frac{|\mathbf{x}|}{c_o}\right) \oint_{S_J} \frac{\partial\varphi^*}{\partial s_\perp}(\mathbf{y})\, dS(\mathbf{y}),$$

where the integration is over the free surface S_J of the jet (Figure 3.3.5). The integral represents the volume flux through S_J of the ideal flow through the aperture defined by the potential function φ^*, with streamline pattern illustrated in Figure 3.3.6 for a circular aperture in a thin plate. Because $\nabla^2\varphi^* = 0$, it follows from (3.3.3) that $\oint_{S_J} \frac{\partial\varphi^*}{\partial s_\perp}(\mathbf{y})\, dS(\mathbf{y}) = A$, and therefore that

$$p_\sigma(\mathbf{x}, t) \approx -\frac{\rho_o U_\sigma}{2\pi\ell|\mathbf{x}|}\, A u_\sigma\left(t - \frac{|\mathbf{x}|}{c_o}\right). \quad (3.3.19)$$

Downloaded from https://www.cambridge.org/core. Charité Universitätsmedizin Berlin, on 20 Dec 2021 at 10:08:47, subject to the Cambridge Core terms of use, available at https://www.cambridge.org/core/terms. https://doi.org/10.1017/CBO9781107360273.004

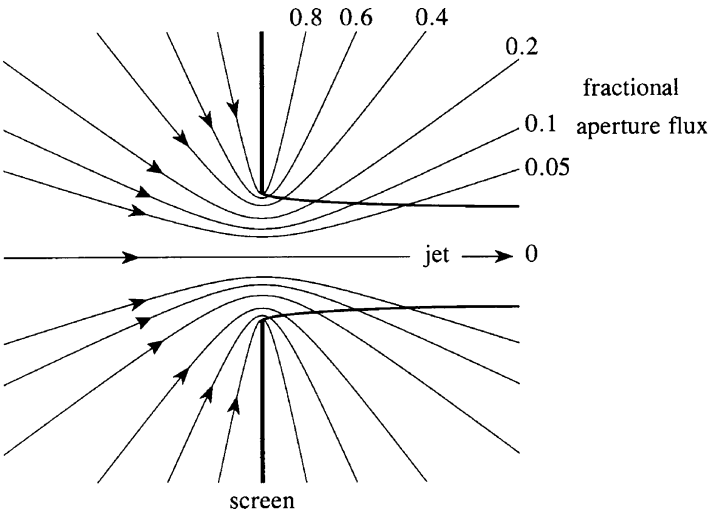

Figure 3.3.6

A typical 'streamtube' of the φ^*-flow through a circular aperture (Figure 3.3.6) is obtained by rotation of a streamline about the x_1 axis of symmetry. A streamline's numerical label in the figure represents the fraction of the total flux A conveyed by the corresponding streamtube. It follows that the section of the jet boundary S_J downstream of its intersection with the streamline labelled 0.1, for example, contributes $0.1A$ to the flux integral $\oint_{S_J} \frac{\partial \varphi^*}{\partial s_\perp}(\mathbf{y})\, dS(\mathbf{y})$. It is clear, therefore, that roughly 90% of the value of this integral is from the section of S_J within a distance from the screen marginally larger than the aperture radius.

The transmitted acoustic pressure is now obtained from equation (3.3.19) and the first of (3.3.17) in the form

$$p(\mathbf{x},t) = p_A + p_\sigma \approx \frac{K_o}{\pi|\mathbf{x}|} p_I\left(t - \frac{|\mathbf{x}|}{c_o}\right) - \frac{\rho_o U_\sigma}{2\pi\sigma\ell|\mathbf{x}|} Q\left(t - \frac{|\mathbf{x}|}{c_o}\right), \quad |\mathbf{x}| \to \infty, \quad x_1 > 0, \tag{3.3.20}$$

where $Q(t) = \sigma A u_\sigma(t)$ is the unsteady volume velocity. This monopole radiation from the aperture must coincide with that given directly in terms of the aperture volume velocity Q by equation (3.3.1). By equating the two results we obtain the linearised *Cummings–Fant* equation

$$\rho_o \frac{dQ}{dt} = 2K_o\, p_I(t) - \frac{\rho_o U_\sigma Q}{\sigma\ell},$$

Downloaded from https://www.cambridge.org/core. Charité Universitätsmedizin Berlin, on 20 Dec 2021 at 10:08:47, subject to the Cambridge Core terms of use, available at https://www.cambridge.org/core/terms. https://doi.org/10.1017/CBO9781107360273.004

which determines $Q(t)$ in terms of the incident pressure $p_I(t)$. It replaces equation (3.3.9) in the absence of bias flow. Experiments (Cummings 1984) indicate that the best agreement with predictions based on this equation are obtained by taking $\sigma \approx 0.75$.

It is usual to write the equation in terms of the average velocity $U_J = \sigma U_\sigma$ of the jet across the area A of the aperture:

$$\rho_o \ell \frac{dQ}{dt} + \frac{\rho_o U_J Q}{\sigma^2} = 2A\, p_I(t). \tag{3.3.21}$$

In the absence of forcing by the incident wave, this equation predicts that any perturbation in Q is exponentially damped like $\mathrm{e}^{-U_J t/\ell\sigma^2}$. This damping is caused by the transfer of energy to kinetic energy of the jet (see §3.3.7).

The energy equation (3.3.11) now assumes the form

$$\frac{d}{dt}\left(\frac{\rho_o Q^2}{2K_o}\right) = 2p_I Q - \frac{\rho_o}{\pi c_o}\left(\frac{dQ}{dt}\right)^2 + \frac{\rho_o}{\pi c_o}\frac{d}{dt}\left(Q\frac{dQ}{dt}\right) - \frac{\rho_o U_J Q^2}{\sigma^2 A},$$

so that the mean rate of dissipation of the incident acoustic energy

$$2\langle p_I Q\rangle = \left\langle \frac{\rho_o}{\pi c_o}\left(\frac{dQ}{dt}\right)^2\right\rangle + \left\langle \frac{\rho_o U_J Q^2}{\sigma^2 A}\right\rangle. \tag{3.3.22}$$

The terms on the right respectively represent the acoustic power in the spherical waves radiated from the aperture on both sides of the screen, and the rate of increase of the kinetic energy of the jet.

3.3.6 The complex conductivity*

The transmitted acoustic pressure for the bias flow problem of Figure 3.3.4 is given by equation (3.3.1), where $Q(t)$ is the solution of equation (3.3.21) which accounts for the interaction of the sound with the jet. The strength of this interaction is frequency-dependent, and we therefore take the incident wave p_I and Q in the time-harmonic forms

$$p_I = \hat{p}_I(\omega)\mathrm{e}^{-i\omega(t-x_1/c_o)}, \quad Q = \hat{Q}(\omega)\mathrm{e}^{-i\omega t}.$$

Substitution into (3.3.21) yields $\hat{Q}(\omega) = (2A\hat{p}_I(\omega)/\rho_o)/(-i\omega\ell + U_J/\sigma^2)$. The corresponding acoustic pressure $\hat{p}(\mathbf{x},\omega)$ in $x_1 > 0$ determined by (3.3.1) supplies the following generalisation of the 'jet-free' formula (3.3.10):

$$\left.\begin{aligned} \hat{p}(\mathbf{x},\omega) &\approx \frac{\hat{K}(\omega)\,\hat{p}_I(\omega)\mathrm{e}^{ik_o|\mathbf{x}|}}{\pi|\mathbf{x}|}, \quad |\mathbf{x}| \to \infty, \\ \hat{K}(\omega) &= \frac{(\omega\ell/U_J)K_o}{(\omega\ell/U_J + i/\sigma^2)}, \end{aligned}\right\} \tag{3.3.23}$$

Downloaded from https://www.cambridge.org/core. Charité Universitätsmedizin Berlin, on 20 Dec 2021 at 10:08:47, subject to the Cambridge Core terms of use, available at https://www.cambridge.org/core/terms. https://doi.org/10.1017/CBO9781107360273.004

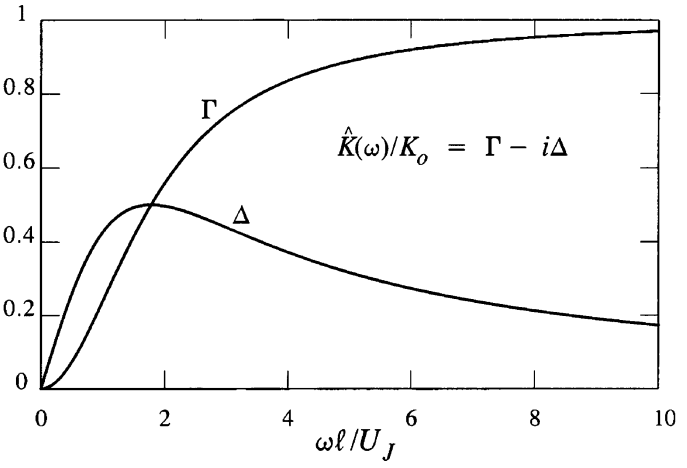

Figure 3.3.7

where $K_o = A/\ell$ is the aperture conductivity in the absence of mean flow. $\hat{K}(\omega)$ is the complex conductivity, which satisfies the following analogue of (3.3.6):

$$\hat{\varphi}_+(\omega) - \hat{\varphi}_-(\omega) = \frac{\hat{Q}(\omega)}{\hat{K}(\omega)}, \tag{3.3.24}$$

where $\hat{\varphi}_+(\omega)$, $\hat{\varphi}_-(\omega)$ respectively represent the time-harmonic components of the acoustic potentials at large distances from the aperture in $x_1 \gtrless 0$, but well within a characteristic acoustic wavelength ($\sim c_o/\omega$). Let $\hat{K}/K_o = \Gamma - i\Delta$. The imaginary part Δ accounts for the absorption of acoustic energy by the jet, and $\hat{K} \to K_o$ when $\omega\ell/U_J$ becomes large – because the alternations in the acoustic field within the aperture are then too rapid to affect vorticity production. The dependences of Γ and Δ on the *Strouhal number* $\omega\ell/U_J$ are shown in Figure 3.3.7 for $\sigma = 0.75$.

Example The bias-flow perforated screen Let the time-harmonic plane wave $\hat{p}_I e^{ik_o x_1}$ of frequency ω be incident on a thin screen (at $x_1 = 0$) which is uniformly perforated with N acoustically compact apertures per unit area (Figure 3.3.8). The distance between neighbouring apertures is small compared to the acoustic wavelength, but large enough for the *hydrodynamics* of neighbouring jets to be independent. There are plane-reflected and transmitted waves $\hat{p}_R e^{-ik_o x_1}$, $\hat{p}_T e^{ik_o x_1}$, respectively.

The volume flux through one aperture is (by (3.3.24))

$$\hat{Q}(\omega) = \frac{\hat{K}(\omega)(\hat{p}_I + \hat{p}_R - \hat{p}_T)}{-i\omega\rho_o}.$$

Downloaded from https://www.cambridge.org/core. Charité Universitätsmedizin Berlin, on 20 Dec 2021 at 10:08:47, subject to the Cambridge Core terms of use, available at https://www.cambridge.org/core/terms. https://doi.org/10.1017/CBO9781107360273.004

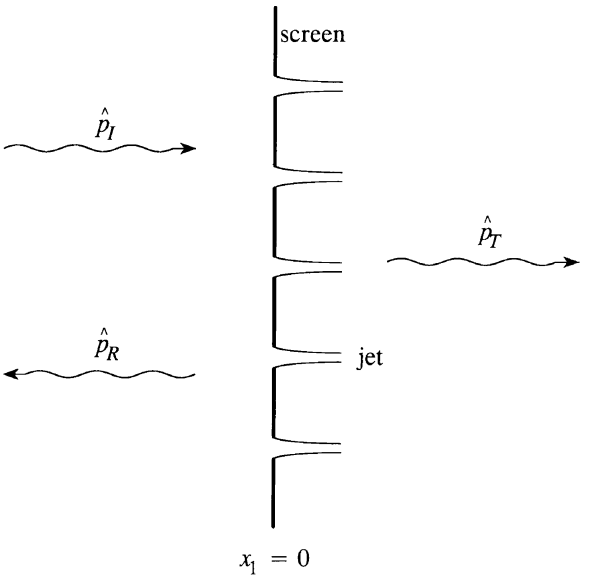

Figure 3.3.8

The volume flux through unit area of the screen is $N\hat{Q}$, and therefore

$$\frac{\hat{p}_T}{\rho_o c_o} = \frac{\hat{p}_I - \hat{p}_R}{\rho_o c_o} = \frac{N\hat{K}(\omega)(\hat{p}_I + \hat{p}_R - \hat{p}_T)}{-i\omega\rho_o},$$

so that $\hat{p}_R = R\hat{p}_I$ and $\hat{p}_T = T\hat{p}_I$, where the reflection and transmission coefficients R, T are

$$R = \frac{k_o}{k_o + 2iN\hat{K}(\omega)}, \quad T = \frac{2iN\hat{K}(\omega)}{k_o + 2iN\hat{K}(\omega)}.$$

The time-averaged acoustic power Π_a dissipated per unit area of the screen is

$$\Pi_a = \frac{|\hat{p}_I|^2}{\rho_o c_o}\Big\langle \mathrm{Re}\Big((1+R)\mathrm{e}^{-i\omega t}\Big)\,\mathrm{Re}\Big((1-R)\mathrm{e}^{-i\omega t}\Big) - \mathrm{Re}\Big(T\mathrm{e}^{-i\omega t}\Big)\,\mathrm{Re}\Big(T\mathrm{e}^{-i\omega t}\Big)\Big\rangle$$

$$= \frac{|\hat{p}_I|^2}{2\rho_o c_o}\left(1 - |R|^2 - |T|^2\right) = \frac{|\hat{p}_I|^2}{2\rho_o c_o}\,\frac{4k_o N K_o \Delta(\omega)}{|k_o + 2iN\hat{K}(\omega)|^2} > 0. \qquad (3.3.25)$$

The fractional dissipated power $1 - |R|^2 - |T|^2$ is plotted against $\omega a/U$ in Figure 3.3.9 for a screen with circular apertures of uniform radius a (so that $\ell = \pi a/2$). The plots are for several values of α/M, where $\alpha = N\pi a^2$ is

Downloaded from https://www.cambridge.org/core. Charité Universitätsmedizin Berlin, on 20 Dec 2021 at 10:08:47, subject to the Cambridge Core terms of use, available at https://www.cambridge.org/core/terms. https://doi.org/10.1017/CBO9781107360273.004

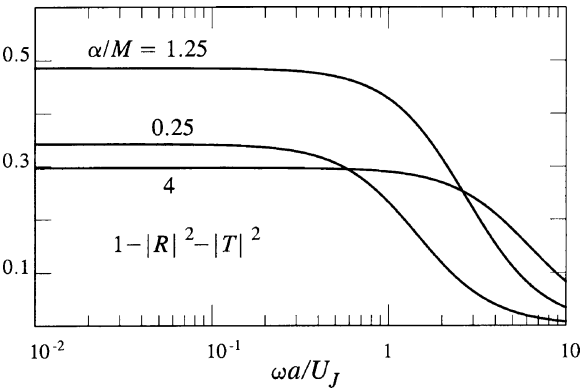

Figure 3.3.9

the *fractional open area* and $M = U_J/c_o$ is the mean jet Mach number in the plane of each aperture. The dissipation attains a maximum of about 0.5 near $\alpha/M = 1.25$ over a broad range of Strouhal numbers $\omega a/U_J < 1$.

3.3.7 Dissipation by vorticity production

At low frequencies the flow within an aperture can be sufficiently slow that viscous-induced dissipation becomes important. If the local Reynolds number is large, however, viscous action can result in the production of 'free' *vorticity* that carries away acoustic energy in the form of hydrodynamic kinetic energy before being subsequently dissipated by viscosity into heat.

At low Mach numbers the rate of production of this kinetic energy can be calculated using Crocco's momentum equation (1.2.10). Let $\mathbf{v}_\omega$ denote the velocity induced by the vorticity $\boldsymbol{\omega}$ as if the flow were incompressible (including any low Mach number *mean* flow velocity; cf. §§4.4, 4.5), and put

$$\mathbf{v} = \mathbf{v}_\omega + \nabla\varphi,$$

where the velocity potential φ accounts for the influence of compressibility, including contributions from incident and diffracted sound waves.

When the typical mean flow Mach number $M \ll 1$ departures of the density from the mean density ρ_o are of order $M^2\rho_o$, and the kinetic energy of the fluid is approximately

$$T = \tfrac{1}{2}\rho_o \int (\mathbf{v}_\omega + \nabla\varphi)^2 d^3\mathbf{x} \equiv \tfrac{1}{2}\rho_o \int \mathbf{v}_\omega^2 d^3\mathbf{x} + \tfrac{1}{2}\rho_o \int (\nabla\varphi)^2 d^3\mathbf{x},$$

where the integrations are over the fluid. The split into the final two integrals follows from the divergence theorem and the conditions that $\operatorname{div}\mathbf{v}_\omega = 0$

Downloaded from https://www.cambridge.org/core. Charité Universitätsmedizin Berlin, on 20 Dec 2021 at 10:08:47, subject to the Cambridge Core terms of use, available at https://www.cambridge.org/core/terms. https://doi.org/10.1017/CBO9781107360273.004

and that the normal component of $\mathbf{v}_\omega$ vanishes on solid boundaries. When $\mathbf{v}_\omega$ includes a mean component of velocity $\mathbf{U}$, say, there is no contribution $\oint_\Sigma \varphi\, \mathbf{U}\cdot d\mathbf{S}$ from a control surface Σ at large distances, because Σ is ultimately sufficiently distant that no sound has arrived.

The kinetic energy is therefore partitioned between the kinetic energy $E = \frac{1}{2}\rho_o \int \mathbf{v}_\omega^2 d^3\mathbf{x}$ of the vortical motion and the kinetic energy of the acoustic field. To calculate the changes in E, the homentropic form of Crocco's equation is written

$$\rho_o \frac{\partial \mathbf{v}_\omega}{\partial t} + \nabla\left(\rho_o\left[B + \frac{\partial \varphi}{\partial t}\right]\right) = -\rho_o \boldsymbol{\omega}\wedge\mathbf{v} - \eta \mathrm{curl}\,\boldsymbol{\omega},$$

and the scalar product is taken with $\mathbf{v}_\omega$:

$$\frac{\partial}{\partial t}\left(\tfrac{1}{2}\rho_o \mathbf{v}_\omega^2\right) + \mathrm{div}\left(\rho_o \mathbf{v}_\omega\left[B + \frac{\partial \varphi}{\partial t}\right]\right) = \rho_o \nabla\varphi\cdot\boldsymbol{\omega}\wedge\mathbf{v} - \eta\mathbf{v}_\omega\cdot\mathrm{curl}\,\boldsymbol{\omega},$$

because $\mathrm{div}\,\mathbf{v}_\omega = 0$, and $\mathbf{v}_\omega\cdot\boldsymbol{\omega}\wedge\mathbf{v} = (\mathbf{v}-\nabla\varphi)\cdot\boldsymbol{\omega}\wedge\mathbf{v} = -\nabla\varphi\cdot\boldsymbol{\omega}\wedge\mathbf{v}$. The argument of the divergence represents the flux of vortical kinetic energy when convection by the acoustic particle velocity is excluded. The first term on the right is a *source* of vorticity kinetic energy arising from the coupling between the vorticity and the sound.

Hence, integration over the fluid region yields

$$\frac{\partial E}{\partial t} + 2\eta \int e_{ij}e_{ij}\, d^3\mathbf{x} = \rho_o \int \nabla\varphi\cdot\boldsymbol{\omega}\wedge\mathbf{v}\, d^3\mathbf{x}, \tag{3.3.26}$$

where e_{ij} is the rate of strain tensor (1.2.6). The left-hand side is the power $\Pi_\omega = \partial E/\partial t$ entering the vortical flow and that dissipated by friction. At high Reynolds numbers, viscous dissipation occurs mainly at solid boundaries where velocity gradients are large. The energy supplied by the source (on the right-hand side) therefore passes to the vortex motions and is not immediately dissipated by viscous action. In the absence of mean flow $\Pi_\omega \sim O(\epsilon^3)$, where ϵ is a measure of the acoustic amplitude, because both $\boldsymbol{\omega}$ and $\mathbf{v}_\omega$ are $O(\epsilon)$. When, however, there is a substantial mean flow component of $\mathbf{v}$, both $\mathbf{v}_\omega$ and $\boldsymbol{\omega}$ can have large mean components that are independent of the sound – mean flow can therefore increase the rate of production of vortical energy at the expense of the sound to $\Pi_\omega \sim O(\epsilon^2)$.

Thus

$$\Pi_\omega \approx \rho_o \int \mathbf{u}\cdot\boldsymbol{\omega}\wedge\mathbf{v}\, d^3\mathbf{x} \tag{3.3.27}$$

is the *rate of dissipation of acoustic energy* by vorticity production, where the acoustic particle velocity $\nabla\varphi$ has been denoted by $\mathbf{u}$.

Downloaded from https://www.cambridge.org/core. Charité Universitätsmedizin Berlin, on 20 Dec 2021 at 10:08:47, subject to the Cambridge Core terms of use, available at https://www.cambridge.org/core/terms. https://doi.org/10.1017/CBO9781107360273.004

Example Power dissipated in a bias-flow jet For the problem of Figure 3.3.4 involving a plane wave incident on a screen with a single aperture, we have from (3.3.18):

$$\boldsymbol{\omega} \wedge \mathbf{v} \approx U_\sigma u_\sigma(t)\delta(s_\perp)\mathbf{n} \equiv \frac{U_J Q(t)}{\sigma^2 A}\delta(s_\perp)\mathbf{n}$$

and the acoustic particle velocity within and near the aperture is given by (3.3.2) as:

$$\mathbf{u} = \frac{Q}{A}\nabla\varphi^*.$$

Hence equation (3.3.27) gives the following expression for the acoustic power dissipated by vorticity production in the jet:

$$\Pi_\omega = \frac{\rho_o U_J Q^2(t)}{\sigma^2 A^2}\oint_{S_J} \nabla\varphi^* \cdot d\mathbf{S} = \frac{\rho_o U_J Q^2(t)}{\sigma^2 A}.$$

This confirms our earlier interpretation of the second term on the right of the energy equation (3.3.22) as the rate of dissipation due to vorticity production in the jet.

Problems 3

3.1. A plane time-harmonic sound wave of frequency ω and pressure $\hat{p} = \hat{p}_I e^{-ik_o x_1}$ is incident from $x_1 > 0$ on an infinite rigid baffle $x_1 = 0$ containing a spring-loaded, circular piston of radius a flush with the baffle and centre at the origin. The piston is acoustically compact and its motion is governed by equation (3.1.17). Show that the spherical wave radiated from the piston is given by

$$\hat{p}(\mathbf{x}, \omega) \approx \frac{3\pi a \hat{p}_I e^{ik_o|\mathbf{x}|}}{8|\mathbf{x}|} \frac{\omega^2 M_a}{\left(\Omega^2 M - \frac{i\omega\rho_o c_o \pi a^2}{2} - \omega^2 (M + M_a)\right)}, \quad |\mathbf{x}| \to \infty,$$

where $M_a = \rho_o \pi a^2 \ell$ ($\ell = 8a/3\pi$) is the piston added mass and ρ_o is the mean fluid density.

3.2.* A narrow air jet impinges at normal incidence on the free surface $x_1 = 0$ of water of infinite depth. The jet exerts an unsteady force $F(t)$ on the interface over a surface area of infinitesimal cross-section, and can be represented by an unsteady surface pressure $p = F(t)\delta(x_2)\delta(x_3)$ applied at the surface at the coordinate origin O. Show that the acoustic pressure in the water at $\mathbf{x}$ is given by

Downloaded from https://www.cambridge.org/core. Charité Universitätsmedizin Berlin, on 20 Dec 2021 at 10:08:47, subject to the Cambridge Core terms of use, available at https://www.cambridge.org/core/terms. https://doi.org/10.1017/CBO9781107360273.004

$$p(\mathbf{x},t) = -\frac{\partial}{\partial x_1}\left[\frac{1}{2\pi|\mathbf{x}|}F\left(t-\frac{|\mathbf{x}|}{c_o}\right)\right]$$
$$\simeq \frac{\cos\theta}{2\pi c_o|\mathbf{x}|}\frac{\partial F}{\partial t}\left(t-\frac{|\mathbf{x}|}{c_o}\right), \quad |\mathbf{x}|\to\infty, \quad \cos\theta = \frac{x_1}{|\mathbf{x}|}.$$

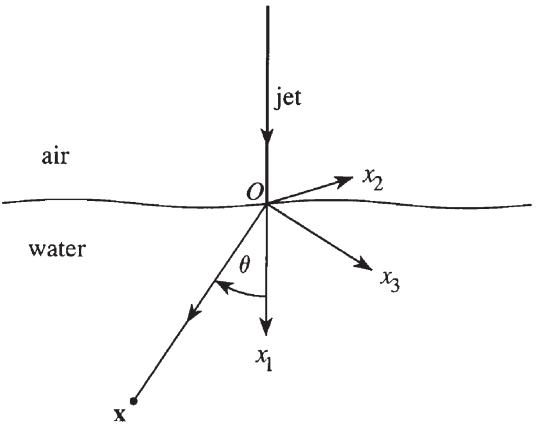

3.3.* The face of a circular piston of radius a is in contact with the free surface $x_1 = 0$ of water of infinite depth with its centre at the origin, where x_1 increases into the water. The piston is in small amplitude motion at normal velocity $U(t)$ (in the x_1 direction) producing sound of characteristic wavelength $\lambda \gg a$. Show that the acoustic pressure at a far field point $\mathbf{x}$ in the water is given approximately by

$$p(\mathbf{x},t) \approx \frac{2\rho_o a^3\cos\theta}{3\pi c_o|\mathbf{x}|}\left[\frac{d^2U}{dt^2}\right], \quad \cos\theta = \frac{x_1}{|\mathbf{x}|},$$

where the square brackets denote evaluation at the retarded time $t - |\mathbf{x}|/c_o$.

3.4. A thin rigid screen $x_1 = 0$ has an aperture centred on the coordinate origin whose shape is defined by the polar equation $\varpi = a|\sin n\theta|$, $0 < \theta < 2\pi$, where $(x_2, x_3) = \varpi(\cos\theta, \sin\theta)$, a is constant and n is an integer. A plane time-harmonic wave $\hat{p}(x_1,\omega) = \hat{p}_I e^{ik_o x_1}$ is incident on the screen from $x_1 < 0$. If $k_o a \gg 1$, use Kirchhoff diffraction theory to calculate the pressure on the positive x_1 axis within the Fresnel zone.

3.5. A thin rigid screen $x_1 = 0$ has a rectangular aperture occupying the region $-a < x_2 < a$, $-b < x_3 < b$. A time-harmonic plane wave $\hat{p}(x_1,\omega) = \hat{p}_I e^{ik_o x_1}$ is incident on the screen from $x_1 < 0$. Use

Downloaded from https://www.cambridge.org/core. Charité Universitätsmedizin Berlin, on 20 Dec 2021 at 10:08:47, subject to the Cambridge Core terms of use, available at https://www.cambridge.org/core/terms. https://doi.org/10.1017/CBO9781107360273.004

Kirchhoff diffraction theory to show that the acoustic intensity I in the Fraunhofer far field on the side $x_1 > 0$ is given by

$$I = I_o \left(\frac{\sin n_2 k_o a}{n_2 k_o a} \right)^2 \left(\frac{\sin n_3 k_o b}{n_3 k_o b} \right)^2, \quad \mathbf{n} = \frac{\mathbf{x}}{|\mathbf{x}|},$$

where I_o is the intensity on the x_1 axis.

3.6.* A plane wave $p_I(t - x_1/c_o)$ is incident from $x_1 < 0$ on a thin, rigid bias-flow screen occupying $x_1 = 0$ with a small aperture of conductivity K_o centred on the coordinate origin. The volume velocity Q through the aperture satisfies equation (3.3.21). Show that the acoustic pressure at large distances in $x_1 > 0$ is given by

$$p(\mathbf{x}, t) \simeq \frac{K_o}{\pi |\mathbf{x}|} \left\{ p_I([t]) - \frac{U_J}{\ell \sigma^2} \int_{-\infty}^{[t]} p_I(\tau) \mathrm{e}^{-U_J([t]-\tau)/\ell\sigma^2} d\tau \right\},$$

$$[t] = t - \frac{|\mathbf{x}|}{c_o}.$$

Calculate and plot the transmitted acoustic waveform when $p_I(t) = p_o \mathrm{e}^{-(t/t_o)^2}$ (p_o, t_o being constants) for a range of values of $U_J t_o/\ell\sigma^2$.

3.7. A Helmholtz resonator consists of a hard-walled, acoustically compact cavity of interior volume V that communicates with the atmosphere by means of a short narrow-necked tube of cross-section A and length $h \ll V^{\frac{1}{3}}$. The system behaves as a simple harmonic oscillator with a reciprocating flow into and out of the cavity through the neck. The pressure fluctuations within the cavity may be assumed to be uniform

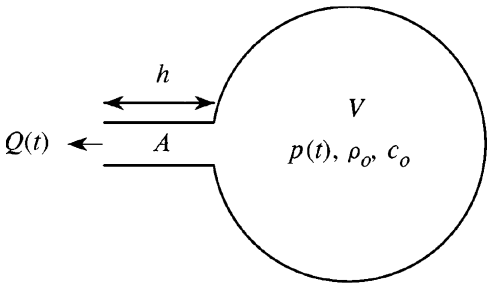

and equal to $p(t)$. Show that in the linearised, ideal fluid approximation, the volume velocity Q of the exit flow in the neck satisfies the equations

$$\frac{V}{\rho_o c_o^2} \frac{dp}{dt} + Q = 0, \quad \rho_o \ell \frac{dQ}{dt} = Ap,$$

where $\ell \sim h$ is the effective slug length of the flow through the neck. Deduce that the resonance frequency is given by $f = (c_o/2\pi)\sqrt{A/V\ell}$.

Downloaded from https://www.cambridge.org/core. Charité Universitätsmedizin Berlin, on 20 Dec 2021 at 10:08:47, subject to the Cambridge Core terms of use, available at https://www.cambridge.org/core/terms. https://doi.org/10.1017/CBO9781107360273.004

4

Aerodynamic Sound

4.1 Lighthill's acoustic analogy

The sound generated by turbulent flow is called *aerodynamic sound*. Most unsteady flows of technological interest are of high Reynolds number and turbulent, and the acoustic radiation is a very small by-product of the motion. The turbulence is usually produced by fluid motion over a solid boundary or by flow instability. Lighthill (1952) investigated aerodynamic sound by transforming the Navier–Stokes and continuity equations to form an exact, inhomogeneous wave equation whose source terms are important only within the turbulent region. He argued that sound is a very small component of the whole motion and that, once generated, its 'back-reaction' on the main flow can usually be ignored. The properties of the unsteady flow in the source region may then be determined by neglecting the production and propagation of the sound, a reasonable approximation if the Mach number M is small, and there are many important flows where the hypothesis is obviously correct, and where the theory leads to unambiguous predictions of the sound.

Lighthill was initially interested in solving the problem illustrated in Figure 4.1.1a, of the sound produced by a turbulent nozzle flow. However, his original theory actually applies to the simpler situation shown in Figure 4.1.1b, in which the sound is imagined to be generated by a finite region of 'rotational' flow in an *unbounded* fluid. This avoids complications caused by the presence of the nozzle. The fluid is assumed to be at rest at infinity, where the mean pressure, density and sound speed are respectively equal to $p_o,\ \rho_o,\ c_o$. Lighthill compared the equations for the production of acoustic *density* fluctuations in the real flow with those in an ideal, linear acoustic medium that coincides with the real fluid at large distances from the sources.

To do this body forces are neglected and the i-component of the momentum equation (1.2.4) is cast in the form

Downloaded from https://www.cambridge.org/core. Charité Universitätsmedizin Berlin, on 20 Dec 2021 at 10:08:47, subject to the Cambridge Core terms of use, available at https://www.cambridge.org/core/terms. https://doi.org/10.1017/CBO9781107360273.005

$$\rho\frac{\partial v_i}{\partial t}+\rho v_j\frac{\partial v_i}{\partial x_j}=-\frac{\partial p}{\partial x_i}+\frac{\partial \sigma_{ij}}{\partial x_j}\equiv-\frac{\partial}{\partial x_j}\left(p\delta_{ij}-\sigma_{ij}\right), \tag{4.1.1}$$

where σ_{ij} is the viscous stress tensor

$$\sigma_{ij}=2\eta\left(e_{ij}-\frac{1}{3}e_{kk}\delta_{ij}\right)+\eta' e_{kk}\delta_{ij}, \tag{4.1.2}$$

and e_{ij} is the rate of strain tensor (1.2.6). Next, multiply the continuity equation (1.2.3) by v_i:

$$v_i\frac{\partial \rho}{\partial t}+v_i\frac{\partial(\rho v_j)}{\partial x_j}=0.$$

By adding this to equation (4.1.1) we obtain *Reynolds form* of the momentum equation

$$\frac{\partial(\rho v_i)}{\partial t}=-\frac{\partial \pi_{ij}}{\partial x_j}, \tag{4.1.3}$$

where

$$\pi_{ij}=\rho v_i v_j+(p-p_o)\delta_{ij}-\sigma_{ij} \tag{4.1.4}$$

is the *momentum flux* tensor, and $\partial\pi_{ij}/\partial x_j$ is the rate at which i-momentum flows out of unit volume of fluid. The constant pressure p_o is inserted for convenience.

In an ideal, linear acoustic medium, the momentum flux tensor contains only the pressure, that is,

$$\pi_{ij}\to\pi^o_{ij}=(p-p_o)\delta_{ij}\equiv c_o^2(\rho-\rho_o)\delta_{ij}, \tag{4.1.5}$$

and the momentum equation then reduces to

$$\frac{\partial(\rho v_i)}{\partial t}+\frac{\partial}{\partial x_i}[c_o^2(\rho-\rho_o)]=0. \tag{4.1.6}$$

By writing the continuity equation (1.2.3) in the slightly modified form

$$\frac{\partial}{\partial t}(\rho-\rho_o)+\frac{\partial(\rho v_i)}{\partial x_i}=0, \tag{4.1.7}$$

the momentum density ρv_i can be eliminated between (4.1.6) and (4.1.7) to give the equation of *linear acoustics* satisfied by the perturbation density $\rho-\rho_o$:

$$\left(\frac{1}{c_o^2}\frac{\partial^2}{\partial t^2}-\nabla^2\right)[c_o^2(\rho-\rho_o)]=0. \tag{4.1.8}$$

Because the turbulence is neglected in this approximation, and there are no externally applied forces or moving boundaries, the unique solution of this

Downloaded from https://www.cambridge.org/core. Charité Universitätsmedizin Berlin, on 20 Dec 2021 at 10:08:47, subject to the Cambridge Core terms of use, available at https://www.cambridge.org/core/terms. https://doi.org/10.1017/CBO9781107360273.005

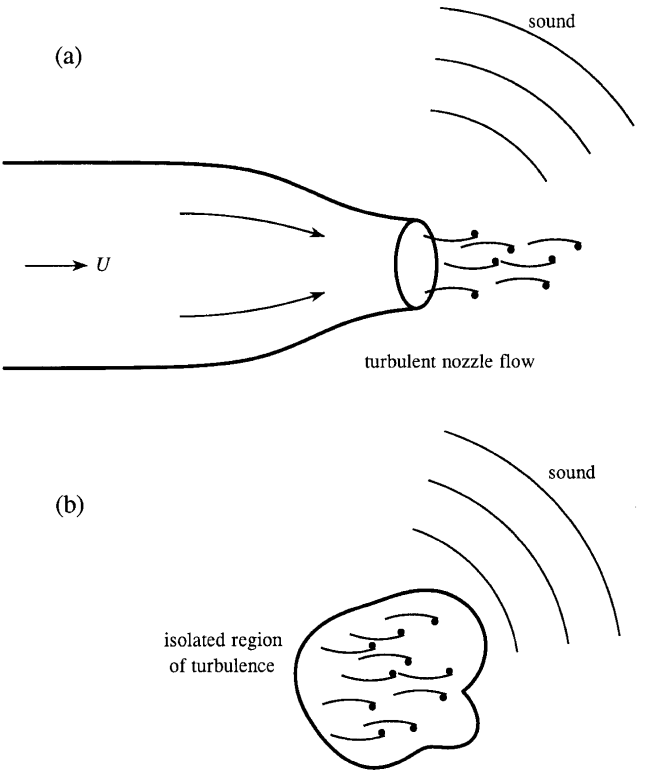

Figure 4.1.1

equation that satisfies the radiation condition of *outgoing wave behaviour* is simply $\rho - \rho_o = 0$.

It can now be asserted that the sound generated by the turbulence in the *real fluid* is exactly equivalent to that produced in the ideal, stationary acoustic medium (which is governed by (4.1.8) in turbulence-free regions) forced by the excess stress distribution

$$\begin{aligned} T_{ij} &= \pi_{ij} - \pi^o_{ij} \\ &= \rho v_i v_j + \Big((p - p_o) - c_o^2 (\rho - \rho_o) \Big) \delta_{ij} - \sigma_{ij}, \end{aligned} \tag{4.1.9}$$

where T_{ij} is called the *Lighthill stress tensor*. This is **Lighthill's acoustic analogy**.

Downloaded from https://www.cambridge.org/core. Charité Universitätsmedizin Berlin, on 20 Dec 2021 at 10:08:47, subject to the Cambridge Core terms of use, available at https://www.cambridge.org/core/terms. https://doi.org/10.1017/CBO9781107360273.005

Indeed, (4.1.3) can be re-cast as the momentum equation of an ideal, stationary acoustic medium of mean density ρ_o and sound speed c_o subject to the externally applied stress T_{ij}:

$$\frac{\partial(\rho v_i)}{\partial t} + \frac{\partial \pi_{ij}^o}{\partial x_j} = -\frac{\partial}{\partial x_j}\left(\pi_{ij} - \pi_{ij}^o\right)$$

$$\text{i.e. } \frac{\partial(\rho v_i)}{\partial t} + \frac{\partial}{\partial x_i}\left[c_o^2(\rho - \rho_o)\right] = -\frac{\partial T_{ij}}{\partial x_j}. \tag{4.1.10}$$

The elimination of the momentum density ρv_i between this and the continuity equation (4.1.7) (the same procedure used above for the linear problem) then yields **Lighthill's equation**

$$\left(\frac{1}{c_o^2}\frac{\partial^2}{\partial t^2} - \nabla^2\right)[c_o^2(\rho - \rho_o)] = \frac{\partial^2 T_{ij}}{\partial x_i \partial x_j}. \tag{4.1.11}$$

This is the *exact*, nonlinear counterpart of (4.1.8). The problem of calculating the turbulence generated sound is therefore equivalent to solving this equation for the radiation into a stationary, ideal fluid produced by a distribution of *quadrupole* sources whose strength per unit volume is the Lighthill stress tensor T_{ij}. The quadrupole character of the turbulence sources is one of the most important conclusions of Lighthill's theory; it implies (see §4.2) that free field turbulence is an extremely weak sound source, and that in a typical low Mach number flow only a tiny fraction of the available flow energy is converted into sound.

In the definition (4.1.9) of T_{ij}, the term $\rho v_i v_j$ is called the *Reynolds stress*. For the simplified problem of Figure 4.1.1b it is a nonlinear quantity that can be neglected except where the motion is turbulent. The second term represents the *excess* of momentum transfer by the pressure over that in the ideal ('linear') fluid of density ρ_o and sound speed c_o. This is produced by wave amplitude nonlinearity, and by mean density variations in the source flow. The viscous stress tensor σ_{ij} is linear in the perturbation quantities, and properly accounts for the attenuation of the sound; in most applications the *Reynolds number* in the source region is very large and σ_{ij} can be neglected, and the viscous attenuation of the radiating sound is usually ignored.

4.2 The v^8-law

The formal solution of Lighthill's equation (4.1.11) with outgoing wave behaviour is given by (1.8.7) with $p(\mathbf{x}, t)$ replaced by $c_o^2(\rho - \rho_o)$:

$$c_o^2(\rho - \rho_o)(\mathbf{x}, t) = \frac{1}{4\pi}\frac{\partial^2}{\partial x_i \partial x_j}\int_{-\infty}^{\infty} \frac{T_{ij}(\mathbf{y}, t - |\mathbf{x} - \mathbf{y}|/c_o)}{|\mathbf{x} - \mathbf{y}|}\, d^3\mathbf{y}. \tag{4.2.1}$$

Downloaded from https://www.cambridge.org/core. Charité Universitätsmedizin Berlin, on 20 Dec 2021 at 10:08:47, subject to the Cambridge Core terms of use, available at https://www.cambridge.org/core/terms. https://doi.org/10.1017/CBO9781107360273.005

This is strictly an alternative, integral equation representation of equation (4.1.11); it provides a useful prediction of the sound only when T_{ij} is known or has been determined by some other means. This is because the terms in the definition (4.1.9) of T_{ij} not only account for the generation of sound but also govern acoustic *self-modulation* caused by acoustic nonlinearity, the *convection* of sound waves by the turbulent velocity, *refraction* caused by sound speed variations, and *attenuation* due to thermal and viscous actions. The influence of acoustic nonlinearity and of thermo-viscous dissipation are usually sufficiently weak to be neglected within the source region, although they may affect propagation to a distant observer. Convection and refraction of sound within and near the source flow can be important, for example in the presence of a mean shear layer (when the Reynolds stress will include terms like $\rho U_i u_j$, where $\mathbf{U}$ and $\mathbf{u}$ respectively denote the mean and fluctuating components of $\mathbf{v}$) or when there are large variations in the mean thermodynamic properties of the medium *within* the source region; such effects are described by the presence of unsteady *linear* terms in T_{ij} (Ffowcs Williams 1974).

Thus, to predict the radiated sound from Lighthill's equation (4.2.1) it is usually necessary to suppose that all of these 'acoustic' effects in the source flow (which really depend on fluid *compressibility*) are in some sense negligible. This means that in practice it must be possible to derive a good approximation for T_{ij} by taking the source flow to be effectively *incompressible*. This is often possible when the characteristic Mach number $M \sim v/c_o$ is small (specifically, when $M^2 \ll 1$), and when the wavelength of the sound is much larger than the size of the source region.

Consider the particular, but important case in which the mean density and sound speed are uniform throughout the fluid. The variations in the density ρ within a low Mach number, high Reynolds number source flow are then of order $\rho_o M^2$ (Batchelor 1967). Thus, $\rho v_i v_j = \rho_o(1 + O(M^2))v_i v_j \approx \rho_o v_i v_j$. Similarly, if $c(\mathbf{x}, t)$ is the local speed of sound in the source region, it may also be shown that $c_o^2/c^2 = 1 + O(M^2)$, so that

$$p - p_o - c_o^2(\rho - \rho_o) \approx (p - p_o)(1 - c_o^2/c^2) \sim O(\rho_o v^2 M^2)$$

Hence, if viscous dissipation is neglected we make the approximation

$$T_{ij} \approx \rho_o v_i v_j, \quad \text{provided that } M^2 \ll 1. \tag{4.2.2}$$

In the acoustic region outside the source flow $c_o^2(\rho - \rho_o) = p - p_o$. If the irrelevant constant pressure p_o is suppressed, the solution (4.2.1) of Lighthill's equation therefore becomes

Downloaded from https://www.cambridge.org/core. Charité Universitätsmedizin Berlin, on 20 Dec 2021 at 10:08:47, subject to the Cambridge Core terms of use, available at https://www.cambridge.org/core/terms. https://doi.org/10.1017/CBO9781107360273.005

$$p(\mathbf{x},t) \approx \frac{\partial^2}{\partial x_i \partial x_j} \int \frac{\rho_o v_i v_j(\mathbf{y}, t - |\mathbf{x}-\mathbf{y}|/c_o)}{4\pi|\mathbf{x}-\mathbf{y}|} d^3\mathbf{y}$$

$$\approx \frac{x_i x_j}{4\pi c_o^2 |\mathbf{x}|^3} \frac{\partial^2}{\partial t^2} \int \rho_o v_i v_j \left(\mathbf{y}, t - \frac{|\mathbf{x}|}{c_o} + \frac{\mathbf{x}\cdot\mathbf{y}}{c_o|\mathbf{x}|}\right) d^3\mathbf{y}, |\mathbf{x}| \to \infty, \quad (4.2.3)$$

where in the second line we have used the formula (1.10.9) for the far field of a quadrupole distribution. Quantitative predictions can be made from this formula provided the behaviour of the Reynolds stress $\rho_o v_i v_j$ is known.

To determine the order of magnitude of p we introduce a characteristic velocity v and length scale ℓ (of the 'energy containing eddies') of the turbulence sources. The value of ℓ depends on the mechanism responsible for turbulence production, such as the width of a jet mixing layer. Fluctuations in $v_i v_j$ occurring in different regions of the turbulent flow separated by distances $> O(\ell)$ will tend to be statistically independent, and the sound may be considered to be generated by a collection of V_o/ℓ^3 independent eddies, where V_o is the volume occupied by the turbulence (Figure 4.2.1). The characteristic frequency of the turbulent fluctuations $f \sim v/\ell$, so that the wavelength (c_o/f) of the sound $\sim \ell/M \gg \ell$ (because $M = v/c_o \ll 1$). Hence, we arrive at the

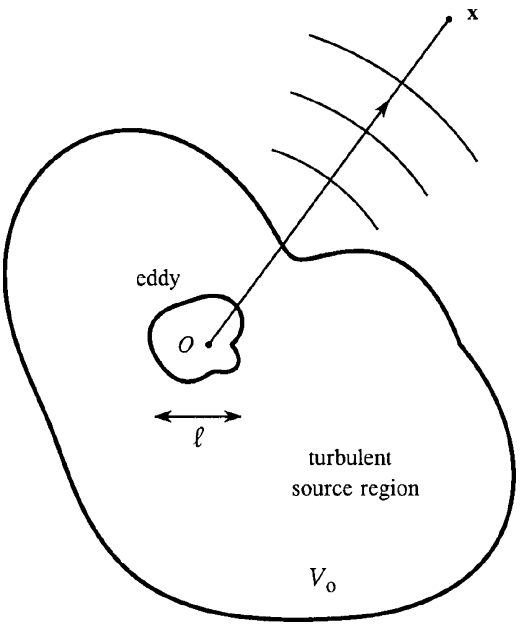

Figure 4.2.1

Downloaded from https://www.cambridge.org/core. Charité Universitätsmedizin Berlin, on 20 Dec 2021 at 10:08:47, subject to the Cambridge Core terms of use, available at https://www.cambridge.org/core/terms. https://doi.org/10.1017/CBO9781107360273.005

important conclusion that the *turbulence eddies are each acoustically compact*. This means that when the integral in (4.2.3) is confined to a single eddy, the retarded time variations $\mathbf{x}\cdot\mathbf{y}/c_o|\mathbf{x}|$ across that eddy can be neglected, that is, if the coordinate origin is temporarily placed at O within the eddy, we can set $\mathbf{x}\cdot\mathbf{y}/c_o|\mathbf{x}| = 0$ in the integration over that eddy. The value of the integral over the eddy may then be estimated to be of order $\rho_o v^2 \ell^3$.

The order of magnitude of the time derivative for changes in the source region is

$$\frac{\partial}{\partial t} \sim \frac{v}{\ell}.$$

It therefore follows from (4.2.3) that, for one eddy, the far field acoustic pressure satisfies

$$p \sim \frac{\ell}{|\mathbf{x}|}\frac{\rho_o v^4}{c_o^2} = \frac{\ell}{|\mathbf{x}|}\rho_o v^2 M^2. \tag{4.2.4}$$

The acoustic *power* radiated by the eddy is determined by the surface integral (1.9.7) taken over a large sphere centred on the eddy. Thus, in order of magnitude,

$$\text{acoustic power radiated by one eddy } \sim 4\pi|\mathbf{x}|^2\frac{p^2}{\rho_o c_o} \sim \frac{\ell^2\rho_o v^8}{c_o^5} = \ell^2\rho_o v^3 M^5 \tag{4.2.5}$$

This is Lighthill's 'eighth power' law.

The *total* power radiated from the whole of the turbulent region of volume V_o, containing V_o/ℓ^3 independent eddies, is

$$\Pi_q \approx \frac{V_o}{\ell^3} \times (\ell^2\rho_o v^3 M^5) = \frac{v}{\ell}\rho_o v^2 M^5 V_o.$$

Dimensional arguments and experiment indicate that the rate Π_o, say, at which energy must be supplied by the action of external forces to maintain the kinetic energy of a statistically steady turbulent field occupying a volume V_o is given in order of magnitude by

$$\Pi_o \sim \frac{v}{\ell}\rho_o v^2 V_o.$$

Therefore, the mechanical *efficiency* with which turbulence kinetic energy is converted into sound is

$$\frac{\Pi_q}{\Pi_o} \sim M^5. \tag{4.2.6}$$

This is smaller than about 0.01 for Mach numbers $M < 0.4$, confirming Lighthill's hypothesis that the flow generated sound is an infinitesimal by-product of the turbulent motion.

Downloaded from https://www.cambridge.org/core. Charité Universitätsmedizin Berlin, on 20 Dec 2021 at 10:08:47, subject to the Cambridge Core terms of use, available at https://www.cambridge.org/core/terms. https://doi.org/10.1017/CBO9781107360273.005

4.3 Curle's theory

In most applications of Lighthill's theory, it is necessary to generalise the solution (4.2.1) to account for the presence of solid bodies in the flow. Indeed, turbulence is frequently generated in the boundary layers and wakes of flow past such bodies (airfoils, flow control surfaces, etc), and the unsteady surface forces ('dipoles') that arise are likely to make a significant contribution to the production of sound. The procedure in such cases is to introduce a system of control surfaces (§2.1) that can be deformed to coincide with the surfaces of the different moving or stationary bodies. Surfaces and solid bodies outside the source region (say, at distances greater than an acoustic wavelength) do not normally affect the efficiency of sound production, but can be responsible for the reflection, scattering or diffraction of the sound. Such effects are usually incorporated by means of a simple modification of the 'free field' solution – an important exception occurs for resonating systems, however, where reflected sound provides 'feedback' to the source favouring the production of sound at certain characteristic frequencies.

4.3.1 Curle's equation

Curle (1955) investigated the influence of *stationary* bodies, and derived the aeroacoustic version of Kirchhoff's formula (2.1.4) (called *Curle's equation*) which formally solves Lighthill's equation (4.1.11) for the sound produced by turbulence in the vicinity of an arbitrary, *fixed* surface S, defined as in §2.1 by an equation $f(\mathbf{x}) = 0$ (Figure 4.3.1). This surface may either enclose a solid body, or merely constitute a control surface used to isolate a fixed region of space containing both solid bodies and fluid or just fluid.

To derive Curle's equation, multiply the momentum equation (4.1.10) by $\mathrm{H} \equiv \mathrm{H}(f)$, and use the definition (4.1.9) of T_{ij} to obtain

$$\frac{\partial}{\partial t}(\rho v_i \mathrm{H}) + \frac{\partial}{\partial x_i}\left(\mathrm{H}c_o^2(\rho - \rho_o)\right) = -\frac{\partial}{\partial x_j}\left(\mathrm{H}T_{ij}\right) + \left(\rho v_i v_j + p'_{ij}\right)\frac{\partial \mathrm{H}}{\partial x_j}, \tag{4.3.1}$$

where

$$p'_{ij} = (p - p_o)\delta_{ij} - \sigma_{ij} \tag{4.3.2}$$

is the *compressive stress* tensor. Repeat this operation for the continuity equation (4.1.7):

$$\frac{\partial}{\partial t}(\mathrm{H}(\rho - \rho_o)) + \frac{\partial}{\partial x_i}(\mathrm{H}\rho v_i) = (\rho v_i)\frac{\partial \mathrm{H}}{\partial x_i}. \tag{4.3.3}$$

The formula $\nabla \mathrm{H} = \nabla f \delta(f)$, shows that equations (4.3.1) and (4.3.3) formally determine the momentum density ρv_i and the density fluctuation $(\rho - \rho_o)$ *in*

Downloaded from https://www.cambridge.org/core. Charité Universitätsmedizin Berlin, on 20 Dec 2021 at 10:08:47, subject to the Cambridge Core terms of use, available at https://www.cambridge.org/core/terms. https://doi.org/10.1017/CBO9781107360273.005

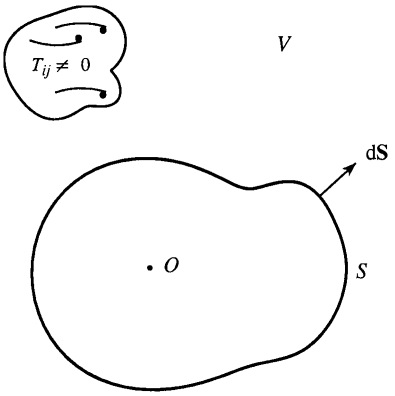

Figure 4.3.1

the exterior region V (where $\mathrm{H}(f) \equiv 1$) in terms of the Lighthill stresses T_{ij} in V and sources distributed over the control surface.

An analogue of Lighthill's equation (4.1.11) is obtained by eliminating $\mathrm{H}\rho v_i$ between (4.3.1) and (4.3.3). This is the differential form of Curle's equation:

$$\left(\frac{1}{c_o^2}\frac{\partial^2}{\partial t^2} - \nabla^2\right)[\mathrm{H}c_o^2(\rho - \rho_o)] = \frac{\partial^2(\mathrm{H}T_{ij})}{\partial x_i \partial x_j} - \frac{\partial}{\partial x_i}\left((\rho v_i v_j + p'_{ij})\frac{\partial \mathrm{H}}{\partial x_j}\right) + \frac{\partial}{\partial t}\left(\rho v_j \frac{\partial \mathrm{H}}{\partial x_j}\right). \tag{4.3.4}$$

The equation is valid throughout all space, including the region enclosed by S where $\mathrm{H}(f)$ vanishes. The second and third terms on the right-hand side respectively represent *dipole* and *monopole* sources distributed over S. They have the following interpretations:

(i) If S is merely an artificial control surface it will enclose fluid, possibly also solid bodies, and may or may not contain turbulence; the surface dipole and monopole sources then represent the influence of this region on the sound radiated in V; in other words the aggregate effect of the dipole and monopole sources accounts for the presence of solid bodies and turbulence within S (when $T_{ij} \neq 0$ in S) and also for the interaction of sound generated outside S with the fluid and solid bodies in S.

(ii) If S is the boundary of a solid body, the surface dipole represents the production of sound by the unsteady surface force that the body exerts on the exterior fluid, whereas the monopole is responsible for the sound produced by surface vibration of the body.

Downloaded from https://www.cambridge.org/core. Charité Universitätsmedizin Berlin, on 20 Dec 2021 at 10:08:47, subject to the Cambridge Core terms of use, available at https://www.cambridge.org/core/terms. https://doi.org/10.1017/CBO9781107360273.005

Curle's form of Lighthill's equation is valid throughout all space, and the general outgoing wave solution can be written as a retarded potential (1.6.6) in the usual way (§2.1), using the special forms (1.8.5), (1.8.7) for dipole and quadrupole sources. When account is taken of the transformation formula (2.1.2) this yields **Curle's equation**

$$\mathrm{H}c_o^2(\rho-\rho_o) = \frac{\partial^2}{\partial x_i \partial x_j}\int_V \Big[T_{ij}\Big]\frac{d^3\mathbf{y}}{4\pi|\mathbf{x}-\mathbf{y}|} - \frac{\partial}{\partial x_i}\oint_S \Big[\rho v_i v_j + p'_{ij}\Big]\frac{dS_j(\mathbf{y})}{4\pi|\mathbf{x}-\mathbf{y}|} + \frac{\partial}{\partial t}\oint_S \Big[\rho v_j\Big]\frac{dS_j(\mathbf{y})}{4\pi|\mathbf{x}-\mathbf{y}|}, \tag{4.3.5}$$

where the square bracket notation $[T_{ij}] \equiv T_{ij}(\mathbf{y}, t-|\mathbf{x}-\mathbf{y}|/c_o)$, etc, implies evaluation at the retarded time. Because $\mathrm{H}(f) \equiv 0$ inside S, the sum of the three integrals on the right hand side vanishes when the field point $\mathbf{x}$ is within S.

4.3.2 Sound produced by turbulence near a compact rigid body

When the surface S (in Figure 4.3.1) is *rigid and fixed*, Curle's equation (4.3.5) reduces to

$$\mathrm{H}c_o^2(\rho-\rho_o) = \frac{\partial^2}{\partial x_i \partial x_j}\int_V \Big[T_{ij}\Big]\frac{d^3\mathbf{y}}{4\pi|\mathbf{x}-\mathbf{y}|} - \frac{\partial}{\partial x_i}\oint_S \Big[p'_{ij}\Big]\frac{dS_j(\mathbf{y})}{4\pi|\mathbf{x}-\mathbf{y}|}. \tag{4.3.6}$$

We now use this solution to determine the order of magnitude of the sound generated by a stationary *compact* body within a turbulent flow. Compactness usually requires the Mach number $M \sim v/c_o \ll 1$, and we shall assume this to be the case in the following.

In the far field the pressure $p(\mathbf{x}, t) = c_o^2(\rho-\rho_o)(\mathbf{x}, t)$ and $\mathrm{H}(f) = 1$. The contribution to the acoustic pressure from the quadrupole integral in (4.3.6) is estimated as in §4.2. To deal with the surface dipole we use the far field dipole approximation (1.10.7) (with the origin at O in Figure 4.3.1) and neglect retarded time variations $\mathbf{x}\cdot\mathbf{y}/c_o|\mathbf{x}|$ because S is compact. The dipole sound pressure p_d, say, is then

$$p_d \approx \frac{x_i}{4\pi c_o|\mathbf{x}|^2}\frac{\partial}{\partial t}\oint_S p'_{ij}\left(\mathbf{y}, t-\frac{|\mathbf{x}|}{c_o}\right)dS_j = \frac{x_j}{4\pi c_o|\mathbf{x}|^2}\frac{\partial F_j}{\partial t}\left(t-\frac{|\mathbf{x}|}{c_o}\right), \quad |\mathbf{x}|\to\infty, \tag{4.3.7}$$

where $\mathbf{F}(t)$ is the unsteady force exerted *on the fluid* by the body.

Downloaded from https://www.cambridge.org/core. Charité Universitätsmedizin Berlin, on 20 Dec 2021 at 10:08:47, subject to the Cambridge Core terms of use, available at https://www.cambridge.org/core/terms. https://doi.org/10.1017/CBO9781107360273.005

For turbulence of velocity v and correlation scale ℓ the orders of magnitude of the pressure and viscous components of the compressive stress tensor

$$p'_{ij} = (p - p_o)\delta_{ij} - \sigma_{ij}$$

are

$$(p - p_o) \sim \rho_o v^2, \quad \sigma \sim \eta \frac{v}{\ell}$$

i.e.

$$\frac{(p - p_o)}{\sigma} \sim \frac{\rho_o v \ell}{\eta} = \frac{v\ell}{\nu}.$$

where $\nu = \eta/\rho_o$ is the kinematic viscosity. The dimensionless ratio $Re = v\ell/\nu$ is the *Reynolds number* and is always very large ($\sim 10^4$ or more) in turbulent flow. This means that viscous contributions to the surface force can be neglected.

The contribution to p_d from a surface element of diameter ℓ within which the turbulence surface pressure fluctuations are correlated is therefore of order

$$\frac{1}{c_o|\mathbf{x}|}\frac{v}{\ell} \times (\rho_o v^2 \ell^2) = \frac{\ell}{|\mathbf{x}|}\rho_o v^2 M,$$

which exceeds by an order of magnitude ($1/M \gg 1$) the sound pressure (4.2.4) produced by a quadrupole in V of length scale ℓ. If A is the total surface area 'wetted' by the turbulence, there are A/ℓ^2 independently radiating surface elements, and the total power radiated by the dipoles is

$$\Pi_d \sim 4\pi|\mathbf{x}|^2 \times \left(\frac{p_d^2}{\rho_o c_o}\right) \sim A\rho_o v^3 M^3. \tag{4.3.8}$$

The direct power radiated by quadrupoles occupying a volume V_o is $\Pi_q \sim (V_o/\ell)\rho_o v^3 M^5$, the same as in the absence of the body (see §4.2). The sound produced by the turbulence near S is therefore dominated by the dipole when M is small, and as $M \to 0$ the acoustic power exceeds the quadrupole power by a factor $\sim 1/M^2 \gg 1$. Precisely how small M should be for this to be true depends on the details of the flow, which determine the appropriate values of A and V_o/ℓ.

This increase in acoustic efficiency brought about by surface dipoles on an acoustically compact body occurs also for arbitrary, *non-compact* bodies when turbulence interacts with compact structural elements, such as edges, corners and protuberances.

4.3.3 The Ffowcs Williams–Hawkings equation (1969)

The equation defining the control surface of Figure 4.3.1 becomes $f(\mathbf{x}, t) = 0$ when S is in motion at velocity $\bar{\mathbf{v}}(\mathbf{x}, t)$ at $\mathbf{x}$ on S. Then $(\partial/\partial t + \bar{v}_j \partial/\partial x_j)\,\mathrm{H}(f)$

Downloaded from https://www.cambridge.org/core. Charité Universitätsmedizin Berlin, on 20 Dec 2021 at 10:08:47, subject to the Cambridge Core terms of use, available at https://www.cambridge.org/core/terms. https://doi.org/10.1017/CBO9781107360273.005

$= 0$, and the procedure of §4.3.1 involving multiplication of the momentum and continuity equations by $\mathrm{H}(f)$ can be repeated to obtain the following modification of Curle's equation (4.3.5):

$$\begin{aligned}\mathrm{H}c_o^2(\rho-\rho_o) = {} & \frac{\partial^2}{\partial x_i \partial x_j}\int_{V(\tau)}\Big[T_{ij}\Big]\frac{d^3\mathbf{y}}{4\pi|\mathbf{x}-\mathbf{y}|} \\ & -\frac{\partial}{\partial x_i}\oint_{S(\tau)}\Big[\rho v_i(v_j-\bar{v}_j)+p'_{ij}\Big]\frac{dS_j(\mathbf{y})}{4\pi|\mathbf{x}-\mathbf{y}|} \\ & +\frac{\partial}{\partial t}\oint_{S(\tau)}\Big[\rho(v_j-\bar{v}_j)+\rho_o\bar{v}_j\Big]\frac{dS_j(\mathbf{y})}{4\pi|\mathbf{x}-\mathbf{y}|}, \quad (4.3.9)\end{aligned}$$

where the quantities in square brackets are evaluated at the retarded time $\tau = t - |\mathbf{x}-\mathbf{y}|/c_o$, and the surface integrals are over the retarded surface $S(\tau)$ defined by $f(\mathbf{y},\tau) = 0$, with the surface element $d\mathbf{S}$ directed into the region $V(\tau)$ where $f > 0$. This extension of Curle's equation is called the *Ffowcs Williams–Hawkings* equation.

4.3.4 Influence of surface vibration

The Ffowcs Williams–Hawkings equation reveals that Curle's formula (4.3.5) remains valid to first order in the surface velocity when a compact body S (Figure 4.3.1) vibrates at *small* amplitude. In a real fluid v_j and $\bar{v}_j$ are equal on S, so that both formulae yield the dipole acoustic pressure p_d of (4.3.7). The monopole contributions (the final integrals in (4.3.5, 4.3.9)) are also the same. Thus, if the body executes small amplitude translational oscillations at velocity $\mathbf{U}(t)$, and taking $\rho = \rho_o(1 + O(M^2)) \sim \rho_o$ in Curle's formula, we find in either case (as in §2.1.3)

$$\frac{\partial}{\partial t}\oint_S\Big[\rho_o v_j\Big]\frac{dS_j(\mathbf{y})}{4\pi|\mathbf{x}-\mathbf{y}|} \simeq \frac{x_j}{4\pi c_o|\mathbf{x}|^2}m_o\frac{\partial^2 U_j}{\partial t^2}\left(t-\frac{|\mathbf{x}|}{c_o}\right), \quad |\mathbf{x}|\to\infty,$$

correct to dipole order, where m_o is the mass of the fluid displaced by S.

This, together with the result (4.3.7), leads to the following generalisation to a real fluid of formula (2.1.5) of §2.1.3: the sound generated by a compact rigid body executing small amplitude vibrations is the formal solution of

$$\left(\frac{1}{c_o^2}\frac{\partial^2}{\partial t^2}-\nabla^2\right)p = -\mathrm{div}\Big(\mathbf{f}(t)\delta(\mathbf{x})\Big), \quad \mathbf{f} = m_o\frac{d\mathbf{U}}{dt}+\mathbf{F}$$

namely,

$$p(\mathbf{x},t) \simeq \frac{x_j}{4\pi c_o|\mathbf{x}|^2}\left[\frac{df_j}{dt}\right] \equiv \frac{x_j}{4\pi c_o|\mathbf{x}|^2}\frac{\partial}{\partial t}\left[m_o\frac{dU_j}{dt}+F_j\right], \quad |\mathbf{x}|\to\infty, \quad (4.3.10)$$

Downloaded from https://www.cambridge.org/core. Charité Universitätsmedizin Berlin, on 20 Dec 2021 at 10:08:47, subject to the Cambridge Core terms of use, available at https://www.cambridge.org/core/terms. https://doi.org/10.1017/CBO9781107360273.005

where the large square brackets indicate evaluation at the retarded time $t - |\mathbf{x}|/c_o$. The dipole strength $\mathbf{f}$ is the force required to accelerate the fluid mass displaced by the body at velocity $\mathbf{U}(t)$ plus the net force exerted on the fluid by the body, including all contributions from the added mass and turbulence surface pressures, and from surface friction.

4.4* Vorticity

Lighthill's theory furnishes an excellent approximation to the sound radiated from low Mach number flow when the quadrupole and surface sources are evaluated as if the motion is *incompressible*. Acoustic energy is produced at the expense of the *hydrodynamic* kinetic energy of the flow. That part of the source flow energy generated by moving boundaries, such as the surface of a vibrating body, is stored only temporarily within the fluid. The remainder is *intrinsic* kinetic energy that exists provided the vorticity $\boldsymbol{\omega} \neq 0$. This fundamental property of the spatial derivative $\boldsymbol{\omega} = \operatorname{curl} \mathbf{v}$ of the velocity is the basis of **Kelvin's** (1867) definition of a vortex in a homogeneous incompressible fluid as *'...a portion of fluid having any motion that it could not acquire by fluid pressure transmitted from its boundary'*.

To understand the mechanisms of sound production by an unsteady flow it is therefore necessary to enquire further into the properties of vorticity.

4.4.1 Kinetic energy of incompressible flow

There can be no vorticity in an ideal, homogeneous fluid that is set in motion by a moving boundary. This is a consequence of **Kelvin's circulation theorem**, that the circulation

$$\Gamma = \oint_C \mathbf{v} \cdot d\mathbf{x} = \int_{S'} \boldsymbol{\omega} \cdot d\mathbf{S},$$

is constant when C is a closed material contour, that is, a contour formed by a 'necklace' of fluid particles that moves with those particles; S' is any two-sided surface bounded by C. Indeed, because the motion is homentropic, with $dp/\rho = dw$ (§1.2.6),

$$\frac{D\Gamma}{Dt} = \frac{D}{Dt} \oint_C \mathbf{v} \cdot d\mathbf{x} \equiv \oint_C \frac{D}{Dt}\left(\mathbf{v} \cdot d\mathbf{x}\right) = \oint_C d\left(-w + \frac{1}{2}v^2\right) \equiv 0,$$

wherein $(D\mathbf{v}/Dt) \cdot d\mathbf{x} = -dp/\rho$ in the absence of body forces, and $D(d\mathbf{x})/Dt = d\mathbf{v}$. It follows by taking C to be an infinitesimal closed circular contour of arbitrary orientation, that vorticity can neither be created nor destroyed in a body of inviscid, homentropic fluid. The theorem remains true

Downloaded from https://www.cambridge.org/core. Charité Universitätsmedizin Berlin, on 20 Dec 2021 at 10:08:47, subject to the Cambridge Core terms of use, available at https://www.cambridge.org/core/terms. https://doi.org/10.1017/CBO9781107360273.005

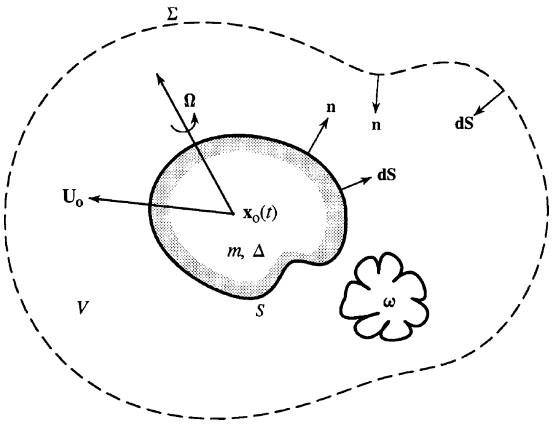

Figure 4.4.1

in the presence of conservative body forces $\mathbf{F} = \rho\nabla\Phi$ defined by a potential Φ (gravity, for example).

Therefore when a homogeneous, ideal incompressible fluid is set in motion by a moving solid boundary S – by 'fluid pressure transmitted from' S, Figure 4.4.1 with $\boldsymbol{\omega} = 0$ – there must exist a velocity potential such that $\mathbf{v}(\mathbf{x}, t) = \nabla\varphi$, where $\operatorname{div}\mathbf{v} \equiv \nabla^2\varphi = 0$ and $\partial\varphi/\partial x_n = U_n$ = the normal component of velocity on S. The kinetic energy T_o of the flow is

$$T_o = \frac{1}{2}\rho_o \int_V (\nabla\varphi)^2 d^3\mathbf{x} = \frac{1}{2}\rho_o \int_V \Big(\operatorname{div}(\varphi\nabla\varphi) - \varphi\nabla^2\varphi\Big) d^3\mathbf{x}$$
$$= -\frac{1}{2}\rho_o \oint_S \varphi \frac{\partial\varphi}{\partial x_n} dS \equiv -\frac{1}{2}\rho_o \oint_S \varphi U_n dS, \tag{4.4.1}$$

where the divergence theorem has been used to obtain the second line (there is no contribution from the surface Σ at 'infinity' in Figure 4.4.1, where at most $\varphi \sim O(1/|\mathbf{x}|)$). This formula confirms that the kinetic energy is stored only temporarily in the fluid, because the motion everywhere ceases instantaneously if S is brought to rest ($U_n \to 0$), when $\int_V (\nabla\varphi)^2 d^3\mathbf{x}$ can vanish only if $\nabla\varphi \equiv 0$. This is never observed in a real fluid because (i) no fluid is perfectly incompressible – 'signals' generated by changes in the boundary conditions propagate at the finite speed of sound, and (ii) diffusion of *vorticity* from the boundary supplies irrecoverable kinetic energy to the fluid.

In a real, uniform incompressible fluid we can put $\mathbf{v} = \nabla\varphi + \mathbf{u}$, where $\boldsymbol{\omega} = \operatorname{curl}\mathbf{u}$, and $\partial\varphi/\partial x_n = U_n$ on S (on which $u_n = 0$). A similar calculation then reveals that the flow kinetic energy T is now

Downloaded from https://www.cambridge.org/core. Charité Universitätsmedizin Berlin, on 20 Dec 2021 at 10:08:47, subject to the Cambridge Core terms of use, available at https://www.cambridge.org/core/terms. https://doi.org/10.1017/CBO9781107360273.005

$$T = T_o + \frac{1}{2}\rho_o \int_V u^2 d^3\mathbf{x}. \tag{4.4.2}$$

This proves Kelvin's theorem (1879) for a fluid of uniform density, that the kinetic energy of a real, incompressible flow always exceeds that of the corresponding ideal flow subject to the same moving boundary condition; irrotational flow therefore characterises the *minimum* possible disturbance to a fluid produced by a moving boundary. The potential flow component of the motion stops instantaneously when the boundary stops moving, but that associated with the rotational velocity $\mathbf{u}$ persists. The crucial difference between rotational and irrotational flows is that, once established, vortical motions proceed irrespective of whether or not the fluid continues to be driven by moving boundaries or other external agencies.

4.4.2 Vortex lines and angular velocity

The velocity within a small spherical fluid particle relative to its centre at O, say, at vector distance $\mathbf{x}'$ from O, includes an irrotational component representing the rate of distortion from spherical to an ellipsoidal shape, together with a solid body rotation about an axis through O at angular velocity $\frac{1}{2}\boldsymbol{\omega}$ (see equation (1.2.7)). If the spherical particle is suddenly solidified without change of angular momentum, it will continue to rotate at this angular velocity, so that $\boldsymbol{\omega}$ may be defined as twice the initial angular velocity of an infinitesimally small sphere of fluid with centre at O that is suddenly solidified without change of angular momentum. Vorticity may therefore be regarded as a measure of the angular momentum of a fluid particle. This is consistent with our conclusion that vorticity is associated with the intrinsic kinetic energy of the flow, and determines the motion that persists in an incompressible fluid when the boundaries are brought to rest.

A **vortex line** is tangential to the vorticity vector at all points along its length. Vortex lines that pass through every point of a simple closed curve define the boundary of a *vortex tube* (Figure 4.4.2). For a tube of small cross-sectional area δS the product $\omega\delta S$ is called the tube strength, and is constant because $\text{div}\,\boldsymbol{\omega} = \text{div}(\text{curl}\,\mathbf{v}) \equiv 0$ and the divergence theorem therefore implies that $\oint \boldsymbol{\omega} \cdot d\mathbf{S} = 0$ for any closed surface, and in particular for the surface formed by two cross-sections of the tube and the tube wall separating them, on the latter of which $\boldsymbol{\omega} \cdot d\mathbf{S} = 0$. It follows that vortex tubes and lines cannot begin or end within the fluid. The 'no-slip' condition (Batchelor 1967) requires the velocity at a boundary to be the same as that of the boundary. A vortex line

Downloaded from https://www.cambridge.org/core. Charité Universitätsmedizin Berlin, on 20 Dec 2021 at 10:08:47, subject to the Cambridge Core terms of use, available at https://www.cambridge.org/core/terms. https://doi.org/10.1017/CBO9781107360273.005

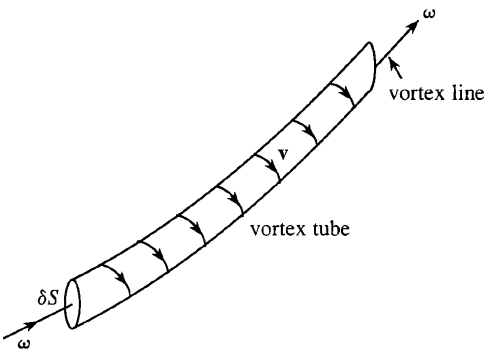

Figure 4.4.2

must therefore form a closed loop, or end on a *rotating* surface S at which $\frac{1}{2}\omega_n = \mathbf{n}\cdot\boldsymbol{\Omega}$, $\boldsymbol{\Omega}$ being the angular velocity of S.

4.4.3 The vorticity equation

Vorticity will now be shown to be transported through the fluid by convection and molecular diffusion. This implies that an initially bounded region of vortex tubes can often be assumed to remain bounded.

When the flow is homentropic, Crocco's equation (1.2.10) in the absence of body forces and of the term in $\operatorname{div}\mathbf{v}$ representing the small effect of compressibility on viscous dissipation, reduces to

$$\frac{\partial \mathbf{v}}{\partial t} + \boldsymbol{\omega}\wedge\mathbf{v} + \nabla B = -\nu \operatorname{curl}\boldsymbol{\omega}. \tag{4.4.3}$$

The curl of this equation and the relation $\operatorname{curl}\operatorname{curl}\boldsymbol{\omega} \equiv -\nabla^2\boldsymbol{\omega}$ yield the **vorticity equation** for a fluid of constant kinematic viscosity:

$$\frac{\partial \boldsymbol{\omega}}{\partial t} + \operatorname{curl}(\boldsymbol{\omega}\wedge\mathbf{v}) = \nu\nabla^2\boldsymbol{\omega}. \tag{4.4.4}$$

For an incompressible fluid $\operatorname{div}\boldsymbol{\omega} = \operatorname{div}\mathbf{v} = 0$ and

$$\operatorname{curl}(\boldsymbol{\omega}\wedge\mathbf{v}) \equiv (\mathbf{v}\cdot\nabla)\boldsymbol{\omega} + \boldsymbol{\omega}\operatorname{div}\mathbf{v} - (\boldsymbol{\omega}\cdot\nabla)\mathbf{v} - \mathbf{v}\operatorname{div}\boldsymbol{\omega} = (\mathbf{v}\cdot\nabla)\boldsymbol{\omega} - (\boldsymbol{\omega}\cdot\nabla)\mathbf{v},$$

therefore, the vorticity equation can also be written

$$\frac{D\boldsymbol{\omega}}{Dt} = (\boldsymbol{\omega}\cdot\nabla)\mathbf{v} + \nu\nabla^2\boldsymbol{\omega}. \tag{4.4.5}$$

The terms on the right represent the mechanisms that change the vorticity of a fluid particle in incompressible flow:

Downloaded from https://www.cambridge.org/core. Charité Universitätsmedizin Berlin, on 20 Dec 2021 at 10:08:47, subject to the Cambridge Core terms of use, available at https://www.cambridge.org/core/terms. https://doi.org/10.1017/CBO9781107360273.005

(a) Stretching and rotation of vortex lines

Consider two neighbouring fluid particles A and B. Let $\mathbf{X}(t)$ denote the vector position of B relative to A. During a small time interval δt the change in $\mathbf{X}$ is given by

$$\delta\mathbf{X} \simeq \Big(\mathbf{v}(\mathbf{x}+\mathbf{X},t) - \mathbf{v}(\mathbf{x},t)\Big)\delta t \;\simeq\; X_j \frac{\partial \mathbf{v}}{\partial x_j}\delta t \;\equiv\; (\mathbf{X}\cdot\nabla)\,\mathbf{v}\,\delta t$$

$$\therefore \quad \frac{D\mathbf{X}}{Dt} = (\mathbf{X}\cdot\nabla)\,\mathbf{v}, \tag{4.4.6}$$

which coincides with the vorticity equation (4.4.5) when $\nu = 0$:

$$\frac{D\boldsymbol{\omega}}{Dt} = (\boldsymbol{\omega}\cdot\nabla)\mathbf{v}. \tag{4.4.7}$$

Let us assume that the fluid particles at $\mathbf{x}$ and $\mathbf{x}+\mathbf{X}$ lie on the same vortex line at $t = 0$. Then there exists a constant ϵ such that $\boldsymbol{\omega} = \epsilon\mathbf{X}$ at $t = 0$. Equations (4.4.6) and (4.4.7) imply that $\mathbf{X}$ and $\boldsymbol{\omega}$ experience the same proportionate change during a short time interval δt. Therefore at time δt we continue to have $\boldsymbol{\omega} = \epsilon\mathbf{X}$ for the *same* constant ϵ for the fluid particle initially at $\mathbf{x}$. It follows that '*vortex lines move with the fluid particles*' and that the magnitude of $\boldsymbol{\omega}$ increases/decreases as the separation distance $|\mathbf{X}|$ increases/decreases. This is the dominant mechanism by which the vortex field evolves in high Reynolds number flows.

For a compressible fluid the same argument is valid with $\boldsymbol{\omega}$ replaced by $\boldsymbol{\omega}/\rho$.

(b) Molecular diffusion of vorticity.

In regions of high shear the term $\nu\nabla^2\boldsymbol{\omega}$ in the vorticity equation (4.4.4) becomes important, in particular near solid boundaries. Very close to a stationary wall the velocity becomes small, nonlinear terms can be neglected (i.e. the Reynolds number $\ll 1$), and the vorticity equation reduces to the classical diffusion equation

$$\frac{\partial\boldsymbol{\omega}}{\partial t} = \nu\nabla^2\boldsymbol{\omega}.$$

Vorticity is generated at solid boundaries, and viscosity is responsible for its diffusion into the body of the fluid, where it can subsequently be convected by the flow.

It should be understood that viscosity merely serves to diffuse the vorticity into the fluid from the surface, and does not generate the vorticity. In an ideal fluid the no-slip condition creates a singular layer of vorticity at the surface called a **vortex sheet**. The strength of the sheet is determined by the tangential velocity difference between the surface and the ideal exterior flow 'slipping'

Downloaded from https://www.cambridge.org/core. Charité Universitätsmedizin Berlin, on 20 Dec 2021 at 10:08:47, subject to the Cambridge Core terms of use, available at https://www.cambridge.org/core/terms. https://doi.org/10.1017/CBO9781107360273.005

over the surface. This vorticity stays on the surface; it would start to diffuse into the fluid if the fluid were suddenly endowed with viscosity. The *rate* of diffusion would depend on the value of ν, but the *amount* of the vorticity available for diffusion from the surface is independent of ν.

4.4.4 The Biot–Savart formula

In an unbounded fluid the velocity $\mathbf{v}$ can always be expressed in terms of scalar and vector potentials φ and $\mathbf{A}$ such that

$$\mathbf{v} = \nabla\varphi + \text{curl}\,\mathbf{A}, \text{ where div}\,\mathbf{A} = 0.$$

The equations determining φ and $\mathbf{A}$ are found by taking in turn the divergence and curl (using the formula curl curl $\mathbf{A}$ = grad div $\mathbf{A} - \nabla^2\mathbf{A}$):

$$\nabla^2\varphi = \text{div}\,\mathbf{v}, \quad \nabla^2\mathbf{A} = -\text{curl}\,\mathbf{v} \equiv -\boldsymbol{\omega}.$$

We can take $\varphi = 0$ for incompressible, unbounded flow which is at rest at infinity. To find $\mathbf{A}$ we use the Green's function for Laplace's equation (the solution (2.3.6) of equation (2.3.3) in the incompressible limit $k_o \to 0$) to obtain

$$\mathbf{A} = \int \frac{\boldsymbol{\omega}(\mathbf{y}, t)d^3\mathbf{y}}{4\pi|\mathbf{x} - \mathbf{y}|}. \tag{4.4.8}$$

The velocity is then given by the **Biot–Savart** formula

$$\mathbf{v}(\mathbf{x}, t) = \text{curl} \int \frac{\boldsymbol{\omega}(\mathbf{y}, t)d^3\mathbf{y}}{4\pi|\mathbf{x} - \mathbf{y}|}. \tag{4.4.9}$$

This is a purely *kinematic* relation between a vector $\mathbf{v}$ that vanishes at infinity and $\boldsymbol{\omega} = \text{curl}\,\mathbf{v}$.

Because vorticity is transported by convection and diffusion, an initially confined region of vorticity will tend to remain within a bounded domain, so that it may be assumed that $\boldsymbol{\omega} \to 0$ as $|\mathbf{x}| \to \infty$. The divergence theorem then shows that

$$\int \omega_i(\mathbf{y}, t)d^3\mathbf{y} = -\oint_\Sigma y_i\omega_j(\mathbf{y}, t)n_j d\mathrm{S}(\mathbf{y}) \equiv 0,$$

where the surface Σ (with inward normal $\mathbf{n}$) is large enough to contain all the vorticity. By using this result and the expansion (1.10.4) for $|\mathbf{x}| \to \infty$ we derive from (4.4.9) the following approximation in the *hydrodynamic far field*:

$$\mathbf{v}(\mathbf{x}, t) \approx \text{curl}\left(\frac{x_j}{4\pi|\mathbf{x}|^3}\int y_j\boldsymbol{\omega}(\mathbf{y}, t)d^3\mathbf{y}\right) \sim O\left(\frac{1}{|\mathbf{x}|^3}\right), \quad |\mathbf{x}| \to \infty. \tag{4.4.10}$$

Downloaded from https://www.cambridge.org/core. Charité Universitätsmedizin Berlin, on 20 Dec 2021 at 10:08:47, subject to the Cambridge Core terms of use, available at https://www.cambridge.org/core/terms. https://doi.org/10.1017/CBO9781107360273.005

Furthermore, the divergence theorem also implies that

$$\int \operatorname{div}\Big(y_i y_j \boldsymbol{\omega}(\mathbf{y},t)\Big)d^3\mathbf{y} = 0 \quad \text{and therefore that}$$
$$\int \Big(y_i \omega_j(\mathbf{y},t) + y_j \omega_i(\mathbf{y},t)\Big)d^3\mathbf{y} = 0.$$

This can be used to express (4.4.10) in either of the following equivalent forms

$$\mathbf{v}(\mathbf{x},t) \approx \operatorname{curl}\operatorname{curl}\left(\frac{\mathbf{I}}{4\pi|\mathbf{x}|}\right) = \operatorname{grad}\operatorname{div}\left(\frac{\mathbf{I}}{4\pi|\mathbf{x}|}\right), \quad |\mathbf{x}| \to \infty,$$
$$\text{where} \qquad \mathbf{I} = \frac{1}{2}\int \mathbf{y} \wedge \boldsymbol{\omega}(\mathbf{y},t)d^3\mathbf{y}, \tag{4.4.11}$$

(Question 4.9 of **Problems 4**). The vector $\mathbf{I}$ is called the *impulse* of the vortex system, and is an *absolute constant* in unbounded flow (Batchelor 1967). These formulae supply alternative representations of $\mathbf{v}$ in the *hydrodynamic* far field (where the motion is entirely irrotational) in terms of either the vector potential $\mathbf{A} = \operatorname{curl}(\mathbf{I}/4\pi|\mathbf{x}|)$ or a scalar potential $\varphi = \operatorname{div}(\mathbf{I}/4\pi|\mathbf{x}|)$.

Very similar conclusions are obtained for incompressible flow in the presence of a solid boundary. In Figure 4.4.1, for example, a rigid body of volume Δ moves in incompressible fluid at rest at infinity with velocity

$$\mathbf{U} = \mathbf{U}_o + \boldsymbol{\Omega} \wedge (\mathbf{x} - \mathbf{x}_o(t)), \tag{4.4.12}$$

where $\mathbf{U}_o = d\mathbf{x}_o/dt$ is the velocity of its centre of volume $\mathbf{x}_o(t)$, and $\boldsymbol{\Omega}(t)$ is its angular velocity. Let $f(\mathbf{x},t)$ vanish on S, with $f > 0$ in the fluid. Then $\mathrm{H}(f)\mathbf{v} + \mathrm{H}(-f)\mathbf{U}$ is the velocity everywhere, in both the fluid and solid. Put

$$\mathrm{H}(f)\mathbf{v} + \mathrm{H}(-f)\mathbf{U} = \nabla\varphi + \operatorname{curl}\mathbf{A}, \ (\operatorname{div}\mathbf{A} = 0).$$

The body has constant volume ($\operatorname{div}\mathbf{U} = 0$), but $\operatorname{curl}\mathbf{U} = 2\boldsymbol{\Omega}$. The no slip condition on S implies that

$$\operatorname{div}(\mathrm{H}(f)\mathbf{v} + \mathrm{H}(-f)\mathbf{U}) = \nabla\mathrm{H}(f)\cdot(\mathbf{v}-\mathbf{U}) \equiv 0$$
$$\operatorname{curl}(\mathrm{H}(f)\mathbf{v} + \mathrm{H}(-f)\mathbf{U}) = \mathrm{H}(f)\boldsymbol{\omega} + \mathrm{H}(-f)2\boldsymbol{\Omega}.$$

Hence, $\varphi \equiv 0$, and the velocity *everywhere* is given by the following modification of the Biot–Savart formula (4.4.9):

$$\mathbf{v}(\mathbf{x},t) = \operatorname{curl}\int_V \frac{\boldsymbol{\omega}(\mathbf{y},t)d^3\mathbf{y}}{4\pi|\mathbf{x}-\mathbf{y}|} + \operatorname{curl}\int_\Delta \frac{2\boldsymbol{\Omega}(t)d^3\mathbf{y}}{4\pi|\mathbf{x}-\mathbf{y}|}, \tag{4.4.13}$$

where V is the volume occupied by the fluid.

This formula predicts that $\mathbf{v} = \mathbf{U}$ when $\mathbf{x}$ lies within the region occupied by the body. Vortex lines may be imagined to continue into the solid. As for an

Downloaded from https://www.cambridge.org/core. Charité Universitätsmedizin Berlin, on 20 Dec 2021 at 10:08:47, subject to the Cambridge Core terms of use, available at https://www.cambridge.org/core/terms. https://doi.org/10.1017/CBO9781107360273.005

unbounded flow, the identity $\int \text{curl}\,(\text{H}(f)\mathbf{v} + \text{H}(-f)\mathbf{U})\,d^3\mathbf{x} = 0$ implies that $\mathbf{v} \sim \text{O}(1/|\mathbf{x}|^3)$ as $|\mathbf{x}| \to \infty$. Similarly, the asymptotic approximations (4.4.11) remain valid provided the integration includes the region occupied by the body (where $\boldsymbol{\omega} = 2\boldsymbol{\Omega}$). Formula (4.4.13) is also applicable in inviscid flow, but the contribution from the 'bound vorticity' in the vortex sheet on the surface of the body must be included in the integrals.

4.5 Vorticity as a source of sound

Lighthill's quadrupole source (4.2.2) in low Mach number, unbounded, homentropic flow can be replaced by the incompressible approximation (§4.4.4):

$$T_{ij} \approx \rho_o u_i u_j, \quad \mathbf{u}(\mathbf{x}, t) = \text{curl} \int \frac{\boldsymbol{\omega}(\mathbf{y}, t) d^3\mathbf{y}}{4\pi |\mathbf{x} - \mathbf{y}|}. \tag{4.5.1}$$

Consider the acoustically compact eddy of Figure 4.2.1 consisting of vorticity of characteristic length ℓ, and take the coordinate origin within the eddy. Put

$$\mathbf{v} = \mathbf{u} + \nabla\varphi;$$

$\mathbf{u}$ is the *incompressible* component of velocity, and $u \sim O(1/|\mathbf{x}|^3)$ as $|\mathbf{x}| \to \infty$ (§4.4.4). Because $\text{div}\,\mathbf{u} = 0$, the scalar potential φ describes compressible motions, and the continuity equation becomes

$$\nabla^2\varphi + \frac{1}{\rho}\frac{D\rho}{Dt} = 0.$$

But, $p - p_o \sim \rho_o u^2$ in the eddy, where the characteristic frequency $\sim u/\ell$. Thus,

$$\frac{Dp}{Dt} \sim \frac{\rho_o u^3}{\ell}, \quad \therefore \quad \frac{1}{\rho}\frac{D\rho}{Dt} = \frac{1}{\rho c^2}\frac{Dp}{Dt} \sim \frac{u}{\ell}M^2, \quad M = \frac{u}{c_o}.$$

Hence, in order of magnitude

$$\nabla\varphi = O(uM^2), \quad \text{within the eddy, where } |\mathbf{x}| \sim \ell. \tag{4.5.2}$$

Now write

$$\frac{\partial^2(u_i u_j)}{\partial x_i \partial x_j} = \text{div}\,(\boldsymbol{\omega} \wedge \mathbf{u}) + \nabla^2\left(\tfrac{1}{2}u^2\right) \tag{4.5.3}$$

and express the solution $p(\mathbf{x}, t) = c_o^2(\rho - \rho_o)$ of Lighthill's equation given by (4.2.1) in the form

$$p(\mathbf{x}, t) = p_1(\mathbf{x}, t) + p_2(\mathbf{x}, t),$$

Downloaded from https://www.cambridge.org/core. Charité Universitätsmedizin Berlin, on 20 Dec 2021 at 10:08:47, subject to the Cambridge Core terms of use, available at https://www.cambridge.org/core/terms. https://doi.org/10.1017/CBO9781107360273.005

where, using (1.10.7) and (1.10.9) as $|\mathbf{x}| \to \infty$,

$$p_1(\mathbf{x},t) = \frac{-\rho_o x_i}{4\pi c_o |\mathbf{x}|^2} \frac{\partial}{\partial t} \int (\boldsymbol{\omega} \wedge \mathbf{u})_i \left(\mathbf{y}, t - \frac{|\mathbf{x}|}{c_o} + \frac{\mathbf{x}\cdot\mathbf{y}}{c_o|\mathbf{x}|} \right) d^3\mathbf{y}, \quad (4.5.4)$$

$$p_2(\mathbf{x},t) = \frac{\rho_o}{4\pi c_o^2 |\mathbf{x}|} \frac{\partial^2}{\partial t^2} \int \tfrac{1}{2} u^2 \left(\mathbf{y}, t - \frac{|\mathbf{x}|}{c_o} + \frac{\mathbf{x}\cdot\mathbf{y}}{c_o|\mathbf{x}|} \right) d^3\mathbf{y}. \quad (4.5.5)$$

When retarded time variations $\mathbf{x}\cdot\mathbf{y}/c_o|\mathbf{x}|$ within the eddy are neglected the identity (4.5.3) and the divergence theorem imply that $\int \boldsymbol{\omega}\wedge\mathbf{u}\, d^3\mathbf{y} \equiv \mathbf{0}$, because $u \sim O(1/|\mathbf{y}|^3)$ as $|\mathbf{y}| \to \infty$. To estimate the value of the integral in (4.5.4) it is therefore necessary to expand the integrand to the next order of approximation in the retarded time:

$$\begin{aligned}(\boldsymbol{\omega} \wedge \mathbf{u}) &\left(\mathbf{y}, t - \frac{|\mathbf{x}|}{c_o} + \frac{\mathbf{x}\cdot\mathbf{y}}{c_o|\mathbf{x}|} \right) \\ &= (\boldsymbol{\omega} \wedge \mathbf{u}) \left(\mathbf{y}, t - \frac{|\mathbf{x}|}{c_o} \right) + \frac{\mathbf{x}\cdot\mathbf{y}}{c_o|\mathbf{x}|} \frac{\partial}{\partial t} \left\{ (\boldsymbol{\omega} \wedge \mathbf{u}) \left(\mathbf{y}, t - \frac{|\mathbf{x}|}{c_o} \right) \right\} + \cdots .\end{aligned}$$

We now find

$$\begin{aligned} p_1(\mathbf{x},t) &\approx \frac{-\rho_o x_i x_j}{4\pi c_o^2 |\mathbf{x}|^3} \frac{\partial^2}{\partial t^2} \int y_i (\boldsymbol{\omega} \wedge \mathbf{u})_j \left(\mathbf{y}, t - \frac{|\mathbf{x}|}{c_o} \right) d^3\mathbf{y} \\ &\sim \frac{\ell}{|\mathbf{x}|} \rho_o u^2 M^2, \quad |\mathbf{x}| \to \infty. \end{aligned} \quad (4.5.6)$$

The order of magnitude of $p_2(\mathbf{x},t)$ is estimated using Crocco's form of the momentum equation (4.4.3). Because $B = \int dp/\rho + \frac{1}{2}v^2$ in homentropic flow, we can write

$$\frac{\partial \mathbf{u}}{\partial t} + \nabla \left(\int \frac{dp}{\rho} + \tfrac{1}{2}v^2 + \frac{\partial \varphi}{\partial t} \right) = -\boldsymbol{\omega} \wedge \mathbf{u} - \boldsymbol{\omega} \wedge \nabla\varphi - \nu \operatorname{curl} \boldsymbol{\omega}.$$

Take the scalar product with $\mathbf{u}$

$$\begin{aligned} &\frac{\partial}{\partial t} \left(\tfrac{1}{2}u^2 \right) + \operatorname{div} \left\{ \mathbf{u} \left(\int \frac{dp}{\rho} + \tfrac{1}{2}v^2 + \frac{\partial \varphi}{\partial t} \right) \right\} \\ &\quad = -\mathbf{u} \cdot \boldsymbol{\omega} \wedge \nabla\varphi - \nu \mathbf{u} \cdot \operatorname{curl} \boldsymbol{\omega} \\ &\quad = -\mathbf{u} \cdot \boldsymbol{\omega} \wedge \nabla\varphi + \nu \left(\operatorname{div} (\mathbf{u} \wedge \boldsymbol{\omega}) - \omega^2 \right) \end{aligned}$$

and integrate over the whole of space. The contributions from the divergence terms vanish because $\mathbf{u}(\int dp/\rho + \frac{1}{2}v^2 + \partial\varphi/\partial t)$ tends to zero at least as fast as $1/|\mathbf{y}|^3$ as $|\mathbf{y}| \to \infty$, where also $\boldsymbol{\omega} = \mathbf{0}$. Hence, using the estimate (4.5.2)

$$\frac{\partial}{\partial t} \int \tfrac{1}{2} u^2(\mathbf{y},t) d^3\mathbf{y} = -\int \left(\mathbf{u} \cdot \boldsymbol{\omega} \wedge \nabla\varphi + \nu\omega^2 \right) (\mathbf{y},t) d^3\mathbf{y} \sim \ell^2 u^3 M^2 + \frac{\ell^2 u^3}{Re} \quad (4.5.7)$$

Downloaded from https://www.cambridge.org/core. Charité Universitätsmedizin Berlin, on 20 Dec 2021 at 10:08:47, subject to the Cambridge Core terms of use, available at https://www.cambridge.org/core/terms. https://doi.org/10.1017/CBO9781107360273.005

where $Re = u\ell/\nu$ typically exceeds 10^4 in turbulent flow. The two terms on the right-hand side nominally represent the dissipation of the turbulent motions respectively by acoustic radiation and by viscous damping. (Equation (4.2.5) actually shows that a more accurate estimate of the radiation damping is $\ell^2 u^3 M^5$.)

Thus, when retarded time variations are neglected in (4.5.5), we find

$$p_2(\mathbf{x}, t) \sim \frac{\ell}{|\mathbf{x}|}\rho_o u^2 M^4 + \frac{\ell}{|\mathbf{x}|}\frac{\rho_o u^2 M^2}{Re},$$

and therefore that $p_2 \ll p_1$ in turbulent flow where $M \ll 1$ and $Re \gg 1$.

We conclude that the component

$$\operatorname{div}(\rho_o \boldsymbol{\omega} \wedge \mathbf{v}) \text{ of the Lighthill quadrupole } \frac{\partial^2(\rho_o v_i v_j)}{\partial x_i \partial x_j}$$

is principal source of sound at low Mach numbers.

4.6 The vortex sound equation

Lighthill's equation (4.1.11) can be recast to emphasise the rôle of vorticity in the production of aerodynamic sound by taking the acoustic variable to be the perturbation of the **total enthalpy** $B = w + \frac{1}{2}v^2$ from its background mean value, in place of Lighthill's $c_o^2(\rho - \rho_o)$. To illustrate this we shall consider homentropic flows for which

$$B = \int \frac{dp}{\rho} + \frac{1}{2}v^2.$$

The total enthalpy occurs naturally in Crocco's momentum equation (1.2.10). In the following the homentropic approximation (4.4.3) of this equation is used, in which the viscous term $(\nu' + \frac{4}{3}\nu)\nabla(\operatorname{div}\mathbf{v})$ is neglected. Indeed, the principal effect of this term is to attenuate the sound once it has been generated and is propagating to a distant observer in the source-free region of the flow. This attenuation can be significant in applications, but is of no particular interest when studying sound generation. All viscous stresses can be ignored in a high Reynolds number source flow *except* possibly within surface boundary layers on bodies immersed in the flow. But surface friction is dominated by the vorticity term $-\nu\operatorname{curl}\boldsymbol{\omega}$, which is retained in (4.4.3).

In irrotational flow Crocco's equation (4.4.3) reduces to

$$\frac{\partial \mathbf{v}}{\partial t} = -\nabla B.$$

Downloaded from https://www.cambridge.org/core. Charité Universitätsmedizin Berlin, on 20 Dec 2021 at 10:08:47, subject to the Cambridge Core terms of use, available at https://www.cambridge.org/core/terms. https://doi.org/10.1017/CBO9781107360273.005

In other words, to within an arbitrary constant,

$$B = -\frac{\partial \varphi}{\partial t} \text{ in regions where } \boldsymbol{\omega} = \mathbf{0}, \tag{4.6.1}$$

where $\varphi(\mathbf{x}, t)$ is the velocity potential that determines the whole motion in the irrotational regions of the fluid. B is *constant* in steady irrotational flow, and at large distances from the acoustic sources perturbations in B represent sound waves.

If the mean flow is at rest in the far field, the acoustic pressure is given by

$$p = \rho_o B \equiv -\rho_o \frac{\partial \varphi}{\partial t}. \tag{4.6.2}$$

To calculate the pressure in terms of B elsewhere in the flow we use the definition

$$\int \frac{dp}{\rho} = B - \frac{1}{2} v^2.$$

Differentiating with respect to time and using Crocco's equation (4.4.3), we have

$$\begin{aligned} \frac{1}{\rho}\frac{\partial p}{\partial t} &= \frac{\partial B}{\partial t} - \mathbf{v} \cdot \frac{\partial \mathbf{v}}{\partial t} \\ &= \frac{\partial B}{\partial t} - \mathbf{v} \cdot \Big(- \nabla B - \boldsymbol{\omega} \wedge \mathbf{v} - \nu \operatorname{curl} \boldsymbol{\omega} \Big) \\ &= \frac{DB}{Dt} + \nu \mathbf{v} \cdot \operatorname{curl} \boldsymbol{\omega}. \end{aligned}$$

The viscous term represents a small correction of relative order $\sim 1/Re$, and can be ignored in high Reynolds number source flows, where p and B can be taken to be related by

$$\frac{1}{\rho}\frac{\partial p}{\partial t} = \frac{DB}{Dt}. \tag{4.6.3}$$

4.6.1 Reformulation of Lighthill's equation

Multiply Crocco's equation (4.4.3) by the density ρ and take the divergence:

$$\operatorname{div}\left(\rho \frac{\partial \mathbf{v}}{\partial t}\right) + \nabla \cdot (\rho \nabla B) = -\operatorname{div}(\rho \boldsymbol{\omega} \wedge \mathbf{v}). \tag{4.6.4}$$

The first term on the left is expressed in terms of B by using the continuity equation in the form

$$\operatorname{div} \mathbf{v} = -\frac{1}{\rho}\frac{D\rho}{Dt}$$

Downloaded from https://www.cambridge.org/core. Charité Universitätsmedizin Berlin, on 20 Dec 2021 at 10:08:47, subject to the Cambridge Core terms of use, available at https://www.cambridge.org/core/terms. https://doi.org/10.1017/CBO9781107360273.005

and writing

$$\begin{aligned}\operatorname{div}\left(\rho\frac{\partial \mathbf{v}}{\partial t}\right) &= \nabla\rho\cdot\frac{\partial \mathbf{v}}{\partial t}+\rho\frac{\partial}{\partial t}\operatorname{div}\mathbf{v} = \nabla\rho\cdot\frac{\partial \mathbf{v}}{\partial t}-\rho\frac{\partial}{\partial t}\left(\frac{1}{\rho}\frac{D\rho}{Dt}\right)\\ &= \nabla\rho\cdot\frac{\partial \mathbf{v}}{\partial t}-\rho\frac{\partial}{\partial t}\left(\frac{1}{\rho}\frac{\partial\rho}{\partial t}\right)-\frac{\partial \mathbf{v}}{\partial t}\cdot\nabla\rho-\rho\mathbf{v}\cdot\nabla\left(\frac{1}{\rho}\frac{\partial\rho}{\partial t}\right)\\ &= -\rho\frac{D}{Dt}\left(\frac{1}{\rho}\frac{\partial\rho}{\partial t}\right)=-\rho\frac{D}{Dt}\left(\frac{1}{\rho c^2}\frac{\partial p}{\partial t}\right)\\ &= -\rho\frac{D}{Dt}\left(\frac{1}{c^2}\frac{DB}{Dt}\right),\end{aligned}$$

where equation (4.6.3) has been used on the last line. Substituting into (4.6.4) and dividing by ρ we obtain the desired **vortex sound equation** for homentropic flow:

$$\left(\frac{D}{Dt}\left(\frac{1}{c^2}\frac{D}{Dt}\right)-\frac{1}{\rho}\nabla\cdot(\rho\nabla)\right)B=\frac{1}{\rho}\operatorname{div}(\rho\boldsymbol{\omega}\wedge\mathbf{v}). \tag{4.6.5}$$

The 'vortex source' on the right-hand side vanishes in irrotational regions; if $\boldsymbol{\omega}=\mathbf{0}$ everywhere, and if there are no moving boundaries, the total enthalpy B is constant, and there are no sound waves propagating in the fluid. If acoustic waves cannot enter from infinity, it follows that the (homentropic) flow can generate sound only if moving vorticity is present, and the right-hand side of (4.6.5) may be identified as the analytical representation of the acoustic sources. The differential operator on the left describes propagation of the sound through the non-uniform flow; as in the case of Lighthill's equation, when the source region is very extensive it will not normally be permissible to neglect the interaction of the sound with the vorticity through which it propagates.

4.6.2 Vortex sound at low Mach numbers

When the characteristic Mach number M is small the local mean values of the density and sound speed are related to their uniform respective values ρ_o and c_o at infinity by relations of the form

$$\frac{c}{c_o}\sim 1+O(M^2),\quad \frac{\rho}{\rho_o}\sim 1+O(M^2).$$

The vortex sound equation (4.6.5) can therefore be simplified by (a) taking $c=c_o$, and $\rho=\rho_o$, and (b) by neglecting nonlinear effects of propagation and the scattering of sound by the vorticity. The production of sound is then governed by the simpler equation

$$\left(\frac{1}{c_o^2}\frac{\partial^2}{\partial t^2}-\nabla^2\right)B=\operatorname{div}(\boldsymbol{\omega}\wedge\mathbf{v}), \tag{4.6.6}$$

Downloaded from https://www.cambridge.org/core. Charité Universitätsmedizin Berlin, on 20 Dec 2021 at 10:08:47, subject to the Cambridge Core terms of use, available at https://www.cambridge.org/core/terms. https://doi.org/10.1017/CBO9781107360273.005

and in the far field the acoustic pressure is given by the linearised approximation

$$p(\mathbf{x}, t) \approx \rho_o B(\mathbf{x}, t). \tag{4.6.7}$$

4.6.3 Sound generation by a spinning vortex pair (Powell 1963)

Two parallel vortex filaments each of circulation Γ and distance 2ℓ apart rotate about the x_3-axis midway between them at angular velocity $\Omega = \Gamma/4\pi\ell^2$ (Figure 4.6.1), provided the Mach number is small enough for the motion to be regarded as incompressible. Their positions at time t are

$$\bar{\mathbf{x}} = (x_1, x_2) = \pm\mathbf{s} \equiv \pm(s_1(t), s_2(t)) = \pm\ell(\cos\Omega t, \sin\Omega t).$$

The vorticity distribution is

$$\boldsymbol{\omega} = \Gamma\mathbf{k}\Big(\delta(\bar{\mathbf{x}} - \mathbf{s}) + \delta(\bar{\mathbf{x}} + \mathbf{s})\Big),$$

where $\mathbf{k}$ is a unit vector in the x_3-direction, parallel to the vortices. The vortex convection velocities are

$$\mathbf{v} = \pm\Omega\mathbf{k} \wedge \mathbf{s}(t) \quad \text{at} \quad \bar{\mathbf{x}} = \pm\mathbf{s}(t), \quad \text{where } U = \Omega\ell \ll c_o.$$

Hence, because $\mathbf{k} \wedge (\mathbf{k} \wedge \mathbf{s}) = -\mathbf{s}$,

$$\boldsymbol{\omega} \wedge \mathbf{v} = -\Gamma\Omega\mathbf{s}(t)\Big[\delta(\bar{\mathbf{x}} - \mathbf{s}) - \delta(\bar{\mathbf{x}} + \mathbf{s})\Big].$$

If this is expanded in powers of the radius ℓ of the circular orbit (and it can be verified that this is equivalent to expanding the acoustic pressure in powers of $M = U/c_o \ll 1$) the i-component of the first non-zero term is

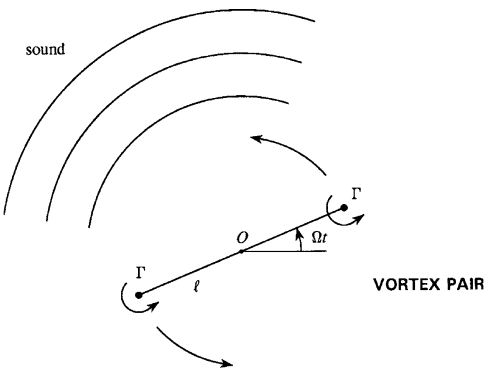

Figure 4.6.1

Downloaded from https://www.cambridge.org/core. Charité Universitätsmedizin Berlin, on 20 Dec 2021 at 10:08:47, subject to the Cambridge Core terms of use, available at https://www.cambridge.org/core/terms. https://doi.org/10.1017/CBO9781107360273.005

$$(\boldsymbol{\omega} \wedge \mathbf{v})_i \approx \frac{\partial}{\partial \bar{x}_j}\Big(2\Gamma\Omega s_i(t) s_j(t) \delta(\bar{\mathbf{x}})\Big),$$

so that the vortex sound source is equivalent to the quadrupole

$$\operatorname{div}(\boldsymbol{\omega} \wedge \mathbf{v}) \approx \frac{\partial^2}{\partial \bar{x}_i \partial \bar{x}_j}\Big(2\Gamma\Omega s_i(t) s_j(t) \delta(\bar{\mathbf{x}})\Big).$$

The solution of the vortex sound equation (4.6.6) for this quadrupole source is (cf. (4.2.1))

$$B = \frac{1}{4\pi} \frac{\partial^2}{\partial \bar{x}_i \partial \bar{x}_j} \int 2\Gamma\Omega\,(s_i s_j)\Big(t - \frac{|\mathbf{x}-\mathbf{y}|}{c_o}\Big) \frac{\delta(\bar{\mathbf{y}}) d^3\mathbf{y}}{|\mathbf{x}-\mathbf{y}|}, \quad \bar{\mathbf{y}} = (y_1, y_2).$$

In the acoustic far field we use (1.10.8):

$$\frac{\partial}{\partial \bar{x}_j} \approx \frac{-\bar{x}_j}{c_o\left(\varpi^2 + (x_3 - y_3)^2\right)^{\frac{1}{2}}} \frac{\partial}{\partial t},$$

where $\varpi = (x_1^2 + x_2^2)^{\frac{1}{2}}$ is the perpendicular distance from the centroid of the vortices (the x_3-axis). Thus, by setting $\xi = y_3 - x_3$, we can write in the acoustic far field, where $B \approx p/\rho_o$,

$$p \approx \frac{\rho_o \Gamma\Omega \bar{x}_i \bar{x}_j}{2\pi c_o^2} \frac{\partial^2}{\partial t^2} \int_{-\infty}^{\infty} (s_i s_j)\Big(t - \frac{(\varpi^2 + \xi^2)^{\frac{1}{2}}}{c_o}\Big) \frac{d\xi}{(\varpi^2 + \xi^2)^{\frac{3}{2}}}, \quad \varpi \to \infty. \tag{4.6.8}$$

In this formula

$$(s_i s_j)(t) = \frac{\ell^2}{2} \begin{pmatrix} 1 + \cos 2\Omega t & \sin 2\Omega t \\ \sin 2\Omega t & 1 - \cos 2\Omega t \end{pmatrix},$$

but the constant terms in the matrix can be omitted because of the time derivatives in (4.6.8). The integration in (4.6.8) can now be performed by the method of stationary phase (§4.6.4) in the limit that $\Omega\varpi/c_o \to \infty$, that is, in the limit in which the radial distance ϖ greatly exceeds the acoustic wavelength:

$$\int_{-\infty}^{\infty} (s_i s_j)\Big(t - \frac{(\varpi^2 + \xi^2)^{\frac{1}{2}}}{c_o}\Big) \frac{d\xi}{(\varpi^2 + \xi^2)^{\frac{3}{2}}} \approx \frac{\ell^2}{2\varpi^2}\Big(\frac{\pi c_o}{\Omega\varpi}\Big)^{\frac{1}{2}} \begin{pmatrix} \cos\big(2\Omega[t] - \frac{\pi}{4}\big) & \sin\big(2\Omega[t] - \frac{\pi}{4}\big) \\ \sin\big(2\Omega[t] - \frac{\pi}{4}\big) & -\cos\big(2\Omega[t] - \frac{\pi}{4}\big) \end{pmatrix},$$

where $[t] = t - \varpi/c_o$. Hence, introducing polar coordinates $\bar{\mathbf{x}} = \varpi(\cos\theta, \sin\theta)$, we find

Downloaded from https://www.cambridge.org/core. Charité Universitätsmedizin Berlin, on 20 Dec 2021 at 10:08:47, subject to the Cambridge Core terms of use, available at https://www.cambridge.org/core/terms. https://doi.org/10.1017/CBO9781107360273.005

$$\bar{x}_i \bar{x}_j \frac{\ell^2}{2\varpi^2} \left(\frac{\pi c_o}{\Omega\varpi}\right)^{\frac{1}{2}} \begin{pmatrix} \cos\left(2\Omega[t] - \frac{\pi}{4}\right) & \sin\left(2\Omega[t] - \frac{\pi}{4}\right) \\ \sin\left(2\Omega[t] - \frac{\pi}{4}\right) & -\cos\left(2\Omega[t] - \frac{\pi}{4}\right) \end{pmatrix}_{ij}$$

$$= \frac{\ell^2}{2} \left(\frac{\pi c_o}{\Omega\varpi}\right)^{\frac{1}{2}} (\cos\theta, \sin\theta) \begin{pmatrix} \cos\left(2\Omega[t] - \frac{\pi}{4}\right) & \sin\left(2\Omega[t] - \frac{\pi}{4}\right) \\ \sin\left(2\Omega[t] - \frac{\pi}{4}\right) & -\cos\left(2\Omega[t] - \frac{\pi}{4}\right) \end{pmatrix} \begin{pmatrix} \cos\theta \\ \sin\theta \end{pmatrix}$$

$$= \frac{\ell^2}{2} \left(\frac{\pi c_o}{\Omega\varpi}\right)^{\frac{1}{2}} \cos\left(2\theta - 2\Omega[t] + \frac{\pi}{4}\right),$$

and therefore (4.6.8) becomes

$$p \approx \frac{-\rho_o \Gamma \Omega^3 \ell^2}{\pi c_o^2} \left(\frac{\pi c_o}{\Omega\varpi}\right)^{\frac{1}{2}} \cos\left[2\theta - 2\Omega\left(t - \frac{\varpi}{c_o}\right) + \frac{\pi}{4}\right]$$

$$= -4\sqrt{\frac{\pi\ell}{\varpi}} \rho_o U^2 M^{3/2} \cos\left[2\theta - 2\Omega\left(t - \frac{\varpi}{c_o}\right) + \frac{\pi}{4}\right], \quad \frac{\Omega\varpi}{c_o} \to \infty. \quad (4.6.9)$$

The amplitude of the sound decreases like $1/\sqrt{\varpi}$ (instead of $1/\varpi$) because the waves are spreading 'cylindrically' in two dimensions. The sound power must now be calculated by considering the integral

$$\int_\Sigma \frac{p^2}{\rho_o c_o} dS$$

over the surface of a large circular cylinder ϖ = constant. Taking the time average, we can show that the acoustic power *per unit length* of the vortices $\sim \ell\rho_o U^3 M^4$. This is nominally larger by one inverse power of the Mach number (M^{-1}) than the power radiated by a compact body of three-dimensional turbulence, and is characteristic of the acoustic power radiated by two-dimensional regions of turbulence *in an unbounded fluid*.

4.6.4 Example: Method of stationary phase

Show that

$$\int_{-\infty}^{\infty} f\left(\frac{\xi}{\varpi}\right) e^{ik_o\sqrt{\varpi^2+\xi^2}} d\xi \approx \varpi f(0) \left(\frac{2\pi}{k_o\varpi}\right)^{\frac{1}{2}} e^{i(k_o\varpi + \frac{\pi}{4})}, \quad k_o\varpi \to \infty. \quad (4.6.10)$$

Put $\xi = \mu\varpi$, then

$$I \equiv \int_{-\infty}^{\infty} f\left(\frac{\xi}{\varpi}\right) e^{ik_o\sqrt{\varpi^2+\xi^2}} d\xi = \varpi \int_{-\infty}^{\infty} f(\mu) e^{ik_o\varpi\sqrt{1+\mu^2}} d\mu.$$

As $k_o\varpi \to \infty$ the exponential factor oscillates increasingly rapidly, and the main contribution to the integral is from the neighbourhood of that value of μ where the oscillations are 'stationary'. This occurs at $\mu = 0$. The integrand

Downloaded from https://www.cambridge.org/core. Charité Universitätsmedizin Berlin, on 20 Dec 2021 at 10:08:47, subject to the Cambridge Core terms of use, available at https://www.cambridge.org/core/terms. https://doi.org/10.1017/CBO9781107360273.005

is therefore expanded about this point. In the first approximation $f(\mu)$ can be replaced by $f(0)$, and

$$e^{ik_o\varpi\sqrt{1+\mu^2}} \approx e^{ik_o\varpi + ik_o\varpi\mu^2/2}$$

$$\therefore \quad I = \varpi \int_{-\infty}^{\infty} f(\mu) e^{ik_o\varpi\sqrt{1+\mu^2}} d\mu$$

$$\approx \varpi f(0) e^{ik_o\varpi} \int_{-\infty}^{\infty} e^{ik_o\varpi\mu^2/2} d\mu = \varpi f(0) e^{ik_o\varpi} \left(\frac{2\pi}{k_o\varpi}\right)^{\frac{1}{2}} e^{\frac{i\pi}{4}},$$

which yields (4.6.10). The general formula

$$\int_{-\infty}^{\infty} e^{i\alpha\mu^2} d\mu = \sqrt{\frac{\pi}{|\alpha|}}\, e^{\frac{i\pi}{4}\mathrm{sgn}(\alpha)}, \quad (\alpha \text{ real}), \tag{4.6.11}$$

has been used to evaluate the last integral, together with the implicit assumption that $k_o > 0$.

In particular

$$\int_{-\infty}^{\infty} \left\{\cos 2\Omega\left(t - \frac{(\varpi^2+\xi^2)^{\frac{1}{2}}}{c_o}\right) - i \sin 2\Omega\left(t - \frac{(\varpi^2+\xi^2)^{\frac{1}{2}}}{c_o}\right)\right\} \frac{d\xi}{(\varpi^2+\xi^2)^{\frac{3}{2}}}$$

$$= e^{-2i\Omega t} \int_{-\infty}^{\infty} e^{i\frac{2\Omega}{c_o}\sqrt{\varpi^2+\xi^2}} \frac{d\xi}{(\varpi^2+\xi^2)^{\frac{3}{2}}}$$

$$\approx \frac{1}{\varpi^2}\left(\frac{\pi c_o}{\Omega\varpi}\right)^{\frac{1}{2}} e^{-i\left[2\Omega\left(t-\frac{\varpi}{c_o}\right)-\frac{\pi}{4}\right]}, \quad \frac{\Omega\varpi}{c_o} \to \infty.$$

Hence

$$\int_{-\infty}^{\infty} \cos 2\Omega\left(t - \frac{(\varpi^2+\xi^2)^{\frac{1}{2}}}{c_o}\right) \frac{d\xi}{(\varpi^2+\xi^2)^{\frac{3}{2}}}$$

$$\approx \frac{1}{\varpi^2}\left(\frac{\pi c_o}{\Omega\varpi}\right)^{\frac{1}{2}} \cos\left[2\Omega\left(t - \frac{\varpi}{c_o}\right) - \frac{\pi}{4}\right]$$

$$\int_{-\infty}^{\infty} \sin 2\Omega\left(t - \frac{(\varpi^2+\xi^2)^{\frac{1}{2}}}{c_o}\right) \frac{d\xi}{(\varpi^2+\xi^2)^{\frac{3}{2}}}$$

$$\approx \frac{1}{\varpi^2}\left(\frac{\pi c_o}{\Omega\varpi}\right)^{\frac{1}{2}} \sin\left[2\Omega\left(t - \frac{\varpi}{c_o}\right) - \frac{\pi}{4}\right].$$

4.7 Vortex-surface interaction noise

The small Mach number vortex sound equation (4.6.6) is now applied to determine the sound generated by vorticity in the neighbourhood of a fixed body

Downloaded from https://www.cambridge.org/core. Charité Universitätsmedizin Berlin, on 20 Dec 2021 at 10:08:47, subject to the Cambridge Core terms of use, available at https://www.cambridge.org/core/terms. https://doi.org/10.1017/CBO9781107360273.005

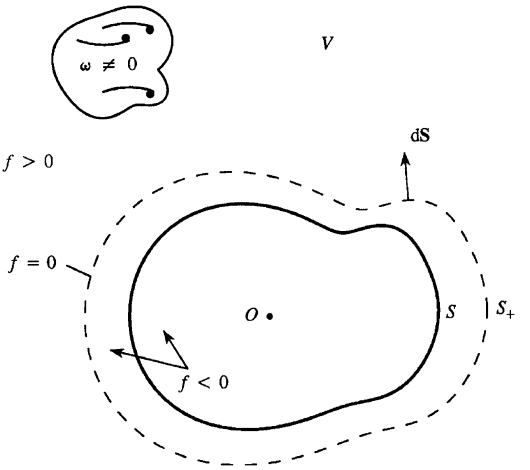

Figure 4.7.1

whose surface S may be vibrating at small amplitude (Figure 4.7.1). The development here follows closely the methods of §2.1 for Kirchhoff's formula and §4.3 for Curle's equation.

Introduce a stationary, closed control surface S_+ on which $f(\mathbf{x}) = 0$, such that $f(\mathbf{x}) \gtrless 0$ according as $\mathbf{x}$ lies outside or within S_+. The body is inside S_+, and S_+ will subsequently shrink down to coincide with S. Multiply equation (4.6.6) by $\mathrm{H} \equiv \mathrm{H}(f)$ and form the inhomogeneous wave equation for the new variable $\mathrm{H}B$:

$$\left(\frac{1}{c_o^2}\frac{\partial^2}{\partial t^2} - \nabla^2\right)(\mathrm{H}B) = -\mathrm{div}\,(B\nabla\mathrm{H}) - \nabla\mathrm{H}\cdot(\nabla B + \boldsymbol{\omega}\wedge\mathbf{v}) + \mathrm{div}\,(\mathrm{H}\boldsymbol{\omega}\wedge\mathbf{v}).$$

Use Crocco's equation (4.4.3) to make the substitution

$$\nabla\mathrm{H}\cdot(\nabla B + \boldsymbol{\omega}\wedge\mathbf{v}) = -\nabla\mathrm{H}\cdot\left(\frac{\partial\mathbf{v}}{\partial t} + \nu\,\mathrm{curl}\,\boldsymbol{\omega}\right) \equiv -\nabla\mathrm{H}\cdot\frac{\partial\mathbf{v}}{\partial t} + \nu\,\mathrm{div}\,(\nabla\mathrm{H}\wedge\boldsymbol{\omega}),$$

thereby obtaining the vortex sound equation in the form

$$\left(\frac{1}{c_o^2}\frac{\partial^2}{\partial t^2} - \nabla^2\right)(\mathrm{H}B) = -\mathrm{div}\,(B\nabla\mathrm{H}) + \nabla\mathrm{H}\cdot\frac{\partial\mathbf{v}}{\partial t} + \mathrm{div}\,(\mathrm{H}\boldsymbol{\omega}\wedge\mathbf{v}) - \nu\,\mathrm{div}\,(\nabla\mathrm{H}\wedge\boldsymbol{\omega}). \tag{4.7.1}$$

The sources on the right-hand side are either concentrated on the control surface S_+ or lie in the fluid outside S_+; they completely determine B outside the control surface. The solution in this region is found by using any Green's function $G(\mathbf{x}, \mathbf{y}, t-\tau)$ that satisfies (1.6.1) for $\mathbf{x}$ and $\mathbf{y}$ anywhere within the

Downloaded from https://www.cambridge.org/core. Charité Universitätsmedizin Berlin, on 20 Dec 2021 at 10:08:47, subject to the Cambridge Core terms of use, available at https://www.cambridge.org/core/terms. https://doi.org/10.1017/CBO9781107360273.005

fluid. In Figure 4.7.1 the fluid occupies the region V *outside* the surface S of the solid body; the control surface S_+ ($f(\mathbf{x}) = 0$) therefore lies *within* V.

Proceeding in the usual way, we obtain the following general solution in the region $f > 0$ outside S_+:

$$\begin{aligned} B(\mathbf{x}, t) = &\oint_{S_+} \left(B(\mathbf{y}, \tau) \frac{\partial G}{\partial y_n}(\mathbf{x}, \mathbf{y}, t-\tau) + G(\mathbf{x}, \mathbf{y}, t-\tau) \frac{\partial v_n}{\partial \tau}(\mathbf{y}, \tau) \right) dS(\mathbf{y}) d\tau \\ &- \int_V \mathrm{H}(f(\mathbf{y}))(\boldsymbol{\omega} \wedge \mathbf{v})(\mathbf{y}, \tau) \cdot \frac{\partial G}{\partial \mathrm{y}}(\mathbf{x}, \mathbf{y}, t-\tau) d^3\mathbf{y} d\tau \\ &+ \nu \oint_{S_+} \boldsymbol{\omega}(\mathbf{y}, \tau) \wedge \frac{\partial G}{\partial \mathbf{y}}(\mathbf{x}, \mathbf{y}, t-\tau) \cdot d\mathbf{S}(\mathbf{y}) d\tau, \end{aligned} \tag{4.7.2}$$

where for brevity we have omitted the integration sign for τ, which is understood to vary over the range $-\infty < \tau < \infty$.

We now choose G to have vanishing normal derivative on the surface S of the body. When this is done the control surface S_+ is allowed to collapse onto S (whereupon the first term in the first integral of (4.7.2) vanishes), and the outgoing wave solution in the fluid becomes

$$\begin{aligned} B(\mathbf{x}, t) = &- \int_V (\boldsymbol{\omega} \wedge \mathbf{v})(\mathbf{y}, \tau) \cdot \frac{\partial G}{\partial \mathbf{y}}(\mathbf{x}, \mathbf{y}, t-\tau) d^3\mathbf{y} d\tau \\ &+ \nu \oint_S \boldsymbol{\omega}(\mathbf{y}, \tau) \wedge \frac{\partial G}{\partial \mathbf{y}}(\mathbf{x}, \mathbf{y}, t-\tau) \cdot d\mathbf{S}(\mathbf{y}) d\tau \\ &+ \oint_S G(\mathbf{x}, \mathbf{y}, t-\tau) \frac{\partial v_n}{\partial \tau}(\mathbf{y}, \tau) dS(\mathbf{y}) d\tau, \\ &\text{where} \quad \frac{\partial G}{\partial y_n}(\mathbf{x}, \mathbf{y}, t-\tau) = 0 \ \text{ on } S. \end{aligned} \tag{4.7.3}$$

In the acoustic far field ($|\mathbf{x}| \to \infty$) $B(\mathbf{x}, t)$ may be replaced by $p(\mathbf{x}, t)/\rho_o$.

The first integral represents the production of sound by vortex sources distributed within the fluid. Green's function takes full account of the influence of the body on the efficiency with which these sources generate sound. The second, surface integral involving the surface vorticity is the contribution from frictional forces on S. To interpret the final term, recall that the control surface S_+ was taken to be fixed in space. This means that fluid can flow through the surface. When S_+ shrinks down to S the implication is that S is also fixed in space. However, the normal velocity v_n can still be non-zero if the surface of the body is *vibrating* at small amplitude, and this term in the solution is equivalent to that in (2.1.6) applied to a vibrating body in the absence of vortex sources.

Downloaded from https://www.cambridge.org/core. Charité Universitätsmedizin Berlin, on 20 Dec 2021 at 10:08:47, subject to the Cambridge Core terms of use, available at https://www.cambridge.org/core/terms. https://doi.org/10.1017/CBO9781107360273.005

The contribution to the sound from surface friction (the first surface integral on the right of (4.7.3)) is nominally of order

$$\frac{1}{Re} \ll 1, \quad Re = \frac{v\ell}{\nu},$$

relative to that from the volume vorticity (the first integral), where ℓ is the characteristic length scale of the turbulence or body and v is a typical velocity. At high Reynolds numbers the acoustic pressure is therefore given by

$$\frac{p(\mathbf{x}, t)}{\rho_o} = \oint_S G(\mathbf{x}, \mathbf{y}, t-\tau) \frac{\partial v_n}{\partial \tau}(\mathbf{y}, \tau) dS(\mathbf{y}) d\tau - \int_V (\boldsymbol{\omega} \wedge \mathbf{v})(\mathbf{y}, \tau) \cdot \frac{\partial G}{\partial \mathbf{y}}(\mathbf{x}, \mathbf{y}, t-\tau) d^3\mathbf{y} d\tau. \quad (4.7.4)$$

4.7.1 Example: Sound produced by vortex motion near a half-plane (Crighton 1972)

A line vortex of strength $\Gamma > 0$ in an ideal fluid is parallel to the unit vector $\mathbf{k}$ in the x_3-direction and adjacent to a rigid half-plane $x_1 < 0,\ x_2 = 0$; Figure 4.7.2. The vortex moves under the influence of 'image vortices' within the half-plane along a trajectory $\mathbf{x} \equiv (x_1, x_2) = (x_{01}(t), x_{02}(t))$ given in the approximation of incompressible motion by

$$\frac{x_{o1}}{\ell} = \frac{1 - (Ut/\ell)^2}{\sqrt{1 + (Ut/\ell)^2}}, \quad \frac{x_{o2}}{\ell} = \frac{-2Ut/\ell}{\sqrt{1 + (Ut/\ell)^2}}, \quad U = \frac{\Gamma}{8\pi\ell}, \quad (4.7.5)$$

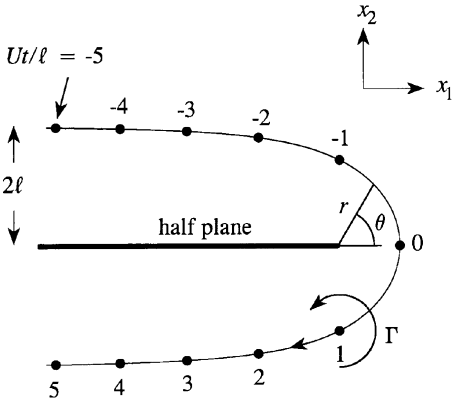

Figure 4.7.2

Downloaded from https://www.cambridge.org/core. Charité Universitätsmedizin Berlin, on 20 Dec 2021 at 10:08:47, subject to the Cambridge Core terms of use, available at https://www.cambridge.org/core/terms. https://doi.org/10.1017/CBO9781107360273.005

where the path crosses the x_1 axis at $t = 0$ at distance ℓ from the edge (see §2.A.3, Example 7). The vortex starts above the half-plane at $t = -\infty$ at $x_{o1} = -\infty$, $x_{o2} = 2\ell$ and translates towards the edge, initially at speed U parallel to the plane. After crossing the x_1-axis it proceeds along a symmetrical path below the half-plane.

The sound generated during the unsteady motion of the vortex around the edge is calculated using the two-dimensional compact Green's function (2.9.9), which can be written

$$G_1(\mathbf{x}, \mathbf{y}, t-\tau) \approx \frac{\sin(\theta/2)\varphi^*(\mathbf{y})}{\pi\sqrt{|\mathbf{x}|}}\delta\left(t - \tau - \frac{|\mathbf{x}|}{c_o}\right), \quad |\mathbf{x}| \to \infty,$$
$$\varphi^*(\mathbf{y}) = \sqrt{r_o}\sin(\theta_o/2), \tag{4.7.6}$$

where $\mathbf{x} = |\mathbf{x}|(\cos\theta, \sin\theta)$, the coordinates being defined as in Figure 4.7.2. This is applicable when the distance r_o from the edge of the source at $(y_1, y_2) = r_o(\cos\theta_o, \sin\theta_o)$ is much smaller than the acoustic wavelength. For a line vortex at (r_o, θ_o) the characteristic frequency $\sim v/r_o$, where v is the vortex translational velocity. The wavelength is therefore of order

$$\frac{r_o}{v} \times c_o = \frac{r_o}{M} \gg r_o \text{ for } M = \frac{v}{c_o} \ll 1,$$

so that low Mach number motion is sufficient to ensure that the wavelength of the sound is much larger than the vortex distance from the edge.

Thus, with $\boldsymbol{\omega} = \Gamma\mathbf{k}\delta(\mathbf{x} - \mathbf{x}_o(t))$ and $\mathbf{v} = d\mathbf{x}_0/dt$ at the vortex core, the two-dimensional version of (4.7.4), with $v_n \equiv 0$ and G given by (4.7.6), yields

$$\begin{aligned} p(\mathbf{x}, t) &\approx \frac{-\rho_o\Gamma\sin(\theta/2)}{\pi\sqrt{|\mathbf{x}|}} \int \mathbf{k} \wedge \frac{d\mathbf{x}_o}{d\tau}(\tau) \cdot \nabla\varphi^*(\mathbf{y}) \\ &\qquad \times \delta\Big(\mathbf{y} - \mathbf{x}_o(\tau)\Big)\delta\left(t - \tau - \frac{|\mathbf{x}|}{c_o}\right) dy_1 dy_2 d\tau \\ &= \frac{-\rho_o\Gamma\sin(\theta/2)}{\pi\sqrt{|\mathbf{x}|}}\left[\mathbf{k} \wedge \frac{d\mathbf{x}_o}{dt} \cdot \nabla\varphi^*\right], \quad |\mathbf{x}| \to \infty, \end{aligned} \tag{4.7.7}$$

where the term in the square brackets is evaluated at the retarded position $\mathbf{x}_o(t - |\mathbf{x}|/c_o)$ of the vortex.

Now $\varphi^*(\mathbf{y})$ is the velocity potential of an ideal, incompressible flow around the edge of the half-plane with streamlines as in Figure 4.7.3, and is the real part of

$$w = \varphi^* + i\psi^* = -i\sqrt{z}, \quad z = y_1 + iy_2.$$

Downloaded from https://www.cambridge.org/core. Charité Universitätsmedizin Berlin, on 20 Dec 2021 at 10:08:47, subject to the Cambridge Core terms of use, available at https://www.cambridge.org/core/terms. https://doi.org/10.1017/CBO9781107360273.005

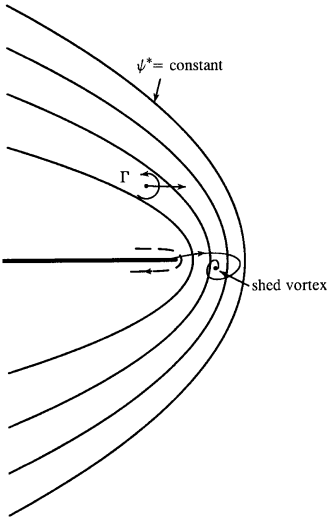

Figure 4.7.3

The *stream function* ψ^* is constant on a streamline, and satisfies (§2.A.1)

$$\frac{\partial \varphi^*}{\partial y_1} = \frac{\partial \psi^*}{\partial y_2}, \quad \frac{\partial \varphi^*}{\partial y_2} = -\frac{\partial \psi^*}{\partial y_1}.$$

These relations imply that

$$\mathbf{k} \wedge \nabla \varphi^* = \nabla \psi^*,$$

and therefore that

$$\mathbf{k} \wedge \frac{d\mathbf{x}_o}{dt} \cdot \nabla \varphi^* = -\frac{d\mathbf{x}_o}{dt} \wedge \mathbf{k} \cdot \nabla \varphi^* = -\frac{d\mathbf{x}_o}{dt} \cdot \mathbf{k} \wedge \nabla \varphi^* = -\frac{d\mathbf{x}_o}{dt} \cdot \nabla \psi^*.$$

The acoustic pressure can therefore be put in the form

$$p(\mathbf{x}, t) \approx \frac{\rho_o \Gamma \sin(\theta/2)}{\pi \sqrt{|\mathbf{x}|}} \left[\frac{d\mathbf{x}_o}{dt} \cdot \nabla \psi^* \right] \equiv \frac{\rho_o \Gamma \sin(\theta/2)}{\pi \sqrt{|\mathbf{x}|}} \left[\frac{D\psi^*}{Dt} \right], \quad |\mathbf{x}| \to \infty, \tag{4.7.8}$$

where $[D\psi^*/Dt]$ is evaluated at the retarded position of the vortex.

Because ψ^* is constant on each of the parabolic streamlines of the ideal flow around the edge defined by φ^* (Figure 4.7.3), a vortex that translated along

Downloaded from https://www.cambridge.org/core. Charité Universitätsmedizin Berlin, on 20 Dec 2021 at 10:08:47, subject to the Cambridge Core terms of use, available at https://www.cambridge.org/core/terms. https://doi.org/10.1017/CBO9781107360273.005

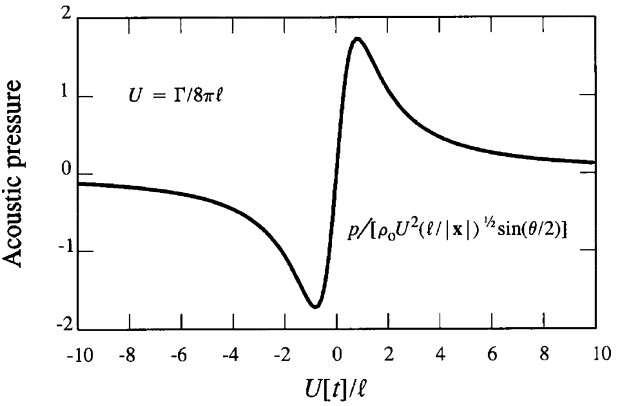

Figure 4.7.4

one of these streamlines would be 'silent'. The actual edge-generated sound depends on the rate $D\psi^*/Dt \equiv (d\mathbf{x}_0/dt)\cdot\nabla\psi^*$ at which the trajectory of the vortex cuts across the streamlines of this ideal edge-flow. This is found as follows (using the formulae (4.7.5)):

$$\nabla\psi^* = \nabla \mathrm{Im}\{-i\sqrt{z}\} = \mathrm{Im}\left(\frac{(-i,1)}{2\sqrt{z}}\right) = \frac{(-1, Ut/\ell)}{2\sqrt{\ell}\left(1+(Ut/\ell)^2\right)^{\frac{3}{4}}};$$

$d\mathbf{x}_0/dt$ is found similarly by differentiation of equations (4.7.5). Performing the calculations we find (see Figure 4.7.4)

$$p(\mathbf{x},t) \approx 4\rho_o U^2 \left(\frac{\ell}{|\mathbf{x}|}\right)^{\frac{1}{2}} \sin\left(\frac{\theta}{2}\right)\left[\frac{Ut/\ell}{[1+(Ut/\ell)^2]^{5/4}}\right]_{t-|\mathbf{x}|/c_o}, \quad |\mathbf{x}|\to\infty.$$

The pressure vanishes at the retarded time $[t]=0$ of closest approach of the vortex to the edge (at 0 in Figure 4.7.2).

4.8 Radiation from an acoustically compact body

When the surface S of Figure 4.7.1 is acoustically compact the compact Green's function (2.9.1) can be used to evaluate the general solution (4.7.3) *in the far field*. When $|\mathbf{x}|\to\infty$ and the origin is within or close to S, we proceed in the way already described in §2.8, by expanding the Green's function to first order in the retarded time:

Downloaded from https://www.cambridge.org/core. Charité Universitätsmedizin Berlin, on 20 Dec 2021 at 10:08:47, subject to the Cambridge Core terms of use, available at https://www.cambridge.org/core/terms. https://doi.org/10.1017/CBO9781107360273.005

$$G(\mathbf{x}, \mathbf{y}, t-\tau) = \frac{1}{4\pi|\mathbf{X}-\mathbf{Y}|}\delta\left(t-\tau-\frac{|\mathbf{X}-\mathbf{Y}|}{c_o}\right) \approx \frac{1}{4\pi|\mathbf{x}|}\delta\left(t-\tau-\frac{|\mathbf{x}|}{c_o}\right)+\frac{x_j Y_j}{4\pi c_o|\mathbf{x}|^2}\delta'\left(t-\tau-\frac{|\mathbf{x}|}{c_o}\right), \quad |\mathbf{x}| \to \infty,$$

where the prime denotes differentiation with respect to t. The first term in this approximation, which is independent of $\mathbf{y}$, clearly makes no contribution to the first two integrals in (4.7.3). It makes a contribution to the final surface integral only if the volume of the body is pulsating. When this happens the resulting monopole radiation from the body is usually large compared to all other sources. We shall therefore ignore this possibility, and consider only surface vibrations for which the volume of S is constant; in particular we shall assume that S vibrates as a rigid body without rotation. In this case, therefore, the first (monopole) term in the Green's function expansion can again be discarded.

Substituting into (4.7.3) and performing the integrations with respect to τ, we find in the acoustic far field (where $B = p/\rho_o$)

$$p(\mathbf{x}, t) \approx \frac{-\rho_o x_j}{4\pi c_o|\mathbf{x}|^2}\frac{\partial}{\partial t}\left[\int_V (\boldsymbol{\omega}\wedge\mathbf{v})\cdot\nabla Y_j d^3\mathbf{y} - \nu\oint_S \boldsymbol{\omega}\wedge\nabla Y_j\cdot d\mathbf{S}(\mathbf{y}) - \oint_S \frac{\partial U_n}{\partial t}Y_j dS(\mathbf{y})\right] \tag{4.8.1}$$

where the large square brackets ([ ]) denote evaluation at the retarded time $t-|\mathbf{x}|/c_o$, and U_n is the normal component of velocity of vibration of S.

We can put $U_n = U_i n_i$ when the body executes translational oscillations at velocity $\mathbf{U}(t)$, where n_i is the i-component of the surface normal directed into the fluid. Then

$$\rho_o\oint_S \frac{\partial U_n}{\partial t}Y_j dS = \rho_o\frac{dU_i}{dt}\oint_S (n_i y_j - n_i\varphi_j^*)dS = \left(m_o\delta_{ij}+M_{ij}\right)\frac{dU_i}{dt},$$

as in §2.8.2, where m_o is the mass of fluid displaced by the body, and M_{ij} is the added mass tensor.

The solution (4.8.1) can therefore be written

$$p(\mathbf{x}, t) \approx \frac{x_j}{4\pi c_o|\mathbf{x}|^2} \times \frac{\partial}{\partial t}\left[M_{ij}\frac{dU_i}{dt} - \rho_o\int(\boldsymbol{\omega}\wedge\mathbf{v})\cdot\nabla Y_j d^3\mathbf{y} + \eta\oint_S \boldsymbol{\omega}\wedge\nabla Y_j\cdot d\mathbf{S}(\mathbf{y})\right] + \frac{x_j}{4\pi c_o|\mathbf{x}|^2}\left[m_o\frac{d^2U_j}{dt^2}\right], \quad |\mathbf{x}| \to \infty. \tag{4.8.2}$$

Downloaded from https://www.cambridge.org/core. Charité Universitätsmedizin Berlin, on 20 Dec 2021 at 10:08:47, subject to the Cambridge Core terms of use, available at https://www.cambridge.org/core/terms. https://doi.org/10.1017/CBO9781107360273.005

It is shown in §4.A.2 of the appendix to this chapter, that a rigid body translating at velocity $\mathbf{U}(t)$ *without rotation* in an incompressible fluid exerts a force $\mathbf{F}(t)$ on the fluid whose ith component is given by

$$F_i = M_{ij}\frac{dU_j}{dt} - \rho_o \int_V \nabla X_i \cdot \boldsymbol{\omega} \wedge \mathbf{v}_{\rm rel} d^3\mathbf{x} + \eta \oint_S \boldsymbol{\omega} \wedge \nabla X_i \cdot d\mathbf{S}, \quad \mathbf{v}_{\rm rel} = \mathbf{v} - \mathbf{U}, \tag{4.8.3}$$

where $\mathbf{v}_{\rm rel}$ is the fluid velocity relative to the translational velocity of S.

The solution (4.8.2) therefore reduces to Curle's form (4.3.10)

$$p(\mathbf{x}, t) \approx \frac{x_j}{4\pi c_o |\mathbf{x}|^2}\frac{\partial}{\partial t}\left[m_o \frac{dU_j}{dt} + F_j\right], \quad |\mathbf{x}| \to \infty, \tag{4.8.4}$$

with the added benefit of an explicit formula for $\mathbf{F}$ in terms of the velocity and vorticity distributions near S.

The relative contributions from the volume and surface distributions of vorticity in (4.8.2) (respectively the second and third integrals) for turbulence of length scale ℓ and velocity v are estimated respectively by

$$\rho_o v^2 M \frac{\ell}{|\mathbf{x}|} \quad \text{and} \quad \rho_o v^2 M \frac{\ell}{|\mathbf{x}|}\frac{1}{Re}, \quad Re = \frac{v\ell}{\nu}.$$

Thus in high Reynolds number turbulent flows the surface frictional contribution to the dipole force $\mathbf{F}$ can usually be neglected. For a *non-vibrating* compact body the principal component of the acoustic pressure in the far field is given by

$$p(\mathbf{x}, t) \approx \frac{-\rho_o x_j}{4\pi c_o |\mathbf{x}|^2}\frac{\partial}{\partial t}\int (\boldsymbol{\omega} \wedge \mathbf{v})\left(\mathbf{y}, t - \frac{|\mathbf{x}|}{c_o}\right) \cdot \nabla Y_j(\mathbf{y}) d^3\mathbf{y}, \quad |\mathbf{x}| \to \infty. \tag{4.8.5}$$

4.8.1 Radiation in two dimensions

When the vortex source distribution is two dimensional and adjacent to a solid cylindrical body of diameter $\sim \ell$ with generators parallel to the vorticity, the sound produced at low Mach number $M \sim v/c_o$ has characteristic wavelength $\sim \ell/M \gg \ell$. At high Reynolds number the acoustic pressure is determined by the two-dimensional version of equation (4.7.4) in terms of the compact Green's function (2.9.19). For the particular case of a *stationary* body we find

$$p(\mathbf{x}, t) \approx \frac{-\rho_o x_j}{2\pi\sqrt{2c_o}|\mathbf{x}|^{\frac{3}{2}}}\frac{\partial}{\partial t}\int_{-\infty}^{t-|\mathbf{x}|/c_o} \frac{d\tau}{\sqrt{t - \tau - |\mathbf{x}|/c_o}} \times \int (\boldsymbol{\omega} \wedge \mathbf{v} \cdot \nabla Y_j)(\mathbf{y}, \tau) dy_1 dy_2, \quad |\mathbf{x}| \to \infty, \tag{4.8.6}$$

Downloaded from https://www.cambridge.org/core. Charité Universitätsmedizin Berlin, on 20 Dec 2021 at 10:08:47, subject to the Cambridge Core terms of use, available at https://www.cambridge.org/core/terms. https://doi.org/10.1017/CBO9781107360273.005

where $\mathbf{x} = (x_1, x_2)$. According to the inviscid form of the formula (4.8.3) applied to a stationary body, this can also be written

$$p(\mathbf{x}, t) \approx \frac{x_j}{2\pi\sqrt{2c_o}|\mathbf{x}|^{\frac{3}{2}}} \frac{\partial}{\partial t} \int_{-\infty}^{t-|\mathbf{x}|/c_o} \frac{F_j(\tau)d\tau}{\sqrt{t-\tau-|\mathbf{x}|/c_o}}, \quad |\mathbf{x}| \to \infty, \quad (4.8.7)$$

where F_j is the force *per unit length of the cylinder* exerted on the fluid in the j-direction.

4.9 Influence of vortex shedding

We can use formula (4.7.8) for the sound produced by a vortex passing an edge to form a qualitative picture of the influence of 'vortex shedding' on sound generation. Let the circulation of the vortex Γ in Figure 4.7.3 be in the indicated anticlockwise sense, so that fluid near the edge is induced to flow in a *clockwise* direction around the edge, as implied by the dashed curve in the figure. When the Reynolds number is large inertial forces actually cause the flow to *separate* from the edge, resulting in the release of vorticity of *opposite* sign from the edge into the 'wake'. Let us assume for simplicity that this shed vorticity rolls up into a concentrated core of strength Γ_s. Equation (4.7.8) then supplies the following prediction for the net acoustic pressure

$$p(\mathbf{x}, t) \approx \frac{\rho_o \sin(\theta/2)}{\pi\sqrt{|\mathbf{x}|}} \left(\Gamma \left[\frac{D\psi^*}{Dt} \right]_\Gamma + \Gamma_s \left[\frac{D\psi^*}{Dt} \right]_{\Gamma_s} \right), \quad |\mathbf{x}| \to \infty,$$

where the derivatives are evaluated at the retarded positions of Γ and Γ_s respectively. Both vortices translate across the curves $\psi^* =$ constant in the direction of decreasing ψ^*, and the derivatives therefore have the same sign. Hence, because Γ and Γ_s have opposite signs, *sound produced by the shed vortex will tend to cancel the edge-generated sound attributable to the incident vortex* Γ *alone*.

This conclusion is applicable to a wide range of fluid-structure interactions. A typical interaction involves a bounded region of vorticity, called a 'gust', swept along in a nominally steady mean flow. The localised velocity field of the gust is determined by the Biot–Savart formula (4.4.9). At high mean flow speeds it is sometimes permissible to neglect changes in the relative configuration of the vorticity distribution during its convection past an observation point: the vorticity is then said to be 'frozen' (at least temporarily) and the induced velocity is steady in a frame translating with the gust. If the mean flow carries the gust past the surface S of a stationary body, the free field-induced velocity determined by the Biot–Savart integral is said to produce an 'upwash' velocity on S; the actual velocity consists of the upwash velocity augmented by the

Downloaded from https://www.cambridge.org/core. Charité Universitätsmedizin Berlin, on 20 Dec 2021 at 10:08:47, subject to the Cambridge Core terms of use, available at https://www.cambridge.org/core/terms. https://doi.org/10.1017/CBO9781107360273.005

velocity field required to satisfy the 'no-slip' condition on S. (In an ideal fluid only the normal component of the upwash velocity is cancelled on S.)

When a gust convects past a stationary airfoil the high Reynolds number surface force (responsible for the sound) is given by (see (4.8.3))

$$F_i = -\rho_o \int_V \nabla Y_i(\mathbf{y}) \cdot (\boldsymbol{\omega} \wedge \mathbf{v})(\mathbf{y}, t) d^3\mathbf{y}, \quad Y_i = y_i - \varphi_i^*(\mathbf{y}). \tag{4.9.1}$$

The vector ∇Y_i is the velocity of an ideal flow past the airfoil that has unit speed in the i-direction at large distances from the airfoil. It is singular (or very large) at the edges of the airfoil. These singularities have the following significance: when the vorticity length scale is small compared to the airfoil chord the principal contribution to the integral is from vorticity in the neighbourhoods of the singularities. For example, for the strip airfoil of Figure 2.6.5

$$Y_2 = \mathrm{Re}\Big(- i\sqrt{z^2 - a^2}\Big), \quad z = y_1 + iy_2,$$

and ∇Y_2 becomes infinite at the leading and trailing edges $z = \mp a$. An incident, small scale gust convecting in the y_1-direction in a mean flow at speed U would in practice induce shedding from the trailing edge at $z = a$. When this shedding is ignored the force calculated from (4.9.1) has two principal components, respectively from gust elements near the leading and trailing edges. To calculate the overall force, however, it is necessary to include the contribution from the shed vorticity, which affects the unsteady hydrodynamic flow only near the trailing edge when the length scale (or 'wavelength') of the wake vorticity is small. In the linearised treatment of this classical *airfoil-gust* interaction problem (Sears 1941) the gust and wake vorticity are taken to convect at the *same* mean velocity U, and it is found that the force component produced by the wake is approximately equal and opposite to that generated by the gust at the trailing edge.

The practical consequence of this cancellation can be approximated without calculating any details of the shed vorticity. This is accomplished by formally deleting the trailing edge singularity from ∇Y_2, and then ignoring the contribution to the integral (4.9.1) from the shed vorticity. To understand this observe that, because the value of the integral is dominated by vorticity near the edges, it is only the behaviours of Y_2 near these edges that must be retained in the integrand, and Y_2 can therefore be replaced by the leading order terms in its expansions about the edges. For the strip airfoil of Figure 2.6.5 we would write

$$Y_2 = \mathrm{Re}\Big(- i\sqrt{z-a}\sqrt{z+a}\Big) \sim \mathrm{Re}\Big(\sqrt{2a}\sqrt{z+a}\Big) + \mathrm{Re}\Big(- i\sqrt{2a}\sqrt{z-a}\Big). \tag{4.9.2}$$

Downloaded from https://www.cambridge.org/core. Charité Universitätsmedizin Berlin, on 20 Dec 2021 at 10:08:47, subject to the Cambridge Core terms of use, available at https://www.cambridge.org/core/terms. https://doi.org/10.1017/CBO9781107360273.005

The last term is singular at the trailing edge; it is deleted and the following approximation is used in (4.9.1) with the wake vorticity ignored:

$$Y_2 \sim \mathrm{Re}\Big(\sqrt{2a}\sqrt{z+a}\Big), \tag{4.9.3}$$

where the branch cut for $\sqrt{z+a}$ is taken along the real axis from $z = -a$ to $z = +\infty$.

4.9.1 Blade-vortex interaction noise in two dimensions

To illustrate the procedure, consider a line vortex of strength Γ parallel to the strip-airfoil occupying $-a < x_1 < a,\ x_2 = 0$ in the presence of a uniform mean stream at speed U in the positive x_1 direction. The vortex is assumed to convect past the airfoil at the mean flow velocity at a constant distance h above the airfoil (Figure 4.9.1). This is the approximation of linearised 'thin airfoil theory', which is applicable when $\Gamma/h \ll U$, i.e. when the influence on the vortex trajectory of the induced velocity ($\sim \Gamma/h$) of 'image' vortices in the body of the airfoil is negligible. As the vortex passes the airfoil new vorticity is shed from the trailing edge into the airfoil wake, which is assumed to consist of a vortex sheet stretching along the x_1-axis from $x_1 = a$ to $x_1 = +\infty$.

Suppose that the vortex passes above the midchord of the airfoil at time $t = 0$, and let us first examine sound generation during 'potential flow interaction' between the vortex and airfoil, when wake vorticity is ignored. Then

$$\boldsymbol{\omega} = \Gamma\mathbf{k}\delta(x_1 - Ut)\delta(x_2 - h), \quad \mathbf{v} = U\mathbf{i}$$
$$\therefore \quad \boldsymbol{\omega} \wedge \mathbf{v} = \Gamma U\mathbf{j}\delta(x_1 - Ut)\delta(x_2 - h), \tag{4.9.4}$$

where $\mathbf{i}$ and $\mathbf{j}$ are unit vectors in the x_1 and x_2 directions. The acoustic pressure is given by (4.8.6) with

$$Y_1 = y_1, \quad Y_2 = \mathrm{Re}\Big(-i\sqrt{z^2 - a^2}\Big), \quad z = y_1 + iy_2.$$

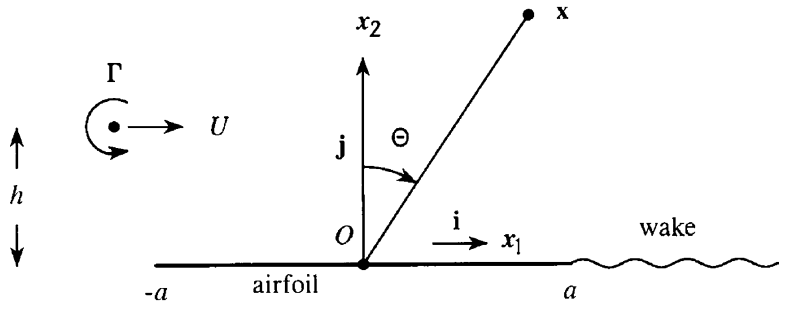

Figure 4.9.1

Downloaded from https://www.cambridge.org/core. Charité Universitätsmedizin Berlin, on 20 Dec 2021 at 10:08:47, subject to the Cambridge Core terms of use, available at https://www.cambridge.org/core/terms. https://doi.org/10.1017/CBO9781107360273.005

Thus, $\nabla Y_1 = \mathbf{i}$ and $\boldsymbol{\omega} \wedge \mathbf{v} \cdot \nabla Y_1 \equiv 0$, and (4.8.6) reduces to

$$p(\mathbf{x}, t) \approx \frac{-\rho_o \Gamma U x_2}{2\pi\sqrt{2c_o}|\mathbf{x}|^{\frac{3}{2}}} \frac{\partial}{\partial t} \int_{-\infty}^{t-|\mathbf{x}|/c_o} \frac{\partial Y_2}{\partial y_2}(U\tau, h) \frac{d\tau}{\sqrt{t-\tau-|\mathbf{x}|/c_o}},$$
$$= \frac{-\rho_o \Gamma U \cos\Theta}{2\pi\sqrt{2c_o}|\mathbf{x}|^{\frac{1}{2}}} \frac{\partial}{\partial t} \int_{-\infty}^{t-|\mathbf{x}|/c_o} \frac{\partial Y_2}{\partial y_2}(U\tau, h) \frac{d\tau}{\sqrt{t-\tau-|\mathbf{x}|/c_o}},$$
$$|\mathbf{x}| \to \infty, \tag{4.9.5}$$

where $\Theta = \cos^{-1}(x_2/|\mathbf{x}|)$ is the angle between the radiation direction $\mathbf{x}$ and the normal to the airfoil (the x_2 axis). The sound can be attributed to a dipole source orientated in the x_2 direction.

The radiation produced when a vortex passes very close to the airfoil (so that $h \ll a$) is likely to be particularly intense. The dominant interactions occur as the vortex passes the edges, where the time scales of the motions $\sim h/U$. Thus, the characteristic frequency

$$\omega \sim \frac{U}{h} \quad \text{and the reduced frequency} \quad \frac{\omega a}{U} \sim \frac{a}{h} \gg 1.$$

We may therefore regard the leading and trailing edges as independent sources of sound, and calculate their individual contributions by using the local approximation (4.9.2). For the acoustic pressure p_{LE}, say, produced at the leading edge ($x_1 = -a$) we take

$$Y_2 \sim \mathrm{Re}\left(\sqrt{2a}\sqrt{z+a}\right),$$

so that (4.9.5) becomes

$$p_{\mathrm{LE}} \approx \frac{-\rho_o \Gamma U \cos\Theta}{2\pi\sqrt{2c_o}|\mathbf{x}|^{\frac{1}{2}}}$$
$$\times \frac{\partial}{\partial t} \int_{-\infty}^{t-|\mathbf{x}|/c_o} \mathrm{Re}\left(\frac{i\sqrt{2a}}{2(U\tau + ih + a)^{\frac{1}{2}}}\right) \frac{d\tau}{\sqrt{t-\tau-|\mathbf{x}|/c_o}}, \quad |\mathbf{x}| \to \infty.$$

To evaluate the integral, make the substitution $\mu = \sqrt{t-\tau-|\mathbf{x}|/c_o}$ and perform the differentiation with respect to time. Then

$$p_{\mathrm{LE}} \approx \frac{-\rho_o \Gamma U \cos\Theta}{2\pi\sqrt{c_o}} \left(\frac{a}{|\mathbf{x}|}\right)^{\frac{1}{2}} \frac{\partial}{\partial t} \int_0^\infty \mathrm{Re}\left[\frac{i}{(U[t] + ih + a - U\mu^2)^{\frac{1}{2}}}\right] d\mu$$
$$= \frac{\rho_o \Gamma U^2 \cos\Theta}{4\pi\sqrt{c_o}} \left(\frac{a}{|\mathbf{x}|}\right)^{\frac{1}{2}} \int_0^\infty \mathrm{Re}\left[\frac{i}{(U[t] + ih + a - U\mu^2)^{\frac{3}{2}}}\right] d\mu,$$
$$\text{where } [t] = t - \frac{|\mathbf{x}|}{c_o}.$$

Downloaded from https://www.cambridge.org/core. Charité Universitätsmedizin Berlin, on 20 Dec 2021 at 10:08:47, subject to the Cambridge Core terms of use, available at https://www.cambridge.org/core/terms. https://doi.org/10.1017/CBO9781107360273.005

The additional substitution $\mu = 1/\xi$ transforms the integrand into an exact differential, leading finally to

$$p_{\mathrm{LE}} \approx \frac{\rho_o \Gamma U^2 \cos\Theta}{4\pi\sqrt{c_o}} \left(\frac{a}{|\mathbf{x}|}\right)^{\frac{1}{2}} \int_0^\infty \mathrm{Re}\left[\frac{i\xi}{[(U[t]+ih+a)\xi^2 - U]^{\frac{3}{2}}}\right] d\xi$$

$$= \frac{\rho_o \Gamma U\sqrt{M}\cos\Theta}{4\pi a}\left(\frac{a}{|\mathbf{x}|}\right)^{\frac{1}{2}} \frac{\left(\frac{U[t]}{a}+1\right)}{\left(\frac{U[t]}{a}+1\right)^2 + \left(\frac{h}{a}\right)^2}, \quad |\mathbf{x}| \to \infty, \tag{4.9.6}$$

where $M = U/c_o$.

The non-dimensional pressure signature

$$p_{\mathrm{LE}} \Big/ \frac{\rho_o \Gamma U\sqrt{M}\cos\Theta}{4\pi a}\left(\frac{a}{|\mathbf{x}|}\right)^{\frac{1}{2}} \tag{4.9.7}$$

is plotted in Figure 4.9.2 as the solid curve when $h/a = 0.2$. The pressure field is generated predominantly as the vortex passes the leading edge of the airfoil at the retarded time $[t] = -a/U$, with characteristic frequency $\omega \sim U/h$. At high reduced frequencies the sound pressure p_{TE}, say, generated by the potential flow interaction of the vortex with the trailing edge is effectively cancelled by that produced by the wake vorticity; the solid curve in Figure 4.9.2 should therefore be representative of the whole of the radiation produced by the blade-vortex interaction.

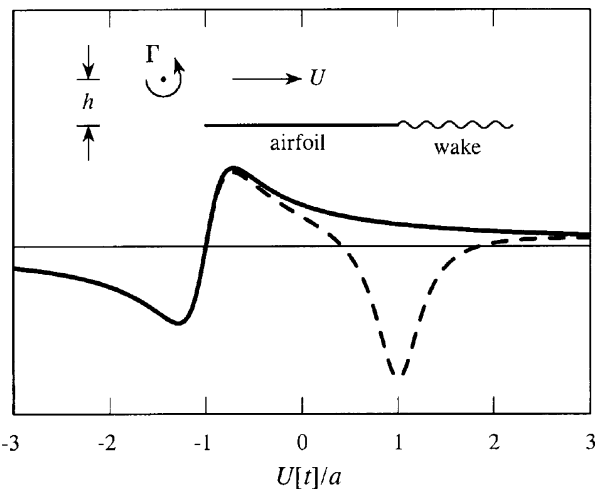

Figure 4.9.2

Downloaded from https://www.cambridge.org/core. Charité Universitätsmedizin Berlin, on 20 Dec 2021 at 10:08:47, subject to the Cambridge Core terms of use, available at https://www.cambridge.org/core/terms. https://doi.org/10.1017/CBO9781107360273.005

To determine $p_{\rm TE}$ the calculation above for $p_{\rm LE}$ is repeated after setting

$$Y_2 = {\rm Re}\Big(- i\sqrt{2a}\sqrt{z-a}\Big)$$

in (4.9.5), leading to

$$\begin{aligned} p_{\rm TE} &\approx \frac{-\rho_o \Gamma U \cos\Theta}{4\pi\sqrt{c_o}} \left(\frac{a}{|\mathbf{x}|}\right)^{\frac{1}{2}} \\ &\quad \times \frac{\partial}{\partial t} \int_{-\infty}^{t-|\mathbf{x}|/c_o} {\rm Re}\left(\frac{1}{(U\tau + ih - a)^{\frac{1}{2}}}\right) \frac{d\tau}{\sqrt{t-\tau-|\mathbf{x}|/c_o}} \\ &= \frac{-\rho_o \Gamma U \sqrt{M}\cos\Theta}{4\pi a} \left(\frac{a}{|\mathbf{x}|}\right)^{\frac{1}{2}} \frac{\left(\frac{h}{a}\right)}{\left(\frac{U[t]}{a}-1\right)^2 + \left(\frac{h}{a}\right)^2}, \ |\mathbf{x}| \to \infty. \quad (4.9.8) \end{aligned}$$

This is large at the retarded times during which the vortex is close to the trailing edge. Thus, when the contribution from the wake is ignored (which is approximately equal and opposite to $p_{\rm TE}$) the overall acoustic pressure signature is given non-dimensionally by

$$(p_{\rm LE} + p_{\rm TE}) \Big/ \frac{\rho_o \Gamma U \sqrt{M}\cos\Theta}{4\pi a} \left(\frac{a}{|\mathbf{x}|}\right)^{\frac{1}{2}},$$

which is plotted as the broken line curve in Figure 4.9.2.

The leading and trailing edge generated components $p_{\rm LE}$ and $p_{\rm TE}$ have different waveforms, even though they are produced by the vortex interacting with geometrically identical airfoil edges. This is because the integral in (4.9.5) determines the acoustic pressure at the retarded time $[t]$ in terms of interactions between the vortex and the airfoil *at all earlier retarded times*; it is a further consequence of the two-dimensional character of the acoustic sources, according to which, after the first arrival of sound from the nearest point on the source, additional contributions to the sound continue to be received *indefinitely in time* from more distant 'spanwise' parts of the source.

4.9.2 Comparison with airfoil-gust interaction theory: Kutta condition

The acoustic pressure $p \simeq p_{\rm LE}$ produced as the vortex convects over the airfoil is plotted in non-dimensional form

$$p \Big/ \frac{\rho_o \Gamma U \sqrt{M}\cos\Theta}{4\pi a} \left(\frac{a}{|\mathbf{x}|}\right)^{\frac{1}{2}}$$

as the solid curves in Figure 4.9.3 for $h/a = 0.2,\ 0.5,\ 1.0$. The approximation (obtained by deleting the trailing edge singularity from Green's function and ignoring the shed vorticity) is expected to be applicable provided $h \ll a$, when

Downloaded from https://www.cambridge.org/core. Charité Universitätsmedizin Berlin, on 20 Dec 2021 at 10:08:47, subject to the Cambridge Core terms of use, available at https://www.cambridge.org/core/terms. https://doi.org/10.1017/CBO9781107360273.005

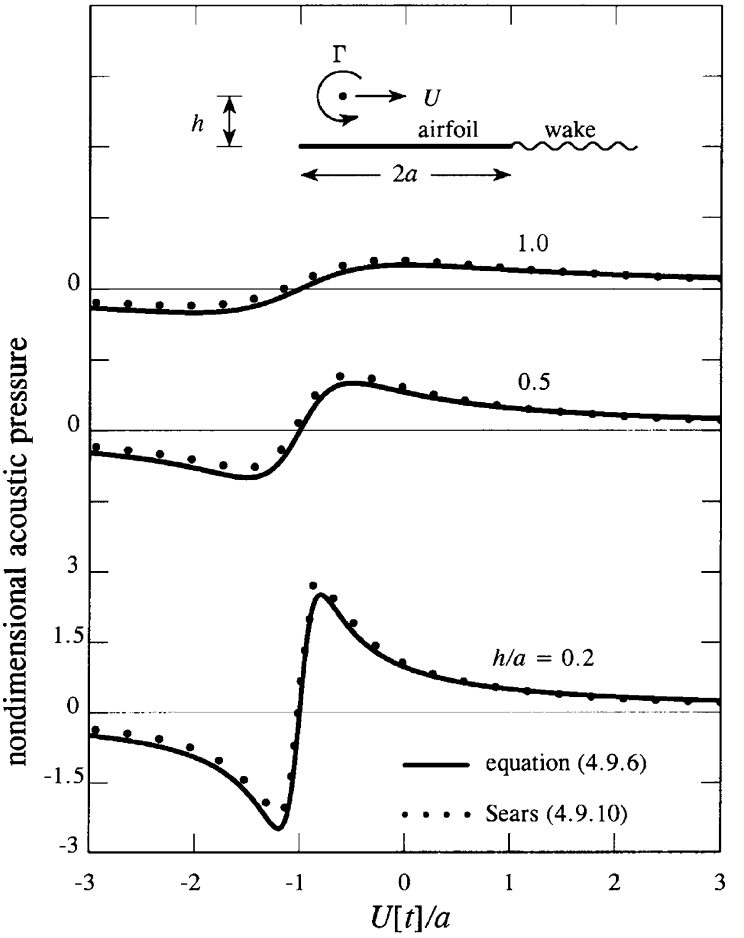

Figure 4.9.3

the contribution to the sound from vortex shedding at the trailing edge roughly cancels the trailing edge (potential flow) component p_{TE} (4.9.8).

According to equation (4.8.7) the radiation can also be expressed in terms of the unsteady force exerted on the fluid by the airfoil during the passage of the vortex. Only the component F_2 is non-zero in the linearised approximation, and the method of calculating this for incompressible flow was developed by Sears (1941) who determined the strength of vorticity shed into a vortex sheet wake by application of the *Kutta* condition that the unsteady velocity at the edge should remain finite. The result was expressed in terms of the *Sears* function $\mathcal{S}(x)$:

$$\mathcal{S}(x) = \frac{2}{\pi x \left[\mathrm{H}_0^{(1)}(x) + i\mathrm{H}_1^{(1)}(x) \right]}. \tag{4.9.9}$$

Downloaded from https://www.cambridge.org/core. Charité Universitätsmedizin Berlin, on 20 Dec 2021 at 10:08:47, subject to the Cambridge Core terms of use, available at https://www.cambridge.org/core/terms. https://doi.org/10.1017/CBO9781107360273.005

where $H_0^{(1)}$, $H_1^{(1)}$ are Hankel functions.

Sear's theory leads to the following representation of the acoustic pressure

$$\frac{p(\mathbf{x},t)}{\rho_o \Gamma U\sqrt{M}\cos\Theta(a/|\mathbf{x}|)^{\frac{1}{2}}/4\pi a} \approx \sqrt{2\pi}\,\mathrm{Re}\int_0^\infty (ik)^{\frac{1}{2}}\mathcal{S}(k)\mathrm{e}^{-k\{h/a+iU[t]/a\}}dk, \quad |\mathbf{x}|\to\infty. \tag{4.9.10}$$

This is plotted as the dotted curves in Figure 4.9.3. The agreement with the approximate theory of equation (4.9.6) is remarkably good even when h/a is as large as unity, when the characteristic reduced frequency $k = \omega a/U$ of the motion is relatively small, and might be expected to lie outside the range for which (4.9.6) is valid.

4.10 Linear theory of vortex-airfoil interaction noise

Consider an inhomogeneous field of vorticity, a 'gust', convected in high Reynolds number, homentropic flow past a stationary rigid airfoil (Figure 4.10.1). The undisturbed flow has speed U in the x_1 direction, where the origin is at a convenient point within the airfoil, with x_3 along the span and x_2 vertically 'upwards'. The Mach number $M = U/c_o$ is sufficiently small that convection of sound by the flow can be ignored and the airfoil chord can be assumed to be acoustically compact.

The vortex sound source $\mathrm{div}(\boldsymbol{\omega}\wedge\mathbf{v})$ includes vorticity in the gust together with any vorticity shed from the airfoil, either in response to excitation by the gust, or as 'tip' vortices responsible for the mean lift. The problem can

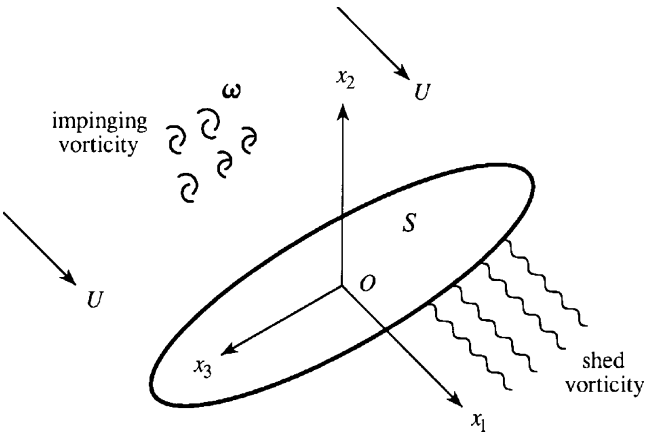

Figure 4.10.1

Downloaded from https://www.cambridge.org/core. Charité Universitätsmedizin Berlin, on 20 Dec 2021 at 10:08:47, subject to the Cambridge Core terms of use, available at https://www.cambridge.org/core/terms. https://doi.org/10.1017/CBO9781107360273.005

be linearised by assuming that $u \ll U$, where curl $\mathbf{u} = \boldsymbol{\omega}$, i.e. by requiring the gust-induced velocity, and the perturbation velocities caused by airfoil thickness, twist, camber, and the angle of attack, to be small. When $\mathrm{div}(\boldsymbol{\omega} \wedge \mathbf{v})$ is expanded about the undisturbed mean flow, only the gust vorticity and additional vorticity shed when the gust encounters the airfoil contribute to the acoustic radiation to first order. That is, airfoil thickness, twist, camber and angle of attack may be ignored, and the airfoil regarded as a rigid lamina in the plane $x_2 = 0$. In this approximation quadrupoles are neglected and vorticity convects as a *frozen* pattern of vortex filaments at the undisturbed mean stream velocity $\mathbf{U} = (U, 0, 0)$. In particular, the wake vorticity is confined to a vortex sheet downstream of the trailing edge.

When convection of sound by the flow is neglected, the linearised form of the vortex sound equation (4.6.6) becomes

$$\left(\frac{1}{c_o^2}\frac{\partial^2}{\partial t^2} - \nabla^2\right) B = \mathrm{div}(\boldsymbol{\omega} \wedge \mathbf{U}), \tag{4.10.1}$$

with solution

$$B(\mathbf{x}, t) = \frac{p(\mathbf{x}, t)}{\rho_o} \approx -\int (\boldsymbol{\omega} \wedge \mathbf{U})(\mathbf{y}, \tau) \cdot \frac{\partial G}{\partial \mathbf{y}}(\mathbf{x}, \mathbf{y}, t - \tau) d^3\mathbf{y} d\tau, \quad |\mathbf{x}| \to \infty, \tag{4.10.2}$$

where $\partial G/\partial y_2 = 0$ on both sides ($y_2 = \pm 0$) of the projection of the airfoil planform onto the $y_1 y_3$-plane. At sufficiently small Mach numbers G may be approximated by the Green's function for an airfoil of compact chord.

The sound produced when a localised, high Reynolds number *frozen* gust $\boldsymbol{\omega}(\mathbf{x} - \mathbf{U}t) \equiv \boldsymbol{\omega}(x_1 - Ut, x_2, x_3)$ is swept past the airfoil of Figure 4.10.1 is therefore given by (4.8.5) with the convection velocity $\mathbf{v}$ replaced by $\mathbf{U}$, and the Kirchhoff vector $\mathbf{Y}$ by

$$Y_1 = y_1, \; Y_2 = y_2 - \varphi_2^*(\mathbf{y}), \; Y_3 = y_3.$$

Thus, because $\int \boldsymbol{\omega} d^3\mathbf{y} \equiv \mathbf{0}$, equation (4.8.5) reduces to

$$p(\mathbf{x}, t) \approx \frac{-\rho_o U \cos\Theta}{4\pi c_o |\mathbf{x}|} \frac{\partial}{\partial t} \int \left[\omega_3 \frac{\partial Y_2}{\partial y_2} - \omega_2 \frac{\partial Y_2}{\partial y_3}\right]_{t - |\mathbf{x}|/c_o} d^3\mathbf{y}, \quad |\mathbf{x}| \to \infty, \tag{4.10.3}$$

where $\Theta = \cos^{-1}(x_2/|\mathbf{x}|)$ is the angle between the radiation direction and the normal to the airfoil, and the origin is taken in the airfoil within the interaction region.

Let the interaction occur at an inboard location where the chord may be regarded as constant, with both the leading and trailing edges at right angles to the mean flow (so that $\partial Y_2/\partial y_3 \ll \partial Y_2/\partial y_2$). The planform in the interaction

Downloaded from https://www.cambridge.org/core. Charité Universitätsmedizin Berlin, on 20 Dec 2021 at 10:08:47, subject to the Cambridge Core terms of use, available at https://www.cambridge.org/core/terms. https://doi.org/10.1017/CBO9781107360273.005

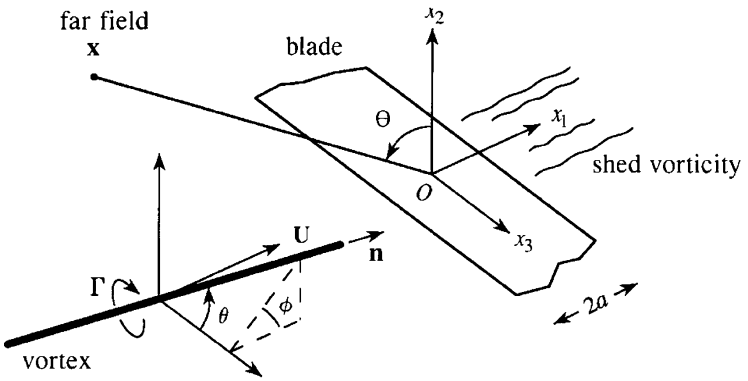

Figure 4.10.2

region is then locally the same as that of the two-dimensional airfoil of Figure 4.10.2, and Y_2 can be approximated as in Table 2.9.1, with $2a$ equal to the local chord of the airfoil. Then (4.10.3) becomes

$$p(\mathbf{x},t) \approx \frac{-\rho_o U\cos\Theta}{4\pi c_o|\mathbf{x}|}\frac{\partial}{\partial t}\int\left[\omega_3\frac{\partial Y_2}{\partial y_2}\right]_{t-|\mathbf{x}|/c_o} d^3\mathbf{y}, \quad |\mathbf{x}|\to\infty, \qquad (4.10.4)$$

which reveals that only the spanwise component of vorticity contributes to the production of sound.

According to equation (4.8.4) (in which we put $dU_j/dt = 0$), this result can also be expressed in the form

$$p(\mathbf{x},t) \approx \frac{\cos\Theta}{4\pi c_o|\mathbf{x}|}\frac{\partial F_2}{\partial t}\left(t-\frac{|\mathbf{x}|}{c_o}\right), \quad |\mathbf{x}|\to\infty,$$
$$F_2(t) = -\rho_o U\int\omega_3(\mathbf{y},t)\frac{\partial Y_2}{\partial y_2}(\mathbf{y})d^3\mathbf{y}, \qquad (4.10.5)$$

where $-F_2$ is the unsteady airfoil *lift* during the interaction when the motion is regarded as incompressible, and the vorticity ω_3 includes contributions from the impinging gust together with any shed into the vortex sheet wake.

4.10.1 Blade-vortex interactions in three dimensions

The calculations can be performed explicitly for a gust in the form of a rectilinear *line vortex*. Let the vortex have circulation Γ and be orientated with its axis in the direction of the unit vector $\mathbf{n}$, as indicated in Figure 4.10.2. The mean flow speed is sufficiently large that the vortex can be assumed to maintain its rectilinear form after being cut by the leading edge of the airfoil. Choose the origin on the airfoil midchord such that the axis of the vortex passes through

Downloaded from https://www.cambridge.org/core. Charité Universitätsmedizin Berlin, on 20 Dec 2021 at 10:08:47, subject to the Cambridge Core terms of use, available at https://www.cambridge.org/core/terms. https://doi.org/10.1017/CBO9781107360273.005

the origin at time $t = 0$. Any point $\mathbf{x}$ on the vortex can then be represented in the parametric form

$$\mathbf{x} = (Ut, 0, 0) + s\mathbf{n}, \quad -\infty < s < \infty, \tag{4.10.6}$$

where s is distance measured along the vortex from its point of intersection with the plane of the airfoil. Then, if $\mathbf{s}_\perp$ denotes vector distance measured in the normal direction from the vortex axis, we can put $\boldsymbol{\omega} = \Gamma\mathbf{n}\delta(\mathbf{s}_\perp)$, where the polar angles $\theta,\ \phi$ in Figure 4.10.2 define the orientation of the unit vector

$$\mathbf{n} = (\sin\theta\cos\phi, \sin\theta\sin\phi, \cos\theta), \quad 0 < \theta < \pi,\ 0 < \phi < 2\pi.$$

Because of vortex shedding from the trailing edge, most of the sound is generated when the vortex is cut by the leading edge. The influence of the shed vorticity can be formally included by the procedure described in §4.9, by expanding Y_2 about its singularity at the leading edge, that is, by setting

$$Y_2 \sim \mathrm{Re}\left(\sqrt{2a}\sqrt{z+a}\right), \quad z = y_1 + iy_2,$$

with the branch cut for the square root taken along the z-axis from $z = -a$ to $z = +\infty$. Thus, by recalling the relation (4.10.6), equation (4.10.4) becomes

$$p(\mathbf{x}, t) \approx \frac{-n_3\rho_o\Gamma U\cos\Theta}{4\pi c_o|\mathbf{x}|}\frac{\partial}{\partial t}\mathrm{Re}\int\left[\delta(\mathbf{s}_\perp)\left(\frac{i\sqrt{2a}}{2\sqrt{y_1+iy_2+a}}\right)\right]_{t-|\mathbf{x}|/c_o} d^2\mathbf{s}_\perp ds$$

$$= \frac{-n_3\rho_o\Gamma U\cos\Theta}{4\sqrt{2}\pi c_o|\mathbf{x}|}\frac{\partial}{\partial t}\mathrm{Re}\int_{-\infty}^{\infty}\left(\frac{i\sqrt{a}}{\sqrt{U[t]+s(n_1+in_2)+a}}\right)ds$$

$$= \frac{n_3\rho_o\Gamma U^2\cos\Theta}{8\sqrt{2}\pi c_o|\mathbf{x}|}\mathrm{Re}\int_{-\infty}^{\infty}\left(\frac{i\sqrt{a}}{(U[t]+s(n_1+in_2)+a)^{\frac{3}{2}}}\right)ds$$

$$= \frac{-n_3\rho_o\Gamma U^2\cos\Theta}{4\sqrt{2}\pi c_o|\mathbf{x}|}\mathrm{Re}\left[\frac{i\sqrt{a}}{(U[t]+s(n_1+in_2)+a)^{\frac{1}{2}}(n_1+in_2)}\right]_{-\infty}^{\infty}, \tag{4.10.7}$$

where $[t] = t - |\mathbf{x}|/c_o$ is the retarded time.

By referring to Figure 4.10.3 it will be seen that the last line of (4.10.7) is zero when

$$U[t] + a < 0,$$

before the vortex is cut by the leading edge of the airfoil. At later times the integration along the vortex axis over the infinite range $-\infty < s < \infty$ must be

Downloaded from https://www.cambridge.org/core. Charité Universitätsmedizin Berlin, on 20 Dec 2021 at 10:08:47, subject to the Cambridge Core terms of use, available at https://www.cambridge.org/core/terms. https://doi.org/10.1017/CBO9781107360273.005

split, as indicated in the figure, into the two parts $-\infty < s < -0,\ +0 < s < \infty$, because the square root in the denominator of the last line of (4.10.7) is

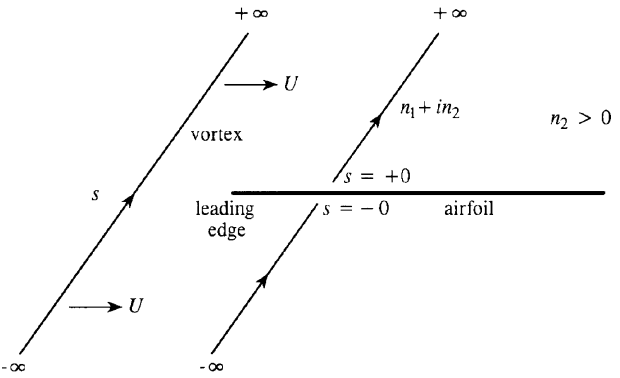

Figure 4.10.3

discontinuous across the airfoil; for example, when $n_2 > 0$ the square root is real and positive on the upper surface ($s = +0$) and real and negative at $s = -0$. Hence, the acoustic pressure becomes

$$p(\mathbf{x}, t) \approx \frac{\rho_o \Gamma U M \cos\Theta}{2^{\frac{3}{2}}\pi |\mathbf{x}|} \frac{|\sin\phi|}{\tan\theta} \frac{\mathrm{H}\left(\frac{U[t]}{a} + 1\right)}{\sqrt{\frac{U[t]}{a} + 1}}. \tag{4.10.8}$$

The pressure pulse accordingly begins with a singular peak at the instant at which the vortex is severed by the leading edge of the airfoil at the retarded time $U[t]/a = -1$. The waveform is illustrated by the dotted curve in Figure 4.10.4, which is a plot of

$$\frac{p(\mathbf{x}, t)}{(\rho_o \Gamma U M \cos\Theta/|\mathbf{x}|)} = \frac{|\sin\phi|}{2^{\frac{3}{2}}\pi \tan\theta} \frac{\mathrm{H}\left(\frac{U[t]}{a} + 1\right)}{\sqrt{\frac{U[t]}{a} + 1}} \quad \text{for } \theta = 85^\circ,\ \phi = 90^\circ.$$

The infinite singularity in the pressure is absent for a vortex of non-zero core radius R, say. If, for example, the vorticity is assumed to be distributed according to the Gaussian formula

$$\boldsymbol{\omega}(\mathbf{x}) = \frac{\Gamma \mathbf{n} e^{-(s_\perp/R)^2}}{\pi R^2},$$

as a function of distance $s_\perp$ from the vortex axis, the acoustic pressure is found to be given by (Howe 1998)

Downloaded from https://www.cambridge.org/core. Charité Universitätsmedizin Berlin, on 20 Dec 2021 at 10:08:47, subject to the Cambridge Core terms of use, available at https://www.cambridge.org/core/terms. https://doi.org/10.1017/CBO9781107360273.005

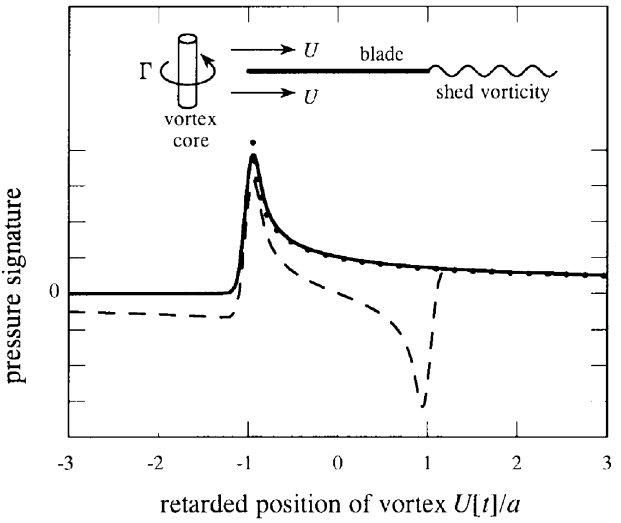

Figure 4.10.4

$$\frac{p(\mathbf{x},t)}{(\rho_o \Gamma U M \cos\Theta/|\mathbf{x}|)} \approx \frac{|\sin\phi|^{\frac{3}{2}}}{8\tan\theta}\left(\frac{a}{\pi R}\right)^{\frac{1}{2}} \Im(\alpha)\,, \quad |\mathbf{x}| \to \infty, \text{ for } R \ll a, \tag{4.10.9}$$

where

$$\Im(\alpha) = |\alpha|^{\frac{1}{2}}\left\{\mathrm{I}_{-\frac{1}{4}}\left(\frac{\alpha^2}{8}\right) + \mathrm{sgn}(\alpha)\mathrm{I}_{\frac{1}{4}}\left(\frac{\alpha^2}{8}\right)\right\}\mathrm{e}^{-\alpha^2/8}, \quad \alpha = \frac{2a|\sin\phi|}{R\left(\frac{U[t]}{a}+1\right)},$$

and $\mathrm{I}_{\pm\frac{1}{4}}$ are modified Bessel functions of the first kind. The pressure signature predicted by (4.10.9) for

$$R = 0.1a,\ \theta = 85^\circ,\ \phi = 90^\circ,$$

is plotted as the solid curve in Figure 4.10.4, and differs negligibly from the line vortex prediction when $U[t]/a > -1$.

The broken-line curve in Figure 4.10.4 represents the pressure signature produced by the *potential flow* interaction between the finite core vortex and airfoil (i.e. when vortex shedding is ignored). It is an odd function of the retarded time [t]. The large negative peak produced as the vortex crosses the trailing edge (at $U[t]/a = 1$) is cancelled by an equal and opposite contribution generated by the wake. The reader can easily show that, when the finite size of the vortex core is ignored, the potential flow, trailing edge generated pressure pulse is given by

$$p(\mathbf{x},t) \approx -\frac{\rho_o \Gamma U M \cos\Theta}{2^{\frac{3}{2}}\pi|\mathbf{x}|}\frac{|\sin\phi|}{\tan\theta}\frac{\mathrm{H}\left(1-\frac{U[t]}{a}\right)}{\sqrt{\frac{1-U[t]}{a}}}.$$

Downloaded from https://www.cambridge.org/core. Charité Universitätsmedizin Berlin, on 20 Dec 2021 at 10:08:47, subject to the Cambridge Core terms of use, available at https://www.cambridge.org/core/terms. https://doi.org/10.1017/CBO9781107360273.005

4.A Appendix: Surface force in incompressible flow

4.A.1 Surface force expressed in terms of vorticity

The unsteady force $\mathbf{F}(t)$ exerted on an incompressible fluid by the moving body of Figure 4.4.1 can be written

$$F_i = \rho_o \frac{d}{dt} \int_V v_i(\mathbf{x}, t) d^3\mathbf{x} - \oint_\Sigma p(\mathbf{x}, t) n_i dS. \tag{4.A.1}$$

It is assumed that the surface Σ is sufficiently distant that it contains all of the vorticity. The integrations on the right can be expressed entirely in terms of the vorticity by making use of the following properties of the Kirchhoff vector X_i: $\mathbf{n} \cdot \nabla X_i = 0$ on S, $\nabla^2 X_i = 0$ in V, to express the component F_i of the force in the form

$$\begin{aligned} F_i = &-\frac{d}{dt} \oint_S \rho_o \varphi_i^* \mathbf{v} \cdot d\mathbf{S} - \oint_S \rho_o \frac{DX_i}{Dt} \mathbf{v} \cdot d\mathbf{S} \\ &-\rho_o \int_V \nabla X_i \cdot \boldsymbol{\omega} \wedge \mathbf{v} \, d^3\mathbf{x} + \eta \oint_S \boldsymbol{\omega} \wedge \nabla X_i \cdot d\mathbf{S}. \end{aligned} \tag{4.A.2}$$

To do this take the divergence of Crocco's equation (4.4.3) (wherein $B = p/\rho_o + \frac{1}{2}v^2$) and consider the pair of equations

$$\nabla^2 \left(p + \tfrac{1}{2}\rho_o v^2 \right) = -\text{div}\,(\rho_o \boldsymbol{\omega} \wedge \mathbf{v}) \tag{4.A.3}$$

$$\nabla^2 X_i = 0. \tag{4.A.4}$$

Multiply these equations respectively by X_i and $(p + \frac{1}{2}\rho_o v^2)$ and apply Green's theorem to obtain

$$\begin{aligned} \oint_{S+\Sigma} \left\{ X_i \left[\nabla \left(p + \tfrac{1}{2}\rho_o v^2 \right) + \rho_o \boldsymbol{\omega} \wedge \mathbf{v} \right] - \left(p + \tfrac{1}{2}\rho_o v^2 \right) \nabla X_i \right\} \cdot d\mathbf{S} \\ = -\rho_o \int_V \nabla X_i \cdot \boldsymbol{\omega} \wedge \mathbf{v} \, d^3\mathbf{x}. \end{aligned} \tag{4.A.5}$$

This is simplified as follows.

Using Crocco's equation (4.4.3), the first term in the brace brackets on the left yields

$$\begin{aligned} &\oint_{S+\Sigma} X_i \left[\nabla \left(p + \tfrac{1}{2}\rho_o v^2 \right) + \rho_o \boldsymbol{\omega} \wedge \mathbf{v} \right] \cdot d\mathbf{S} \\ &= -\oint_{S+\Sigma} X_i \left(\rho_o \frac{\partial \mathbf{v}}{\partial t} + \eta \text{curl}\, \boldsymbol{\omega} \right) \cdot d\mathbf{S} \\ &= -\oint_{S+\Sigma} X_i \rho_o \frac{\partial \mathbf{v}}{\partial t} \cdot d\mathbf{S} - \eta \oint_S \boldsymbol{\omega} \wedge \nabla X_i \cdot d\mathbf{S}, \end{aligned} \tag{4.A.6}$$

Downloaded from https://www.cambridge.org/core. Charité Universitätsmedizin Berlin, on 20 Dec 2021 at 10:08:47, subject to the Cambridge Core terms of use, available at https://www.cambridge.org/core/terms. https://doi.org/10.1017/CBO9781107360273.005

because $X_i \operatorname{curl} \boldsymbol{\omega} = \operatorname{curl}(X_i \boldsymbol{\omega}) + \boldsymbol{\omega} \wedge \nabla X_i$, and $\boldsymbol{\omega} = \mathbf{0}$ on Σ. Furthermore,

$$\oint_{S+\Sigma} X_i \rho_o \frac{\partial \mathbf{v}}{\partial t} \cdot d\mathbf{S} = \oint_{S+\Sigma} \frac{\partial}{\partial t}\Big(\rho_o X_i \mathbf{v}\Big) \cdot d\mathbf{S} - \oint_S \rho_o \frac{\partial X_i}{\partial t} \mathbf{v} \cdot d\mathbf{S},$$

and

$$\begin{aligned}
&\oint_{S+\Sigma} \frac{\partial}{\partial t}\Big(\rho_o X_i \mathbf{v}\Big) \cdot d\mathbf{S} \\
&\quad = -\frac{d}{dt} \int_V \operatorname{div}\Big(\rho_o X_i \mathbf{v}\Big) d^3\mathbf{x} - \oint_{S+\Sigma} \operatorname{div}\Big(\rho_o X_i \mathbf{v}\Big) \mathbf{v} \cdot d\mathbf{S} \\
&\quad = -\frac{d}{dt} \int_V \rho_o v_i \, d^3\mathbf{x} - \frac{d}{dt} \oint_S \rho_o \varphi_i^* \mathbf{v} \cdot d\mathbf{S} - \oint_S \rho_o (\mathbf{v} \cdot \nabla X_i) \mathbf{v} \cdot d\mathbf{S}.
\end{aligned}$$

Therefore, (4.A.6) becomes

$$\begin{aligned}
&\oint_{S+\Sigma} X_i \Big[\nabla\Big(p + \tfrac{1}{2}\rho_o v^2\Big) + \rho_o \boldsymbol{\omega} \wedge \mathbf{v}\Big] \cdot d\mathbf{S} \\
&\quad = \frac{d}{dt} \int_V \rho_o v_i \, d^3\mathbf{x} + \frac{d}{dt} \oint_S \rho_o \varphi_i^* \mathbf{v} \cdot d\mathbf{S} + \oint_S \rho_o \frac{DX_i}{Dt} \mathbf{v} \cdot d\mathbf{S} \\
&\qquad\qquad - \eta \oint_S \boldsymbol{\omega} \wedge \nabla X_i \cdot d\mathbf{S}. \qquad (4.A.7)
\end{aligned}$$

The contribution from S of the second term in the brace brackets on the left of (4.A.5) vanishes identically because $\nabla X_i \cdot \mathbf{n} = 0$. On Σ this term supplies $-\oint_\Sigma p n_i dS$, and equation (4.A.2) is finally obtained by inserting this and (4.A.7) into (4.A.5) and using (4.A.1).

4.A.2 Solid body in translational motion

The velocity of a typical point $\mathbf{x}$ within the rigid body of Figure 4.4.1 is

$$\mathbf{U} = \mathbf{U}_o + \boldsymbol{\Omega} \wedge (\mathbf{x} - \mathbf{x}_o(t))$$

where $\mathbf{U}_o = d\mathbf{x}_o/dt$ is the velocity of its centre of volume $\mathbf{x}_o(t)$, and $\boldsymbol{\Omega}(t)$ is its angular velocity. For a body in translational motion $\mathbf{U} = \mathbf{U}_o$ and $\boldsymbol{\Omega} = \mathbf{0}$. Then $\oint_S (DX_i/Dt)\mathbf{v} \cdot d\mathbf{S} \equiv 0$, and the no-slip condition on S and the identity

$$\nabla X_i \cdot \boldsymbol{\omega} \wedge \mathbf{U}_o = \operatorname{div}\Big(\mathbf{U}_o(\mathbf{v} \cdot \nabla X_i) - \mathbf{v}(\mathbf{U}_o \cdot \nabla X_i) - (\mathbf{v} \cdot \mathbf{U}_o)\nabla X_i\Big)$$

imply that $\int_V \nabla X_i \cdot \boldsymbol{\omega} \wedge \mathbf{U}_o \, d^3\mathbf{x} = 0$, so that (4.A.2) reduces to

$$F_i = M_{ij} \frac{dU_{oj}}{dt} - \rho_o \int_V \nabla X_i \cdot \boldsymbol{\omega} \wedge \mathbf{v}_{\text{rel}} \, d^3\mathbf{x} + \eta \oint_S \boldsymbol{\omega} \wedge \nabla X_i \cdot d\mathbf{S}, \quad \mathbf{v}_{\text{rel}} = \mathbf{v} - \mathbf{U}_o, \qquad (4.A.8)$$

Downloaded from https://www.cambridge.org/core. Charité Universitätsmedizin Berlin, on 20 Dec 2021 at 10:08:47, subject to the Cambridge Core terms of use, available at https://www.cambridge.org/core/terms. https://doi.org/10.1017/CBO9781107360273.005

where $\mathbf{v}_{\text{rel}}$ is the fluid velocity relative to the translational velocity of S, and we have used the definition $M_{ij} = M_{ji} = -\rho_o \oint_S n_j \varphi_i^* dS$ of the added mass coefficient.

The first term on the right of (4.A.8) represents the *inviscid* component of the surface force associated with the added mass. The volume integral furnishes the component produced by 'free' vorticity *within* the fluid interacting with the surface; the surface integral represents the net contribution from frictional effects on S. Because $\mathbf{v}_{\text{rel}} = \mathbf{0}$ on S, the contribution to the volume integral from vorticity close to and on S is negligible; even in the inviscid limit there is no contribution to this integral from the surface vortex sheet forming the 'bound vorticity' on S, because ∇X_i and $\boldsymbol{\omega} \wedge \mathbf{v}_{\text{rel}}$ are orthogonal on S.

The contribution from surface friction has two components:

$$\eta \boldsymbol{\omega} \wedge \nabla X_i \cdot d\mathbf{S} = -\eta (\boldsymbol{\omega} \wedge d\mathbf{S})_i + \eta \nabla \varphi_i^* \cdot \boldsymbol{\omega} \wedge d\mathbf{S}.$$

The first term on the right corresponds to the usual surface frictional force, tangential to S, whereas $\eta \oint_S \nabla \varphi_i^* \cdot \boldsymbol{\omega} \wedge d\mathbf{S}$ may be attributed to the normal pressure forces on S produced by the frictional stress. Thus (because $X_i = x_i - \varphi_i^*$) the net contribution of the normal pressure forces on S associated with vorticity is represented in (4.A.8) by the terms

$$-\rho_o \int_V \nabla X_i \cdot \boldsymbol{\omega} \wedge \mathbf{v}_{\text{rel}} d^3\mathbf{x} + \eta \oint_S \nabla \varphi_i^* \cdot \boldsymbol{\omega} \wedge d\mathbf{S}.$$

The viscous component is comparable in magnitude to the skin friction.

4.A.3 Surface force in irrotational flow with sources

Incompressible motion of a uniform, ideal fluid in the absence of vorticity is governed by a velocity potential $\varphi(\mathbf{x}, t)$ satisfying

$$\nabla^2 \varphi = q(\mathbf{x}, t), \tag{4.A.9}$$

where $q(\mathbf{x}, t)$ is a distribution of volume sources. Let the sources be in the neighbourhood of a moving solid boundary S defined by the equation $f(\mathbf{x}, t) = 0$ (with $f \gtrless 0$ according as $\mathbf{x}$ is outside or within S, as in Figure 2.1.2). Then the force $\mathbf{F}(t)$ exerted on the fluid by the body is given by

$$\mathbf{F}(t) = -\rho_o \frac{d}{dt} \oint_S (\mathbf{n}\varphi)(\mathbf{x}, t)\, dS - \rho_o \int_V (q \nabla \varphi)(\mathbf{x}, t)\, d^3\mathbf{x}, \tag{4.A.10}$$

where the surface unit normal $\mathbf{n}$ is directed into the fluid region V.

To prove this we use Bernoulli's equation

$$\frac{\partial \varphi}{\partial t} + \frac{p}{\rho_o} + \tfrac{1}{2}(\nabla \varphi)^2 = 0, \tag{4.A.11}$$

Downloaded from https://www.cambridge.org/core. Charité Universitätsmedizin Berlin, on 20 Dec 2021 at 10:08:47, subject to the Cambridge Core terms of use, available at https://www.cambridge.org/core/terms. https://doi.org/10.1017/CBO9781107360273.005

obtained by integration of the inviscid, irrotational form of Crocco's equation (4.4.3), i.e. of $\nabla\Big(\partial\varphi/\partial t + B\Big) = 0$, subject to the condition that flow perturbations vanish at infinity. The surface $f(\mathbf{x}, t) = 0$ moves with the fluid particles in contact with S, and therefore satisfies

$$\frac{\partial \mathrm{H}}{\partial t} + \frac{\partial \varphi}{\partial x_j}\frac{\partial \mathrm{H}}{\partial x_j} = 0, \quad \text{where} \quad \mathrm{H} \equiv \mathrm{H}(f).$$

Then

$$\begin{aligned}
&-\frac{d}{dt}\oint_{\mathrm{S}} \mathbf{n}\varphi \, d\mathrm{S} \\
&= -\frac{d}{dt}\int_{-\infty}^{\infty} \varphi \nabla \mathrm{H}\, d^3\mathbf{x} = -\int_{-\infty}^{\infty}\left(\frac{\partial \varphi}{\partial t}\nabla \mathrm{H} + \varphi \nabla \frac{\partial \mathrm{H}}{\partial t}\right) d^3\mathbf{x} \\
&= -\oint_{\mathrm{S}} \mathbf{n}\frac{\partial \varphi}{\partial t} d\mathrm{S} - \int_{-\infty}^{\infty}\left\{\nabla\left[\varphi\frac{\partial \mathrm{H}}{\partial t}\right] + \frac{\partial}{\partial x_i}\left[\mathrm{H}\nabla\varphi\frac{\partial \varphi}{\partial x_i}\right]\right. \\
&\qquad\qquad \left. -\nabla\left[\tfrac{1}{2}\mathrm{H}(\nabla\varphi)^2\right] + \tfrac{1}{2}(\nabla\varphi)^2\nabla\mathrm{H} - \mathrm{H}\nabla\varphi\,\nabla^2\varphi\right\} d^3\mathbf{x} \\
&= -\oint_{\mathrm{S}} \mathbf{n}\frac{\partial \varphi}{\partial t} d\mathrm{S} + 0 + 0 + 0 - \int_{-\infty}^{\infty}\left(\tfrac{1}{2}(\nabla\varphi)^2\nabla\mathrm{H} - \mathrm{H}\nabla\varphi\,\nabla^2\varphi\right) d^3\mathbf{x},
\end{aligned}$$

where the '0' terms vanish because $\mathbf{v} = \nabla\varphi$ decreases at least as fast as $1/|\mathbf{x}|^2$ as $|\mathbf{x}| \to \infty$, and because $\partial \mathrm{H}/\partial t$ also vanishes there.

Hence, using equations (4.A.9) and (4.A.11), we find

$$\begin{aligned}
-\frac{d}{dt}\oint_{\mathrm{S}} \mathbf{n}\varphi \, d\mathrm{S} - \int_V \nabla\varphi \, q(\mathbf{x}, t) d^3\mathbf{x} &= -\oint_{\mathrm{S}} \mathbf{n}\left[\frac{\partial \varphi}{\partial t} + \tfrac{1}{2}(\nabla\varphi)^2\right] d\mathrm{S} \\
&= \oint_{\mathrm{S}} \frac{p}{\rho_o}\mathbf{n}\, d\mathrm{S} \equiv \frac{\mathbf{F}}{\rho_o}.
\end{aligned}$$

Problems 4

4.1. In a region of low Mach number, homogeneous turbulent flow the pressure fluctuation $p - p_o$ relative to the background mean pressure $\sim O(\rho_o v^2)$. Use the ideal gas formula $c^2 = \gamma \mathrm{R}T$ and the isentropic relation $c_p dT = dp/\rho \approx dp/\rho_o$ (molecular diffusion of heat being negligible at high Reynolds number) to deduce that

$$p - p_o - c_o^2(\rho - \rho_o) \approx (p - p_o)(1 - c_o^2/c^2) \sim O(\rho_o v^2 M^2), \quad M \sim \frac{v}{c_o}.$$

4.2.* Show that the acoustic efficiency of a compact sphere of radius R executing small amplitude translational oscillations at velocity $U = U_o \sin(\omega t)$ is

Downloaded from https://www.cambridge.org/core. Charité Universitätsmedizin Berlin, on 20 Dec 2021 at 10:08:47, subject to the Cambridge Core terms of use, available at https://www.cambridge.org/core/terms. https://doi.org/10.1017/CBO9781107360273.005

$$\frac{\Pi_a}{\Pi_o} \sim (k_o R)^3, \quad k_o = \frac{\omega}{c_o},$$

where

$$\Pi_a = \frac{\pi \omega R^3}{6} \rho_o U_o^2 (k_o R)^3, \quad \Pi_o = \frac{2\omega R^3}{3} \rho_o U_o^2,$$

are, respectively, the average acoustic and hydrodynamic powers fed into the fluid during the *quarter* cycle $0 < \omega t < \frac{\pi}{2}$.

Explain the significance of averaging only over $0 < \omega t < \frac{\pi}{2}$.

4.3.* What is the efficiency in Problem 4.2 when the sphere pulsates with small amplitude normal velocity $v_n = U_o \sin(\omega t)$?

4.4.* The wake behind a bluff, rigid body fixed in a nominally steady, low Mach number flow at speed U produces a drag force equal to $C_D A \frac{1}{2} \rho_o U^2$, where C_D is the *drag coefficient* (which may be regarded as constant) and A is the projected cross-sectional area of the body in the flow direction. If the body is acoustically compact, derive an approximate formula for the far field acoustic pressure radiated from the body when U contains a small amplitude, time-harmonic component such that $U = U_o + u \cos(\omega t)$, where U_o and u are constant and $u \ll U_o$.

Explain how the formula is modified if the flow produces small amplitude translational vibrations of the body at speed $v(t)$ parallel to the direction of the mean flow.

4.5.* An acoustically compact, rigid sphere of radius a executes small amplitude translational oscillations about the origin in the x_1 direction at speed $U(t)$ in an ideal acoustic medium. Use the formula $\varphi = -a^3 x_1 U(t)/2|\mathbf{x}|^3$ for the potential of the *incompressible* motion produced by the moving sphere and the *linearised* form of Curle's equation (4.3.5), namely

$$\mathrm{H} c_o^2 (\rho - \rho_o) = -\frac{\partial}{\partial x_i} \oint_S \left[p'_{ij} \right] \frac{dS_j(\mathbf{y})}{4\pi |\mathbf{x} - \mathbf{y}|} + \frac{\partial}{\partial t} \oint_S \left[\rho_o v_j \right] \frac{dS_j(\mathbf{y})}{4\pi |\mathbf{x} - \mathbf{y}|},$$

to show that the acoustic pressure in the far field is given by

$$p(\mathbf{x}, t) = \frac{\rho_o a^3 \cos\Theta}{2c_o |\mathbf{x}|} \frac{\partial^2 U}{\partial t^2} \Big(t - |\mathbf{x}|/c_o \Big), \quad \text{where } \cos\Theta = \frac{x_1}{|\mathbf{x}|}.$$

4.6. Show that in inviscid, homentropic flow (where $\operatorname{div} \mathbf{v} \neq 0$) the vorticity equation (4.4.7) takes the form

$$\frac{D}{Dt} \left(\frac{\boldsymbol{\omega}}{\rho} \right) = \left(\frac{\boldsymbol{\omega}}{\rho} \cdot \nabla \right) \mathbf{v}.$$

Downloaded from https://www.cambridge.org/core. Charité Universitätsmedizin Berlin, on 20 Dec 2021 at 10:08:47, subject to the Cambridge Core terms of use, available at https://www.cambridge.org/core/terms. https://doi.org/10.1017/CBO9781107360273.005

4.7.* Let $d\mathbf{S}$ denote a vectororial material surface element in an incompressible fluid. Suppose the point A lies at the centroid of $d\mathbf{S}$, and consider the infinitesimal volume $\mathbf{X} \cdot d\mathbf{S}$ of the inclined cylinder with axis $\mathbf{X}$ starting at A and ending at the neighbouring material point B.
Then

$$\frac{D}{Dt}(\mathbf{X} \cdot d\mathbf{S}) \equiv X_j \frac{D}{Dt}(dS_j) + dS_j \frac{DX_j}{Dt} = 0.$$

It follows by use of equation (4.4.6) that

$$X_j \left(\frac{D}{Dt}(dS_j) + dS_i \frac{\partial v_i}{\partial x_j} \right) = 0,$$

and therefore, because $\mathbf{X}$ is an arbitrary infinitesimal vector, that

$$\frac{D}{Dt}(dS_j) = -dS_i \frac{\partial v_i}{\partial x_j} \quad \text{for an incompressible fluid.}$$

Mass conservation in a compressible fluid implies that $\frac{D}{Dt}(\rho \mathbf{X} \cdot d\mathbf{S}) = 0$. Deduce in this case that

$$\frac{D}{Dt}(dS_j) = dS_j \operatorname{div} \mathbf{v} - dS_i \frac{\partial v_i}{\partial x_j}.$$

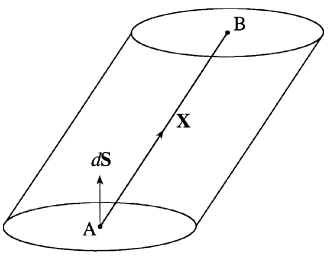

4.8.* Use the result of Question 4.7 to show that $\frac{D}{Dt}(\boldsymbol{\omega} \cdot d\mathbf{S}) = 0$ where $d\mathbf{S}$ is a material surface element in an ideal, compressible fluid. Deduce from this *Kelvin's circulation theorem*

$$\frac{D}{Dt} \oint_C \mathbf{v} \cdot d\mathbf{x} = 0,$$

where the integration is around a closed material contour C.

4.9. Complete the derivation of equations (4.4.11) from (4.4.10).

Downloaded from https://www.cambridge.org/core. Charité Universitätsmedizin Berlin, on 20 Dec 2021 at 10:08:47, subject to the Cambridge Core terms of use, available at https://www.cambridge.org/core/terms. https://doi.org/10.1017/CBO9781107360273.005

4.10. Sound waves propagating in uniform flow at speed U in the x direction are governed by

$$\left[\frac{1}{c_o^2}\left(\frac{\partial}{\partial t}+U\frac{\partial}{\partial x}\right)^2-\nabla^2\right]\varphi'=0,$$

where c_o is the uniform mean sound speed. Show that plane waves propagating parallel to the x axis have the general form

$$\varphi'=f\left(t-\frac{x}{c_o(1+M)}\right)+g\left(t+\frac{x}{c_o(1-M)}\right),\quad M=\frac{U}{c_o},$$

for arbitrary functions $f,\ g$.

4.11.* **Kirchhoff's spinning vortex:** A columnar vortex parallel to the x_3-axis has elliptic cross-section defined by the polar equation $r = a\{1+\epsilon\cos(2\theta-\Omega t/2)\}$, where $\epsilon \ll 1$ and Ω is the uniform vorticity in the core. The ellipse rotates at angular velocity $\frac{1}{4}\Omega$, and the velocity distribution within the core is given by,

$$\mathbf{v}=(v_1,v_2)=-\frac{1}{2}\Omega r\Big(\sin\theta+\epsilon\sin(\theta-\Omega t/2),\\ -\cos\theta+\epsilon\cos(\theta-\Omega t/2)\Big).$$

Show that to first order in ϵ the vortex is equivalent to the two-dimensional quadrupole

$$\mathrm{div}(\boldsymbol{\omega}\wedge\mathbf{v})\approx\frac{\partial^2}{\partial x_i\partial x_j}\left(T_{ij}\delta(x_1)\delta(x_2)\right),\quad i,\ j=1,\ 2$$

where

$$T_{ij}=\frac{\epsilon\pi\Omega^2a^4}{8}\begin{pmatrix}\cos(\Omega t/2) & \sin(\Omega t/2)\\ \sin(\Omega t/2) & -\cos(\Omega t/2)\end{pmatrix}$$

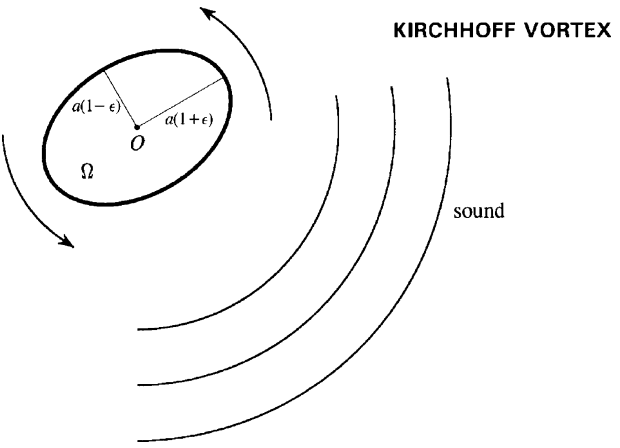

Downloaded from https://www.cambridge.org/core. Charité Universitätsmedizin Berlin, on 20 Dec 2021 at 10:08:47, subject to the Cambridge Core terms of use, available at https://www.cambridge.org/core/terms. https://doi.org/10.1017/CBO9781107360273.005

and that the acoustic pressure is,

$$p \approx -\frac{\epsilon}{8}\sqrt{\frac{2\pi a}{r}}\rho_o U^2 M^{3/2}\cos\left[2\theta - \frac{\Omega}{2}\left(t - \frac{r}{c_o}\right) + \frac{\pi}{4}\right], \quad \frac{\Omega r}{c_o} \to \infty,$$

where $U = \frac{1}{2}a\Omega$ and $M = U/c_o$.

4.12. **Coaxial vortex rings:** Use equation (4.6.6) to calculate the sound produced by the unsteady motions of an acoustically compact system of N vortex rings coaxial with the x_1-axis. Take the vorticity of the nth vortex to be $\boldsymbol{\omega}_n = \Gamma_n \delta(x_1 - X_n(t))\delta(r - R_n(t))\mathbf{i}_\theta$, where (r, θ, x_1) are cylindrical polar coordinates, $R_n(t)$ being the vortex ring radius, $X_n(t)$ its location in the x_1-direction, and $\mathbf{i}_\theta$ is a unit vector in the azimuthal direction. Show that

$$p \approx \frac{\rho_o}{8c_o^2|\mathbf{x}|}(3\cos^2\Theta - 1)\frac{\partial^2}{\partial t^2}\left[\sum_n \Gamma_n X_n \frac{dR_n^2}{dt}\right], \quad |\mathbf{x}| \to \infty,$$

where Θ is the angle between the observer direction and the positive x_1-axis and the term in square braces is evaluated at $\tau = t - |\mathbf{x}|/c_o$.

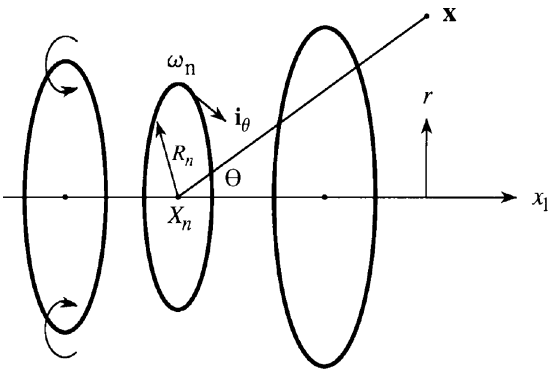

In an ideal, incompressible fluid conservation of energy and momentum implies that

$$\sum_n \Gamma_n R_n\left(R_n\frac{dX_n}{dt} - X_n\frac{dR_n}{dt}\right) = \text{constant}, \quad \sum_n \Gamma_n R_n^2 = \text{constant}.$$

Use these equations to show that

Downloaded from https://www.cambridge.org/core. Charité Universitätsmedizin Berlin, on 20 Dec 2021 at 10:08:47, subject to the Cambridge Core terms of use, available at https://www.cambridge.org/core/terms. https://doi.org/10.1017/CBO9781107360273.005

$$p \approx \frac{\rho_o}{12c_o^2|\mathbf{x}|}(3\cos^2\Theta - 1)\left[\frac{d^3S}{dt^3}\right], \quad |\mathbf{x}| \to \infty.$$

where $S(t) = \sum_n \Gamma_n R_n^2 X_n$.

4.13. The free space Green's function in two dimensions, that is, the solution of

$$\left(\frac{1}{c_o^2}\frac{\partial^2}{\partial t^2} - \nabla^2\right)G = \delta(x_1 - y_1)\delta(x_2 - y_2)\delta(t-\tau), \text{ where } G = 0 \text{ for } t < \tau,$$

can be derived by integrating the three-dimensional Green's function

$$\frac{1}{4\pi|\mathbf{x}-\mathbf{y}|}\delta\left(t - \tau - \frac{|\mathbf{x}-\mathbf{y}|}{c_o}\right) \quad \text{over} \quad -\infty < y_3 < \infty.$$

Deduce that

$$G(\mathbf{x}, \mathbf{y}, t-\tau) = \frac{\mathrm{H}(t - \tau - |\mathbf{x}-\mathbf{y}|/c_o)}{2\pi\sqrt{(t-\tau)^2 - (\mathbf{x}-\mathbf{y})^2/c_o^2}},$$
$$\mathbf{x} = (x_1, x_2), \quad \mathbf{y} = (y_1, y_2),$$

and that near the wavefront, where $|\mathbf{x} - \mathbf{y}| \approx c_o(t-\tau)$

$$G(\mathbf{x}, \mathbf{y}, t-\tau) \approx \frac{\mathrm{H}(t - \tau - |\mathbf{x}-\mathbf{y}|/c_o)}{2\pi\sqrt{2|\mathbf{x}-\mathbf{y}|/c_o}\sqrt{(t-\tau) - |\mathbf{x}-\mathbf{y}|/c_o}}.$$

4.14. Starting from the formula

$$G_2 \approx \frac{\bar{\mathbf{x}}\cdot\mathbf{Y}}{2\pi c_o}\frac{\partial}{\partial t}\int_0^\infty \delta\left(t - \tau - \frac{\sqrt{|\bar{\mathbf{x}}|^2 + \xi^2}}{c_o}\right)\frac{d\xi}{(|\bar{\mathbf{x}}|^2 + \xi^2)},$$

derive the far field approximation (2.9.19) for the dipole component of the two-dimensional compact Green's function by writing

$$\delta\left(t - \tau - \frac{\sqrt{|\bar{\mathbf{x}}|^2 + \xi^2}}{c_o}\right) = \frac{1}{2\pi}\int_{-\infty}^{\infty} \mathrm{e}^{-i\omega\left(t-\tau-\frac{\sqrt{|\bar{\mathbf{x}}|^2+\xi^2}}{c_o}\right)}d\omega,$$

and applying the formula (4.6.10).

Downloaded from https://www.cambridge.org/core. Charité Universitätsmedizin Berlin, on 20 Dec 2021 at 10:08:47, subject to the Cambridge Core terms of use, available at https://www.cambridge.org/core/terms. https://doi.org/10.1017/CBO9781107360273.005

4.15. A vortex line of circulation Γ is adjacent to a parallel circular, rigid cylinder of radius a whose axis coincides with the x_3 axis. The vortex moves along a circular trajectory around the cylinder of radius r_o at angular velocity Ω (clockwise when viewed from the direction of the positive x_3 axis). If the motion occurs at infinitesimal Mach number, show that the far field acoustic pressure is given by

$$p(\mathbf{x},t) \approx -\frac{\rho_o \Gamma |\Omega| r_o}{2\pi (2c_o|\mathbf{x}|)^{\frac{1}{2}}}\left(1-\frac{a^2}{r_o^2}\right)\frac{\partial}{\partial t}\int_{-\infty}^{t-|\mathbf{x}|/c_o}\frac{\cos(\theta+|\Omega|\tau)d\tau}{\sqrt{t-\tau-|\mathbf{x}|/c_o}}, \quad |\mathbf{x}|\to\infty,$$

where $\mathbf{x} = |\mathbf{x}|(\cos\theta, \sin\theta)$.
Use the formula

$$\int_{-\infty}^{t-|\mathbf{x}|/c_o}\frac{\cos(\theta+|\Omega|\tau)d\tau}{\sqrt{t-\tau-|\mathbf{x}|/c_o}} = \left(\frac{\pi}{|\Omega|}\right)^{\frac{1}{2}}\cos\left\{\theta+|\Omega|\left[t-\frac{|\mathbf{x}|}{c_o}\right]-\frac{\pi}{4}\right\}$$

to deduce that

$$p(\mathbf{x},t) \approx \rho_o U^2\sqrt{M}\sqrt{\frac{\pi r_o}{2|\mathbf{x}|}}\left(\frac{r_o}{a}\right)^2\left(1-\frac{a^2}{r_o^2}\right)^2 \times \sin\left\{\theta+|\Omega|\left[t-\frac{|\mathbf{x}|}{c_o}\right]-\frac{\pi}{4}\right\}, \quad |\mathbf{x}|\to\infty,$$

where $U = |\Omega| r_o$ is the vortex speed and $M = U/c_o$.

4.16.* A 'small' vortex ring with an infinitesimal core, circulation Γ and radius a is located with its centre on the x_1 axis and translates in the positive x_1 direction at speed U, as indicated in the figure on the next page. If the vortex centre coincides with the coordinate origin at time $t = 0$, show that the corresponding vortex sound source $\mathrm{div}(\boldsymbol{\omega}\wedge\mathbf{v})$ can be approximated (for small a) by the point quadrupole

$$\mathrm{div}(\boldsymbol{\omega}\wedge\mathbf{v}) \simeq -\pi a^2\Gamma U\left(\frac{\partial^2}{\partial x_2^2}+\frac{\partial^2}{\partial x_3^2}\right)\{\delta(x_1-Ut)\delta(x_2)\delta(x_3)\}.$$

Downloaded from https://www.cambridge.org/core. Charité Universitätsmedizin Berlin, on 20 Dec 2021 at 10:08:47, subject to the Cambridge Core terms of use, available at https://www.cambridge.org/core/terms. https://doi.org/10.1017/CBO9781107360273.005

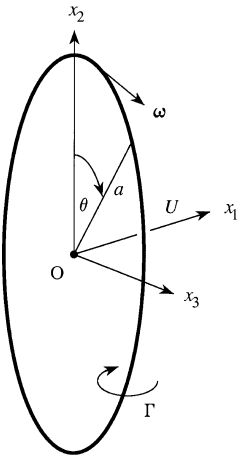

4.17. The vortex ring of Question 4.16 is orientated with its axis parallel to the $+x_1$ axis and is convected in a low Mach number mean flow at speed U in the x_1 direction past the edge of the rigid half-plane $x_1 < 0,\ x_2 = 0,\ -\infty < x_3 < \infty$. Use the compact Green's function (2.9.7) to calculate the sound produced as the vortex passes the edge when the influence of the half-plane on the motion of the ring is ignored. Ignore any vorticity shed from the edge.

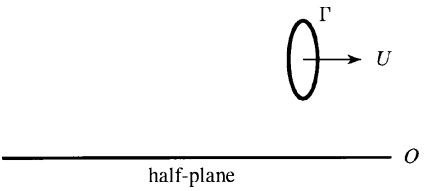

4.18.* A *small* vortex ring of radius a and circulation Γ is orientated with its axis in the x_1 direction and translates at constant velocity $\mathbf{v} = U\mathbf{i}$ in the positive x_1 direction with its centre on the line $x_2 = h,\ x_3 = 0$, where $U \ll c_o$. The vortex passes a fixed, rigid sphere of radius $R < h$ with centre at the origin; assume that the influence of the sphere on the path and velocity of motion of the vortex can be ignored, and that the vortex is directly above the sphere (i.e. its centre is at $x_1 = 0$) at time $t = 0$.

Show that the sound generated as the vortex passes the sphere can be attributed to two dipole sources at the origin, a 'drag' dipole with its axis in the x_1 direction and a 'lift' dipole with axis in the x_2 direction. Use the compact Green's function to calculate the acoustic pressure at large distances $|\mathbf{x}|$ from the sphere in the plane of symmetry $x_3 = 0$.

Downloaded from https://www.cambridge.org/core. Charité Universitätsmedizin Berlin, on 20 Dec 2021 at 10:08:47, subject to the Cambridge Core terms of use, available at https://www.cambridge.org/core/terms. https://doi.org/10.1017/CBO9781107360273.005

Show that if p_d and p_ℓ are the component sound pressures produced by the drag and lift dipoles, then (for $x_3 = 0$)

$$p_d(\mathbf{x}, t) \simeq -\frac{\rho_o \Gamma U M \cos\Theta}{|\mathbf{x}|}\left(\frac{a^2R^3}{h^5}\right)\frac{3(3-24T^2+8T^4)}{8(1+T^2)^{\frac{9}{2}}}$$

$$p_\ell(\mathbf{x}, t) \simeq \frac{\rho_o \Gamma U M \sin\Theta}{|\mathbf{x}|}\left(\frac{a^2R^3}{h^5}\right)\frac{15T(3-4T^2)}{8(1+T^2)^{\frac{9}{2}}}$$

$$\text{where} \quad (\cos\Theta, \sin\Theta) = \frac{(x_1, x_2)}{|\mathbf{x}|}, \quad T = \frac{U[t]}{h} \equiv \frac{U}{h}\left(t - \frac{|\mathbf{x}|}{c_o}\right).$$

Give simple sketch graphs of the corresponding pressure variations as functions of T.

4.19.* Repeat Question 4.17 when a vortex ring of radius $R \ll a$ convects at speed U in the x_1 direction over the strip airfoil of chord $2a$ shown in the figure at distance $h \gg R$ above the airfoil, such that its centre at time t is at $(Ut, h, 0)$. Show that when the Kutta condition is applied at the trailing edge of the airfoil

$$p(\mathbf{x}, t) \approx \frac{3}{16\sqrt{2}}\left(\frac{R}{a}\right)^2 \frac{\rho_o U^2 \Gamma \cos\Theta}{c_o|\mathbf{x}|}\,\mathrm{Re}\left\{\frac{1}{\left(\frac{U[t]}{a}+1+\frac{ih}{a}\right)^{\frac{5}{2}}}\right\},$$

$$|\mathbf{x}| \to \infty,$$

where Θ is the angle between the radiation direction $\mathbf{x}$ and the normal to the airfoil. The pressure signature is plotted as the solid curve in the

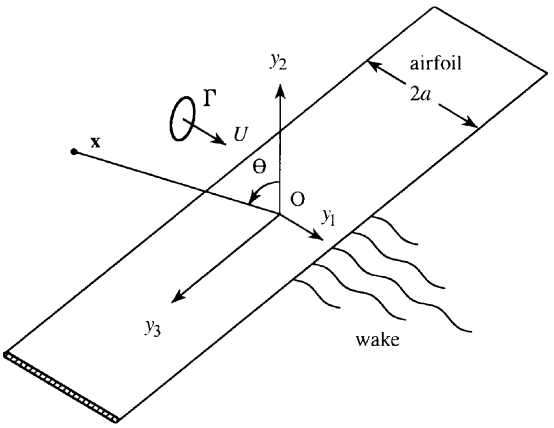

Downloaded from https://www.cambridge.org/core. Charité Universitätsmedizin Berlin, on 20 Dec 2021 at 10:08:47, subject to the Cambridge Core terms of use, available at https://www.cambridge.org/core/terms. https://doi.org/10.1017/CBO9781107360273.005

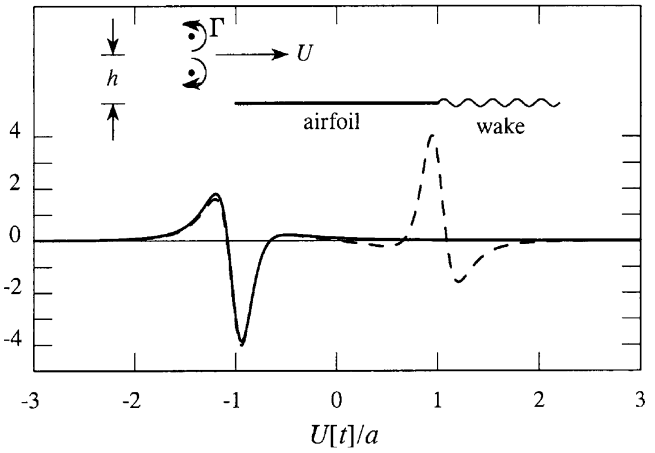

figure above; the broken line curve is the pressure for 'potential flow' interaction between the vortex and airfoil.

4.20. Calculate the sound produced within and outside a semi-finite circular cylindrical rigid pipe when a vortex ring exhausts axisymmetrically from the open end. Neglect the influence of the pipe walls on the motion of the vortex and ignore any change in the vortex radius at the exit.

4.21. Use the result of Question 2.12 (**Problems 2**) to calculate the sound produced in an ideal fluid during the 'head on' collision of two equal 'vortex pairs'.

4.22. A point source of constant strength Q is distance $h > 0$ from a plane rigid wall $x_2 = 0$ in an ideal, incompressible fluid of uniform density ρ_o. Show (i) by integration of the surface pressure, and (ii) by means of formula (4.A.10), that the wall experiences a suction force $F_2 = \rho_o Q^2/16\pi h^2$.

Downloaded from https://www.cambridge.org/core. Charité Universitätsmedizin Berlin, on 20 Dec 2021 at 10:08:47, subject to the Cambridge Core terms of use, available at https://www.cambridge.org/core/terms. https://doi.org/10.1017/CBO9781107360273.005

5

Aperture and Duct Problems

5.1 Rayleigh's approximation for the conductivity

The sound transmitted through a compact aperture in a screen is governed by the conductivity K_o. Transmission through a thin screen with one or more circular apertures is investigated in §3.3 in terms of K_o calculated from the velocity potential φ^* of §2.9.1g. But this is exceptional; for example, K_o is not usually known when the screen spans a cross-section of a narrow duct, or when the aperture is not circular. A more or less precise determination of the conductivity will then involve the evaluation of the corresponding φ^* from a numerical solution of Laplace's equation. For many geometries, however, a sufficient approximation (to within one or two per cent) can be found by appeal to Kelvin's theorem (§4.4.1), that of all possible incompressible flows through the aperture, the kinetic energy attains its minimum value when the flow is irrotational.

5.1.1 Circular aperture in a thin screen (Rayleigh 1870)

The basic idea will be illustrated for the known case of a circular aperture of radius a in a thin screen (Figure 3.3.1 with $h = 0$). Suppose a volume velocity Q through the aperture is created instantaneously from rest by simultaneous radial contraction and expansion of large hemispherical boundaries (Σ in the figure) respectively on the 'left' and 'right' sides of the screen. The initial motion is always irrotational, and the kinetic energy is $T = \rho_o Q^2/2K_o$ (equation (3.3.7)). The effective slug length of fluid in motion through the aperture is $\ell = A/K_o$, where $A = \pi a^2$ is the aperture area. According to Kelvin's theorem

$$\frac{1}{K_o} \equiv \frac{\ell}{A} = \frac{2T}{\rho_o Q^2} \leq \frac{2T'}{\rho_o Q^2}, \tag{5.1.1}$$

Downloaded from https://www.cambridge.org/core. Charité Universitätsmedizin Berlin, on 20 Dec 2021 at 10:08:47, subject to the Cambridge Core terms of use, available at https://www.cambridge.org/core/terms. https://doi.org/10.1017/CBO9781107360273.006

where T' is the kinetic energy of any other possible (rotational) motion through the aperture consistent with the boundary conditions on Σ.

Let the screen occupy the plane $x_1 = 0$ with the aperture centre at the origin, and let $v_n(\mathbf{x})$ denote the normal velocity within the aperture in the $+x_1$ direction. In the absence of volume sources $q(\mathbf{x}, t)$, the potential φ of the motion in $x_1 > 0$ can be deduced from (2.1.10) by taking for G the hard wall Green's function (2.1.7) in which we let $c_o \to \infty$ for incompressible flow. Then, if $\varphi \to 0$ as $x_1 \to +\infty$ we find

$$\varphi(\mathbf{x}) = -\frac{1}{2\pi} \oint_{y_1=+0} \frac{v_n(\mathbf{y})\, dS(\mathbf{y})}{|\mathbf{x}-\mathbf{y}|}, \quad x_1 > 0, \tag{5.1.2}$$

the integration being over the plane $y_1 = +0$ of the aperture. Thus, $\varphi \approx -Q/2\pi|\mathbf{x}|$ at large distances $|\mathbf{x}|$ on the right of the aperture. According to (3.3.3), at large distances on the left of the screen ($x_1 \to -\infty$)

$$\varphi \approx \frac{Q}{2\pi|\mathbf{x}|} - \frac{Q\ell}{A},$$

where ℓ is the slug length of (5.1.1).

The kinetic energy of the whole motion (equal to twice that on the right-hand side of the screen) can be calculated in terms of the values of φ and $\partial\varphi/\partial x_1 = v_n$ at $x_1 = 0$ by application of the divergence theorem:

$$T = \rho_o \int_{x_1>0} (\nabla\varphi)^2 d^3\mathbf{x} = -\rho_o \oint_{x_1=+0} \varphi \frac{\partial\varphi}{\partial x_1} dS(\mathbf{x}) \equiv -\rho_o \oint_{x_1=+0} \varphi\, v_n\, dS(\mathbf{x}). \tag{5.1.3}$$

It follows from the exact solution (§§3.3.1, 3.3.2) that

$$v_n = \frac{Q}{2\pi a\sqrt{a^2 - \varpi^2}}, \quad 0 < \varpi < a, \quad \varpi = (x_2^2 + x_3^2)^{\frac{1}{2}}, \tag{5.1.4}$$

and therefore from (5.1.2), (5.1.3) that $T = \rho_o Q^2/4a$. Then (5.1.1) yields $K_o = 2a$ and $\ell = \frac{\pi}{2}a$.

In the absence of a knowledge of (5.1.4) one might postulate the two-parameter approximation

$$v_n = \bar{v}\left(1 + \mu\frac{\varpi^2}{a^2} + \mu'\frac{\varpi^4}{a^4}\right), \quad 0 < \varpi < a, \tag{5.1.5}$$

where the coefficients μ, μ' are to be determined to give a 'best fit' to the velocity. Continuity requires

$$Q = \int_{x_1=+0} v_n\, dS(\mathbf{x}) = 2\pi\bar{v} \int_0^a \left(1 + \mu\frac{\varpi^2}{a^2} + \mu'\frac{\varpi^4}{a^4}\right) \varpi\, d\varpi,$$

Downloaded from https://www.cambridge.org/core. Charité Universitätsmedizin Berlin, on 20 Dec 2021 at 10:08:47, subject to the Cambridge Core terms of use, available at https://www.cambridge.org/core/terms. https://doi.org/10.1017/CBO9781107360273.006

so that

$$\bar{v} = \frac{Q}{\pi a^2 \left(1 + \frac{\mu}{2} + \frac{\mu'}{3}\right)}. \tag{5.1.6}$$

The resulting motion calculated from (5.1.2) and (5.1.5) is irrotational for $x_1 \gtrless 0$, with potential φ', say, but the plane $x_1 = 0$ of the aperture is spanned by a vortex sheet. The kinetic energy T' must therefore exceed that for irrotational flow, and according to equation (5.1.1) will furnish an *upper bound* for the slug length ℓ. The formula (5.1.5) lacks the singular behaviour $\sim 1/(a^2 - \varpi^2)^{\frac{1}{2}}$ of the irrotational solution (5.1.4) at the edge of the aperture, but it should supply a good approximation for ℓ provided the minimum value of the kinetic energy T', obtained by suitable choice of the values of μ and μ', is a close approximation to the irrotational kinetic energy T. Indeed, the much simpler 'piston' approximation $\bar{v} = Q/\pi a^2,\ \mu = 0,\ \mu' = 0$ yields the estimate $\ell \approx 16a/3\pi \approx 1.7a$, which is only about 8% larger than the true value $\ell = \pi a/2 \approx 1.57a$.

To evaluate T', we have

$$T' = -\rho_o \oint_{x_1=+0} \varphi'\, v_n \, dS(\mathbf{x}) = \frac{\rho_o}{2\pi} \oint_{x_1=+0} \oint_{y_1=+0} \frac{v_n(\mathbf{x}) v_n(\mathbf{y})}{|\mathbf{x} - \mathbf{y}|} dS(\mathbf{y}) dS(\mathbf{x}),$$

where φ' is defined as in (5.1.2) with v_n given by (5.1.5), and the surface integrals are over the positive face of the aperture. The symmetry of the integrands is similar to that encountered in §3.1.4 in calculating the reaction force on a circular piston so that, as in (3.1.14),

$$T' = \frac{\rho_o}{\pi} \oint_{|\mathbf{x}|<a} v_n(\mathbf{x}) dS(\mathbf{x}) \oint_{|\mathbf{y}|<|\mathbf{x}|} \frac{v_n(\mathbf{y})}{|\mathbf{x} - \mathbf{y}|} dS(\mathbf{y}).$$

Put $r = |\mathbf{x} - \mathbf{y}|$ and use polar coordinates (r, θ) for the $\mathbf{y}$ integration with pole at $\mathbf{x}$, then $\varpi^2(\mathbf{y}) = |\mathbf{x}|^2 + r^2 - 2|\mathbf{x}| r \cos\theta$ (where $|\mathbf{x}| \equiv \varpi(\mathbf{x}) = (x_2^2 + x_3^2)^{\frac{1}{2}}$, see Figure 5.1.1).

Then

$$\begin{aligned}
&\oint_{|\mathbf{y}|<|\mathbf{x}|} \frac{v_n(\mathbf{y})}{|\mathbf{x} - \mathbf{y}|} dS(\mathbf{y}) \\
&\quad = \bar{v} \int_{-\frac{\pi}{2}}^{\frac{\pi}{2}} d\theta \int_0^{2|\mathbf{x}|\cos\theta} \left(1 + \mu \frac{\varpi^2}{a^2} + \mu' \frac{\varpi^4}{a^4}\right) dr \\
&\quad = \bar{v} \left(4\varpi(\mathbf{x}) + \frac{20}{9} \frac{\mu \varpi^3(\mathbf{x})}{a^2} + \frac{356}{225} \frac{\mu' \varpi^5(\mathbf{x})}{a^4}\right)
\end{aligned}$$

Downloaded from https://www.cambridge.org/core. Charité Universitätsmedizin Berlin, on 20 Dec 2021 at 10:08:47, subject to the Cambridge Core terms of use, available at https://www.cambridge.org/core/terms. https://doi.org/10.1017/CBO9781107360273.006

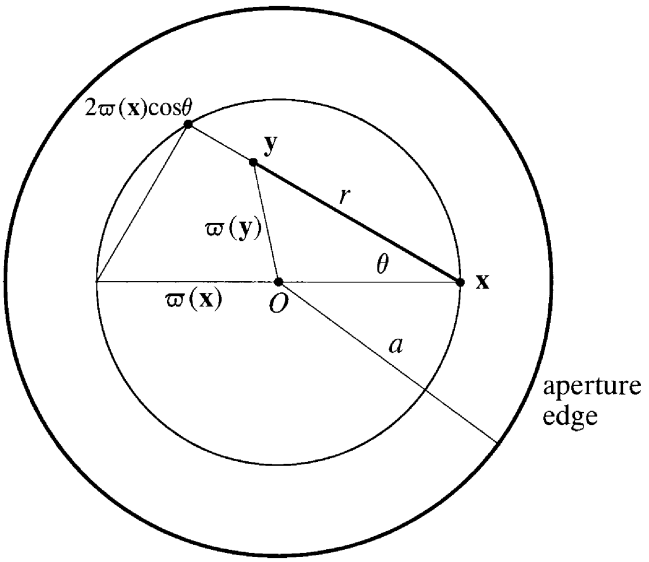

Figure 5.1.1

$$\therefore \quad T' = 2\rho_o \bar{v}^2 \int_0^a \left(1 + \mu \frac{\varpi^2}{a^2} + \mu' \frac{\varpi^4}{a^4}\right) \times \left(4\varpi + \frac{20}{9}\frac{\mu \varpi^3}{a^2} + \frac{356}{225}\frac{\mu' \varpi^5}{a^4}\right) \varpi \, d\varpi$$
$$= \rho_o \bar{v}^2 \frac{8a^3}{3}\left(1 + \frac{14\mu}{15} + \frac{5\mu^2}{21} + \frac{314\mu'}{525} + \frac{214\mu\mu'}{675} + \frac{89\mu'^2}{825}\right).$$

Hence, (5.1.1) and (5.1.6) give

$$\frac{1}{K_o} \equiv \frac{\ell}{A} \leq \frac{2T'}{\rho_o Q^2} = \frac{16\left(1 + \frac{14\mu}{15} + \frac{5\mu^2}{21} + \frac{314\mu'}{525} + \frac{214\mu\mu'}{675} + \frac{89\mu'^2}{825}\right)}{3\pi^2 a \left(1 + \frac{\mu}{2} + \frac{\mu'}{3}\right)^2}. \tag{5.1.7}$$

The values of μ, μ' that minimise the ratio on the right-hand side (calculated by the method of §5.1.3) are shown in the first row of Table 5.1.1. The corresponding estimates $\ell/a \simeq 1.5894$ and $K_o/a \simeq 1.9766$ (obtained by replacing '$\leq$' by '$=$' in (5.1.7)) are also given; they are respectively about 1.2 per cent larger and smaller than the exact values. The table also lists alternative (and less accurate) estimates of ℓ/a, K_o/a obtained when either or both of μ, μ' vanishes.

Downloaded from https://www.cambridge.org/core. Charité Universitätsmedizin Berlin, on 20 Dec 2021 at 10:08:47, subject to the Cambridge Core terms of use, available at https://www.cambridge.org/core/terms. https://doi.org/10.1017/CBO9781107360273.006

Table 5.1.1

μ	μ'	ℓ/a	K_o/a	error %
−2.84211	5.2105	1.5894	1.9766	1.2
7.0000	0.0	1.6096	1.9518	2.4
0.0	4.1831	1.5960	1.9685	1.6
0.0	0.0	1.6976	1.8506	7.5
exact values		$\frac{\pi}{2} \simeq 1.5708$	2.0	

5.1.2 Annular aperture*

The same procedure can be applied to an annular aperture in a thin screen. Let the screen be at $x_1 = 0$ with the aperture centred on the origin with inner and outer radii respectively equal to a and b (Figure 5.1.2).

Consider the one-parameter approximation

$$v_n = \bar{v}\left(1 + \mu\frac{\varpi^2}{b^2}\right), \quad a < \varpi < b,$$

where

$$\bar{v} = \frac{Q}{\pi(b^2 - a^2)\left(1 + \frac{\mu(b^2+a^2)}{2b^2}\right)}.$$

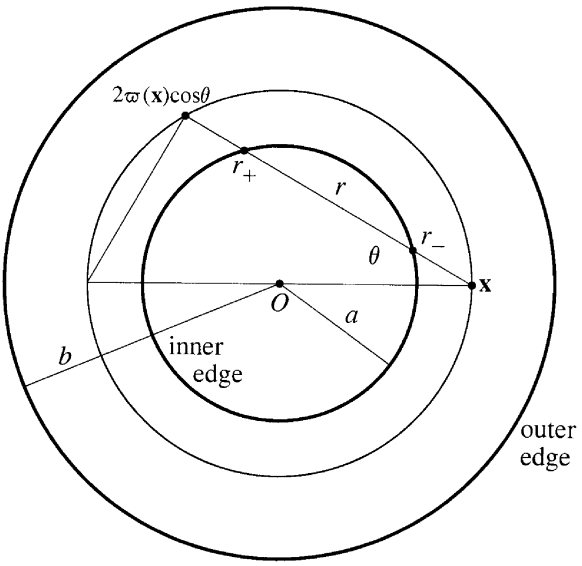

Figure 5.1.2

Downloaded from https://www.cambridge.org/core. Charité Universitätsmedizin Berlin, on 20 Dec 2021 at 10:08:47, subject to the Cambridge Core terms of use, available at https://www.cambridge.org/core/terms. https://doi.org/10.1017/CBO9781107360273.006

The kinetic energy is calculated as before

$$T' = \frac{\rho_o}{\pi} \oint_{a<|\mathbf{x}|<b} v_n(\mathbf{x}) dS(\mathbf{x}) \oint_{a<|\mathbf{y}|<|\mathbf{x}|} \frac{v_n(\mathbf{y})}{|\mathbf{x}-\mathbf{y}|} dS(\mathbf{y}),$$

in which

$$\begin{aligned}
&\oint_{a<|\mathbf{y}|<|\mathbf{x}|} \frac{v_n(\mathbf{y})}{|\mathbf{x}-\mathbf{y}|} dS(\mathbf{y}) \\
&\quad = \left(\int_{-\frac{\pi}{2}}^{-\theta'} d\theta + \int_{\theta'}^{\frac{\pi}{2}} d\theta \right) \int_0^{2|\mathbf{x}|\cos\theta} v_n(r,\theta) dr \\
&\qquad + \int_{-\theta'}^{\theta'} d\theta \left(\int_0^{r_-} v_n(r,\theta) dr + \int_{r_+}^{2|\mathbf{x}|\cos\theta} v_n(r,\theta) dr \right),
\end{aligned}$$

where $\theta' = \sin^{-1}(a/|\mathbf{x}|)$ and $r_\pm = |\mathbf{x}|\cos\theta \pm (a^2 - |\mathbf{x}|^2 \sin^2\theta)^{\frac{1}{2}}$. Then

$$\frac{1}{K_o} = \frac{\ell}{\pi(b^2-a^2)} \le \frac{2T'}{\rho_o Q^2} = \frac{16b^3}{3\pi^2(b^2-a^2)^2} \frac{(A\mu^2 + 2G\mu + C)}{\left(1 + \frac{\mu(b^2+a^2)}{2b^2}\right)^2}, \quad (5.1.8)$$

where, putting $\xi = a/b$,

$$\begin{aligned}
A &= \frac{1}{3}\left(\frac{5(1+\xi^7)}{7} \right. \\
&\qquad \left. -\xi^4 \int_0^{\frac{\pi}{2}} \cos^2\phi\,(1+2\sin^2\phi)(1+2\xi^2\sin^2\phi)\sqrt{1-\xi^2\sin^2\phi}\, d\phi \right) \\
G &= \frac{1}{2}\left(\frac{14(1+\xi^5)}{15} \right. \\
&\qquad \left. -\xi^2 \int_0^{\frac{\pi}{2}} \cos^2\phi\,(1+\xi^2[1+4\sin^2\phi])\sqrt{1-\xi^2\sin^2\phi}\, d\phi \right) \\
C &= 1+\xi^3 - 3\xi^2 \int_0^{\frac{\pi}{2}} \cos^2\phi \sqrt{1-\xi^2\sin^2\phi}\, d\phi\,.
\end{aligned}$$

The approximation for ℓ is now found by first writing (5.1.8) in the form

$$\frac{\ell}{b} \le \frac{16\mathcal{Z}}{3\pi(1-\xi^2)}, \quad \text{where } \mathcal{Z} = \frac{A\mu^2 + 2G\mu + C}{\left(1 + \frac{\mu}{2}(1+\xi^2)\right)^2}. \quad (5.1.9)$$

The ratio of quadratics $\mathcal{Z}(\mu)$ attains its minimum value of

$$\mathcal{Z} = \frac{AC - G^2}{A - (1+\xi^2)G + (1+\xi^2)^2 C/4} \quad \text{when } \mu = \frac{(1+\xi^2)C - 2G}{2A - (1+\xi^2)G},$$

Downloaded from https://www.cambridge.org/core. Charité Universitätsmedizin Berlin, on 20 Dec 2021 at 10:08:47, subject to the Cambridge Core terms of use, available at https://www.cambridge.org/core/terms. https://doi.org/10.1017/CBO9781107360273.006

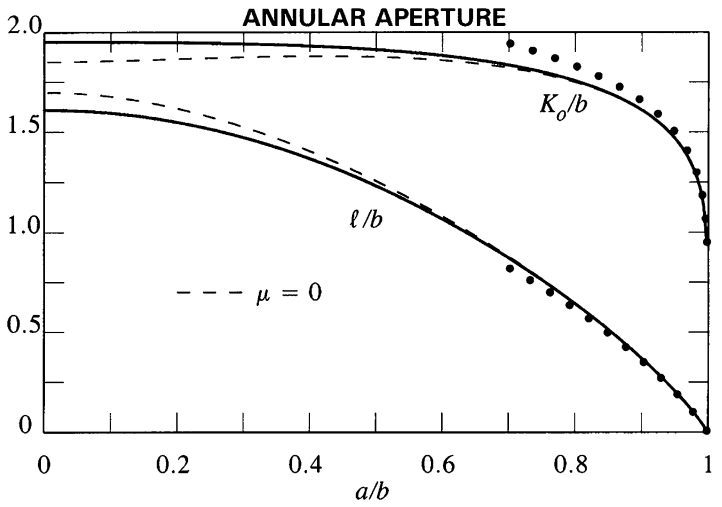

Figure 5.1.3

and the corresponding estimate of ℓ is obtained by replacing '$\leq$' by '$=$' in (5.1.9).

The variations of ℓ/b and $K_o/b = \pi(1-\xi^2)/(\ell/b)$ are plotted in Figure 5.1.3 for $0 < \xi = a/b < 1$. The conductivity increases towards $K_o = 1.9518\,b$ as $a/b \to 0$, which is 2.4% smaller than the exact value for a circular aperture of radius b (as in the second row of Table 5.1.1). The broken line curves are the corresponding predictions when $\mu \equiv 0$.

The dotted curves in Figure 5.1.3 correspond to the asymptotic formulae

$$\frac{\ell}{b} \approx \frac{2(1-\xi)}{\pi} \ln\left(\frac{32}{1-\xi}\right), \quad \frac{K_o}{b} \approx \frac{\pi^2(1+\xi)}{2\,\ln\left(\frac{32}{1-\xi}\right)},$$

for a narrow annulus, when $(b-a) \ll a$ ($\xi = a/b \sim 1$) (Question 5.7, **Problems 5**).

5.1.3 Minimum of a ratio of quadratic functions

Consider

$$\mathcal{Z} = \frac{A\mu^2 + B\mu'^2 + C + 2F\mu' + 2G\mu + 2H\mu\mu'}{(\gamma + \alpha\mu + \beta\mu')^2} \tag{5.1.10}$$

for prescribed values of the coefficients $A,\ B,\ C,\ F,\ G,\ H,\ \alpha,\ \beta,\ \gamma$.

Clearing fractions leads to the bi-quadratic

$$A\mu^2 + B\mu'^2 + C + 2F\mu' + 2G\mu + 2H\mu\mu' - \mathcal{Z}\left(\gamma + \alpha\mu + \beta\mu'\right)^2 = 0. \quad \text{(a)}$$

Downloaded from https://www.cambridge.org/core. Charité Universitätsmedizin Berlin, on 20 Dec 2021 at 10:08:47, subject to the Cambridge Core terms of use, available at https://www.cambridge.org/core/terms. https://doi.org/10.1017/CBO9781107360273.006

The derivatives $\partial\mathcal{Z}/\partial\mu,\ \partial\mathcal{Z}/\partial\mu' = 0$ at a stationary value of $\mathcal{Z}$.

$$\therefore \quad A\mu + H\mu' + G - \alpha\mathcal{Z}\left(\gamma + \alpha\mu + \beta\mu'\right) = 0 \qquad \text{(b)}$$

$$\text{and} \quad H\mu + B\mu' + F - \beta\mathcal{Z}\left(\gamma + \alpha\mu + \beta\mu'\right) = 0 \qquad \text{(c)}$$

$$\text{and also} \quad G\mu + F\mu' + C - \gamma\mathcal{Z}\left(\gamma + \alpha\mu + \beta\mu'\right) = 0, \qquad \text{(d)}$$

where (d) is obtained by subtracting $\mu \times$ (b) and $\mu' \times$ (c) from (a). After using (d) to eliminate $\mathcal{Z}$ from (b) and (c) we can write

$$\left.\begin{aligned}(\gamma A - \alpha G)\mu + (\gamma H - \alpha F)\mu' + \gamma G - \alpha C = 0\\ (\gamma H - \beta G)\mu + (\gamma B - \beta F)\mu' + \gamma F - \beta C = 0\\ (G - \alpha\gamma\mathcal{Z})\mu + (F - \beta\gamma\mathcal{Z})\mu' + C - \gamma^2\mathcal{Z} = 0.\end{aligned}\right\} \qquad (5.1.11)$$

These equations yield consistent values of $\mu,\ \mu'$ provided

$$\begin{vmatrix} \gamma A - \alpha G & \gamma H - \alpha F & \gamma G - \alpha C \\ \gamma H - \beta G & \gamma B - \beta F & \gamma F - \beta C \\ G - \alpha\gamma\mathcal{Z} & F - \beta\gamma\mathcal{Z} & C - \gamma^2\mathcal{Z} \end{vmatrix} = 0,$$

so that

$$\begin{aligned}\mathcal{Z} &= \begin{vmatrix} A & H & G \\ H & B & F \\ G & F & C \end{vmatrix} \div \left(\alpha \begin{vmatrix} \alpha & \beta & \gamma \\ H & B & F \\ G & F & C \end{vmatrix} + \beta \begin{vmatrix} \alpha & \beta & \gamma \\ G & F & C \\ A & H & G \end{vmatrix} + \gamma \begin{vmatrix} \alpha & \beta & \gamma \\ A & H & G \\ H & B & F \end{vmatrix} \right) \\ &= \frac{A(BC - F^2) + H(FG - HC) + G(HF - BG)}{\left(\begin{array}{c} \alpha^2(BC - F^2) + \beta^2(CA - G^2) + \gamma^2(AB - H^2) \\ +2\alpha\beta(FG - HC) + 2\beta\gamma(GH - FA) + 2\gamma\alpha(HF - BG) \end{array} \right)}. \end{aligned} \qquad (5.1.12)$$

5.2 Impulsive motion of an incompressible fluid

A deeper understanding of the significance of Kelvin's theorem depends on the concept of *impulsive pressure*. Suppose that an incompressible fluid is at rest a time t when it is suddenly set in motion by movement of a solid boundary at a finite velocity. Incompressible motion starts everywhere instantaneously by the transmission of an impulsive pressure $\Omega(\mathbf{x})$ to all points $\mathbf{x}$ of the fluid, where

$$\Omega = \lim_{\epsilon \to +0} \int_t^{t+\epsilon} p\, dt.$$

The resulting velocity $\mathbf{v}$, velocity gradients, and viscous forces are all finite, but $\mathbf{v}$ changes discontinuously so that $\partial\mathbf{v}/\partial t$ as well as p are initially infinite.

Thus, recalling that $D\rho/Dt = 0$ for an inhomogeneous, incompressible fluid, it follows by integrating the momentum equation (1.2.4) from t to $t + \epsilon$ and taking the limit $\epsilon \to 0$, that the initial distribution of *momentum* density is

$$\rho\mathbf{v} = -\nabla\Omega.$$

Downloaded from https://www.cambridge.org/core. Charité Universitätsmedizin Berlin, on 20 Dec 2021 at 10:08:47, subject to the Cambridge Core terms of use, available at https://www.cambridge.org/core/terms. https://doi.org/10.1017/CBO9781107360273.006

The initial motion is therefore irrotational in a fluid of uniform density $\rho = \rho_o$, with velocity potential $-\Omega/\rho_o$. Vortex sheets are always formed instantaneously at any surfaces, however, and vorticity will subsequently diffuse into the body of a viscous fluid. When ρ is not uniform, the initial motion is generally not irrotational because vorticity is generated across density gradients. In a compressible fluid an impulsive boundary motion would generate sound. The sound speed is infinite in an incompressible fluid so that the impulsive pressure is transmitted instantaneously to every point of the fluid.

5.2.1 Remarks on Kelvin's theorem (1879)

The general form of Kelvin's 'minimum energy' theorem asserts, that when an *incompressible* fluid at rest within a closed surface Σ is suddenly set in motion by the imposition of a prescribed normal velocity distribution on Σ, the motion assumed by the fluid has less kinetic energy than any other motion consistent with continuity and the boundary conditions. This is true whether or not the fluid is viscous, and whether or not the density is uniform.

Let V denote the fluid region within Σ and let $\Omega(\mathbf{x})$ be the impulsive pressure produced by the boundary motion. The velocity $\mathbf{v}(\mathbf{x})$ excited in V satisfies $\rho(\mathbf{x})\mathbf{v}(\mathbf{x}) = -\nabla\Omega$. Let this motion have kinetic energy T and let $\mathbf{v}'$ and T' respectively denote the velocity and kinetic energy of any other possible motion consistent with conditions on Σ. Then $T' \geq T$, because

$$\begin{aligned} T' - T &= \frac{1}{2}\int_V \rho(v'^2 - v^2)d^3\mathbf{x} = \frac{1}{2}\int_V \Big(2\rho\mathbf{v}\cdot(\mathbf{v}'-\mathbf{v}) + \rho(\mathbf{v}'-\mathbf{v})^2\Big)d^3\mathbf{x} \\ &= -\int_V \mathrm{div}\{\Omega(\mathbf{v}'-\mathbf{v})\}d^3\mathbf{x} + \frac{1}{2}\int_V \rho(\mathbf{v}'-\mathbf{v})^2 d^3\mathbf{x} \\ &= -\oint_\Sigma \Omega(\mathbf{v}'-\mathbf{v})\cdot d\mathbf{S} + \frac{1}{2}\int_V \rho(\mathbf{v}'-\mathbf{v})^2 d^3\mathbf{x} \\ &= \frac{1}{2}\int_V \rho(\mathbf{v}'-\mathbf{v})^2 d^3\mathbf{x} \;\geq\; 0, \end{aligned}$$

where the divergence theorem has been used, noting that $\mathrm{div}(\mathbf{v}' - \mathbf{v}) = 0$, and the surface integral vanishes because the normal components of $\mathbf{v}'$ and $\mathbf{v}$ are equal on Σ.

Corollary 1 If the density $\rho(\mathbf{x})$ is *reduced* in some regions of V the new minimum kinetic energy is *smaller* than before.

Because, when $\rho(\mathbf{x})$ is reduced in some regions, the kinetic energy will be reduced if the velocity field $\mathbf{v}(\mathbf{x})$ is unchanged. This constitutes a *possible* motion of the fluid with the new density distribution, but its kinetic energy is necessarily greater than or equal to the new minimum kinetic energy.

Downloaded from https://www.cambridge.org/core. Charité Universitätsmedizin Berlin, on 20 Dec 2021 at 10:08:47, subject to the Cambridge Core terms of use, available at https://www.cambridge.org/core/terms. https://doi.org/10.1017/CBO9781107360273.006

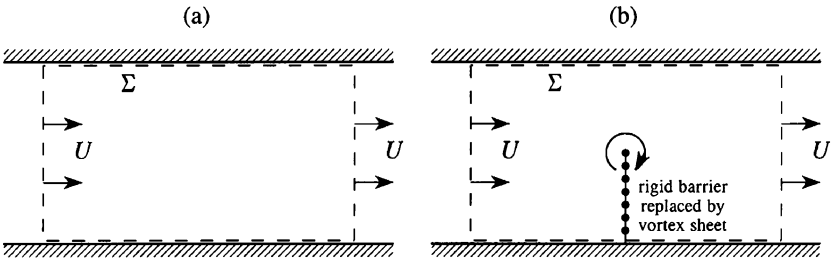

Figure 5.2.1

Corollary 2 If the density $\rho(\mathbf{x})$ is *increased* in some regions of V the new minimum kinetic energy is *increased*.

Corollary 3 A thin, rigid barrier placed in V always increases the minimum kinetic energy. Because the new motion may be conceived as derived from the original merely by increasing indefinitely the density of the fluid layer that would be replaced by the barrier. Alternatively, for a fluid of uniform density, the new motion in the presence of the barrier can be regarded as a possible motion within V *in the absence of the barrier* produced by replacing the barrier by a stationary vortex sheet of appropriate strength. Therefore, the new motion necessarily has greater kinetic energy than in the absence of the vorticity. Figure 5.2.1 illustrates this for a barrier in a rigid duct of uniform cross-section. A normal velocity U is imposed in the same direction at the end-faces of Σ; the vertical barrier in case (b) is imagined to be replaced by a vortex sheet.

Similarly, a rigid obstacle V' of finite volume placed in V always increases the kinetic energy – because the new motion can be regarded as a possible one in which the density of the fluid that would be displaced by the obstacle is increased indefinitely, or because V' can be regarded as a region of stationary fluid separated from the exterior potential flow by a vortex sheet.

A particularly useful consequence is: if an infinitely thin, massless layer of fluid is assumed to occupy the plane of an aperture, the kinetic energy will be *reduced* relative to the case of uniform mean density. The impulsive pressure and velocity gradients vanish in the plane of the layer, so that the motion just upstream and downstream of the layer is normal to the layer. This result often permits a *lower bound* to be derived for the slug length ℓ.

5.3 Duct problems

5.3.1 Circular aperture in a duct (Fock 1941)

Many practical problems involve the transmission of sound through an aperture in a baffle plate spanning a duct. The simple case discussed below in §5.3.3 is

Downloaded from https://www.cambridge.org/core. Charité Universitätsmedizin Berlin, on 20 Dec 2021 at 10:08:47, subject to the Cambridge Core terms of use, available at https://www.cambridge.org/core/terms. https://doi.org/10.1017/CBO9781107360273.006

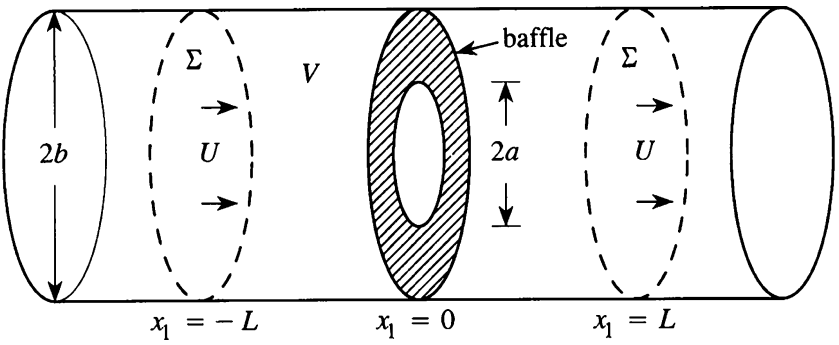

Figure 5.3.1

based on the model of Figure 5.3.1 where the duct is circular cylindrical of radius b and the aperture is circular of radius a placed symmetrically at the centre of a rigid baffle.

Take the x_1 axis along the centre of the duct, directed to the right in the figure, with the origin at the aperture centre. Let a uniform impulsive normal velocity U be imposed over the end-faces of the control surface Σ at $x_1 = \pm L$ enclosing the section V of the duct. When the baffle plate is absent the kinetic energy of incompressible irrotational flow in V is

$$T_o = \frac{\rho_o}{2} \int_V (\nabla\varphi)^2 \, d^3\mathbf{x} = \frac{\rho_o}{2} Q(\varphi_{x_1=L} - \varphi_{x_1=-L})$$

where $\varphi = Ux_1$ is the velocity potential, and $Q = A_d U$ ($A_d = \pi b^2$) is the volume velocity, that is,

$$T_o = \frac{\rho_o}{2} Q^2 \left(\frac{2L}{A_d}\right)$$

In the presence of the baffle and aperture the kinetic energy T will exceed T_o and we can write

$$\frac{2T}{\rho_o Q^2} = \frac{1}{A_d}(2L + \ell_d), \quad \ell_d > 0. \tag{5.3.1}$$

The length ℓ_d governs the kinetic energy as $L \to 0$, when T is wholly determined by the kinetic energy $\rho_o Q^2/2K_o$ of the motion through the aperture, where K_o is the aperture conductivity. Thus

$$K_o \equiv \frac{A}{\ell} = \frac{A_d}{\ell_d}, \tag{5.3.2}$$

where $A = \pi a^2$ is the aperture area, and ℓ is the usual effective slug length of the energised fluid in motion through the aperture.

Downloaded from https://www.cambridge.org/core. Charité Universitätsmedizin Berlin, on 20 Dec 2021 at 10:08:47, subject to the Cambridge Core terms of use, available at https://www.cambridge.org/core/terms. https://doi.org/10.1017/CBO9781107360273.006

The details of potential flow through the aperture are largely uninfluenced by the presence of the duct wall when the aperture is very small, so that $K_o \simeq 2a$ when $a \ll b$. For larger values of a/b, K_o is given by Fock's (1941) analytical approximation

$$K_o = \frac{2a}{1 + \sum_{n=1}^{12} \alpha_n \xi^n}, \quad 0 \le \xi \equiv \frac{a}{b} < 0.95, \tag{5.3.3}$$

where

$$\begin{aligned} \alpha_1 &= -1.40925 & \alpha_7 &= 0.03015 \\ \alpha_2 &= 0 & \alpha_8 &= -0.01641 \\ \alpha_3 &= 0.33818 & \alpha_9 &= 0.01729 \\ \alpha_4 &= 0 & \alpha_{10} &= -0.01248 \\ \alpha_5 &= 0.06793 & \alpha_{11} &= 0.01205 \\ \alpha_6 &= -0.02287 & \alpha_{12} &= -0.00985 \end{aligned}$$

The corresponding variations of K_o/a and ℓ_d/b with a/b are plotted as solid-line curves in Figure 5.3.2.

5.3.2 Rayleigh's method applied to Fock's problem*

The exact potential describing the irrotational flow can be put in the form

$$\varphi = U\left(x_1 + \frac{\ell_d}{2}\mathrm{sgn}(x_1) + \mathrm{sgn}(x_1)\sum_{n=1}^{\infty} A_n \mathrm{J}_0\left(\lambda_n \frac{\varpi}{b}\right) \mathrm{e}^{-\lambda_n |x_1|/b}\right),$$

$$\varpi = \sqrt{x_2^2 + x_3^2}, \tag{5.3.4}$$

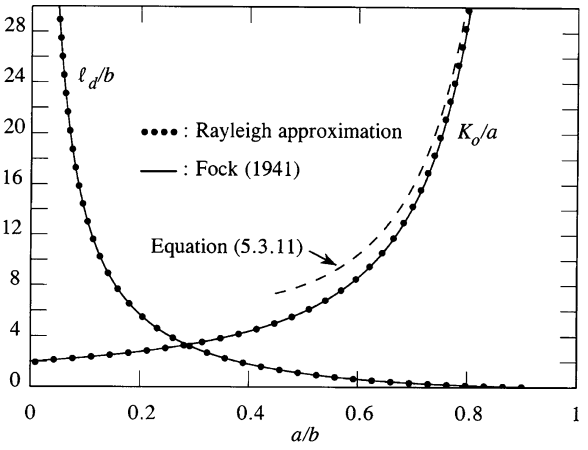

Figure 5.3.2

Downloaded from https://www.cambridge.org/core. Charité Universitätsmedizin Berlin, on 20 Dec 2021 at 10:08:47, subject to the Cambridge Core terms of use, available at https://www.cambridge.org/core/terms. https://doi.org/10.1017/CBO9781107360273.006

where J_ν is the Bessel function of order ν. This satisfies the axisymmetric form of Laplace's equation and has vanishing normal derivative on the duct wall $\varpi = b$ provided λ_n is the nth positive root of $d\mathrm{J}_0(\lambda)/d\lambda \equiv -\mathrm{J}_1(\lambda) = 0$. It is an odd function of x_1, so that $\varphi = 0$ in the plane of the aperture ($x_1 = 0,\ \varpi < a$); the coefficients A_n and ℓ_d are therefore determined from the *dual* conditions

$$\left.\begin{aligned} \varphi &= 0, \quad 0 < \varpi < a \\ \frac{\partial \varphi}{\partial x_1} &= 0, \quad a < \varpi < b \end{aligned}\right\} x_1 = 0.$$

An approximation for ℓ_d can be determined by the method of §5.1.1 by representing the normal velocity within the aperture by

$$v_n = \bar{v} f(\varpi), \quad f(0) = 1, \quad 0 < \varpi < a,$$

for some suitable function $f(\varpi)$. This defines a velocity potential φ' in $x_1 \gtrless 0$ satisfying

$$\left(\frac{\partial \varphi'}{\partial x_1}\right)_{x_1=0} = \begin{cases} \bar{v} f(\varpi), & 0 < \varpi < a \\ 0, & a < \varpi < b, \end{cases} \tag{5.3.5}$$

where

$$\varphi' = U x_1 + \alpha_0 + \sum_{n=1}^{\infty} \alpha_n \mathrm{J}_0\left(\lambda_n \frac{\varpi}{b}\right) \mathrm{e}^{-\lambda_n x_1/b}, \quad \varpi = \sqrt{x_2^2 + x_3^2}, \quad 0 < x_1 < L. \tag{5.3.6}$$

Then $\partial\varphi'/\partial x_1 = U$ at the end-face $x_1 = L$ of Σ, provided L/b is sufficiently large.

The orthogonality condition (Abramowitz & Stegun 1970):

$$\int_0^b \varpi \mathrm{J}_0\left(\lambda_n \frac{\varpi}{b}\right) \mathrm{J}_0\left(\lambda_m \frac{\varpi}{b}\right) d\varpi = \begin{cases} 0, & n \neq m \\ \frac{b^2}{2} \mathrm{J}_0{}^2(\lambda_n), & n = m, \end{cases} \tag{5.3.7}$$

is valid for all $n,\ m \geq 0$, with $\lambda_0 = 0$. When applied to the velocity condition (5.3.5) it yields

$$\left.\begin{aligned} \alpha_n &= \frac{-2\bar{v}}{b\lambda_n \mathrm{J}_0{}^2(\lambda_n)} \int_0^a \varpi f(\varpi) \mathrm{J}_0\left(\lambda_n \tfrac{\varpi}{b}\right) d\varpi, \quad n \geq 1, \\ \bar{v} &= Q \Big/ 2\pi \int_0^a \varpi f(\varpi)\, d\varpi, \quad Q = U A_d, \quad n = 0, \end{aligned}\right\} \tag{5.3.8}$$

The kinetic energy T' of the whole flow in $-L < x_1 < L$ is twice that in $0 < x_1 < L$, i.e.

$$T' = 2\pi\rho_o \int_0^b \left[\left(\varphi' \frac{\partial \varphi'}{\partial x_1}\right)_{x_1=L} - \left(\varphi' \frac{\partial \varphi'}{\partial x_1}\right)_{x_1=0}\right] \varpi\, d\varpi$$

Downloaded from https://www.cambridge.org/core. Charité Universitätsmedizin Berlin, on 20 Dec 2021 at 10:08:47, subject to the Cambridge Core terms of use, available at https://www.cambridge.org/core/terms. https://doi.org/10.1017/CBO9781107360273.006

$$\therefore \quad \frac{2T'}{\rho_o Q^2} = \frac{2L}{A_d} - \frac{4\pi\bar{v}}{Q^2}\sum_{n=1}^{\infty}\alpha_n \int_0^a \varpi f(\varpi) \mathrm{J}_0\left(\lambda_n \frac{\varpi}{b}\right) d\varpi.$$

Hence, combining this result with (5.3.1), (5.3.2), (5.3.8) and Kelvin's theorem that $T \leq T'$, we find

$$\frac{1}{K_o} = \frac{\ell_d}{A_d} \leq \frac{2}{\pi b\left(\int_0^a \varpi f(\varpi)\, d\varpi\right)^2} \sum_{n=1}^{\infty} \frac{\left(\int_0^a \varpi f(\varpi) \mathrm{J}_0\left(\lambda_n \frac{\varpi}{b}\right) d\varpi\right)^2}{\lambda_n \mathrm{J}_0^2(\lambda_n)}. \tag{5.3.9}$$

Two-parameter approximation

The approximation

$$f(\varpi) = \frac{1}{\sqrt{1-\varpi^2/a^2}}\left(1 + \mu\frac{\varpi^2}{a^2} + \mu'\frac{\varpi^4}{a^4}\right), \quad 0 < \varpi < a,$$

exhibits the kind of singularity expected at the edge of an aperture (cf. (5.1.4)). In this case (5.3.9) becomes

$$\frac{1}{K_o} = \frac{\ell_d}{A_d} \leq \frac{2b}{\pi a^2\left(1 + \frac{2\mu}{3} + \frac{8\mu'}{15}\right)^2} \sum_{n=1}^{\infty} \frac{\left(\sin\lambda_n' + \mu\chi(\lambda_n') + \mu'\chi'(\lambda_n')\right)^2}{\lambda_n^3 \mathrm{J}_0^2(\lambda_n)} \tag{5.3.10}$$

where $\lambda_n' = \lambda_n a/b$ and

$$\chi(\lambda_n') = \sin\lambda_n' - \frac{(\sin\lambda_n' - \lambda_n'\cos\lambda_n')}{\lambda_n'^2}$$

$$\chi'(\lambda_n') = \sin\lambda_n' - \frac{2(\sin\lambda_n' - \lambda_n'\cos\lambda_n')}{\lambda_n'^2} + \frac{3\{(3-\lambda_n'^2)\sin\lambda_n' - 3\lambda_n'\cos\lambda_n'\}}{\lambda_n'^4}.$$

Predictions of K_o and the slug length $\ell = \ell_d A/A_d$ are obtained by minimising the right hand side of (5.3.10) (by the method of §5.1.3), and replacing '$\leq$' by '$=$'. The results (• • • in Figure 5.3.2) agree well with Fock's formula (5.3.3) except when $a \sim b$. In this limit it is found (Question 5.2, **Problems 5**) that

$$\frac{1}{K_o} = \frac{\ell_d}{A_d} \sim \frac{1}{b}\left(1 - \frac{a}{b}\right)^2. \tag{5.3.11}$$

K_o/a calculated from this formula is also shown in Figure 5.3.2 (- - - -).

5.3.3 Example: Sound transmission through a baffle-plate aperture

This is similar to the example in §3.3.6, but without the bias flow. A long wavelength, time-harmonic pressure wave $\hat{p}_I e^{ik_o x_1}$ is incident from $x_1 < 0$

Downloaded from https://www.cambridge.org/core. Charité Universitätsmedizin Berlin, on 20 Dec 2021 at 10:08:47, subject to the Cambridge Core terms of use, available at https://www.cambridge.org/core/terms. https://doi.org/10.1017/CBO9781107360273.006

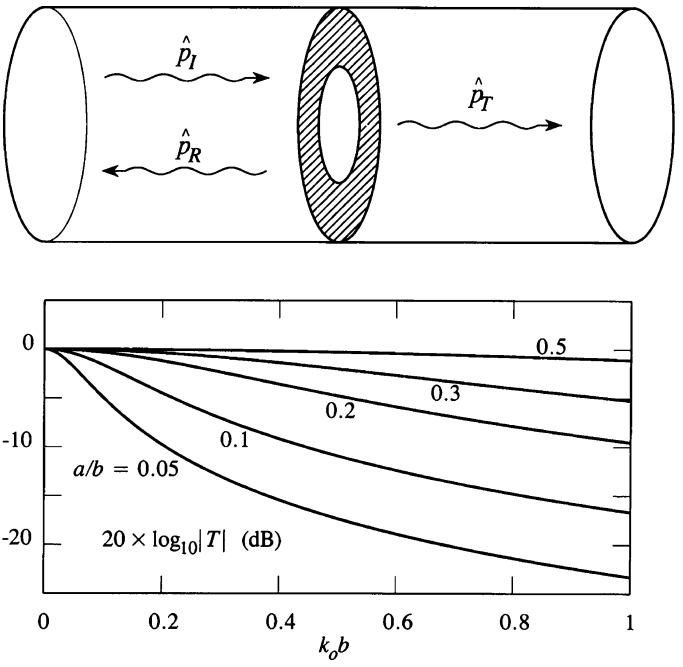

Figure 5.3.3

on the baffle, producing reflected and transmitted waves $\hat{p}_R e^{-ik_o x_1}$, $\hat{p}_T e^{ik_o x_1}$ (Figure 5.3.3).

The volume flux through the aperture is

$$\hat{Q} = \frac{K_o(\hat{p}_I + \hat{p}_R - \hat{p}_T)}{-i\omega\rho_o} = \frac{\hat{p}_T A_d}{\rho_o c_o} = \frac{(\hat{p}_I - \hat{p}_R)A_d}{\rho_o c_o}.$$

Therefore $\hat{p}_R = R\hat{p}_I$ and $\hat{p}_T = T\hat{p}_I$, where the reflection and transmission coefficients R, T are given by

$$R = \frac{k_o \ell_d}{(2i + k_o \ell_d)}, \quad T = \frac{2i}{(2i + k_o \ell_d)},$$

and $\ell_d = A_d/K_o$ is determined in terms of a/b by Fock's formula (5.3.3). There is no mechanism for dissipating energy in this problem, so that the attenuation $20 \times \log_{10}|T|$ dB of the transmitted sound is caused by reflection alone. It is plotted as a function of $k_o b$ in the figure for several values of a/b. The long wavelength assumption implies that $k_o b$ must be smaller than about 1, but $k_o \ell_d$ can still be very large when a/b is small. The attenuation becomes minimal when $a/b \geq 0.5$.

Downloaded from https://www.cambridge.org/core. Charité Universitätsmedizin Berlin, on 20 Dec 2021 at 10:08:47, subject to the Cambridge Core terms of use, available at https://www.cambridge.org/core/terms. https://doi.org/10.1017/CBO9781107360273.006

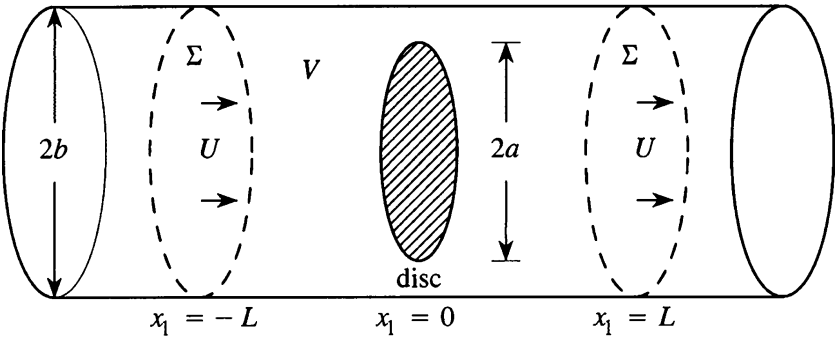

Figure 5.3.4

5.3.4 Duct with an annular aperture*

There is no simple formula for K_o when the baffle plate is replaced by a rigid disc of radius $a < b$ (Figure 5.3.4). This is a primitive model of a *flame holder* in an industrial burner – a uniform fuel-air mixture flowing along the duct from the left (say) is ignited at the disc, producing a nominally axisymmetric flame trailing downstream from the edge of the disc. An understanding of the acoustic properties of this system depends on a knowledge of the conductivity.

Rayleigh's formula (5.3.9) becomes

$$\frac{1}{K_o} = \frac{\ell_d}{A_d} \leq \frac{2}{\pi b\left(\int_a^b \varpi f(\varpi)\, d\varpi\right)^2} \sum_{n=1}^{\infty} \frac{\left(\int_a^b \varpi f(\varpi) \mathrm{J}_0\left(\lambda_n \frac{\varpi}{b}\right) d\varpi\right)^2}{\lambda_n \mathrm{J}_0^2(\lambda_n)}, \tag{5.3.12}$$

where $v_n = \bar{v} f(\varpi)$ represents an assumed normal velocity distribution in the annular region $x_1 = 0,\ a < \varpi < b$ between the edge of the disc and the duct wall.

Let

$$y = b - \varpi, \quad h = b - a, \quad \epsilon = \frac{h}{b}$$

and consider

$$f(\varpi) = \frac{1}{\sqrt{1 - y^2/h^2}} \left(1 + \mu \frac{y^2}{h^2} + \mu' \frac{y^4}{h^4}\right), \quad a < \varpi < b, \quad (0 < y < h),$$

which has the usual edge singularity, but is finite elsewhere between the disc and the duct wall. Then (5.3.12) supplies

Downloaded from https://www.cambridge.org/core. Charité Universitätsmedizin Berlin, on 20 Dec 2021 at 10:08:47, subject to the Cambridge Core terms of use, available at https://www.cambridge.org/core/terms. https://doi.org/10.1017/CBO9781107360273.006

$$\frac{1}{K_o} = \frac{\ell_d}{A_d} \leq \frac{2}{\pi b\left\{\frac{\pi}{2} - \epsilon + \mu\left(\frac{\pi}{4} - \frac{2\epsilon}{3}\right) + \mu'\left(\frac{3\pi}{16} - \frac{8\epsilon}{15}\right)\right\}^2} \times \sum_{n=1}^{\infty} \frac{\left(I_{0n} + \mu I_{2n} + \mu' I_{4n}\right)^2}{\lambda_n \mathrm{J}_0^2(\lambda_n)}$$

where

$$I_{mn} = \int_0^{\frac{\pi}{2}} \sin^m\theta(1 - \epsilon\sin\theta)\mathrm{J}_0\Big(\lambda_n(1 - \epsilon\sin\theta)\Big)\,d\theta.$$

The corresponding predictions of K_o/b and ℓ_d/b are displayed (• • •) in Figure 5.3.5. Independent confirmation is obtained by numerical solution of Laplace's equation $\nabla^2\varphi = 0$, where $\varphi(x_1, \varpi)$ is the velocity potential of flow along the duct past the disc, normalised such that $\partial\varphi/\partial x_1 \to 1$ when $|x_1|/b$ is large. Then (cf. equation (5.3.4))

$$\ell_d = \int_{-\infty}^{\infty}\left(\frac{\partial\varphi}{\partial x_1}(x_1, \varpi) - 1\right)dx_1,$$

where the integration path is parallel to the x_1 axis with $a < \varpi < b$. The results (——— in Figure 5.3.5) are in good agreement with Rayleigh's approximation.

Evidently, the potential flow resistance offered by the disc does not become significant until $a \sim b$; indeed, $K_o/b > 3$ when $a/b < 0.9$.

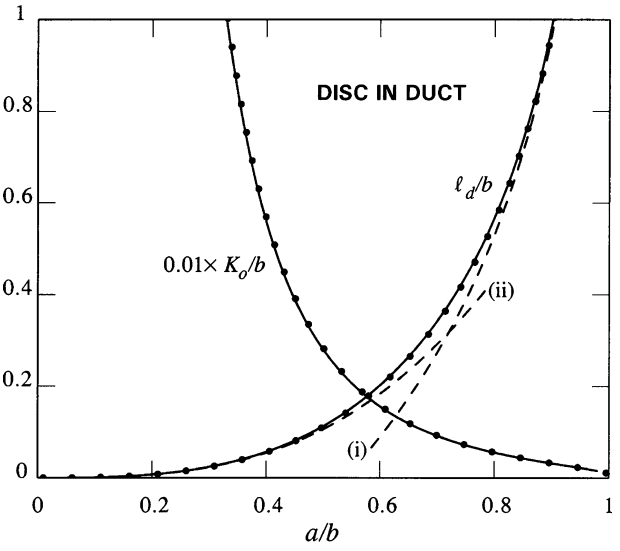

Figure 5.3.5

Downloaded from https://www.cambridge.org/core. Charité Universitätsmedizin Berlin, on 20 Dec 2021 at 10:08:47, subject to the Cambridge Core terms of use, available at https://www.cambridge.org/core/terms. https://doi.org/10.1017/CBO9781107360273.006

5.3.5* *Example: Analytical approximations for the annular aperture*

Consider the limiting cases (i) $1-\xi \ll 1$ and (ii) $\xi \ll 1$, where $\xi = a/b$.

(i) Narrow gap, $1-\xi \ll 1$

A narrow gap between the disc and the duct wall behaves as a circumferential ring source of strength $Q/2\pi b$ per unit length, in terms of which the velocity potential in $x_1 > 0$ at distances $x_1 \gg b-a$ can be assumed to satisfy $\partial\varphi/\partial x_1 = (Q/2\pi b)\delta(\varpi - b + 0)$ as $x_1 \to +0$, so that (cf. (5.3.4))

$$\varphi = Ux_1 + \frac{U\ell_d}{2} - \frac{Q}{\pi b}\sum_{n=1}^{\infty}\frac{\mathrm{J}_0(\lambda_n\varpi/b)}{\lambda_n \mathrm{J}_0(\lambda_n)}\mathrm{e}^{-\lambda_n x_1/b}, \quad x_1 > 0,$$

$$\sim \frac{U\ell_d}{2} + \frac{1.5301Q}{2\pi b} + \frac{Q}{\pi^2 b}\ln\left(\frac{\pi x_1}{8b}\right), \text{ for } x_1 \ll b,\ \varpi = b, \quad (5.3.13)$$

where $U = Q/\pi b^2$.

Similarly, in the immediate neighbourhood of the gap between the disc and duct wall the velocity potential is locally two dimensional and can be approximated by conformal mapping. By selecting the particular solution that vanishes at $x_1 = 0,\ a < \varpi < b$ (so that φ is an odd function of x_1), we find

$$\varphi \sim \frac{Q}{\pi^2 b}\ln\left(\frac{2x_1}{b-a}\right), \text{ for } x_1 \gg h,\ \varpi = b.$$

This will agree with (5.3.13) provided

$$\frac{\ell_d}{b} = \frac{2}{\pi}\ln\left(\frac{0.4604}{1-\xi}\right), \quad (\xi = a/b).$$

(ii) Wide gap, $\xi \equiv a/b \ll 1$

The exact velocity potential can be expanded as in (5.3.4)

$$\varphi = U\left(x_1 + \frac{\ell_d}{2} + \sum_{n=1}^{\infty} A_n \mathrm{J}_0\left(\lambda_n\frac{\varpi}{b}\right)\mathrm{e}^{-\lambda_n x_1/b}\right), \quad x_1 > 0, \qquad (5.3.14)$$

where $\varphi = 0$ in the plane of the gap between the disc and the duct wall. When the disc is very small $\varphi/U \approx X_1 =$ the x_1 component of the Kirchhoff vector for a disc (defined as in §2.9.1f). This vanishes in the plane of the disc when $\varpi > a$, and $X_1 = \frac{2}{\pi}\sqrt{a^2 - \varpi^2}$ on the face $x_1 = +0$ of the disc. Hence, setting $x_1 = +0$ in (5.3.14) and replacing the left hand side by $\varphi = \frac{2U}{\pi}\sqrt{a^2 - \varpi^2}$, the orthogonality relation (5.3.7) applied for $n = 0$ yields the small disc approximation

$$\frac{\ell_d}{b} = \frac{8\xi^3}{3\pi}, \quad \xi \equiv \frac{a}{b} \ll 1.$$

Downloaded from https://www.cambridge.org/core. Charité Universitätsmedizin Berlin, on 20 Dec 2021 at 10:08:47, subject to the Cambridge Core terms of use, available at https://www.cambridge.org/core/terms. https://doi.org/10.1017/CBO9781107360273.006

The small and large gap approximations are plotted as the broken line curves in Figure 5.3.5, labelled (i) and (ii) respectively. A smooth transition between the two is given by

$$\frac{\ell_d}{b} = \frac{0.05 \ln\left\{e^{f_0(\xi)} + e^{f_1(\xi)}\right\}}{1 - 0.55\xi}, \tag{5.3.15}$$

where

$$f_0(\xi) = 16.98(1 - 0.55\xi)\xi^3, \quad f_1(\xi) = 12.73(1 - 0.55\xi) \ln\left(\frac{0.4604}{1 - \xi}\right),$$

which provides an excellent approximation to the numerical results of Figure 5.3.5.

5.4 The end correction

A time-harmonic wave $p = \hat{p}_I e^{ik_o x_1}$ (with implied time dependence $e^{-i\omega t}$) is incident from within on the open end of a circular cylindrical duct of acoustically compact radius b (Figure 5.4.1). The coordinate origin is at the centre O of the open end and the negative x_1 axis extends back into the duct. A plane wave $p_R = R\hat{p}_I e^{-ik_o x_1}$ is reflected at the open end, from which sound is also radiated into free space.

It is convenient to work in terms of the velocity potential φ rather than the pressure. In the compact approximation the motion in region A of the opening can be regarded as incompressible, and can be expressed in terms of the potential of axisymmetric flow from a circular cylindrical duct (§2.9.1e). Outside

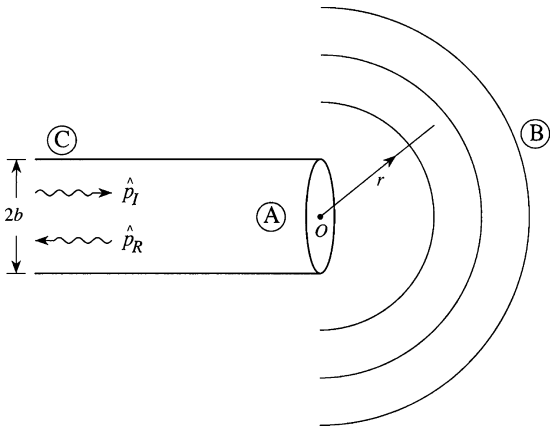

Figure 5.4.1

Downloaded from https://www.cambridge.org/core. Charité Universitätsmedizin Berlin, on 20 Dec 2021 at 10:08:47, subject to the Cambridge Core terms of use, available at https://www.cambridge.org/core/terms. https://doi.org/10.1017/CBO9781107360273.006

the duct at B, at distances $r = |\mathbf{x}| \gg b$ the potential φ resembles that for a point source $\propto \mathrm{e}^{ik_o r}/4\pi r$. Therefore, for an incident wave of unit amplitude we can put

$$\varphi = \mathrm{e}^{ik_o x_1} + R\mathrm{e}^{-ik_o x_1} \quad \text{for } |x_1| \gg b \text{ within the duct at C} \tag{5.4.1a}$$

$$= \alpha + \beta\varphi^*(\mathbf{x}) \quad \text{at A} \tag{5.4.1b}$$

$$= -\frac{\gamma A_d \mathrm{e}^{ik_o r}}{4\pi r} \quad \text{at B,} \tag{5.4.1c}$$

where the reflection coefficient R and the constants $\alpha,\ \beta,\ \gamma$ are to be determined, $A_d = \pi b^2$ is the duct cross-sectional area, and $\varphi^*(\mathbf{x})$ is the velocity potential of incompressible axisymmetric flow from the open end, normalised such that

$$\left.\begin{aligned} \varphi^*(\mathbf{x}) &\approx x_1 - \ell_E \quad \text{as } x_1 \to -\infty \text{ within the duct,} \\ &\approx -A_d/4\pi r \quad \text{as } |\mathbf{x}| \to \infty \text{ outside the duct.} \end{aligned}\right\} \tag{5.4.2}$$

The length ℓ_E ($\simeq 0.6127b$) is called the *end correction* (see Question 5.5, **Problems 5**).

The coefficients in (5.4.1a–c) are found by 'matching' the different expressions for φ in regions of overlap. Thus, within the duct in the interval $b \ll |x_1| \ll \lambda$ (where $\lambda = 2\pi/k_o$ is the acoustic wavelength) the formulae (5.4.1a, b) yield

$$\varphi \approx 1 + R + ik_o x_1(1 - R) = \alpha + \beta(x_1 - \ell_E).$$

Therefore

$$1 + R = \alpha - \beta\ell_E, \quad ik_o(1 - R) = \beta.$$

Similarly, in the interval $b \ll r \ll \lambda$ outside the duct we find from (5.4.1b, c)

$$\alpha = -\frac{i\gamma k_o A_d}{4\pi}, \quad \beta = \gamma.$$

In particular, the solutions of these simultaneous equations give for the reflection coefficient (correct to $O(k_o^2 b^2)$)

$$R = -\left(\frac{1 + ik_o(\ell_E + ik_o A_d/4\pi)}{1 - ik_o(\ell_E + ik_o A_d/4\pi)}\right) \approx -\mathrm{e}^{2ik_o(\ell_E + ik_o A_d/4\pi)}. \tag{5.4.3}$$

Thus the pressure in the duct becomes

$$p = \hat{p}_I\left(\mathrm{e}^{ik_o x_1} + R\mathrm{e}^{-ik_o x_1}\right), \quad x_1 \ll 0,$$

and the fraction of the incident acoustic power $A_d|\hat{p}_I|^2/2\rho_o c_o$ radiated from the open end is

$$1 - |R|^2 = 1 - \mathrm{e}^{-k_o^2 A_d/\pi} \sim (k_o b)^2.$$

Downloaded from https://www.cambridge.org/core. Charité Universitätsmedizin Berlin, on 20 Dec 2021 at 10:08:47, subject to the Cambridge Core terms of use, available at https://www.cambridge.org/core/terms. https://doi.org/10.1017/CBO9781107360273.006

When this radiation damping is ignored ($k_o^2 b^2 \ll 1$) the pressure within the duct can be written

$$p = \hat{p}_I \left(e^{ik_o x_1} - e^{-ik_o(x_1 - 2\ell_E)} \right) \equiv 2i\,\hat{p}_I e^{ik_o \ell_E} \sin\Big(k_o(x_1 - \ell_E)\Big),$$

which formally vanishes at $x_1 = \ell_E$ *outside* the duct. In other words, to this order of approximation the solution coincides with that obtained by requiring that $p = 0$ at $x_1 = \ell_E$, so that the classical low frequency theory (§1.3.3) remains valid provided the effective length of the duct is increased by ℓ_E.

The end correction is proportional to the kinetic energy of the non-uniform fluid motion near the open end, in just the same way that the length ℓ_d determines the kinetic energy of incompressible motion near a barrier in a duct. Indeed, if $L \gg \ell_E$ and T denotes the kinetic energy in a compact section of the duct $-L < x_1 < 0$ and in the exit flow, produced by motion of a plane boundary Σ at $x_1 = -L$ at speed U in the x_1 direction, then because $\varphi^* \approx x_1 - \ell_E$ near Σ,

$$\frac{2T}{\rho_o Q^2} \equiv \frac{1}{A_d^2} \int_V (\nabla \varphi^*)^2 \, d^3\mathbf{x} = -\frac{1}{A_d^2} \int_\Sigma \varphi^* \frac{\partial \varphi^*}{\partial x_1} dS \equiv \frac{1}{A_d}(L + \ell_E), \tag{5.4.4}$$

where V is the fluid region to the right of Σ, including the flow outside the duct exit, and $Q = A_d U$.

5.4.1* *Cylindrical duct with a small axisymmetric opening*

Rayleigh's method is not easily applied to determine ℓ_E for the cylindrical duct (Figure 5.4.1) because there is no simple formula for the kinetic energy of the exterior flow. However, for this and the more general case (Figure 5.4.2) where the opening consists of an axisymmetric circular aperture of radius $a < b$ in a rigid baffle spanning the duct exit, equation (5.4.2) implies that

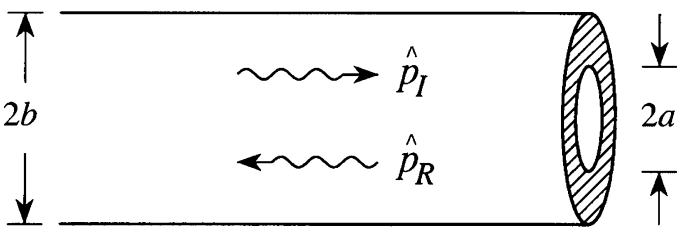

Figure 5.4.2

Downloaded from https://www.cambridge.org/core. Charité Universitätsmedizin Berlin, on 20 Dec 2021 at 10:08:47, subject to the Cambridge Core terms of use, available at https://www.cambridge.org/core/terms. https://doi.org/10.1017/CBO9781107360273.006

$$\ell_E = \int_{-\infty}^{0} \left(\frac{\partial \varphi *}{\partial x_1} - 1 \right) dx_1 + \int_0^{\infty} \frac{\partial \varphi *}{\partial x_1} \, dx_1, \tag{5.4.5}$$

where the integration is along any parallel to the duct axis passing through the aperture. The integrals can be evaluated by determining φ^* by numerical integration of Laplace's equation $\nabla^2 \varphi^* = 0$.

The potential $\varphi^* = \varphi^*(x_1, \varpi)$, $\varpi = (x_2^2 + x_3^2)^{\frac{1}{2}}$, defines an axisymmetric flow for which $\partial \varphi^* / \partial x_1 = 1$ at $x_1 = -L$ within the duct when $L \gg b$, and $\varphi^* \sim -A_d / 4\pi r$ at large distance r outside the duct. A simpler numerical problem is obtained by introducing the associated Stokes stream function $\psi^*(x_1, \varpi)$ defined by

$$\frac{\partial \varphi^*}{\partial x_1} = \frac{1}{\varpi} \frac{\partial \psi^*}{\partial \varpi}, \quad \frac{\partial \varphi^*}{\partial \varpi} = -\frac{1}{\varpi} \frac{\partial \psi^*}{\partial x_1}. \tag{5.4.6}$$

The Laplace equation $\nabla^2 \varphi^* = 0$ is then satisfied identically and the condition curl $\mathbf{v} = 0$ that the flow is irrotational implies that

$$\frac{\partial^2 \psi^*}{\partial x_1^2} + \frac{\partial^2 \psi^*}{\partial \varpi^2} - \frac{1}{\varpi} \frac{\partial \psi^*}{\partial \varpi} = 0. \tag{5.4.7}$$

This equation is solved by finite differences inside a large rectangular region of the $x_1 \varpi$-plane indicated (- - - -) in Figure 5.4.3, the lower side of which extends from $x_1 = -L$ to $x_1 = x_R \gg b$ along the x_1-axis of symmetry. Uniform flow at unit speed within the duct requires that $\psi^* = \frac{1}{2} \varpi^2$ on the section Σ_L ($x_1 = -L$, $0 < \varpi < b$) of the rectangle. The stream function is constant along streamlines of the flow, so that $\psi^* = 0$ on the x_1 axis, and $\psi^* = \frac{1}{2} b^2$ on Σ_D, the interior and exterior surfaces of duct wall and the solid section ($x_1 = 0$, $a < \varpi \leq b$) of the duct exit. The exterior flow at large distances from the aperture resembles that of a point source at $\mathbf{x} = 0$ with $\varphi^* \simeq -A_d / 4\pi r$, for which

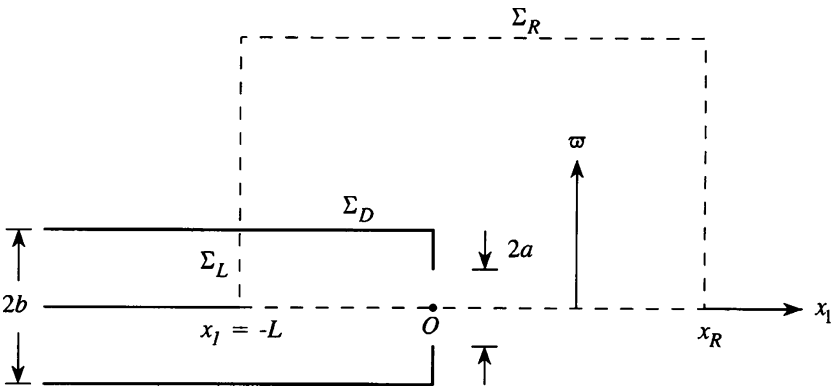

Figure 5.4.3

Downloaded from https://www.cambridge.org/core. Charité Universitätsmedizin Berlin, on 20 Dec 2021 at 10:08:47, subject to the Cambridge Core terms of use, available at https://www.cambridge.org/core/terms. https://doi.org/10.1017/CBO9781107360273.006

$$\psi^* \simeq \frac{A_d}{4\pi}\left(1 - \frac{x_1}{(x_1^2 + \varpi^2)^{\frac{1}{2}}}\right).$$

This formula can be used to define the boundary values of ψ^* on the distant exterior edges Σ_R of the rectangle, provided L and x_R are sufficiently large.

The numerical solution determines ψ^* inside the rectangle in terms of the boundary values and the value of ψ^* on Σ_D. The following approximation to (5.4.5) is then evaluated

$$\ell_E \approx \int_{-L}^{0}\left(\frac{1}{\varpi}\frac{\partial\psi^*}{\partial\varpi}(x_1, \varpi) - 1\right) dx_1 + \int_0^{x_R} \frac{1}{\varpi}\frac{\partial\psi^*}{\partial\varpi}(x_1, \varpi)\, dx_1 + \frac{A_d}{4\pi\left(x_R^2 + \varpi^2\right)^{\frac{1}{2}}} \tag{5.4.8}$$

where the path of integration passes through the aperture parallel to the duct axis. The solid line curves (———) in Figure 5.4.4 show the calculated values of ℓ_E/b and $K_o/b = \pi b/\ell_E$ plotted as functions of $\xi = a/b$. The numerical results are well approximated (• • • in Figure 5.4.4) by the formula

$$\frac{\pi b}{\ell_E} = \frac{K_o}{b} \simeq \frac{2\xi(1 - 1.2032\xi^8 + 0.8844\xi^9)}{1 - 0.735\xi}, \quad \xi = \frac{a}{b}. \tag{5.4.9}$$

When $a = b$ ($\xi = 1$) the end correction coincides with $\ell_E \simeq 0.6127b$ obtained using the exact formula for irrotational flow from a cylinder (Question 5.5, **Problems 5**). For a very small aperture ($a \ll b$) the conductivity

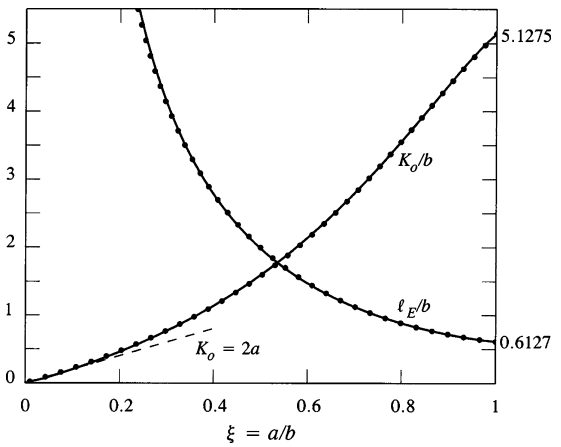

Figure 5.4.4

Downloaded from https://www.cambridge.org/core. Charité Universitätsmedizin Berlin, on 20 Dec 2021 at 10:08:47, subject to the Cambridge Core terms of use, available at https://www.cambridge.org/core/terms. https://doi.org/10.1017/CBO9781107360273.006

$K_o \sim 2a$ (- - - - in Figure 5.4.4) and ℓ_E increases indefinitely. Therefore, $k_o \ell_E$ is not necessarily small for long wavelength sound $p = \hat{p}_I e^{ik_o x_1}$ incident from within on the open end of the duct. If $k_o^2 b^2 \ll 1$ the reflection coefficient (5.4.3) becomes

$$R = -\left(\frac{1 + ik_o\ell_E}{1 - ik_o\ell_E}\right) = -e^{2i\Theta}, \quad \text{where} \quad \Theta = \tan^{-1}(k_o\ell_E).$$

Thus $\Theta = \frac{\pi}{2}$ when $\xi \to 0$, and the reflection coefficient reverts to its value $R = 1$ for a closed end. Similarly, the pressure near the open end is now

$$p = \hat{p}_I \left(e^{ik_o x_1} - e^{-i(k_o x_1 - 2\Theta)}\right) \equiv 2i\hat{p}_I e^{i\Theta} \sin\left(k_o x_1 - \Theta\right),$$

so that the effective acoustic end correction is frequency-dependent and equal to $\Theta/k_o = \tan^{-1}(k_o\ell_E)/k_o < \lambda/4$, where $\lambda = 2\pi/k_o$ is the acoustic wavelength.

5.4.2 End correction for a flanged duct (Rayleigh 1870)*

Rayleigh's method is easily applied to determine ℓ_E when the exit geometry of an open duct is modified by the addition of a large *flange* (Figure 5.4.5). Let the duct be circular cylindrical of radius b, and consider the two-parameter model (5.1.5) (with a replaced by b) for the exit plane velocity (at $x_1 = 0$), with a control surface Σ in the duct a $x_1 = -L$. When Σ is set in motion at speed U towards the open end the kinetic energy T_E of the motion outside the

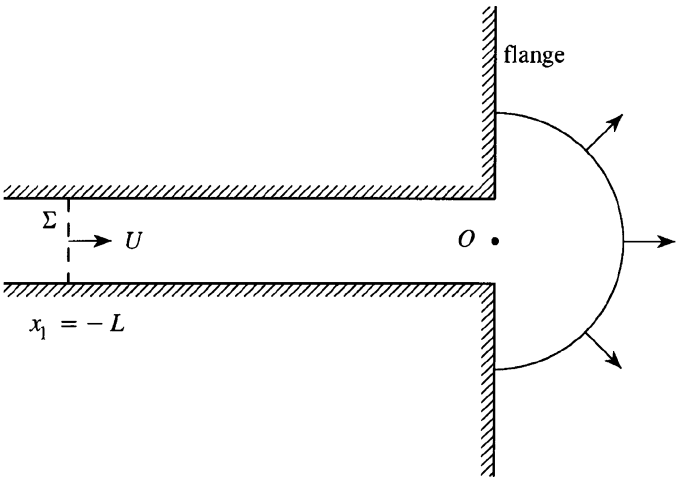

Figure 5.4.5

Downloaded from https://www.cambridge.org/core. Charité Universitätsmedizin Berlin, on 20 Dec 2021 at 10:08:47, subject to the Cambridge Core terms of use, available at https://www.cambridge.org/core/terms. https://doi.org/10.1017/CBO9781107360273.006

duct is obtained by taking *half* of that in the corresponding formula (5.1.7) and replacing a by b:

$$\frac{2T_E}{\rho_o Q^2} = \frac{8\left(1+\frac{14\mu}{15}+\frac{5\mu^2}{21}+\frac{314\mu'}{525}+\frac{214\mu\mu'}{675}+\frac{89\mu'^2}{825}\right)}{3\pi^2 b\left(1+\frac{\mu}{2}+\frac{\mu'}{3}\right)^2},$$

where $Q = A_d U$.

Within the duct

$$\varphi(\mathbf{x}) = Ux_1 + \alpha_0 + \frac{4Ub}{\left(1+\frac{\mu}{2}+\frac{\mu'}{3}\right)}\sum_{n=1}^{\infty}\frac{\left\{\mu+2\mu'\left(1-\frac{8}{\lambda_n^2}\right)\right\}\mathrm{J}_0\left(\lambda_n\frac{\varpi}{b}\right)}{\lambda_n^3\mathrm{J}_0(\lambda_n)}\mathrm{e}^{\lambda_n x_1/b},$$

$$x_1 < 0, \quad \varpi < b,$$

and the kinetic energy T_I of the interior flow in the interval $-L < x_1 < 0$ is therefore

$$\frac{2T_I}{\rho_o Q^2} = \frac{L}{A_d} + \frac{16}{\pi b\left(1+\frac{\mu}{2}+\frac{\mu'}{3}\right)^2}\sum_{n=1}^{\infty}\frac{\left[\mu+2\mu'\left(1-\frac{8}{\lambda_n^2}\right)\right]^2}{\lambda_n^5}.$$

Hence, because the kinetic energy of irrotational flow $T \le T_I + T_E$ we have from (5.4.4)

$$\frac{\ell_E}{b} \le \left\{\frac{8}{3\pi}\left[1+\frac{14\mu}{15}+\frac{5\mu^2}{21}+\frac{314\mu'}{525}+\frac{214\mu\mu'}{675}+\frac{89\mu'^2}{825}\right]\right.$$
$$\left. + 16\sum_{n=1}^{\infty}\frac{1}{\lambda_n^5}\left[\mu+2\mu'\left(1-\frac{8}{\lambda_n^2}\right)\right]^2\right\}\Big/\left(1+\frac{\mu}{2}+\frac{\mu'}{3}\right)^2.$$

The right hand side assumes its minimum value when $\mu = -1.0120$, $\mu' = 1.9515$, leading to the approximation $\ell_E = 0.8242b$. This exceeds the end correction $\sim 0.6127b$ for the *unflanged* duct (Figure 5.4.4), as expected from Corollary 3 of Kelvin's theorem (§5.2.1) that the introduction of any kind of barrier *increases* the minimum kinetic energy. We can further assert that ℓ_E must exceed $\pi b/4 \sim 0.785b$, because the kinetic energy of ideal flow is *decreased* when a thin massless layer of fluid is interposed in the plane of the duct mouth. In this case the motion within the duct has uniform velocity U with $2T_I/\rho_o Q^2 \equiv L/A_d$, but the exterior motion is exactly the same as that on one side of a circular aperture in a thin wall, for which $\ell/b = \frac{\pi}{4}$ (equal to half of the 'exact value' in Table 5.1.1).

The end correction for a flanged circular cylindrical duct of radius b that communicates with free space via an axisymmetric circular aperture of radius $a < b$ (Figure 5.4.6) is given approximately by the formula

Downloaded from https://www.cambridge.org/core. Charité Universitätsmedizin Berlin, on 20 Dec 2021 at 10:08:47, subject to the Cambridge Core terms of use, available at https://www.cambridge.org/core/terms. https://doi.org/10.1017/CBO9781107360273.006

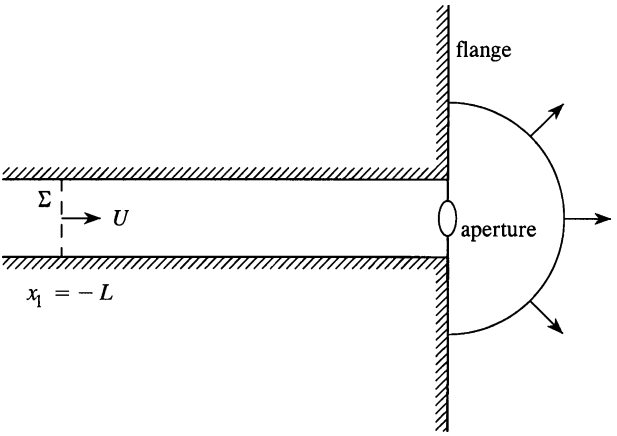

Figure 5.4.6

$$\frac{\pi b}{\ell_E} = \frac{K_o}{b} \simeq \frac{2\xi(1 - 0951\xi^6 + 0.618\xi^7)}{1 - 0.65\xi}, \quad \xi = \frac{a}{b}. \tag{5.4.10}$$

K_o/b and ℓ_E/b are plotted against ξ (• • •) in the figure accompanying Question 5.3 of **Problems 5**.

5.5 Duct of variable diameter

The effective slug length for a circular cylindrical aperture in a wall of finite thickness h was discussed in §3.3.2. If the end correction is ℓ_E then to a good approximation

$$\ell \equiv \frac{A}{K_o} = h + 2\ell_E,$$

where A is the aperture cross-sectional area.

The contribution $2\ell_E$ of the end correction is often negligible when h is large. Upper and lower bounds for ℓ, or more precisely for $1/K_o$, for the more general case of an axisymmetric, elongated and approximately straight duct (Figure 5.5.1) can be deduced from Kelvin's theorem. The introduction of an infinite number of imaginary plane, massless, fluid laminae perpendicular to the axis of symmetry and of area $S(x_1)$ equal to the local cross-section corresponds to a new system of *reduced* kinetic energy and can therefore be used to obtain a *lower* bound for $1/K_o$. The contribution to this reduced kinetic energy T'', say, from a section of the duct between two laminae separated by dx_1 is given by

Downloaded from https://www.cambridge.org/core. Charité Universitätsmedizin Berlin, on 20 Dec 2021 at 10:08:47, subject to the Cambridge Core terms of use, available at https://www.cambridge.org/core/terms. https://doi.org/10.1017/CBO9781107360273.006

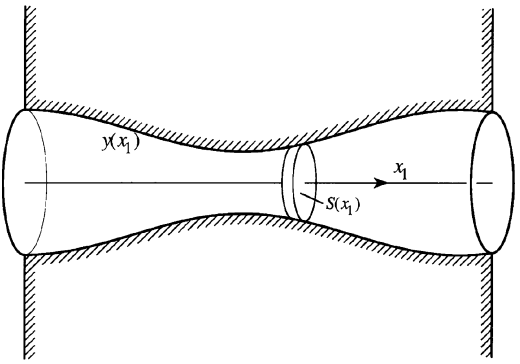

Figure 5.5.1

$$d\left(\frac{2T''}{\rho_o Q^2}\right) = \frac{dx_1}{S(x_1)}.$$

If T denotes the actual (irrotational) kinetic energy of the motion *within the duct* then $T'' \leq T$, where equality occurs only for a uniform duct when $\ell_E \ll h$. Therefore

$$\frac{1}{K_o} \geq \int \frac{dx_1}{S(x_1)},$$

the integration being along the axis of the channel.

An upper limit is found by calculating the kinetic energy of any other incompressible motion through the channel that is compatible with the boundary conditions. This can be done by introducing constraints in the form of massless, *rigid* pistons (or vortex sheets), causing the axial component of velocity u to be constant over each piston, such that $u(x_1) = Q/S(x_1)$. The radial velocity v, say, is also required to calculate the kinetic energy. This is done by using the continuity equation

$$\frac{1}{\varpi}\frac{\partial}{\partial \varpi}(\varpi v) + \frac{\partial}{\partial x_1}\left(\frac{Q}{S(x_1)}\right) = 0,$$

which yields the radial velocity

$$v = -\frac{\varpi}{2}\frac{\partial}{\partial x_1}\left(\frac{Q}{S(x_1)}\right).$$

This corresponds to a distribution of azimuthal vorticity of strength

$$\frac{\partial v}{\partial x_1} = -\frac{\varpi}{2}\frac{\partial^2}{\partial x_1^2}\left(\frac{Q}{S(x_1)}\right).$$

Downloaded from https://www.cambridge.org/core. Charité Universitätsmedizin Berlin, on 20 Dec 2021 at 10:08:47, subject to the Cambridge Core terms of use, available at https://www.cambridge.org/core/terms. https://doi.org/10.1017/CBO9781107360273.006

Hence, the kinetic energy T' ($\geq T$) is

$$\frac{2T'}{\rho_o Q^2} = 2\pi \int \left[\frac{1}{S^2} + \frac{\varpi^2}{4S^4} \left(\frac{\partial S}{\partial x_1} \right)^2 \right] \varpi \, d\varpi \, dx_1$$
$$= \int \frac{dx_1}{S(x_1)} + \frac{1}{2\pi} \int \frac{1}{y^2} \left(\frac{dy}{dx_1} \right)^2 dx_1,$$

where $y(x_1)$ is the duct radius ($S = \pi y^2$). Thus,

$$\int \frac{dx_1}{S(x_1)} \leq \frac{1}{K_o} \leq \int \frac{dx_1}{S(x_1)} + \frac{1}{2\pi} \int \frac{1}{y^2} \left(\frac{dy}{dx_1} \right)^2 dx_1, \tag{5.5.1}$$

and we can take

$$\frac{1}{K_o} = \int \frac{dx_1}{S(x_1)} \tag{5.5.2}$$

subject to an error no larger than $\frac{1}{2\pi} \int \frac{1}{y^2} \left(\frac{dy}{dx_1} \right)^2 dx_1$.

Rayleigh has shown that the actual value of $1/K_o$ is closer to the upper limit in (5.5.1).

5.6* Effect of mean flow

5.6.1 The Cummings–Fant equation

The method of §3.3.5 can be extended to estimate the influence of flow on the transmission of low frequency sound through a duct aperture (Figure 5.6.1). Consider first the case of Figure 5.6.1a of a duct of radius b and an axisymmetric aperture of radius a in a thin 'orifice plate' situated at $x_1 = 0$. In the absence of sound the flow is steady, of low Mach number and uniform at speed U_o in the upstream section of the duct. A jet is formed at the aperture, and the mean flow Mach number $M_o = U_o/c_o$ is assumed to be sufficiently small that the jet flow can be regarded as incompressible, with fully contracted mean velocity $U_\sigma \simeq U_o(b^2/\sigma a^2)$, σ being the jet contraction ratio. Further downstream the jet mixes into a nominally homogeneous, turbulent mean flow at speed U_o. This turbulence is a source of weak quadrupole sound, which is ignored.

The acoustic frequency is small enough that only plane waves can propagate in the duct, and a plane sound wave of pressure $p_I(t - x_1/c_o)$ (for $M_o \ll 1$) is assumed to be incident on the aperture from upstream ($x_1 < 0$). Reflected and transmitted waves $p_R(t + x_1/c_o)$ and $p_T(t - x_1/c_o)$ are formed at the plate (§5.3.3), so that the unsteady pressures $p_\mp(t)$ just upstream and downstream of the plate, at distances small compared to the acoustic wavelength yet large compared to the aperture radius a, are given by

$$p_-(t) = p_I(t) + p_R(t), \quad p_+(t) = p_T(t).$$

Downloaded from https://www.cambridge.org/core. Charité Universitätsmedizin Berlin, on 20 Dec 2021 at 10:08:47, subject to the Cambridge Core terms of use, available at https://www.cambridge.org/core/terms. https://doi.org/10.1017/CBO9781107360273.006

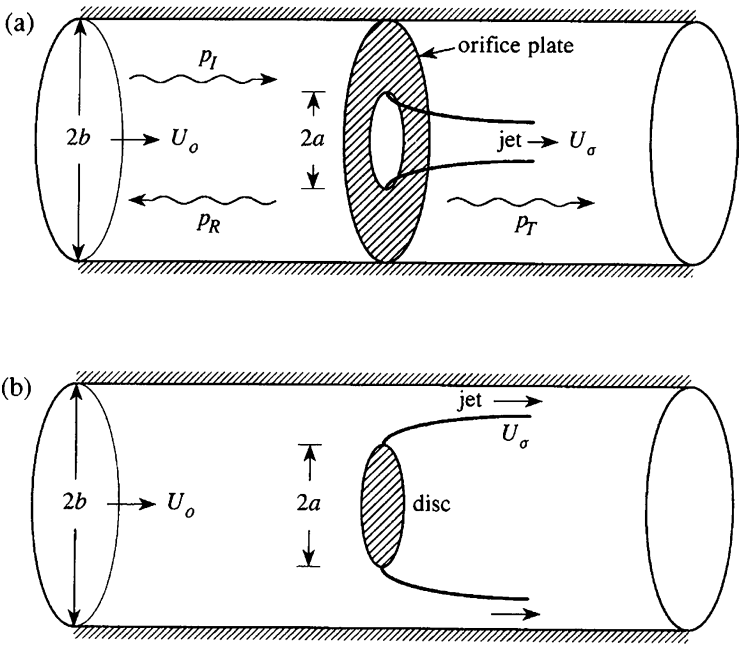

Figure 5.6.1

These pressures 'drive' the unsteady motion through the aperture.

The reflected and transmitted waves are determined by the unsteady component of the volume velocity $Q(t)$ through the aperture. The aperture behaves as a 'source' of strength $Q(t)$ of the transmitted wave, such that

$$p_T(t - x_1/c_o) = \frac{\rho_o c_o}{A_d}\, Q(t - x_1/c_o), \quad A_d = \pi b^2, \quad x_1 > 0. \tag{5.6.1}$$

Total reflection occurs if the aperture is closed ($a = 0$), when $p_R = p_I(t + x_1/c_o)$. When $a \neq 0$, however, this is supplemented by the wave produced by an aperture source of strength $-Q(t)$, so that

$$p_R(t + x_1/c_o) = p_I(t + x_1/c_o) - \frac{\rho_o c_o}{A_d}\, Q(t + x_1/c_o), \quad x_1 < 0. \tag{5.6.2}$$

The equation governing $Q(t)$ is derived by equating the sum of the rate of increase of the kinetic energy $\rho_o Q^2/2K_o$ within the aperture (equation (3.3.7)) and its rate of dissipation by vorticity production (equation (3.3.27)) to the rate of working of the upstream and downstream pressures $p_\mp(t)$:

$$\frac{d}{dt}\left(\frac{\rho_o Q^2}{2K_o}\right) + \rho_o \int \mathbf{u} \cdot (\boldsymbol{\omega} \wedge \mathbf{v})'\, d^3\mathbf{x} = Q\Big(p_-(t) - p_+(t)\Big), \tag{5.6.3}$$

Downloaded from https://www.cambridge.org/core. Charité Universitätsmedizin Berlin, on 20 Dec 2021 at 10:08:47, subject to the Cambridge Core terms of use, available at https://www.cambridge.org/core/terms. https://doi.org/10.1017/CBO9781107360273.006

where $(\boldsymbol{\omega} \wedge \mathbf{v})' \equiv (\boldsymbol{\omega} \wedge \mathbf{v})'(\mathbf{x}, t)$ denotes the perturbation value. The acoustic particle velocity $\mathbf{u}(\mathbf{x}, t)$ within and near the aperture can be replaced by

$$\mathbf{u}(\mathbf{x}, t) = \frac{Q(t)}{A_d} \nabla \varphi^*(\mathbf{x}),$$

provided the aperture is acoustically compact, where $\varphi^* = \varphi^*(\mathbf{x})$ is the velocity potential of incompressible, irrotational flow through the aperture normalised such that $\partial \varphi^* / \partial x_1 \to 1$ at large distances from the aperture in the uniform sections of the duct.

$\varphi^*(\mathbf{x})$ can be adjusted to satisfy

$$\varphi^* \sim \begin{cases} x_1 + \ell_d/2 & \text{for } x_1/b \text{ large and positive} \\ x_1 - \ell_d/2 & \text{for } x_1/b \text{ large and negative} \end{cases}$$

$$\text{where} \quad \ell_d = \frac{A_d}{K_o} = \int_{-\infty}^{\infty} \left(\frac{\partial \varphi^*}{\partial x_1} - 1 \right) dx_1,$$

the path of integration passing through the aperture parallel to the x_1 axis. The energy equation (5.6.3) therefore reduces to

$$\rho_o \ell_d \frac{dQ}{dt} + \rho_o \int \frac{\partial \varphi^*}{\partial \mathbf{x}} \cdot (\boldsymbol{\omega} \wedge \mathbf{v})' d^3\mathbf{x} = A_d \Big(p_-(t) - p_+(t) \Big). \tag{5.6.4}$$

This is the *Cummings–Fant* equation of §3.3.5. The right hand side can be written in terms of Q and the incident pressure $p_I(t)$ by substitution from equations (5.6.1), (5.6.2).

5.6.2 Linearisation of the dissipation integral

The integration in (5.6.4) is confined to the jet and the turbulent 'mixing region' downstream of the aperture, and accounts for dissipation of the sound by vorticity production. In a first approximation the downstream turbulence can be ignored, because in this region the vorticity convects primarily in the direction of the mean stream (parallel to $\nabla \varphi^*$, and therefore makes a negligible contribution to the integral). The contribution from the jet will be evaluated as in §3.3.5 for the bias flow aperture (see Figure 3.3.5), using the linearised, quasi-static representation (3.3.18) of $\boldsymbol{\omega} \wedge \mathbf{v}$. This gives

$$\int \nabla \varphi^* \cdot (\boldsymbol{\omega} \wedge \mathbf{v})' \, d^3\mathbf{x} \simeq Q(t) U_o \frac{A_d}{\sigma A_a} \left(\frac{A_d}{\sigma A_a} - 1 \right) \tag{5.6.5}$$

where $A_a = \pi a^2$ is the aperture area.

Downloaded from https://www.cambridge.org/core. Charité Universitätsmedizin Berlin, on 20 Dec 2021 at 10:08:47, subject to the Cambridge Core terms of use, available at https://www.cambridge.org/core/terms. https://doi.org/10.1017/CBO9781107360273.006

The substitution of (5.6.1), (5.6.2) and (5.6.5) into (5.6.4) yields the linearised Cummings–Fant equation

$$\ell_d \frac{dQ}{dt} + 2c_o Q + \frac{A_d}{\sigma A_a}\left(\frac{A_d}{\sigma A_a} - 1\right) U_o Q = \frac{2A_d p_I(t)}{\rho_o}. \tag{5.6.6}$$

5.6.3 Time-harmonic sound

For time-harmonic sound $\propto \mathrm{e}^{-i\omega t}$ the incident wave $p_I = \hat{p}_I \mathrm{e}^{ik_o x_1}$, and the reflected and transmitted waves are $p_R = R\hat{p}_I \mathrm{e}^{-ik_o x_1}$, $p_T = T\hat{p}_I \mathrm{e}^{ik_o x_1}$, where R, T are suitable reflection and transmission coefficients. Substitute $Q(t) = \hat{Q}\mathrm{e}^{-i\omega t}$ into (5.6.6) to obtain

$$\frac{\rho_o c_o \hat{Q}}{A_d} = \frac{2\hat{p}_I}{2 + M_o \frac{A_d}{\sigma A_a}\left(\frac{A_d}{\sigma A_a} - 1\right) - ik_o \ell_d}.$$

Equations (5.6.1) and (5.6.2) supply the reflection and transmission coefficients

$$R = \frac{M_o \frac{A_d}{\sigma A_a}\left(\frac{A_d}{\sigma A_a} - 1\right) - ik_o \ell_d}{2 + M_o \frac{A_d}{\sigma A_a}\left(\frac{A_d}{\sigma A_a} - 1\right) - ik_o \ell_d}, \quad T = \frac{2}{2 + M_o \frac{A_d}{\sigma A_a}\left(\frac{A_d}{\sigma A_a} - 1\right) - ik_o \ell_d}. \tag{5.6.7}$$

The fraction of the incident wave energy absorbed by vorticity production at the aperture is

$$\alpha \equiv 1 - |R|^2 - |T|^2 = \frac{4M_o \frac{A_d}{\sigma A_a}\left(\frac{A_d}{\sigma A_a} - 1\right)}{\left(2 + M_o \frac{A_d}{\sigma A_a}\left(\frac{A_d}{\sigma A_a} - 1\right)\right)^2 + (k_o \ell_d)^2},$$

which vanishes in the absence of mean flow. It is plotted against the aperture Strouhal number fa/U ($f = \omega/2\pi$, $U = U_o A_d/A_a$ = mean jet speed in the aperture) in Figure 5.6.2 when $M_o = 0.05$, $\sigma = 0.75$ and for several values of $\xi = a/b$. The slug length ℓ_d is calculated from Fock's formula (5.3.3). The peak dissipation occurs at very small Strouhal numbers, α attaining a maximum value of $\frac{1}{2}$ when $a/b = \left(2/\sigma[1 + \sqrt{1 + 8/M_o}]\right)^{\frac{1}{2}} \simeq 0.441$ (cf. Figure 3.3.9 for the bias flow screen).

5.6.4 Absorption at an annular aperture

The formulae for R, T and α for case (b) of Figure 5.6.1 are identical with those for the orifice plate provided the aperture area A_a is replaced by the area $A_g = \pi(b^2 - a^2) = A_d(1 - \xi^2)$ of the annular gap. The relevant Strouhal number fh/U is now based on the width $h = b - a$ of the annular gap,

Downloaded from https://www.cambridge.org/core. Charité Universitätsmedizin Berlin, on 20 Dec 2021 at 10:08:47, subject to the Cambridge Core terms of use, available at https://www.cambridge.org/core/terms. https://doi.org/10.1017/CBO9781107360273.006

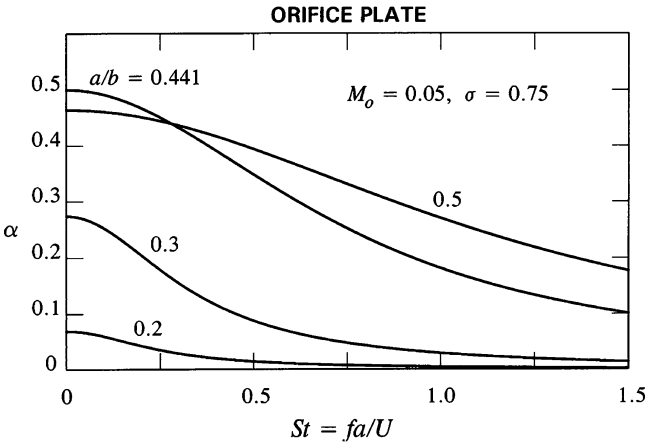

Figure 5.6.2

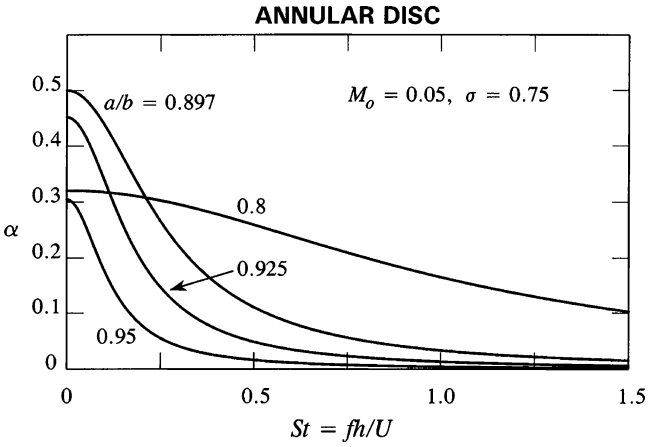

Figure 5.6.3

and the dependence of the fractional attenuation α on fh/U is shown in Figure 5.6.3 for $M_o = 0.05$, $\sigma = 0.75$, and several values of $\xi = a/b$, the slug length ℓ_d being determined by (5.3.15). The peak dissipation ($\alpha = \frac{1}{2}$) occurs at

$$\frac{a}{b} = \left[1 - \frac{2}{\sigma\left(1 + \sqrt{1 + \frac{8}{M_o}}\right)}\right]^{\frac{1}{2}} \quad \text{when} \quad \frac{fh}{U} \to 0,$$

that is, at $a/b \simeq 0.897$.

Downloaded from https://www.cambridge.org/core. Charité Universitätsmedizin Berlin, on 20 Dec 2021 at 10:08:47, subject to the Cambridge Core terms of use, available at https://www.cambridge.org/core/terms. https://doi.org/10.1017/CBO9781107360273.006

5.7* Sound produced by a synthetic jet

The absorption of sound at a bias-flow aperture has been treated (§§3.3, 5.6) by using a free streamline model of the mean jet formed at the aperture. The strength of the vortex sheet at the edge of the jet is assumed to be modulated by the sound without affecting the overall structure of the jet. When there is no bias flow, however, the aperture flow generated by the sound alternates in direction, causing vorticity to be ejected in jet-like 'puffs' from both sides of the aperture, each puff developing into a vortex ring moving away from the aperture and each carrying energy and momentum extracted from the sound. The same mechanism is involved in the operation of a *synthetic jet device*, a simplified example of which consists of a short cylindrical cavity closed at its left hand end in Figure 5.7.1 and open at $x_1 = 0$ via a small circular aperture. A snugly fitting piston vibrates at small amplitude at $x_1 = -L$ resulting in the periodic ejection of vortex rings from the cavity and producing a quasi-steady jet whose energy and momentum are supplied by the piston. The jet is unaffected by the return flow into the cavity, because the spherically symmetric, sink-like inflow occurs at low speed, and does not attain its peak values until the most recently ejected vortex ring is far from the aperture.

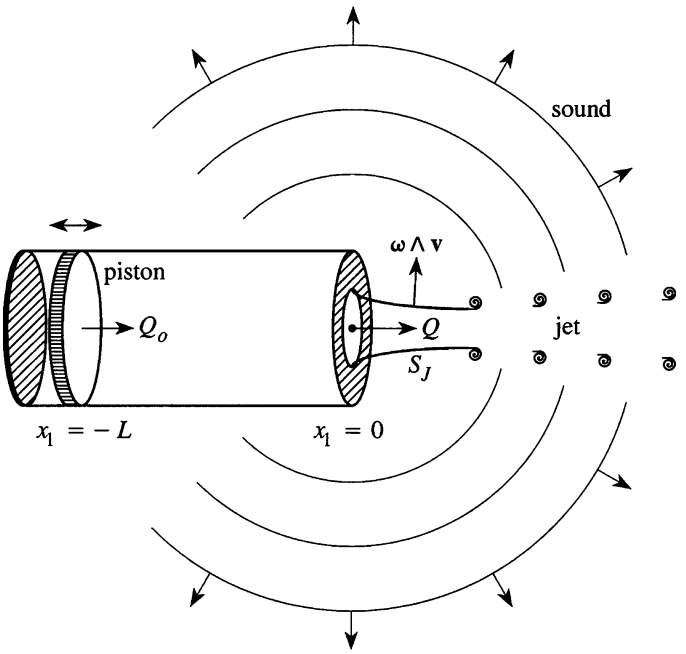

Figure 5.7.1

Downloaded from https://www.cambridge.org/core. Charité Universitätsmedizin Berlin, on 20 Dec 2021 at 10:08:47, subject to the Cambridge Core terms of use, available at https://www.cambridge.org/core/terms. https://doi.org/10.1017/CBO9781107360273.006

The synthetic jet is important because no external source of fluid is required to maintain the jet, making it an ideal stand-alone flow control device for promoting fluid mixing and heat transfer in engineering systems. The aerodynamic sound radiated from the cavity by the exit flow is evidently of monopole type and can be much more significant than the usual quadrupole or dipole noise sources (§§4.2, 4.3).

5.7.1 Representation of the monopole sound

Let the cavity be circular cylindrical of working length L and radius b, and let the opening at $x_1 = 0$ be a concentric circular aperture of radius a. All of the cavity walls are rigid and of negligible thickness, and the coordinate origin is taken in the centre of the aperture. The operating frequency of the piston is usually close to the minimum cavity resonance frequency f_c. At this frequency the acoustic wavelength greatly exceeds the cavity diameter. Therefore the cavity cross-section is acoustically compact and the pressure in the acoustic far field is

$$p(\mathbf{x}, t) = \frac{\rho_o}{4\pi|\mathbf{x}|}\frac{\partial Q}{\partial t}\left(t - \frac{|\mathbf{x}|}{c_o}\right), \quad |\mathbf{x}| \to \infty, \tag{5.7.1}$$

where $Q(t)$ is the volume velocity at the cavity exit. This equation cannot be used by itself for making predictions until $Q(t)$ has been found from the appropriate Cummings–Fant equation.

To do this for complex systems of the present type equation (4.7.4) is first used to derive an alternative formula for the sound in terms of aerodynamic sources by putting $p(\mathbf{x}, t) = p_s(\mathbf{x}, t) + p_\omega(\mathbf{x}, t)$, where

$$\begin{aligned} p_s(\mathbf{x}, t) &= \rho_o \int_{-\infty}^{\infty} \oint_S G \frac{\partial \mathbf{v}}{\partial \tau} \cdot d\mathbf{S}(\mathbf{y}) d\tau, \\ p_\omega(\mathbf{x}, t) &= -\rho_o \int_{-\infty}^{\infty} \int_V \frac{\partial G}{\partial \mathbf{y}} \cdot \boldsymbol{\omega} \wedge \mathbf{v}\, d^3\mathbf{y} d\tau. \end{aligned} \tag{5.7.2}$$

The components p_s, p_ω correspond respectively to the contributions from the surface S of the piston, which may be assumed to have uniform normal velocity with overall volume velocity $Q_o(t)$, say, and from vortex sources close to the aperture. This high Reynolds number approximation ignores the explicit contribution to the sound of surface viscous sources – except in so far as viscosity plays an essential role in releasing vorticity into the jet shear layer, and thereby contributes to the dominant flow noise component p_ω. The Cummings–Fant equation is obtained by expressing the vortex sources in terms of Q and equating the pressure $p(\mathbf{x}, t)$ determined by (5.7.2) to the right-hand side of (5.7.1).

Downloaded from https://www.cambridge.org/core. Charité Universitätsmedizin Berlin, on 20 Dec 2021 at 10:08:47, subject to the Cambridge Core terms of use, available at https://www.cambridge.org/core/terms. https://doi.org/10.1017/CBO9781107360273.006

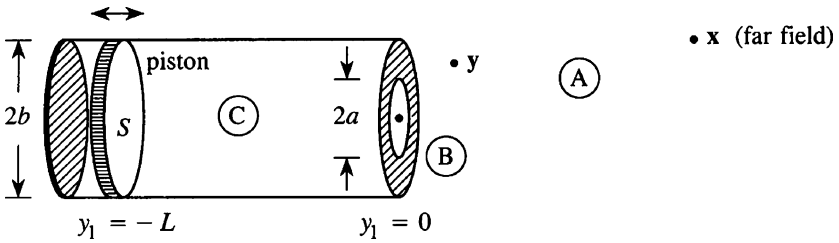

Figure 5.7.2

5.7.2 *Green's function and the calculation of* p_s *and* p_ω

Green's function $G(\mathbf{x}, \mathbf{y}, t-\tau)$ must satisfy $\partial G/\partial y_n = 0$ on all solid boundaries (including the mean position of the face of the piston) and will be found by the method of §3.3.4 for source points $\mathbf{y}$ in regions B and C of Figure 5.7.2, for $\mathbf{x}$ in the acoustic far field, and in the compact approximation where the relevant acoustic wavelengths $\lambda \gg$ the cavity radius b.

Assume that $b \ll |\mathbf{y}| \ll \lambda$ in the free space region A (Figure 5.7.2). Then, correct to monopole order,

$$G \simeq \frac{1}{4\pi|\mathbf{x}-\mathbf{y}|}\,\delta\left(t-\tau-\frac{|\mathbf{x}-\mathbf{y}|}{c_o}\right)+\frac{1}{4\pi|\mathbf{y}|}\,\Phi\left(\tau+\frac{|\mathbf{y}|}{c_o}\right), \qquad |\mathbf{y}|\to\infty$$
$$\sim \frac{1}{4\pi|\mathbf{x}|}\,\delta\left(t-\tau-\frac{|\mathbf{x}|}{c_o}\right)+\frac{\Phi(\tau)}{4\pi|\mathbf{y}|}+\frac{\Phi'(\tau)}{4\pi c_o} \qquad \text{for } \mathbf{y} \text{ in A}, \tag{5.7.3}$$

where $\Phi(\tau+|\mathbf{y}|/c_o)/4\pi|\mathbf{y}|$ is an advanced potential converging on the cavity exit. Φ also depends on $(\mathbf{x}, t)$ but this is suppressed for brevity in this and similar functions to be introduced.

In the compact region B

$$G \simeq \alpha(\tau)+\beta(\tau)\varphi^*(\mathbf{y}) \sim \begin{cases} \alpha(\tau)-\beta(\tau)A_d/4\pi|\mathbf{y}| & \text{in A} \\ \alpha(\tau)+\beta(\tau)(y_1-\ell_E) & \text{in C} \end{cases} \tag{5.7.4}$$

where $\varphi^*(\mathbf{y})$ is the potential function defined as in (5.4.2) and $A_d = \pi b^2$ is the cavity cross-sectional area.

Only plane waves can propagate in the cavity region C when $\lambda \gg b$. Therefore, because $\partial G/\partial y_n = 0$ on the cavity walls including the piston at $y_1 = -L$, we can put

$$G \simeq \int_{-\infty}^{\infty} \mathcal{F}(k_o)\,\cos\{k_o(y_1+L)\}\mathrm{e}^{i\omega\tau}\,d\omega$$
$$\sim \int_{-\infty}^{\infty} \mathcal{F}(k_o)\,\cos(k_oL)\mathrm{e}^{i\omega\tau}\,d\omega - y_1\int_{-\infty}^{\infty}\mathcal{F}(k_o)\,k_o\sin(k_oL)\mathrm{e}^{i\omega\tau}\,d\omega$$
$$\text{as } y_1 \to -0, \tag{5.7.5}$$

where $k_o = \omega/c_o$ and the dependence of $\mathcal{F}(k_o)$ on $\mathbf{x}$ and t is suppressed.

Downloaded from https://www.cambridge.org/core. Charité Universitätsmedizin Berlin, on 20 Dec 2021 at 10:08:47, subject to the Cambridge Core terms of use, available at https://www.cambridge.org/core/terms. https://doi.org/10.1017/CBO9781107360273.006

Formulae (5.7.3), (5.7.4) and (5.7.5) are consistent provided they agree in the respective regions of overlap A and $y_1 \sim -0$ within the cavity. This leads to the following compatibility relations

$$\alpha + \frac{A_d}{4\pi c_o}\frac{\partial \beta}{\partial \tau} = \frac{1}{4\pi |\mathbf{x}|}\,\delta\left(t - \tau - \frac{|\mathbf{x}|}{c_o}\right) \tag{5.7.6}$$

$$\alpha(\tau) = \ell_E \beta(\tau) - \frac{1}{2\pi}\int_{-\infty}^{\infty} \frac{\beta(\tau')\cos(k_o L)}{k_o \sin(k_o L)}\,\mathrm{e}^{-i\omega(\tau'-\tau)} d\omega d\tau', \tag{5.7.7}$$

$$\mathcal{F}(k_o) = \frac{-1}{2\pi k_o \sin(k_o L)}\int_{-\infty}^{\infty} \beta(\tau)\mathrm{e}^{-i\omega\tau} d\tau, \tag{5.7.8}$$

where the causality condition that $G(\mathbf{x}, \mathbf{y}, t-\tau)$ should vanish when $\tau > t$ requires the path of integration in the ω plane to pass above the singularities on the real axis in (5.7.7).

The solution of these simultaneous equations determines the explicit forms of G in the source regions B and C, but this step is not necessary to obtain the Cummings–Fant equation. Instead (5.7.4) and the first line of (5.7.5) applied at $y_1 = -L$ with (5.7.8) are used respectively in (5.7.2) to evaluate p_ω and p_s, and to deduce that

$$p(\mathbf{x}, t) \simeq \rho_o \int_{-\infty}^{\infty} \beta(\tau)\left\{\frac{ic_o}{2\pi}\int_{-\infty}^{\infty}\frac{Q_o(\tau')}{\sin(k_o L)}\mathrm{e}^{-i\omega(\tau-\tau')} d\omega d\tau' - \int_V (\nabla\varphi^* \cdot \boldsymbol{\omega} \wedge \mathbf{v})(\mathbf{y}, \tau)\, d^3\mathbf{y}\right\} d\tau, \tag{5.7.9}$$

where V is the region occupied by the vortex sources.

This is to be equated to the monopole expression (5.7.1) for the pressure. But because of the presence of $\beta(\tau)$ in the integrand of (5.7.9) it is necessary to use (5.7.6), (5.7.7) and integration by parts (recalling that $\beta(\tau) = 0,\ Q(\tau) = 0$ respectively at $\tau = \pm\infty$) to re-cast (5.7.1) as follows

$$\begin{aligned} p(\mathbf{x}, t) &= \rho_o \int_{-\infty}^{\infty} \frac{dQ(\tau)}{d\tau}\frac{1}{4\pi|\mathbf{x}|}\delta\left(t - \tau - \frac{|\mathbf{x}|}{c_o}\right) d\tau \\ &\equiv \rho_o \int_{-\infty}^{\infty}\left(\alpha(\tau) + \frac{A_d}{4\pi c_o}\frac{\partial\beta(\tau)}{\partial\tau}\right)\frac{dQ(\tau)}{d\tau}\, d\tau \\ &\equiv \rho_o \int_{-\infty}^{\infty}\beta(\tau)\left\{\frac{-A_d}{4\pi c_o}\frac{d^2Q}{d\tau^2} + \ell_E\frac{dQ}{d\tau} + \frac{ic_o}{2\pi}\int_{-\infty}^{\infty}\frac{\cos(k_o L)}{\sin(k_o L)}\, Q(\tau')\mathrm{e}^{-i\omega(\tau-\tau')} d\omega d\tau'\right\} d\tau. \end{aligned} \tag{5.7.10}$$

Downloaded from https://www.cambridge.org/core. Charité Universitätsmedizin Berlin, on 20 Dec 2021 at 10:08:47, subject to the Cambridge Core terms of use, available at https://www.cambridge.org/core/terms. https://doi.org/10.1017/CBO9781107360273.006

5.7.3 Cummings–Fant equation

Equations (5.7.9) and (5.7.10) are consistent provided the expressions in the brace brackets of the two integrands can be equated. This yields the Cummings–Fant equation

$$\frac{-A_d}{4\pi c_o}\frac{d^2Q}{dt^2} + \ell_E\frac{dQ}{dt} + \int_V (\nabla\varphi^*\cdot\boldsymbol{\omega}\wedge\mathbf{v})(\mathbf{y},t)\,d^3\mathbf{y} = \frac{ic_o}{2\pi}\int_{-\infty}^{\infty}\left(\frac{Q_o(\tau)-Q(\tau)\cos(k_oL)}{\sin(k_oL)}\right)\mathrm{e}^{-i\omega(t-\tau)}d\omega d\tau, \qquad (5.7.11)$$

which determines $Q(t)$ in terms of the piston volume velocity $Q_o(t)$ and the jet vorticity. It has the same structure as equation (5.6.4) for the duct problems of Figure 5.6.1. The reader can easily verify that the right-hand side of (5.7.11) is equal to $A_d p_-/\rho_o$, where p_- is the cavity pressure just to the left of the aperture ($x_1 = -0$). Similarly, $-(A_d/4\pi c_o)d^2Q/dt^2 = A_d p_+/\rho_o$, where p_+ is the exterior, uniform near field acoustic pressure (cf. §3.3.3).

The energy equation is obtained by multiplication by $\rho_o Q/A_d$ and averaging over time (denoted by angle brackets $< >$):

$$\langle Qp_-\rangle = \frac{\rho_o}{4\pi c_o}\left\langle\left(\frac{dQ}{dt}\right)^2\right\rangle + \left\langle\rho_o\int_V \mathbf{u}\cdot\boldsymbol{\omega}\wedge\mathbf{v}\,d^3\mathbf{y}\right\rangle, \qquad (5.7.12)$$

where $\mathbf{u} = (Q/A_d)\nabla\varphi^*$ is the acoustic particle velocity at the aperture. $\langle Qp_-\rangle$ is the net rate of working of the piston, because dissipation within the cavity has been ignored, and (5.7.12) equates this respectively to the radiation losses and the power absorbed by vorticity production, both within the synthetic jet and within the cavity during inflow phases of the motion.

An integrable form of (5.7.11) can be derived by means of the quasi-static approximation of §3.3.5 (Figure 3.3.5) that expresses $\boldsymbol{\omega}\wedge\mathbf{v}$ in terms of Q. We can set $U_\sigma = 0$ in equation (3.3.18) in the absence of a mean flow to obtain $\boldsymbol{\omega}\wedge\mathbf{v} \simeq \frac{1}{2}u_\sigma^2(t)\delta(s_\perp)\mathbf{n}$. Therefore during outflow from the cavity ($Q > 0$): $\int_V \nabla\varphi^*\cdot\boldsymbol{\omega}\wedge\mathbf{v}d^3\mathbf{y} \approx \frac{1}{2}u_\sigma^2\oint_{S_J}(\partial\varphi^*/\partial y_n)dS = \frac{1}{2}A_d u_\sigma^2$, where $\oint_{S_J}(\partial\varphi^*/\partial y_n)dS$ is the net flux A_d of the hypothetical flow defined by $\varphi^*(\mathbf{y})$ through the edge S_J of the jet. The same calculation performed for $Q < 0$ during inflow yields the same result with the sign reversed, and both cases are therefore included in

$$\int_V \nabla\varphi^*\cdot\boldsymbol{\omega}\wedge\mathbf{v}d^3\mathbf{y} \simeq \frac{A_d}{2\sigma^2A_a^2}Q(t)|Q(t)| \qquad (5.7.13)$$

where $Q = \sigma A_a u_\sigma$ and $A_a = \pi a^2$ is the aperture cross-section.

Downloaded from https://www.cambridge.org/core. Charité Universitätsmedizin Berlin, on 20 Dec 2021 at 10:08:47, subject to the Cambridge Core terms of use, available at https://www.cambridge.org/core/terms. https://doi.org/10.1017/CBO9781107360273.006

The ω-integration on the right of (5.7.11) can be evaluated in terms of the residues of the simple poles at the zeros of $\sin(k_o L)$ at

$$\omega = \omega_n = \frac{n\pi c_o}{L}, \quad n = 0,\ \pm 1,\ \pm 2,\ \dots\ , \tag{5.7.14}$$

which correspond to the resonance frequencies of a cavity of length L *closed* at both ends. Using this and formula (5.7.13) the Cummings–Fant equation becomes

$$\frac{-A_d}{4\pi c_o}\frac{d^2Q}{dt^2} + \ell_E \frac{dQ}{dt} + \frac{AQ|Q|}{2\sigma^2 A_a^2} + \frac{c_o^2}{L}\sum_{n=0}^{\infty}\int_{-\infty}^{t} \gamma_n \Big[Q(\tau) - (-1)^n Q_o(\tau)\Big]\cos\{\omega_n(t-\tau)\}\,d\tau = 0, \tag{5.7.15}$$

where $\gamma_0 = 1$ and $\gamma_n = 2,\ n \geq 1$.

5.7.4 Time-harmonic piston motion

Let the piston execute small amplitude oscillations at velocity $v_o \sin(2\pi f_p t)$, v_o being the peak velocity and f_p the frequency. The cavity response depends on the proximity of f_p to a resonant frequency of the cavity. In practice f_p is close to the minimum cavity resonance frequency f_c, which is the smallest positive root of

$$\frac{\ell_E}{L}(k_o L)\sin(k_o L) - \cos(k_o L) = 0, \quad k_o = \frac{2\pi f}{c_o}. \tag{5.7.16}$$

This is the characteristic equation of the linearised, homogeneous form of the Cummings–Fant equation (5.7.11) when $(k_o b)^2 \ll 1$, namely:

$$\ell_E \frac{dQ}{dt} + \frac{ic_o}{2\pi}\int_{-\infty}^{\infty} \frac{\cos(k_o L)}{\sin(k_o L)}\, Q(\tau) \mathrm{e}^{-i\omega(t-\tau)} d\omega d\tau = 0, \tag{5.7.17}$$

where the end correction ℓ_E is given in terms of $\xi = a/b$ by equation (5.4.9). The solution f_c of (5.7.16) can be approximated by the Helmholtz resonator formula $f_c = c_o/(2\pi\sqrt{\ell_E L})$ provided $\ell_E \gg L$, i.e. when $\xi \ll 1$.

If we now write $Q_o(t) = \bar{Q}_o \sin(2\pi f_p t)$ where $\bar{Q}_o = v_o A_d$, and put

$$T = f_p t, \quad \hat{Q} = \frac{Q}{\bar{Q}_o}, \quad M_o = \frac{v_o}{c_o}, \tag{5.7.18}$$

the Cummings–Fant equation (5.7.15) assumes the non-dimensional form

$$-\frac{f_p b}{4c_o}\frac{d^2\hat{Q}}{dT^2} + \frac{\ell_E}{b}\frac{d\hat{Q}}{dT} = \frac{-1}{(f_p b/c_o)}\left\{\frac{M_o}{2\sigma^2\xi^4}\hat{Q}|\hat{Q}| + \frac{(b/L)}{(f_p b/c_o)}\sum_{n=0}^{\infty}\gamma_n Z_n(T)\right\}, \tag{5.7.19}$$

Downloaded from https://www.cambridge.org/core. Charité Universitätsmedizin Berlin, on 20 Dec 2021 at 10:08:47, subject to the Cambridge Core terms of use, available at https://www.cambridge.org/core/terms. https://doi.org/10.1017/CBO9781107360273.006

where

$$Z_n(T) = \int_{-\infty}^{T} [\hat{Q}(T') - (-1)^n \sin(2\pi T')] \cos[\Omega_n(T - T')] dT',$$
$$\Omega_n = \frac{n\pi(b/L)}{(f_p b/c_o)}, \quad n \geq 0. \tag{5.7.20}$$

This is solved by Runge–Kutta integration by the method of Question 5.8, **Problems 5**, by assuming the system starts from rest at $T = 0$ and continuing the integration until a periodic limit cycle solution is attained.

As an illustration consider a device for which

$$\frac{b}{L} = 0.2, \quad \frac{a}{b} = 0.3, \quad v_o = 1\,\text{m/s} \ \ (M_0 = 0.0029), \quad \sigma = 0.75, \tag{5.7.21}$$

where $c_o \simeq 340$ m/s in air. For these conditions $\ell_E/b = 4.082$ and $f_c b/c_o = 0.029$.

The acoustic pressure (5.7.1) is periodic of frequency f_p and can be written

$$p(\mathbf{x}, t) = \frac{b}{4|\mathbf{x}|} \left(\frac{f_p b}{c_o}\right) \rho_o c_o v_o \left[\frac{d\hat{Q}}{dT}\right], \tag{5.7.22}$$

where the square brackets indicate evaluation at the retarded non-dimensional time $T - f_p|\mathbf{x}|/c_o$. Four cycles of the non-dimensional pressure profile $d\hat{Q}/dT$ are plotted in Figure 5.7.3a for the case where $f_p = f_c$, the minimum cavity resonance frequency. The amplitude of $Q(t)$ is controlled predominantly by flow nonlinearity, the nonlinear nature of the wave profile being evident from the figure. The aperture exit velocity $U = Q(t)/A_a$ averaged over the aperture cross-section is given by $U/v_o = \hat{Q}(T)/\xi^2$; for the conditions (5.7.21) the limit cycle solution yields the root mean square value of $U = 16.3$ m/s.

Introduce the Fourier representation

$$\frac{d\hat{Q}}{dT} = \sum_{n=1}^{\infty} \Big(a_n \cos(2\pi n f_p t) + b_n \sin(2\pi n f_p t)\Big),$$

where $(a_n, b_n) = 2\int (d\hat{Q}/dT)\{\cos(2\pi nT), \sin(2\pi nT)\}\, dT$, the integration being over one complete cycle. The radiated sound power Π_a is then given by

$$\frac{\Pi_a}{\rho_o c_o^3 A_d} = \frac{M_o^2}{4} \left(\frac{f_p b}{c_o}\right)^2 \left\langle \left(\frac{d\hat{Q}}{dT}\right)^2 \right\rangle = \frac{M_o^2}{8} \left(\frac{f_p b}{c_o}\right)^2 \sum_{n=1}^{\infty} c_n^2, \quad c_n^2 = a_n^2 + b_n^2, \tag{5.7.23}$$

so that the magnitude of c_n^2 determines the component of acoustic power at frequency nf_p. The calculated power distribution for conditions (5.7.21)

Downloaded from https://www.cambridge.org/core. Charité Universitätsmedizin Berlin, on 20 Dec 2021 at 10:08:47, subject to the Cambridge Core terms of use, available at https://www.cambridge.org/core/terms. https://doi.org/10.1017/CBO9781107360273.006

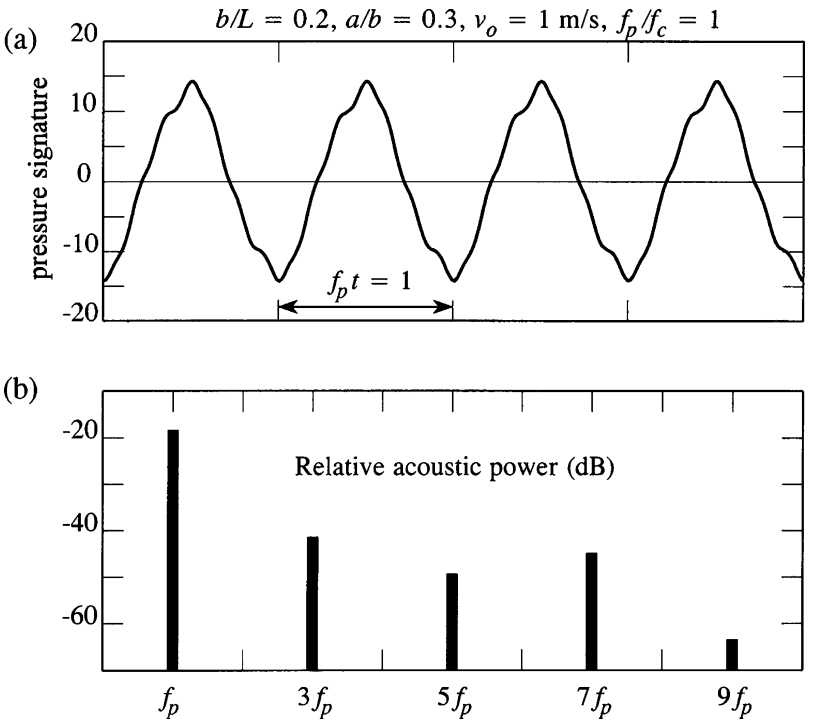

Figure 5.7.3

is plotted as $10 \times \log_{10}\{c_n^2 M_o^2 (f_p b/c_o)^2/8\}$ (dB) in Figure 5.7.3b for $n = 1-9$. Only the odd modes are significant, with most of the energy transmitted at the fundamental frequency f_p. The third harmonic is essentially 20 dB smaller.

The net rate of working of the piston Π_o is given by (5.7.12), with non-dimensional representation

$$\frac{\Pi_o}{\rho_o c_o^3 A_d} = \frac{M_o^2}{4}\left(\frac{f_p b}{c_o}\right)^2 \left\langle \left(\frac{d\hat{Q}}{dT}\right)^2 \right\rangle + \frac{M_o^3}{2\sigma^2 \xi^4} \langle \hat{Q}^2 |\hat{Q}| \rangle, \tag{5.7.24}$$

the second term on the right being the energy lost to vorticity production. The efficiency of sound production is therefore Π_a/Π_o. The dependence of this and the acoustic power Π_a on the piston frequency f_p are plotted for conditions (5.7.21) in Figure 5.7.4a. The acoustic power exhibits a maximum close to f_c and also near $f_p \simeq 3.76 f_c$, the second cavity resonance frequency. The acoustic efficiency is seen to increase steadily with frequency – 30% or more of the piston power being radiated as sound when $f_p > 2 f_c$. This is also evident

Downloaded from https://www.cambridge.org/core. Charité Universitätsmedizin Berlin, on 20 Dec 2021 at 10:08:47, subject to the Cambridge Core terms of use, available at https://www.cambridge.org/core/terms. https://doi.org/10.1017/CBO9781107360273.006

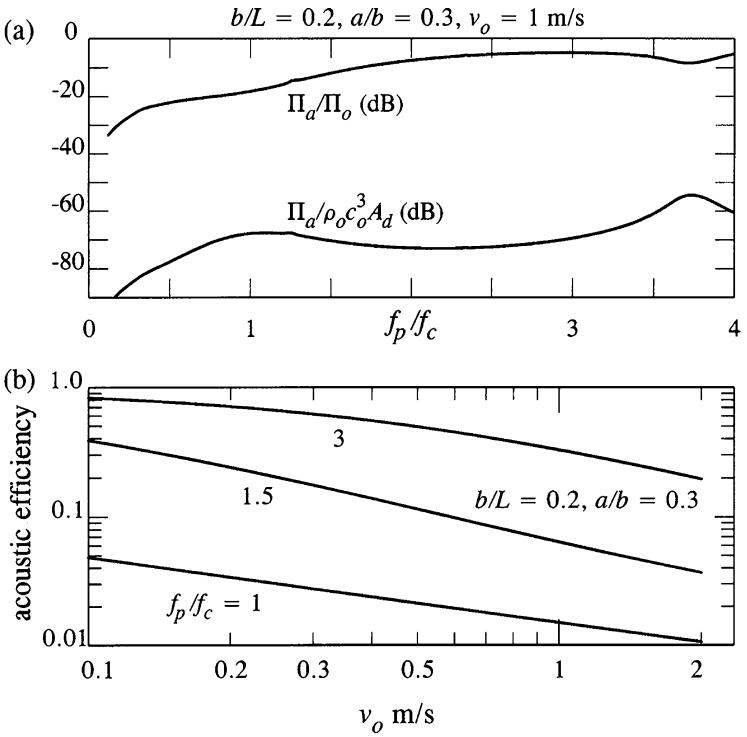

Figure 5.7.4

from the dependence of the efficiency on the piston velocity v_o, which is plotted in Figure 5.7.4b for $f_p/f_c = 1,\ 1.5,\ 3$.

Problems 5

5.1. Use the two-parameter representation

$$v_n = \bar{v}\left(1 + \mu\frac{\varpi^2}{b^2} + \mu'\frac{\varpi^4}{b^4}\right), \quad a < \varpi < b,$$

to improve the approximation of §5.1.2 for the conductivity of an annular aperture in a thin screen.

5.2.* Consider ideal, incompressible flow at speed U in the x direction above a rigid wall $y = 0$. A thin rigid barrier of height h occupies the strip $x = 0,\ 0 < y < h$, and the complex potential of the flow past the barrier is $w = U\sqrt{z^2 + h^2},\ z = x + iy$. Use this formula with $h = b - a$ to derive the approximation (5.3.11) by the method of §5.3.5 (ii). Assume that the velocity potential for incompressible flow through the duct is

Downloaded from https://www.cambridge.org/core. Charité Universitätsmedizin Berlin, on 20 Dec 2021 at 10:08:47, subject to the Cambridge Core terms of use, available at https://www.cambridge.org/core/terms. https://doi.org/10.1017/CBO9781107360273.006

given exactly by

$$\varphi = Ux_1 + \operatorname{sgn}(x_1)\left(\frac{U\ell_d}{2} + \sum_{n=1}^{\infty} A_n \mathrm{J}_0\left(\lambda_n \frac{\varpi}{b}\right) \mathrm{e}^{-\lambda_n |x_1|/b}\right),$$

$$\varpi = \sqrt{x_2^2 + x_3^2},$$

where $\varphi = 0$ in the plane of the aperture $x_1 = 0,\ 0 < \varpi < a$.

5.3.* Use Rayleigh's method with the two parameter approximation

$$v_n = \bar{v}\left(1 + \mu\frac{\varpi^2}{a^2} + \mu'\frac{\varpi^4}{a^4}\right), \quad 0 < \varpi < a,$$

to obtain the graphical representations plotted in the figure (———) of the end correction ℓ_E and conductivity K_o for a flanged, circular cylindrical duct of radius b which communicates with free space via an axisymmetric circular aperture of radius $a < b$ (Figure 5.4.6). Check your results against the approximation (5.4.10) (• • • in the figure).

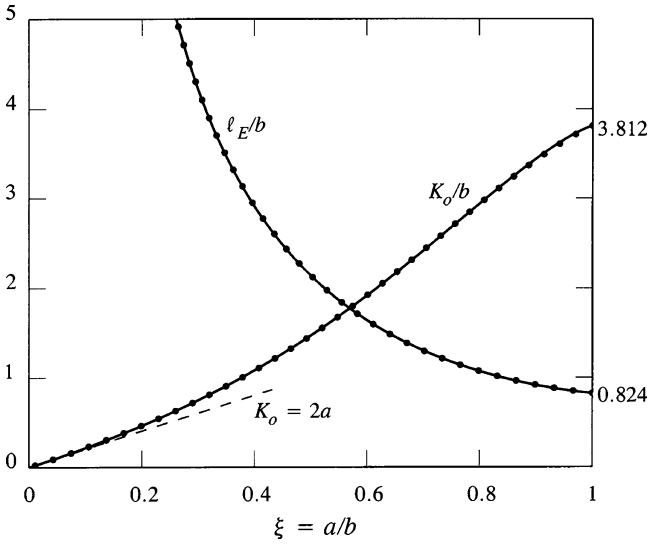

5.4. Use Rayleigh's method to show that the end correction of a flanged semi-infinite duct of square cross section of side a is $\ell_E \approx 0.813R$ where R is the radius of a circular duct of the same cross-sectional area ($R = a/\sqrt{\pi}$). Assume that in the square exit plane ($x_1 = 0$) of the duct

$$v_n = \bar{v}\left(1 + \frac{\mu(x_2^4 + x_3^4)}{a^4}\right), \quad -\frac{a}{2} < x_2,\ x_3 < \frac{a}{2}.$$

Downloaded from https://www.cambridge.org/core. Charité Universitätsmedizin Berlin, on 20 Dec 2021 at 10:08:47, subject to the Cambridge Core terms of use, available at https://www.cambridge.org/core/terms. https://doi.org/10.1017/CBO9781107360273.006

5.5. The potential φ^* for incompressible flow from an *unflanged* circular cylindrical duct of radius a, normalised as in (5.4.2), is defined by (cf. §2.9.1e)

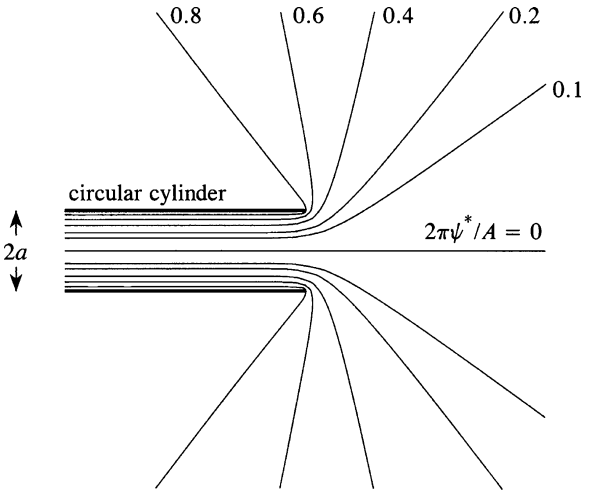

$$\frac{\partial\varphi^*}{\partial x_1}(\varpi, x_1) = \frac{1}{2} - \frac{1}{2\pi}\int_0^\infty \mathrm{I}_0\left(\lambda\frac{\varpi}{a}\right)\sqrt{\frac{2\mathrm{K}_1(\lambda)}{\mathrm{I}_1(\lambda)}} \times \sin\left(\lambda\left[\frac{x_1}{a} + \mathcal{Z}(\lambda)\right]\right) d\lambda, \quad \varpi < a,$$

where $\mathcal{Z}(\lambda) = \dfrac{1}{\pi}\displaystyle\int_0^\infty \frac{\ln[\mathrm{K}_1(\mu)\mathrm{I}_1(\mu)/\mathrm{K}_1(\lambda)\mathrm{I}_1(\lambda)]}{\mu^2 - \lambda^2}\, d\mu.$

Show that

$$\begin{aligned}\ell_E &= \int_{-\infty}^0 \left(\frac{\partial\varphi^*}{\partial x_1}(0, x_1) - 1\right) dx_1 + \int_0^\infty \frac{\partial\varphi^*}{\partial x_1}(0, x_1)\, dx_1 \\ &\equiv \frac{1}{2\pi}\int_{-\infty}^\infty dx_1 \int_0^\infty \left[\frac{2}{\lambda}\sin\left(\frac{\lambda x_1}{a}\right) - \sqrt{\frac{2\mathrm{K}_1(\lambda)}{\mathrm{I}_1(\lambda)}}\sin\left(\lambda\left[\frac{x_1}{a} + \mathcal{Z}(\lambda)\right]\right)\right] d\lambda\end{aligned}$$

Use the formula

$$\begin{aligned}\int_{-\infty}^\infty \sin\left[\lambda\left(\frac{x_1}{a} + \mathcal{Z}(\lambda)\right)\right] dx_1 &= \mathrm{Im}\left\{2\pi a\delta(\lambda)\mathrm{e}^{i\{\lambda\mathcal{Z}(\lambda)\}}\right\} \\ &= 2\pi a\delta(\lambda)\sin\left(\lambda\mathcal{Z}(\lambda)\right)\end{aligned}$$

Downloaded from https://www.cambridge.org/core. Charité Universitätsmedizin Berlin, on 20 Dec 2021 at 10:08:47, subject to the Cambridge Core terms of use, available at https://www.cambridge.org/core/terms. https://doi.org/10.1017/CBO9781107360273.006

to deduce that

$$\ell_E = -a\mathcal{Z}(0) = -\frac{a}{\pi}\int_0^\infty \frac{\ln[2\mathrm{K}_1(\mu)\mathrm{I}_1(\mu)]}{\mu^2}\,d\mu \;\approx\; 0.6127a.$$

5.6. Use equation (5.5.2) to estimate the conductivity of a conical channel in a wall of thickness h when the minimum and maximum radii of the channel are respectively a and b. Show that the fractional error is smaller than $(b-a)^2/2h^2$.

5.7.* The complex potential of incompressible flow from the lower to the upper $\zeta = x' + iy$ plane through a slit in the interval $-h < x' < h$ in a thin rigid wall coinciding with $y = 0$ is given by

$$w = \frac{q}{\pi}\ln\left(\frac{\zeta}{h} + \sqrt{\frac{\zeta^2}{h^2} - 1}\right),$$

where q is the volume velocity per unit span of the slit. Use this formula to evaluate the velocity potential of flow through a narrow annulus (Figure 5.1.2 with $b - a \ll a$) at distances $|\zeta|$ large compared to $b - a$, but small compared to the disc radius a.

In the usual notation, if U is the mean normal velocity in the plane of the slit, the approximation

$$\varphi(\mathbf{x}) = \mathrm{sgn}(y)\left(\frac{-q}{2\pi}\int_S \frac{\delta(\varpi' - \bar{b})dS(\mathbf{y}')}{|\mathbf{x} - \mathbf{y}'|} + \frac{U\ell}{2}\right), \quad \mathbf{x} = (x, y, z),$$

may be used to evaluate the potential at distances $\gg b-a$ from the annular aperture, where $\bar{b} = \frac{1}{2}(a + b)$, and the integration is over the plane S of the wall, on which $\varpi' = |\mathbf{y}'|$ denotes distance from the geometrical centre of the annulus. Evaluate the integral at a point $\mathbf{x}$ very close to the annular slit.

Hence, by taking $q = U(b^2-a^2)/2\bar{b}$ deduce the following asymptotic approximations

$$\frac{\ell}{b} \;\approx\; \frac{2(1-\xi)}{\pi}\ln\left(\frac{32}{1-\xi}\right), \quad \frac{K_o}{b} \;\approx\; \frac{\pi^2(1+\xi)}{2\,\ln\left(\frac{32}{1-\xi}\right)}, \quad \xi = \frac{a}{b} \sim 1,$$

which define the dotted curves in Figure 5.1.3.

Downloaded from https://www.cambridge.org/core. Charité Universitätsmedizin Berlin, on 20 Dec 2021 at 10:08:47, subject to the Cambridge Core terms of use, available at https://www.cambridge.org/core/terms. https://doi.org/10.1017/CBO9781107360273.006

5.8. When $f_p/f_c \sim O(1)$ limit cycle solutions of the Cummings–Fant equation (5.7.19) are periodic with period 1 in $T = f_p t$, with most of the acoustic energy contained in the first Fourier components $\propto e^{\pm 2\pi i f_p t}$. The radiation damping term on the left hand side can then be approximated by $(\pi^2 f_p b/c_o)\hat{Q}$ and (5.7.19) reduced to

$$\frac{d\hat{Q}}{dT} = \frac{-1}{(\ell_E/b)(f_p b/c_o)} \left\{ \left(\frac{\pi f_p b}{c_o}\right)^2 \hat{Q} + \frac{M_o}{2\sigma^2\xi^4}\hat{Q}|\hat{Q}| + \frac{(b/L)}{(f_p b/c_o)} \sum_{n=0}^{\infty} \gamma_n Z_n(T) \right\}.$$

Show that the solution of this equation can be obtained by regarding the Z_n as independent variables that are to be determined by the simultaneous solution of the system of equations

$$\frac{dZ_n}{dT} = \hat{Q}(T) - (-1)^n \sin(2\pi T) - \Omega_n Z_n', \quad \frac{dZ_n'}{dT} = \Omega_n Z_n, \quad n \geq 0,$$

where $Z_n'(T) = \int_{-\infty}^{T} [\hat{Q}(T') - (-1)^n \sin(2\pi T')] \sin[\Omega_n(T - T')] dT'$. By truncating the infinite system at $n = 7$, say, and taking the initial conditions to be $\hat{Q} = 0$, $Z_n = Z_n' = 0$ at $T = 0$, use Runge–Kutta integration to confirm the graphical results of §5.7.4.

Downloaded from https://www.cambridge.org/core. Charité Universitätsmedizin Berlin, on 20 Dec 2021 at 10:08:47, subject to the Cambridge Core terms of use, available at https://www.cambridge.org/core/terms. https://doi.org/10.1017/CBO9781107360273.006

6

Solutions of Starred Problems

6.1 Problems 1

1.1 Fluctuations in p, ρ, T, and v propagate as sound waves, whereas the specific entropy s remains uniform throughout the fluid. Therefore each of p, ρ, T, v is a function of $t \pm x/c_o$, where the $\pm$ sign is taken according as the wave propagates in the $\mp x$ direction (i.e. to the 'left' or 'right').

First, for such waves the momentum equation yields

$$\frac{\partial v}{\partial t} = -\frac{1}{\rho_o}\frac{\partial p}{\partial x} = \mp\frac{1}{\rho_o c_o}\frac{\partial p}{\partial t} \quad \text{i.e.} \quad v\left(t \pm x/c_o\right) = \mp\frac{p\left(t \pm x/c_o\right)}{\rho_o c_o}.$$

Second, the adiabatic relation $\delta\rho = \delta p/c_o^2$ implies that $\rho\left(t \pm x/c_o\right) = p\left(t \pm x/c_o\right)/c_o^2$.

Next, the formula $dw = dp/\rho + Tds$ applied to a perfect gas with $ds = 0$ and enthalpy $w = c_p T$, supplies $T\left(t \pm x/c_o\right) = p\left(t \pm x/c_o\right)/\rho_o c_p$.

1.3 Put $\varphi = \Phi(t - |x|/c_o)$ and substitute into

$$\left(\frac{1}{c_o^2}\frac{\partial^2}{\partial t^2} - \frac{\partial^2}{\partial x^2}\right)\varphi = \delta(x)\delta(t)$$

to obtain

$$\frac{1}{c_o^2}\Phi''\left(t - \frac{|x|}{c_o}\right) - \frac{1}{c_o^2}\Phi''\left(t - \frac{|x|}{c_o}\right) + \frac{2}{c_o}\delta(x)\Phi'(t) = \delta(x)\delta(t),$$

because

$$\frac{\partial^2\Phi}{\partial x^2}\left(t - \frac{|x|}{c_o}\right) = \frac{\partial}{\partial x}\left[\frac{-1}{c_o}\frac{\partial|x|}{\partial x}\Phi'\left(t - \frac{|x|}{c_o}\right)\right]$$

Downloaded from https://www.cambridge.org/core. Charité Universitätsmedizin Berlin, on 20 Dec 2021 at 10:08:46, subject to the Cambridge Core terms of use, available at https://www.cambridge.org/core/terms. https://doi.org/10.1017/CBO9781107360273.007

$$= \frac{\partial}{\partial x}\left[\frac{-\mathrm{sgn}(x)}{c_o}\Phi'\left(t - \frac{|x|}{c_o}\right)\right]$$
$$= -\frac{2}{c_o}\delta(x)\Phi'(t) + \frac{1}{c_o^2}\Phi''\left(t - \frac{|x|}{c_o}\right),$$

where the primes denote differentiation with respect to the argument, and $\frac{\partial}{\partial x}\mathrm{sgn}(x) = \frac{\partial}{\partial x}\{2\mathrm{H}(x) - 1\} = 2\delta(x)$.
Hence

$$\Phi'(t) = \frac{c_o}{2}\delta(t), \quad \therefore \quad \Phi(t) = \frac{c_o}{2}\mathrm{H}(t) + C \quad (C = \text{constant}).$$

The condition $\varphi = 0,\ t < 0$ implies that $C = 0$,

$$\therefore \quad \varphi = \Phi\left(t - \frac{|x|}{c_o}\right) \equiv \frac{c_o}{2}\mathrm{H}\left(t - \frac{|x|}{c_o}\right).$$

1.5 Consider the region $x_1 > h$. From (1.7.4):

$$p(\mathbf{x}, t) = \frac{\partial}{\partial t}\Big(t\,\bar{f}(c_o t)\Big).$$

This formula is evidently independent of the position of P in any plane $x_1 = $ constant (parallel to boundaries of the initial high pressure region), and represents a plane wave $p = p(t - x_1/c_o)$.
Now

$$\bar{f} = 0 \ \text{ for } c_o t < r_1;$$
$$= \frac{p_o}{2}\int_0^{\Theta_2} \sin\theta\, d\theta = \frac{p_o}{2}(1 - \cos\Theta_2)$$
$$= \frac{p_o}{2}\left(1 - \frac{r_1}{c_o t}\right) \text{ for } r_1 < c_o t < r_1 + h;$$
$$= \frac{p_o}{2}\int_{\Theta_1}^{\Theta_2} \sin\theta\, d\theta = \frac{p_o}{2}(\cos\Theta_1 - \cos\Theta_2)$$
$$= \frac{p_o}{2}\left(\frac{r_1 + h}{c_o t} - \frac{r_1}{c_o t}\right) \text{ for } c_o t > r_1 + h;$$

$$\therefore \quad p(\mathbf{x}, t) = \frac{\partial}{\partial t}\Big(t\,\bar{f}(c_o t)\Big) = \begin{cases} 0, & c_o t < r_1 \\ p_o/2, & r_1 < c_o t < r_1 + h \\ 0, & c_o t > r_1 + h \end{cases}$$

$$\text{i.e.} \quad p(\mathbf{x}, t) = \frac{p_o}{2}\Big(\mathrm{H}(t - r_1/c_o) - \mathrm{H}(t - [r_1 + h]/c_o)\Big), \quad x_1 > h.$$

Downloaded from https://www.cambridge.org/core. Charité Universitätsmedizin Berlin, on 20 Dec 2021 at 10:08:46, subject to the Cambridge Core terms of use, available at https://www.cambridge.org/core/terms. https://doi.org/10.1017/CBO9781107360273.007

Because $r_1 = x_1 - h$ when $x_1 > h$, this formula represents a plane wave pulse of amplitude $\frac{1}{2}p_o$ and thickness h (duration h/c_o) propagating in the x_1 direction.

1.8 The acoustic wavelength is much larger than the radius R and therefore the axial velocity in the exit plane of the duct $v \simeq 2p_I \cos(\omega t)/\rho_o c_o$, so that $Q = \pi R^2 v = (2\pi R^2 p_I/\rho_o c_o)\cos(\omega t)$.

The duct opening behaves as a monopole source, with spherically symmetric pressure at large distances r given by equation (1.8.1):

$$p(\mathbf{x}, t) = \frac{\rho_o}{4\pi|\mathbf{x}|}\left[\frac{dQ}{dt}\right] = -\frac{k_o R^2 p_I}{2r}\sin(\omega[t]), \quad [t] = t - r/c_o.$$

$$\therefore \quad \langle p^2 \rangle = \frac{(k_o R^2 p_I)^2}{4r^2}\langle \sin^2(\omega[t])\rangle = \frac{(k_o R^2 p_I)^2}{8r^2},$$

where $\langle\ \rangle$ denotes a time average. The free space sound power is therefore

$$\Pi = 4\pi r^2 \frac{\langle p^2 \rangle}{\rho_o c_o} = \frac{\pi R^2 (k_o R)^2 p_I^2}{2\rho_o c_o}.$$

The acoustic power of the incident wave is

$$\Pi_I = \pi R^2 \frac{\langle p_I^2 \cos^2\{\omega(t - x_1/c_o)\}\rangle}{\rho_o c_o} = \frac{\pi R^2 p_I^2}{2\rho_o c_o}.$$

Hence the fraction of the incident power radiated from the duct is $\Pi/\Pi_I = (k_o R)^2$.

1.12 Consider the trial solution

$$\varphi = \frac{A}{r}\mathrm{e}^{-i\omega(t - r/c_o)}, \quad r > a,$$

where A is a constant to be determined. This is an outgoing spherically symmetric solution of the wave equation (§1.4.2).

A is found from the condition $(\partial\varphi/\partial r)_{r=a} = u\mathrm{e}^{-i\omega t}$,

$$\text{i.e.} \quad \frac{\partial\varphi}{\partial r} = A\left(-\frac{1}{r^2} + \frac{ik_o}{r}\right)\mathrm{e}^{-i\omega(t - r/c_o)} = u\mathrm{e}^{-i\omega t}, \ \text{ at } r = a,$$

$$\therefore \quad A = \frac{-a^2 u \mathrm{e}^{-ik_o a}}{(1 - ik_o a)}.$$

$$\text{and} \quad \varphi = \frac{-a^2 u}{r(1 - ik_o a)}\mathrm{e}^{-i\omega(t - r/c_o) - ik_o a} \equiv \frac{-Q_o\,\mathrm{e}^{-i\omega\{t - (r-a)/c_o\}}}{4\pi r(1 - ik_o a)}.$$

Downloaded from https://www.cambridge.org/core. Charité Universitätsmedizin Berlin, on 20 Dec 2021 at 10:08:46, subject to the Cambridge Core terms of use, available at https://www.cambridge.org/core/terms. https://doi.org/10.1017/CBO9781107360273.007

In the compact limit $k_o a \to 0$, and $\varphi \sim -(Q_o/4\pi r)\mathrm{e}^{-i\omega(t-r/c_o)}$, which is the outgoing solution of (§1.5.1)

$$\left(\frac{1}{c_o^2}\frac{\partial^2}{\partial t^2} - \nabla^2\right)\varphi = -Q_o \mathrm{e}^{-i\omega t}\delta(\mathbf{x}).$$

1.14 Because the normal velocity on the sphere $u_n = \mathrm{Re}\{u\mathrm{e}^{-i\omega t}\}$ it follows from Question 1.12 that

$$\varphi = \mathrm{Re}\left\{\frac{-a^2 u\, \mathrm{e}^{-i\omega[t-(r-a)/c_o]}}{(1-ik_o a)r}\right\}.$$

$$\therefore \quad p = -\rho_o\frac{\partial\varphi}{\partial t} = \mathrm{Re}\left\{\frac{-i\omega\rho_o a^2 u\, \mathrm{e}^{-i\omega[t-(r-a)/c_o]}}{(1-ik_o a)\, r}\right\}$$

$$\text{and} \qquad \Pi_a = \oint_S \frac{\langle p^2\rangle}{\rho_o c_o} dS\,,$$

where the integration is over the surface of a sphere of radius $r > a$.

Put $p = \mathrm{Re}\{\alpha\mathrm{e}^{-i\omega t}\}$, then $p = \frac{1}{2}\{\alpha\mathrm{e}^{-i\omega t} + \alpha^*\mathrm{e}^{i\omega t}\}$, where α^* is the complex conjugate of α, and

$$\langle p^2\rangle = \langle\frac{1}{4}(\alpha\mathrm{e}^{-i\omega t} + \alpha^*\mathrm{e}^{i\omega t})(\alpha\mathrm{e}^{-i\omega t} + \alpha^*\mathrm{e}^{i\omega t})\rangle = \frac{1}{4}(|\alpha|^2 + |\alpha|^2)$$
$$= \frac{|\alpha|^2}{2},$$

because $\langle\mathrm{e}^{-2i\omega t}\rangle \equiv \langle\mathrm{e}^{2i\omega t}\rangle \equiv 0$.

Hence

$$\Pi_a = \frac{4\pi r^2}{2\rho_o c_o}\left|\frac{-i\omega\rho_o a^2 u}{(1-ik_o a)\, r}e^{ik_o(r-a)}\right|^2 = \frac{2\pi}{\rho_o c_o}\frac{\omega^2\rho_o^2 a^4 u^2}{\left(1+k_o^2 a^2\right)}$$

$$\therefore \quad \Pi_a = \frac{(k_o a)^2}{\left(1+(k_o a)^2\right)}\left(4\pi a^2\right)c_o\left(\frac{1}{2}\rho_o u^2\right),$$

$$\text{where} \quad \Pi_a \sim (k_o a)^2\left(4\pi a^2\right)c_o\left(\frac{1}{2}\rho_o u^2\right) \quad \text{for } k_o a \ll 1,$$

$$\sim \left(4\pi a^2\right)c_o\left(\frac{1}{2}\rho_o u^2\right) \quad \text{for } k_o a \gg 1.$$

Downloaded from https://www.cambridge.org/core. Charité Universitätsmedizin Berlin, on 20 Dec 2021 at 10:08:46, subject to the Cambridge Core terms of use, available at https://www.cambridge.org/core/terms. https://doi.org/10.1017/CBO9781107360273.007

1.16 Using the Fraunhofer approximation in the acoustic far field

$$\varphi(\mathbf{x},t) \approx \frac{1}{4\pi a|\mathbf{x}|}\int_{-\infty}^{\infty} \mathrm{sgn}(y_1)\mathrm{H}(a-|\mathbf{y}|)U\left(t-\frac{|\mathbf{x}|}{c_o}+\frac{\mathbf{x}\cdot\mathbf{y}}{c_o|\mathbf{x}|}\right)d^3\mathbf{y}$$

$$= \frac{1}{4\pi a|\mathbf{x}|}\int_{|\mathbf{y}|<a} \mathrm{sgn}(y_1)U\left(t-\frac{|\mathbf{x}|}{c_o}+\frac{\mathbf{x}\cdot\mathbf{y}}{c_o|\mathbf{x}|}\right)d^3\mathbf{y}$$

$$= \frac{1}{4\pi a|\mathbf{x}|}\int_{|\mathbf{y}|<a} \mathrm{sgn}(y_1)U\left(t-\frac{|\mathbf{x}|}{c_o}\right)d^3\mathbf{y}$$
$$+\frac{1}{4\pi a|\mathbf{x}|}\int_{|\mathbf{y}|<a} \mathrm{sgn}(y_1)\frac{\mathbf{x}\cdot\mathbf{y}}{c_o|\mathbf{x}|}\frac{\partial U}{\partial t}\left(t-\frac{|\mathbf{x}|}{c_o}\right)d^3\mathbf{y}+\cdots$$

$$= \text{monopole} + \text{dipole} + \cdots$$

$$= 0 + \frac{x_j}{4\pi a c_o|\mathbf{x}|^2}\frac{\partial U}{\partial t}\left(t-\frac{|\mathbf{x}|}{c_o}\right)\int_{|\mathbf{y}|<a}\mathrm{sgn}(y_1)y_j d^3\mathbf{y}+\cdots$$
$$(\text{integral } = 0 \text{ for } j\neq 1)$$

$$= \frac{\cos\theta}{4\pi a c_o|\mathbf{x}|}\frac{\partial U}{\partial t}\left(t-\frac{|\mathbf{x}|}{c_o}\right)\int_{|\mathbf{y}|<a}|y_1|d^3\mathbf{y}+\cdots$$

$$= \frac{\cos\theta}{4\pi a c_o|\mathbf{x}|}\frac{\partial U}{\partial t}\left(t-\frac{|\mathbf{x}|}{c_o}\right)2\pi\int_0^{\pi}|\cos\vartheta|\sin\vartheta\,d\vartheta\int_0^a r^3\,dr$$
$$\left(\begin{array}{l} y_1 = r\cos\vartheta \\ d^3\mathbf{y} = r^2\sin\vartheta\,d\vartheta d\phi dr \end{array}\right)$$

$$\int_0^{\pi}(\cdot)\,d\vartheta = 2\int_0^{\frac{\pi}{2}}\cos\vartheta\sin\vartheta\,d\vartheta = 1, \quad \int_0^a r^3\,dr = \frac{a^4}{4}.$$

$$\therefore\quad \varphi(\mathbf{x},t) \simeq \frac{a^3\cos\theta}{8c_o|\mathbf{x}|}\frac{\partial U}{\partial t}\left(t-\frac{|\mathbf{x}|}{c_o}\right), \quad |\mathbf{x}|\to\infty.$$

1.17 Let the source move along the x_1 axis in the direction of the unit vector $\mathbf{i}$, so that $\mathbf{U} = U\mathbf{i}$.

The solution with outgoing wave behaviour is found using the free space Green's function (1.6.2) to be

$$\varphi = -\frac{1}{4\pi}\int_{-\infty}^{\infty}\frac{1}{|\mathbf{x}-\mathbf{y}|}\,\delta\left(t-\tau-\frac{|\mathbf{x}-\mathbf{y}|}{c_o}\right)q_o(\tau)\,\delta(\mathbf{y}-\mathbf{U}\tau)\,d^3\mathbf{y}d\tau$$

$$= -\frac{1}{4\pi}\int_{-\infty}^{\infty} q_o(\tau)\,\frac{\delta\left(t-\tau-\frac{|\mathbf{x}-U\mathbf{i}\tau|}{c_o}\right)}{|\mathbf{x}-U\mathbf{i}\tau|}\,d\tau$$

Downloaded from https://www.cambridge.org/core. Charité Universitätsmedizin Berlin, on 20 Dec 2021 at 10:08:46, subject to the Cambridge Core terms of use, available at https://www.cambridge.org/core/terms. https://doi.org/10.1017/CBO9781107360273.007

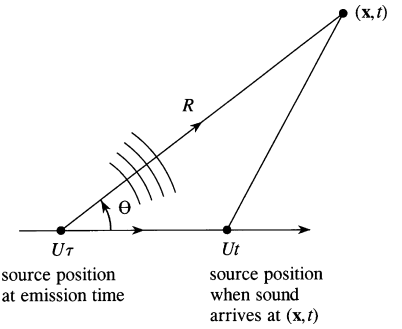

Figure 6.1.1

The 'spike' of the δ function occurs at the root τ of the equation $c_o\,(t-\tau) = |\mathbf{x} - U\mathbf{i}\tau|$. This value of τ is the time of emission of sound by the source which is received at the distant point $\mathbf{x}$ at the later time t. The travel distance of this sound is $R = c_o(t-\tau) \equiv |\mathbf{x} - U\mathbf{i}\tau|$, so that $\tau = t - R/c_o$. The remaining integration is performed by use of the formula $\int_{-\infty}^{\infty} F(\tau)\delta[f(\tau)]\,d\tau = F(\tau_o)/|f'(\tau_o)|$, where $f(\tau) = 0$ at $\tau = \tau_o$ (a 'simple' zero).

Thus:

$$\varphi(\mathbf{x}, t) = -\frac{1}{4\pi}\frac{q_o(t - R/c_o)}{R\left|\frac{\partial}{\partial\tau}\left(t - \tau - \frac{|\mathbf{x}-U\mathbf{i}\tau|}{c_o}\right)\right|}$$

At the spike

$$\frac{\partial}{\partial\tau}|\mathbf{x} - U\mathbf{i}\tau| = -\frac{U\mathbf{i}\cdot(\mathbf{x} - U\mathbf{i}\tau)}{|\mathbf{x} - U\mathbf{i}\tau|} = \frac{-U(x_1 - U\tau)}{R} = -U\cos\Theta$$

$$\therefore\ \varphi(\mathbf{x}, t) = -\frac{1}{4\pi}\frac{q_o(t - R/c_o)}{R|\,-1 + M\cos\Theta|},\ \text{where}\ M = U/c_o < 1,$$

that is,

$$\varphi(\mathbf{x}, t) = \frac{-q_o(t - R/c_o)}{4\pi R(1 - M\cos\Theta)}$$

Note: When $M < 1$ the equation $c_o(t-\tau) = |\mathbf{x} - U\mathbf{i}\tau|$ has only one root τ for which $R \equiv c_o(t-\tau) > 0$. There are two non-trivial roots during supersonic motion ($M > 1$).

6.2 Problems 2

2.4 A dipole source of constant strength convecting uniformly at subsonic speed generates only a near field disturbance in the fluid, the velocity potential decaying like the inverse square of distance from the dipole.

Downloaded from https://www.cambridge.org/core. Charité Universitätsmedizin Berlin, on 20 Dec 2021 at 10:08:46, subject to the Cambridge Core terms of use, available at https://www.cambridge.org/core/terms. https://doi.org/10.1017/CBO9781107360273.007

The sound produced when this near field impinges on an obstacle in the medium, such as the rigid cylinder of this problem, is called **diffraction radiation**; it is significant only at the retarded times at which the dipole is close to the obstacle. For the cylinder the sound has characteristic frequency $\sim U/h$ and wavelength $\lambda \sim h/M \gg h$ when M is small, so that the problem can be solved using the compact Green's function.

For $\mathbf{x}$ in the far field of the interaction region

$$G(\mathbf{x}, \mathbf{y}, t-\tau) \approx \frac{1}{4\pi|\mathbf{x}|}\delta\left(t-\tau-\frac{|\mathbf{x}|}{c_o}\right) + \frac{\mathbf{x}\cdot\mathbf{Y}}{4\pi c_o|\mathbf{x}|^2}\delta'\left(t-\tau-\frac{|\mathbf{x}|}{c_o}\right),$$

$$\text{where} \quad Y_{1,2} = y_{1,2}\left(1+\frac{a^2}{y_1^2+y_2^2}\right), \quad Y_3 = y_3.$$

Then, for $|\mathbf{x}| \to \infty$

$$\varphi \simeq \frac{-f_2 x_j}{4\pi c_o|\mathbf{x}|^2}\frac{\partial}{\partial t}\int Y_j(\mathbf{y})\frac{\partial}{\partial y_2}\{\delta(y_1-U[t])\delta(y_2-h)\delta(y_3)\}\,d^3\mathbf{y},$$

$$[t] = t - |\mathbf{x}|/c_o.$$

$$\therefore \quad \varphi \simeq \frac{f_2 x_j}{4\pi c_o|\mathbf{x}|^2}\frac{\partial}{\partial t}\left(\frac{\partial Y_j}{\partial y_2}\right)_{(U[t],h,0)}$$

$$= \frac{-a^2 f_2 x_1}{2\pi c_o|\mathbf{x}|^2}\frac{\partial}{\partial t}\left(\frac{2U[t]h}{(U^2[t]^2+h^2)^2}\right) + \frac{f_2 x_2}{4\pi c_o|\mathbf{x}|^2}\frac{\partial}{\partial t}\left(1+\frac{a^2(U^2[t]^2-h^2)}{(U^2[t]^2+h^2)^2}\right)$$

$$= \frac{f_2 M a^2}{2\pi|\mathbf{x}|(h^2+U^2[t]^2)^3} \times \left\{\frac{x_1 h}{|\mathbf{x}|}(3U^2[t]^2-h^2) + \frac{x_2 U[t]}{|\mathbf{x}|}(3h^2-U^2[t]^2)\right\}.$$

2.5 The velocity potential associated with a uniformly translating point source in free space is the solution of Problem 1.17 This must be excluded from the calculation of the diffraction radiation $\varphi_s(\mathbf{x}, t)$, say, produced as the source passes the sphere, which is acoustically compact

Downloaded from https://www.cambridge.org/core. Charité Universitätsmedizin Berlin, on 20 Dec 2021 at 10:08:46, subject to the Cambridge Core terms of use, available at https://www.cambridge.org/core/terms. https://doi.org/10.1017/CBO9781107360273.007

when $M \ll 1$. To do this the compact Green's function is expanded to first order in φ_i^*:

$$G(\mathbf{x},\mathbf{y},t-\tau) \approx \frac{1}{4\pi|\mathbf{x}-\mathbf{Y}|}\delta\left(t-\tau-\frac{|\mathbf{x}-\mathbf{Y}|}{c_o}\right)$$
$$\approx \frac{1}{4\pi|\mathbf{x}-\mathbf{y}|}\delta\left(t-\tau-\frac{|\mathbf{x}-\mathbf{y}|}{c_o}\right)$$
$$-\frac{x_j\varphi_j^*}{4\pi c_o|\mathbf{x}|^2}\delta'\left(t-\tau-\frac{|\mathbf{x}|}{c_o}\right),$$
$$\text{where}\quad \varphi_j^* = -\frac{a^3 y_j}{2|\mathbf{y}|^3}.$$

Then, for $|\mathbf{x}| \to \infty$

$$\varphi_s \simeq \frac{q_o x_j}{4\pi c_o|\mathbf{x}|^2}\frac{\partial}{\partial t}\int \varphi_j^*(\mathbf{y})\delta(y_1-U[t])\delta(y_2-h)\delta(y_3)\,d^3\mathbf{y},$$
$$[t] = t - |\mathbf{x}|/c_o.$$
$$\therefore\quad \varphi_s \simeq \frac{q_o x_j}{4\pi c_o|\mathbf{x}|^2}\frac{\partial}{\partial t}\varphi_j^*(U[t],h,0)$$
$$= \frac{-q_o x_1}{4\pi c_o|\mathbf{x}|^2}\frac{\partial}{\partial t}\left(\frac{a^3U[t]}{2(U^2[t]^2+h^2)^{\frac{3}{2}}}\right)$$
$$-\frac{q_o x_2}{4\pi c_o|\mathbf{x}|^2}\frac{\partial}{\partial t}\left(\frac{a^3 h}{2(U^2[t]^2+h^2)^{\frac{3}{2}}}\right)$$
$$= \frac{q_o M a^3}{8\pi|\mathbf{x}|(h^2+U^2[t]^2)^{\frac{5}{2}}}\left\{\frac{x_1}{|\mathbf{x}|}(2U^2[t]^2-h^2)+\frac{x_2}{|\mathbf{x}|}3hU[t]\right\}.$$

2.6 We have to solve

$$\left(\frac{1}{c_o^2}\frac{\partial^2}{\partial t^2}-\nabla^2\right)p = \rho_o\frac{\partial}{\partial t}\Big(q_o\delta(x_1-Ut)\delta(x_2)\delta(x_3)\Big)$$

If the neck has characteristic length ℓ the acoustic frequency $\sim U/\ell$ and wavelength $\sim \ell/M \gg \ell$, that is, the neck is acoustically compact, with compact Green's function

$$G(\mathbf{x},\mathbf{y},t-\tau) = \frac{c_o}{2A}\mathrm{H}\left(t-\tau-\frac{|X_1-Y_1|}{c_o}\right), \quad |\mathbf{x}-\mathbf{y}| \gg \sqrt{A}.$$

Downloaded from https://www.cambridge.org/core. Charité Universitätsmedizin Berlin, on 20 Dec 2021 at 10:08:46, subject to the Cambridge Core terms of use, available at https://www.cambridge.org/core/terms. https://doi.org/10.1017/CBO9781107360273.007

Now,

$$Y_1 - y_1 = \int_0^{y_1} \left(\frac{A}{S(\xi)} - 1 \right) d\xi \to \int_0^{\infty} \left(\frac{A}{S(\xi)} - 1 \right) d\xi \sim O(\ell), \quad \text{as } |y_1| \to \infty.$$

Therefore, when $|x_1|$ is far from the neck

$$\begin{aligned} |X_1 - Y_1| &\approx |x_1 - y_1 - (Y_1 - y_1)| \\ &= |x_1 - y_1| \left| 1 - \frac{(Y_1 - y_1)}{(x_1 - y_1)} \right| \\ &= |x_1 - y_1| - \operatorname{sgn}(x_1 - y_1)(Y_1 - y_1), \\ &\qquad \text{because } (Y_1 - y_1)/(x_1 - y_1) \ll 1, \end{aligned}$$

$$\begin{aligned} \therefore \quad G(\mathbf{x}, \mathbf{y}, t - \tau) &\approx \frac{c_o}{2A} \mathrm{H} \left(t - \tau - \frac{|x_1 - y_1|}{c_o} \right. \\ &\qquad \left. + \frac{\operatorname{sgn}(x_1 - y_1)(Y_1 - y_1)}{c_o} \right) \\ &\approx \frac{c_o}{2A} \mathrm{H} \left(t - \tau - \frac{|x_1 - y_1|}{c_o} \right) \\ &\qquad + \frac{\operatorname{sgn}(x_1)(Y_1 - y_1)}{2A} \delta \left(t - \tau - \frac{|x_1|}{c_o} \right). \end{aligned}$$

The first term is the Green's function in a uniform duct, the second determines the diffraction radiation from the neck, and its gradient is negligible when $|y_1| > \ell$. Hence, the pressure wave generated during passage through the neck is

$$\begin{aligned} p_{neck} &\approx \frac{\rho_o q_o \operatorname{sgn}(x_1)}{2A} \frac{\partial}{\partial t} \int (Y_1 - y_1) \delta \left(t - \tau - \frac{|x_1|}{c_o} \right) \\ &\qquad \times \delta(y_1 - U\tau) \delta(y_2) \delta(y_3) d^3\mathbf{y} d\tau \\ &= \frac{\rho_o q_o \operatorname{sgn}(x_1)}{2A} \frac{\partial}{\partial t} \left\{ \int_0^{U[t]} \frac{A d\xi}{S(\xi)} - U[t] \right\}, \\ &\qquad \text{where } [t] = t - |x_1|/c_o, \\ \therefore \quad p_{neck} &\approx \frac{\rho_o q_o U \operatorname{sgn}(x_1)}{2A} \left\{ \frac{A}{S(U[t])} - 1 \right\}. \end{aligned}$$

Example Suppose $S(x_1) = A\{1 - \alpha \mathrm{e}^{-(x_1/\ell)^2}\}$, then

$$p_{neck} \approx \frac{\rho_o q_o U \operatorname{sgn}(x_1) \alpha \mathrm{e}^{-(U[t]/\ell)^2}}{2A \left(1 - \alpha \mathrm{e}^{-(U[t]/\ell)^2} \right)}.$$

Downloaded from https://www.cambridge.org/core. Charité Universitätsmedizin Berlin, on 20 Dec 2021 at 10:08:46, subject to the Cambridge Core terms of use, available at https://www.cambridge.org/core/terms. https://doi.org/10.1017/CBO9781107360273.007

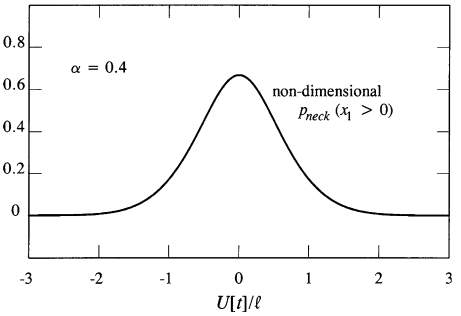

Figure 6.2.1

The figure shows $p_{neck}/(\rho_o q_o U/2A)$ plotted against $U[t]/\ell$ for $\alpha = 0.4$ and $x_1 > 0$. An equal but negative pulse is propagated to $x_1 = -\infty$.

Note: A stationary source in a uniform duct generates a uniform far field pressure $p_o = \rho_o c_o q_o/2A$. When the source is in steady motion, the uniform-duct part of the Green's function gives the pressure

$$p_o(x_1, t) \approx \frac{\rho_o c_o q_o}{2A\{1 - \mathrm{sgn}(x_1 - Ut)M\}}.$$

2.9 In the far field

$$G(\mathbf{x}, \mathbf{y}, t-\tau) \approx \frac{1}{4\pi|\mathbf{x}|}\delta\left(t - \tau - \frac{|\mathbf{x}|}{c_o}\right) + \frac{\mathbf{x}\cdot\mathbf{Y}}{4\pi c_o|\mathbf{x}|^2}\delta'\left(t - \tau - \frac{|\mathbf{x}|}{c_o}\right).$$

$$\therefore\ p(\mathbf{x}, t) \approx \rho_o \frac{\partial}{\partial t}\oint G(\mathbf{x}, \mathbf{y}, t-\tau) v_n(\mathbf{y}, \tau) dS(\mathbf{y}) d\tau \quad \text{(from (2.1.6))}$$

$$= \frac{\rho_o x_j}{4\pi c_o|\mathbf{x}|^2}\left[\frac{d^2U_i}{dt^2}\right]\oint_S (n_i y_j - n_i \varphi_j^*) dS(\mathbf{y}),$$

$$\left[\ \cdot\ \right] = \text{evaluation at } t - |\mathbf{x}|/c_o,$$

$$= \frac{\rho_o \cos\theta}{\pi^2 c_o|\mathbf{x}|}\left[\frac{d^2U}{dt^2}\right] 2\pi \int_0^a \sqrt{a^2 - \varpi^2}\, \varpi\, d\varpi,$$

$$\varpi = (y_2^2 + y_3^2)^{\frac{1}{2}},$$

$$\text{i.e.} \quad p(\mathbf{x}, t) \approx \frac{2\rho_o a^3 \cos\theta}{3\pi c_o|\mathbf{x}|}\left[\frac{d^2U}{dt^2}\right], \quad |\mathbf{x}| \to \infty.$$

2.11 The scattered pressure satisfies

$$\left(\frac{1}{c_o^2}\frac{\partial^2}{\partial t^2} - \nabla^2\right) p_s = 0,$$

Downloaded from https://www.cambridge.org/core. Charité Universitätsmedizin Berlin, on 20 Dec 2021 at 10:08:46, subject to the Cambridge Core terms of use, available at https://www.cambridge.org/core/terms. https://doi.org/10.1017/CBO9781107360273.007

where

$$p_s(\mathbf{x},t) = \rho_o \frac{\partial}{\partial t} \oint v_{sn}(\mathbf{y},\tau) G(\mathbf{x},\mathbf{y},t-\tau) dS(\mathbf{y}) d\tau.$$

In the far field

$$G(\mathbf{x},\mathbf{y},t-\tau) \approx \frac{1}{4\pi|\mathbf{x}|}\delta\left(t-\tau-\frac{|\mathbf{x}|}{c_o}\right) + \frac{\mathbf{x}\cdot\mathbf{Y}}{4\pi c_o|\mathbf{x}|^2}\delta'\left(t-\tau-\frac{|\mathbf{x}|}{c_o}\right).$$

$$\therefore \quad p_s = p_m + p_d$$

$$\text{where} \quad p_m = \frac{\rho_o}{4\pi|\mathbf{x}|}\frac{\partial}{\partial t}\oint \left[v_{sn}\right] dS$$

$$\text{and} \quad p_d = \frac{\rho_o x_j}{4\pi c_o|\mathbf{x}|^2}\frac{\partial^2}{\partial t^2}\oint \left[v_{sn}\right] Y_j \, dS,$$

$$[\cdot] = \text{ evaluation at } t - |\mathbf{x}|/c_o.$$

Neglect compressibility to calculate the motion of the compact sphere. The incident acoustic particle velocity $v_I = p_I(t)/\rho_o c_o$ causes the sphere to move at speed $U(t)$ in the x_1 direction and produces a local flow with velocity potential

$$\varphi = v_I(t)x_1 + \frac{(v_I(t) - U(t))a^3 x_1}{2|\mathbf{x}|^3},$$

where $\mathbf{x} = 0$ at the centre of the sphere. Using this to calculate the pressure $p = -\rho_o \partial\varphi/\partial t$ on the surface of the sphere we find (from the equation of motion of the sphere) that

$$U(t) = \frac{3m_o v_I(t)}{2m + m_o}$$

in the x_1 direction.

Therefore, on the sphere with unit normal $\mathbf{n} = (n_1, n_2, n_3)$,

$$\begin{aligned} v_{sn} &= -v_I(t - y_1/c_0)n_1 + U(t)n_1 \\ &\approx \frac{y_1 n_1}{c_o}\frac{\partial v_I(t)}{\partial t} + (U(t) - v_I(t))n_1 \\ &= \left(\frac{1}{\rho_o c_o^2}\frac{\partial p_I(t)}{\partial t}\right) y_1 n_1 + \left(\frac{3m_o}{2m+m_o} - 1\right)\frac{p_I(t)}{\rho_o c_o} n_1 \\ &= \left(\frac{1}{\rho_o c_o^2}\frac{\partial p_I(t)}{\partial t}\right) y_1 n_1 - \frac{2(m-m_o)}{(2m+m_o)}\frac{p_I(t)}{\rho_o c_o} n_1. \end{aligned}$$

Downloaded from https://www.cambridge.org/core. Charité Universitätsmedizin Berlin, on 20 Dec 2021 at 10:08:46, subject to the Cambridge Core terms of use, available at https://www.cambridge.org/core/terms. https://doi.org/10.1017/CBO9781107360273.007

Evaluating p_m and p_d correct to *quadrupole order*, we find

$$p_m \approx \frac{\rho_o}{4\pi|\mathbf{x}|}\frac{\partial}{\partial t}\oint\left[\left(\frac{1}{\rho_o c_o^2}\frac{\partial p_I(t)}{\partial t}\right)y_1 n_1 - \frac{2(m-m_o)}{(2m+m_o)}\frac{p_I(t)}{\rho_o c_o}n_1\right]dS$$

$$= \frac{m_o}{4\pi\rho_o c_o^2|\mathbf{x}|}\left[\frac{\partial^2 p_I(t)}{\partial t^2}\right] + 0,$$

and $$p_d \approx -\frac{\rho_o x_j}{4\pi\rho_o c_o^2|\mathbf{x}|^2}\frac{2(m-m_o)}{(2m+m_o)}\left[\frac{\partial^2 p_I(t)}{\partial t^2}\right]\oint n_1 Y_j(\mathbf{y})dS$$

$$= -\frac{a\rho_o x_j}{4\pi\rho_o c_o^2|\mathbf{x}|^2}\frac{3(m-m_o)}{(2m+m_o)}\left[\frac{\partial^2 p_I(t)}{\partial t^2}\right]\oint n_1 n_j(\mathbf{y})dS,$$

because $Y_j = \dfrac{3an_j}{2}$ on the sphere,

$$= -\frac{m_o\cos\theta}{4\pi\rho_o c_o^2|\mathbf{x}|}\frac{3(m-m_o)}{(2m+m_o)}\left[\frac{\partial^2 p_I(t)}{\partial t^2}\right].$$

Hence

$$p_s = p_m + p_d \approx \frac{m_o}{4\pi\rho_o c_o^2|\mathbf{x}|}\left(1 - \frac{3(m-m_o)}{(2m+m_o)}\cos\theta\right)\left[\frac{\partial^2 p_I(t)}{\partial t^2}\right], \quad |\mathbf{x}| \to \infty.$$

2.12 The motion of vortex A (Figure 6.2.2) at $z = z_o(t)$ is governed by the velocity potential of the other three vortices, so that

$$W = \frac{i\Gamma}{2\pi}\left\{\ln\left(z - z_o^*\right) + \ln\left(z + z_o^*\right) - \ln\left(z + z_o\right)\right\}$$

and $$\left(\frac{dW}{dz}\right)_{z_o} = \frac{i\Gamma}{2\pi}\left\{\frac{1}{z - z_o^*} + \frac{1}{z + z_o^*} - \frac{1}{z + z_o}\right\}_{z=z_o}.$$

Let $z_o = x + iy$ ($z_o^* = x - iy$), then

$$\left.\begin{aligned} \tfrac{dx}{dt} - i\tfrac{dy}{dt} &= \tfrac{i\Gamma}{2\pi}\left\{\tfrac{-i}{2y} + \tfrac{1}{2x} - \tfrac{(x-iy)}{2(x^2+y^2)}\right\} \\ \tfrac{dx}{dt} &= \tfrac{\Gamma}{4\pi}\tfrac{x^2}{y(x^2+y^2)} \\ \tfrac{dy}{dt} &= -\tfrac{\Gamma}{4\pi}\tfrac{y^2}{x(x^2+y^2)} \\ \therefore\ \tfrac{dy}{dx} &= -\tfrac{y^3}{x^3} \\ \tfrac{dx}{x^3} + \tfrac{dy}{y^3} &= 0. \end{aligned}\right\} \qquad (6.2.1)$$

Downloaded from https://www.cambridge.org/core. Charité Universitätsmedizin Berlin, on 20 Dec 2021 at 10:08:46, subject to the Cambridge Core terms of use, available at https://www.cambridge.org/core/terms. https://doi.org/10.1017/CBO9781107360273.007

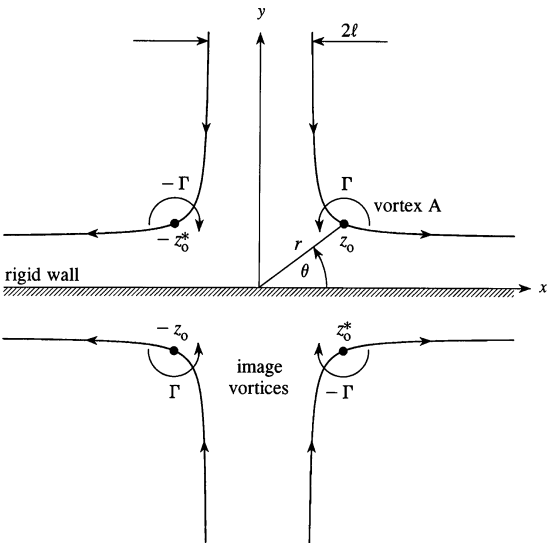

Figure 6.2.2

The Cartesian equation of the trajectory is therefore

$$\frac{1}{x^2} + \frac{1}{y^2} = \frac{1}{\ell^2} \tag{6.2.2}$$

where 2ℓ is the initial distance between the vortices (as $y \to \infty$) and ℓ is the final distance of each vortex from the wall (as $|x| \to \infty$). In terms of polar coordinates $x = r\cos\theta$, $y = r\sin\theta$

$$\frac{r^2}{\ell^2} = \frac{1}{\cos^2\theta} + \frac{1}{\sin^2\theta} = \frac{4\left(\cos^2\theta + \sin^2\theta\right)}{(2\sin\theta\cos\theta)^2} = \frac{4}{\sin^2 2\theta},$$

so that the polar form of the trajectory is

$$r\sin 2\theta = 2\ell. \tag{6.2.3}$$

To determine the time dependence of the vortex position we have from equations (6.2.1)

$$x\frac{dx}{dt} + y\frac{dy}{dt} = \frac{\Gamma}{4\pi}\left(\frac{x^3}{yr^2} - \frac{y^3}{xr^2}\right)$$

$$\frac{1}{2}\frac{d}{dt}\left(x^2 + y^2\right) = \frac{\Gamma}{4\pi}\frac{\left(x^4 - y^4\right)}{xyr^2}$$

Downloaded from https://www.cambridge.org/core. Charité Universitätsmedizin Berlin, on 20 Dec 2021 at 10:08:46, subject to the Cambridge Core terms of use, available at https://www.cambridge.org/core/terms. https://doi.org/10.1017/CBO9781107360273.007

$$r\frac{dr}{dt} = \frac{\Gamma}{4\pi}\frac{\left(\cos^4\theta - \sin^4\theta\right)}{\sin\theta\cos\theta} = \frac{\Gamma\cos 2\theta}{2\pi\sin 2\theta}. \quad (6.2.4)$$

From (6.2.3)

$$\frac{\cos 2\theta}{\sin 2\theta} = \frac{r}{2\ell}\sqrt{1-\left(\frac{2\ell}{r}\right)^2},$$

so that (6.2.4) becomes

$$\frac{dr}{dt} = \frac{\Gamma}{4\pi\ell}\sqrt{1-\frac{4\ell^2}{r^2}}$$

$$\therefore \quad \frac{rdr}{\sqrt{r^2-4\ell^2}} = \frac{\Gamma}{4\pi\ell}dt$$

$$\sqrt{r^2-4\ell^2} = \frac{\Gamma t}{4\pi\ell} + \text{Constant}.$$

Let the minimum value of $r = r_{min} = 2\ell$ occur at $t = 0$ (from equation (6.2.3) the corresponding $\theta = \theta_{min} = \pi/4$). Then the constant of integration is zero and

$$r = 2\ell\left(1+\left(\frac{\Gamma t}{8\pi\ell^2}\right)^2\right)^{1/2},$$

$$\sin 2\theta = \frac{2\ell}{r} = \frac{1}{\sqrt{1+\left(\frac{\Gamma t}{8\pi\ell^2}\right)^2}}, \quad \cos 2\theta = \frac{\frac{\Gamma t}{8\pi\ell^2}}{\sqrt{1+\left(\frac{\Gamma t}{8\pi\ell^2}\right)^2}}.$$

Hence if $T = \Gamma t/8\pi\ell^2$, $-\infty < T < \infty$, the trajectory of vortex A is given by

$$r/\ell = 2\sqrt{1+T^2},$$

$$\cos\theta = \left(\frac{T+\sqrt{1+T^2}}{2\sqrt{1+T^2}}\right)^{1/2}, \sin\theta = \left(\frac{\sqrt{1+T^2}-T}{2\sqrt{1+T^2}}\right)^{1/2},$$

$$x/\ell = 2^{1/2}\left(1+T^2\right)^{1/4}\left(T+\sqrt{1+T^2}\right)^{1/2},$$

$$y/\ell = 2^{1/2}\left(1+T^2\right)^{1/4}\left(\sqrt{1+T^2}-T\right)^{1/2}.$$

Downloaded from https://www.cambridge.org/core. Charité Universitätsmedizin Berlin, on 20 Dec 2021 at 10:08:46, subject to the Cambridge Core terms of use, available at https://www.cambridge.org/core/terms. https://doi.org/10.1017/CBO9781107360273.007

2.13 The complex potential in the ζ plane is

$$w = -\frac{i\Gamma}{2\pi}\ln(\zeta - \zeta_o) + \frac{i\Gamma}{2\pi}\ln(\zeta - \zeta_o^*)$$

$$\therefore \quad W(z) = -\frac{i\Gamma}{2\pi}\ln(\zeta - \zeta_o) + \frac{i\Gamma}{2\pi}\ln(z - z_o) + \frac{i\Gamma}{2\pi}\ln(\zeta - \zeta_o^*),$$

where $W(z)$ is defined as in equation (2.A.2).

Next

$$\zeta'(z) = \frac{z}{a(z^2 + a^2)^{\frac{1}{2}}}, \quad \zeta''(z) = \frac{a}{(z^2 + a^2)^{\frac{3}{2}}}$$

$$\therefore \quad -\frac{i\Gamma\zeta''(z_o)}{4\pi\zeta'(z_o)} = -\frac{i\Gamma a^2}{4\pi z_o(z_o^2 + a^2)}$$

$$\text{and} \quad F'(z) = \frac{d}{dz}\left(\frac{i\Gamma}{2\pi}\ln(\zeta - \zeta_o^*)\right) = \frac{i\Gamma z}{2\pi a(\zeta - \zeta_o^*)(z^2 + a^2)^{\frac{1}{2}}},$$

$$\text{But} \quad \frac{1}{(\zeta_o - \zeta_o^*)} = \frac{a}{(z_o^2 + a^2)^{\frac{1}{2}} - \{(z_o^2 + a^2)^{\frac{1}{2}}\}^*}$$

$$= \frac{a(z_o^2 + a^2)^{\frac{1}{2}}}{(z_o^2 + a^2) - |z_o^2 + a^2|}.$$

$$\therefore \quad \frac{dz_o^*}{dt} = -\frac{i\Gamma\zeta''(z_o)}{4\pi\zeta'(z_o)} + F'(z_o)$$

$$= -\frac{i\Gamma}{4\pi}\left\{\frac{a^2}{z_o(z_o^2 + a^2)} - \frac{2z_o}{z_o^2 + a^2 - |z_o^2 + a^2|}\right\}.$$

6.3 Problems 3

3.2 Small amplitude pressure fluctuations $p(\mathbf{x}, t)$ in the water satisfy the homogeneous form of equation (2.1.1) (with $q = 0$, $\mathbf{F} = 0$). The surface force $F(t)$ concentrated at the origin corresponds to a singular distribution of applied surface pressure on $x_1 = 0$ equal to $F(t)\delta(x_2)\delta(x_3)$. The very large difference in the mean gas and water densities implies that pressure fluctuations occurring elsewhere on the free surface can be ignored.

Downloaded from https://www.cambridge.org/core. Charité Universitätsmedizin Berlin, on 20 Dec 2021 at 10:08:46, subject to the Cambridge Core terms of use, available at https://www.cambridge.org/core/terms. https://doi.org/10.1017/CBO9781107360273.007

According to Kirchhoff's formula (2.1.6)

$$p(\mathbf{x},t)=\iint\!\!\!\!\!\!\diamondsuit_{y_1=0}\left(\frac{\partial G}{\partial t}\rho_o v_1+\frac{\partial G}{\partial y_1}p\right)dy_2dy_3d\tau,\quad x_1>0. \quad (6.3.1)$$

The integral involving the unknown normal velocity v_1 is eliminated by taking G to be the plane-wall, 'pressure release' Green's function (2.1.8) (which vanishes on $y_1=0$)

$$G(\mathbf{x},\mathbf{y},t-\tau)=\frac{1}{4\pi|\mathbf{x}-\mathbf{y}|}\delta\left(t-\tau-\frac{|\mathbf{x}-\mathbf{y}|}{c_o}\right)$$
$$-\frac{1}{4\pi|\bar{\mathbf{x}}-\mathbf{y}|}\delta\left(t-\tau-\frac{|\bar{\mathbf{x}}-\mathbf{y}|}{c_o}\right),$$

where $\bar{\mathbf{x}}=(-x_1,x_2,x_3)$ for the present orientation of the coordinates. The remaining integral is evaluated by setting $p=F(\tau)\delta(y_2)\delta(y_3)$ in the integrand. This reveals that the acoustic pressure in the water is given (without approximation) by the dipole formula

$$p(\mathbf{x},t)=-\frac{\partial}{\partial x_1}\left[\frac{1}{2\pi|\mathbf{x}|}F\left(t-\frac{|\mathbf{x}|}{c_o}\right)\right],\quad x_1>0.$$

3.3 The representation (6.3.1) can be used to express the pressure in the form

$$p(\mathbf{x},t)=\rho_o\frac{\partial}{\partial t}\iint\!\!\!\!\!\!\diamondsuit_{\varpi<a}G(\mathbf{x},\mathbf{y},t-\tau)U(\tau)\,dy_2dy_3d\tau,\quad x_1>0, \quad (6.3.2)$$

provided G satisfies

$$G=0\text{ for }y_1=+0,\ \varpi>a;\quad \frac{\partial G}{\partial y_1}=0\text{ for }y_1=+0,\ \varpi<a,$$

where $\varpi=(y_2^2+y_3^2)^{\frac{1}{2}}$. To determine G set $G=G_o+G'$, where G_o is defined as in Question 3.2. Then, as $y_1\to+0$,

$$G_o(\mathbf{x},\mathbf{y},t-\tau)\ \simeq\ \frac{y_1\cos\theta}{2\pi c_o|\mathbf{x}|}\delta'\left(t-\tau-\frac{|\mathbf{x}|}{c_o}\right),\quad |\mathbf{x}|\to\infty,$$

which vanishes on the free surface of the water and on the surface of the piston. The correction G' that takes account of the presence of the piston *in the compact approximation* is obtained by replacing y_1 in this formula by $Y_1=y_1-\varphi_1^*$ defined as in (2.9.16), because $Y_1=0$ on $y_1=0,\ \varpi>a$, and $\partial Y_1/\partial y_1=0$ on the piston $y_1=0,\ \varpi<a$.

Downloaded from https://www.cambridge.org/core. Charité Universitätsmedizin Berlin, on 20 Dec 2021 at 10:08:46, subject to the Cambridge Core terms of use, available at https://www.cambridge.org/core/terms. https://doi.org/10.1017/CBO9781107360273.007

According to §2.9.1f, $Y_1 = (2/\pi)\mathrm{H}\Big(a-\varpi\Big)\Big(a^2-\varpi^2\Big)^{\frac{1}{2}}$ when $y_1 = +0$, i.e.

$$G(\mathbf{x},\mathbf{y},t,\tau) \simeq \frac{\cos\theta}{\pi^2 c_o|\mathbf{x}|}\mathrm{H}\Big(a-\varpi\Big)\Big(a^2-\varpi^2\Big)^{\frac{1}{2}}\delta'\left(t-\tau-\frac{|\mathbf{x}|}{c_o}\right), \qquad y_1 = +0,\ |\mathbf{x}|\to\infty.$$

Therefore (6.3.2) yields

$$p(\mathbf{x},t) \simeq \frac{\rho_o\cos\theta}{\pi^2 c_o|\mathbf{x}|}\left[\frac{d^2U}{dt^2}\right]2\pi\int_0^a \varpi\,(a^2-\varpi^2)^{\frac{1}{2}}\,d\varpi$$
$$= \frac{2\rho_o a^3\cos\theta}{3\pi c_o|\mathbf{x}|}\left[\frac{d^2U}{dt^2}\right], \quad |\mathbf{x}|\to\infty,\ x_1>0.$$

3.6 Equation (3.3.21) written in the form

$$\frac{dQ}{dt}+\frac{U_J Q}{\ell\sigma^2} = \frac{2K_o}{\rho_o}p_I(t), \quad (K_o = A/\ell),$$

is solved by multiplication by the integrating factor $\mathrm{e}^{U_J t/\ell\sigma^2}$, to obtain

$$\frac{d}{dt}\left(Q\,\mathrm{e}^{U_J t/\ell\sigma^2}\right) = \frac{2K_o}{\rho_o}p_I(t)\mathrm{e}^{U_J t/\ell\sigma^2}.$$

Assuming that $p_I(t)\to 0$ as $t\to-\infty$, we find

$$Q = \frac{2K_o}{\rho_o}\int_{-\infty}^{t} p_I(\tau)\mathrm{e}^{-\frac{U_J}{\ell\sigma^2}(t-\tau)}\,d\tau.$$

The pressure in the far field ($x_1\to+\infty$) is found from (3.3.1) or (3.3.20), each of which gives

$$p(\mathbf{x},t) \simeq \frac{K_o}{\pi|\mathbf{x}|}\left\{p_I([t]) - \frac{U_J}{\ell\sigma^2}\int_{-\infty}^{[t]} p_I(\tau)\mathrm{e}^{-\frac{U_J}{\ell\sigma^2}([t]-\tau)}d\tau\right\},\ [t] = t-\frac{|\mathbf{x}|}{c_o}.$$

The influence of the jet on the transmitted sound can be understood by considering the idealised case of an incident sound pulse $p_I(t) = p_o\delta(t/t_o)$, where p_o is the pressure amplitude, and t_o is introduced to make the delta function dimensionless. Then

$$p(\mathbf{x},t) \simeq \frac{K_o p_o}{\pi|\mathbf{x}|}\left\{\delta\left(\frac{[t]}{t_o}\right) - \frac{U_J t_o}{\ell\sigma^2}\mathrm{H}\left(\frac{[t]}{t_o}\right)\exp\left(-\frac{U_J t_o}{\ell\sigma^2}\frac{[t]}{t_o}\right)\right\},$$

which consists of a pulsatile wavefront proportional to the incident pressure followed by an expansionary 'tail' of initial amplitude proportional to $U_J t_o/\ell\sigma^2$, as illustrated in Figure 6.3.1 for $U_J t_o/\ell\sigma^2 = 0.5$. When $p_I(t) = p_o\mathrm{e}^{-(t/t_o)^2}$,

Downloaded from https://www.cambridge.org/core. Charité Universitätsmedizin Berlin, on 20 Dec 2021 at 10:08:46, subject to the Cambridge Core terms of use, available at https://www.cambridge.org/core/terms. https://doi.org/10.1017/CBO9781107360273.007

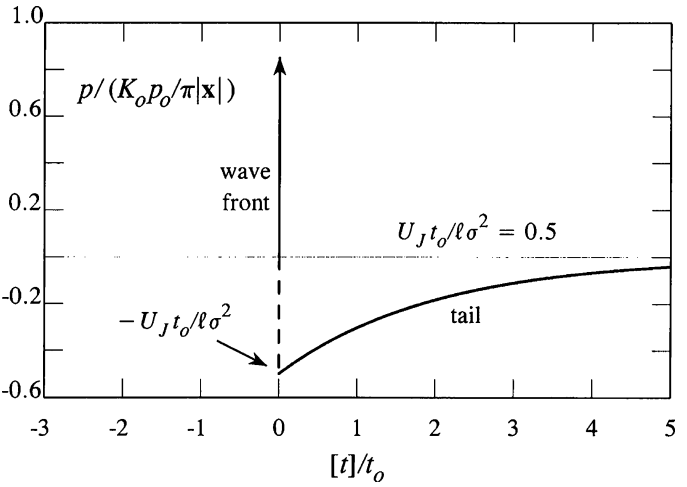

Figure 6.3.1

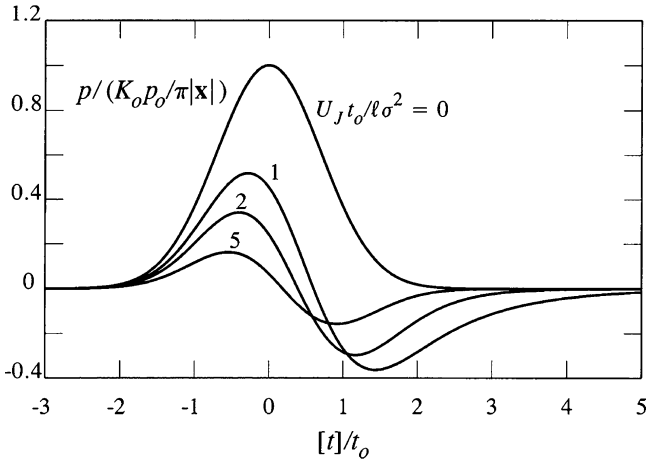

Figure 6.3.2

$$\frac{p(\mathbf{x},t)}{(K_o p_o/\pi|\mathbf{x}|)} = \mathrm{e}^{-([t]/t_o)^2} - \frac{U_J t_o}{\ell\sigma^2}\int_{-\infty}^{[t]/t_o} \exp\left\{-\frac{U_J t_o}{\ell\sigma^2}\left(\frac{[t]}{t_o}-\xi\right)-\xi^2\right\} d\xi.$$

Numerical evaluation of the integral for different values of $U_J t_o/\ell\sigma^2$ yields the wave profiles of Figure 6.3.2. These profiles are diffusive versions of the transmitted wave of Figure 6.3.1 for an incident pulse of

Downloaded from https://www.cambridge.org/core. Charité Universitätsmedizin Berlin, on 20 Dec 2021 at 10:08:46, subject to the Cambridge Core terms of use, available at https://www.cambridge.org/core/terms. https://doi.org/10.1017/CBO9781107360273.007

infinitesimal width. The incident pressure $p_o e^{-(t/t_o)^2}$ is smooth with temporal width $\sim 2t_o$, and its interaction with the jet produces the smoothed, negative tail of the transmitted sound.

6.4 Problems 4

4.2 From §1.8.5 the potential for a compact sphere is

$$\varphi = -\frac{R^3 \cos\theta}{2r^2} U\,(t - r/c_o) - \frac{R^3 \cos\theta}{2c_o r}\frac{\partial U}{\partial t}\,(t - r/c_o)\,.$$

In the far field

$$p = -\rho_o \frac{\partial \varphi}{\partial t} = \frac{\rho_o R^3 \cos\theta}{2c_o r}\frac{\partial^2 U}{\partial t^2}\,(t - r/c_o)$$

where $\frac{\partial^2 U}{\partial t^2} = -\omega^2 U_o \sin\omega\,(t - r/c_o)$.

$$\therefore\ \Pi_a = \oint_S \frac{\langle p^2\rangle}{\rho_o c_o} dS = \frac{\rho_o R^6}{4c_o^3 r^2}\left(\omega^4 U_o^2\right)\oint_S \langle \sin^2\omega\,(t - r/c_o)\rangle \cos^2\theta dS$$

where $\langle \sin^2\omega\,(t - r/c_o)\rangle = \frac{1}{2}$ and the integration is over the surface S of a large sphere centred on the origin O. On S: $dS = r^2 \sin\theta d\theta d\phi$

$$\therefore\ \ \Pi_a = \frac{\rho_o R^6 \omega^4 U_o^2}{8c_o^3}\int_0^{2\pi} d\phi \int_0^{\pi} \cos^2\theta \sin\theta d\theta = \frac{\pi\omega R^3}{6}\rho_o U_o^2 (k_o R)^3.$$

The hydrodynamic power $\Pi_o = \oint_S \langle pv\rangle\, dS$, where the integration is over the surface of the sphere at its mean position. Using near field values:

$$\begin{aligned} v &= \left(\frac{\partial\varphi}{\partial r}\right)_{r=R} &&= U(t)\cos\theta \\ p &= \left(-\rho_o\frac{\partial\varphi}{\partial t}\right)_{r=R} &&= \frac{\rho_o R}{2}\dot{U}(t)\cos\theta \qquad \left(\dot{U} = dU/dt\right) \\ \therefore\ \ \Pi_o &= \left(\frac{\rho_o R}{2}\right)\langle U(t)\dot{U}(t)\rangle \int_0^{2\pi} d\phi \int_0^{\pi} R^2\cos^2\theta\sin\theta d\theta \\ &= \frac{2\pi}{3}\rho_0 R^3 \langle \dot{U}U\rangle. \end{aligned}$$

Now $\langle \dot{U}U\rangle \equiv 0$, when the average is taken over a multiple of half a complete cycle. Therefore, we average over a quarter-cycle only in order to obtain a non-trivial measure of the mechanical energy flux between the sphere and the hydrodynamic flow (without changing the average value of Π_a):

Downloaded from https://www.cambridge.org/core. Charité Universitätsmedizin Berlin, on 20 Dec 2021 at 10:08:46, subject to the Cambridge Core terms of use, available at https://www.cambridge.org/core/terms. https://doi.org/10.1017/CBO9781107360273.007

$$\langle \dot{U}U \rangle_{\frac{1}{4}} = \left(U_o^2\omega\right)\frac{2\omega}{\pi}\int_0^{\frac{\pi}{2\omega}} \sin\omega t\cos\omega t\, dt = \left(U_o^2\omega\right)\frac{2\omega}{\pi}\left[\frac{\sin^2\omega t}{2\omega}\right]_0^{\frac{\pi}{2\omega}}$$
$$= \frac{\omega}{\pi}U_0^2.$$

$$\therefore \quad \Pi_o = \frac{2}{3}\omega R^3\rho_o U_0^2, \quad \text{so that} \quad \frac{\Pi_a}{\Pi_o} = \frac{\pi}{4}(k_o R)^3.$$

4.3

$$\Pi_a = c_o\left(\tfrac{1}{2}\rho_o U_o^2\right)(4\pi R^2)(k_o R)^2, \quad \Pi_o = 8\omega R^3\left(\tfrac{1}{2}\rho_o U_o^2\right),$$
$$\therefore \quad \frac{\Pi_a}{\Pi_o} = \frac{\pi}{2}(k_o R).$$

4.4 We may solve the equation

$$\left(\frac{1}{c_o^2}\frac{\partial^2}{\partial t^2} - \nabla^2\right)p = -\frac{\partial}{\partial x}[F(t)\delta(\mathbf{x})]$$

where $F(t) = -\frac{C_D A}{2}\rho_o(U_o + u\cos\omega t)^2$ is the force in the x direction exerted *on the fluid* by the body, with the body centroid at $\mathbf{x} = 0$, or quote formula (4.3.7) from Curle's theory. In either case the pressure in the far field is given by

$$p = \frac{\cos\theta}{4\pi c_o|\mathbf{x}|}\frac{\partial F}{\partial t}\left(t - \frac{|\mathbf{x}|}{c_o}\right), \quad \cos\theta = \frac{x}{|\mathbf{x}|}.$$

When $u \ll U_o$

$$F \simeq -\frac{C_D A\rho_o U_o^2}{2} - C_D A\rho_o U_o u\cos(\omega t)$$

$$\therefore \quad p \simeq \frac{\omega C_D A\rho_o U_o u\cos\theta}{4\pi c_o|\mathbf{x}|}\sin\omega\left(t - \frac{|\mathbf{x}|}{c_o}\right), \quad |\mathbf{x}| \to \infty.$$

When the body vibrates at speed $v(t)$ in the x direction there is an additional component of the dipole sound pressure equal to

$$\frac{m_o\cos\theta}{4\pi c_o|\mathbf{x}|}\frac{\partial^2 v}{\partial t^2}\left(t - \frac{|\mathbf{x}|}{c_o}\right), \quad |\mathbf{x}| \to \infty,$$

where m_o is the fluid mass displaced by the body.

Downloaded from https://www.cambridge.org/core. Charité Universitätsmedizin Berlin, on 20 Dec 2021 at 10:08:46, subject to the Cambridge Core terms of use, available at https://www.cambridge.org/core/terms. https://doi.org/10.1017/CBO9781107360273.007

4.5 From the linearised Curle formula

$$p(\mathbf{x},t) \simeq -\frac{\partial}{\partial x_i}\oint_S \frac{\left[p'_{ij}\right]dS_j}{4\pi|\mathbf{x}-\mathbf{y}|} + \frac{\partial}{\partial t}\oint_S \frac{\left[\rho_o v_j\right]dS_j}{4\pi|\mathbf{x}-\mathbf{y}|},$$

where S is the surface of the sphere at its undisturbed position. On S (where $|\mathbf{y}| = a$):

$$\text{normal velocity} = v_n = U(t)\cos\theta, \quad \cos\theta = \frac{y_1}{|\mathbf{y}|},$$

and

$$\varphi = -\frac{a}{2}\cos\theta\, U(t), \quad p = -\rho_o\frac{\partial\varphi}{\partial t} = \frac{\rho_o a\cos\theta}{2}\dot{U}(t) \quad \left(\dot{U} = dU/dt\right).$$

Then:

$$-\frac{\partial}{\partial x_i}\oint_S \frac{\left[p'_{ij}\right]dS_j}{4\pi|\mathbf{x}-\mathbf{y}|} = -\frac{\partial}{\partial x_i}\oint_S \frac{\rho_o a\cos\theta\left[\dot{U}(t)\right]\delta_{ij}}{2}\frac{dS_j}{4\pi|\mathbf{x}-\mathbf{y}|}$$

$$= -\frac{\partial}{\partial x_i}\oint_S \frac{\rho_o a\cos\theta}{8\pi|\mathbf{x}-\mathbf{y}|}\dot{U}\left(t - \frac{|\mathbf{x}-\mathbf{y}|}{c_o}\right)dS_i$$

$$\simeq \frac{1}{8\pi|\mathbf{x}|}\frac{x_i}{|\mathbf{x}|}\frac{1}{c_o}\frac{\partial}{\partial t}\oint \rho_o a\cos\theta\,\dot{U}\left(t - \frac{|\mathbf{x}|}{c_o}\right)dS_i,$$

where $dS_i = n_i a^2\sin\theta d\phi d\theta$, $\mathbf{n} = (\cos\theta, \sin\theta\cos\phi, \sin\theta\sin\phi)$, $0 < \theta < \pi$, $0 < \phi < 2\pi$. The integrations over $0 < \phi < 2\pi$ vanish except for $n_1 = \cos\theta$ $(i = 1)$,

$$\therefore \quad -\frac{\partial}{\partial x_i}\oint \frac{\left[p'_{ij}\right]dS_j}{4\pi|\mathbf{x}-\mathbf{y}|} = \frac{\rho_o a^3\cos\Theta}{8\pi|\mathbf{x}|}\frac{1}{c_o}\frac{\partial^2 U}{\partial t^2}\left(t - \frac{|\mathbf{x}|}{c_o}\right)$$

$$\times \int \sin\theta\cos^2\theta d\theta d\phi$$

$$= \frac{\rho_o a^3\cos\Theta}{6c_o|\mathbf{x}|}\left[\frac{\partial^2 U}{\partial t^2}\right], \quad \text{where } \cos\Theta = \frac{x_1}{|\mathbf{x}|}.$$

Next:

$$\frac{\partial}{\partial t}\int \frac{\left[\rho_o v_j\right]dS_j}{4\pi|\mathbf{x}-\mathbf{y}|} \simeq \frac{\rho_o}{4\pi|\mathbf{x}|}\rho_o\frac{\partial}{\partial t}\oint v_n\left(\mathbf{y}, t - \frac{|\mathbf{x}|}{c_o} + \frac{\mathbf{x}\cdot\mathbf{y}}{c_o|\mathbf{x}|}\right)dS$$

$$= \frac{\rho_o}{4\pi|\mathbf{x}|}\frac{\partial}{\partial t}\oint U\left(t - \frac{|\mathbf{x}|}{c_o} + \frac{\mathbf{x}\cdot\mathbf{y}}{c_o|\mathbf{x}|}\right)\cos\theta\, dS$$

Downloaded from https://www.cambridge.org/core. Charité Universitätsmedizin Berlin, on 20 Dec 2021 at 10:08:46, subject to the Cambridge Core terms of use, available at https://www.cambridge.org/core/terms. https://doi.org/10.1017/CBO9781107360273.007

$$\simeq \frac{\rho_o}{4\pi|\mathbf{x}|}\frac{\partial}{\partial t}\left\{U\left(t-\frac{|\mathbf{x}|}{c_o}\right)\oint \cos\theta\, dS + \dot{U}\left(t-\frac{|\mathbf{x}|}{c_o}\right)\oint \cos\theta\,\frac{x_i y_i}{c_o|\mathbf{x}|}dS\right\}$$

$$= \frac{\rho_o}{4\pi|\mathbf{x}|}\left\{0+\frac{a}{c_o}\left[\ddot{U}\right]\oint \cos\theta\,\frac{\mathbf{x}\cdot\mathbf{n}}{|\mathbf{x}|}dS\right\}$$

because $\mathbf{y} = a\mathbf{n}$ on the sphere. Only the component $n_1 = \cos\theta$ yields a non-zero contribution because $dS = a^2\sin\theta d\theta d\phi$,

$$\therefore \quad \frac{\partial}{\partial t}\int \frac{\left[\rho_o v_j\right]dS_j}{4\pi|\mathbf{x}-\mathbf{y}|} \simeq \frac{\rho_o a^3}{3c_o|\mathbf{x}|}\cos\Theta\left[\frac{\partial^2 U}{\partial t^2}\right].$$

The combined contributions from the surface pressure and normal velocity integrals therefore give

$$p(\mathbf{x},t) \simeq \frac{\rho_o a^3}{6c_o|\mathbf{x}|}\cos\Theta\left[\frac{\partial^2 U}{\partial t^2}\right]+\frac{\rho_o a^3}{3c_o|\mathbf{x}|}\cos\Theta\left[\frac{\partial^2 U}{\partial t^2}\right] = \frac{\rho_o a^3}{2c_o|\mathbf{x}|}\cos\Theta\left[\frac{\partial^2 U}{\partial t^2}\right].$$

4.7 Expand the mass conservation formula $D(\rho X_j dS_j)/Dt = 0$ to obtain

$$X_j dS_j \frac{1}{\rho}\frac{D\rho}{Dt} + X_j\frac{D}{Dt}\left(dS_j\right) + dS_j\frac{DX_j}{Dt} = 0.$$

The continuity equation and equation (4.4.6) imply that

$$X_j\left(-dS_j \mathrm{div}\,\mathbf{v} + \frac{D}{Dt}\left(dS_j\right) + dS_i\frac{\partial v_i}{\partial x_j}\right) = 0.$$

Therefore, because $\mathbf{X}$ is an arbitrary infinitesimal vector

$$\frac{D}{Dt}\left(dS_j\right) = dS_j\,\mathrm{div}\,\mathbf{v} - dS_i\frac{\partial v_i}{\partial x_j}.$$

4.8

$$\frac{D}{Dt}(\boldsymbol{\omega}\cdot d\mathbf{S}) \equiv \frac{D}{Dt}\left[\rho\left(\frac{\boldsymbol{\omega}}{\rho}\right)\cdot d\mathbf{S}\right] = \frac{1}{\rho}\frac{D\rho}{Dt}(\boldsymbol{\omega}\cdot d\mathbf{S}) + \rho d\mathbf{S}\cdot\frac{D}{Dt}\left(\frac{\boldsymbol{\omega}}{\rho}\right) + \boldsymbol{\omega}\cdot\frac{D}{Dt}d\mathbf{S}$$

Downloaded from https://www.cambridge.org/core. Charité Universitätsmedizin Berlin, on 20 Dec 2021 at 10:08:46, subject to the Cambridge Core terms of use, available at https://www.cambridge.org/core/terms. https://doi.org/10.1017/CBO9781107360273.007

This vanishes because the continuity equation, the vorticity equation of Question 4.6 and the result of Question 4.7 imply that the right-hand side is equivalent to

$$-\text{div}\,\mathbf{v}\,(\boldsymbol{\omega}\cdot d\mathbf{S}) + d\mathbf{S}\cdot(\boldsymbol{\omega}\cdot\nabla)\mathbf{v} + (\boldsymbol{\omega}\cdot d\mathbf{S})\text{div}\,\mathbf{v} - d\mathbf{S}\cdot(\boldsymbol{\omega}\cdot\nabla)\mathbf{v} \equiv 0.$$

Thus, for any material closed contour C bounding an open material surface S in the fluid

$$\Gamma = \oint_C \mathbf{v}\cdot d\mathbf{x} = \int_S \boldsymbol{\omega}\cdot d\mathbf{S} = \sum_n (\boldsymbol{\omega}\cdot d\mathbf{S})_n$$

$$\therefore \quad \frac{D\Gamma}{Dt} = \sum_n \frac{D}{Dt}(\boldsymbol{\omega}\cdot d\mathbf{S})_n \equiv 0.$$

4.11 **Kirchhoff's spinning vortex:** The vorticity is non-zero only within the elliptic region $r < a\,\{1+\epsilon\cos(2\theta-\Omega t/2)\}$, that is,

$$\boldsymbol{\omega} = \Omega\mathbf{k}\text{H}\Big(a - r + a\epsilon\cos(2\theta-\Omega t/2)\Big),$$

where $\text{H}(\cdot)$ is the Heaviside step function and $\mathbf{k}$ is a unit vector in the x_3 direction.

$$\therefore \quad \boldsymbol{\omega}\wedge\mathbf{v} = |\boldsymbol{\omega}|\mathbf{k}\wedge\mathbf{v} = |\boldsymbol{\omega}|(-v_2, v_1)$$

$$= -\tfrac{1}{2}\Omega^2 r\,\text{H}\Big(a - r + a\epsilon\cos(2\theta-\Omega t/2)\Big)$$

$$\times\Big(\cos\theta - \epsilon\cos(\theta-\Omega t/2), \sin\theta + \epsilon\sin(\theta-\Omega t/2)\Big).$$

Expand this to first order in ϵ:

$$\boldsymbol{\omega}\wedge\mathbf{v} \simeq -\tfrac{1}{2}\Omega^2 r\,\text{H}(a-r)(\cos\theta,\ \sin\theta)$$

$$-\tfrac{1}{2}\epsilon\Omega^2 r\,\text{H}(a-r)[-\cos(\theta-\Omega t/2),\ \sin(\theta-\Omega t/2)]$$

$$-\tfrac{1}{2}\epsilon\Omega^2 a^2\,\delta(a-r)\cos(2\theta-\Omega t/2)(\cos\theta,\ \sin\theta). \quad (6.4.1)$$

The first term on the right may be discarded because it does not depend on time and therefore makes no contribution to the sound.

A quadrupole representation T_{ij} of the vortex source is found by introducing a test function $f(x_1, x_2)$ and considering the integral

Downloaded from https://www.cambridge.org/core. Charité Universitätsmedizin Berlin, on 20 Dec 2021 at 10:08:46, subject to the Cambridge Core terms of use, available at https://www.cambridge.org/core/terms. https://doi.org/10.1017/CBO9781107360273.007

$$I = \iint_{-\infty}^{\infty} f(x_1, x_2)\,\mathrm{div}(\boldsymbol{\omega} \wedge \mathbf{v})\,dx_1 dx_2$$

$$= -\iint_{-\infty}^{\infty} \frac{\partial f}{\partial x_\alpha}(x_1, x_2)\,(\boldsymbol{\omega} \wedge \mathbf{v})_\alpha\,dx_1 dx_2$$

$$= -\iint_{-\infty}^{\infty} \left\{ \left(\frac{\partial f}{\partial x_\alpha}\right)_0 + x_\beta \left(\frac{\partial^2 f}{\partial x_\alpha \partial x_\beta}\right)_0 + \cdots \right\} (\boldsymbol{\omega} \wedge \mathbf{v})_\alpha\,dx_1 dx_2$$

$$= 0 - \iint_{-\infty}^{\infty} \left(\frac{\partial^2 f}{\partial x_\alpha \partial x_\beta}\right)_0 x_\beta (\boldsymbol{\omega} \wedge \mathbf{v})_\alpha\,dx_1 dx_2 + \cdots$$

$$\approx -\left(\frac{\partial^2 f}{\partial x_\alpha \partial x_\beta}\right)_0 \Big(A_{\alpha\beta} + B_{\alpha\beta}\Big), \quad \text{correct to order } \epsilon, \tag{6.4.2}$$

where the repeated Greek subscripts α, β are summed over the 1, 2 directions only.

The two-dimensional matrices (tensors) $A_{\alpha\beta}$, $B_{\alpha\beta}$ correspond respectively to the contributions from the second and third terms on the right of expression (6.4.1) for $\boldsymbol{\omega} \wedge \mathbf{v}$. In terms of polar coordinates $x_\beta = r(\cos\theta, \sin\theta)_\beta$, and

$$A_{\alpha\beta} = -\tfrac{1}{2}\epsilon\Omega^2 \iint_{-\infty}^{\infty} r^2\,\mathrm{H}(a-r)[-\cos(\theta - \Omega t/2), \sin(\theta - \Omega t/2)]_\alpha (\cos\theta, \sin\theta)_\beta\,dx_1 dx_2$$

$$= -\tfrac{1}{2}\epsilon\Omega^2 \int_0^{2\pi}\int_0^a r^3\,[-\cos(\theta - \Omega t/2),\ \sin(\theta - \Omega t/2)]_\alpha \times (\cos\theta, \sin\theta)_\beta\,dr d\theta$$

$$= -\tfrac{1}{8}\epsilon\Omega^2 a^4 \int_0^{2\pi} \begin{pmatrix} -\cos^2\theta\,\cos(\Omega t/2) - \sin^2\theta\,\sin(\Omega t/2) \\ -\cos^2\theta\,\sin(\Omega t/2) \quad \sin^2\theta\,\cos(\Omega t/2) \end{pmatrix}_{\alpha\beta} d\theta$$

$$\therefore\ A_{\alpha\beta} = \tfrac{\pi}{8}\epsilon\Omega^2 a^4 \begin{pmatrix} \cos(\Omega t/2) & \sin(\Omega t/2) \\ \sin(\Omega t/2) & -\cos(\Omega t/2) \end{pmatrix}_{\alpha\beta}.$$

Similarly

$$B_{\alpha\beta} = -\tfrac{1}{2}\epsilon\Omega^2 a^2 \int_0^{2\pi}\int_0^{\infty} \delta(a-r)\cos(2\theta - \Omega t/2)(\cos\theta,\ \sin\theta)_\alpha \times (\cos\theta,\ \sin\theta)_\beta\,r^2 dr d\theta$$

Downloaded from https://www.cambridge.org/core. Charité Universitätsmedizin Berlin, on 20 Dec 2021 at 10:08:46, subject to the Cambridge Core terms of use, available at https://www.cambridge.org/core/terms. https://doi.org/10.1017/CBO9781107360273.007

$$= -\tfrac{1}{2}\epsilon\Omega^2 a^4 \int_0^{2\pi} \cos(2\theta - \Omega t/2) \begin{pmatrix} \cos^2\theta & \sin\theta\cos\theta \\ \sin\theta\cos\theta & \sin^2\theta \end{pmatrix}_{\alpha\beta} d\theta$$

$$= -\tfrac{1}{4}\epsilon\Omega^2 a^4 \int_0^{2\pi} \cos(2\theta - \Omega t/2) \begin{pmatrix} 1+\cos 2\theta & \sin 2\theta \\ \sin 2\theta & 1-\cos 2\theta \end{pmatrix}_{\alpha\beta} d\theta$$

$$= -\tfrac{\pi}{4}\epsilon\Omega^2 a^4 \begin{pmatrix} \cos(\Omega t/2) & \sin(\Omega t/2) \\ \sin(\Omega t/2) & -\cos(\Omega t/2) \end{pmatrix}_{\alpha\beta}.$$

Hence

$$A_{\alpha\beta} + B_{\alpha\beta} = -\tfrac{\pi}{8}\epsilon\Omega^2 a^4 \begin{pmatrix} \cos(\Omega t/2) & \sin(\Omega t/2) \\ \sin(\Omega t/2) & -\cos(\Omega t/2) \end{pmatrix}_{\alpha\beta}.$$

Therefore (6.4.2) becomes

$$I = \tfrac{\pi}{8}\epsilon\Omega^2 a^4 \left(\frac{\partial^2 f}{\partial x_\alpha \partial x_\beta}\right)_0 \begin{pmatrix} \cos(\Omega t/2) & \sin(\Omega t/2) \\ \sin(\Omega t/2) & -\cos(\Omega t/2) \end{pmatrix}_{\alpha\beta}$$

$$\equiv \iint_{-\infty}^{\infty} f(x_1, x_2) \frac{\partial^2}{\partial x_\alpha \partial x_\beta} \left(T_{\alpha\beta}\delta(x_1)\delta(x_2)\right) dx_1 dx_2.$$

This means, that to first order in ϵ the **vortex sound source** is

$$\operatorname{div}(\boldsymbol{\omega} \wedge \mathbf{v}) \simeq \frac{\partial^2}{\partial x_i \partial x_j} \left(T_{ij}\delta(x_1)\delta(x_2)\right), \quad i,\ j = 1,\ 2$$

where $$T_{ij} = \frac{\epsilon\pi\Omega^2 a^4}{8} \begin{pmatrix} \cos(\Omega t/2) & \sin(\Omega t/2) \\ \sin(\Omega t/2) & -\cos(\Omega t/2) \end{pmatrix}.$$

Calculation of the sound: The acoustic radiation is approximated by the solution of

$$\left(\frac{1}{c_o^2}\frac{\partial^2}{\partial t^2} - \nabla^2\right) B = \frac{\partial^2}{\partial x_i \partial x_j} \left(T_{ij}(t)\delta(x_1)\delta(x_2)\right).$$

By using the free space retarded potential solution for a quadrupole (§1.10.2) we write

$$B = \frac{1}{4\pi}\frac{\partial^2}{\partial \bar{x}_i \partial \bar{x}_j} \int_{-\infty}^{\infty} T_{ij}\left(t - \frac{|\mathbf{x}-\mathbf{y}|}{c_o}\right) \frac{\delta(y_1)\delta(y_2)\, d^3\mathbf{y}}{|\mathbf{x}-\mathbf{y}|} \quad (\bar{\mathbf{x}} = (x_1, x_2))$$

$$= \frac{1}{4\pi}\frac{\partial^2}{\partial \bar{x}_i \partial \bar{x}_j} \int_{-\infty}^{\infty} T_{ij}\left(t - \frac{\sqrt{r^2+\xi^2}}{c_o}\right) \frac{d\xi}{\sqrt{r^2+\xi^2}} \quad (r = |\bar{\mathbf{x}}|).$$

Downloaded from https://www.cambridge.org/core. Charité Universitätsmedizin Berlin, on 20 Dec 2021 at 10:08:46, subject to the Cambridge Core terms of use, available at https://www.cambridge.org/core/terms. https://doi.org/10.1017/CBO9781107360273.007

When $r \to \infty$ $\quad \dfrac{\partial}{\partial \bar{x}_i} \simeq \dfrac{-\bar{x}_i}{c_o\sqrt{r^2+\xi^2}} \dfrac{\partial}{\partial t}$,

$$\therefore \quad B \simeq \frac{\bar{x}_i \bar{x}_j}{4\pi c_o^2} \frac{\partial^2}{\partial t^2} \int_{-\infty}^{\infty} T_{ij}\left(t - \frac{\sqrt{r^2+\xi^2}}{c_o}\right) \frac{d\xi}{(r^2+\xi^2)^{\frac{3}{2}}}$$

$$= \frac{-\epsilon\, \Omega^4 a^4 \bar{x}_i \bar{x}_j}{2^7 c_o^2} \int_{-\infty}^{\infty} \begin{pmatrix} \cos(\Omega[t]/2) & \sin(\Omega[t]/2) \\ \sin(\Omega[t]/2) & -\cos(\Omega[t]/2) \end{pmatrix}_{ij} \times \frac{d\xi}{(r^2+\xi^2)^{\frac{3}{2}}}, \tag{6.4.3}$$

where $[t] = t - \dfrac{\sqrt{r^2+\xi^2}}{c_o}$.

The integral is approximated by the method of stationary phase (§4.6.4) in the limit as $k_o r \to \infty$, where $k_o = \Omega/2c_o$. Consider

$$\int_{-\infty}^{\infty} \{\cos(\Omega[t]/2) - i\sin(\Omega[t]/2)\} \frac{d\xi}{(r^2+\xi^2)^{\frac{3}{2}}}$$

$$= \frac{\mathrm{e}^{-i\Omega t/2}}{r^2} \int_{-\infty}^{\infty} \frac{\mathrm{e}^{ik_o r\sqrt{1+\mu^2}} d\mu}{(1+\mu^2)^{\frac{3}{2}}}$$

$$\simeq \frac{\mathrm{e}^{-i\frac{\Omega}{2}\left(t-\frac{r}{c_o}\right)}}{r^2} \int_{-\infty}^{\infty} \mathrm{e}^{\frac{ik_o r\mu^2}{2}} d\mu$$

$$= \frac{1}{r^2}\left(\frac{2\pi}{k_o r}\right)^{\frac{1}{2}} \mathrm{e}^{-i\frac{\Omega}{2}\left(t-\frac{r}{c_o}\right)+i\frac{\pi}{4}},$$

that is, taking real and imaginary parts

$$\int_{-\infty}^{\infty} \begin{pmatrix} \cos(\Omega[t]/2) \\ \sin(\Omega[t]/2) \end{pmatrix} \frac{d\xi}{(r^2+\xi^2)^{\frac{3}{2}}}$$

$$\simeq \frac{1}{r^2}\left(\frac{4\pi c_o}{\Omega r}\right)^{\frac{1}{2}} \begin{pmatrix} \cos\left[\frac{\Omega}{2}\left(t-\frac{r}{c_o}\right)-\frac{\pi}{4}\right] \\ \sin\left[\frac{\Omega}{2}\left(t-\frac{r}{c_o}\right)-\frac{\pi}{4}\right] \end{pmatrix}, \quad \frac{\Omega r}{c_o} \to \infty.$$

Hence, by putting $\bar{\mathbf{x}} = r(\cos\theta, \sin\theta)$ in equation (6.4.3), we find

Downloaded from https://www.cambridge.org/core. Charité Universitätsmedizin Berlin, on 20 Dec 2021 at 10:08:46, subject to the Cambridge Core terms of use, available at https://www.cambridge.org/core/terms. https://doi.org/10.1017/CBO9781107360273.007

$$B = \frac{p}{\rho_o} \simeq \frac{-\epsilon\,\Omega^4 a^4}{2^7 c_o^2}\left(\frac{4\pi c_o}{\Omega r}\right)^{\frac{1}{2}} \cos\left\{\frac{\Omega}{2}\left(t-\frac{r}{c_o}\right)-2\theta-\frac{\pi}{4}\right\}$$

$$\therefore\ p(r,\theta,t) \simeq -\frac{\epsilon}{8}\rho_o U^2 M^{\frac{3}{2}}\left(\frac{2\pi a}{r}\right)^{\frac{1}{2}} \cos\left\{2\theta-\frac{\Omega}{2}\left(t-\frac{r}{c_o}\right)+\frac{\pi}{4}\right\},$$
$$r\to\infty,$$

where $U = \Omega a/2,\ M = U/c_o$.

4.16 Put $\boldsymbol{\omega} = \Gamma\delta(x_1-Ut)\delta(r-a)\hat{\boldsymbol{\theta}}$, where $r = (x_2^2+x_3^2)^{\frac{1}{2}}$ and $\hat{\boldsymbol{\theta}}$ is a unit vector tangential to the vortex ring. Also, put $\mathbf{v} = U\mathbf{i}$ where $\mathbf{i}$ is a unit vector in the x_1 direction. Then $\boldsymbol{\omega}\wedge\mathbf{v} = \Gamma U\delta(x_1-Ut)\delta(r-a)\hat{\mathbf{r}}$, where $\hat{\mathbf{r}}$ is a unit vector in the radial direction in the x_2x_3-plane, and

$$\operatorname{div}(\boldsymbol{\omega}\wedge\mathbf{v}) = \frac{1}{r}\frac{\partial}{\partial r}\{r\Gamma U\delta(x_1-Ut)\delta(r-a)\}$$

$$\equiv \frac{a\Gamma U\delta(x_1-Ut)}{r}\frac{\partial}{\partial r}\{\delta(r-a)\}.$$

Let $f(x_2,x_3)$ be a 'test' function and consider

$$I = \iint_{-\infty}^{\infty} f(x_2,x_3)\frac{1}{r}\frac{\partial}{\partial r}\{\delta(r-a)\}\,dx_2dx_3$$

$$= \iint_{-\infty}^{\infty}\left(f(\mathbf{0}) + x_\alpha\frac{\partial f}{\partial x_\alpha} + \frac{1}{2}x_\alpha x_\beta\frac{\partial^2 f}{\partial x_\alpha x_\beta}+\cdots\right)$$
$$\times\frac{1}{r}\frac{\partial}{\partial r}\{\delta(r-a)\}\,dx_2dx_3,$$

where in the double Taylor series expansion of f about the origin each repeated Greek subscript is to be summed over the 2, 3 directions only. The integration is performed by transforming to polar coordinates (r,θ) such that $(x_2,x_3) = (r\cos\theta, r\sin\theta)$ and $dx_2dx_3 = rdrd\theta$, to obtain

$$I = \int_0^{2\pi}\int_0^{\infty}\Big(f(\mathbf{0}) + r(\cos\theta,\sin\theta)_\alpha\frac{\partial f}{\partial x_\alpha}$$
$$+\frac{1}{2}r^2(\cos\theta,\sin\theta)_\alpha(\cos\theta,\sin\theta)_\beta\frac{\partial^2 f}{\partial x_\alpha x_\beta}+\cdots\Big)$$
$$\times\frac{1}{r}\frac{\partial}{\partial r}\{\delta(r-a)\}\,rdrd\theta$$

Downloaded from https://www.cambridge.org/core. Charité Universitätsmedizin Berlin, on 20 Dec 2021 at 10:08:46, subject to the Cambridge Core terms of use, available at https://www.cambridge.org/core/terms. https://doi.org/10.1017/CBO9781107360273.007

$$= 0 + 0 \; - \; a \int_0^{2\pi} (\cos\theta, \sin\theta)_\alpha (\cos\theta, \sin\theta)_\beta \frac{\partial^2 f}{\partial x_\alpha x_\beta} \, d\theta$$

$$= -a\pi \delta_{\alpha\beta} \frac{\partial^2 f}{\partial x_\alpha x_\beta} \; \equiv \; -a\pi \left(\frac{\partial^2}{\partial x_2^2} + \frac{\partial^2}{\partial x_3^2} \right) f.$$

Hence, for any test function $f(x_2, x_3)$

$$\iint_{-\infty}^{\infty} f(x_2, x_3) \mathrm{div}(\boldsymbol{\omega} \wedge \mathbf{v}) dx_2 dx_3$$
$$= -\pi a^2 \Gamma U \delta(x_1 - Ut) \left(\left[\frac{\partial^2}{\partial x_2^2} + \frac{\partial^2}{\partial x_3^2} \right] f \right)_{x_2 = x_3 = 0}$$

$$\therefore \quad \mathrm{div}(\boldsymbol{\omega} \wedge \mathbf{v}) \simeq -\pi a^2 \Gamma U \left(\frac{\partial^2}{\partial x_2^2} + \frac{\partial^2}{\partial x_3^2} \right) \{\delta(x_1 - Ut)\delta(x_2)\delta(x_3)\}.$$

4.18 When the vortex radius $a \ll h$ its vortex sound source representation can be approximated by the quadrupole (see Question 4.16)

$$\mathrm{div}(\boldsymbol{\omega} \wedge \mathbf{v}) \simeq -\pi a^2 \Gamma U \left(\frac{\partial^2}{\partial x_2^2} + \frac{\partial^2}{\partial x_3^2} \right) \{\delta(x_1 - Ut)\delta(x_2 - h)\delta(x_3)\}.$$

The overall acoustic pressure is

$$p(\mathbf{x}, t) \simeq \rho_o \iint G(\mathbf{x}, \mathbf{y}, t, \tau) \mathrm{div}(\boldsymbol{\omega} \wedge \mathbf{v}) \, d^3\mathbf{y} d\tau$$

$$\simeq -\rho_o \pi a^2 \Gamma U \iint G(\mathbf{x}, \mathbf{y}, t, \tau)$$
$$\times \left(\frac{\partial^2}{\partial y_2^2} + \frac{\partial^2}{\partial y_3^2} \right) \{\delta(y_1 - U\tau)\delta(y_2 - h)\delta(y_3)\} \, d^3\mathbf{y} d\tau$$

$$= -\rho_o \pi a^2 \Gamma U \iint \delta(y_1 - U\tau)\delta(y_2 - h)\delta(y_3)$$
$$\times \left(\frac{\partial^2}{\partial y_2^2} + \frac{\partial^2}{\partial y_3^2} \right) G(\mathbf{x}, \mathbf{y}, t, \tau) \, d^3\mathbf{y} d\tau$$

$$= -\rho_o \pi a^2 \Gamma U \int \left[\left(\frac{\partial^2}{\partial y_2^2} + \frac{\partial^2}{\partial y_3^2} \right) G(\mathbf{x}, \mathbf{y}, t, \tau) \right]_{\mathbf{y} = (U\tau, h, 0)} d\tau. \tag{6.4.4}$$

In the acoustic far field ($|\mathbf{x}| \to \infty$) the compact Green's function is approximated as follows:

Downloaded from https://www.cambridge.org/core. Charité Universitätsmedizin Berlin, on 20 Dec 2021 at 10:08:46, subject to the Cambridge Core terms of use, available at https://www.cambridge.org/core/terms. https://doi.org/10.1017/CBO9781107360273.007

$$G = \frac{1}{4\pi|\mathbf{X}-\mathbf{Y}|}\,\delta\left(t-\tau-\frac{|\mathbf{X}-\mathbf{Y}|}{c_o}\right)$$

$$\simeq \frac{1}{4\pi|\mathbf{x}|}\,\delta\left(t-\tau-\frac{|\mathbf{x}|}{c_o}+\frac{\mathbf{x}\cdot\mathbf{Y}}{c_o|\mathbf{x}|}\right)$$

$$\simeq \frac{1}{4\pi|\mathbf{x}|}\left\{\delta\left(t-\tau-\frac{|\mathbf{x}|}{c_o}\right)+\frac{x_jY_j}{c_o|\mathbf{x}|}\delta'\left(t-\tau-\frac{|\mathbf{x}|}{c_o}\right)\right\}. \quad (6.4.5)$$

Only the second term in the curly brackets of (6.4.5) makes a non-trivial contribution to (6.4.4), which becomes

$$p(\mathbf{x},t) \simeq \frac{-\rho_o a^2\Gamma U x_j}{4c_o|\mathbf{x}|^2}\int\left[\left(\frac{\partial^2}{\partial y_2^2}+\frac{\partial^2}{\partial y_3^2}\right)Y_j\right]_{\mathbf{y}=(U\tau,h,0)} \times\delta'\left(t-\tau-\frac{|\mathbf{x}|}{c_o}\right)d\tau$$

$$= \frac{-\rho_o a^2\Gamma U x_j}{4c_o|\mathbf{x}|^2}\frac{\partial}{\partial t}\left[\left(\frac{\partial^2}{\partial y_2^2}+\frac{\partial^2}{\partial y_3^2}\right)Y_j\right]_{\mathbf{y}=(U[t],h,0)}$$

$$= \frac{\rho_o a^2\Gamma U x_j}{4c_o|\mathbf{x}|^2}\frac{\partial}{\partial t}\left[\frac{\partial^2 Y_j}{\partial y_1^2}\right]_{\mathbf{y}=(U[t],h,0)}, \quad (6.4.6)$$

because $\nabla^2 Y_j = 0$.

For a sphere of radius R with centre at the origin

$$Y_j = y_j\left(1+\frac{R^3}{2|\mathbf{y}|^3}\right)$$

in which we can put $y_2 = h,\ y_3 = 0$ for use in (6.4.6). Therefore only the components Y_1 and Y_2 contribute to the sound, corresponding respectively to drag and lift dipole sources. Taking the two cases $j = 1$ and $j = 2$ in (6.4.6) we obtain (for $\mathbf{x}$ in the median plane $x_3 = 0$), respectively,

$$p_d(\mathbf{x},t) = \frac{\rho_o a^2\Gamma U\cos\Theta}{4c_o|\mathbf{x}|}\frac{\partial}{\partial t}\left[\frac{\partial^2 Y_1}{\partial y_1^2}\right]_{\mathbf{y}=(U[t],h,0)},$$

$$p_\ell(\mathbf{x},t) = \frac{\rho_o a^2\Gamma U\sin\Theta}{4c_o|\mathbf{x}|}\frac{\partial}{\partial t}\left[\frac{\partial^2 Y_2}{\partial y_1^2}\right]_{\mathbf{y}=(U[t],h,0)}.$$

Downloaded from https://www.cambridge.org/core. Charité Universitätsmedizin Berlin, on 20 Dec 2021 at 10:08:46, subject to the Cambridge Core terms of use, available at https://www.cambridge.org/core/terms. https://doi.org/10.1017/CBO9781107360273.007

Now

$$\left(\frac{\partial^2 Y_1}{\partial y_1^2}\right)_{(y_1,h,0)} = \frac{3R^3 y_1(2y_1^2 - 3h^2)}{2(y_1^2 + h^2)^{\frac{7}{2}}}$$

$$\therefore \quad p_d(\mathbf{x}, t) \simeq \frac{3\rho_o a^2 R^3 \Gamma U \cos\Theta}{8c_o|\mathbf{x}|} \frac{\partial}{\partial t}\left(\frac{U[t](2U^2[t]^2 - 3h^2)}{(U^2[t]^2 + h^2)^{\frac{7}{2}}}\right)$$

$$= \frac{-\rho_o \Gamma U M \cos\Theta}{|\mathbf{x}|}\left(\frac{a^2 R^3}{h^5}\right)\frac{3(3 - 24T^2 + 8T^4)}{8(1 + T^2)^{\frac{9}{2}}},$$

where T denotes the non-dimensional retarded time $U[t]/h$ and $M = U/c_o$.

For the lift dipole

$$\left(\frac{\partial^2 Y_2}{\partial y_1^2}\right)_{(y_1,h,0)} = \frac{3hR^3(4y_1^2 - h^2)}{2(y_1^2 + h^2)^{\frac{7}{2}}}$$

$$\therefore \quad p_\ell(\mathbf{x}, t) \simeq \frac{3\rho_o a^2 h R^3 \Gamma U \sin\Theta}{8c_o|\mathbf{x}|} \frac{\partial}{\partial t}\left(\frac{4U^2[t]^2 - h^2}{(U^2[t]^2 + h^2)^{\frac{7}{2}}}\right)$$

$$= \frac{\rho_o \Gamma U M \sin\Theta}{|\mathbf{x}|}\left(\frac{a^2 R^3}{h^5}\right)\frac{15T(3 - 4T^2)}{8(1 + T^2)^{\frac{9}{2}}}.$$

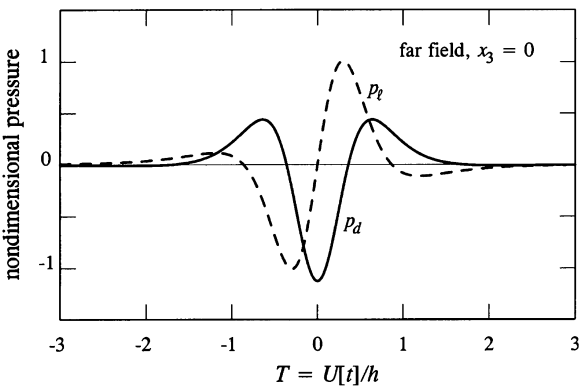

Figure 6.4.1

Downloaded from https://www.cambridge.org/core. Charité Universitätsmedizin Berlin, on 20 Dec 2021 at 10:08:46, subject to the Cambridge Core terms of use, available at https://www.cambridge.org/core/terms. https://doi.org/10.1017/CBO9781107360273.007

The figure illustrates the calculated non-dimensional pressure signatures

$$p_d \Big/ \left(\frac{\rho_o \Gamma U M \cos\Theta}{|\mathbf{x}|} \frac{a^2 R^3}{h^5} \right) \quad \text{and} \quad p_\ell \Big/ \left(\frac{\rho_o \Gamma U M \sin\Theta}{|\mathbf{x}|} \frac{a^2 R^3}{h^5} \right)$$

4.19 From Problem 4.16 we can take

$$(\boldsymbol{\omega} \wedge \mathbf{v})_1 = 0,$$
$$(\boldsymbol{\omega} \wedge \mathbf{v})_\alpha = -\pi R^2 \Gamma U \frac{\partial}{\partial x_\alpha} \{\delta(x_1 - Ut)\delta(x_2 - h)\delta(x_3)\}, \quad \alpha = 2,\ 3.$$

The $\mathbf{y}$-dependent part of the compact Green's function is

$$G(\mathbf{x}, \mathbf{y}, t - \tau) = \frac{x_j Y_j}{4\pi c_o |\mathbf{x}|^2} \delta' \left(t - \tau - \frac{|\mathbf{x}|}{c_o} \right), \quad |\mathbf{x}| \to \infty,$$

where

$$Y_1 = y_1,\ Y_2 = \mathrm{Re}\Big(-i\sqrt{z^2 - a^2} \Big),\ Y_3 = y_3 \quad (z = y_i + iy_2),$$

and the far field acoustic pressure is

$$p(\mathbf{x}, t) \simeq -\frac{\rho_o x_j}{4\pi c_o |\mathbf{x}|^2} \frac{\partial}{\partial t} \int \left[\boldsymbol{\omega} \wedge \mathbf{v} \cdot \frac{\partial Y_j}{\partial \mathbf{y}} \right] d^3\mathbf{y},$$

the square brackets denoting evaluation at the retarded time $t - |\mathbf{x}|/c_o$.

Substituting for $\boldsymbol{\omega} \wedge \mathbf{v}$ and evaluating the integral, we find

$$p(\mathbf{x}, t) \simeq -\frac{R^2 \Gamma U \cos\Theta}{4c_o |\mathbf{x}|} \frac{\partial}{\partial t} \left(\frac{\partial^2 Y_2}{\partial y_\alpha^2} \right)_{(U[t], h, 0)}$$
$$\equiv \frac{R^2 \Gamma U \cos\Theta}{4c_o |\mathbf{x}|} \frac{\partial}{\partial t} \left(\frac{\partial^2 Y_2}{\partial y_1^2} \right)_{(U[t], h, 0)},$$

because $\nabla^2 Y_2 = 0$, and where $\cos\Theta = x_2/|\mathbf{x}|$.

The acoustic pressure produced by the 'potential flow interaction' of the vortex ring with the airfoil (no vortex shedding) is obtained by taking $Y_2 = \mathrm{Re}\Big(-i\sqrt{z^2 - a^2} \Big)$. To apply the Kutta condition at the trailing edge the singularity of Y_2 at $z = a$ is formally deleted by putting

$$Y_2 \simeq \sqrt{2a}\mathrm{Re}\Big(\sqrt{z + a} \Big)$$

in the acoustic pressure formula. This yields the solid-line pressure signature in the figure of Question 4.19.

Downloaded from https://www.cambridge.org/core. Charité Universitätsmedizin Berlin, on 20 Dec 2021 at 10:08:46, subject to the Cambridge Core terms of use, available at https://www.cambridge.org/core/terms. https://doi.org/10.1017/CBO9781107360273.007

6.5 Problems 5

5.2 When $h = b - a \ll b$ the velocity potential $\varphi = \mathrm{Re}\, w$ governs the local flow in the vicinity of the narrow, annular strip that forms the baffle. Take coordinate axes (x, y) with origin at O (Figure 6.5.1). Then $w = i\sqrt{y^2 - h^2}$ in the plane of the aperture (- - - -) where $y > h$, so that $\varphi = 0$ there. The complex potential accordingly defines φ as an odd function of x. On the faces $x = \pm 0,\ 0 < y < h$ of the baffle, $\varphi = \pm U\sqrt{h^2 - y^2}$.

This behaviour of φ at $x = 0$ must be replicated by the formal solution

$$\varphi = Ux_1 + \mathrm{sgn}(x_1)\left(\frac{U\ell_d}{2} + \sum_{n=1}^{\infty} A_n \mathrm{J}_0\left(\lambda_n \frac{\varpi}{b}\right) \mathrm{e}^{-\lambda_n |x_1|/b}\right),$$

$$\varpi = \sqrt{x_2^2 + x_3^2},$$

at $x_1 \equiv x = 0$. By equating the two representations at $x = 0$ and applying the orthogonality condition (5.3.7) for $n = 0$, it follows that

$$\frac{\ell_d b^2}{4} = \int_{b-h}^{b} \sqrt{h^2 - y^2}\, \varpi\, d\varpi \equiv \int_0^h \sqrt{h^2 - y^2}\,(b - y)dy$$

$$\simeq \frac{\pi b h^2}{4} \quad (b \gg h),$$

and therefore that $\ell_d/b = \pi\,(1 - a/b)^2$. This gives the approximation (5.3.11), where $A_d = \pi b^2$.

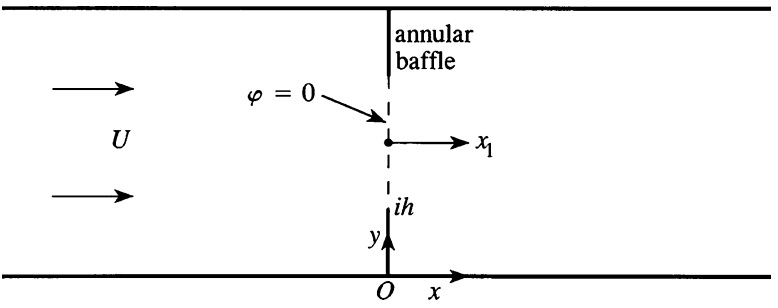

Figure 6.5.1

5.3 Consider the region V consisting of the fluid outside the duct and within a section of the duct of length $L \gg b$ bounded internally by a piston of equal area $A_d = \pi b^2$ that can move freely (Figure 5.4.6). Let the piston be set in motion impulsively at speed U towards the open end. The fluid is assumed to be ideal and *incompressible*, and moves irrotationally with

Downloaded from https://www.cambridge.org/core. Charité Universitätsmedizin Berlin, on 20 Dec 2021 at 10:08:46, subject to the Cambridge Core terms of use, available at https://www.cambridge.org/core/terms. https://doi.org/10.1017/CBO9781107360273.007

velocity potential $U\varphi(\mathbf{x})$, where $\varphi(\mathbf{x})$ is the solution of Laplace's equation with the properties

$$\varphi(\mathbf{x}) \sim \begin{cases} -A_d/2\pi|\mathbf{x}|, & |\mathbf{x}| \gg b \ \text{ in free space,} \\ x_1 - \ell_E, & x_1 \ll -b \ \text{ in the duct;} \end{cases}$$

ℓ_E is the required end correction. The energy T of the motion in V is entirely kinetic, and

$$T \equiv \frac{\rho_o U^2}{2}\int_V (\nabla\varphi)^2\, d^3\mathbf{x} = -\frac{\rho_o U^2}{2}\int_{S_p} \varphi \frac{\partial\varphi}{\partial x_1}\, dS = \frac{\rho_o U^2}{2} A_d(L+\ell_E),$$

where S_p is the face of the piston, at which $\varphi = -(L+\ell_E)$.

We now proceed by Rayleigh's method for the flanged cylindrical duct (Figure 5.4.5). For any compatible motion with kinetic energy T'

$$\frac{L}{A_d} + \frac{\ell_E}{A_d} \le \frac{2T'}{\rho_o Q^2}, \quad Q = UA_d. \tag{6.5.1}$$

Consider an approximation φ' whose normal derivative $\partial\varphi'/\partial x_1$ within the plane of the aperture satisfies

$$\frac{\partial\varphi'}{\partial x_1} = v_n \equiv \bar{v}\left(1 + \frac{\mu\varpi^2}{a^2} + \frac{\mu'\varpi^4}{a^4}\right), \tag{6.5.2}$$
$$x_1 = 0,\ 0 < \varpi = \sqrt{x_2^2 + x_3^2} < a.$$

Continuity requires that $A_d = \int_{S_0} v_n dS$, the integration being over the circular aperture of Figure 5.4.6, so that

$$\bar{v} = \frac{A_d}{\pi a^2\left(1 + \frac{\mu}{2} + \frac{\mu'}{3}\right)}.$$

Within the duct we can put

$$\varphi'(\mathbf{x}) = x_1 + \alpha_0 + \sum_{n=1}^{\infty} \alpha_n \mathrm{J}_0\left(\lambda_n \frac{\varpi}{b}\right) \mathrm{e}^{\lambda_n x_1/b}, \quad x_1 < 0, \quad \varpi < b,$$

where λ_n is the nth *positive* root of $d\mathrm{J}_0(\lambda)/d\lambda \equiv -\mathrm{J}_1(\lambda) = 0$.

Insert this into the left-hand side of equation (6.5.2) and use the orthogonality condition (5.3.7) to obtain

$$\alpha_n = \frac{2\bar{v}}{b\lambda_n \mathrm{J}_0^2(\lambda_n)} \int_0^a \left(1 + \frac{\mu\varpi^2}{a^2} + \frac{\mu'\varpi^4}{a^4}\right) \mathrm{J}_0\left(\lambda_n \frac{\varpi}{b}\right) \varpi\, d\varpi, \quad n \ge 1, \tag{6.5.3}$$

Downloaded from https://www.cambridge.org/core. Charité Universitätsmedizin Berlin, on 20 Dec 2021 at 10:08:46, subject to the Cambridge Core terms of use, available at https://www.cambridge.org/core/terms. https://doi.org/10.1017/CBO9781107360273.007

in which

$$\int_0^a \left(1+\frac{\mu\varpi^2}{a^2}+\frac{\mu'\varpi^4}{a^4}\right) \mathrm{J}_0\left(\lambda_n\frac{\varpi}{b}\right)\varpi\, d\varpi = \frac{ab}{\lambda_n}\left(\mathrm{J}_1(\bar\lambda_n)+\mu\mathcal{I}_n+\mu'\mathcal{I}'_n\right) \tag{6.5.4}$$

$$\mathcal{I}_n = \frac{(\bar\lambda_n^2-4)\mathrm{J}_1(\bar\lambda_n)+2\bar\lambda_n\mathrm{J}_0(\bar\lambda_n)}{\bar\lambda_n^2}$$

$$\mathcal{I}'_n = \frac{(\bar\lambda_n^2-8)[(\bar\lambda_n^2-8)\mathrm{J}_1(\bar\lambda_n)+4\bar\lambda_n\mathrm{J}_0(\bar\lambda_n)]}{\bar\lambda_n^4}$$

where $\bar\lambda_n = \xi\lambda_n, \quad \xi = \dfrac{a}{b}.$

The kinetic energy T_I of the motion within the section V_I, say, of the duct in the interval $-L < x_1 < 0$ (where $L \gg b$) is given by

$$\begin{aligned}\frac{2T_I}{\rho_o Q^2} &= \frac{1}{A_d^2}\int_{V_I}(\nabla\varphi')^2 d^3\mathbf{x}\\ &\equiv \frac{2\pi}{A_d^2}\int_0^b\left[\left(\varphi\frac{\partial\varphi'}{\partial x_1}\right)_{x_1=0}-\left(\varphi'\frac{\partial\varphi'}{\partial x_1}\right)_{x_1=-L}\right]\varpi\, d\varpi\\ &= \frac{L}{A_d}+\frac{2\pi\bar v}{A_d^2}\sum_{n=1}^{\infty}\alpha_n\int_0^a\left(1+\frac{\mu\varpi^2}{a^2}+\frac{\mu'\varpi^4}{a^4}\right)\mathrm{J}_0\left(\lambda_n\frac{\varpi}{b}\right)\varpi\, d\varpi\end{aligned}$$

i.e. using (6.5.3, 4),

$$\frac{2T_I}{\rho_o Q^2} = \frac{L}{A_d}+\frac{4b}{\pi a^2\left(1+\frac{\mu}{2}+\frac{\mu'}{3}\right)^2}\sum_{n=1}^{\infty}\frac{\left(\mathrm{J}_1(\bar\lambda_n)+\mu\mathcal{I}_n+\mu'\mathcal{I}'_n\right)^2}{\lambda_n^3\mathrm{J}_0^2(\lambda_n)}\,.$$

The expression for the kinetic energy T_E of the exterior motion is the same as for the flanged duct of §5.4.2 with b replaced by a, that is,

$$\frac{2T_E}{\rho_o Q^2} = \frac{8}{3\pi^2 a}\frac{\left(1+\frac{14\mu}{15}+\frac{5\mu^2}{21}+\frac{314\mu'}{525}+\frac{214\mu\mu'}{675}+\frac{89\mu'^2}{825}\right)}{\left(1+\frac{\mu}{2}+\frac{\mu'}{3}\right)^2}.$$

The relation (6.5.1) satisfied by $T' = T_I + T_E$ therefore becomes

Downloaded from https://www.cambridge.org/core. Charité Universitätsmedizin Berlin, on 20 Dec 2021 at 10:08:46, subject to the Cambridge Core terms of use, available at https://www.cambridge.org/core/terms. https://doi.org/10.1017/CBO9781107360273.007

$$\frac{\ell_E}{b} \le \left\{ \frac{8}{3\pi\xi}\left(1 + \frac{14\mu}{15} + \frac{5\mu^2}{21} + \frac{314\mu'}{525} + \frac{214\mu\mu'}{675} + \frac{89\mu'^2}{825}\right) + \frac{4}{\xi^2}\sum_{n=1}^{\infty}\left(\mathrm{J}_1(\bar{\lambda}_n) + \mu\mathcal{I}_n + \mu'\mathcal{I}'_n\right)^2 / \lambda_n^3 \mathrm{J}_0^2(\lambda_n)\right\} \Big/ \left(1 + \frac{\mu}{2} + \frac{\mu'}{3}\right)^2 .$$

For each fixed value of $\xi = a/b$, Rayleigh's approximation to the end correction ℓ_E is obtained by minimising the right-hand side of this expression with respect to its dependence on μ and μ' and replacing '$\le$' by '$=$'. When $a = b$ the minimum occurs at $\mu = -1.0120,\ \mu' = 1.9515$, for which $\ell_E/b = 0.8242$, in agreement with Rayleigh's calculation in §5.4.2.

The minima are determined by the method of §5.1.3. This yields the curves for ℓ_E/b and $K_o/b = \pi/(\ell_E/b)$ in the figure of Question 5.3.

5.7 Let the plane of the annular aperture be $y = 0$ (Figure 6.5.2) and consider flow through the aperture in the direction of increasing y with volume velocity $Q = UA$, where $A = \pi(b^2 - a^2)$ and U is the mean normal velocity in the aperture. For a narrow, slit-like aperture with $2h \equiv b - a$ ($\ll a$) the flux per unit length is $q = Q/2\pi\bar{b}$, $\bar{b} = (b + a)/2$, so that at distances $\ll a$ from a section of the slit we can put $\varphi = \mathrm{Re}\, w$, where

$$w = \frac{Q}{2\pi^2\bar{b}} \ln\left(\frac{\zeta}{h} + \sqrt{\frac{\zeta^2}{h^2} - 1}\right), \quad \zeta = x' + iy,$$

the coordinate origin being at the midpoint of the slit section with a local x'-axis parallel to the radius from the centre of the annulus.

Now, $\varphi = \mathrm{Re}\, w = 0$ within the plane of the slit ($|x'| < h, y = 0$), because

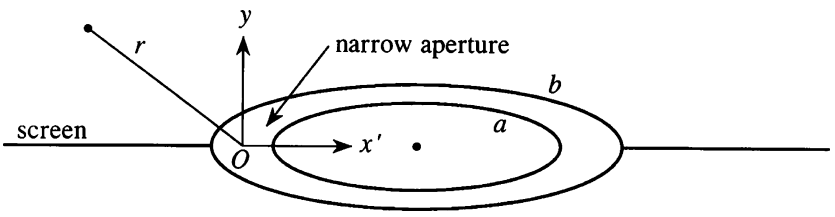

Figure 6.5.2

Downloaded from https://www.cambridge.org/core. Charité Universitätsmedizin Berlin, on 20 Dec 2021 at 10:08:46, subject to the Cambridge Core terms of use, available at https://www.cambridge.org/core/terms. https://doi.org/10.1017/CBO9781107360273.007

$$w = \frac{Q}{2\pi^2\bar{b}} \ln\left(\frac{x'}{h} + i\sqrt{1 - \frac{x'^2}{h^2}}\right)$$
$$= \frac{Q}{2\pi^2\bar{b}} \ln(\cos\theta + i\sin\theta) = \frac{Q}{2\pi^2\bar{b}} \ln\left(e^{i\theta}\right) = \frac{i\theta Q}{2\pi^2\bar{b}},$$

where $\cos\theta = x'/h,\ 0 < \theta < \pi$. This means that φ defined by w is an odd function of y. Thus, when $h \ll |\zeta| = r = \sqrt{x'^2 + y^2} \ll a$

$$\varphi \sim \mathrm{sgn}(y)\,\mathrm{Re}\,\frac{Q}{2\pi^2\bar{b}} \ln\left(\frac{2\zeta}{h}\right) = -\mathrm{sgn}(y)\,\frac{Q}{2\pi^2\bar{b}} \ln\left(\frac{h}{2r}\right). \quad (6.5.5)$$

This formula must match the 'inner' limit $|\mathbf{x}| \to a,\ (y \to \pm 0)$ of the narrow aperture approximation

$$\varphi(\mathbf{x}) = \mathrm{sgn}(y)\left(\frac{-Q}{(2\pi)^2\bar{b}} \int_S \frac{\delta(\varpi - \bar{b})dS(\mathbf{y}')}{|\mathbf{x} - \mathbf{y}'|} + \frac{U\ell}{2}\right).$$

When $y = 0$ and $|\mathbf{x}| < \bar{b}$ the integral can be evaluated in terms of the complete elliptic integral of the first kind $\mathbf{K}(p)$ $(= \frac{1}{2}\int_0^\pi d\theta/(1 \pm 2p\cos\theta + p^2)^{\frac{1}{2}}$, $|p| < 1$, Abramowitz & Stegun 1970), yielding

$$\varphi(\mathbf{x}) = \mathrm{sgn}(y)\left[\frac{-Q}{\pi^2\bar{b}}\,\mathbf{K}\left(\frac{|\mathbf{x}|}{\bar{b}}\right) + \frac{U\ell}{2}\right]$$
$$\sim \mathrm{sgn}(y)\left[\frac{-Q}{2\pi^2\bar{b}} \ln\left(\frac{16\bar{b}^2}{\bar{b}^2 - |\mathbf{x}|^2}\right) + \frac{U\ell}{2}\right], \quad \text{as } |\mathbf{x}| \to \bar{b}.$$

In the final expression $\bar{b} - |\mathbf{x}| = r$ when $y = 0$, so that $16\bar{b}^2/(\bar{b}^2 - |\mathbf{x}|^2) \simeq 8\bar{b}/r$, as $|\mathbf{x}| \to \bar{b}$, i.e.

$$\varphi(\mathbf{x}) \sim \mathrm{sgn}(y)\left[\frac{-Q}{2\pi^2\bar{b}} \ln\left(\frac{8\bar{b}}{r}\right) + \frac{U\ell}{2}\right], \quad y \to \pm 0.$$

This must coincide with the final term on the right of (6.5.5), which implies that $\ell/2 = (A/2\pi^2\bar{b})\ln(16\bar{b}/h)$, and therefore that

$$\frac{\ell}{b} \sim \frac{2(1-\xi)}{\pi} \ln\left(\frac{32}{1-\xi}\right), \quad \xi = \frac{a}{b} \sim 1.$$

The corresponding formula for the conductivity is deduced from $K_o = A/\ell$.

Downloaded from https://www.cambridge.org/core. Charité Universitätsmedizin Berlin, on 20 Dec 2021 at 10:08:46, subject to the Cambridge Core terms of use, available at https://www.cambridge.org/core/terms. https://doi.org/10.1017/CBO9781107360273.007

Downloaded from https://www.cambridge.org/core. Charité Universitätsmedizin Berlin, on 20 Dec 2021 at 10:08:46, subject to the Cambridge Core terms of use, available at https://www.cambridge.org/core/terms. https://doi.org/10.1017/CBO9781107360273.007

Bibliography

Abramowitz, M. and Stegun, I. A. 1970. *Handbook of Mathematical Functions*. Ninth corrected printing, U.S. Department of Commerce, National Bureau of Standard Applied Mathematics Series No. 55.

Baker, B. B. and Copson, E. T. 1969. *The Mathematical Theory of Huygens' Principle*. Second edition. Oxford: Oxford University Press.

Batchelor, G. K. 1967. *An Introduction to Fluid Dynamics*. Cambridge: Cambridge University Press.

Birkhoff, G. 1955. *Hydrodynamics – A Study in Logic, Fact and Similitude.* New York: Dover Publications (republication of edition published by Princeton University Press, 1950).

Birkhoff, G. and Zarantonello, E. H. 1957. *Jets, Wakes and Cavities*. New York: Academic Press.

Crighton, D. G. 1972. Radiation from vortex filament motion near a half plane. *Journal of Fluid Mechanics* **51**: 357–62.

Crighton D. G. 1975. Basic principles of aerodynamic noise generation. *Progress in Aerospace Sciences* **16**: 31–96.

Crighton, D. G. 1985. The Kutta condition in unsteady flow. *Annual Reviews of Fluid Mechanics* **17**: 411–45.

Crighton, D. G., Dowling, A. P., Ffowcs Williams, J. E., Heckl, M. and Leppington, F. G. 1992. *Modern Methods in Analytical Acoustics (Lecture Notes)*. London: Springer-Verlag.

Cummings, A. 1984. Acoustic nonlinearities and power losses at orifices. *American Institute of Aeronautics and Astronautics Journal* **22**: 786–92.

Curle, N. 1955. The influence of solid boundaries upon aerodynamic sound. *Proceedings of the Royal Society of London* **A231**: 505–14.

Dowling, A. P. and Ffowcs Williams, J. E. 1983. *Sound and Sources of Sound*. Chichester, UK: Ellis Horwood.

Fant, G. 1960. *Acoustic Theory of Speech Production*. The Hague: Mouton.

Ffowcs Williams, J. E. and Hawkings, D. L. 1969. Sound generation by turbulence and surfaces in arbitrary motion. *Philosophical Transactions of the Royal Society of London* **A264**: 321–42.

Ffowcs Williams, J. E. and Hall, L. H. 1970. Aerodynamic sound generation by turbulent flow in the vicinity of a scattering half-plane. *Journal of Fluid Mechanics* **40**: 657–70.

Downloaded from https://www.cambridge.org/core. Charité Universitätsmedizin Berlin, on 20 Dec 2021 at 10:08:47, subject to the Cambridge Core terms of use, available at https://www.cambridge.org/core/terms. https://doi.org/10.1017/CBO9781107360273.008

Ffowcs Williams, J. E. 1974. Sound production at the edge of a steady flow. *Journal of Fluid Mechanics* **66**: 791–816.

Fock, V. A. 1941. A theoretical investigation of the acoustical conductivity of a circular aperture in a wall put across a tube. *Comptes Rendus (Doklady) de l'Academie des Sciences de l'URSS* **31**: 875–8.

Goldstein, M. E. 1976. *Aeroacoustics*. New York: McGraw-Hill.

Goldstein, S. 1960. *Lectures on Fluid Mechanics*. New York: Interscience.

Gurevich, M. I. 1965. *Theory of Jets in Ideal Fluids*. New York: Academic Press.

Hadamard, J. 1952. *Lectures on Cauchy's Problem in linear partial differential equations*. New York: Dover Publications.

Howe, M. S. 1975. The generation of sound by aerodynamic sources in an inhomogeneous steady flow. *Journal of Fluid Mechanics* **67**: 579–610.

Howe, M. S. 1975. Contributions to the theory of aerodynamic sound, with application to excess jet noise and the theory of the flute. *Journal of Fluid Mechanics* **71**: 625–73.

Howe, M. S. 1989. On unsteady surface forces, and sound produced by the normal chopping of a rectilinear vortex. *Journal of Fluid Mechanics* **206**: 131–53.

Howe, M. S. 1995. On the force and moment exerted on a body in an incompressible fluid, with application to rigid bodies and bubbles at high and low Reynolds numbers. *Quarterly Journal of Mechanics and Applied Mathematics* **48**: 401–26.

Howe, M. S. 1998. *Acoustics of Fluid-Structure Interactions*. Cambridge: Cambridge University Press.

Howe, M. S. 2003. *Theory of Vortex Sound*. Cambridge: Cambridge University Press.

Huang, Z. 2014. *On the Sound Produced by a Synthetic Jet Device*. Master of Science thesis, Boston University, Department of Mechanical Engineering.

Kelvin, Lord. 1867. On vortex motion. *Transactions of the Royal Society of Edinburgh* **25**: 217–60.

Kelvin, Lord. 1867. On vortex atoms. *Philosophical Magazine* **34**: 15–24.

Kelvin, W. T. and Tate, P. G. 1879. *Treatise on Natural Philosophy*. Cambridge: Cambridge University Press.

Lamb, Horace. 1932. *Hydrodynamics*. Sixth edition. Cambridge: Cambridge University Press.

Landau, L. D. and Lifshitz, E. M. 1987. *Fluid Mechanics*. Second edition. Oxford: Pergamon.

Lebedeva, I. V. and Grushin, A. E. 2003. Amplitude and frequency characteristics of acoustic jets. *Acoustical Physics* **49**: 300–4.

Levine, H. and Schwinger, J. 1948. On the radiation of sound from an unflanged circular pipe. *Physical Review* **73**: 383–406.

Lighthill, M. J. 1952. On sound generated aerodynamically. Part I: General theory. *Proceedings of the Royal Society of London* **A211**: 564–87.

Lighthill, M. J. 1958. *An Introduction to Fourier Analysis and Generalised Functions*. Cambridge: Cambridge University Press.

Lighthill, James. 1978. *Waves in Fluids*. Cambridge: Cambridge University Press.

Milne-Thomson, L. M. 1968. *Theoretical Hydrodynamics*. Fifth edition. London: Macmillan.

Möhring, W. 1978. On vortex sound at low Mach number. *Journal of Fluid Mechanics* **85**: 685–91.

Downloaded from https://www.cambridge.org/core. Charité Universitätsmedizin Berlin, on 20 Dec 2021 at 10:08:47, subject to the Cambridge Core terms of use, available at https://www.cambridge.org/core/terms. https://doi.org/10.1017/CBO9781107360273.008

Möhring, W. 1980. Modelling low Mach number noise. In *Mechanics of Sound Generation in Flows*, ed. E.-A. Müller, pp. 85–96. Berlin: Springer-Verlag.

Noble, B. 1958. *Methods Based on the Wiener-Hopf Technique*. London: Pergamon Press.

Pierce, A. D. 1989. *Acoustics: An Introduction to Its Principles and Applications*. Woodbury, New York: American Institute of Physics.

Powell, A. 1963. *Mechanisms of Aerodynamic Sound Production.* AGARD Report No. 466.

Powell, A. 1964. Theory of vortex sound. *Journal of the Acoustical Society of America* **36**: 177–95.

Rayleigh, Lord. 1870. On the theory of resonance. *Philosophical Transactions of the Royal Society of London* **161**: 77–118.

Rayleigh, Lord. 1873. Harmonic echoes. *Nature* VIII, 319–20.

Rayleigh, Lord. 1945. *Theory of Sound*, Volumes 1 and 2. New York: Dover.

Saffman, P. G. 1993. *Vortex Dynamics*. Cambridge: Cambridge University Press.

Sears, W. R. 1941. Some aspects of non-stationary airfoil theory and its practical applications. *Journal of the Aeronautical Sciences* **8**: 104–8.

Smith, B. L. and Glezer, A. 1998. The formation and evolution of synthetic jets. *Physics of Fluids* **10**: 2281–97.

Downloaded from https://www.cambridge.org/core. Charité Universitätsmedizin Berlin, on 20 Dec 2021 at 10:08:47, subject to the Cambridge Core terms of use, available at https://www.cambridge.org/core/terms. https://doi.org/10.1017/CBO9781107360273.008

Downloaded from https://www.cambridge.org/core. Charité Universitätsmedizin Berlin, on 20 Dec 2021 at 10:08:47, subject to the Cambridge Core terms of use, available at https://www.cambridge.org/core/terms. https://doi.org/10.1017/CBO9781107360273.008

Index

acoustic, analogy, 143
  energy density, 32
  far field, 37
  intensity, 31, 34, 107
  particle velocity, 6, 9
  power, 34
  wavenumber, 12
added mass, piston, 115
  sphere, 81
  tensor, 80, 177, 193
advanced potential, 48
  compact Green's function, 129
  derivation of Kirchhoff's formula, 57
airfoil, 180 et seq.

baffle, 105
baffle-plate aperture, 218
bias flow, 131
  energy equation, 135
  perforated screen, 136
Biot-Savart formula, 160
blade-vortex interaction, 181, 188
bursting balloon, 21, 35
Babinet's principle, 119
Batchelor, 65, 79, 80, 131, 147, 157, 161
Bernoulli's equation, 102, 194

Cauchy's problem, 21
Cauchy-Riemann equations, 94
causality, 14
clover leaf quadrupole pattern, 40
combustion, 27
compact, acoustically, 13
  aperture, 124
  sphere, 14, 30
  turbulent eddy, 149
compact Green's function, preliminary definition, 63, 66
  circular aperture, 90, 129
  circular cylinder, 72, 85
  circular disc, 90
  cylindrical bodies, 70
  definition for Helmholtz equation, 75
  definition for wave equation, 76
  deletion of trailing edge singularity, 180, 184, 189
  disc at air-water interface, 266
  duct open end, 88
  duct with neck, 87
  general form, 84
  half-plane, 87
  incompressible limit, 102
  rigid strip, 72, 85
  sphere, 68, 85
  surface irregularity, 84
  symmetric, 74
  synthetic jet device, 239
  two dimensional, 91
compressive stress, 150
complex potential, definition, 94
  circular cylinder, 94
  for strip, 73
  uniform flow, 94
  vortex, 95
complex velocity, 94
conductivity, defined, 126
  annular aperture in a duct, 220
  annular aperture, 211, 284
  aperture in a duct, 214

Downloaded from https://www.cambridge.org/core. Charité Universitätsmedizin Berlin, on 20 Dec 2021 at 10:08:46, subject to the Cambridge Core terms of use, available at https://www.cambridge.org/core/terms. https://doi.org/10.1017/CBO9781107360273

circular aperture, 127, 205
complex, 135
duct of variable diameter, 232
duct with flanged exit, 228
duct with small axisymmetric opening, 225
duct with small flanged exit, 228, 246
Rayleigh's approximation, 205
conformal transformation, 96
half-plane, 96
of sources and vortices, 96
continuity equation, 2
linearised, 7
contraction ratio, 131, 135
control surface, 49
Crighton, 173
Crocco's equation, 5, 138, 158, 164
Cummings, 135
Cummings-Fant equation, 134
synthetic jet, 241
with mean flow, 234
Curle, 150
Curle's equation, 152
differential form, 151

D'Alembert, 9
damping by vorticity production, 135, 139
at circular and annular duct apertures, 235
linearised approximation, 135, 140, 234
perforated screen, 136, 140
decibel, 6
descent, Hadamard's method, 20
diffraction, Kirchhoff theory, 116
aperture, 119
disc, 120
edge, 121
diffraction radiation, 256
disc, vibrating, 104
drag coefficient, 196

efficiency, pulsating sphere, 269
surface dipole, 153
synthetic jet, 244
turbulence sound source, 149
vibrating sphere, 35, 269
eighth power law, 149
end correction, 223
circular duct exit, 224, 247
duct with flanged exit, 228
duct with small axisymmetric opening, 225
duct with small flanged exit, 228, 246, 281
energy, compressional, 32
density, 32
equation for aperture flow, 128
equation, 3
flux, 32, 34, 169
for aperture flow in a duct, 233
for synthetic jet device, 241
internal, 5
kinetic, 32
power, 34
enthalpy, definition, 5
perfect gas, 6
entropy, 4
equation of state, 4

far field, 31, 37
Fraunhofer, 38, 119, 254
Fresnel transition region, 42, 119, 120
hydrodynamic, 160
Ffowcs Williams, 147
Ffowcs Williams-Hawkings equation, 154
flame holder, 220
fluid particle, 2
Fock, 214
Fock's problem, 214
solved by Rayleigh's method, 216
force, for body in translational motion, 193
in potential flow, 194
in terms of added mass, 80
in terms of vorticity, 178, 192
Fourier transform, 58
Fraunhofer far field, 38, 119, 254
dipole source, 38
quadrupole source, 40
Fresnel zone, 42, 109, 119
aperture, 119
baffled piston, 110
disc, 120

generalised function, 17
Green's function, see also compact Green's function
definition, 19
for hard wall, 54
for pressure-release surface, 54, 265
free space, 19
in one dimension, 20
in two dimensions, 21
time-domain, 19, 59
time-harmonic, 59
gust, 179, 187

Downloaded from https://www.cambridge.org/core. Charité Universitätsmedizin Berlin, on 20 Dec 2021 at 10:08:46, subject to the Cambridge Core terms of use, available at https://www.cambridge.org/core/terms. https://doi.org/10.1017/CBO9781107360273

Hadamard, 20
harmonic echoes, 83
Heaviside function, definition, 20
  in surface/volume integrals, 48
Helmholtz, equation, 59
  resonator, 142, 242
homentropic motion, 5
  approximation, 7
Howe, 190
Huygens' principle, 116, 117

ideal fluid, definition, 7
  in two dimensions, 93
impedance, 61
impulse, vortex, 161
impulsive pressure, 212
incompressible fluid, 14
intensity, 31, 34, 107

Kelvin, circulation theorem, 155, 197
  definition of vorticity, 155
  minimum energy theorem, 157, 205
  theorem for impulsive motion, 213
kinetic energy, acoustic, 32
  incompressible and irrotational, 126, 156
  Kelvin's theorem, 157, 205, 213
Kirchhoff, vector, 66
  spinning vortex 198, 272
Kirchhoff diffraction theory, 116
  aperture, 119
  disc, 120
  edge, 121
Kirchhoff formula, 50
  applied to vibrating body, 51
  for velocity potential, 55
  generalised, 52, 58
  in frequency domain, 60
Kutta condition, 185
  see also singularities

Laplace equation, 13
  axisymmetric, 67
  cylindrically symmetric, 71
  two dimensions, 93
Lighthill, 17
Lighthill's, acoustic analogy, 145
  equation, 146
  v^8-law, 146
  stress tensor, 145
  theory reformulated in terms of vorticity, 165
loudspeaker, 104

material derivative, 2
momentum equation, 3
  Crocco's form, 5
  linearised, 7
  Reynolds form, 144
momentum, density, 150, 212
  flux tensor, 144
monopole, 25
multipole expansion, 41

Navier-Stokes equation, 3
near field, 31
  hydrodynamic, 31
no-slip condition, 157, 180
Noble, 124

Ohm's law, 126
orifice plate, 232
outgoing wave, 16, 18

piston, baffled, 105
  in uniform tube, 10
  surface force, 113
  time-harmonic vibrations, 106
plane wave, 9
point source, 16
  impulsive, 18
Poisson, 22, 121
potential flow interaction, 184, 191
Powell, 167
power, acoustic, 34
pressure, impulsive, 212
  in terms of potential, 8
  thermodynamic, 5

quadrupole, 28
  Lighthill's, 146

radiation condition, 14
rate of strain tensor, 4, 139, 144
Rayleigh, 61, 81, 83, 115, 205, 228, 282
Rayleigh's integral, 106
reciprocal theorem, 62, 64, 74
reduced frequency, 182
reflection, from closed end, 10
  open end, 10
resonance frequency, open ended tube, 11
retarded, potential, 20
  time, 15

Downloaded from https://www.cambridge.org/core. Charité Universitätsmedizin Berlin, on 20 Dec 2021 at 10:08:46, subject to the Cambridge Core terms of use, available at https://www.cambridge.org/core/terms. https://doi.org/10.1017/CBO9781107360273

Reynolds, equation, 144
number, 153
stress, 146, 147
Runge-Kutta integration, 100, 243

scattering, Rayleigh, 81
sphere, 83
Sears, 180, 185
Sears function, 185
self potential, vortex, 97
singularities, deleting from Green's function, 180, 182, 184, 189
slug length, 126
annular aperture, 211, 284
annular aperture in a duct, 220
aperture in a duct, 214, 281
circular aperture, 127, 205
relation to kinetic energy, 205
source, dipole, 27
impulsive, 18
monopole, 25
quadrupole, 28
volume, 7
speed of sound, 6, 8
nonlinear, 10
perfect gas, 9
values in air and water, 9
sphere, compact, 14, 68
modelled by point source, 17
near dipole source, 68
pulsating, 13
radiated power, 34
vibrating, 30, 78
stationary phase, method, 112, 169, 275
Stokesian fluid, 3
stream function, 94, 175
equation, 226
stress, compressive, 150
Lighthill's, 145
Reynolds, 146–148
viscous, 144
Strouhal number, 133, 136
synthetic jet, 237
characteristic equation, 242

test function, 17, 272, 276
thermodynamic pressure, 5
time-harmonic, Green's function, 59
wave equation, 59
trailing edge, singularity, 180
total enthalpy, definition, 6
as acoustic variable, 164
homentropic flow, 164
relation to pressure, 165, 167
relation to velocity potential, 165
turbulence, source of sound, 143, 145
eddy, 148
near compact body, 152
gust, 179

uniqueness, outgoing wave solution, 56

vibrating compact body, 51, 77, 81, 154
disc, 104
sphere, 30, 78, 81
viscosity, bulk, 3
kinematic, 3
shear, 3
values for air and water, 4
velocity potential, 8
volume, flux, 15
point source, 16
source, 7
velocity, 15
vortex, complex potential, 95
equation of motion, 97
impulse, 161
motion near half-plane, 98, 173
pair motion towards a plane, 261
ring, 199, 201
sheet, 131
spinning pair, 167
surface interaction noise, 170, 181, 186, 188
tube, 157
vortex shedding, 179, 181
influence on sound generation, 179
vortex line, 157
interaction with blade, 181, 188
molecular diffusion, 159
stretching and rotation, 159
vortex sound, at high Reynolds number, 173
equation, 166
from compact body, 176
general solution, 172
linearised, 187
produced by blade-vortex interaction, 181, 188
produced by vortex near an edge, 173
two-dimensions, 178

Downloaded from https://www.cambridge.org/core. Charité Universitätsmedizin Berlin, on 20 Dec 2021 at 10:08:46, subject to the Cambridge Core terms of use, available at https://www.cambridge.org/core/terms. https://doi.org/10.1017/CBO9781107360273

vorticity, definition, 3
damping of sound, 139
equation, 158
frozen, 179, 187
generated by sound, 131
measure of angular velocity, 157
molecular diffusion, 159
quasi-static approximation, 133
sound source, 164
stretching and rotation, 159
wave equation, ideal fluid, 7
inhomogeneous, 8
initial value problem, 21
of classical acoustics, 8
of linear acoustics, 144
one dimensional, 9, 14
solution in free space, 29
vortex-sound, 166
wavenumber, acoustic, 12

Downloaded from https://www.cambridge.org/core. Charité Universitätsmedizin Berlin, on 20 Dec 2021 at 10:08:46, subject to the Cambridge Core terms of use, available at https://www.cambridge.org/core/terms. https://doi.org/10.1017/CBO9781107360273